SCUOLA DI DOTTORATO
UNIVERSITÀ DEGLI STUDI DI MILANO-BICOCCA

Department of Medicine and Surgery

PhD program in Translational and Molecular Medicine
XXXVI cycle

Study of the immunological landscape in Myelodysplastic Syndromes: a multi-omics approach

Elena Riva

Registration Number: 791898

Tutor: Prof. Matteo Giovanni Della Porta

Coordinator: Prof. Francesco Mantegazza

ACADEMIC YEAR 2022/2023

Table of Contents

Chapter 1

General Introduction

1.1 Myelodysplastic Syndromes

Myelodysplastic syndromes (MDS) are a heterogeneous group of hematopoietic stem cell (HSC) clonal disorders characterized by abnormal cell morphology (myelodysplasia), ineffective hematopoiesis which leads to peripheral blood cytopenia, recurrent genetic abnormalities and an increased risk of evolution to acute myeloid leukemia (AML), called secondary acute myeloid leukemia (sAML) (Cazzola M., 2020; Corey et al., 2007). Approximately 30% of MDS patients progress to leukemia, and secondary AML accounts for 19-25% of total AML cases, showing also a worse outcome compared to de novo AML (Enrico et al., 2017; Granfeldt Østgård et al., 2015; Hulegårdh et al., 2015; Xu et al., 2014).

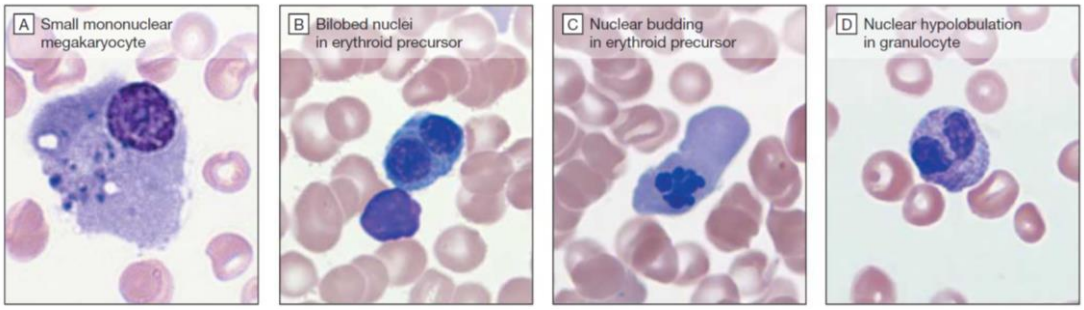

Figure 1

Examples of common morphologic alterations in MDS. Figure from Olnes et al., 2011.

1.1.1 Diagnosis and clinical classification

MDS are among the most common hematological malignancies, with an incidence in the United States between 5.3 and 13.1 cases per 100,000 persons (Cogle, 2015) which is expected to substantially increase due to the progressive population aging. The median age at diagnosis is 71–76 years (Ma et al., 2007; Sekeres et al., 2011) and while no difference in MDS incidence based on sex has been observed in patients <40 years of age, a marked male predominance exists in those >40 years of age (Li et al., 2022).

Although some patients can be asymptomatic at diagnosis and are identified only by the incidental discovery of cytopenia, the most common symptoms for MDS finding are fatigue and weakness (often related to anemia), easy bruising and bleeding (owing to thrombocytopenia) and recurrent bacterial and fungal infections (as a result of neutropenia).

Until 2022, MDS diagnosis and classification were made according to the World Health Organization (WHO) guidelines of 2016 (Arber et al., 2016).

The key diagnostic criteria were (Cazzola, 2020; Montalban-Bravo et al., 2018):

- persistent cytopenia in one or more peripheral-blood cell lineages, assessed by peripheral blood cell count
- morphologic dysplasia in one or more bone marrow cell lineages (the frequency of dysplastic cells must be ≥ 10%) and presence of blasts, assessed by bone marrow aspirate and biopsy
- chromosomal aberrations, assessed by cytogenetic analyses

The subtypes of MDS were classified on the basis of the number of dysplastic lineages (single- or multi-lineage dysplasia), presence or absence of ring sideroblasts, percentage of bone marrow and peripheral-blood blasts, and type of cytogenetic abnormality, in particular the deletion of the chromosome 5 long arm (5q) was considered as a distinct MDS entity (table 1).

Myeloblasts must have a frequency less than 20% on total nucleated cells in the bone marrow: over that threshold, a diagnosis of secondary AML is made (Cazzola M., 2020; Arber et al., 2016).

Disorder	Diagnostic Criteria
Myeloid neoplasms with myelodysplasia	
MDS	Persistent cytopenia in one or more peripheral-blood cell lineages and morphologic dysplasia (≥10% dysplastic cells) in one or more bone marrow cell lineages; on the basis of morphologic and cytogenetic abnormalities, MDS are categorized into the following subtypes: MDS with single-lineage dysplasia MDS with multilineage dysplasia MDS with ring sideroblasts and single-lineage dysplasia or multilineage dysplasia MDS with isolated del(5q) MDS with excess blasts type 1 or type 2 MDS, unclassifiable†
Myelodysplastic–myeloproliferative neoplasms	Myeloid neoplasms with clinical, laboratory, and morphologic features that overlap those of MDS and myeloproliferative neoplasms; myelodysplastic–myeloproliferative neoplasms are divided into the following subtypes: Chronic myelomonocytic leukemia *BCR-ABL1*–negative atypical chronic myeloid leukemia Myelodysplastic–myeloproliferative neoplasm with ring sideroblasts and thrombocytosis Juvenile myelomonocytic leukemia
Therapy-related myeloid neoplasms[9]	MDS, myelodysplastic–myeloproliferative neoplasms, and acute myeloid leukemia that occur as late complications of chemotherapy or radiotherapy
MDS precursor conditions	
CHIP	Normal peripheral-blood cell counts with a somatic mutation, at a variant allele frequency of at least 2%, in a gene that is recurrently mutated in myeloid neoplasms‡
CCUS	Unexplained cytopenia in one or more peripheral-blood cell lineages; a somatic mutation, at a variant allele frequency of at least 20%, in one or more genes that are recurrently mutated in myeloid neoplasms; and insufficient WHO criteria for a diagnosis of MDS, essentially because of lack of overt dysplasia (<10% dysplastic cells in any bone marrow cell lineage), excess blasts, and MDS-defining chromosomal abnormalities[8]§

Table 1

Diagnostic criteria for Myeloid Neoplasms with Myelodysplasia and precursor conditions for MDS, based on WHO 2016 classification. Table from Cazzola, 2020

In 2022, two independent novel classification of myeloid neoplasms and leukemias were published: the WHO 2022 (Khoury et al., 2022) and the International Consensus Classification (ICC) 2022 (Arber et al., 2022).

The WHO 2022 classification has introduced the term “myelodysplastic neoplasms” (always abbreviated as MDS) in place of myelodysplastic syndromes and maintains the threshold for dysplasia at 10% for all lineages. This classification divides MDS in two different branches (table 2): those with defined genetic abnormalities and those defined by morphology. The genetic abnormalities that are taken into account are the isolated 5q deletion (MDS 5q-), the mutation in SF3B1 gene (MDS-SF3B1) and the biallelic inactivation of TP53 gene (MDS-biTP53). Among morphologically defined category, MDS are classified on the basis of blast percentage (MDS with low blast – LB –, MDS with increased blast – IB1/IB2 –), hypoplasia (MDS-h), the presence of fibrosis (MDS-f) or ring sideroblast (MDS-RS). The number of dysplastic lineages (single- or multi-) has been removed from classification criteria.

	Blasts	Cytogenetics	Mutations
MDS with defining genetic abnormalities			
MDS with low blasts and isolated 5q deletion (MDS-5q)	<5% BM and <2% PB	5q deletion alone, or with 1 other abnormality other than monosomy 7 or 7q deletion	
MDS with low blasts and *SF3B1* mutation[a] (MDS-*SF3B1*)		Absence of 5q deletion, monosomy 7, or complex karyotype	*SF3B1*
MDS with biallelic *TP53* inactivation (MDS-bi*TP53*)	<20% BM and PB	Usually complex	Two or more *TP53* mutations, or 1 mutation with evidence of *TP53* copy number loss or cnLOH
MDS, morphologically defined			
MDS with low blasts (MDS-LB)	<5% BM and <2% PB		
MDS, hypoplastic[b] (MDS-h)			
MDS with increased blasts (MDS-IB)			
MDS-IB1	5–9% BM or 2–4% PB		
MDS-IB2	10-19% BM or 5–19% PB or Auer rods		
MDS with fibrosis (MDS-f)	5–19% BM; 2–19% PB		

[a]Detection of ≥15% ring sideroblasts may substitute for *SF3B1* mutation. Acceptable related terminology: MDS with low blasts and ring sideroblasts.
[b]By definition, ≤25% bone marrow cellularity, age adjusted.
BM bone marrow, *PB* peripheral blood, *cnLOH* copy neutral loss of heterozygosity.

Table 2

MDS WHO 2022 classification. Table from Khoury et al., 2022

ICC2022 instead maintained the single- or multi- lineage dysplasia when no otherwise is specified (MDS NOS-SLD and MDS NOS-MLD) but does not consider the presence of ring sideroblast. Furthermore, this classification divides MDS in two different classes on the basis of blast percentage: those with 5-9% of blasts are classified as MDS with excess blasts (MDS-EB), whereas those with a blast percentage of 10-19% are classified as MDS/AML, underlying the disease continuum and similarities among MDS and sAML (table 3). The genetic abnormalities that are considered as relevant for this classification are the isolated 5q deletion (MDS-del(5q)), the SF3B1 mutation (MDS-SF3B1) and the TP53 mutation that should be multi-hit or copy number loss in MDS with < 9% blasts or any mutation with a VAF > 10% in MDS/AML (table 4).

	Dysplastic lineages	Cytopenias	Cytoses*	BM and PB Blasts	Cytogenetics†	Mutations
MDS with mutated *SF3B1* (MDS-*SF3B1*)	Typically ≥1‡	≥1	0	<5% BM <2% PB	Any, except isolated del(5q), −7/del(7q), abn3q26.2, or complex	*SF3B1* (≥ 10% VAF), without multi-hit *TP53*, or *RUNX1*
MDS with del(5q) [MDS-del(5q)]	Typically ≥1‡	≥1	Thrombocytosis allowed	<5% BM <2% PB§	del(5q), with up to 1 additional, except −7/del(7q)	Any, except multi-hit *TP53*
MDS, NOS without dysplasia	0	≥1	0	<5% BM <2% PB§	−7/del(7q) or complex	Any, except multi-hit *TP53* or *SF3B1* (≥ 10% VAF)
MDS, NOS with single lineage dysplasia	1	≥1	0	<5% BM <2% PB§	Any, except not meeting criteria for MDS-del(5q)	Any, except multi-hit *TP53*;not meeting criteria for MDS-*SF3B1*
MDS, NOS with multilineage dysplasia	≥2	≥1	0	<5% BM <2% PB§	Any, except not meeting criteria for MDS-del(5q)	Any, except multi-hit *TP53*,; not meeting criteria for MDS-*SF3B1*
MDS with excess blasts (MDS-EB)	Typically ≥1‡	≥1	0	5-9% BM, 2-9% PB§	Any	Any, except multi-hit *TP53*
MDS/AML	Typically ≥1‡	≥1	0	10-19% BM or PB‖	Any, except AML-defining¶	Any, except *NPM1*, bZIP *CEBPA* or *TP53*

*Cytoses: Sustained white blood count ≥ 13 × 10^9/L, monocytosis (≥0.5 × 10^9/L and ≥10% of leukocytes) or platelets ≥450 × 10^9/L; thrombocytosis is allowed in MDS-del(5q) or in any MDS case with inv(3) or t(3;3) cytogenetic abnormality.

†*BCR::ABL1* rearrangement or any of the rearrangements associated with myeloid/lymphoid neoplasms with eosinophilia and tyrosine kinase gene fusions exclude a diagnosis of MDS, even in the context of cytopenia.

‡Although dysplasia is typically present in these entities, it is not required.

§Although 2% PB blasts mandates classification of an MDS case as MDS-EB, the presence of 1% PB blasts confirmed on 2 separate occasions also qualifies for MDS-EB.

‖For pediatric patients (<18 y), the blast thresholds for MDS-EB are 5% to 19% in BM and 2% to 19% in PB, and the entity MDS/AML does not apply.

¶AML-defining cytogenetics are listed in the AML section.

Table 3

MDS ICC 2022 classification. Table from Arber et al., 2022.

Type	Cytopenia	Blasts	Genetics
MDS with mutated *TP53*	Any	0-9% bone marrow and blood blasts	Multi-hit TP53 mutation* or *TP53* mutation (VAF > 10%) and complex karyotype often with loss of 17p†
MDS/AML with mutated *TP53*	Any	10-19% bone marrow or blood blasts	Any somatic *TP53* mutation (VAF > 10%)
AML with mutated *TP53*	Not required	≥20% bone marrow or blood blasts or meets criteria for pure erythroid leukemia	Any somatic *TP53* mutation (VAF > 10%)

*Defined as 2 distinct *TP53* mutations (each VAF > 10%) OR a single *TP53* mutation with (1) 17p deletion on cytogenetics; (2) VAF of >50%; or (3) Copy-neutral LOH at the 17p *TP53* locus.

†If *TP53* locus LOH information is not available.

Table 4

ICC 2022 criteria for TP53 mutations. Table from Arber et al., 2022.

It is thus evident that both novel classifications aim to integrate mutational data into MDS stratification, according to the huge number of papers supporting the impact of such mutations on patients' survival, disease phenotype, therapeutic decision making and clinical outcome. In fact, SF3B1 mutation has been associated to good prognosis and generally identifies the ring sideroblast phenotype (Malcovati et al., 2015; Malcovati et al., 2020), whereas mutations in TP53 gene were instead associated with worse prognosis, a more aggressive disease phenotype, an increased risk of sAML evolution and shorter treatment response duration, especially when multi-hit and with a high VAF (Bernard et al., 2020; Sallman et al., 2016; Takahashi et al., 2016).

MDS are frequently anteceded by clonal hematopoiesis of indeterminate potential (CHIP) or clonal cytopenias of undetermined significance (CCUS), pre-malignant conditions both characterized by the clonal expansion of somatically mutated clones but absence of dysplasia, excess of blasts and MDS-defining chromosomal abnormalities (Steensma et al., 2015; Steensma DP., 2019). These biological states are very common with aging (they were found in almost 10% of over 65) and are associated with an increased risk for subsequent hematologic cancers (Genovese et al., 2014; Jaiswal et al., 2014). In CHIP patients, the somatic mutation occurs in a gene which is frequently mutated in myeloid neoplasms (especially DNMT3A, TET2 and ASXL1) and is found with a variant allele frequency (VAF) of at least 2%. CCUS patients show instead a VAF of at least 20%, and for this reason have a greater risk of malignancy evolution and show a natural history similar to MDS (Steensma DP., 2019; Malcovati et al., 2017). Another important difference between CHIP and CCUS is the fact that CHIP patients are not cytopenic, whereas CCUS is characterized by cytopenia in one or more blood cell lineages.

In the end, there is a third clinical condition which is characterized by persistent cytopenia in absence of clonal hematopoiesis and without meeting the minimal criteria for MDS: this peculiar phenotype is called idiopathic cytopenia of undetermined significance (ICUS) and fall into the category of "unexplained cytopenias", since no karyotypic abnormalities or gene defects are detected in most of the cases (Valent et al., 2012). Rarely, some patients showed clonal hematopoiesis (detected by Fluorescent in situ hybridization - FISH) but often these clones are very small (Wimazal et al., 2007; Schroeder et al., 2010). Since some ICUS patients could develop MDS or leukemia, especially the ones carrying karyotypic alterations, a long-term follow up is recommended.

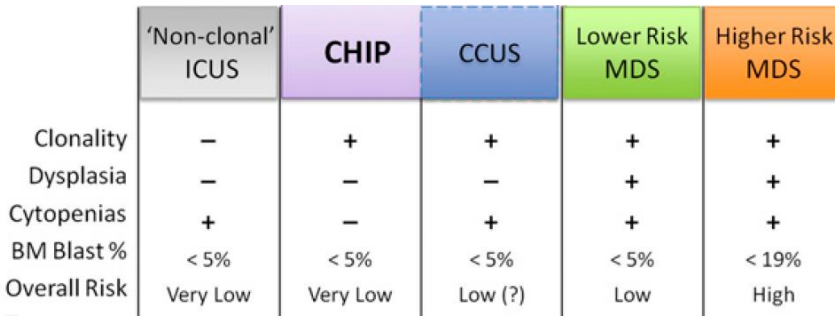

Figure 2

The different spectrum of clonal hematopoiesis and cytopenia. Figure re-adapted from Steensma et al., 2015.

1.1.2 Risk stratification: IPSS-R and IPSS-M

In MDS patients, morbidity and mortality are primarily related to complications arising from cytopenias and transformation to leukemia. However, clinical course is very variable among patients: some live for many years with minimal supportive care, whereas other progress in few months to AML. Due to this variability, several risk stratification systems have been developed in the past decades. In 1997, a collaborative study headed by Greenberg at Stanford University, established the International Prognostic Scoring System (IPSS) with the aim to estimate the risk of evolution to AML and expected survival on the basis of the degree of cytopenia, percentage of bone marrow blasts and cytogenetic features (Greenberg P et al., 1997). This scoring system was subsequently revised in 2012 (IPSS-R) with the addition of novel clinical and biological criteria such as the inclusion of a broader set of chromosomal aberrations and blast percentages, patient age, serum ferritin, hemoglobin and lactate dehydrogenase level. The IPSS-R stratifies patients into five risk groups, whereas the original IPSS had four (Greenberg P et al., 2012; Cazzola M., 2020):

- Very low risk MDS: IPSS-R score ≤ 1.5; median overall survival 8.8 years
- Low risk MDS: IPSS-R score 1.5-3; median overall survival 5.3 years
- Intermediate risk MDS: IPSS-R score 3-4.5; median overall survival 3 years
- High risk MDS: IPSS-R score 4.5-6; median overall survival 1.6 years
- Very high risk MDS: IPSS-R score > 6; median overall survival 0.8 years

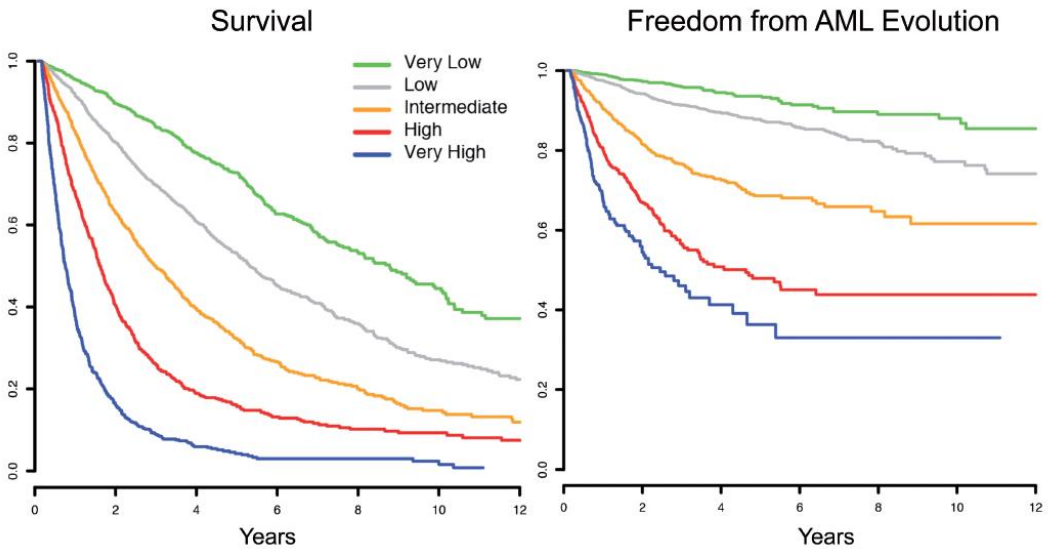

Figure 3

Clinical outcomes of patients with myelodysplastic syndrome in relation to Revised International Prognostic Scoring System prognostic risk-based categories. Figure from Hellström-Lindberg et al., 2020.

The evaluation of recurrent chromosomal abnormalities is very important for diagnosis and prognostication of MDS. Those alterations are detected, by metaphase karyotyping, in about half of patients (Haase et al., 2007). Most of abnormalities are unbalanced changes resulting in loss or gain (called copy number alterations – CNAs) of a large amount of chromosomal material (Ogawa, 2019). The most frequent among these are -7/del(7q) and -5/del(5q), followed by trisomy 8, dup(1q), del(20q), del(11q), del(12p)/t(12p), del(17p)/iso(17q), del(18q), +21q gains, del(13q), and +der(1;7)(q10;p10). These are secondary genetic events deriving from the genomic instability caused by the genetic driver mutations: the only exception is represented by del(5q), which characterizes the 5q- syndrome. Many chromosomal lesions can cooccur as a part of complex abnormalities, designated as complex karyotypes (CKs): complex karyotype is often accompanied by TP53 mutations and is associated with poor prognosis (Haase et al., 2019; Misawa et al., 1996; Ren et al., 2020). By contrast, del(5q), del(12p), del(20q) and the presence of >1 abnormality including del(5q) are associated with favorable prognosis. Cytogenetic abnormalities are categorized into 5 prognostic subgroups (table 5) that possess significant prognostic power for overall survival, risk of sAML evolution and allogeneic hematopoietic stem cell transplantation outcome (Bochtler et al., 2015; Deeg et al., 2012; Schanz et al., 2012). The risk score associated with cytogenetics is included among the IPSS-R criteria.

Risk cohort	Cytogenetic abnormality	Frequency	Median survival (years)
Very good	Del(11q), del(Y)	<5%	5.4
Good	Normal, del(5q) alone or with one other anomaly, del(12p) or del(20q)	65–75%	4.8
Intermediate	Del(7q), trisomy 8, trisomy 19, isochromosome 17q, and any other single or double abnormality not listed	15–20%	2.7
Poor	Abnormal 3q, monosomy 7 and del(7q), double abnormalities including monosomy 7 and del(7q), and complex cytogenetics with three abnormalities	5%	1.5
Very poor	Complex cytogenetics with more than three abnormalities	5–10%	0.7

Table 5

IPSS-R chromosomal risk categories. Figure from Li et al., 2022.

Other risk stratification systems such as the World Health Organization Classification-Based Prognostic Scoring System (WPSS) (Malcovati et al., 2007) and the MD Anderson Prognostic Scoring System (MDPSS) (Kantarjian et al., 2008; Garcia-Manero et al., 2008) have been developed, but since the introduction of IPSS-R, this last one remains the most widely used (Sperling et al., 2017; Steensma DP and Stone RM, 2020) as it showed the best predictive power (Jonas et al., 2014; Moreno Berggren et al., 2018).

Importantly, none of this prognostic scoring systems include information about somatic mutations in individual genes, although (as mentioned before) some mutations can independently predict prognosis. This represents an important limit if we consider that recurrent chromosomal abnormalities are detected in 50% of cases, whereas when cytogenetics is combined with gene sequencing, a range from 78 to 90% of patients are found to carry a clonal genetic lesion (Haferlach et al., 2014; Papaemmanuil et al., 2013). Another important limit associated to these scoring systems is their incapacity to predict patient outcomes and response to therapies with hypomethylating agents (Zeidan et al., 2016).

Given the increasing evidence that genetic aberrations can independently possess prognostic significance and refine classification and prognostication, the International Working Group for the prognosis of MDS (IWG-PM) recently developed the Molecular International Prognostic Scoring System (IPSS-M) (Bernard et al., 2022), a clinical and molecular prognostic model which integrates genomic profiling with cytogenetic and hematologic parameters for risk stratification intended as leukemia-free survival, leukemic transformation, and overall survival. In addition to cytogenetics, percentage of bone marrow blast, hemoglobin level and platelets count, the IPSS-M scoring includes the mutational status of 31 genes that are recurrently mutated in MDS, for a total of 37 different parameters required for risk calculation. The top genetic predictors were identified in multi-hit TP53 mutations (derived from combination of mutations, deletions or copy number loss), FLT3 mutations, MLL partial tandem duplication (MLL^{PTD}) and three different patterns of co-mutations for SF3B1. This ranking system stratifies patients into six different risk categories, defined as very low (VL), low (L), moderate low (ML), moderate high (MH), high (H) and very high (VH) (Fig.4A).The IPSS-M categories re-stratify 46% of patients (of these, 74% were upstaged and 26% down-staged) (Fig. 4B) and show a strong capacity of patient separation for leukemia-free survival (LFS) and overall survival (OS) probability (Fig.4C-D).

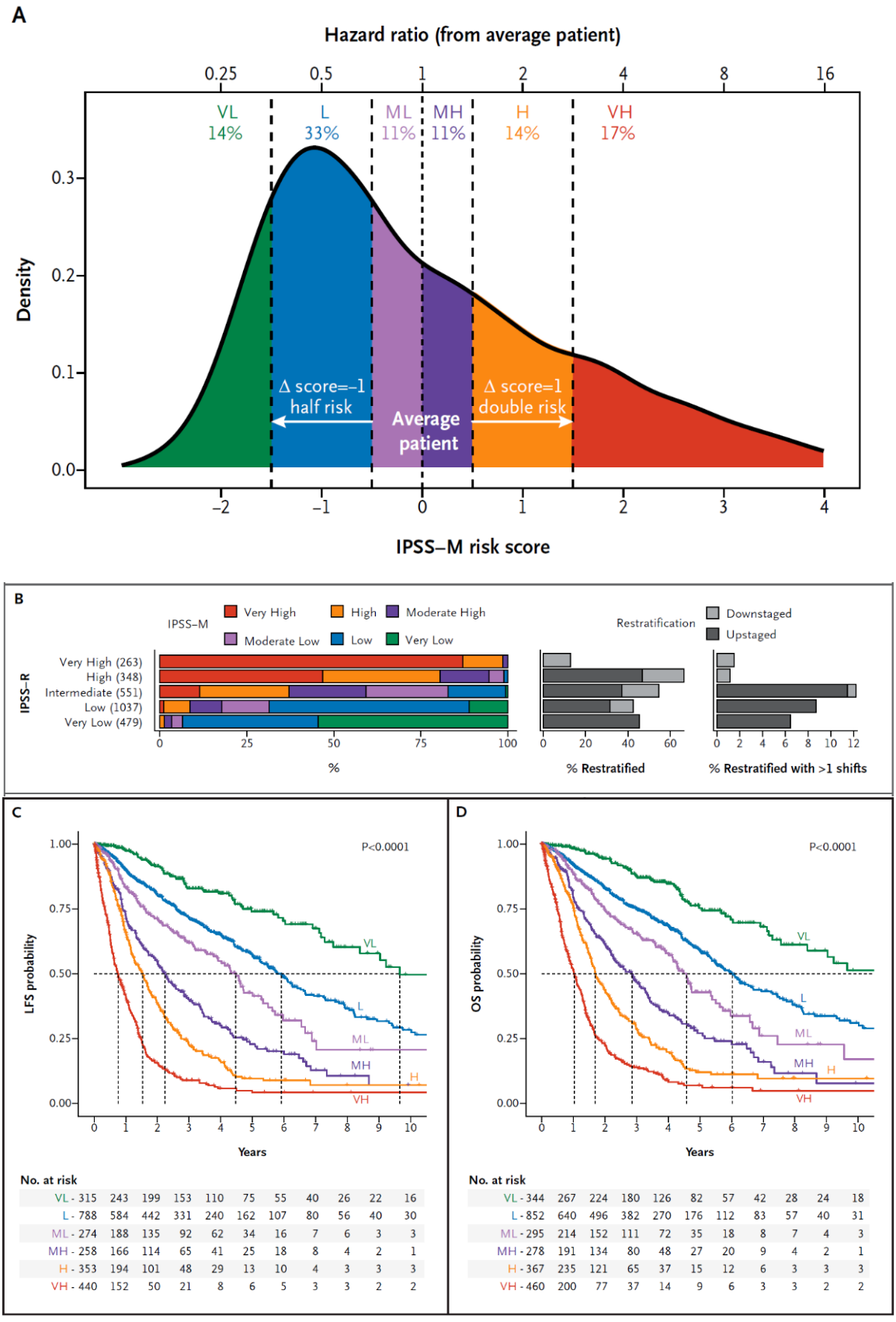
A
Hazard ratio (from average patient)
0.25
0.5
1
2
4
8
16
VL
14%
L
33%
ML
11%
MH
11%
H
14%
VH
17%
Density
0.3
0.2
0.1
0.0
Δ score=−1
half risk
Average
patient
Δ score=1
double risk
−2
−1
0
1
2
3
4
IPSS–M risk score
B
IPSS–M
Very High
High
Moderate High
Moderate Low
Low
Very Low
IPSS–R
Very High (263)
High (348)
Intermediate (551)
Low (1037)
Very Low (479)
0
25
50
75
100
%
Restratification
Downstaged
Upstaged
0
20
40
60
% Restratified
0
2
4
6
8
10
12
% Restratified with >1 shifts
C
P<0.0001
LFS probability
1.00
0.75
0.50
0.25
0.00
VL
L
ML
MH
H
VH
0
1
2
3
4
5
6
7
8
9
10
Years
No. at risk
VL - 315 243 199 153 110 75 55 40 26 22 16
L - 788 584 442 331 240 162 107 80 56 40 30
ML - 274 188 135 92 62 34 16 7 6 3 3
MH - 258 166 114 65 41 25 18 8 4 2 1
H - 353 194 101 48 29 13 10 4 3 3 3
VH - 440 152 50 21 8 6 5 3 3 2 2
D
P<0.0001
OS probability
1.00
0.75
0.50
0.25
0.00
VL
L
ML
MH
H
VH
0
1
2
3
4
5
6
7
8
9
10
Years
No. at risk
VL - 344 267 224 180 126 82 57 42 28 24 18
L - 852 640 496 382 270 176 112 83 57 40 31
ML - 295 214 152 111 72 35 18 8 7 4 3
MH - 278 191 134 80 48 27 20 9 4 2 1
H - 367 235 121 65 37 15 12 6 3 3 3
VH - 460 200 77 37 14 9 6 3 3 2 2

Figure 4

Panel A. Density plot showing the frequency of the six IPSS-M categories. The bottom x-axis shows the IPSS-M score and the top x-axis shows the corresponding hazard ratio from the hypothetical average patient. Vertical dashed lines represent cutoffs that are applied to the score to define the risk categories.

Panel B. Stacked bar plots showing the restratification of IPSS-R to IPSS-M for 2678 patients where both scores could be calculated. Each row corresponds to one IPSS-R category, and colors represent the IPSS-M categories. The gray bar plots represent the percentage of restratified patients in each IPSS-R stratum, counting either any shift (left) or cases with more than one shifts (right).

Panels C and D. Kaplan–Meier probability estimating the leukemia free survival (LFS) and overall survival (OS) across IPSS-M risk categories. Dashed lines highlight the median values. P-values are from the log-rank test.

Figure re-adapted from Bernard et al., 2022

Among restratified patients, 24% possessed one mutated gene and 62% had two or more, meaning that the restratification was the result of cumulative prognostic power of each single mutation. Most of the patients that were upstaged showed two or more IPSS-M adverse genes, whereas only a small fraction of donwstaged patients carried adverse genes. The only two genes that displayed a stable risk category association and concordance between IPSS-R and IPSS-M were $TP53^{multihit}$ and SF3B1, respectively associated with very high/high and low/very low categories.

After the publication of IPSS-M, our and other groups validated it in independent large patient cohorts (Aguirre et al., 2023; Baer et al., 2023; Kewan et al., 2023; Sauta et al., 2023). All the independent validations confirmed the increased prognostic assessment of IPSS-M compared to IPSS-R in terms of overall survival, leukemia free-survival and leukemic transformation prediction, opening a new era in MDS stratification. In our published study, we also assessed the IPSS-M accuracy in cases with missing molecular information, defining a minimum set of 15 genes that are relevant for the score performance. Moreover, we tested both the predictive (= probability of response) and prognostic (= probability of survival) values of IPSS-M in patients receiving specific treatments, in particular hypomethylating agents (HMAs) and hematopoietic stem cell transplantation (HSCT). Interestingly, the molecular score was able to significantly improve the prediction of survival probability and disease relapse in patients treated with HSCT but not in ones treated with HMAs.

1.2 Biology and genetic basis of MDS

Myelodysplastic syndromes are clonal diseases arising from the growth and spread of a somatically mutated HSC clone. This model of clonal evolution generally begins with CHIP and the transition to MDS is the result of a complex interplay between genetic mutations, epigenetic alterations, a corrupted bone marrow microenvironment and immune system dysfunctions. This is a multi-step process, which can develop over many years and whose main phases are the following:

1. A local clone acquires a selective advantage thanks to somatic genetic lesions, termed driver mutations. The initiating mutation occurs in a hematopoietic stem cell capable of self-renewal and frequently hits genes involved in DNA methylation and histone modification, typically TET2, ASXL1 and DNMT3A, which are in fact the ones found mutated in CHIP patients. It is established that both DNA methylation and histone modifications are key regulator factors during hematopoietic differentiation (Cedar et al., 2011; Rodrigues et al., 2020) and that HSC aging is linked to epigenetic changes (Bocker et al., 2011; Chambers et al., 2007). Epigenetic flexibility due to an alteration in these genes can confer enhanced cell adaptability and phenotypic diversification compared to other genetic mutations. Deregulated gene expression of key pathways such as self-renewal, stress response, survival

and cell cycle gives a competitive advantage to the mutated HSC, which prevaricate healthy stem cells and establish its clone in the niche. Aberrant methylation thus contributes to MDS initiation and progression (Itzykson et al., 2013; Jiang et al., 2008).

2. In the second phase, the mutant cells migrate out the bone marrow and, through peripheral blood, seed into other bone marrow districts creating new local clones. The mechanisms by which neoplastic hematopoietic cells leave the primary site and migrate to other bone marrow districts remain poorly elucidated (Papayannopoulou et al., 2007), but it seems that 2 pathways are involved in the bone marrow retention: one dependent on α4β1 integrin (Papayannopoulou et al., 1993; Priestley et al., 2006; Scott et al., 2003) and the other one on CXCR4/CXCL12 signaling (Burger et al., 2008; De Lourdes Perim et al., 2015).
3. The third phase is the first clinically evident and is characterized by the dominance of the mutated clone in the bone marrow. At the onset of clinical disease, the median number of driver mutations is 2 to 3 and the vast majority of circulating mature cells derive from the dominant clone (Cazzola et al., 2013). As the disease progresses, mutant cells acquire additional mutations and cytogenetic abnormalities arise (Lindsley et al., 2013). At this point, mutated HSC clones have acquired the capacity to convert the bone marrow niche to their favor, allowing disease progression and further clonal expansion at the expense of non-malignant HSCs.
4. The fourth and last phase is characterized by clonal selection and leukemic transformation: the emergence and expansion of preexisting subclones with increasingly aggressive phenotype and impaired differentiation capacity leads to an increase of blasts percentage in the bone marrow.

1.2.1 The bone marrow niche

The bone marrow niche is a complex tissue composed of many cellular and noncellular components that collectively cooperate to HSCs maintenance, proliferation, localization, and differentiation. However, under certain circumstances, the same components can also favor neoplastic processes. The cellular types inhabiting the bone marrow microenvironment are extremely heterogeneous and include mesenchymal stromal cells, endothelial cells, fibroblasts, adipocytes, osteolineage cells (osteoclasts, osteoblasts and osteocytes), non-myelinating Schwann Cells, megakaryocytes and several immune cells (macrophages, dendritic cells, NK cells, B and T lymphocytes). These diverse cell types create different special structures within the bone marrow (Ghobrial et al., 2018; Wilson et al., 2006):

- The vascular niche is composed by central regions enriched in endothelial cells and pericytes which compose blood vessels. These regions are rich of oxygen and are involved in HSCs mobilization, proliferation and differentiation.
- The reticular niche regulates the production of stem cell factors and is enriched in a particular type of reticular cells termed CXCL12-abundant reticular (CAR) cells, which are distributed throughout the bone marrow and possess long processes that create a network. The chemokine CXCL12, also known as stromal cell-derived factor [SDF]-1, is a strong chemotactic molecule that induces migration of hematopoietic progenitor and stem cells, endothelial cells and most leukocytes by interacting with its receptors CXC chemokine receptor 4 (CXCR4) (Janssens et al., 2018). The CXCL12-CXCR4 signaling is essential for homing and maintenance of HSCs and development of immune cells, and HSCs have been shown to be in contact with CAR cell processes in the marrow (Sugiyama et al., 2006).
- The endosteal niche is composed by bone marrow zones enriched in osteolineage cells. These are hypoxic environments (oxygen tension < 5%) and are the site of HSCs homing, long-term retention and self-renewal. HSCs are well-adapted to tolerate low oxygen levels thanks to the expression of HIF transcription factors (HIFs) which activate the transcription of genes containing hypoxia-

responsive elements (HREs) and that regulate a variety of biological processes such as angiogenesis, non-oxidative glycolysis, and matrix formation (Reagan et al., 2016; Schipani et al., 2013).

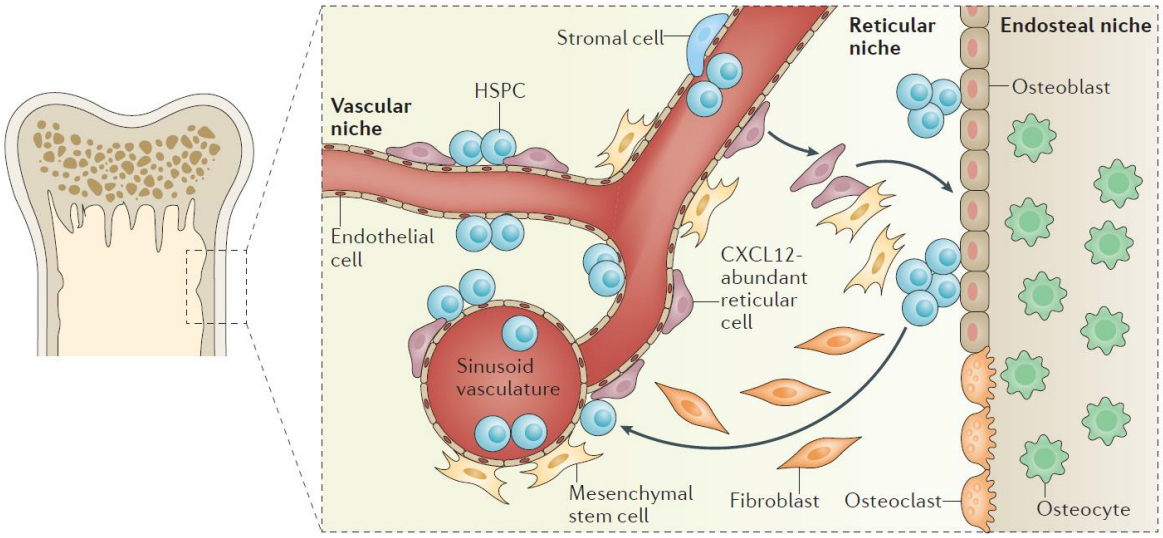

Figure 5

Stem cell niches in healthy bone marrow. Figure from Ghobrial et al., 2018.

As I mentioned before, not only genetic and epigenetic factors are responsible of disease pathogenesis, but also bone marrow microenvironment gives an important contribution. It has been shown that myelodysplastic clones are able to reprogram mesenchymal stromal cells (MSCs) in the niche to support their own growth (Medyouf et al., 2014; Pronk et al., 2019) and to release cytokines, chemokines and other soluble factors able to alter the functions and properties of immune cells (Sarhan et al., 2020; Schroeder et al., 2016). Moreover, many other molecules that are released from tumor cells have been found implied in tumor growth and dissemination (Reagan et al., 2016). Among them, the vascular endothelial growth factor (VEGF) plays a key role in increasing bone marrow vascularity that allows blast cells to proliferate and survive (Legros et al., 2012; Wimazal et al., 2006; Xiong et al., 2021). Also the expression and secretion of MMP-2 and -9 matrix metalloproteinases have been shown to be upregulated and involved in tissue remodeling and tumor invasion and migration (Chaudhary et al., 2016; Ries et al., 1999; Travaglino et al., 2008). Other molecules that can play a role are activin-A with the TGF-β family citokines (Verma et al., 2020) and endothelin-1 (Yachoui et al., 2015).

Altered MSCs display inhibited osteogenesis and enhanced osteogenic capacity which leads to the accumulation of altered osteoblasts in the niche as a myelofibrotic cells (Reagan et al., 2016). Moreover, MSCs also exert immunomodulatory capacities (Zheng et al., 2022), regulating both adaptive and innate immune cells functions and exhibiting different characteristics depending on the stage of the disease: in low-risk MDS they display a global activation of inflammatory programs through the release of pro-inflammatory cytokines such as IL-1β and NFkB (Chen et al., 2016; Sallman et al., 2019), whereas in higher risk MDS they demonstrate higher apoptotic and immunosuppressive properties (Wang et al., 1013; Zhao et al., 2012). Also endothelial progenitor cells seem to be dysfunctional and to contribute to vascular niche dysfunction (Teofili et al., 2015).

Both AML and MDS display a hypercellular bone marrow due to an increased cell proliferation and lack of mature blood cells. Usually, in AML all the three main lineages (red blood cells, granulocytes and platelets)

are reduced, whereas in MDS there might be a loss of one, two or all the three lineages. However, the mechanisms at the basis of peripheral cytopenia is different: in AML, blast cells show a block in the differentiation at an early stage and reduced cell death, whereas in MDS the progenitor cells proceed in their maturation pathways, but the final stage is dysplastic and exhibit increased apoptosis (Corey et al., 2007; Sperling et al., 2016). Apoptosis rate changes along disease progression: early stage and low-risk MDS are characterized by high rate of apoptosis, whereas in higher-risk MDS the intramedullary apoptosis decreases and blast cells begin to accumulate in the bone marrow (Greenberg, 1998; Westwood et al., 2003). The reduction of apoptotic rate in advanced stages of MDS is correlated to a decreased ratio of pro- versus anti-apoptotic Bcl-2-family proteins (Parker et al., 2000; Parker et al., 1998).

1.2.2 Genetic landscape of MDS

Thanks to the advent and massive use of next generation sequencing (NGS) technologies, the genetic landscape of MDS is now quite well elucidated. Two important studies sequenced the largest cohorts of MDS patients (Papaemmanuil et al., 2013; Haferlach et al., 2014) and found 50 recurrently mutated genes that can be classified in six different categories:

- DNA methylation: DNMT3A, TET2, IDH1, IDH2
- Chromatin modification: EZH2, ASXL1
- RNA splicing: SF3B1, U2AF1, SRSF2, ZRSR2
- Regulation of transcription: RUNX1, GATA2, ETV6, BCOR
- Signaling and DNA repair: TP53, JAK2, KRAS, NRAS, CBL
- Cohesin complex: STAG2, RAD21, SMC1A, CTCF

Haferlach et al. found that about 90% of samples carry at least one mutation, with a median of 3 (in a range from 0 to 12) per patient. Papaemmanuil et al. found instead at least one oncogenic mutation in 74% of cases. Both the papers agree on the fact that the combination of sequencing and cytogenetics analysis is able to detect oncogenic lesions in a greater fraction compared to cytogenetics alone.

Only six genes were found to be consistently mutated with a frequency >10%: SF3B1 (24-33%), TET2 (22-32%), ASXL1 (23%), RSF2 (14-17%), DNMT3A (13%) and RUNX1 (11%). Other less frequent mutations (from 2 to 10% of cases) were found in U2AF1, ZRSR2, STAG2, TP53, EZH2, IDH2, CBL, NRAS, BCOR, JAK2, IDH1 and KRAS (Fig.6A). Looking to the gene categories, the most frequently targeted was RNA splicing (64% of the cases), followed by DNA methylation (47%) and chromatin modification (28%) (Fig 6B). Interestingly, the mutation frequency of these genes categories was correlated with specific WHO subtypes: for example, splicing genes were found enriched in MDS with ring sideroblast RARS and RCMD-RS, whereas cohesin complex, RAS pathways and DNA repair were mostly found in higher risk categories with excess of blasts (RAEB-1 and RAEB-2). The mean number of mutations also correlated with severity of the disease: the more severe is the disease, the more is the fraction of samples with high (≥4) number of mutations (Fig. 6C).

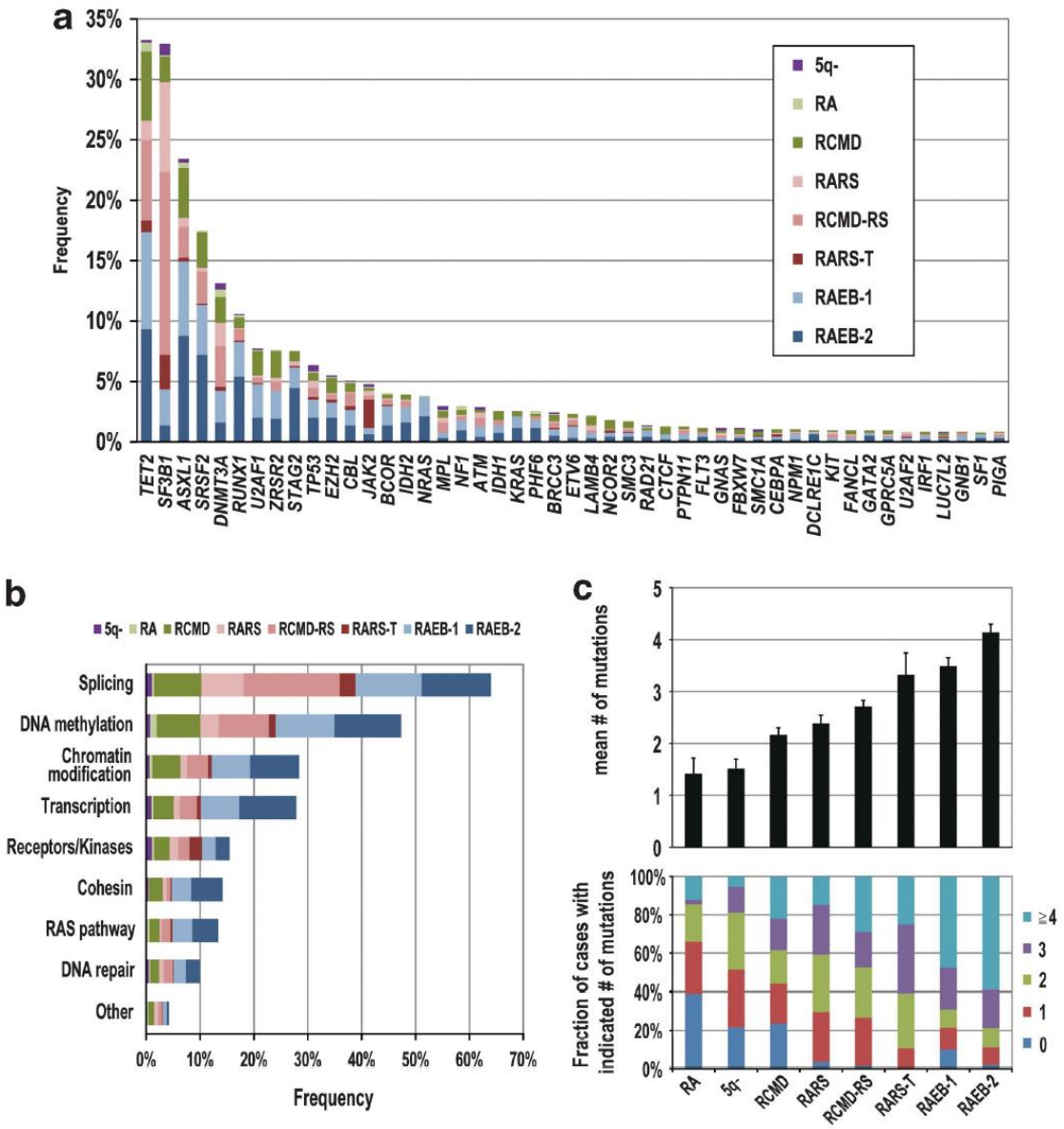

Figure 6

Panel A. Frequency of mutations in 47 significantly mutated genes in 944 cases across several WHO subtypes, shown in different colors. Panel B. Frequency of gene mutations involved in common functional pathways. Panel C. Number of gene mutations detected in different MDS subtypes. Figure from Haferlach et al., 2014.

Papaemmanuil et al. also found the number of driver oncogenic mutations per patient as one of the strongest predictors of outcome in terms of leukemia free survival (LFS) and incidence of AML transformation. In fact, this study highlighted that the number of driver mutations is negatively correlated with LFS (fig.7A) and positively correlated with AML transformation rates (fig. 7B).

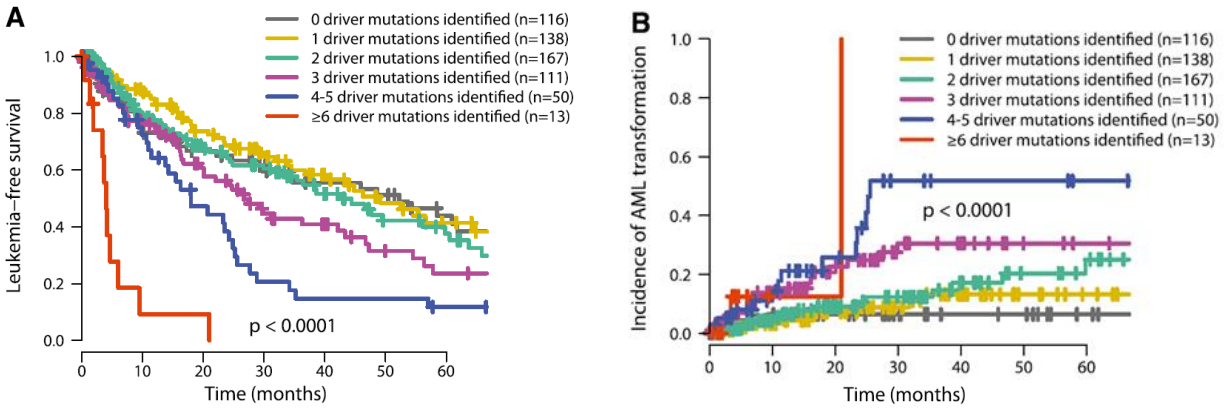

Figure 7

(A) Leukemia-free survival in MDS patients classified on the basis of how many oncogenic mutations they carry (including both point mutations and cytogenetic lesions). (B) Incidence of transformation to acute leukemia in MDS patients classified on the basis of how many oncogenic mutations they carry. Figure re-adapted from Papaemmanuil et al., 2013.

Further analyses showed that genes have tendencies of co-occurrence or mutual exclusivity: in general, genes belonging to the same biological pathway do not show co-occurrence suggesting that a second mutation in the same group provides no additional selective advantage to the tumor due to functional redundancy or is not tolerated (Haferlach et al., 2014; Walter et al., 2013). In particular, SF3B1 is negatively correlated with every common mutated gene other than DNMT3A and JAK2 (Fig.8). Other negative correlations include SRSF2 with DNMT3A, EZH2 and IRF1 and ASXL1 with DNMT3A. Positive correlation was instead observed among STAG2, IDH2, ASXL1, RUNX1 and BCOR and among TET2 with SRSF2 and ZRSR2.

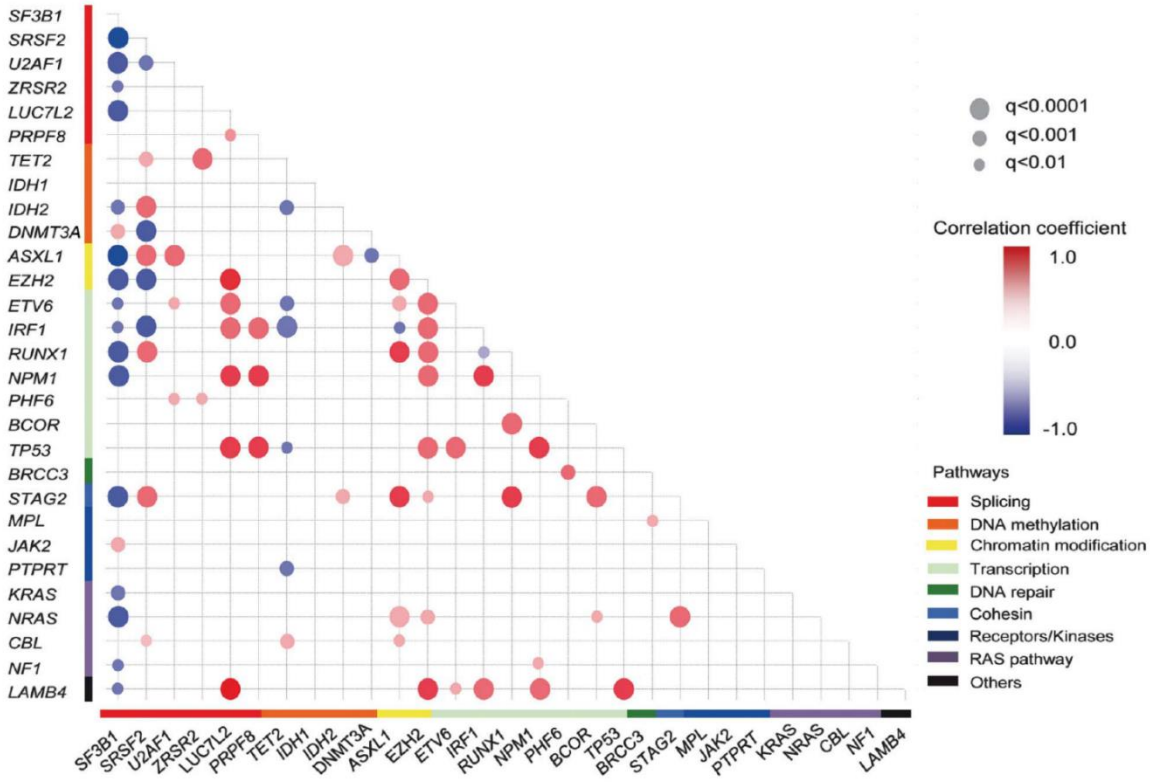

Figure 8

Correlation plot between major genetic lesions. Correlation coefficients are indicated by a color gradient and q-values by circle diameters. Genes are divided for pathways, indicated in different colors. Figure from Haferlach et al., 2014.

Mutational exclusivity implies that the mutation taken in consideration is sufficient by itself to confer a gain of function to the cell, and no additional advantage is achieved from the accumulation of other mutations. By contrast, mutational co-occurrence indicates the presence of functional interactions among the mutations for MDS pathogenesis. However, some genes show mutual exclusivity even if they operate in different pathways (for example, EZH2 and SRSF or IDH2 and SF3B1), meaning that functional redundancy is not the unique factor to consider. Another reason why some genes show mutual exclusivity is that these gene mutations can be tumorigenic only in specific genomic contexts: in fact, the set of commutated genes of genes involved in the same pathways (for example SF3B1 and SRSF2) can be very different, meaning that the functional consequences of mutations in genes belonging to the same category cannot be the same and can also result in different disease phenotype. This led to the formulation of an hypothesis of "genetic predestination", according to which the earliest mutations affect and shrink the downstream repertoire of cooperating genetic lesions (Papaemmanuil et al., 2013).

1.2.3 TP53 mutated MDS

As previously mentioned, TP53-mutated myelodysplastic syndrome forms a distinct group with dismal outcomes due to a more aggressive disease phenotype, an increased risk of sAML evolution and shorter treatment response duration (Bernard et al., 2020; Sallman et al., 2016; Takahashi et al., 2016).

TP53 is a 20-kb tumor suppressor gene located on chromosome 17p13.1, which encodes for the transcription factor p53, called "the guardian of the genome." The protein has five functional domains: the transactivation domain, a proline-rich domain in the N-terminal region, the oligomerization domain, the regulatory domain in the C-terminal region and finally the DNA-binding domain (DBD) in the central core (Harms et al., 2006). The p53 protein is involved in several cellular processes of fundamental importance such as genomic stability, cell cycling, proliferation, differentiation, apoptosis, senescence, autophagy, metabolism, and stem cell homeostasis (Fig.9). TP53 is the most frequently mutated gene across human cancers and 90% of TP53 mutations are characterized by structural losses of both alleles which leads to complete or partial loss of function of p53 protein (Donehower et al., 2019). The loss of function of p53 implies its inability to trigger p21 and subsequent cell cycle arrest, apoptosis and DNA damage repair, and the up-regulation of proteins involved in cell-cycle progression (for example cyclin B1, cyclin E1, FOXM1, CDK1).

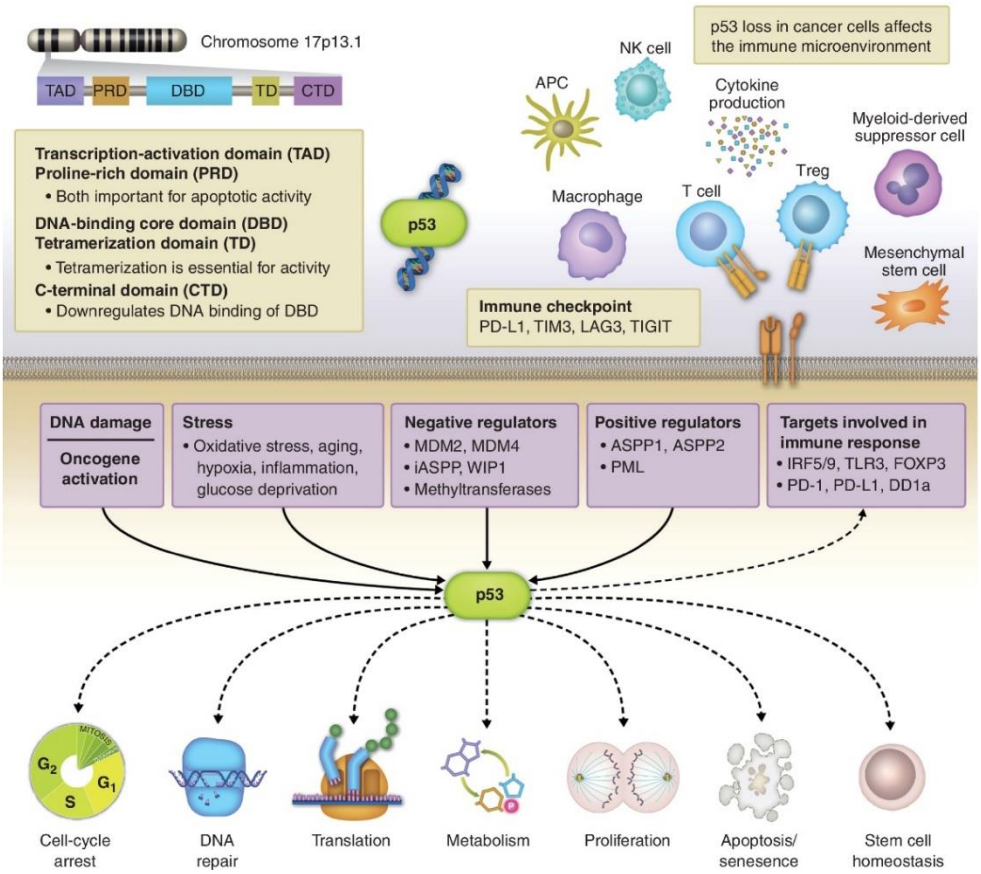

Figure 9

P53 protein and its pathways. Figure from Daver et al., 2022.

TP53 abnormalities are found in 5% to 10% of patients with de novo MDS (Bernard et al., 2020; Lindsley et al., 2017), but their frequency further increases to 70% to 80% in patients with complex karyotype and/or with 5q and 7q deletions (Haase et al., 2017; Kulasekararaj et al., 2013; Pitel et al., 2021; Weinberg et al., 2022). The majority of TP53 mutations are missense variants localized within the DBD. Consistent with its role as a tumor suppressor gene, bi-allelic targeting is very frequent: in fact, more than 91% of TP53-mutant cancers exhibit second allele loss due to mutation, chromosomal deletion, or copy-neutral LOH (Donehower et al., 2019). Multi-hit TP53 mutations or biallelic defects, occurring in 2/3 of patients, show few co-occurring mutations, evolve to become dominant clones and confer therapy resistance, thus resulting in very poor clinical outcomes (Bernard et al., 2020; Lindsley et al., 2017). Monoallelic TP53 mutations occurs in 1/3 of patients and show patterns of co-mutation with TET2 (29%), SF3B1 (27%), ASXL1 (16%), and DNMT3A (16%) and are likely to be subclonal events with less impact on outcomes (Bernard et al., 2020).

Beyond single- or multi- hit TP53 mutations, also mutational burden has emerged as a significant prognostic factor in MDS. A VAF over 6% was indeed associated with inferior overall survival (OS) and progression-free survival in lower-risk MDS (Belickova et al., 2016). In higher-risk MDS patients, increasing VAF strongly correlates with risk of complex cytogenetics, and a VAF >40% was shown to be an independent predictor for poor OS (Montalban-Bravo et al., 2020; Sallman et al., 2016).

For these reasons, the MDS diagnosis workflow should be implemented to better characterize the TP53 allelic state, coupling karyotype analysis with NGS in order to evaluate the copy-number status of the TP53 gene, its mutational profile, and the variant allele frequency (VAF) of the mutations identified. However, NGS still remains a time-consuming and expensive procedure for diagnostic routine. On the other hand, immunohistochemistry (IHC) is a fast, cheap and reproducible technique that is already implemented in

diagnostic procedures and that can be used to estimate p53 protein expression in bone marrow biopsies (McGraw et al., 2016). In fact, IHC cannot normally detect the WT p53 protein, since its half-life is short. Mutated p53 instead possess a longer half-life and accumulates in the nucleus, and hence ca be usually easily detected in formalin-fixed and paraffine-embedded tissues (Kerns et al., 1992). P53 detection by IHC is therefore indicative of underlying mutations in the TP53 gene and a correlation between p53 nuclear overexpression in MDS and survival was observed in several studies (Molteni et al., 2019; Nishiwaki et al., 2016; Pich et al., 2017).

1.2.4 SF3B1 mutated MDS

The spliceosome is a large, dynamic ribonucleoprotein complex composed of small nuclear RNAs associated with proteins, whose function is the removal of introns from precursor mRNA (premRNA) to generate mature, spliced mRNAs. SF3B1 is the largest subunit of the spliceosome factor 3b (SF3B) complex, which is a core component of spliceosomes.

In MDS, SF3B1 is one of the most frequently mutated genes and the most common among the ones involved in splicing process (Papaemmanuil et al., 2013; Yoshida et al., 2011; Haferlach et al., 2014). As anticipated before, SF3B1 mutations are associated with peculiar ring sideroblasts phenotype (Malcovati et al., 2011; Papaemmanuil et al., 2011), ineffective erythropoiesis and indolent disease course with rare progression to sAML, which results in good prognosis (Huber et al., 2022; Malcovati et al., 2015; Malcovati et al., 2020; Pellagatti et al., 2016). Due to its peculiar characteristics, SF3B1-mutated patients are recognized, as TP53-mutated ones, a distinct MDS subtype.

Interestingly, mutations in other genes involved in splicing machinery such as SRSF2 or U2AF1 are instead associated with shorter patient survival and AML transformation (Graubert et al., 2011; Makishima et al., 2012; Pellagatti et al., 2016; Thol et al., 2012). Splicing factor mutations are generally mutually exclusive (Papaemmanuil et al., 2013; Yoshida et al., 2011) and are found to occur early in the disease, thus representing founder mutations (Makishima et al., 2017; Mian et al., 2013; Papaemmanuil et al., 2013). A recent study deeply investigated the genomic landscape of SF3B1 mutated MDS and found that the most frequent additional mutations in $SF3B1^{mut}$ patients are TET2 (29%), DNMT3A (16%) and ASXL1 (9%), whereas mutations in ASXL1, RUNX1, TP53, ZRSR2, SRSF2 and STAG2 were significantly less frequent in $SF3B1^{mut}$ patients compared to $SF3B1^{WT}$ (Huber et al., 2022). Moreover, the study also analyzed the prognostic contribution of additional mutations and cytogenetic alterations in $SF3B1^{mut}$ patients, finding that only RUNX1 mutations and del(5q) were independent prognostic factors associated to shorter OS and thus highlighting the necessity to further characterize $SF3B1^{mut}$ category to better stratify patients.

Hematopoietic cells are heterozygous for the SF3B1 mutation, meaning that, in each cell, about half of the splicing events are operated by spliceosomes with a mutant SF3B1 factor (Cazzola, 2020). These mutations are generally missense substitutions that in more than half of cases involves an A to G transition that results in a lysine to glutamic acid substitution at amino acid position 700 (K700E) (Papaemmanuil et al., 2011; Yoshida et al., 2011). The mutation induces the SF3B1 protein to preferentially use cryptic and aberrant 3' splice sites that cluster within 10 to 30 bp upstream of canonical ones (Obeng et al., 2016), resulting in insertion of nucleotides at the exon-exon junctions (Pellagatti et al., 2018; Shiozawa et al., 2018). Most of these aberrant transcripts are degraded by nonsense-mediated decay due to the insertion of premature stop codon, leading to the reduced transcript production of several genes; in other cases, a mutant protein is translated and could result in aberrant activity (Fig.10). An example comes from ERFE gene, encoding Erythroferrone, whose variant produced by SF3B1 mutated erythroblasts contributes to parenchymal iron loading through the suppression of hepcidin hormone (Bondu et al., 2019).

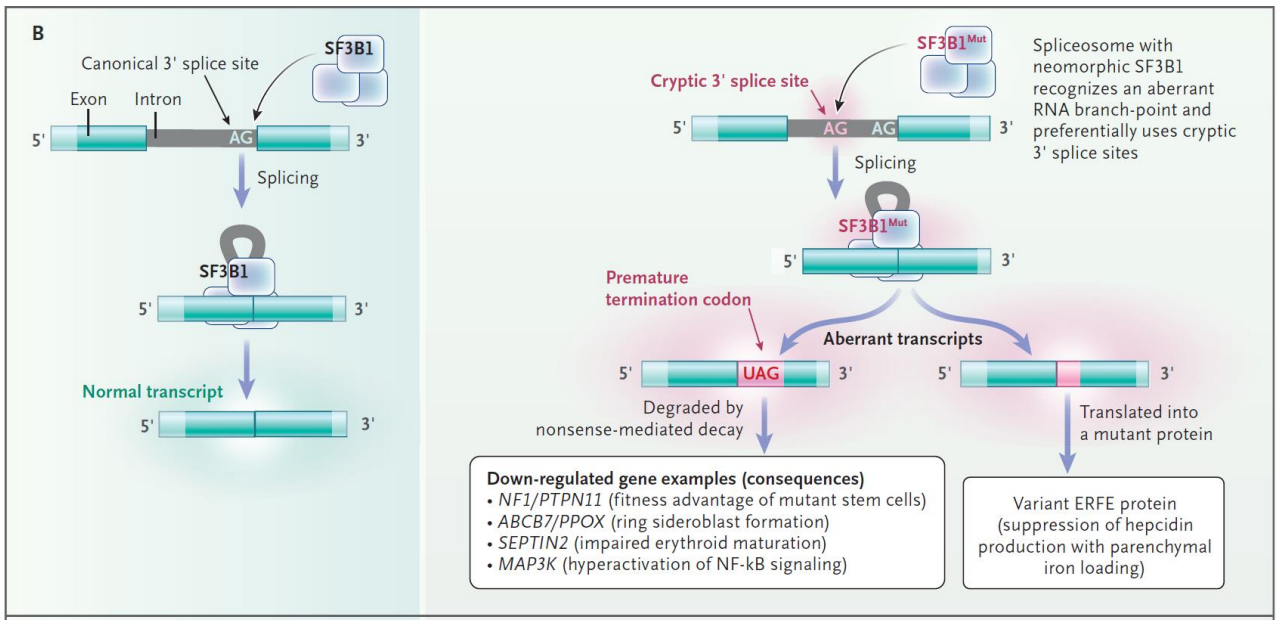

Figure 10

The role of production of abnormal gene transcripts in the pathophysiology of SF3B1-mutated MDS. Figure from Cazzola, 2020.

Another consequence of aberrant splicing is the generation of neoantigens that could be presented through HLA molecules and thus can be used as novel and specific targets to eliminate the tumoral clone (Xie et al., 2023). One study on MDS identified a candidate SF3B1^{mut} epitope that is naturally processed and presented on HLA-B molecules and that showed an immunogenic activity (Biernacki et al., 2020), opening a new field of research for targeted treatment of splicing factors-mutated patients.

1.2.5 Clonal evolution of MDS

Somatic mutations normally occur with low frequency in HSCs genomes during DNA duplication: although most of the mistakes are immediately corrected by cellular DNA repair mechanisms, some of them can persist and be propagated along HSCs division and self-renewal. It has been calculated that HSCs accumulate coding mutations at a rate of about 0.13 per year (Welch et al., 2012), meaning that at the median age of MDS diagnosis each HSC has accumulated 9 mutations: most of them are harmless and non-tumorigenic, so they

are called “passenger mutations”. However, the more mutations accumulate, the greater is the likelihood of one of them being tumorigenic: it has been estimated that 5-6% of people older than 70 years carry mutations that could represent premalignant events leading to clonal expansion (Xie et al., 2014).

The first mutation which gives a clonal dominance to the cell is termed “driver”, whereas the next ones who provide an increased aggressiveness and adaptation to the environment are called “secondary mutations”. Tumor subclones compete with each other and with healthy cells for nutrients and resources within the bone marrow niche: during this Darwinian selection, mutations that confers a strong selective advantage allow a clone to expand and dominate the hematopoietic compartment, however, unexpected changes imposed on this ecosystem (for example, the beginning of a treatment) will alter the relative competitiveness of cancer cell clones, conferring selective advantage to new clones and causing the disappearance of the previous dominant ones. Generally, driver mutations are maintained throughout disease evolution (Corces-Zimmerman et al., 2014; Walter et al., 2012) whereas secondary oncogenic mutations change along time and drive sequential waves of clonal expansion. These complex dynamics of continuous and variable pattern of genetic diversity and clonal architecture are called clonal evolution. There are two main types of clonal evolution:

- the linear evolution, in which the founding mutations are carried forward from daughter subclones with increasing number of mutations and outcompeting the preexisting clone (Fig. 11-A)
- the branched evolution, in which distinct clones carrying different mutations arise from the same ancestral clone and diverge into separate lineages (Fig. 11-B).

Therapy may influence clonal evolution patterns creating an “evolutionary bottleneck” that can either push the founding clone to acquire new mutations (Fig.11-C) or favor the emergence of preexisting subclones (Fig. 11-D).

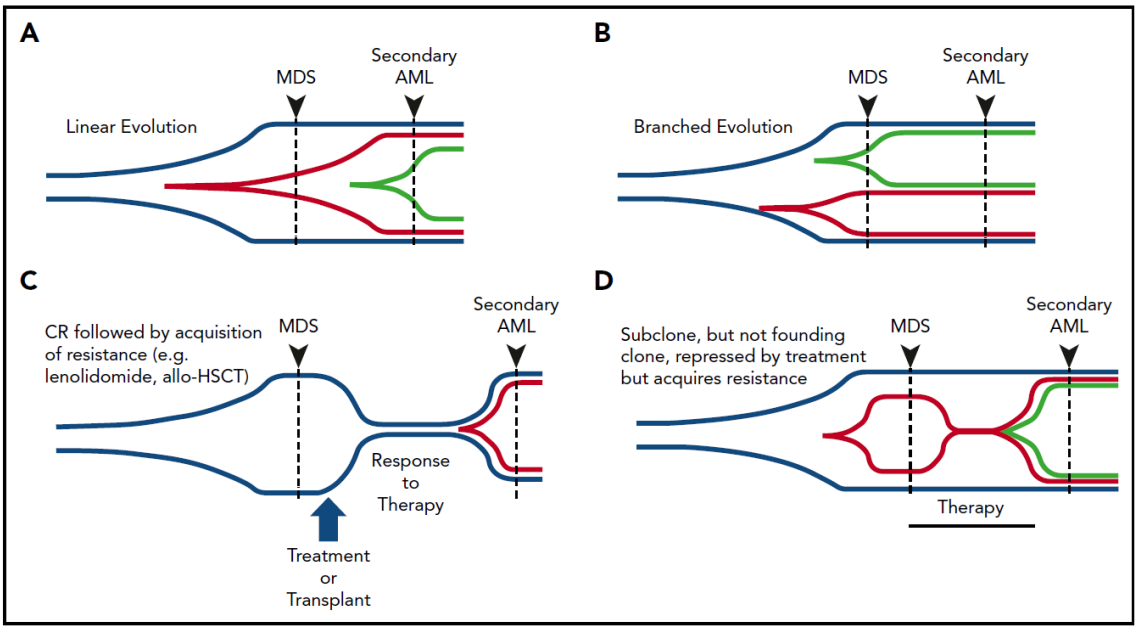

Figure 11

Patterns of clonal evolution during the progression of MDS to secondary AML. Figure from Menssen and Walter, 2020.

Variant allele frequency can be employed to estimate the rate of tumor cells carrying a mutation of interest and to identify, through different models, which mutations are associated with initial clonal proliferation and

which are involved in subclonal evolution. In this way, the VAF allows to estimate the temporal order of mutations acquisition, the hierarchical organization of malignant clones and the mutational trajectories assumed by the tumor during disease progression and evolution upon specific therapies (Da Silva-Coelho et al., 2017; Mossner et al., 2016). Moreover, VAF can also be used to predict MDS phenotype, refine prognostication and to monitor residual disease (Makishima et al., 2017; Sallman and Padron, 2016). The limit of using VAF mainly emerge when mutations are present at a low burden: in these cases, in fact, imputing an accurate clonal architecture is challenging since is not possible to understand whether mutations co-occur in the same cell or exist in parallel subclones. To understand clonal architecture in case of mutations with low VAF, single-cell sequencing is the finest and most reliable option, even if the "allele dropout" (ADO) and amplification artifacts phenomena could occur in targeted sequencing and deeply affect the results (Luquette et al., 2019; Shestak et al., 2021).

Both bone marrow (BM) and peripheral blood (PB) can be employed for monitoring tumor mutational burden in hematological cancers: in fact, several studies confirmed a high concordance between the two tissues, with a high sensitivity of PB in identifying all BM variants, even if with a lower VAF (Jumniensuk et al., 2022; Lucas et al., 2020; Takahashi et al., 2013; Tong et al., 2015). The same was confirmed in studies on MDS patients (Da Silva-Coelho et al., 2017; Duncavage et al., 2017; Mohamedali et al., 2014). This makes clonal evolution phenomenon easier to study in hematological malignancies than solid cancers, especially for the feasibility to collect blood samples during the disease and the treatment history of the patient.

In MDS, mutations in genes involved in DNA methylation and RNA splicing were found to occur as early events and thus represent driver mutations (Makishima et al., 2017; Mian et al., 2013; Papaemmanuil et al., 2013), whereas mutations in genes involved in signaling and chromatin modification were often found to occur later and to drive subclonal evolution (Kim et al., 2017; Menssen et al., 2022; Mossner et al., 2016; Takahashiet al., 2013). Several studies implying whole-exome/targeted deep sequencing (Da Silva-Coelho et al., 2017; Makishima et al., 2017; Mossner et al., 2016; Uy et al., 2017; Walter et al., 2012) or single cell genotyping (Guess et al., 2022; Menssen et al., 2022) have tried to elucidate the complex clonal dynamics in MDS and sAML. In these studies, both patterns of linear and branching clonal evolution were documented in MDS patients during MDS progression and transformation to sAML and when the disease relapses after the treatment.

Illustrative examples of MDS clonal evolution came from Da Silva-Coelho et al. study, in which they performed clonal evolution analysis in six MDS patients receiving only supportive care and five patients treated with lenalidomide and other drugs. The figure shows the clonal turnover in the patients without pharmacological treatments and highlights that both the linear (Fig. 12 B-C) and the more complex branched (Fig. 12 D-E-F) evolution patterns occur. Only one patient showed no clonal evolution during 8 years of follow-up (Fig. 12 A).

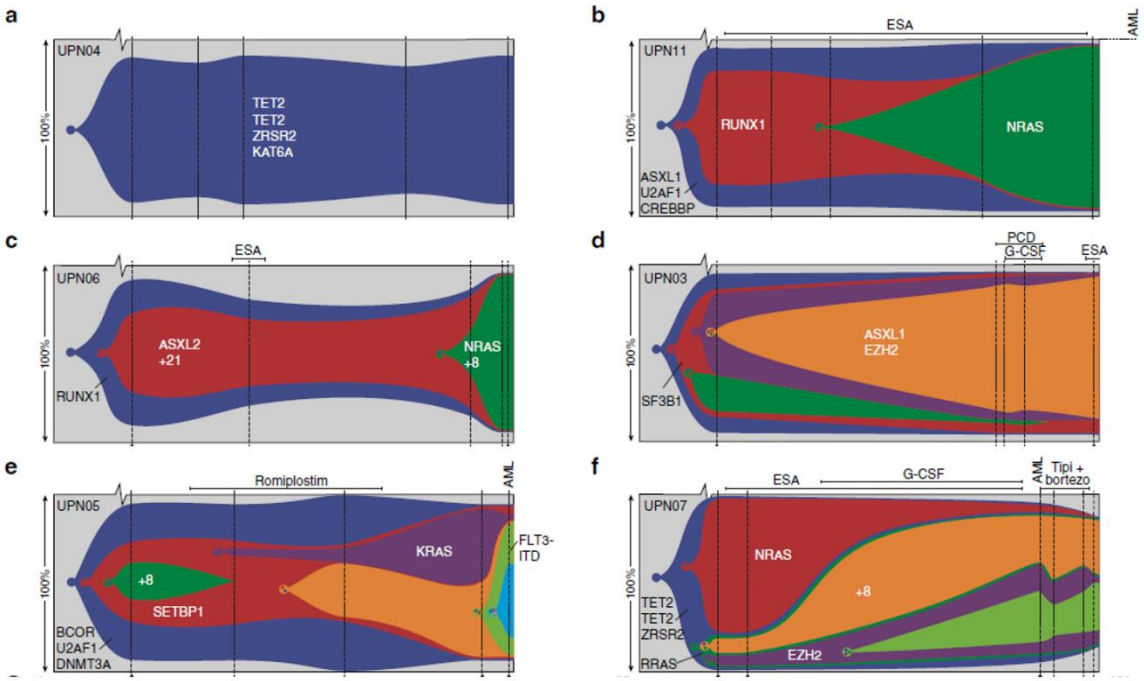

Figure 12

Clonal evolution patterns in the bone marrow of MDS patients who received only supportive care. Figure re-adapted from Da Silva-Coelho et al., 2017.

Patients that undergo pharmacological treatment showed instead highly dynamic shifts in their clonal composition. In fact, despite an initial clinical response due to the reduction of the founding clone, patient's bone marrow remained clonal allowing the subsequent outgrowth of the founder clone, a preexisting or fully independent/unrelated clones to drive drug resistance and disease relapse.

In the first case (Fig. 13-A, patient UPN01), the therapy suppressed the original clone and selected the acquisition of TP53 mutation, that was undetectable before treatment. In the other three patients (Fig. 13 B-C-D, patients UPN08-09-10), small preexisting clones carrying mutations not shared with the founding clone expanded: in these cases, the evolutionary bottleneck caused by the pharmacological therapy created space in the niche and may have favored the bone marrow repopulation by HSCS harboring other driver mutations.

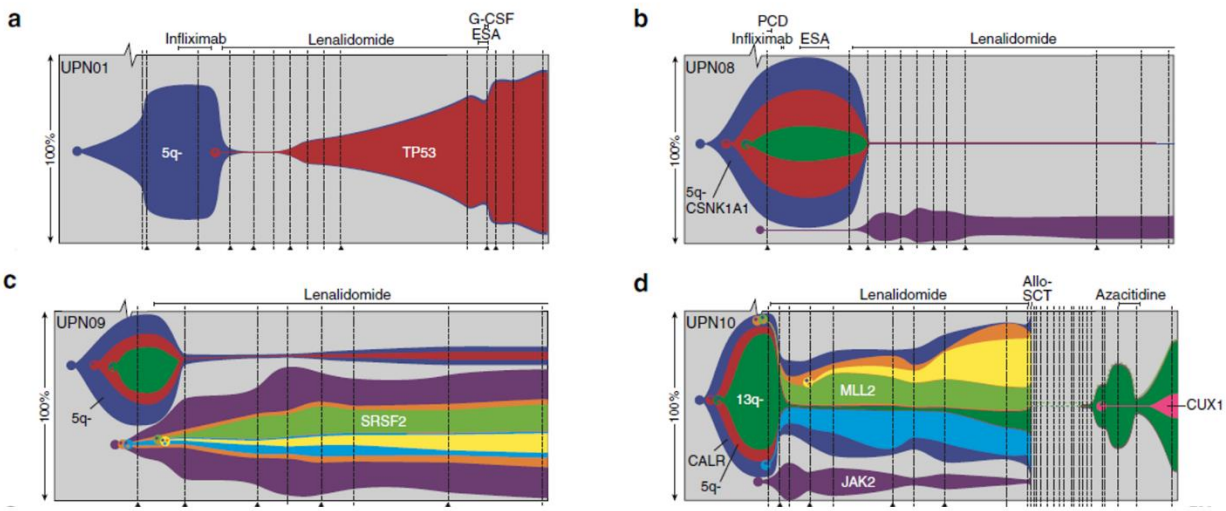

Figure 13

Clonal evolution patterns in the bone marrow of MDS patients who were treated with lenalidomide. Figure re-adapted from Da Silva-Coelho et al., 2017.

Interestingly, the frequencies variation and emergence/disappearance of specific clones were correlated with changes of clinical parameters such as hemoglobin level, the dependence from erythrocyte transfusion and leukocyte and platelet count, highlighting functional properties linked to the different driver mutations (Da Silva-Coelho et al., 2017; Mossner et al., 2016).

Studies on AML evolution from MDS demonstrated that despite MDS and sAML are considered distinct clinical entities, they show a large degree of mutational overlap and thus represent a disease continuum that undergoes clonal evolution. In Walter et al. study of sAML clonal architecture, each of the 7 patients studied were characterized by the persistence of an antecedent myelodysplastic founding clone and the emergence of at least one new subclone (Walter et al., 2012). Another study from Guess et. al instead identified two classes of patients: who have a relatively stable patterns of clonality ("Static group") and who show overwhelming changes ("Dynamic group"). The static group is characterized by minimal changes in architecture along sAML evolution and show founder mutation in DNA methylation genes (DNMT3A/TET2/IDH1/2), suggesting that alterations in epigenome more than genomic evolution can block cell maturation and drive tumor proliferation. In contrast, the dynamic group displayed clonal architecture changes either in terms of chromosomal alterations or clonal changes (Guess et al., 2022). In chromosomal alteration group, the karyotypes displayed increasing complexity during disease progression and an enrichment in TP53 mutations. In cases of clonal changes, the new mutations were generally found in signaling genes: this data is in line with another published paper in which it was observed the enrichment in signaling genes mutations in sAML samples compared to MDS (Menssen et al., 2022).

1.3 Therapeutic approaches

At clinical presentation, patients mainly complain symptoms derived from anemia, which causes dyspnea and fatigue, whereas bleeding complications and infections become more pronounced during the course of the disease. Those clinical manifestations heavily impact on the quality of life (QoL) of MDS patients, causing distress and interfering with patients' ability to deal with symptoms and treatments (Heptinstall et al., 2008; Troy et al., 2018).

The IPSS-R score is the standard evaluation method for determining the more appropriate treatment and designing new therapeutic strategies and clinical trials. In addition to IPSS-R, also age and performance status (for example, presence of comorbidities) are essential for risk estimation and evaluation of available therapies. Each patient is thus individually evaluated, and the patient-centered care model represents the best approach for the treatment of MDS. The first assessment is to decide whether a therapy is necessary and what type of treatment is the best on the basis of the therapeutic goal. The benefit-to-risk ratio is always carefully evaluated before starting any therapy.

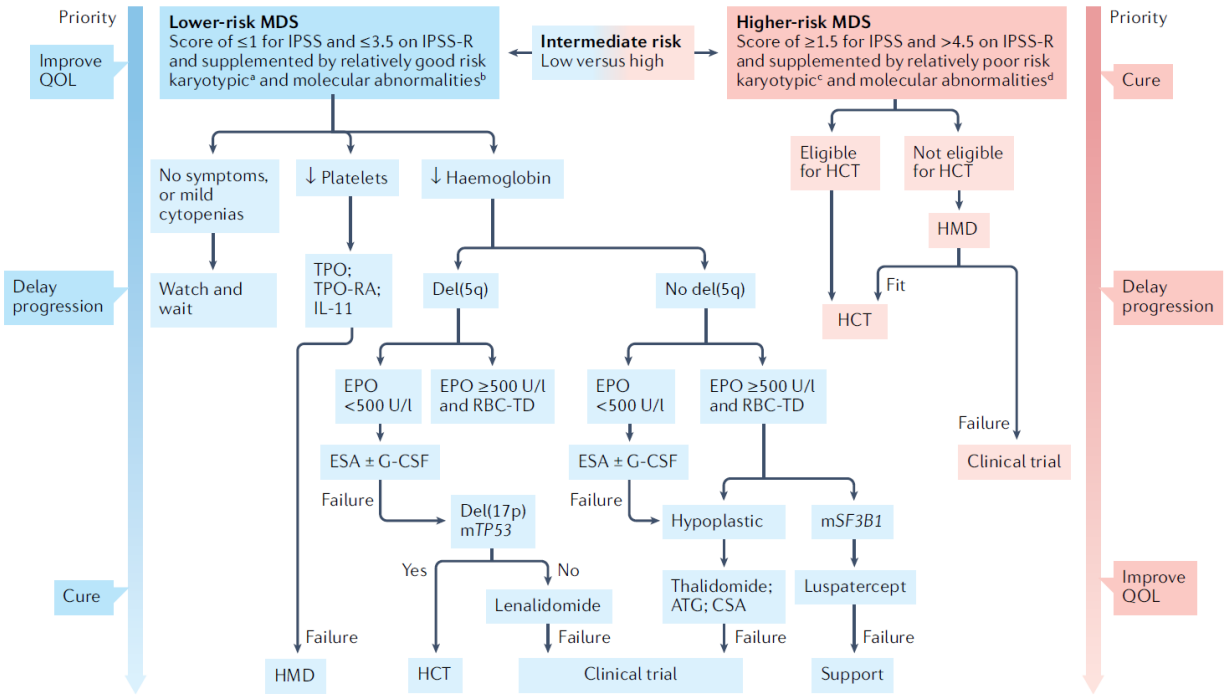

Figure 14

Treatment recommendations for lower and higher-risk MDS. Figure from Li et al., 2022.

1.3.1 Treatments for low-risk MDS patients

In patients with low-risk MDS, the main goal is to ameliorate cytopenia and improve quality of life. Patients with slight cytopenia do not necessarily require a therapy due to mild symptoms and are just regularly followed with blood count to monitor disease progression. People suffering from anemia are generally treated with erythropoiesis-stimulating agents such as erythropoietin (EPO) to increase red cell production (Fenaux et al., 2018), those suffering of thrombocytopenia receive thrombopoietin (TPO) analogues and the ones with granulocytopienia may receive granulocyte-colony stimulating factors (G-CSF) or granulocyte-macrophage colony-stimulating factor (GM-CSF). Patients with del(5q) typically receive Lenalidomide, an immunomodulatory drug that enhance host immunity functions, and which leads to cytogenetic remissions in most of the cases (Fenaux et al., 2011). However, after 2-3 years, the disease often reoccurs thanks to the selection of resistant hematopoietic cells which carry mutations in TP53 or RUNX1 (Jädersten et al., 2011; Martinez-Høyer et al., 2020; Tehranchi et al., 2010). Ring sideroblasts MDS are instead treated with Luspatercept (Schulz et al., 2021), a protein which binds to ligands for TGFβ superfamily receptors, avoiding activation of SMAD2/3 signalling pathways that are linked to impaired erythroid maturation by induction of apoptosis and cell cycle arrest (Kubasch et al., 2021). The treatment with Luspatercept is generally well

tolerated and have been shown to result in transfusion independence in around 40% of cases (Fenaux et al., 2020; Komrokji et al., 2022). During the clinical course, in fact, the vast majority of MDS patients become dependent on regular red blood cells (RBC) transfusions and this could lead to parenchymal iron overload, that must be treated with iron chelation (Angelucci et al., 2020; Cazzola et al., 2008). Patients with hypoplastic bone marrow whose diagnosis is uncertain between aplastic anemia or low-risk MDS can receive a trial of immunosuppressive therapy with anti-thymocyte globulin (ATG) plus oral cyclosporine, which have showed, in a phase 3 clinical trial, a good overall response (around 50%) but no significant improvements in overall survival and leukemia-free survival (Nakao et al., 2016; Passweg et al., 2011). Hematopoietic stem cell transplantation (HSCT) is rarely considered in lower-risk MDS, and only in cases when other therapies have failed.

1.3.2 Treatments for high-risk MDS patients: hematopoietic stem cell transplantation

In patients with high-risk MDS, the aim of the treatment is to eradicate the disease to prevent AML evolution and prolong survival. The first assessment in all cases of high-risk MDS diagnosis is to check the patient's eligibility for HSCT, that represents the only potentially curative treatment. This therapeutic strategy is composed of two different phases:

- Remission induction therapy: represent the first part and is composed by chemotherapy or radiotherapy. The goal of this phase is to eliminate the large majority of blasts in the blood and in the bone marrow, putting the disease into morphological remission (= no evidence of malignant blasts at bone marrow evaluation).
- Consolidation therapy: the second part of the treatment is essential and starts when complete remission is achieved. Hematopoietic stem cell transplantation strategies could be autologous, in which the hematopoietic stem cells source is the patient himself, or allogeneic, in which the HSCs comes from a different individual that can be related or unrelated to the patient. After HSCT, the patients enter into another very delicate phase characterized by bone marrow aplasia and thus absence of immune cells, that make them very vulnerable to any infections and viral re-activation.

Both autologous and allogeneic HSCT present pros and cons. The autologous HSC is associated with a higher risk of disease recurrence: this is due to the concrete risk to harvest not only healthy HSCs from the patient, but also leukemic blasts, which could possibly contribute to the development of post-transplantation relapses. For this reason, patients affected by AML and MDS usually do not undergo auto-HSCT, whereas it is indicated for the treatment of other hematological malignancies, including lymphomas and multiple myeloma. Moreover, the HLA-identical setting of the autologous HSCT do not allow to the new developed immune system to recognize the possible residual disease present in the patient. Nevertheless, no risk of transplant rejection or organ toxicity exist in this case. On the other hand, the allogeneic HSCT represents the strongest antineoplastic therapy due to the synergism between pre-transplantation conditioning and the immunologic antileukemic Graft versus Leukemia (GvL) effect. In fact, the HLA mismatches between donor and recipient and the different minor Histocompatibility Antigens (mHAg) allow the donor immune system to recognize and eliminate the residual leukemic cells which survived the chemotherapy. However, the alloreactive lymphocytes (in particular T lymphocytes and NK cells) recognize not only the residual tumor cells, but also the healthy tissues of the patients, giving rise to a dangerous clinical manifestation called Graft versus Host Disease (GvHD). This collateral effect can be acute (aGvHD) or chronic (cGvHD) on the basis of the timing of the event and tissue/organs involved. Acute GvHD occurs within the first month after the transplant whereas Chronic GvHD can occur also one year after the HSCT. The tissue and organs involved in aGvHD are principally intestine, skin and liver. The cGvHD hit the same sites of aGvHD with the addition of lungs, oral tract, eyes and joints. For this reason, post-transplantation treatment with cyclophosphamide (an immune system suppressor drug) is generally performed to avoid massive immune cells activation and inflammation.

Even if HSCT represent the only resolutive treatment, is performed in less than 10% of MDS patients (Li et al., 2022) for several reasons: first of all, the conditioning regiment is a toxic treatment and all the process per se is associated with high morbidity and mortality, and thus is not affordable for everyone. Second, sometimes is difficult to estimate prognosis with or without HSCT and third, is not always possible to find a donor. Patients with good performance status, no or few comorbidities, poor risk cytogenetic/molecular features and under the age limit for transplantation (around 70 years) are the best candidates (de Witte et al., 2017; Saber et al., 2016). In the last decade, the transplantation has become more accessible also to older patients thanks to the introduction of conditioning regimens of lower intensity (Belkacémi et al., 2007; de Witte et al., 2017; Kröger et al., 2017). Transplant outcomes can vary widely, but generally about 40-50% of patients survive from 2 to 5 years after transplantation. Factors that correlate with transplant outcome and survival include: the pre-transplantation hematological parameters (for example, the % of blasts), the HCT comorbidity index (HCT-CI), the age, the type of donor and the presence of some mutations. A study reported a worse prognosis associated with TP53, RAS pathway and JAK2 mutations (Lindsley et al., 2017; Yoshizato et al., 2017), whereas other studies found a correlation with TP53, ASXL1 and RUNX1 (Della Porta et al., 2016) and with TP53, TET2 and DNMT3A (Bejar et al., 2014). Throughout the studies, strong negative effects of TP53 mutations on outcome and survival were reproducible findings, whereas no unanimous results were obtained for other mutations. The worse overall survival and highest frequency of relapse and AML transformation was mainly observed when TP53 was mutated in a biallelic status (multi-hit) and in association with complex karyotype (Bernard et al., 2020; Della Porta et al., 2016; Lindsley et al., 2017; Yoshizato et al., 2017).

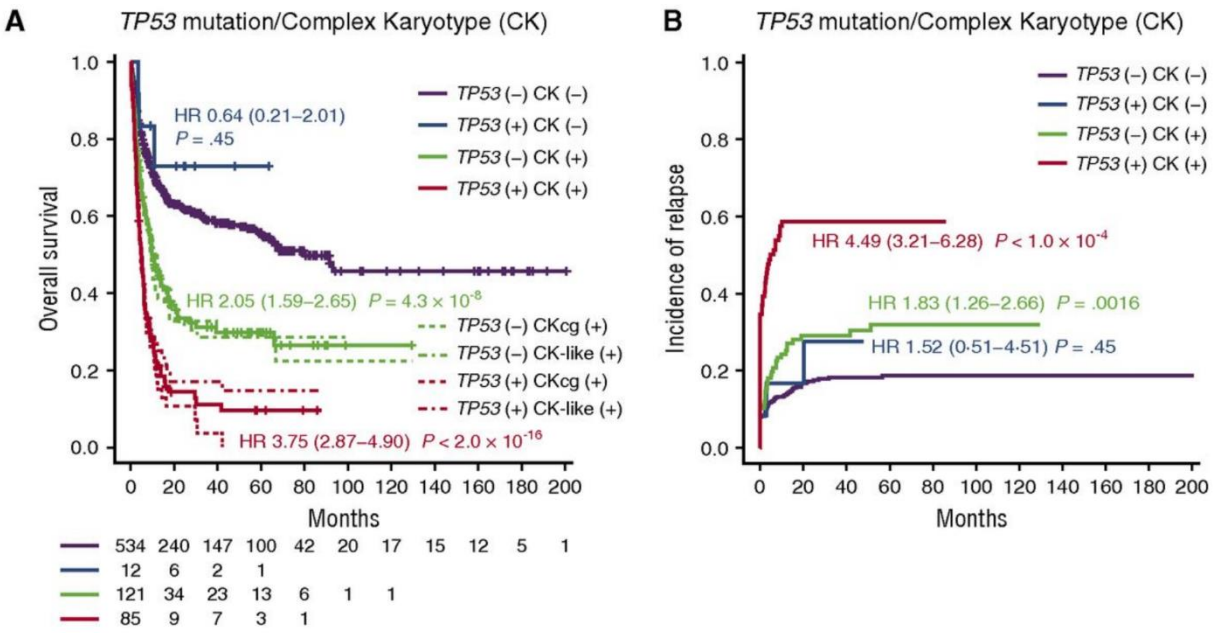

Figure 15

Effects of TP53 mutation and complex karyotype (CK) on overall survival (A) and incidence of relapse after HSCT (B). Figure from Yoshizato et al., 2017.

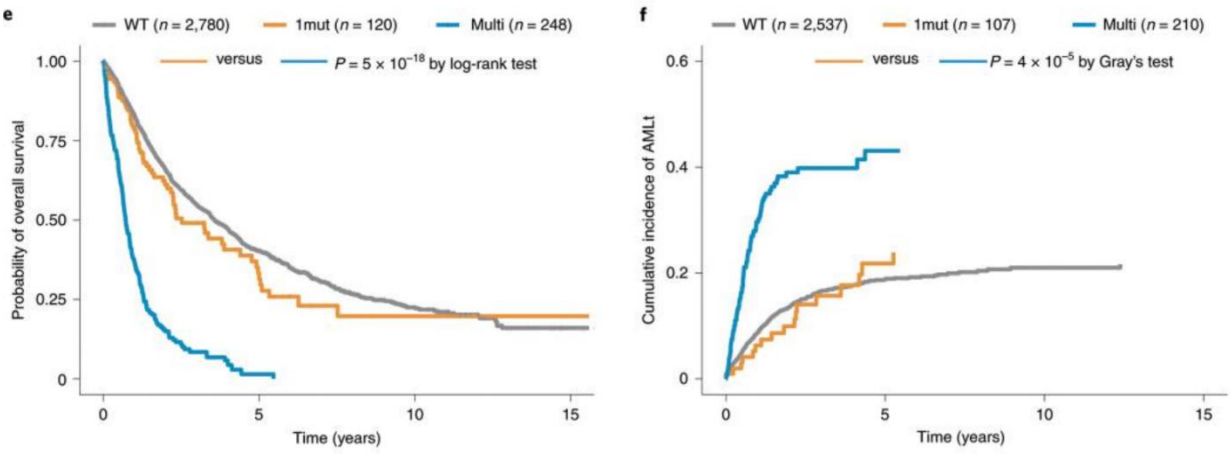

Figure 16

Kaplan–Meier probability estimating the overall survival (E) and cumulative AML transformation (F) per TP53 allelic state. Figure from Bernard et al., 2020.

1.3.3 Treatments for high-risk MDS patients: hypomethylating agents

If the patient is ineligible to transplantation, the pharmacological treatment of higher-risk MDS is actually dominated by monotherapy with hypomethylating agents azacytidine (AZA) or decitabine (DAC). A phase III study reported that azacytidine increased survival by 9 months compared to conventional care (best supportive care, low-dose cytarabine, or intensive chemotherapy) and about half of the patients showed an hematological response (Fenaux et al., 2009). Another study reported a seven months increased survival in 2/3 of patients receiving at least 4 cycles of therapy (Mozessohn et al., 2018). The sum of the available data suggests that azacytidine must be administered for long-term periods (at least 6 cycles) to reach therapeutic benefits (Dinmohamed et al., 2015; Mozessohn et al., 2018; Silverman et al., 2011), even if the survival benefits are in the order of few months and, unfortunately, in most of the cases does not eliminate the founder clone which continue to drive clonal hematopoiesis, and is therefore non curative (Nannya et al., 2023; Schnegg-Kaufmann et al., 2023; Unnikrishnan et al., 2017). The rate of relapse after AZA treatment has been reported to be around 40% (Prébet et al., 2011).

For what concern decitabine, a phase III clinical trial comparing low-dose decitabine with best supportive care did not show any improvement in overall survival but a significant increased progression-free survival and quality of life parameters, and lower risk of AML transformation (Lübbert et al., 2011). Similar results were previously reported from another phase III study (Kantarjian et al., 2006).

It thus seems that azacytidine possesses a best performance compared to decitabine: this is still a controversial aspect, since comparative studies reported different results. One study claimed that azacytidine and decitabine showed comparable efficacy since there were no significant differences in overall survival, event-free survival and rate of leukemia transformation, even if in patients ≥ 65 years of age survival was significantly improved in the azacytidine group (Lee et al., 2013). Other comparative studies found an improved OS and AML-free survival of azacytidine compared to decitabine and thus recommended the use of the first one as first-line hypomethylating agent, especially in older patients (Liu et al., 2021; Xie et al., 2015). Those observed differences in clinical efficacy may rely on different trial design and administration doses rather than a real different efficacy, even if is important to remember that their mechanisms of action are different. Both of them are DNA methyltransferase (DNMT) inhibitors, acting in two ways: as direct inhibitors of DNMT enzymes through irreversible binding and degradation (Jüttermann et al., 1994; Patel et

al., 2010) and as cytidine analogs that, after cellular uptake, thanks to their molecular structure can't act as acceptor of the methyl group (-CH3), and thus prevent methylation operated by DNMT enzymes. Both azacytidine and decitabine possess an identical ring structure, however, the ring is attached to a ribose sugar in AZA and to a deoxyribose in DAC (Fig.17): in this way, after uptake into the cell, they are converted to their metabolically active forms through phosphorylation respectively by deoxycytidine kinase (DCK) and uridine-cytidine kinase (UCK), but since DAC contains deoxyribose, 100% of it is incorporated directly into DNA, whereas only about 10–20% of AZA is converted into a deoxyribonucleotide and binds DNA. The remaining 80–90% of AZA is incorporated into RNA (Cruijsen et al., 2014; Jasielec et al., 2014).

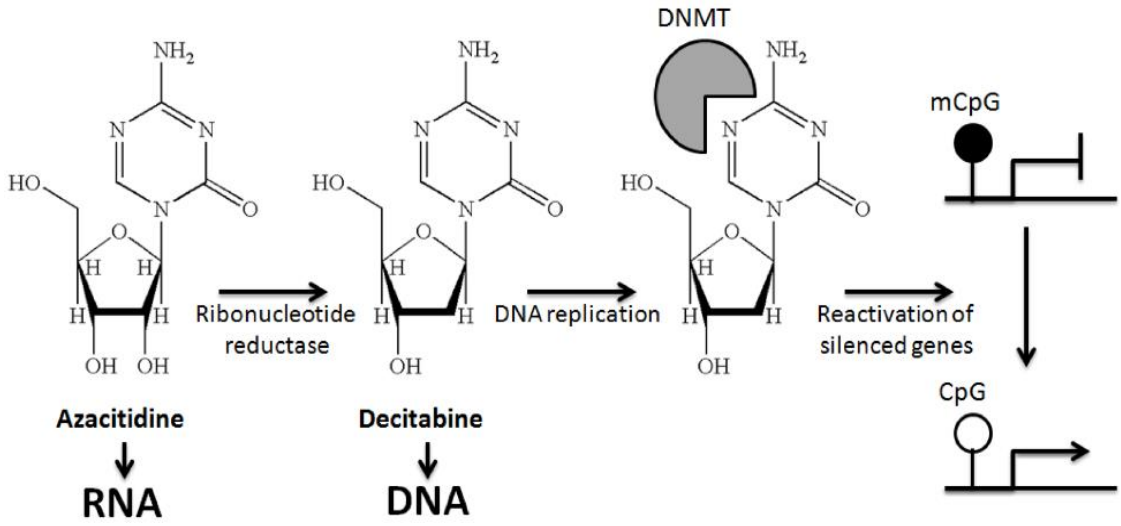

Figure 17

Different structure and mechanism of action of hypomethylating agents Azacytidine and Decitabine. Figure from Cruijsen et al., 2014.

The final result of DNMT enzymes inhibition is the hypomethylation and up-regulation/reactivation of silenced genes involved in multiple pathways including cell cycle arrest, apoptosis, immune response and recognition, renewal and stemness, angiogenesis, cell differentiation and tumor suppressor genes (Itzykson and Fenaux, 2014; Wolff et al., 2017). HMAs have also been shown to re-induce the expression of tumor-associated antigens (TAAs) (Almstedt et al., 2010; Atanackovic et al., 2011; Weber et al., 1994), leading to the activation of tumor-specific cytotoxic T lymphocytes and the subsequent reduction of tumor cells (Goodyear et al., 2010; Guo et al., 2006; Klar et al., 2015). The rationale at the basis of hypomethylating agents use in MDS therapy rely on many evidences that epigenetics changes play an important role in oncogenesis and thus also in hematological cancers and clonal hematopoiesis (Blecua et al., 2002; Jones and Baylin., 2002; Jones and Baylin., 2007). As previously discussed, mutations in genes involved in DNA methylation (DNMT3A, TET2, IDH1, IDH2) are in fact frequently mutated in AML and MDS patients and these mutations are found to occur as early events, indicating a pivotal role in the development of such diseases. Moreover, several studies found aberrant DNA methylation in MDS and sAML patients (Figueroa et al., 2009), with increased methylation level in sAML as compared with matched MDS stage (Gonçalves et al., 2021; Zhou et al., 2020), providing additional theoretical basis for the usage of demethylation drugs in MDS patients against disease progression.

HMA failure in MDS is generally categorized into primary or secondary based on the patient's initial response to treatment: primary failure is defined as the lack of blast reduction or improvement in blood counts after

at least four to six cycles of initial therapy, or MDS progression to higher-risk categories or transformation to AML. Secondary failure occurs in patients who experience a worsening blood counts or progression of MDS to higher-risk categories or AML despite their initial response to HMA. The precise molecular mechanisms involved in HMA therapy resistance and failure are unknown, but different factors – both intrinsic and extrinsic to hematopoietic stem and progenitor cells – have been proposed. Among intrinsic factors, the pathways involved in HMA metabolism were investigated. One study on response to decitabine reported a higher CDA/DCK ratio (where CDA is the enzyme responsible for the inactivation of cytidine analogs) in non-responders than responders, but no significant differences at relapse, suggesting that this could be a mechanism of primary resistance (Qin et al., 2011). Also for AZA, lower expression of UCK enzyme was observed in patients who do not respond to treatment, but the difference in the enzyme expression was not influenced by methylation of its promoter (Valencia et al., 2014). However, a later study using mass spectrometry quantified the active metabolites of AZA in MDS and CMML concluded that primary resistance was not due to impaired of AZA metabolism (Unnikrishnan et al., 2018). Another study, always focused on metabolism, found that DNMT1 was not depleted at relapse and thus suggested that relapse might be result of changes of pyrimidine metabolism that prevents DNMT1 degradation (Gu et al., 2021). An additional intrinsic factor found involved in HMA resistance and relapse is the cell cycle activity of hematopoietic cells, which were observed to be more quiescent in patients with primary resistance. Cell quiescence was mediated by integrin α5 (ITGA5) signaling, making it an interesting molecule to target with integrin α5 inhibitor for overcoming HMA resistance (Unnikrishnan et al., 2017). One study identified 167 differentially methylated regions (DMRs) of DNA at baseline that distinguished responders from non-responders CMML patients treated with decitabine, and through transcriptional analysis found the overexpression of CXCL4 and CXCL7 in the bone marrow of non-responders (Meldi et al., 2015). Interestingly, the treatment with these two chemokines, which regulates the cell cycle activity of hematopoietic stem cells, was able to abrogate the effect of decitabine on primary CMML cells, suggesting that their upregulation is involved in primary resistance. In another study, the anti-apoptotic Bcl-2 member BCL2L10 was found to correlate with AZA treatment resistance (Cluzeau et al., 2012) and resulted, in a retrospective study, correlated with response to AZA and overall survival, with a potential impact in clinical practice (Vidal ed al., 2017).

The action of hypomethylating agents is genome-wide and not directed to specific genomic regions, preferentially affecting the most heavily methylated genes (Klco et al., 2013). Since the activity is not targeted, undesirable off-target actions could have adverse effects and compromise their efficacy. For example, one study reported a reactivation of the oncogene SALL4 upon treatment with azacytidine in 40% of the patients, which also displayed worse outcome (Liu et al., 2022). Other studies linked the use of hypomethylating agents and the induction of immune checkpoint inhibitors expression PD/PD-L1 axis and CTLA-4, which was correlated with resistance to HMA treatment, disease progression and shorter OS likely due to T cell exhaustion and tumor immune evasion (Ørskov et al., 2015; Yang et al., 2014).

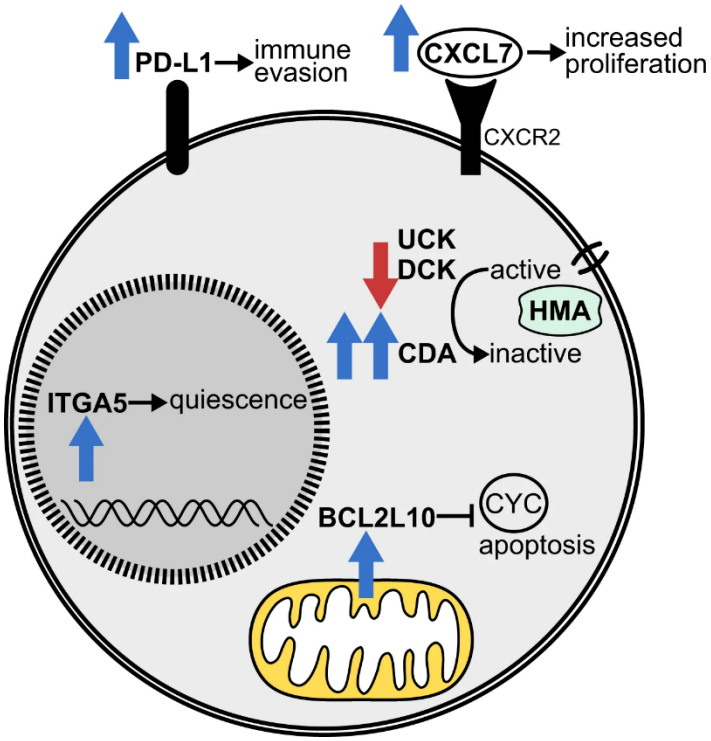

Figure 18

Cell-intrinsic factors associated with HMA resistance in myeloid malignancies. Figure from Stomper et al., 2021.

In addition to cell-intrinsic factors, HMAs exert their effects also on immune cells and the bone marrow niche components, whose behavior can contribute to both HMA response and failure. Among bone marrow niche cells, the effect of HMAs on mesenchymal stem cells was particularly investigated. It was observed that *in-vitro* treatment of MSCs with AZA significantly restored their normal properties (osteogenic differentiation, proliferation, gene expression) and their ability to support the *in-vivo* engraftment of hematopoietic cells (Poon et al.,2018). Similar findings were reported in another study, where AZA was observed to exert a direct effect on healthy as well as MDS-derived MSCs to favor support of healthy over malignant clonal HSPC expansion in coculture experiments (Wenk et al., 2018). An additional *in-vitro* study reported a decrease in IL-6 production in MSCs from MDS patients to levels found in normal controls after AZA treatment (Boada et al., 2021). However, AZA treatment was also linked to augmented immune-modulation functions of MSCs, that showed increased immunosuppressive effects through the secretion of PGE_2 due to the demethylation of the COX2 and PTGES promoters (Lee S et al., 2015). Several studies demonstrated the effects of HMAs on immune cells, as I will discuss in a separate chapter.

Beyond the research for understanding the resistance mechanisms to HMA, many groups tried to discover biomarkers and/or genetic features that could be predictive for treatment outcome and survival. Somatic gene mutations were investigated in numerous studies; however, the obtained results were discordant regarding the prognostic and predictive value of mutations (Stomper et al., 2021; Zhao et al., 2021). For example, some studies shown that TET2 and DNMT3A mutations correlates with improved response to HMAs (Bejar et al., 2014; Itzykson et al., 2011; Metzeler et al., 2011; Traina et al., 2014), and two studies reported correlation between complete response to decitabine and TP53 mutations (Chang et al., 2017; Welch et al., 2016). By contrast, another study on 127 Korean MDS patients found instead the opposite, correlating DNMT3A and TP53 mutations with poor prognosis (Jung et al., 2016). Some studies indicated that abnormalities of chromosome 7, alone or with complex karyotype, was predictive of response to HMA

(Lübbert et al., 2001; Raj et al., 2007). Other two studies respectively on 128 and 700 MDS patients did not find any prognostic genetic mutation and cytogenetic aberrations (Kuendgen et al., 2018; Sébert et al., 2017). Very recently, another paper claimed that the evaluation of post-treatment clone size, together with the pretreatment mutational profile (in particular multi-hit TP53, EZH2 and DDX41 mutations) improves prognostication of azacitidine-treated patients (Nannya et al., 2023). Beyond mutations and cytogenetic alterations, one study focused on methylation signatures and defined a panel of 200 regions with differential methylation patterns at diagnosis that correlate with survival and HMA response (Cabezón et al., 2021). Within these regions, three genes (CPT1C, PRRT1 and LYPD3) had their promoters more methylated in patients with shorter survival and four genes (CRADD, RDH13, BRDT and PACRG) were differentially methylated between responding and nonresponding patients to AZA treatment. However, this type of analyses is difficult to implement in diagnostic processes and routine clinic. A second study longitudinally assessed constitutive and ligand-induced phospho-Stat3/5 signaling activation (STAT3 and STAT5 proteins are oncogenic downstream mediators of the JAK-STAT pathway, whose deregulation promotes cancer cell proliferation and survival) by multiparametric flow cytometry in 74 patients with MDS and low blast count AML undergoing azacitidine therapy, finding that the pre-treatment Stat3/5 signaling profiles in CD34+ cells correlated with response and independently predicted event-free survival (Miltiades et al., 2016). Lastly, the dynamics of PD-1 expression (measured by quantitative PCR) have been associated with treatment efficacy and prognosis in patients with high-risk MDS: in particular, PD-1 expression values higher or equal to 75.9 after 2 cycles of HMA treatment was observed to be an independent negative prognostic factor in predicting AML transformation and survival and could help to identify patients who will potentially benefit from the combined therapy of HMA and PD-1 inhibitors (Geng et al., 2022).

In the last few years, a combination therapy of HMAs and the drug Venetoclax showed encouraging results. Venetoclax is an oral selective inhibitor of the anti-apoptotic protein BCL-2 that play an important role in leukemias and more generally in hematological malignancies, providing the initial rationale for its use also in MDS (Garcia et al., 2020). Preclinical studies previously demonstrated that BCL-2 is overexpressed in high-risk MDS, and that BCL-2 inhibition induces apoptosis in MDS progenitor cells (Jilg et al., 2016; Parker et al, 2000). A recent clinical study reported an overall response of 59% (14% of complete response), with a median OS of 19.5 months for the entire cohort and 11.4 months among patients with HMA failure. Moreover, allogeneic stem cell transplantation was performed in most of the patients who achieved a response and they had significantly longer median OS (Ball et al., 2020). However, very poor-risk cytogenetics and the presence of TP53 mutation were factors associated with decreased survival. Other clinical trials showed similar results, highlighting the improved efficacy, less rate of AML transformation and increased survival probability after HSCT of the combined therapy on both naïve and pre-treated MDS patients (Azizi et al, 2020; Bazinet et al., 2022; Komrokji et al., 2022; Wei et al., 2019; Zeidan et al., 2023). Thus, Venetoclax seems to be a promising agent in treatment of MDS patients, even with some limits in TP53 mutated/ high-risk cytogenetic patients. Further prospective clinical trials are still ongoing to investigate its safety and impact on overall survival, in particular in those patients who proceed to transplantation.

To sum up, only half of MDS patients show an hematological response to HMA treatment, but the gain in terms of overall survival is in the order of 7-9 months since the therapy does not eradicate the neoplastic clones. The HMA effect is transient and lasts from 6 to 24 months (Santini, 2019; Zeidan et al., 2014), whereas long-lasting remissions are rare. The prognosis of refractory/relapsed patients is very poor (less than 6 months), also due to the limited availability of alternative treatments (Jabbour et al., 2015; Prébet et al., 2011). Thus, there is still an important unmet clinical need in finding prognostic and predictive biomarkers for treatment response, as well as in developing innovative therapies for primary and secondary failures.

1.3.4 Emerging therapeutic strategies for refractory/relapsed patients

Recent progresses have led to the emergence of innovative therapeutic strategies that could improve the outcome in refractory/relapsed patients, especially the ones that carry mutations in TP53 (Cumbo et al., 2020; Daver et al., 2022). Those immunotherapies and mutant p53–directed approaches can be either cell-extrinsic or cell-intrinsic; and the most promising are:

- Magrolimab: this monoclonal antibody is directed to CD47 molecule, whose over-expression in cancer cells prevent them from phagocytosis. CD47 in fact acts as "don't eat me signal": through its binding to the signal receptor protein-α (SIRPα) on macrophages and dendritic cells, it enables immune evasion by inhibiting prophagocytic receptors like complement receptor 3, Fc receptors, and SLAMF7 (Huang et al., 2022; Veillette et al., 2019). Moreover, CD47 is particularly expressed by leukemic stem cells (LSC), meaning that the therapy should target only cancer cells while sparing normal HSCs (Eladl et al., 2020; Galli et al., 2015; Huang et al., 2020). This receptor was also found upregulated on granulocyte-macrophage progenitors (GMPs) in high-risk MDS (Pang et al., 2013). In a phase-II study, the combination of magrolimab and Azacytidine showed a good tolerance and promising efficacy in TP53-mutant patients, in which 40% achieved CR with a median OS of 16.3 months (Sallman et al., 2023). A second clinical trial always on the combination of magrolimab and azacytidine showed a CR rate of 33%. The median duration of response (DOR) was 8.7 months, and the median OS was 10.8 months (Daver et al., 2022).
- Flotetuzumab: this bispecific antibody targets both CD3 and the IL-3 receptor CD123, whose downstream signaling promotes hematopoietic progenitor cell proliferation through activation of the PI3K/MAPK pathway and upregulation of antiapoptotic proteins (Al-Hussaini et al., 2016). In this way, it mediates T-cell activation and proliferation, resulting in the eradication of CD123-expressing primary AML blasts *in vitro* and *in vivo* (Chichili et al, 2015; Al-Hussaini et al., 2016). A recent study on AML identified a patient subgroup, characterized by TP53 abnormalities, that benefit from immunotherapy with flotetuzumab and showed a response of 47% with a median OS of 10.3 months (Vadakekolathu et al., 2020). Previous preliminary studies in relapsed/refractory (R/R) AML and MDS patients showed evidence of anti-leukemic activity, increase in T cell infiltration and activation, and a good safety profile. However, the T cell activation was accompanied by upregulation of PD-L1 on leukemic blasts. In fact, AML cells in patients that progressed on flotetuzumab or with residual disease were found to be PD-L1 positive, suggesting that combination with anti-PD1/PD-L1 therapy may enhance the effect of flotetuzumab (Retting et al., 2017; Uy et al., 2017).
- Sabatolimab: this monoclonal antibody is specific for TIM3, an immune checkpoint inhibitor that induces T cell exhaustion (Das et al., 2017; Wolf et al.,2020) and is also involved in an autocrine signaling loop via galectin-9, which promotes leukemic stem cells renewal and leukemic progression (Kikushige et al., 2015). A phase Ib trial evaluated sabatolimab with HMA in newly diagnosed patients with HR-MDS or AML unfit for intensive therapy. The treatment showed good safety and tolerability profile and demonstrated a CR rate of 20% and a median duration of response (DOR) of 17 months. Specifically, also HR-MDS with TP53 mutations and AML patients with at least 1 adverse-risk mutation (TP53/RUNX1/ASXL1), showed durable clinical response (Brunner et al., 2021).
- Eprenetapopt (APR-246): this small molecule have been shown to restore p53 protein function through its covalent binding to cysteine residues in the core DNA domain of mutant p53, which induce the correct protein folding to the wild-type conformation (Lambert et al., 2009; Wiman, 2010). Other proposed mechanisms of action of this class of molecules include induction of cell death via reactive oxygen species (Tessoulin et al., 2014), ferroptosis (Birsen et al., 2022; Fujihara et al., 2022), depletion of antioxidant enzymes (Fujihara et al., 2022; Peng et al., 2017) and perturbation of endoplasmic reticulum stress (Teoh et al., 2016). Two recent studies evaluated eprenetapopt with azacitidine in TP53-mutated MDS and AML patients. Both trials highlighted high response rate (71%

and 62%, respectively) and CR rate (44% and 47%, respectively). Moreover, patients with isolated TP53 mutations showed the highest rate of CR and significant reduction in TP53 VAF and p53 expression by immunohistochemistry. Median overall survival was between 10 and 13 months (Cluzeau et al., 2021; Sallman et al., 2021). Furthermore, patients who proceeded to allo-SCT after remission and/or clearing of TP53 mutation had favorable outcomes with a median overall survival of 14.7 months (Sallman et al., 2021). Consistent with the mechanism by which eprenetapopt restores wild-type function to the misfolded mutant p53 protein, the level of bone marrow p53 protein assessed by immunohistochemistry (ICH) acted as predictive biomarker: in fact, patients with low p53 levels on baseline BM biopsies (< 10% p53 IHC+ on BM mononuclear cells) had significantly lower rates of CR than those who were p53-positive (13% v 66%, respectively).

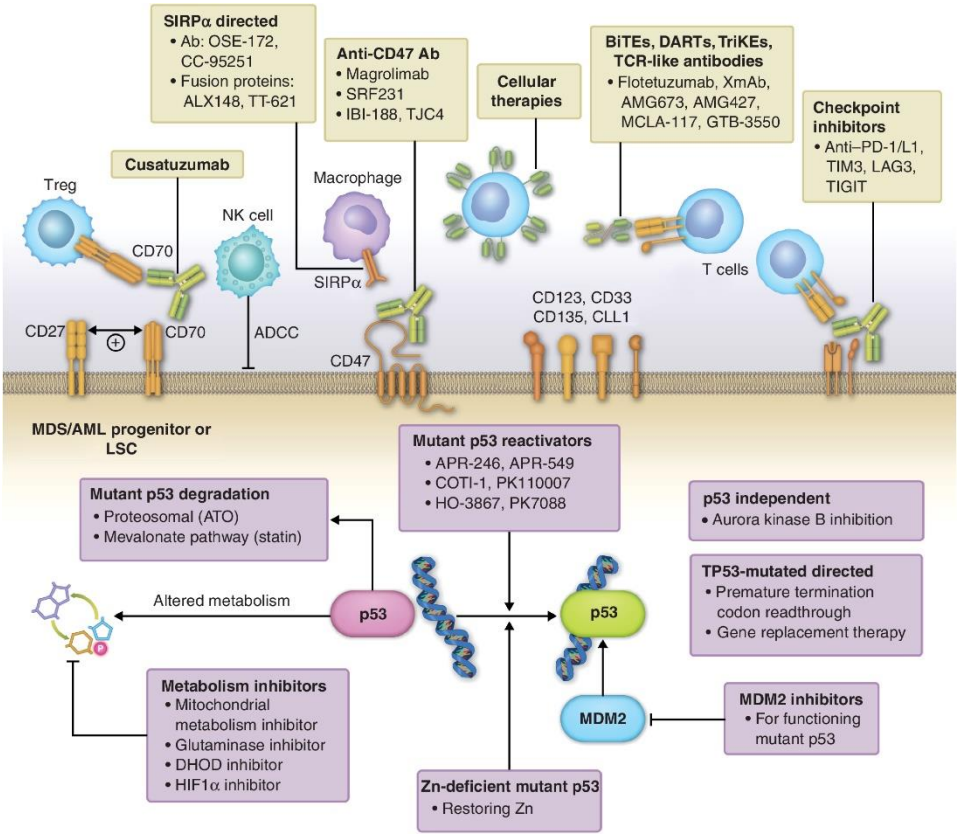

Figure 19

Novel therapies for TP53-mutated and R/R MDS and AML. Cell-extrinsic immunotherapeutic approaches include targeting cell-surface markers including LSC markers, macrophage and T-cell checkpoints, bispecific engagers, and adoptive cellular therapies including unmodified and chimeric antigen receptor–modified cells. Cell-intrinsic approaches include mutant p53 reactivators, mutant p53 degraders, metabolism-targeting agents, GSPT1 degraders, and others. Figure from Daver et al., 2022.

1.4 Immune landscape of MDS

Bone marrow is a sophisticated organ which, besides the main function of hematopoiesis, also serve as an active organ of the immune system, supporting it through lymphopoiesis and myelopoiesis and acting as a sanctuary for plasma cells and lymphoid cells (Mercier et al., 2011). For a long time, the BM had been considered an immune-privileged organ protected from immune damages and inflammation in order to

ensure blood cell production and immune homeostasis. Accumulating evidences have instead demonstrated that niche changes due to autoimmunity, inflammation or infections can occur and can influence the function of HSCs and other BM environmental cells (Sezaki et al., 2020), and those alterations are associated with hematological malignancies (Méndez-Ferrer et al., 2020).

Also in MDS, the bone marrow immune landscape significantly changes and drives normal HSCs suppression and disease progression. However, these niche changes are different depending on the stage of the disease and result in immune peculiarities in low-risk compared to high-risk MDS.

1.4.1 Immune dysregulation in low-risk MDS

Low-risk MDS have been associated to aberrant immune system activation and pro-inflammatory environment that leads to both ineffective hematopoiesis, excessive cellular death and autoimmune manifestations (Gonzalez-Lugo et al., 2022). From a clinical point of view, systemic inflammatory and autoimmune diseases (SIADs) are frequently observed in MDS patients, with an incidence ranging from 10 to 28% in the overall MDS population (Komrokji et al., 2016; Mekinian et al., 2016). Inflammation have been widely described to be associated with MDS pathogenesis (Barreyro et al., 2018; Sallman et al., 2019), and several predisposing factors, extrinsic or intrinsic of the malignant clone, contribute and drive such immune hyperactivation.

Among those factors there are aging and chronic inflammation, which are strictly linked and the term "inflammaging" was introduced to describe this close relationship between the two phenomena (Franceschi et al., 2000). In fact, from a biological point of view, aging is a physiological process of tissue degeneration due to chronic inflammation (López-Otín et al., 2013). The term inflammaging thus describes the chronic, sterile and systemic inflammation with self-reactivity in the absence of acute infection which occur in the old people. The result is reduced adaptive immunity (de Mol et al., 2021; Mittelbrunn et al., 2021), exacerbated pro-inflammatory reactions and autoimmunity (Boren et al., 2004; Stubbins et al., 2022). Moreover, inflammaging has also been linked to HSCs dysfunction, causing loss of quiescence (Agarwal et al., 2019; Ho et al.,2022), reduced self-renewal capacity (Bogeska et al., 2022; Bousounis et al., 2021) and inducing a myeloid differentiation bias - called myeloid skewing - (Beerman et al., 2010; Oduro et al., 2012; Stubbins et al., 2021), thus providing a predisposition to clonal hematopoiesis/expansion and malignancies (Avagyan et al., 2021; Avagyan and Zon; 2023; Crusz et al., 2015; Serrano-López et al., 2021).

Innate immune signaling is central in the pathogenesis of MDS, and genes related to immune signaling are found overexpressed in more than 50% of MDS patients (Hofmann et al., 2002; Pellagatti et al., 2010). The innate immune system recognizes pathogen associated molecular patterns (PAMPs) and host damage associated molecular patterns (DAMPs) by pattern recognition receptors (PRRs), whose first subtype that was discovered is represented by the Toll-like receptors (TLR) family. Upon ligand binding, TLRs recruit cytosolic adaptor proteins that are then responsible for the subsequent activation of other downstream proteins (mainly kinases) which further propagate and amplify the signal. The final result is the upregulation of genes linked to cytokine production with a general activation of the adaptive immunity branch. It was demonstrated in a murine model that chronically activated TLR signaling and consequent prolonged inflammation can alter the bone marrow microenvironment and damage HSCs (Esplin et al., 2011). Moreover, it was described that hematopoietic progenitor cells are mutated for TLRs or overexpress them in MDS patients compared to healthy donors (Maratheftis et al., 2007; Wei Y et al., 2013). The TLRs upregulation was observed in low/intermediate MDS but not in high-risk patients, highlighting the main role of inflammation in the early pathogenesis phases of the disease (Paracatu et al., 2022). The downstream effectors of TLRs signaling MyD88, IRAK1/4 and TRAF6 were also found overexpressed and hyperactivated in MDS (Dimicoli et al., 2013; Fang et al., 2017; Rhyasen et al., 2013), whereas negative regulators such as miR-145, miR-146a, and TIFAB were observed downregulated or deleted in del(5q) MDS (Kumar et al., 2011; Starczynowski et al., 2010; Varney et al., 2015). TLRs massive activation and the consequent formation of the Myddosome

complex (Fig.20) is associated to the elevated transcription and production levels of pro-inflammatory cytokines such as TNFα, IL-6, IL-1β and IL-18 that have been observed in low-risk MDS (Gañán-Gómez et al., 2015; Shi et al., 2019).

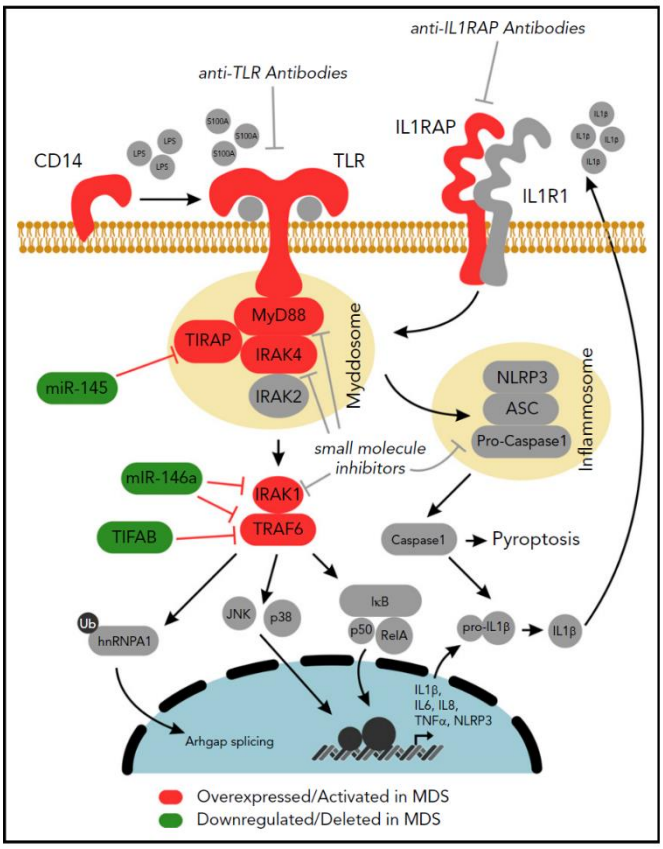

Figure 20

Dysregulation of innate immune signaling in MDS HSCs. *TLRs and interleukin-1 receptor (IL 1R)/IL1RAP recruit MyD88 and IRAK4/2 (Myddosome complex) upon ligand binding. The adaptor protein TIRAP increases the efficiency of Myddosome assembly by binding MyD88. The kinase IRAK4 activates IRAK2 and/or IRAK1 through IRAK4-dependent phosphorylation. IRAK1 activates the ubiquitin (Ub) ligase, TRAF6, which mediates signaling to NF-kB, MAPK, and RNA binding proteins leading to expression of proinflammatory cytokines and NLRP3. microRNA-146a (miR-146a) suppresses IRAK1 and TRAF6 protein expression, whereas miR-145 suppresses TIRAP protein expression. TIFAB suppresses TRAF6 protein stability. Inflammosome activation results in caspase1–dependent IL-1b processing and pyroptosis. Proteins and genes in green are downregulated and/or deleted in MDS. Proteins and genes in red are overexpressed and/or activated in MDS. Steps of the signaling pathway that have been pharmacologically inhibited are indicated. Figure from Barreyro et al., 2018.*

Beyond the induction of pro-inflammatory cytokines transcription, the TLRs signaling is also responsible for the recruitment of the Inflammosome complex. The inflammosome consists of a family of Nod-like receptors (NLRs), whose activation and aggregation leads to the activation of pro-IL1β into its active form, and trigger also a specific program of pro-inflammatory cell death called pyroptosis, characterized by lytic cell death with loss of plasma membrane integrity (Bergsbaken et al., 2009). Among the NLRs family, NLRP3 is the inflammasome sensor that is most strongly associated with the development of uncontrolled inflammation and autoimmunity (Bertheloot et al., 2021). NLRP3 is activated by DAMPs signals, among which alarmins S100A8 and S100A9 are of particular importance in MDS, since they were found in excess in MDS HSPCs and bone marrow plasma (Basiorka et al., 2016). Pharmacologic inhibition of NLRP3 and neutralization of S100A9 were shown to restore normal hematopoiesis (Basiorka et al., 2016). Also Lenalidomide treatment was seen to reduce the steady-state generation of S100A9, thereby increasing the levels of Epo and promoting erythropoiesis (Cluzeau et al., 2017). Interestingly, in addition to DAMPs, the aberrant activation of inflammosome pathway has been associated with common MDS mutations in spliceosome or epigenetic genes as SRSF2, TET2, IDH2, SF3B1, ASXL1 and U2AF1, and with del(5q) cytogenetic aberration (Basiorka et al., 2016; Pollyea et al., 2019; Smith et al., 2019; Zhao LP, Boy M et al., 2021; Zhao LP, Schell B et al., 2021). A recent study on a large and genetically characterized cohort of treatment-naïve MDS patients confirmed the major activation of inflammatory pathways mediated by caspase-1, interleukin IL-1β and IL-18 in low-risk BM compared to high-risk and CHIP patients and found different inflammatory signatures between distinct LR-MDS subgroups: in particular, one cluster associated to lower IL-1β was enriched in SF3B1-mutated patients, whereas the second cluster, associated with higher IL-1β levels, was completely composed of del(5q) cases (Schneider et al., 2023).

Cellular immune response dysregulation is another important immunological mechanism driving MDS pathogenesis, which closely interacts with the coexisting inflammatory microenvironment. For example, it has been observed that S100A8 and S100A9, by binding of CD33, stimulates the expansion of Myeloid-derived suppressor cells (MDSCs), which in turn secrete suppressive cytokines IL-10 and TGF-β that inhibit effector T cells function and proliferation, therefore favoring the malignant clone expansion (Chen X et al., 2013). Moreover, it has been recently published that S100A9 increases the expression of PD-1 on HSPCs and PD-L1 on MDSCs in MDS versus healthy donors, which lead to HSPCs dead and thus contribute to ineffective hematopoiesis (Cheng et al., 2019).

Remaining in the myeloid compartment, the cells of the macrophage/monocyte lineage have been reported to contribute to the inflammatory process in MDS through impaired phagocytosis of the apoptotic hemopoietic cells and abnormal production of cytokines (Allampallam et al., 2002). Monocytes represent 2-12% of leukocytes in the blood and are generally characterized by the strong expression of CD14 and the lack of CD16 expression. Monocytes with this phenotype are called "classical" and represent the majority (80-95%) of circulating monocytes. The remaining part is composed by two minor subsets which can express CD16: the intermediate monocytes (CD14+CD16+) and nonclassical ($CD14^{dim/neg}$CD16+) ones, that represent the 2-11% and 2-8% of the total monocytes, respectively. Classical monocytes are critical for the initial inflammatory response, intermediate monocytes are mainly pro-inflammatory too, whereas nonclassical monocytes have been mostly described as anti-inflammatory (Kapellos et al., 2019; Narasimhan et al., 2019). One study form Velegraky et. al reported a decreased number of classical monocytes and an increased frequency of intermediate monocytes with abnormal functional characteristics in low-risk MDS compared to age- and se- matched healthy individuals. Intermediate monocytes in fact displayed increased release of TNFα after stimulation with LPS and transcriptional profiling found 43 differentially expressed genes involved in immune signaling, cell adhesion and hematopoiesis (Velegraki et al., 2021). A previous study always from Velegraki et al. showed that monocytes from MDS patients over-express TLR4 and its downstream signaling which leads to the production of inflammatory cytokines. Moreover, monocytes had an impaired capacity to engulf the apoptotic BM cells which maintains and enhances an inflammatory environment through an excessive release of high mobility group box-1 protein (HMGB1) by dying cells (Velefraki et al., 2013).

Also monocyte-derived dendritic cells in low-risk MDS were found to be defective, showing reduced membrane upregulation of costimulatory ligands in response to pro-inflammatory stimuli and an altered cytokine profile (Ma L et al., 2007). Fluorescence in situ hybridization (FISH) analysis on purified dendritic cells in MDS patients revealed that DCs carry the same cytogenetic abnormality of the malignant clone (Ma L et al., 2004; Rigolin et al., 1999). Both CD34+ progenitors and monocytes from MDS patients showed impaired capacity of DCs generation (Micheva et al., sept 2004; Micheva et al., dec 2004), and monocyte-derived dendritic cells (MoDCs) showed reduced expression of CD80 and CD1a, lower ability to stimulate T cells, reduced endocytic capacity and ineffective maturation following TNF-stimulation (Micheva et al., dec 2004; Rigolin et al., 1999).

Among T cells compartment, Th17 cells are a subset of CD4+ effector cells, named by their signature cytokine IL-17, which were found to play an important role in in the pathogenesis of inflammatory and autoimmune diseases as well as in tumor immunity (Ye et al., 2013). IL-17, in fact, mediates activation of the adaptive T-cell response inducing an inflammatory cytokine environment. Both Th17 T cells and their secreted cytokine IL-17 have been observed increased in Low-risk MDS compared to High-risk (Kordasti et al., 2009; Li J et al., 2016; Zhang et al., 2013). In literature, Th17 have been both linked to increased function of CD8+ T cells and antitumor effects on one side (Li J et al., 2016), and pro-inflammatory and autoimmunity-associated features on the other one (McGinley et al., 2020). Both CD4+ and CD8+ T cells expansion were described in LR-MDS, and this expansion was mostly polyclonal in the CD4+ subset and oligoclonal in the CD8+ subset: such difference could reflect the selective involvement of effector T cells either in the anti-tumor response or in an autoreactive effect (Fozza et al., 2009). Another important subset of CD4+ T cells is the one of regulatory

T cells (Tregs), who is physiologically involved in the negative control of immune response: those cells are in fact the responsible of "turning off" inflammatory responses, avoiding chronic inflammation and autoimmune T cells expansion (Sakaguchi, 2004). On the other side, excessive expansion of such cells and their recruitment at tumoral sites can suppress anticancer immunity and promote tumor development and progression (Togashi et al., 2019). In low-risk MDS, Tregs are reduced in number compared to healthy controls and high-risk MDS, possibly representing a further mechanism of cytotoxic T cell expansion (Giovazzino et al., 2019), and have also been shown to be dysfunctional both in their suppressive function and in their bone marrow homing capacity (Kotsianidis et al., 2009).

1.4.2 Immune dysregulation in high-risk MDS and AML

In contrast to what observed in low-risk MDS, high-risk and AML patients exhibit decreased apoptosis and an anti-inflammatory and immunosuppressive microenvironment that favor the expansion of malignant cells due to immune evasion mechanisms.

NK cells aberration in high-risk MDS and AML represents an important aspect of defective immune surveillance. In fact, several studies reported reduced NK cell number, impaired NK maturation (higher proportion of immature $CD56^{brigt}$ $CD16^{dim}$ NK cells, with immunomodulatory function, compared to $CD56^{dim}$ $CD16^{high}$ mature cells, with cytotoxic activity) and reduced cytotoxic activity due to down-regulation of the activating receptors NKp30 and NKG2D, up-regulation of inhibitory receptors or reduced levels of perforin and granzyme B (Aggarwal et al., 2016; Cianga et al., 2021; Epling-Burnette et al., 2007; Hejazi et al., 2015; Zhang W et al., 2018). Defects in the NK cell compartment was associated with excess blasts, adverse clinical outcome and blast transcriptional signatures of immune evasion (Chretien et al., 2017; Khaznadar et al., 2015). The evidence of shared genetic lesions between MDS clone and NK cells might explain the intrinsic defects of NK functionality (Arends et al., 2018; Boy et al., 2023; Carlsten et al., 2019).

One of the reasons of the conversion to an immune suppressive and evasive microenvironment is the overexpression of immune checkpoint inhibitors on T cells, in particular the programmed cell death 1 (PD-1) and cytotoxic T-lymphocyte-associated protein 4 (CTLA-4) which lead to T cell exhaustion, loss of function (intended as impaired proliferation and cytokine release, and downregulation of the T-cell receptor TcR) and apoptosis (Coats et al., 2016; Haroun et al., 2017; Radwan et al., 2020; Tcvetkov et al., 2020; Yang X et al., 2022). Those receptors are physiologically expressed on activated T cells, preventing immune over-activations. However, this protective function can be used and improved by tumors to maintain an immunosuppressive niche that favors malignant cell expansion (Yi et al., 2021). In parallel with PD-1 overexpression, also its ligand PD-L1 has been found overexpressed on blast cells (Coats et al., 2016; Tcvetkov et al., 2020; Williams et al., 2019). Other immunomodulatory receptors such as T-cell immunoglobulin and mucin-domain containing-3 (TIM3), T cell immunoglobulin and ITIM domain (TIGIT) and Lymphocyte activation gene 3 (LAG-3) have also been observed upregulated in high-risk MDS and/or AML patients (Abdelhakim et al., 2018; Fu et al., 2019; Meng et al., 2020; Williams et al., 2019; Wolf et al., 2019). The overexpression of such immune checkpoint molecules not only decreases the cytotoxic function and survival capacity of T cells (Sand et al., 2016; Tao et al., 2016) but is also involved in NK cell dysfunction (Beldi-Ferchiou et al., 2017; D'Silva et al., 2023; Gallois et al., 2015; Meng et al., 2020; Ndhlovu et al., 2012; Zhang Q et al., 2018).

An additional reason of the increased immunosuppressive BM environment in advanced stages of the disease is the expansion of Tregs in both BM and PB. In high-risk MDS and AML, Tregs have been shown to maintain their function and homing capacity, and to be a feature of disease progression and aggressiveness (Kordasti et al., 2009; Kotsianidis et al., 2009; Wan et al., 2020). Moreover, Kotsianidis et al showed that Tregs follow the disease course and are significantly reduced in patients who responded to chemotherapy. A recent study reported that Tregs also promote the stemness of leukemic stem cells through the activation of PI3K/AKT following their release of IL-10 (Xu Y et al., 2022). There are several mechanisms by which Tregs can mediate

immunosuppression (Fig. 21) (Togashi et al., 2019). For example, through their high expression level of CD25 receptor, they bind with high affinity and deplete from their surroundings IL-2, a cytokine essential for complete T cell activation, thus reducing its availability for effector T cells (Teff). They also constitutively express CTLA-4, whose binding to CD80 and CD86 on antigen-presenting cells (APCs) lead to the suppression of APC function and reduction of their capacity to activate Teff cells. Moreover, CTLA-4 possess a higher affinity to CD80/86 than the co-stimulatory receptor CD28, further disrupting Teff priming and activation. Tregs also release immunosuppressive cytokines such as IL-10, TGFβ and IL-35, and extracellular ATP, which is converted by CD39 and CD73 enzymes to AMP that provides an immunosuppressive signal to Teff and APCs via A_{2A} receptor. In the end, Tregs can also directly kill Teff cells through release of granzyme and perforin. In high-risk MDS, an increase in IL-10, compared to low-risk, was observed. Moreover, the same study found a positive correlation between IL-10 and TGFβ cytokines level in the serum and FOXP3 expression (the transcription factor expressed by Tregs), and a negative correlation between IL-10 expression and numbers of CD8+ T cells (Lopes et al., 2013).

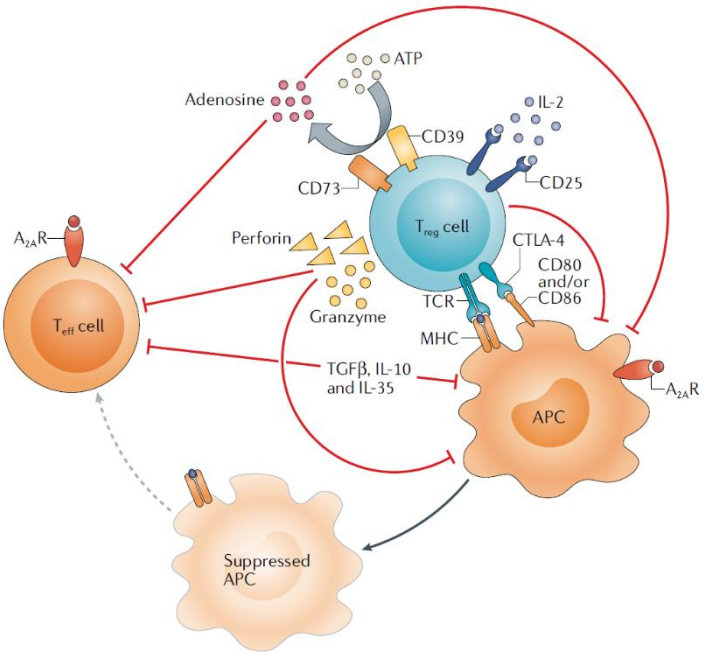

Figure 21

Mechanisms of Tregs-mediated immunosuppression. Figure from Togashi et al., 2019

Another immunosuppressive immune population that has been observed expanded in high-risk MDS and AML is represented by Myeloid-derived suppressor cells. MDSCs overproduce suppressive cytokines, express immune checkpoint inhibitors and secrete reactive oxygen and nitrogen species, thus reducing the function of several immune cells such as T cells, NK cells, Dendritic cells (DCs) and B cells (Lechner et al., 2010; Li K et al., 2021). As I mentioned before, the initial MDSCs expansion in Low-risk MDS is driven by the interaction of pro-inflammatory molecules S100A8/9 with CD33, that results in the release of suppressive cytokines IL-10 and TGF-β. In this way, further proliferation of MDSCs in high-risk MDS (Chee et al., 2022; Velegraki et al., 2022) leads to the prevarication of their immunosuppressive activity over the release of pro-inflammatory molecules. Importantly, the expansion of MDSCs in high-risk MDS have been correlated with the concomitant increased number of Tregs and associated to disease progression (Kittang et al., 2015). MDSCs have been described in MDS to inhibit CD8+ T cells function through TIM3/Gal-9 pathway (Tao et al., 2020) and STAT3-ARG1 pathway (Qi et al., 2021), and to hamper NK cell activity via the TIGIT/CD155 pathway (Yue et al., 2023). Also in AML, MDSCs numbers are increased compared to healthy controls (Lv et al., 2021; Pyzer et al., 2017),

and can be induced by leukemic blasts via the production of MUC1 oncoprotein, which is released through extracellular vescicles (EV) and, when uptaked by MDSCs, increases cMYC expression and cell proliferation (Pyzer et al., 2017). Another study showed the role of extracellular vescicle release from AML blast to induce MDSCs expansion, demonstrating that the palmitoylated proteins on the AML-EV surface can activate Toll-like receptor 2 and the subsequent activation of Akt/mTOR pathway (Tohumeken et al., 2020).

Further myeloid cell subtype are macrophages, a class of plastic cells with different roles in immunity, development and tissue homeostasis and repair. Macrophages differentiate from monocytes that leave the circulation to reside in different tissue, where they acquire specific morphological and transcriptomic profiles to adapt to the tissue of residency (Wynn et al., 2013). In response to IFNs, Toll-like receptor engagement, or IL-4/IL-13 signaling, macrophages can undergo M1 (classical) or M2 (alternative) activation, with M1 having a pro-inflammatory and antitumor effects and M2 an anti-inflammatory and pro-tumoral effect (Sica and Mantovani, 2012). Macrophages that are found within the tumor mass or inside the tumoral niche are called tumor-associated macrophages (TAMs) and play an important role in the pathophysiology of human malignancies, supporting cancer cells by enhancing angiogenesis, promoting tumor cell survival and hampering immune reactions (Cassetta and Pollard 2023). In MDS, monocytes displayed impaired ability to differentiate into macrophages, and mature macrophages were characterized by reduced phagocytic capacity, lower expression of CD206 and signal regulatory protein alpha (SIRPα), and higher secretion levels of inducible nitric oxide synthase (iNOS) (Han et al., 2016). Two studies showed that CD163+CD2016+ M2-TAMs were enriched in HR-MDS patients compared to LR-MDS, that were instead characterized by pro-inflammatory M1 macrophages expressing iNOS (Yang Y and Wu, 2018; Zhang G et al., 2021). It was shown that AML leukemic blasts can reprogram macrophages towards pro-leukemia M2 phenotype with different mechanisms (Miari et al., 2021), for example by the release of arginase (Mussai et al., 2013) or through the expression of the transcriptional repressor Growth factor independence 1 (Al-Matary et al., 2016).

Very little is published about classical and nonclassical monocytes in high-risk MDS and AML, and results are discordant. One paper observed increased non-classical monocytes (ncMono) frequencies in higher-risk MDS compared to low-risk (Chee et al., 2022), whereas a second one did not observe any difference in the frequency of classical, intermediate, and nonclassical monocytes in MDS patients compared to healthy controls (Pollyea et al., 2018). A third paper found a reduction of ncMono in MDS bone marrow compared to normal bone marrow samples, without looking to the differences within MDS subtypes (Van Leeuwen-Kerkhoff et al., 2022). Two papers reported an increased frequency of non-classical monocytes in chronic lymphocytic leukemia (CLL) (Maffei et al., 2013; Pollyea et al., 2018). Classical monocytes in MDS patients exhibited normal innate immune functions compared to monocytes from healthy control subjects (Pollyea et al., 2018); however, accumulation of classical monocytes in MDS was associated with poor prognosis (Wu et al., 2021) and higher frequency of leukemic evolution (Selimoglu-Buet et al., 2017). Monocytes that express low levels of HLA-DR, called CD14+HLA-DRlo/neg monocytes, have recently emerged as important mediators of tumor-induced immunosuppression (Mengos et al., 2019). Two studies described an increased frequency of CD14+HLA-DRlo/neg monocytes in CLL and one of them associated these cells with suppressed in vitro T-cell activation and induction of Tregs (Jitschin et al., 2014; Pollyea et al., 2018).

Dendritic cells were found reduced in numbers in high-risk MDS compared to low-risk MDS and healthy controls (Saft et al., 2013; Van Leeuwen-Kerkhoff et al., 2022). Moreover, DCs derived from high-risk MDS and CMML patient's monocytes were found to be defective, with difficulty in developing dendritic projections and reduced expression of HLA-DR and CD86, suggesting an impairment in antigen processing and presentation to T cells (Bento et al., 2020). Microarray transcriptional analysis on dendritic cells from MDS patients and healthy donors revealed several under-represented transcripts involved in innate in immunity and danger response in MDS, suggesting that this gene expression disruption could lead to diminished immune responsiveness of DCs and favor immune escape of the myeloid clone (Van Leeuwen-Kerkhoff et al., 2022).

Importantly, TP53-mutated MDS and AML have shown to possess a particularly enhanced immunosuppressive environment, characterized by increased expression of PD-L1 on HSCs, TIM3 on MDSC and LAG3 and TIGIT on bone marrow blasts, expansion of ICOS High/PD-1neg Treg and PD-1low myeloid-derived suppressor cells, as well as reduced number of bone marrow-infiltrating OX40+ cytotoxic T cells and helper T cells and decreased ICOS+ and 4-1BB+ natural killer cells (Bewersdorf et al., 2022; Sallman et al., 2020; Williams et al., 2019).

To conclude, immune system plays a critical role in MDS pathogenesis, and both innate and adaptive immune pathways are dysregulated. However, immune microenvironment and immune dysfunctions dynamically change across disease evolution from low-risk to high-risk MDS (Fig.22). Thus, monitoring the immune system represents a new field of research for a deeper and more complete characterization of this disease group.

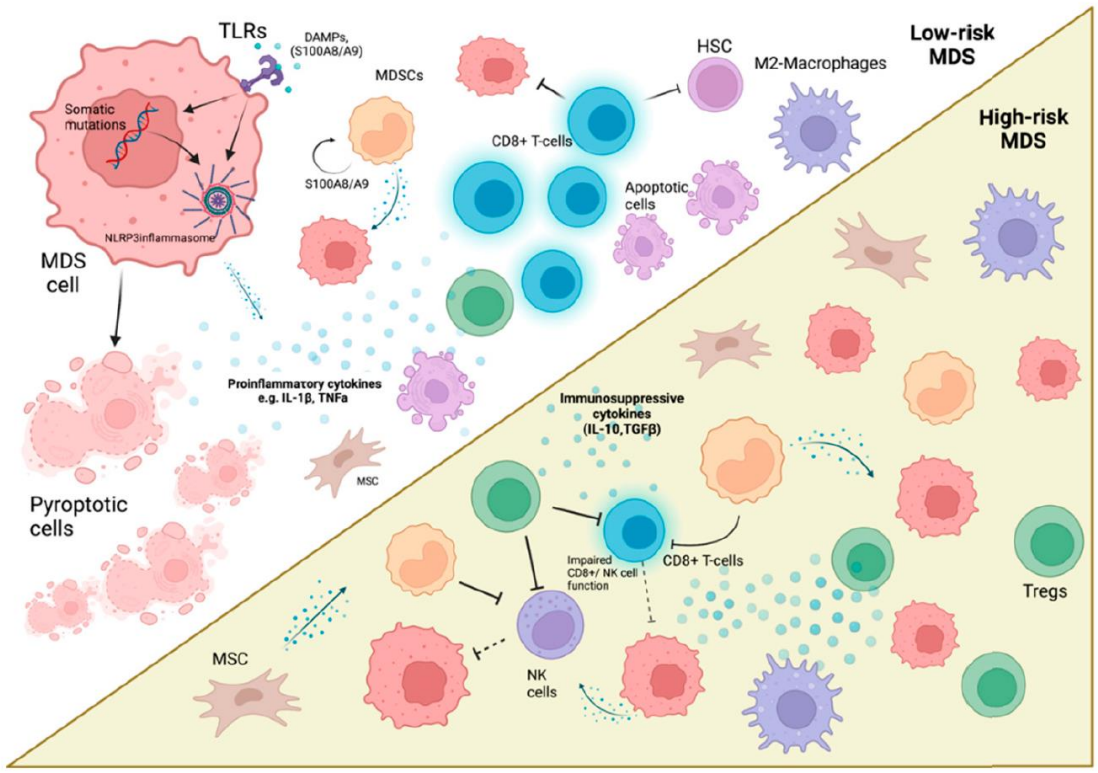

Figure 22

The different immune landscape in LR-MDS vs HR-MDS. Figure from Barakos and Hatzimichael, 2022.

1.4.3 Effects of hypomethylating agents on immune cells and possible combinations with immunotherapies

As previously mentioned, in addition to their direct effects on the malignant clone, HMAs also demonstrated effects on cells of the bone marrow niche, including the ones belonging to immune system (Lindblad et al., 2017), and both the clinical benefits/anti-tumor response and treatment failures/resistance may be the result of the combination of such direct and indirect actions.

A study compared the frequency of the major immune components (CD4 T cells, CD8 T cells, Tregs, NK cells, NKT cells, B cells, dendritic cells, monocytes and MDSCs) in 14 AML patients before and after treatment with decitabine, finding that DEC did not significantly affect the frequency of such immune cell populations. However, both CD4 and CD8 T cells showed an increase in CD38 expression, which was negatively correlated with IFNγ production and positively correlated with the up-regulation of co-inhibitory molecules (PD-1, TIGIT,

LAG3) by CD8+ T cells, indicating a decreased T cell function (Zhao C et al., 2020). Moreover, the high expression of CD38 on both CD8 and CD4 T cells was strongly associated with failure of response to decitabine treatment and poor clinical outcome. A previous study in a chronically infected WT and DNMT3A KO murine model reported a reversion of exhausted T cell phenotype and CD8+ T cell rejuvenation after exposure to decitabine combined with anti-PD1 (Ghoneim et al., 2017). The expression of PD-1 and its ligands is epigenetically regulated (Bally et al., 2016), and patients with MDS or AML treated with HMAs showed hypomethylation in the PD-1 locus and increased expression of PD-1, CTL-A4 and PD-L1/2 on T cells and CD34+ stem cells, respectively (Ørskov et al., 2015; Yang H et al., 2014).

Signal transducer and activator of transcription (STAT) signaling plays a critical role in immune system and controls the epigenetic tuning of CD4 T-cell differentiation and polarization (Seif et al., 2017). One recent study characterized the CD4+ T cells compartment from 73 HR-MDS patients undergoing AZA therapy by using functional proteomic and transcriptomic, finding that responding patients downregulated the pro-inflammatory IL-6/STAT3 axis and the downregulation of IL-6 mediated STAT3 phosphorylation was associated with better disease outcome (Lamprianidou et al., 2021). The aberrant IL-6/STAT signaling in T cells is known to exert effects on antitumor immunity by different mechanisms such as expansion of Tregs and suppression of Th1 responses (Johnson et al., 2018; Tsukamoto et al., 2018). The paper further observed a significant increase of both PD1+CD4+ and PD1+CD8+ T cells in patients upregulating IL-6/STAT3 after 6 cycles of AZA.

Several independent studies described an increase of Tregs frequency upon AZA treatment in murine models of transplantation (Choi et al., 2010; Cooper et al., 2017; Sánchez-Abarca et al., 2010) and in 27 AML patients after allogeneic stem cell transplantation (Goodyear et al., 2012). The induction of Tregs was explained as a consequence of FOXP3 promoter demethylation (Choi et al., 2010; Sánchez-Abarca et al., 2010). All papers underlined the effect of azacytidine on effector T lymphocytes activity and Tregs expansion, illustrating its role in the allogeneic transplantation setting as an immunomodulatory drug and describing a new way to prevent graft-versus-host disease while maintaining the graft-versus-leukemia effect. In non-transplantation setting, Tregs numbers was shown to correlate with HMA response in high-risk MDS patients, where those who responded to hypomethylating treatment with azacitidine were found to have fewer regulatory T-cells in circulation at long-term follow-up than before treatment and appeared more similar to healthy donors in regulatory T-cell frequency (Costantini et al., 2013). Moreover, the absolute numbers of T-helper 1 and T-helper 2, but not T-helper 17, cells were observed to be significantly reduced following 12 months of treatment. Conversely, in a separate cohort of MDS and AML patients the effect of AZA appeared to transiently increase FOXP3+ regulatory T-cells and decrease the Th17 population in both *in vivo* treatment and *in vitro* experiments (Bontkes et al., 2012). Another study observed an impaired T-cell mediated antileukemic activity *in vitro* against leukemic target cells after AZA administration, confirming the results in patients treated with AZA after allo-HSCT, reporting an increased Tregs frequency and a reduction of both effector CD8+ T cells and pro-inflammatory Th1 cells (Stübig et al., 2014).

Treatment with hypomethylating agents showed also good effects on T cells: for example, a study on MDS demonstrated that AZA increased the T cell repertoire (measured as T-cell receptor (TCR) variability) in MDS and AML patients, counteracting immune derangement and TCR skewing (Fozza et al., 2015). A similar result was observed in a clinical trial protocol on four patients with solid tumors treated with decitabine who showed increased TCR diversity in comparison to pre-treatment levels (Nie et al., 2016). Another study observed an enhanced T-cell mediated tumor cell recognition thanks to the upregulation of cancer-testis antigens after AZA treatment on a cohort of MDS, AML and CMML patients (Gang et al., 2014).

In breast cancer cell lines, administration of guadecitabine (a novel experimental hypomethylating drug) upregulated MHC-I in tumor cells promoting recruitment of CD8+ T cells. Moreover, MHC-I genes were found upregulated also in breast cancer patients treated with hypomethylating agents (Luo et al., 2018). This

mechanism of action should be investigated also in hematological malignancies. One in vitro study tested the expression of HLA class I molecules upon treatment with azacytidine or decitabine on several tumor cell lines, among which the leukemic cell line NALM-6, and found a stronger up-regulation of such molecules with decitabine compared to azacytidine (Fazio et al., 2018).

DNA methylation not only affects development, differentiation and activity of T cells: also NK cell maturation and functionality is deeply affected by the DNA methylation status of genes coding for cytokine secretion, surface markers and several receptors with activator or inhibitory function (Cichocki et al., 2013). Various groups have investigated the effects of HMA on the number and function of natural killer (NK) cells in both *in vivo* and *in vitro*. Two *in vitro* studies showed impaired function of NK cells against leukemic cell lines after AZA treatment as a consequence of overexpression of inhibitory receptors, impaired granzyme and perforin release, reduced cytokine mRNA synthesis and enhanced NK-cell apoptosis (Gao et al., 2009; Schmiedel et al., 2011). However, an *in vivo* study on 17 patients with high-risk MDS or AML treated with AZA did not observe any significant changes in both NK cells frequency and functionality, but only a decreasing tendency in a subpopulation of NK cells expressing the inhibitory receptor CD158b. Interestingly, in the same study, when NK cells were subjected to 5-Azacytidine treatment *in vitro*, it was observed a remarkable decrease in killing capacity of NK cells in a dose-dependent manner (Gang et al., 2014). Since this inhibitory effect was clearly evident only *in vitro* despite the concentration was mimicking the peak plasma concentration *in vivo*, the authors suggested that NK cells may be less vulnerable *in vivo*, or the plasma concentration is not sufficiently high during extended periods of time to confer this effect *in vivo*. An additional study investigated the influence of AZA *in vitro* and in patients with high-risk MDS and observed a significant increase in expression of multiple KIRs (inhibitory receptors), but only in cells that had undergone several rounds of cell division (Ki67+); however, in contrast to other studies, these proliferating 5-aza exposed NK cells exhibited increased IFN-γ production and degranulation towards tumor target cells (Sohlberg et al., 2015).

Not only azacytidine effects were evaluated, but also decitabine was investigated. One study exposed NK cells to increasing doses of decitabine and observed an upregulation of KIRs and the activating receptor NKp44, accompanied with decrease of viability, proliferation, and lower expression of the activating receptor NKG2D. Since decitabine affected the expression of activating and inhibitory receptors in NK cells at low concentrations while high doses decreased NK cell proliferation and viability, this study highlighted a biphasic effect of decitabine treatment on overall NK cell lytic function, which was correlated with a biphasic pattern of global hypomethylation (the percentage of methylation decreased linearly until 0.3uM concentrations, then began to rise with increasing doses of decitabine), suggesting that optimal immunomodulation with decitabine occurs at low dose ranges and that high doses abrogate this effect through inhibition of proliferation and direct toxicity to NK cells (Kopp et al., 2013). Finally, one paper compared the effects of azacytidine and decitabine finding opposite effects of the two drugs on NK cells: NK cytotoxicity and IFN-γ production were observed to be significantly impaired by azacytidine but enhanced by decitabine (Schmiedel et al., 2011). One *in vitro* study further reported a synergized effect between decitabine and anti-CD33 antibody against AML blasts through the increased NKG2D ligand (NKG2DL) expression, augmented NK degranulation and NK-mediated antibody-dependent cellular cytotoxicity (ADCC) (Vasu et al., 2016).

It is therefore clear that there is no consensus on the effects of hypomethylating agents on NK cell functionality: this is likely due to different *in vitro* and *ex vivo* conditions, variable concentrations of administered HMAs, lack of consistency in functional assays across groups, as well as the different sources of NK cells used in each study.

Compared to lymphoid cells, the impact of hypomethylating agents on the myeloid cells compartment is still poorly investigated. A genome-wide base-resolution mapping study of 5-methylcytosine in purified monocytes and in monocyte-derived immature and mature DCs showed that dendritic cell development and maturation were associated with a great loss of DNA methylation across many regions, most of them were

enhancers and binding sites for known transcription factors affiliated with DC lineage specification and response to immune stimuli; and this loss could be attributed to the noted down-regulation of the three DNA methyltransferases DNMT1, DNMT3A, and DNMT3B (Zhang X et al., 2014). An *in vitro* study on PBMC-derived DCs found that the treatment with AZA upregulated CD40 and CD86 expression on mature DCs, whereas cytokine secretion of IL-6, IL-12p70, IL-23 and TNFα was comparable to control untreated DCs except for IL-10 and IL-27, that were less released by treated DCs (Frikeche et al., 2011). CD40 expression on DCs is acquired during their maturation process, and its binding with CD40L on antigen-specific CD4+ Th1 cells license dendritic cells to promote antitumor T cell activation. CD86 is a co-stimulatory ligand on DCs that mediates polarization of T-cells upon interaction with MHC II-peptide complexes on DCs: this interaction is necessary for a complete activation of T cells, without which T-cells would become anergic rather than activated. The same study further investigated the peripheral blood of 8 AML and 6 high-risk MDS patients before and after AZA treatment, reporting a significant decrease of IL-4 secreting CD4+ T cells and increase of 17 and IL-21 ones, indicative of a Th17 response and suggesting that azacytidine affects T cell polarization through DCs. A recent study in a murine graft-versus-leukemia model demonstrated that decitabine can prime allogeneic immune reactions of donor lymphocytes by activating DCs and increased IFNγ and CD28 levels, and that the GvL effects can be promoted without causing severe GvHD through an optimal timing of lymphocyte administration on the basis of IFN-γ expression levels (Kwon et al., 2020). In contrast, MDSCs have been shown to be reduced upon decitabine treatment in leukemia-bearing mice, allowing the activation of the adaptive T cell immune response (Zhou J et al., 2017). Same results about decitabine negative effect on MDSCs were reported in mouse models of myeloma, melanoma, colon and breast cancer (Kim et al., 2014; Triozzi et al., 2012; Zhou J et al., 2019).

To summarize, hypomethylating agents have been shown to exert a profound effect on both innate and adaptive branches of immune system:

- NK cells respond to HMA treatment by modulating the expression of inhibitory and activating receptors on the cell surface, in particular increased expression of inhibitory KIR proteins and decreased expression of the activating receptor NKG2D, but the functional effects on cytotoxicity have not been firmly established.
- Within T cell subsets, methylation is critical to regulate expression of the immune checkpoint inhibitors PD-1 and CTLA4, co-stimulatory molecules including CD28 and CD80, and the developmental pathway that favor Tregs differentiation through FOXP3 promoter demethylation at the expense of pro-inflammatory Th1, that are instead reduced.
- Dendritic cells respond to hypomethylating agents by increasing the expression of CD40 and CD86 co-stimulatory molecules on the cell surface, allowing T cell priming and activation.
- MDSCs frequency decreases due to a direct pro-apoptotic effect.
- Direct effects of hypomethylating agents also include increased expression of tumor-associated antigens and MHC-I molecules on tumor cells, leading to increased tumor antigen presentation and activation/expansion of tumor-specific T cells.

Given the wide immunomodulatory properties of hypomethylating agents, there is eager interest in combining HMAs with immunotherapies to provide synergic immune-mediated anti-tumor effects (Wong et al., 2021). For example, the HMA-induced upregulation of tumor-associated antigens such as NY-ESO-1 can enhance anti-cancer vaccine immunogenicity in MDS patients through the induction of antigen-specific T lymphocytes (Griffiths et al., 2018). Infusion of autologous DC- based cellular vaccine for AML have been shown to have enhanced immunogenicity in combination with HMAs, augmenting both antigen processing and presentation (Nahas et al., 2019). Also adoptive NK cell transfer seems to be promising in hematologic malignancies: in a recent phase I study, haploidentical NK cell infusion and IL-2 administration after decitabine treatment in R/R AML patients demonstrated higher NK cell cytotoxicity; the cytotoxic activity of NK cells was further increased by administration of CD33 mAb (Mani et al., 2020). Priming of patients with

AZA before donor-lymphocyte infusion (DLI) showed improved remission rates in MDS and AML patients that relapsed after transplantation, including patients with previous azacytidine failure and with high leukemic burden (Lübbert et al., 2010; Schroeder et al., 2013; Sommer et al., 2018). The increased expression of PD-1, PD-L1/2, CTLA-4 and TIGIT after HMA therapy gives the rationale basis to combine HMA treatment with immune checkpoint blockade (ICB) therapy (anti-PD-1/L1 or -CTLA-4 antibodies). An early phase clinical trial (NCT03358719) investigating the combination of decitabine with the NY-ESO-1 vaccine and nivolumab (anti-PD-1 mAb) in AML and MDS patients has concluded, but the results are still not available.

Since CD123 expression is typically very low or absent in normal hematopoietic cells but broadly expressed in MDS and AML at various intensities (Aldoss et al., 2020; Yue LZ et al., 2010; Zhang W et al., 2015), it represents a good target in immunotherapy and different anti-CD123 monoclonal and bispecific antibodies have been developed and tested (Talacotuzumab, Flotetuzumab, Videcotamab) (Isidori et al., 2021). Tagraxofusp is an engineered fusion protein comprising of IL-3 (CD123 ligand) fused with the diphtheria toxin (DT): in this way, the fusion protein triggers cellular cytotoxicity by delivering DT to CD123+ tumor cells. A phase I/II trial assessed tagraxofusp monotherapy in AML patients in first remission but with high risk of relapse showing good safety profile and reduction of minimal residual disease (Lane et al., 2016). However, resistance or relapse after clinical response have been observed in trials on other types of cancer. Phase I study of tagraxofusp in combination with azacytidine R/R AML and high-risk MDS patients is currently ongoing to determine the MTD and response rates (NCT03113643); the estimated Primary Completion Date is on May 2024 whereas the estimated Study Completion Date is set for May 2026. Recently, a paper proposed CD123 as a target for chimeric antigen receptor (CAR) T-cell therapy in high-risk MDS patients and demonstrated that, with the use of lentiviral vectors, the CAR can be expressed on both healthy donor and MDS patient-derived T lymphocytes with high efficiency, leading to the successful elimination of MDS stem cells both *in vitro* and in patient-derived xenografts (Stevens et al., 2019). An experimental study demonstrated that decitabine significantly enhanced anti-AML effects of CD123 CAR-T cells *in vitro* (THP1 cells) and *in vivo* (NSG mice bearing THP1 tumor xenografts) through epigenetic reprograming of the CAR-T cells. In particular, the inhibition of DNMT3A and DNMT1 expression and the increased DNA hypomethylation caused the upregulation of genes that favored naïve and memory T cells differentiation, resulting in enhanced CD123 CAR-T cells anti-leukemia responses (You et al., 2020).

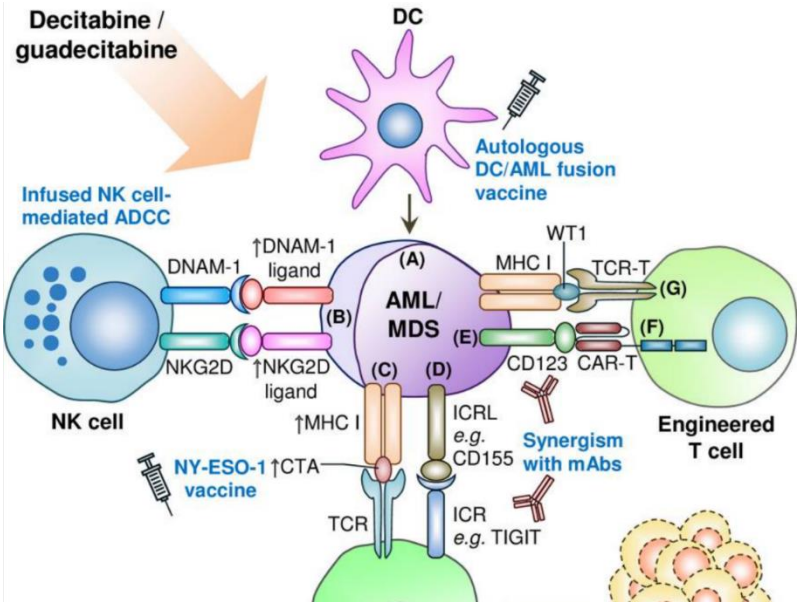

Figure 23

Combination strategies of HMA treatment and immunotherapies for a synergic and improved anti-tumor effect. Figure from Wong et al., 2021.

To conclude, for patients with high-risk MDS or AML with relapsed/refractory disease, or who are unable to undergo hematopoietic stem cell transplantation, or are unsuitable for intensive chemotherapy, there is a pressing clinical need to develop novel, effective therapies. As described above, hypomethylating agents have shown both *in vitro* and *in vivo* effects not only on malignant cells, but also on NK cells, T cells, DCs and MDSCs, and such immunomodulatory properties has prompted interest in these therapies and in combining them with current immunotherapies. However, much work is still needed to fully uncover the impact of HMAs on immune cells and tumor microenvironment: only by elucidating the functional consequences of hypomethylating therapies it will be possible to identify patients who will likely benefit from it and to identify new combination treatments for an improved anti-tumor effect.

Chapter 2

Aim of the thesis

Myelodysplastic Syndromes (MDS) are a group of blood diseases primarily affecting elderly people that are characterized by bone marrow dysplasia, peripheral cytopenia associated to ineffective hematopoiesis, recurrent cytogenetic abnormalities and/or genomic mutations and malignant clonal expansion, which can transform to acute myeloid leukemia (AML).

MDS clinical outcomes can vary greatly even between patients classified in the same disease subtype, highlighting that MDS possess marked heterogeneity regarding prognosis and the risk of disease progression. To overcome this heterogeneity, the Revised International Prognostic Scoring System (IPSS-R) and, more recently, the Molecular International Prognostic Scoring System (IPSS-M) were introduced to provide prognostic assessment for overall survival (OS) and risk of progression to AML (Bernard et al., 2022; Greenberg P et al., 2012).

Since MDS are diseases of hematopoietic stem cells, allogeneic hematopoietic stem cell transplantation (allo-HSCT) represents the unique resolutive treatment for patients with high risk of AML evolution; however, only a small part of them can afford it due to the old age and high treatment-related morbidity and mortality (Li et al., 2022). Thus, the medical treatment of higher-risk MDS patients ineligible for transplantation is actually dominated by monotherapy with hypomethylating agents azacytidine (AZA) or decitabine (DAC). Unfortunately, about half of the patients do not have a hematological response (Fenaux et al., 2009) and the survival benefits are in the order of few months since the treatment does not eliminate the founder clone which continue to drive clonal hematopoiesis and leads to disease relapse in around 40% of patients (Nannya et al., 2023; Prébet et al., 2011; Schnegg-Kaufmann et al., 2023; Unnikrishnan et al., 2017).

Despite IPSS-M, compared to IPSS-R, showed increased capacity of patient stratification and superior prognostic power thanks to the integration of genomic mutations information for risk score calculation, it still fails to reliably predict treatment response, especially to HMAs (Blum et al., 2016; Sauta et al., 2022; Zeidan et al., 2016).

It is well established that immune dysregulation plays a major role in MDS pathogenesis and progression (Barakos and Hatzimichael, 2022; Sallman et al., 2019). In particular, earlier phases of the disease are associated with excessive inflammation and activation of the innate immune system that leads to massive apoptosis of stem/progenitor cells within bone marrow and autoimmune manifestations (Barreyro et al., 2018), while advanced stages are characterized by immune suppression and impaired response of both innate and adaptive branches of immunity, that favor tumor outgrowth (Barakos et al., 2022). Despite all the studies linking immune cell functions to MDS pathogenesis, severity and progression, information about the immune status (the so-called “immunome”) of the patients are currently omitted from MDS classification and risk stratification since there is still no widely accepted method for evaluating the patient’s immune composition, and heterogeneity in immune status evaluation often leads to controversial results. Moreover, even if it is known that hypomethylating agents exert an important immunomodulatory effect (Lindblad et al., 2017), there are not standard ways for monitoring the immune response in treated MDS patients, and more in general it does not exist any prognostic marker for predicting the response to HMA therapy.

The aim of my PhD project was to perform a multi-omic analysis to characterize the immune features of a large cohort of MDS patients, taking advantage of high-dimensional flow cytometry integrated with RNA sequencing, DNA mutations and clinical information, in order to investigate the immune pathways that are dysregulated during MDS progression and upon treatment with HMAs.

We believe that the addition of comprehensive immunologic data to prognostic models could, similar to mutational data for IPSS-M, further help to refine risk stratification across lower- and higher-risk MDS and improve patient’s classification. Moreover, immune signatures could help monitoring and predicting the response to HMA treatment, as well as identifying immune evasion mechanisms that could be targeted with more specific therapies.

References for Chapters 1 and 2

1. Abdelhakim H, Dunavin N, Li M, Braun M, Elkhanany A, Lin TL, Godwin AK. LAG3 Promotes Acute Myeloid Leukemia-Induced Immune Suppression. Blood 2018; 132 (Supplement 1): 2414. doi: https://doi.org/10.1182/blood-2018-99-117784
2. Aguirre LE, Al Ali N, Sallman DA, Ball S, Jain AG, Chan O, Tinsley-Vance SM, Kuykendall A, Sweet K, Lancet JE, Padron E, Komrokji RS. Assessment and validation of the molecular international prognostic scoring system for myelodysplastic syndromes. Leukemia. 2023 May 5. doi: 10.1038/s41375-023-01910-3. Epub ahead of print. PMID: 37147425.
3. Al-Hussaini M, Rettig MP, Ritchey JK, Karpova D, Uy GL, Eissenberg LG, Gao F, Eades WC, Bonvini E, Chichili GR, Moore PA, Johnson S, Collins L, DiPersio JF. Targeting CD123 in acute myeloid leukemia using a T-cell-directed dual-affinity retargeting platform. Blood. 2016 Jan 7;127(1):122-31. doi: 10.1182/blood-2014-05-575704. Epub 2015 Nov 3. PMID: 26531164; PMCID: PMC4705603.
4. Al-Matary YS, Botezatu L, Opalka B, Hönes JM, Lams RF, Thivakaran A, Schütte J, Köster R, Lennartz K, Schroeder T, Haas R, Dührsen U, Khandanpour C. Acute myeloid leukemia cells polarize macrophages towards a leukemia supporting state in a Growth factor independence 1 dependent manner. Haematologica. 2016 Oct;101(10):1216-1227. doi: 10.3324/haematol.2016.143180. Epub 2016 Jul 7. PMID: 27390361; PMCID: PMC5046651.
5. Aldoss I, Clark M, Song JY, Pullarkat V. Targeting the alpha subunit of IL-3 receptor (CD123) in patients with acute leukemia. Hum Vaccin Immunother. 2020 Oct 2;16(10):2341-2348. doi: 10.1080/21645515.2020.1788299. Epub 2020 Jul 21. PMID: 32692611; PMCID: PMC7644204.
6. Allampallam K, Shetty V, Mundle S, Dutt D, Kravitz H, Reddy PL, Alvi S, Galili N, Saberwal GS, Anthwal S, Shaikh MW, York A, Raza A. Biological significance of proliferation, apoptosis, cytokines, and monocyte/macrophage cells in bone marrow biopsies of 145 patients with myelodysplastic syndrome. Int J Hematol. 2002 Apr;75(3):289-97. doi: 10.1007/BF02982044. PMID: 11999358.
7. Almstedt M, Blagitko-Dorfs N, Duque-Afonso J, Karbach J, Pfeifer D, Jäger E, Lübbert M. The DNA demethylating agent 5-aza-2'-deoxycytidine induces expression of NY-ESO-1 and other cancer/testis antigens in myeloid leukemia cells. Leuk Res. 2010 Jul;34(7):899-905. doi: 10.1016/j.leukres.2010.02.004. Epub 2010 Apr 10. PMID: 20381863.
8. Agarwal P, Isringhausen S, Li H, Paterson AJ, He J, Gomariz Á, Nagasawa T, Nombela-Arrieta C, Bhatia R. Mesenchymal Niche-Specific Expression of Cxcl12 Controls Quiescence of Treatment-Resistant Leukemia Stem Cells. Cell Stem Cell. 2019 May 2;24(5):769-784.e6. doi: 10.1016/j.stem.2019.02.018. Epub 2019 Mar 21. Erratum in: Cell Stem Cell. 2020 Jan 2;26(1):123. PMID: 30905620; PMCID: PMC6499704.
9. Aggarwal N, Swerdlow SH, TenEyck SP, Boyiadzis M, Felgar RE. Natural killer cell (NK) subsets and NK-like T-cell populations in acute myeloid leukemias and myelodysplastic syndromes. Cytometry B Clin Cytom. 2016 Jul;90(4):349-57. doi: 10.1002/cyto.b.21349. Epub 2016 Feb 3. PMID: 26648320.
10. Angelucci E, Li J, Greenberg P, Wu D, Hou M, Montano Figueroa EH, Rodriguez MG, Dong X, Ghosh J, Izquierdo M, Garcia-Manero G; TELESTO Study Investigators. Iron Chelation in Transfusion-Dependent Patients With Low- to Intermediate-1-Risk Myelodysplastic Syndromes: A Randomized Trial. Ann Intern Med. 2020 Apr 21;172(8):513-522. doi: 10.7326/M19-0916. Epub 2020 Mar 24. PMID: 32203980.
11. Arber DA, Orazi A, Hasserjian R, et al. The 2016 revision to the World Health Organization classification of myeloid neoplasms and acute leukemia. Blood. 2016;127(20):2391-2405. Blood. 2016 Jul 21;128(3):462-463. doi: 10.1182/blood-2016-06-721662. PMID: 31659364.
12. Arber DA, Orazi A, Hasserjian RP, Borowitz MJ, Calvo KR, Kvasnicka HM, Wang SA, Bagg A, Barbui T, Branford S, Bueso-Ramos CE, Cortes JE, Dal Cin P, DiNardo CD, Dombret H, Duncavage EJ, Ebert BL, Estey EH, Facchetti F, Foucar K, Gangat N, Gianelli U, Godley LA, Gökbuget N, Gotlib J, Hellström-Lindberg E, Hobbs GS, Hoffman R, Jabbour EJ, Kiladjian JJ, Larson RA, Le Beau MM, Loh ML,

Löwenberg B, Macintyre E, Malcovati L, Mullighan CG, Niemeyer C, Odenike OM, Ogawa S, Orfao A, Papaemmanuil E, Passamonti F, Porkka K, Pui CH, Radich JP, Reiter A, Rozman M, Rudelius M, Savona MR, Schiffer CA, Schmitt-Graeff A, Shimamura A, Sierra J, Stock WA, Stone RM, Tallman MS, Thiele J, Tien HF, Tzankov A, Vannucchi AM, Vyas P, Wei AH, Weinberg OK, Wierzbowska A, Cazzola M, Döhner H, Tefferi A. International Consensus Classification of Myeloid Neoplasms and Acute Leukemias: integrating morphologic, clinical, and genomic data. Blood. 2022 Sep 15;140(11):1200-1228. doi: 10.1182/blood.2022015850. PMID: 35767897; PMCID: PMC9479031.

13. Arends CM, Galan-Sousa J, Hoyer K, Chan W, Jäger M, Yoshida K, Seemann R, Noerenberg D, Waldhueter N, Fleischer-Notter H, Christen F, Schmitt CA, Dörken B, Pelzer U, Sinn M, Zemojtel T, Ogawa S, Märdian S, Schreiber A, Kunitz A, Krüger U, Bullinger L, Mylonas E, Frick M, Damm F. Hematopoietic lineage distribution and evolutionary dynamics of clonal hematopoiesis. Leukemia. 2018 Sep;32(9):1908-1919. doi: 10.1038/s41375-018-0047-7. Epub 2018 Mar 1. PMID: 29491455.
14. Atanackovic D, Luetkens T, Kloth B, Fuchs G, Cao Y, Hildebrandt Y, Meyer S, Bartels K, Reinhard H, Lajmi N, Hegewisch-Becker S, Schilling G, Platzbecker U, Kobbe G, Schroeder T, Bokemeyer C, Kröger N. Cancer-testis antigen expression and its epigenetic modulation in acute myeloid leukemia. Am J Hematol. 2011 Nov;86(11):918-22. doi: 10.1002/ajh.22141. Epub 2011 Sep 2. PMID: 21898529.
15. Avagyan S, Henninger JE, Mannherz WP, Mistry M, Yoon J, Yang S, Weber MC, Moore JL, Zon LI. Resistance to inflammation underlies enhanced fitness in clonal hematopoiesis. Science. 2021 Nov 5;374(6568):768-772. doi: 10.1126/science.aba9304. Epub 2021 Nov 4. PMID: 34735227.
16. Avagyan S, Zon LI. Clonal hematopoiesis and inflammation - the perpetual cycle. Trends Cell Biol. 2023 Aug;33(8):695-707. doi: 10.1016/j.tcb.2022.12.001. Epub 2022 Dec 31. PMID: 36593155; PMCID: PMC10310890.
17. Azizi A, Ediriwickrema A, Dutta R, Patel SA, Shomali W, Medeiros B, Iberri D, Gotlib J, Mannis G, Greenberg P, Majeti R, Zhang T. Venetoclax and hypomethylating agent therapy in high risk myelodysplastic syndromes: a retrospective evaluation of a real-world experience. Leuk Lymphoma. 2020 Nov;61(11):2700-2707. doi: 10.1080/10428194.2020.1775214. Epub 2020 Jun 16. PMID: 32543932.
18. Baer C, Huber S, Hutter S, Meggendorfer M, Nadarajah N, Walter W, Platzbecker U, Götze KS, Kern W, Haferlach T, Hoermann G, Haferlach C. Risk prediction in MDS: independent validation of the IPSS-M-ready for routine? Leukemia. 2023 Apr;37(4):938-941. doi: 10.1038/s41375-023-01831-1. Epub 2023 Feb 1. PMID: 36725896; PMCID: PMC10079546.
19. Ball BJ, Famulare CA, Stein EM, Tallman MS, Derkach A, Roshal M, Gill SI, Manning BM, Koprivnikar J, McCloskey J, Testi R, Prebet T, Al Ali NH, Padron E, Sallman DA, Komrokji RS, Goldberg AD. Venetoclax and hypomethylating agents (HMAs) induce high response rates in MDS, including patients after HMA therapy failure. Blood Adv. 2020 Jul 14;4(13):2866-2870. doi: 10.1182/bloodadvances.2020001482. PMID: 32589727; PMCID: PMC7362378.
20. Bally AP, Austin JW, Boss JM. Genetic and Epigenetic Regulation of PD-1 Expression. J Immunol. 2016 Mar 15;196(6):2431-7. doi: 10.4049/jimmunol.1502643. PMID: 26945088; PMCID: PMC4780223.
21. Barakos GP, Hatzimichael E. Microenvironmental Features Driving Immune Evasion in Myelodysplastic Syndromes and Acute Myeloid Leukemia. Diseases. 2022 Jun 10;10(2):33. doi: 10.3390/diseases10020033. PMID: 35735633; PMCID: PMC9221594.
22. Barreyro L, Chlon TM, Starczynowski DT. Chronic immune response dysregulation in MDS pathogenesis. Blood. 2018 Oct 11;132(15):1553-1560. doi: 10.1182/blood-2018-03-784116. Epub 2018 Aug 13. PMID: 30104218; PMCID: PMC6182269.
23. Basiorka AA, McGraw KL, Eksioglu EA, Chen X, Johnson J, Zhang L, Zhang Q, Irvine BA, Cluzeau T, Sallman DA, Padron E, Komrokji R, Sokol L, Coll RC, Robertson AA, Cooper MA, Cleveland JL, O'Neill LA, Wei S, List AF. The NLRP3 inflammasome functions as a driver of the myelodysplastic syndrome

phenotype. Blood. 2016 Dec 22;128(25):2960-2975. doi: 10.1182/blood-2016-07-730556. Epub 2016 Oct 13. PMID: 27737891; PMCID: PMC5179338.

24. Bazinet A, Darbaniyan F, Jabbour E, Montalban-Bravo G, Ohanian M, Chien K, Kadia T, Takahashi K, Masarova L, Short N, Alvarado Y, Yilmaz M, Ravandi F, Andreeff M, Kanagal-Shamanna R, Ganan-Gomez I, Colla S, Qiao W, Huang X, McCue D, Mirabella B, Kantarjian H, Garcia-Manero G. Azacitidine plus venetoclax in patients with high-risk myelodysplastic syndromes or chronic myelomonocytic leukaemia: phase 1 results of a single-centre, dose-escalation, dose-expansion, phase 1-2 study. Lancet Haematol. 2022 Oct;9(10):e756-e765. doi: 10.1016/S2352-3026(22)00216-2. Epub 2022 Sep 2. PMID: 36063832.
25. Beerman I, Bhattacharya D, Zandi S, Sigvardsson M, Weissman IL, Bryder D, Rossi DJ. Functionally distinct hematopoietic stem cells modulate hematopoietic lineage potential during aging by a mechanism of clonal expansion. Proc Natl Acad Sci U S A. 2010 Mar 23;107(12):5465-70. doi: 10.1073/pnas.1000834107. Epub 2010 Mar 18. PMID: 20304793; PMCID: PMC2851806.
26. Bejar R, Lord A, Stevenson K, Bar-Natan M, Pérez-Ladaga A, Zaneveld J, Wang H, Caughey B, Stojanov P, Getz G, Garcia-Manero G, Kantarjian H, Chen R, Stone RM, Neuberg D, Steensma DP, Ebert BL. TET2 mutations predict response to hypomethylating agents in myelodysplastic syndrome patients. Blood. 2014 Oct 23;124(17):2705-12. doi: 10.1182/blood-2014-06-582809. Epub 2014 Sep 15. PMID: 25224413; PMCID: PMC4208285.
27. Bejar R, Stevenson KE, Caughey B, Lindsley RC, Mar BG, Stojanov P, Getz G, Steensma DP, Ritz J, Soiffer R, Antin JH, Alyea E, Armand P, Ho V, Koreth J, Neuberg D, Cutler CS, Ebert BL. Somatic mutations predict poor outcome in patients with myelodysplastic syndrome after hematopoietic stem-cell transplantation. J Clin Oncol. 2014 Sep 1;32(25):2691-8. doi: 10.1200/JCO.2013.52.3381. Epub 2014 Aug 4. PMID: 25092778; PMCID: PMC4207878.
28. Beldi-Ferchiou A, Caillat-Zucman S. Control of NK Cell Activation by Immune Checkpoint Molecules. Int J Mol Sci. 2017 Oct 12;18(10):2129. doi: 10.3390/ijms18102129. PMID: 29023417; PMCID: PMC5666811.
29. Belickova M, Vesela J, Jonasova A, Pejsova B, Votavova H, Merkerova MD, Zemanova Z, Brezinova J, Mikulenkova D, Lauermannova M, Valka J, Michalova K, Neuwirtova R, Cermak J. TP53 mutation variant allele frequency is a potential predictor for clinical outcome of patients with lower-risk myelodysplastic syndromes. Oncotarget. 2016 Jun 14;7(24):36266-36279. doi: 10.18632/oncotarget.9200. PMID: 27167113; PMCID: PMC5094999.
30. Belkacémi Y, Labopin M, Hennequin C, Hoffstetter S, Mungai R, Wygoda M, Lundell M, Finke J, Aktinson C, Lorchel F, Durdux C, Basara N. Reduced-intensity conditioning regimen using low-dose total body irradiation before allogeneic transplant for hematologic malignancies: Experience from the European Group for Blood and Marrow Transplantation. Int J Radiat Oncol Biol Phys. 2007 Feb 1;67(2):544-51. doi: 10.1016/j.ijrobp.2006.08.049. Epub 2006 Dec 4. PMID: 17141976.
31. Bernard E, Nannya Y, Hasserjian RP, Devlin SM, Tuechler H, Medina-Martinez JS, Yoshizato T, Shiozawa Y, Saiki R, Malcovati L, Levine MF, Arango JE, Zhou Y, Solé F, Cargo CA, Haase D, Creignou M, Germing U, Zhang Y, Gundem G, Sarian A, van de Loosdrecht AA, Jädersten M, Tobiasson M, Kosmider O, Follo MY, Thol F, Pinheiro RF, Santini V, Kotsianidis I, Boultwood J, Santos FPS, Schanz J, Kasahara S, Ishikawa T, Tsurumi H, Takaori-Kondo A, Kiguchi T, Polprasert C, Bennett JM, Klimek VM, Savona MR, Belickova M, Ganster C, Palomo L, Sanz G, Ades L, Della Porta MG, Elias HK, Smith AG, Werner Y, Patel M, Viale A, Vanness K, Neuberg DS, Stevenson KE, Menghrajani K, Bolton KL, Fenaux P, Pellagatti A, Platzbecker U, Heuser M, Valent P, Chiba S, Miyazaki Y, Finelli C, Voso MT, Shih LY, Fontenay M, Jansen JH, Cervera J, Atsuta Y, Gattermann N, Ebert BL, Bejar R, Greenberg PL, Cazzola M, Hellström-Lindberg E, Ogawa S, Papaemmanuil E. Implications of TP53 allelic state for genome stability, clinical presentation and outcomes in myelodysplastic syndromes. Nat Med. 2020 Oct;26(10):1549-1556. doi: 10.1038/s41591-020-1008-z. Epub 2020 Aug 3. Erratum in: Nat Med.

2021 Mar;27(3):562. Erratum in: Nat Med. 2021 May;27(5):927. PMID: 32747829; PMCID: PMC8381722.
32. Bernard E, Tuechler H, Greenberg PL, et al: Molecular international prognostic scoring system for myelodysplastic syndromes. NEJM Evid 1:2022, DOI: 10.1056/EVIDoa2200008
33. Bergsbaken T, Fink SL, Cookson BT. Pyroptosis: host cell death and inflammation. Nat Rev Microbiol. 2009 Feb;7(2):99-109. doi: 10.1038/nrmicro2070. PMID: 19148178; PMCID: PMC2910423.
34. Bertheloot D, Latz E, Franklin BS. Necroptosis, pyroptosis and apoptosis: an intricate game of cell death. Cell Mol Immunol. 2021 May;18(5):1106-1121. doi: 10.1038/s41423-020-00630-3. Epub 2021 Mar 30. PMID: 33785842; PMCID: PMC8008022.
35. Bewersdorf JP, Hasle V, Shallis RM, Thompson EG, Lopes de Menezes D, Rose S, Boss IW, Halene S, Haferlach T, Fox B, Zeidan AM. Molecular, Epigenetic, and Immune Landscape of TP53-mutated (TP53-M) Acute Myeloid Leukemia (AML) and Higher Risk Myelodysplastic Syndromes (HR-MDS). Blood 2022; 140 (Supplement 1): 6247–6249. doi: https://doi.org/10.1182/blood-2022-156460
36. Biernacki MA, Foster KA, Clough C, Busch S, Cummings C, Oehler VG, Stirewalt D, Doulatov S, Bleakley M. A Shared SF3B1 Neoantigen Is Presented on Primary Malignant Cells and Induced Pluripotent Stem Cell-Derived Hematopoietic Lines. Blood. 2020 Nov;136(1):13-14. https://doi.org/10.1182/blood-2020-139907. ISSN 0006-4971
37. Birsen R, Larrue C, Decroocq J, Johnson N, Guiraud N, Gotanegre M, Cantero-Aguilar L, Grignano E, Huynh T, Fontenay M, Kosmider O, Mayeux P, Chapuis N, Sarry JE, Tamburini J, Bouscary D. APR-246 induces early cell death by ferroptosis in acute myeloid leukemia. Haematologica. 2022 Feb 1;107(2):403-416. doi: 10.3324/haematol.2020.259531. PMID: 33406814; PMCID: PMC8804578.
38. Blecua P, Martinez-Verbo L, Esteller M. The DNA methylation landscape of hematological malignancies: an update. Mol Oncol. 2020 Aug;14(8):1616-1639. doi: 10.1002/1878-0261.12744. Epub 2020 Jul 3. PMID: 32526054; PMCID: PMC7400809.
39. Blum S, Gattermann N, Martins F, Nachtkamp K, Kuendgen A, Kobbe G, Germing U. Is the IPSS-R Useful for Patients with MDS Receiving Disease-Modifying Treatment?. Blood 2016; 128 (22): 5526. doi: https://doi.org/10.1182/blood.V128.22.5526.5526
40. Boada M, Echarte L, Guillermo C, Diaz L, Touriño C, Grille S. 5-Azacytidine restores interleukin 6-increased production in mesenchymal stromal cells from myelodysplastic patients. Hematol Transfus Cell Ther. 2021 Jan-Mar;43(1):35-42. doi: 10.1016/j.htct.2019.12.002. Epub 2020 Jan 27. PMID: 32008984; PMCID: PMC7910176.
41. Bochtler T, Fröhling S, Krämer A. Role of chromosomal aberrations in clonal diversity and progression of acute myeloid leukemia. Leukemia. 2015 Jun;29(6):1243-52. doi: 10.1038/leu.2015.32. Epub 2015 Feb 12. PMID: 25673237.
42. Bocker MT, Hellwig I, Breiling A, Eckstein V, Ho AD, Lyko F. Genome-wide promoter DNA methylation dynamics of human hematopoietic progenitor cells during differentiation and aging. Blood. 2011 May 12;117(19):e182-9. doi: 10.1182/blood-2011-01-331926. Epub 2011 Mar 22. PMID: 21427290.
43. Bogeska R, Mikecin AM, Kaschutnig P, Fawaz M, Büchler-Schäff M, Le D, Ganuza M, Vollmer A, Paffenholz SV, Asada N, Rodriguez-Correa E, Frauhammer F, Buettner F, Ball M, Knoch J, Stäble S, Walter D, Petri A, Carreño-Gonzalez MJ, Wagner V, Brors B, Haas S, Lipka DB, Essers MAG, Weru V, Holland-Letz T, Mallm JP, Rippe K, Krämer S, Schlesner M, McKinney Freeman S, Florian MC, King KY, Frenette PS, Rieger MA, Milsom MD. Inflammatory exposure drives long-lived impairment of hematopoietic stem cell self-renewal activity and accelerated aging. Cell Stem Cell. 2022 Aug 4;29(8):1273-1284.e8. doi: 10.1016/j.stem.2022.06.012. Epub 2022 Jul 19. PMID: 35858618; PMCID: PMC9357150.
44. Bondu S, Alary AS, Lefèvre C, Houy A, Jung G, Lefebvre T, Rombaut D, Boussaid I, Bousta A, Guillonneau F, Perrier P, Alsafadi S, Wassef M, Margueron R, Rousseau A, Droin N, Cagnard N, Kaltenbach S, Winter S, Kubasch AS, Bouscary D, Santini V, Toma A, Hunault M, Stamatoullas A, Gyan

E, Cluzeau T, Platzbecker U, Adès L, Puy H, Stern MH, Karim Z, Mayeux P, Nemeth E, Park S, Ganz T, Kautz L, Kosmider O, Fontenay M. A variant erythroferrone disrupts iron homeostasis in SF3B1-mutated myelodysplastic syndrome. Sci Transl Med. 2019 Jul 10;11(500):eaav5467. doi: 10.1126/scitranslmed.aav5467. PMID: 31292266; PMCID: PMC8005358.

45. Bontkes HJ , Ruben JM , Alhan C , Westers TM , Ossenkoppele GJ , van de Loosdrecht AA . Azacitidine differentially affects CD4(pos) T-cell polarization in vitro and in vivo in high risk myelodysplastic syndromes. Leuk Res, 36(7), 921–930 (2012).22503132
46. Boren E, Gershwin ME. Inflamm-aging: autoimmunity, and the immune-risk phenotype. Autoimmun Rev. 2004 Jul;3(5):401-6. doi: 10.1016/j.autrev.2004.03.004. PMID: 15288008.
47. Bousounis P, Bergo V, Trompouki E. Inflammation, Aging and Hematopoiesis: A Complex Relationship. Cells. 2021; 10(6):1386. https://doi.org/10.3390/cells10061386
48. Boy M, Bisio V, Zhao LP, Guidez F, Schell B, Lereclus E, Henry G, Villemonteix J, Rodrigues-Lima F, Gagne K, Retiere C, Larcher L, Kim R, Clappier E, Sebert M, Mekinian A, Fain O, Caignard A, Espeli M, Balabanian K, Toubert A, Fenaux P, Ades L, Dulphy N. Myelodysplastic Syndrome associated TET2 mutations affect NK cell function and genome methylation. Nat Commun. 2023 Feb 3;14(1):588. doi: 10.1038/s41467-023-36193-w. PMID: 36737440; PMCID: PMC9898569.
49. Brunner AM, Esteve J, Porkka K, Knapper S, Traer E, Scholl S, Garcia-Manero G, Vey N, Wermke M, Janssen J, Narayan R, Loo S, Kontro M, Ottmann O, Naidu P, Pelletier M, Han M, Lewandowski A, Zhang N, Mohammed A, Rinne ML, Borate U, Wei AH, Tovar N. Efficacy and Safety of Sabatolimab (MBG453) in Combination with Hypomethylating Agents (HMAs) in Patients (Pts) with Very High/High-Risk Myelodysplastic Syndrome (vHR/HR-MDS) and Acute Myeloid Leukemia (AML): Final Analysis from a Phase Ib Study. Blood 2021; 138 (Supplement 1): 244. doi: https://doi.org/10.1182/blood-2021-146039
50. Burger JA, Peled A. CXCR4 antagonists: targeting the microenvironment in leukemia and other cancers. Leukemia. 2009 Jan;23(1):43-52. doi: 10.1038/leu.2008.299. Epub 2008 Nov 6. PMID: 18987663.
51. Cabezón M, Malinverni R, Bargay J, Xicoy B, Marcé S, Garrido A, Tormo M, Arenillas L, Coll R, Borras J, Jiménez MJ, Hoyos M, Valcárcel D, Escoda L, Vall-Llovera F, Garcia A, Font LL, Rámila E, Buschbeck M, Zamora L; CETLAM group. Different methylation signatures at diagnosis in patients with high-risk myelodysplastic syndromes and secondary acute myeloid leukemia predict azacitidine response and longer survival. Clin Epigenetics. 2021 Jan 14;13(1):9. doi: 10.1186/s13148-021-01002-y. PMID: 33446256; PMCID: PMC7809812.
52. Carlsten M, Järås M. Natural Killer Cells in Myeloid Malignancies: Immune Surveillance, NK Cell Dysfunction, and Pharmacological Opportunities to Bolster the Endogenous NK Cells. Front Immunol. 2019 Oct 11;10:2357. doi: 10.3389/fimmu.2019.02357. PMID: 31681270; PMCID: PMC6797594.
53. Cassetta L, Pollard JW. A timeline of tumour-associated macrophage biology. Nat Rev Cancer. 2023 Apr;23(4):238-257. doi: 10.1038/s41568-022-00547-1. Epub 2023 Feb 15. PMID: 36792751.
54. Cazzola M. Myelodysplastic Syndromes. N Engl J Med. 2020 Oct 1;383(14):1358-1374. doi: 10.1056/NEJMra1904794. PMID: 32997910.
55. Cazzola M, Della Porta MG, Malcovati L. Clinical relevance of anemia and transfusion iron overload in myelodysplastic syndromes. Hematology Am Soc Hematol Educ Program. 2008:166-75. doi: 10.1182/asheducation-2008.1.166. PMID: 19074076.
56. Cazzola M, Della Porta MG, Malcovati L. The genetic basis of myelodysplasia and its clinical relevance. Blood. 2013 Dec 12;122(25):4021-34. doi: 10.1182/blood-2013-09-381665. Epub 2013 Oct 17. PMID: 24136165; PMCID: PMC3862275.
57. Cedar H, Bergman Y. Epigenetics of haematopoietic cell development. Nat Rev Immunol. 2011 Jun 10;11(7):478-88. doi: 10.1038/nri2991. PMID: 21660052.

58. Chambers SM, Shaw CA, Gatza C, Fisk CJ, Donehower LA, Goodell MA. Aging hematopoietic stem cells decline in function and exhibit epigenetic dysregulation. PLoS Biol. 2007 Aug;5(8):e201. doi: 10.1371/journal.pbio.0050201. PMID: 17676974; PMCID: PMC1925137.
59. Chang CK, Zhao YS, Xu F, Guo J, Zhang Z, He Q, Wu D, Wu LY, Su JY, Song LX, Xiao C, Li X. TP53 mutations predict decitabine-induced complete responses in patients with myelodysplastic syndromes. Br J Haematol. 2017 Feb;176(4):600-608. doi: 10.1111/bjh.14455. Epub 2016 Dec 16. PMID: 27984642.
60. Chaudhary AK, Chaudhary S, Ghosh K, Shanmukaiah C, Nadkarni AH. Secretion and Expression of Matrix Metalloproteinase-2 and 9 from Bone Marrow Mononuclear Cells in Myelodysplastic Syndrome and Acute Myeloid Leukemia. Asian Pac J Cancer Prev. 2016;17(3):1519-29. doi: 10.7314/apjcp.2016.17.3.1519. PMID: 27039800.
61. Chee L, Ritchie D, Ludford-Menting M, Ripley J, Chung J, Park D, Norton S, Kenealy M, Koldej R. Dysregulation of immune cell and cytokine signalling correlates with clinical outcomes in myelodysplastic syndrome (MDS). Eur J Haematol. 2022 Apr;108(4):342-353. doi: 10.1111/ejh.13742. Epub 2022 Feb 3. PMID: 34963023.
62. Chen S, Zambetti NA, Bindels EMJ, et al. Massive parallel RNA sequencing of highly purified mesenchymal elements in low-risk MDS reveals tissue-context-dependent activation of inflammatory programs. Leukemia. 2016;30(9):1938-1942.
63. Chen X, Eksioglu EA, Zhou J, Zhang L, Djeu J, Fortenbery N, Epling-Burnette P, Van Bijnen S, Dolstra H, Cannon J, Youn JI, Donatelli SS, Qin D, De Witte T, Tao J, Wang H, Cheng P, Gabrilovich DI, List A, Wei S. Induction of myelodysplasia by myeloid-derived suppressor cells. J Clin Invest. 2013 Nov;123(11):4595-611. doi: 10.1172/JCI67580. PMID: 24216507; PMCID: PMC3809779.
64. Cheng P, Eksioglu EA, Chen X, Kandell W, Le Trinh T, Cen L, Qi J, Sallman DA, Zhang Y, Tu N, Adams WA, Zhang C, Liu J, Cleveland JL, List AF, Wei S. S100A9-induced overexpression of PD-1/PD-L1 contributes to ineffective hematopoiesis in myelodysplastic syndromes. Leukemia. 2019 Aug;33(8):2034-2046. doi: 10.1038/s41375-019-0397-9. Epub 2019 Feb 8. PMID: 30737486; PMCID: PMC6687540.
65. Chichili GR, Huang L, Li H, Burke S, He L, Tang Q, Jin L, Gorlatov S, Ciccarone V, Chen F, Koenig S, Shannon M, Alderson R, Moore PA, Johnson S, Bonvini E. A CD3xCD123 bispecific DART for redirecting host T cells to myelogenous leukemia: preclinical activity and safety in nonhuman primates. Sci Transl Med. 2015 May 27;7(289):289ra82. doi: 10.1126/scitranslmed.aaa5693. PMID: 26019218.
66. Chretien AS, Fauriat C, Orlanducci F, Galseran C, Rey J, Bouvier Borg G, Gautherot E, Granjeaud S, Hamel-Broza JF, Demerle C, Ifrah N, Lacombe C, Cornillet-Lefebvre P, Delaunay J, Toubert A, Gregori E, Luche H, Malissen M, Arnoulet C, Nunes JA, Vey N, Olive D. Natural Killer Defective Maturation Is Associated with Adverse Clinical Outcome in Patients with Acute Myeloid Leukemia. Front Immunol. 2017 May 29;8:573. doi: 10.3389/fimmu.2017.00573. PMID: 28611767; PMCID: PMC5447002.
67. Cianga VA, Campos Catafal L, Cianga P, Pavel Tanasa M, Cherry M, Collet P, Tavernier E, Guyotat D, Rusu C, Aanei CM. Natural Killer Cell Subpopulations and Inhibitory Receptor Dynamics in Myelodysplastic Syndromes and Acute Myeloid Leukemia. Front Immunol. 2021 Apr 27;12:665541. doi: 10.3389/fimmu.2021.665541. PMID: 33986753; PMCID: PMC8112610.
68. Cichocki F, Miller JS, Anderson SK, Bryceson YT. Epigenetic regulation of NK cell differentiation and effector functions. Front Immunol. 2013 Feb 28;4:55. doi: 10.3389/fimmu.2013.00055. PMID: 23450696; PMCID: PMC3584244.
69. Cluzeau T, Robert G, Mounier N, Karsenti JM, Dufies M, Puissant A, Jacquel A, Renneville A, Preudhomme C, Cassuto JP, Raynaud S, Luciano F, Auberger P. BCL2L10 is a predictive factor for resistance to azacitidine in MDS and AML patients. Oncotarget. 2012 Apr;3(4):490-501. doi: 10.18632/oncotarget.481. PMID: 22577154; PMCID: PMC3380582.

70. Cluzeau T, McGraw KL, Irvine B, Masala E, Ades L, Basiorka AA, Maciejewski J, Auberger P, Wei S, Fenaux P, Santini V, List A. Pro-inflammatory proteins S100A9 and tumor necrosis factor-α suppress erythropoietin elaboration in myelodysplastic syndromes. Haematologica. 2017 Dec;102(12):2015-2020. doi: 10.3324/haematol.2016.158857. Epub 2017 Oct 5. PMID: 28983059; PMCID: PMC5709100.
71. Cluzeau T, Sebert M, Rahmé R, Cuzzubbo S, Lehmann-Che J, Madelaine I, Peterlin P, Bève B, Attalah H, Chermat F, Miekoutima E, Rauzy OB, Recher C, Stamatoullas A, Willems L, Raffoux E, Berthon C, Quesnel B, Loschi M, Carpentier AF, Sallman DA, Komrokji R, Walter-Petrich A, Chevret S, Ades L, Fenaux P. Eprenetapopt Plus Azacitidine in TP53-Mutated Myelodysplastic Syndromes and Acute Myeloid Leukemia: A Phase II Study by the Groupe Francophone des Myélodysplasies (GFM). J Clin Oncol. 2021 May 10;39(14):1575-1583. doi: 10.1200/JCO.20.02342. Epub 2021 Feb 18. PMID: 33600210; PMCID: PMC8099409.
72. Coats T, Smith A, Mourikis TP, Irish JM, Kordasti S, Mufti GJ. Mass cytometry reveals PD1 upregulation is an early step in MDS disease progression. Blood. 2016;128(22):4296.
73. Cogle CR. Incidence and Burden of the Myelodysplastic Syndromes. Curr Hematol Malig Rep. 2015 Sep;10(3):272-81. doi: 10.1007/s11899-015-0269-y. PMID: 26134527; PMCID: PMC4553145.
74. Corces-Zimmerman MR, Hong WJ, Weissman IL, Medeiros BC, Majeti R. Preleukemic mutations in human acute myeloid leukemia affect epigenetic regulators and persist in remission. Proc Natl Acad Sci U S A. 2014 Feb 18;111(7):2548-53. doi: 10.1073/pnas.1324297111. Epub 2014 Feb 3. PMID: 24550281; PMCID: PMC3932921.
75. Corey SJ, Minden MD, Barber DL, Kantarjian H, Wang JC, Schimmer AD. Myelodysplastic syndromes: the complexity of stem-cell diseases. Nat Rev Cancer. 2007 Feb;7(2):118-29. doi: 10.1038/nrc2047. PMID: 17251918.
76. Costantini B , Kordasti SY , Kulasekararaj AG The effects of 5-azacytidine on the function and number of regulatory T cells and T-effectors in myelodysplastic syndrome. Haematologica, 98(8), 1196–1205 (2013).23242597
77. Cruijsen M, Lübbert M, Wijermans P, Huls G. Clinical Results of Hypomethylating Agents in AML Treatment. J Clin Med. 2014 Dec 25;4(1):1-17. doi: 10.3390/jcm4010001. PMID: 26237015; PMCID: PMC4470235.
78. Crusz SM, Balkwill FR. Inflammation and cancer: advances and new agents. Nat Rev Clin Oncol. 2015 Oct;12(10):584-96. doi: 10.1038/nrclinonc.2015.105. Epub 2015 Jun 30. PMID: 26122183.
79. Cumbo C, Tota G, Anelli L, Zagaria A, Specchia G, Albano F. TP53 in Myelodysplastic Syndromes: Recent Biological and Clinical Findings. Int J Mol Sci. 2020 May 13;21(10):3432. doi: 10.3390/ijms21103432. PMID: 32414002; PMCID: PMC7279310.
80. D'Silva SZ, Singh M, Pinto AS. NK cell defects: implication in acute myeloid leukemia. Front Immunol. 2023 May 9;14:1112059. doi: 10.3389/fimmu.2023.1112059. PMID: 37228595; PMCID: PMC10203541.
81. Da Silva-Coelho P, Kroeze LI, Yoshida K, Koorenhof-Scheele TN, Knops R, van de Locht LT, de Graaf AO, Massop M, Sandmann S, Dugas M, Stevens-Kroef MJ, Cermak J, Shiraishi Y, Chiba K, Tanaka H, Miyano S, de Witte T, Blijlevens NMA, Muus P, Huls G, van der Reijden BA, Ogawa S, Jansen JH. Clonal evolution in myelodysplastic syndromes. Nat Commun. 2017 Apr 21;8:15099. doi: 10.1038/ncomms15099. PMID: 28429724; PMCID: PMC5530598.
82. Das M, Zhu C, Kuchroo VK. Tim-3 and its role in regulating anti-tumor immunity. Immunol Rev. 2017 Mar;276(1):97-111. doi: 10.1111/imr.12520. PMID: 28258697; PMCID: PMC5512889.
83. Daver NG, Maiti A, Kadia TM, Vyas P, Majeti R, Wei AH, Garcia-Manero G, Craddock C, Sallman DA, Kantarjian HM. TP53-Mutated Myelodysplastic Syndrome and Acute Myeloid Leukemia: Biology, Current Therapy, and Future Directions. Cancer Discov. 2022 Nov 2;12(11):2516-2529. doi:

10.1158/2159-8290.CD-22-0332. Erratum in: Cancer Discov. 2022 Dec 2;12(12):2954. PMID: 36218325; PMCID: PMC9627130.

84. Daver NG, Vyas P, Kambhampati S, Al Malki MM, Larson R, Asch A, et al. Tolerability and efficacy of the first-in-class anti-CD47 antibody magrolimab combined with azacitidine in frontline patients with TP53-mutated acute myeloid leukemia: phase 1b results. HemaSphere 2022;6:33–4. Abstr S132.
85. De Lourdes Perim A, Amarante MK, Guembarovski RL, de Oliveira CE, Watanabe MA. CXCL12/CXCR4 axis in the pathogenesis of acute lymphoblastic leukemia (ALL): a possible therapeutic target. Cell Mol Life Sci. 2015 May;72(9):1715-23. doi: 10.1007/s00018-014-1830-x. Epub 2015 Jan 9. PMID: 25572297.
86. de Mol J, Kuiper J, Tsiantoulas D, Foks AC. The Dynamics of B Cell Aging in Health and Disease. Front Immunol. 2021 Oct 5;12:733566. doi: 10.3389/fimmu.2021.733566. PMID: 34675924; PMCID: PMC8524000.
87. de Witte T, Bowen D, Robin M, Malcovati L, Niederwieser D, Yakoub-Agha I, Mufti GJ, Fenaux P, Sanz G, Martino R, Alessandrino EP, Onida F, Symeonidis A, Passweg J, Kobbe G, Ganser A, Platzbecker U, Finke J, van Gelder M, van de Loosdrecht AA, Ljungman P, Stauder R, Volin L, Deeg HJ, Cutler C, Saber W, Champlin R, Giralt S, Anasetti C, Kröger N. Allogeneic hematopoietic stem cell transplantation for MDS and CMML: recommendations from an international expert panel. Blood. 2017 Mar 30;129(13):1753-1762. doi: 10.1182/blood-2016-06-724500. Epub 2017 Jan 17. PMID: 28096091; PMCID: PMC5524528.
88. Deeg HJ, Scott BL, Fang M, Shulman HM, Gyurkocza B, Myerson D, Pagel JM, Platzbecker U, Ramakrishnan A, Radich JP, Sandmaier BM, Sorror M, Stirewalt DL, Wilson WA, Storb R, Appelbaum FR, Gooley T. Five-group cytogenetic risk classification, monosomal karyotype, and outcome after hematopoietic cell transplantation for MDS or acute leukemia evolving from MDS. Blood. 2012 Aug 16;120(7):1398-408. doi: 10.1182/blood-2012-04-423046. Epub 2012 Jul 5. PMID: 22767498; PMCID: PMC3478516.
89. Della Porta MG, Gallì A, Bacigalupo A, Zibellini S, Bernardi M, Rizzo E, Allione B, van Lint MT, Pioltelli P, Marenco P, Bosi A, Voso MT, Sica S, Cuzzola M, Angelucci E, Rossi M, Ubezio M, Malovini A, Limongelli I, Ferretti VV, Spinelli O, Tresoldi C, Pozzi S, Luchetti S, Pezzetti L, Catricalà S, Milanesi C, Riva A, Bruno B, Ciceri F, Bonifazi F, Bellazzi R, Papaemmanuil E, Santoro A, Alessandrino EP, Rambaldi A, Cazzola M. Clinical Effects of Driver Somatic Mutations on the Outcomes of Patients With Myelodysplastic Syndromes Treated With Allogeneic Hematopoietic Stem-Cell Transplantation. J Clin Oncol. 2016 Oct 20;34(30):3627-3637. doi: 10.1200/JCO.2016.67.3616. PMID: 27601546; PMCID: PMC6366344.
90. Dimicoli S, Wei Y, Bueso-Ramos C, Yang H, Dinardo C, Jia Y, Zheng H, Fang Z, Nguyen M, Pierce S, Chen R, Wang H, Wu C, Garcia-Manero G. Overexpression of the toll-like receptor (TLR) signaling adaptor MYD88, but lack of genetic mutation, in myelodysplastic syndromes. PLoS One. 2013 Aug 15;8(8):e71120. doi: 10.1371/journal.pone.0071120. PMID: 23976989; PMCID: PMC3744562.
91. Dinmohamed AG, van Norden Y, Visser O, Posthuma EF, Huijgens PC, Sonneveld P, van de Loosdrecht AA, Jongen-Lavrencic M. Effectiveness of azacitidine for the treatment of higher-risk myelodysplastic syndromes in daily practice: results from the Dutch population-based PHAROS MDS registry. Leukemia. 2015 Dec;29(12):2449-51. doi: 10.1038/leu.2015.220. Epub 2015 Sep 15. PMID: 26369829.
92. Donehower LA, Soussi T, Korkut A, Liu Y, Schultz A, Cardenas M, Li X, Babur O, Hsu TK, Lichtarge O, Weinstein JN, Akbani R, Wheeler DA. Integrated Analysis of TP53 Gene and Pathway Alterations in The Cancer Genome Atlas. Cell Rep. 2019 Sep 10;28(11):3010. doi: 10.1016/j.celrep.2019.08.061. Erratum for: Cell Rep. 2019 Jul 30;28(5):1370-1384.e5. PMID: 31509758.
93. Duncavage EJ, Uy GL, Petti AA, Miller CA, Lee YS, Tandon B, Gao F, Fronick CC, O'Laughlin M, Fulton RS, Wilson RK, Jacoby MA, Cashen AF, Wartman LD, Walter MJ, Westervelt P, Link DC, DiPersio JF,

Ley TJ, Welch JS. Mutational landscape and response are conserved in peripheral blood of AML and MDS patients during decitabine therapy. Blood. 2017 Mar 9;129(10):1397-1401. doi: 10.1182/blood-2016-10-745273. Epub 2017 Jan 12. PMID: 28082444; PMCID: PMC5345736.

94. Eladl E, Tremblay-LeMay R, Rastgoo N, Musani R, Chen W, Liu A, Chang H. Role of CD47 in Hematological Malignancies. J Hematol Oncol. 2020 Jul 16;13(1):96. doi: 10.1186/s13045-020-00930-1. PMID: 32677994; PMCID: PMC7364564.
95. Enrico A, Bestach Y, Flores MG, Arbelbide J, Serale C, Novoa V, Crisp R, Rivas MM, Larripa I, Belli C. Influence of Acute Myeloid Leukemia Progression on the Prognosis of 831 Patients With Myelodysplastic Syndromes From the Argentine Database. Clin Lymphoma Myeloma Leuk. 2017 Nov;17(11):743-752.e5. doi: 10.1016/j.clml.2017.06.024. Epub 2017 Jun 23. PMID: 28797621.
96. Epling-Burnette PK, Bai F, Painter JS, Rollison DE, Salih HR, Krusch M, Zou J, Ku E, Zhong B, Boulware D, Moscinski L, Wei S, Djeu JY, List AF. Reduced natural killer (NK) function associated with high-risk myelodysplastic syndrome (MDS) and reduced expression of activating NK receptors. Blood. 2007 Jun 1;109(11):4816-24. doi: 10.1182/blood-2006-07-035519. Epub 2007 Mar 6. PMID: 17341666; PMCID: PMC1885518.
97. Esplin BL, Shimazu T, Welner RS, Garrett KP, Nie L, Zhang Q, Humphrey MB, Yang Q, Borghesi LA, Kincade PW. Chronic exposure to a TLR ligand injures hematopoietic stem cells. J Immunol. 2011 May 1;186(9):5367-75. doi: 10.4049/jimmunol.1003438. Epub 2011 Mar 25. PMID: 21441445; PMCID: PMC3086167.
98. Fang J, Bolanos LC, Choi K, Liu X, Christie S, Akunuru S, Kumar R, Wang D, Chen X, Greis KD, Stoilov P, Filippi MD, Maciejewski JP, Garcia-Manero G, Weirauch MT, Salomonis N, Geiger H, Zheng Y, Starczynowski DT. Ubiquitination of hnRNPA1 by TRAF6 links chronic innate immune signaling with myelodysplasia. Nat Immunol. 2017 Feb;18(2):236-245. doi: 10.1038/ni.3654. Epub 2016 Dec 26. Erratum in: Nat Immunol. 2017 Mar 22;18(4):474. PMID: 28024152; PMCID: PMC5423405.
99. Fazio C, Covre A, Cutaia O, Lofiego MF, Tunici P, Chiarucci C, Cannito S, Giacobini G, Lowder JN, Ferraldeschi R, Taverna P, Di Giacomo AM, Coral S, Maio M. Immunomodulatory Properties of DNA Hypomethylating Agents: Selecting the Optimal Epigenetic Partner for Cancer Immunotherapy. Front Pharmacol. 2018 Dec 7;9:1443. doi: 10.3389/fphar.2018.01443. PMID: 30581389; PMCID: PMC6293200.
100. Fenaux P, Giagounidis A, Selleslag D, Beyne-Rauzy O, Mufti G, Mittelman M, Muus P, Te Boekhorst P, Sanz G, Del Cañizo C, Guerci-Bresler A, Nilsson L, Platzbecker U, Lübbert M, Quesnel B, Cazzola M, Ganser A, Bowen D, Schlegelberger B, Aul C, Knight R, Francis J, Fu T, Hellström-Lindberg E; MDS-004 Lenalidomide del5q Study Group. A randomized phase 3 study of lenalidomide versus placebo in RBC transfusion-dependent patients with Low-/Intermediate-1-risk myelodysplastic syndromes with del5q. Blood. 2011 Oct 6;118(14):3765-76. doi: 10.1182/blood-2011-01-330126. Epub 2011 Jul 13. PMID: 21753188.
101. Fenaux P, Mufti GJ, Hellstrom-Lindberg E, Santini V, Finelli C, Giagounidis A, Schoch R, Gattermann N, Sanz G, List A, Gore SD, Seymour JF, Bennett JM, Byrd J, Backstrom J, Zimmerman L, McKenzie D, Beach C, Silverman LR; International Vidaza High-Risk MDS Survival Study Group. Efficacy of azacitidine compared with that of conventional care regimens in the treatment of higher-risk myelodysplastic syndromes: a randomised, open-label, phase III study. Lancet Oncol. 2009 Mar;10(3):223-32. doi: 10.1016/S1470-2045(09)70003-8. Epub 2009 Feb 21. PMID: 19230772; PMCID: PMC4086808.
102. Fenaux P, Platzbecker U, Mufti GJ, Garcia-Manero G, Buckstein R, Santini V, Díez-Campelo M, Finelli C, Cazzola M, Ilhan O, Sekeres MA, Falantes JF, Arrizabalaga B, Salvi F, Giai V, Vyas P, Bowen D, Selleslag D, DeZern AE, Jurcic JG, Germing U, Götze KS, Quesnel B, Beyne-Rauzy O, Cluzeau T, Voso MT, Mazure D, Vellenga E, Greenberg PL, Hellström-Lindberg E, Zeidan AM, Adès L, Verma A, Savona MR, Laadem A, Benzohra A, Zhang J, Rampersad A, Dunshee DR, Linde PG, Sherman ML, Komrokji

RS, List AF. Luspatercept in Patients with Lower-Risk Myelodysplastic Syndromes. N Engl J Med. 2020 Jan 9;382(2):140-151. doi: 10.1056/NEJMoa1908892. PMID: 31914241.

103. Fenaux P, Santini V, Spiriti MAA, Giagounidis A, Schlag R, Radinoff A, Gercheva-Kyuchukova L, Anagnostopoulos A, Oliva EN, Symeonidis A, Berger MH, Götze KS, Potamianou A, Haralampiev H, Wapenaar R, Milionis I, Platzbecker U. A phase 3 randomized, placebo-controlled study assessing the efficacy and safety of epoetin-α in anemic patients with low-risk MDS. Leukemia. 2018 Dec;32(12):2648-2658. doi: 10.1038/s41375-018-0118-9. Epub 2018 Mar 30. PMID: 29895954; PMCID: PMC6286328.

104. Figueroa ME, Skrabanek L, Li Y, Jiemjit A, Fandy TE, Paietta E, Fernandez H, Tallman MS, Greally JM, Carraway H, Licht JD, Gore SD, Melnick A. MDS and secondary AML display unique patterns and abundance of aberrant DNA methylation. Blood. 2009 Oct 15;114(16):3448-58. doi: 10.1182/blood-2009-01-200519. Epub 2009 Aug 3. PMID: 19652201; PMCID: PMC2765680.

105. Fozza C, Contini S, Galleu A, Simula MP, Virdis P, Bonfigli S, Longinotti M. Patients with myelodysplastic syndromes display several T-cell expansions, which are mostly polyclonal in the CD4(+) subset and oligoclonal in the CD8(+) subset. Exp Hematol. 2009 Aug;37(8):947-55. doi: 10.1016/j.exphem.2009.04.009. Epub 2009 May 4. PMID: 19409953.

106. Fozza C, Corda G, Barraqueddu F, Virdis P, Contini S, Galleu A, Isoni A, Dore F, Angelucci E, Longinotti M. Azacitidine improves the T-cell repertoire in patients with myelodysplastic syndromes and acute myeloid leukemia with multilineage dysplasia. Leuk Res. 2015 Sep;39(9):957-63. doi: 10.1016/j.leukres.2015.06.007. Epub 2015 Jun 26. PMID: 26209197.

107. Franceschi C, Bonafè M, Valensin S, Olivieri F, De Luca M, Ottaviani E, De Benedictis G. Inflamm-aging. An evolutionary perspective on immunosenescence. Ann N Y Acad Sci. 2000 Jun;908:244-54. doi: 10.1111/j.1749-6632.2000.tb06651.x. PMID: 10911963.

108. Frikeche J, Clavert A, Delaunay J, Brissot E, Grégoire M, Gaugler B, Mohty M. Impact of the hypomethylating agent 5-azacytidine on dendritic cells function. Exp Hematol. 2011 Nov;39(11):1056-63. doi: 10.1016/j.exphem.2011.08.004. Epub 2011 Aug 18. PMID: 21856273.

109. Fu R, Li L, Hu J, Wang Y, Tao J, Liu H, Liu Z, Zhang W. Elevated TIM3 expression of T helper cells affects immune system in patients with myelodysplastic syndrome. J Investig Med. 2019 Dec;67(8):1125-1130. doi: 10.1136/jim-2019-001059. Epub 2019 Sep 11. Erratum in: J Investig Med. 2020 Jan 23;: PMID: 31511310.

110. Fujihara KM, Zhang BZ, Jackson TD, Ogunkola MO, Nijagal B, Milne JV, Sallman DA, Ang CS, Nikolic I, Kearney CJ, Hogg SJ, Cabalag CS, Sutton VR, Watt S, Fujihara AT, Trapani JA, Simpson KJ, Stojanovski D, Leimkühler S, Haupt S, Phillips WA, Clemons NJ. Eprenetapopt triggers ferroptosis, inhibits NFS1 cysteine desulfurase, and synergizes with serine and glycine dietary restriction. Sci Adv. 2022 Sep 16;8(37):eabm9427. doi: 10.1126/sciadv.abm9427. Epub 2022 Sep 14. PMID: 36103522; PMCID: PMC9473576.

111. Galli S, Zlobec I, Schürch C, Perren A, Ochsenbein AF, Banz Y. CD47 protein expression in acute myeloid leukemia: A tissue microarray-based analysis. Leuk Res. 2015 Jul;39(7):749-56. doi: 10.1016/j.leukres.2015.04.007. Epub 2015 Apr 20. PMID: 25943033.

112. Gallois A, Silva I, Osman I, Bhardwaj N. Reversal of natural killer cell exhaustion by TIM-3 blockade. Oncoimmunology. 2015 Jan 7;3(12):e946365. doi: 10.4161/21624011.2014.946365. PMID: 25964857; PMCID: PMC4353130.

113. Gañán-Gómez I, Wei Y, Starczynowski DT, Colla S, Yang H, Cabrero-Calvo M, Bohannan ZS, Verma A, Steidl U, Garcia-Manero G. Deregulation of innate immune and inflammatory signaling in myelodysplastic syndromes. Leukemia. 2015 Jul;29(7):1458-69. doi: 10.1038/leu.2015.69. Epub 2015 Mar 12. PMID: 25761935; PMCID: PMC4857136.

114. Gang AO, Frosig TM , Brimnes MK 5-Azacytidine treatment sensitizes tumor cells to T-cell mediated cytotoxicity and modulates NK cells in patients with myeloid malignancies. Blood cancer journal, 4, e197 (2014).24681961
115. Gao XN, Lin J, Wang LL, Yu L. Demethylating treatment suppresses natural killer cell cytolytic activity. Mol Immunol. 2009 Jun;46(10):2064-70. doi: 10.1016/j.molimm.2009.02.033. Epub 2009 Apr 25. PMID: 19394699.
116. Garcia JS. Prospects for Venetoclax in Myelodysplastic Syndromes. Hematol Oncol Clin North Am. 2020 Apr;34(2):441-448. doi: 10.1016/j.hoc.2019.10.005. Epub 2019 Dec 11. PMID: 32089221.
117. Garcia-Manero G, Shan J, Faderl S, Cortes J, Ravandi F, Borthakur G, Wierda WG, Pierce S, Estey E, Liu J, Huang X, Kantarjian H. A prognostic score for patients with lower risk myelodysplastic syndrome. Leukemia. 2008 Mar;22(3):538-43. doi: 10.1038/sj.leu.2405070. Epub 2007 Dec 13. PMID: 18079733.
118. Geng S, Xu R, Huang X, Li M, Deng C, Lai P, Wang Y, Wu P, Chen X, Weng J, Du X. Dynamics of PD-1 expression are associated with treatment efficacy and prognosis in patients with intermediate/high-risk myelodysplastic syndromes under hypomethylating treatment. Front Immunol. 2022 Aug 8;13:950134. doi: 10.3389/fimmu.2022.950134. PMID: 36003379; PMCID: PMC9393298.
119. Genovese G, Kähler AK, Handsaker RE, Lindberg J, Rose SA, Bakhoum SF, Chambert K, Mick E, Neale BM, Fromer M, Purcell SM, Svantesson O, Landén M, Höglund M, Lehmann S, Gabriel SB, Moran JL, Lander ES, Sullivan PF, Sklar P, Grönberg H, Hultman CM, McCarroll SA. Clonal hematopoiesis and blood-cancer risk inferred from blood DNA sequence. N Engl J Med. 2014 Dec 25;371(26):2477-87. doi: 10.1056/NEJMoa1409405. Epub 2014 Nov 26. PMID: 25426838; PMCID: PMC4290021.
120. Ghobrial IM, Detappe A, Anderson KC, Steensma DP. The bone-marrow niche in MDS and MGUS: implications for AML and MM. Nat Rev Clin Oncol. 2018 Apr;15(4):219-233. doi: 10.1038/nrclinonc.2017.197. Epub 2018 Jan 9. PMID: 29311715.
121. Ghoneim HE, Fan Y, Moustaki A, Abdelsamed HA, Dash P, Dogra P, Carter R, Awad W, Neale G, Thomas PG, Youngblood B. De Novo Epigenetic Programs Inhibit PD-1 Blockade-Mediated T Cell Rejuvenation. Cell. 2017 Jun 29;170(1):142-157.e19. doi: 10.1016/j.cell.2017.06.007. Epub 2017 Jun 22. PMID: 28648661; PMCID: PMC5568784.
122. Giovazzino A, Leone S, Rubino V, Palatucci AT, Cerciello G, Alfinito F, Pane F, Ruggiero G, Terrazzano G. Reduced regulatory T cells (Treg) in bone marrow preferentially associate with the expansion of cytotoxic T lymphocytes in low risk MDS patients. Br J Haematol. 2019 Apr;185(2):357-360. doi: 10.1111/bjh.15496. Epub 2018 Jul 16. PMID: 30010189.
123. Gonçalves AC, Alves R, Baldeiras I, Marques B, Oliveiros B, Pereira A, Nascimento Costa JM, Cortesão E, Mota Vieira L, Sarmento Ribeiro AB. DNA Methylation Is Correlated with Oxidative Stress in Myelodysplastic Syndrome-Relevance as Complementary Prognostic Biomarkers. Cancers (Basel). 2021 Jun 23;13(13):3138. doi: 10.3390/cancers13133138. PMID: 34201739; PMCID: PMC8268426.
124. Gonzalez-Lugo JD, Verma A. Targeting inflammation in lower-risk MDS. Hematology Am Soc Hematol Educ Program. 2022 Dec 9;2022(1):382-387. doi: 10.1182/hematology.2022000350. PMID: 36485128; PMCID: PMC9821551.
125. Goodyear O, Agathanggelou A, Novitzky-Basso I, Siddique S, McSkeane T, Ryan G, Vyas P, Cavenagh J, Stankovic T, Moss P, Craddock C. Induction of a CD8+ T-cell response to the MAGE cancer testis antigen by combined treatment with azacitidine and sodium valproate in patients with acute myeloid leukemia and myelodysplasia. Blood. 2010 Sep 16;116(11):1908-18. doi: 10.1182/blood-2009-11-249474. Epub 2010 Jun 8. PMID: 20530795.
126. Granfeldt Østgård LS, Medeiros BC, Sengeløv H, Nørgaard M, Andersen MK, Dufva IH, Friis LS, Kjeldsen E, Marcher CW, Preiss B, Severinsen M, Nørgaard JM. Epidemiology and Clinical

Significance of Secondary and Therapy-Related Acute Myeloid Leukemia: A National Population-Based Cohort Study. J Clin Oncol. 2015 Nov 1;33(31):3641-9. doi: 10.1200/JCO.2014.60.0890. Epub 2015 Aug 24. PMID: 26304885.

127. Graubert TA, Shen D, Ding L, Okeyo-Owuor T, Lunn CL, Shao J, Krysiak K, Harris CC, Koboldt DC, Larson DE, McLellan MD, Dooling DJ, Abbott RM, Fulton RS, Schmidt H, Kalicki-Veizer J, O'Laughlin M, Grillot M, Baty J, Heath S, Frater JL, Nasim T, Link DC, Tomasson MH, Westervelt P, DiPersio JF, Mardis ER, Ley TJ, Wilson RK, Walter MJ. Recurrent mutations in the U2AF1 splicing factor in myelodysplastic syndromes. Nat Genet. 2011 Dec 11;44(1):53-7. doi: 10.1038/ng.1031. PMID: 22158538; PMCID: PMC3247063.

128. Greenberg P, Cox C, LeBeau MM, Fenaux P, Morel P, Sanz G, Sanz M, Vallespi T, Hamblin T, Oscier D, Ohyashiki K, Toyama K, Aul C, Mufti G, Bennett J. International scoring system for evaluating prognosis in myelodysplastic syndromes. Blood. 1997 Mar 15;89(6):2079-88.

129. Greenberg PL. Apoptosis and its role in the myelodysplastic syndromes: implications for disease natural history and treatment. Leuk Res. 1998 Dec;22(12):1123-36. doi: 10.1016/s0145-2126(98)00112-x. PMID: 9922076.

130. Greenberg PL, Tuechler H, Schanz J, Sanz G, Garcia-Manero G, Solé F, Bennett JM, Bowen D, Fenaux P, Dreyfus F, Kantarjian H, Kuendgen A, Levis A, Malcovati L, Cazzola M, Cermak J, Fonatsch C, Le Beau MM, Slovak ML, Krieger O, Luebbert M, Maciejewski J, Magalhaes SM, Miyazaki Y, Pfeilstöcker M, Sekeres M, Sperr WR, Stauder R, Tauro S, Valent P, Vallespi T, van de Loosdrecht AA, Germing U, Haase D. Revised international prognostic scoring system for myelodysplastic syndromes. Blood. 2012 Sep 20;120(12):2454-65. doi: 10.1182/blood-2012-03-420489. Epub 2012 Jun 27. PMID: 22740453; PMCID: PMC4425443.

131. Griffiths EA, Srivastava P, Matsuzaki J, Brumberger Z, Wang ES, Kocent J, Miller A, Roloff GW, Wong HY, Paluch BE, Lutgen-Dunckley LG, Martens BL, Odunsi K, Karpf AR, Hourigan CS, Nemeth MJ. NY-ESO-1 Vaccination in Combination with Decitabine Induces Antigen-Specific T-lymphocyte Responses in Patients with Myelodysplastic Syndrome. Clin Cancer Res. 2018 Mar 1;24(5):1019-1029. doi: 10.1158/1078-0432.CCR-17-1792. Epub 2017 Sep 25. PMID: 28947565; PMCID: PMC5844797.

132. Gu X, Tohme R, Tomlinson B, Sakre N, Hasipek M, Durkin L, Schuerger C, Grabowski D, Zidan AM, Radivoyevitch T, Hong C, Carraway H, Hamilton B, Sobecks R, Patel B, Jha BK, Hsi ED, Maciejewski J, Sauntharajah Y. Decitabine- and 5-azacytidine resistance emerges from adaptive responses of the pyrimidine metabolism network. Leukemia. 2021 Apr;35(4):1023-1036. doi: 10.1038/s41375-020-1003-x. Epub 2020 Aug 7. PMID: 32770088; PMCID: PMC7867667.

133. Guo ZS, et al. De novo induction of a cancer/testis antigen by 5-aza-2'-deoxycytidine augments adoptive immunotherapy in a murine tumor model. Cancer Res. 2006;66:1105–13. doi:10.1158/0008-5472.CAN-05-3020.

134. Guess T, Potts CR, Bhat P, Cartailler JA, Brooks A, Holt C, Yenamandra A, Wheeler FC, Savona MR, Cartailler JP, Ferrell PB. Distinct Patterns of Clonal Evolution Drive Myelodysplastic Syndrome Progression to Secondary Acute Myeloid Leukemia. Blood Cancer Discov. 2022 Jul 6;3(4):316-329. doi: 10.1158/2643-3230.BCD-21-0128. PMID: 35522837.

135. Haase D, Germing U, Schanz J, Pfeilstöcker M, Nösslinger T, Hildebrandt B, Kundgen A, Lübbert M, Kunzmann R, Giagounidis AA, Aul C, Trümper L, Krieger O, Stauder R, Müller TH, Wimazal F, Valent P, Fonatsch C, Steidl C. New insights into the prognostic impact of the karyotype in MDS and correlation with subtypes: evidence from a core dataset of 2124 patients. Blood. 2007 Dec 15;110(13):4385-95. doi: 10.1182/blood-2007-03-082404. Epub 2007 Aug 28. PMID: 17726160.

136. Haase D, Stevenson KE, Neuberg D, Maciejewski JP, Nazha A, Sekeres MA, Ebert BL, Garcia-Manero G, Haferlach C, Haferlach T, Kern W, Ogawa S, Nagata Y, Yoshida K, Graubert TA, Walter MJ, List AF, Komrokji RS, Padron E, Sallman D, Papaemmanuil E, Campbell PJ, Savona MR, Seegmiller A, Adès L, Fenaux P, Shih LY, Bowen D, Groves MJ, Tauro S, Fontenay M, Kosmider O, Bar-Natan M,

Steensma D, Stone R, Heuser M, Thol F, Cazzola M, Malcovati L, Karsan A, Ganster C, Hellström-Lindberg E, Boultwood J, Pellagatti A, Santini V, Quek L, Vyas P, Tüchler H, Greenberg PL, Bejar R; International Working Group for MDS Molecular Prognostic Committee. TP53 mutation status divides myelodysplastic syndromes with complex karyotypes into distinct prognostic subgroups. Leukemia. 2019 Jul;33(7):1747-1758. doi: 10.1038/s41375-018-0351-2. Epub 2019 Jan 11. PMID: 30635634; PMCID: PMC6609480.

137. Haferlach T, Nagata Y, Grossmann V, Okuno Y, Bacher U, Nagae G, Schnittger S, Sanada M, Kon A, Alpermann T, Yoshida K, Roller A, Nadarajah N, Shiraishi Y, Shiozawa Y, Chiba K, Tanaka H, Koeffler HP, Klein HU, Dugas M, Aburatani H, Kohlmann A, Miyano S, Haferlach C, Kern W, Ogawa S. Landscape of genetic lesions in 944 patients with myelodysplastic syndromes. Leukemia. 2014 Feb;28(2):241-7. doi: 10.1038/leu.2013.336. Epub 2013 Nov 13. PMID: 24220272; PMCID: PMC3918868.

138. Han, Y.;Wang, H.; Shao, Z. Monocyte-Derived Macrophages Are Impaired in Myelodysplastic Syndrome. J. Immunol. Res. 2016,2016, 5479013.

139. Harms KL, Chen X. The functional domains in p53 family proteins exhibit both common and distinct properties. Cell Death Differ. 2006 Jun;13(6):890-7. doi: 10.1038/sj.cdd.4401904. PMID: 16543939.

140. Haroun F, Solola SA, Nassereddine S, Tabbara I. PD-1 signaling and inhibition in AML and MDS. Ann Hematol. 2017 Sep;96(9):1441-1448. doi: 10.1007/s00277-017-3051-5. Epub 2017 Jun 22. PMID: 28643044.

141. Hejazi M, Manser AR, Fröbel J, Kündgen A, Zhao X, Schönberg K, Germing U, Haas R, Gattermann N, Uhrberg M. Impaired cytotoxicity associated with defective natural killer cell differentiation in myelodysplastic syndromes. Haematologica. 2015 May;100(5):643-52. doi: 10.3324/haematol.2014.118679. Epub 2015 Feb 14. PMID: 25682594; PMCID: PMC4420213.

142. Hellström-Lindberg E, Tobiasson M, Greenberg P. Myelodysplastic syndromes: moving towards personalized management. Haematologica. 2020 Jul;105(7):1765-1779. doi: 10.3324/haematol.2020.248955. Epub 2020 May 21. PMID: 32439724; PMCID: PMC7327628.

143. Heptinstall K; Myelodysplastic Syndromes Foundation, Inc. Quality of life in myelodysplastic syndromes. A special report from the Myelodysplastic Syndromes Foundation, Inc. Oncology (Williston Park). 2008 Feb;22(2 Suppl Nurse Ed):13-8; discussion 19. PMID: 18434977.

144. Ho NP, Takizawa H. Inflammation Regulates Haematopoietic Stem Cells and Their Niche. Int J Mol Sci. 2022 Jan 20;23(3):1125. doi: 10.3390/ijms23031125. PMID: 35163048; PMCID: PMC8835214.

145. Hofmann WK, de Vos S, Komor M, Hoelzer D, Wachsman W, Koeffler HP. Characterization of gene expression of CD34+ cells from normal and myelodysplastic bone marrow. Blood. 2002 Nov 15;100(10):3553-60. doi: 10.1182/blood.V100.10.3553. PMID: 12411319.

146. Huang CY, Ye ZH, Huang MY, Lu JJ. Regulation of CD47 expression in cancer cells. Transl Oncol. 2020 Dec;13(12):100862. doi: 10.1016/j.tranon.2020.100862. Epub 2020 Sep 10. PMID: 32920329; PMCID: PMC7494507.

147. Huang J, Liu F, Li C, Liang X, Li C, Liu Y, Yi Z, Zhang L, Fu S, Zeng Y. Role of CD47 in tumor immunity: a potential target for combination therapy. Sci Rep. 2022 Jun 13;12(1):9803. doi: 10.1038/s41598-022-13764-3. PMID: 35697717; PMCID: PMC9192775.

148. Huber S, Haferlach T, Meggendorfer M, Hutter S, Hoermann G, Baer C, Kern W, Haferlach C. SF3B1 mutated MDS: Blast count, genetic co-abnormalities and their impact on classification and prognosis. Leukemia. 2022 Dec;36(12):2894-2902. doi: 10.1038/s41375-022-01728-5. Epub 2022 Oct 19. PMID: 36261576; PMCID: PMC9712089.

149. Hulegårdh E, Nilsson C, Lazarevic V, Garelius H, Antunovic P, Rangert Derolf Å, Möllgård L, Uggla B, Wennström L, Wahlin A, Höglund M, Juliusson G, Stockelberg D, Lehmann S.

Characterization and prognostic features of secondary acute myeloid leukemia in a population-based setting: a report from the Swedish Acute Leukemia Registry. Am J Hematol. 2015 Mar;90(3):208-14. doi: 10.1002/ajh.23908. Epub 2015 Jan 16. PMID: 25421221.

150. Isidori A, Cerchione C, Daver N, DiNardo C, Garcia-Manero G, Konopleva M, Jabbour E, Ravandi F, Kadia T, Burguera AF, Romano A, Loscocco F, Visani G, Martinelli G, Kantarjian H, Curti A. Immunotherapy in Acute Myeloid Leukemia: Where We Stand. Front Oncol. 2021 May 10;11:656218. doi: 10.3389/fonc.2021.656218. PMID: 34041025; PMCID: PMC8143531.

151. Itzykson R, Fenaux P. Epigenetics of myelodysplastic syndromes. Leukemia. 2014 Mar;28(3):497-506. doi: 10.1038/leu.2013.343. Epub 2013 Nov 19. PMID: 24247656.

152. Itzykson R, Kosmider O, Cluzeau T, Mansat-De Mas V, Dreyfus F, Beyne-Rauzy O, Quesnel B, Vey N, Gelsi-Boyer V, Raynaud S, Preudhomme C, Adès L, Fenaux P, Fontenay M; Groupe Francophone des Myelodysplasies (GFM). Impact of TET2 mutations on response rate to azacitidine in myelodysplastic syndromes and low blast count acute myeloid leukemias. Leukemia. 2011 Jul;25(7):1147-52. doi: 10.1038/leu.2011.71. Epub 2011 Apr 15. PMID: 21494260.

153. Jabbour EJ, Garcia-Manero G, Strati P, Mishra A, Al Ali NH, Padron E, Lancet J, Kadia T, Daver N, O'Brien S, Steensma DP, Sekeres MA, Gore SD, Dezern A, Roboz GJ, List AF, Kantarjian HM, Komrokji RS. Outcome of patients with low-risk and intermediate-1-risk myelodysplastic syndrome after hypomethylating agent failure: a report on behalf of the MDS Clinical Research Consortium. Cancer. 2015 Mar 15;121(6):876-82. doi: 10.1002/cncr.29145. Epub 2014 Nov 19. PMID: 25410759; PMCID: PMC4378905.

154. Jädersten M, Saft L, Smith A, Kulasekararaj A, Pomplun S, Göhring G, Hedlund A, Hast R, Schlegelberger B, Porwit A, Hellström-Lindberg E, Mufti GJ. TP53 mutations in low-risk myelodysplastic syndromes with del(5q) predict disease progression. J Clin Oncol. 2011 May 20;29(15):1971-9. doi: 10.1200/JCO.2010.31.8576. Epub 2011 Apr 25. PMID: 21519010.

155. Jaiswal S, Fontanillas P, Flannick J, Manning A, Grauman PV, Mar BG, Lindsley RC, Mermel CH, Burtt N, Chavez A, Higgins JM, Moltchanov V, Kuo FC, Kluk MJ, Henderson B, Kinnunen L, Koistinen HA, Ladenvall C, Getz G, Correa A, Banahan BF, Gabriel S, Kathiresan S, Stringham HM, McCarthy MI, Boehnke M, Tuomilehto J, Haiman C, Groop L, Atzmon G, Wilson JG, Neuberg D, Altshuler D, Ebert BL. Age-related clonal hematopoiesis associated with adverse outcomes. N Engl J Med. 2014 Dec 25;371(26):2488-98. doi: 10.1056/NEJMoa1408617. Epub 2014 Nov 26. PMID: 25426837; PMCID: PMC4306669.

156. Janssens R, Struyf S, Proost P. The unique structural and functional features of CXCL12. Cell Mol Immunol. 2018 Apr;15(4):299-311. doi: 10.1038/cmi.2017.107. Epub 2017 Oct 30. PMID: 29082918; PMCID: PMC6052832.

157. Jasielec J, Saloura V, Godley LA. The mechanistic role of DNA methylation in myeloid leukemogenesis. Leukemia. 2014 Sep;28(9):1765-73. doi: 10.1038/leu.2014.163. Epub 2014 May 20. PMID: 24913729.

158. Jiang Y, Dunbar A, Gondek LP, Mohan S, Rataul M, O'Keefe C, Sekeres M, Saunthararajah Y, Maciejewski JP. Aberrant DNA methylation is a dominant mechanism in MDS progression to AML. Blood. 2009 Feb 5;113(6):1315-25. doi: 10.1182/blood-2008-06-163246. Epub 2008 Oct 2. PMID: 18832655; PMCID: PMC2637194.

159. Jilg S, Reidel V, Müller-Thomas C, et al. Blockade of BCL-2 proteins efficiently induces apoptosis in progenitor cells of high-risk myelodysplastic syndromes patients. Leukemia. 2016;30(1):112-123.

160. Jitschin R, Braun M, Büttner M, Dettmer-Wilde K, Bricks J, Berger J, Eckart MJ, Krause SW,. Oefner PJ, Le Blanc K, Mackensen A, Mougiakakos D; CLL-cells induce IDOhi CD14+HLA-DRlo myeloid-derived suppressor cells that inhibit T-cell responses and promote TRegs. Blood 2014; 124 (5): 750–760. doi: https://doi.org/10.1182/blood-2013-12-546416

161. Johnson DE, O'Keefe RA, Grandis JR. Targeting the IL-6/JAK/STAT3 signalling axis in cancer. Nat Rev Clin Oncol. 2018;15(4):234-248.
162. Jonas BA, Greenberg PL. MDS prognostic scoring systems – past, present, and future. Best Pract Res Clin Haematol. 2015 Mar;28(1):3-13. doi: 10.1016/j.beha.2014.11.001. Epub 2014 Nov 11. PMID: 25659725; PMCID: PMC4324398.
163. Jones PA, Baylin SB. The fundamental role of epigenetic events in cancer. Nat Rev Genet. 2002 Jun;3(6):415-28. doi: 10.1038/nrg816. PMID: 12042769.
164. Jones PA, Baylin SB. The Epigenomics of Cancer. Cell. 2007 Feb;128(4):683-92. doi:https://doi.org/10.1016/j.cell.2007.01.029
165. Jumniensuk C, Nobori A, Lee T, Senaratne TN, Rao D, Pullarkat S. Concordance of Peripheral Blood and Bone Marrow Next-Generation Sequencing in Hematologic Neoplasms. Adv Hematol. 2022 Mar 26;2022:8091746. doi: 10.1155/2022/8091746. PMID: 35378848; PMCID: PMC8976630.
166. Jung SH, Kim YJ, Yim SH, Kim HJ, Kwon YR, Hur EH, Goo BK, Choi YS, Lee SH, Chung YJ, Lee JH. Somatic mutations predict outcomes of hypomethylating therapy in patients with myelodysplastic syndrome. Oncotarget. 2016 Aug 23;7(34):55264-55275. doi: 10.18632/oncotarget.10526. PMID: 27419369; PMCID: PMC5342416.
167. Jüttermann R, Li E, Jaenisch R. Toxicity of 5-aza-2'-deoxycytidine to mammalian cells is mediated primarily by covalent trapping of DNA methyltransferase rather than DNA demethylation. Proc Natl Acad Sci U S A. 1994 Dec 6;91(25):11797-801. doi: 10.1073/pnas.91.25.11797. PMID: 7527544; PMCID: PMC45322.
168. Kantarjian H, Issa JP, Rosenfeld CS, Bennett JM, Albitar M, DiPersio J, Klimek V, Slack J, de Castro C, Ravandi F, Helmer R 3rd, Shen L, Nimer SD, Leavitt R, Raza A, Saba H. Decitabine improves patient outcomes in myelodysplastic syndromes: results of a phase III randomized study. Cancer. 2006 Apr 15;106(8):1794-803. doi: 10.1002/cncr.21792. PMID: 16532500.
169. Kantarjian H, O'Brien S, Ravandi F, Cortes J, Shan J, Bennett JM, List A, Fenaux P, Sanz G, Issa JP, Freireich EJ, Garcia-Manero G. Proposal for a new risk model in myelodysplastic syndrome that accounts for events not considered in the original International Prognostic Scoring System. Cancer. 2008 Sep 15;113(6):1351-61. doi: 10.1002/cncr.23697. PMID: 18618511; PMCID: PMC4188533.
170. Kapellos TS, Bonaguro L, Gemünd I, Reusch N, Saglam A, Hinkley ER, Schultze JL. Human Monocyte Subsets and Phenotypes in Major Chronic Inflammatory Diseases. Front Immunol. 2019 Aug 30;10:2035. doi: 10.3389/fimmu.2019.02035. PMID: 31543877; PMCID: PMC6728754.
171. Kerns BJ, Jordan PA, Moore MB, Humphrey PA, Berchuck A, Kohler MF, Bast RC Jr, Iglehart JD, Marks JR. p53 overexpression in formalin-fixed, paraffin-embedded tissue detected by immunohistochemistry. J Histochem Cytochem. 1992 Jul;40(7):1047-51. doi: 10.1177/40.7.1607637. PMID: 1607637.
172. Kewan T, Bahaj W, Durmaz A, Aly M, Ogbue OD, Carraway HE, Sekeres MA, Visconte V, Gurnari C, Maciejewski JP. Validation of the Molecular International Prognostic Scoring System in patients with myelodysplastic syndromes. Blood. 2023 Apr 6;141(14):1768-1772. doi: 10.1182/blood.2022018896. PMID: 36720101.
173. Khaznadar Z, Boissel N, Agaugué S, Henry G, Cheok M, Vignon M, Geromin D, Cayuela JM, Castaigne S, Pautas C, Raffoux E, Lachuer J, Sigaux F, Preudhomme C, Dombret H, Dulphy N, Toubert A. Defective NK Cells in Acute Myeloid Leukemia Patients at Diagnosis Are Associated with Blast Transcriptional Signatures of Immune Evasion. J Immunol. 2015 Sep 15;195(6):2580-90. doi: 10.4049/jimmunol.1500262. Epub 2015 Aug 5. PMID: 26246143.
174. Khoury JD, Solary E, Abla O, Akkari Y, Alaggio R, Apperley JF, Bejar R, Berti E, Busque L, Chan JKC, Chen W, Chen X, Chng WJ, Choi JK, Colmenero I, Coupland SE, Cross NCP, De Jong D, Elghetany MT, Takahashi E, Emile JF, Ferry J, Fogelstrand L, Fontenay M, Germing U, Gujral S, Haferlach T, Harrison C, Hodge JC, Hu S, Jansen JH, Kanagal-Shamanna R, Kantarjian HM, Kratz CP, Li XQ, Lim MS,

Loeb K, Loghavi S, Marcogliese A, Meshinchi S, Michaels P, Naresh KN, Natkunam Y, Nejati R, Ott G, Padron E, Patel KP, Patkar N, Picarsic J, Platzbecker U, Roberts I, Schuh A, Sewell W, Siebert R, Tembhare P, Tyner J, Verstovsek S, Wang W, Wood B, Xiao W, Yeung C, Hochhaus A. The 5th edition of the World Health Organization Classification of Haematolymphoid Tumours: Myeloid and Histiocytic/Dendritic Neoplasms. Leukemia. 2022 Jul;36(7):1703-1719. doi: 10.1038/s41375-022-01613-1. Epub 2022 Jun 22. PMID: 35732831; PMCID: PMC9252913.

175. Kikushige Y, Miyamoto T, Yuda J, Jabbarzadeh-Tabrizi S, Shima T, Takayanagi S, Niiro H, Yurino A, Miyawaki K, Takenaka K, Iwasaki H, Akashi K. A TIM-3/Gal-9 Autocrine Stimulatory Loop Drives Self-Renewal of Human Myeloid Leukemia Stem Cells and Leukemic Progression. Cell Stem Cell. 2015 Sep 3;17(3):341-52. doi: 10.1016/j.stem.2015.07.011. Epub 2015 Aug 13. PMID: 26279267.

176. Kim K, Skora AD, Li Z, Liu Q, Tam AJ, Blosser RL, Diaz LA Jr, Papadopoulos N, Kinzler KW, Vogelstein B, Zhou S. Eradication of metastatic mouse cancers resistant to immune checkpoint blockade by suppression of myeloid-derived cells. Proc Natl Acad Sci U S A. 2014 Aug 12;111(32):11774-9. doi: 10.1073/pnas.1410626111. Epub 2014 Jul 28. PMID: 25071169; PMCID: PMC4136565.

177. Kim T, Tyndel MS, Kim HJ, Ahn JS, Choi SH, Park HJ, Kim YK, Yang DH, Lee JJ, Jung SH, Kim SY, Min YH, Cheong JW, Sohn SK, Moon JH, Choi M, Lee M, Zhang Z, Kim DDH. The clonal origins of leukemic progression of myelodysplasia. Leukemia. 2017 Sep;31(9):1928-1935. doi: 10.1038/leu.2017.17. Epub 2017 Jan 16. PMID: 28090092.

178. Kittang AO, Kordasti S, Sand KE, Costantini B, Kramer AM, Perezabellan P, Seidl T, Rye KP, Hagen KM, Kulasekararaj A, Bruserud Ø, Mufti GJ. Expansion of myeloid derived suppressor cells correlates with number of T regulatory cells and disease progression in myelodysplastic syndrome. Oncoimmunology. 2015 Jun 24;5(2):e1062208. doi: 10.1080/2162402X.2015.1062208. PMID: 27057428; PMCID: PMC4801428.

179. Klar AS, Gopinadh J, Kleber S, Wadle A, Renner C. Treatment with 5-Aza-2'-Deoxycytidine Induces Expression of NY-ESO-1 and Facilitates Cytotoxic T Lymphocyte-Mediated Tumor Cell Killing. PLoS One. 2015 Oct 8;10(10):e0139221. doi: 10.1371/journal.pone.0139221. PMID: 26447882; PMCID: PMC4598131.

180. Klco JM, Spencer DH, Lamprecht TL, Sarkaria SM, Wylie T, Magrini V, Hundal J, Walker J, Varghese N, Erdmann-Gilmore P, Lichti CF, Meyer MR, Townsend RR, Wilson RK, Mardis ER, Ley TJ. Genomic impact of transient low-dose decitabine treatment on primary AML cells. Blood. 2013 Feb 28;121(9):1633-43. doi: 10.1182/blood-2012-09-459313. Epub 2013 Jan 7. PMID: 23297133; PMCID: PMC3587326.

181. Komrokji RS, Kulasekararaj A, Al Ali NH, Kordasti S, Bart-Smith E, Craig BM, Padron E, Zhang L, Lancet JE, Pinilla-Ibarz J, List AF, Mufti GJ, Epling-Burnette PK. Autoimmune diseases and myelodysplastic syndromes. Am J Hematol. 2016 May;91(5):E280-3. doi: 10.1002/ajh.24333. Epub 2016 Apr 4. PMID: 26875020.

182. Komrokji R.S., Najla Al Ali, Somedeb Ball, Onyee Chan, Andrew Kuykendall, Kendra Sweet, Jeffrey E. Lancet, Eric Padron, David A. Sallman; Luspatercept for Treatment of Lower Risk Myelodysplastic Syndromes: Real World Data Replicates Medalist Study Results and Confirms Activity Among Hypomethylating Agents and Lenalidomide Treated Patients. Blood 2022; 140 (Supplement 1): 4039–4041. doi: https://doi.org/10.1182/blood-2022-169690

183. Komrokji RS, Singh AM, Ali NA, Chan O, Padron E, Sweet K, Kuykendall A, Lancet JE, Sallman DA. Assessing the role of venetoclax in combination with hypomethylating agents in higher risk myelodysplastic syndrome. Blood Cancer J. 2022 Nov 4;12(11):148. doi: 10.1038/s41408-022-00744-z. PMID: 36329025; PMCID: PMC9633639.

184. Kopp LM, Ray A, Denman CJ, Senyukov VS, Somanchi SS, Zhu S, Lee DA. Decitabine has a biphasic effect on natural killer cell viability, phenotype, and function under proliferative conditions.

Mol Immunol. 2013 Jul;54(3-4):296-301. doi: 10.1016/j.molimm.2012.12.012. Epub 2013 Jan 16. PMID: 23328088.

185. Kordasti SY, Ingram W, Hayden J, Darling D, Barber L, Afzali B, Lombardi G, Wlodarski MW, Maciejewski JP, Farzaneh F, Mufti GJ. CD4+CD25high Foxp3+ regulatory T cells in myelodysplastic syndrome (MDS). Blood. 2007 Aug 1;110(3):847-50. doi: 10.1182/blood-2007-01-067546. Epub 2007 Apr 5. PMID: 17412885.

186. Kordasti SY, Afzali B, Lim Z, Ingram W, Hayden J, Barber L, Matthews K, Chelliah R, Guinn B, Lombardi G, Farzaneh F, Mufti GJ. IL-17-producing CD4(+) T cells, pro-inflammatory cytokines and apoptosis are increased in low risk myelodysplastic syndrome. Br J Haematol. 2009 Apr;145(1):64-72. doi: 10.1111/j.1365-2141.2009.07593.x. Epub 2009 Feb 3. PMID: 19210506.

187. Kotsianidis I, Bouchliou I, Nakou E, Spanoudakis E, Margaritis D, Christophoridou AV, Anastasiades A, Tsigalou C, Bourikas G, Karadimitris A, Tsatalas C. Kinetics, function and bone marrow trafficking of CD4+CD25+FOXP3+ regulatory T cells in myelodysplastic syndromes (MDS). Leukemia. 2009 Mar;23(3):510-8. doi: 10.1038/leu.2008.333. Epub 2008 Nov 20. PMID: 19020538.

188. Kröger N, Iacobelli S, Franke GN, Platzbecker U, Uddin R, Hübel K, Scheid C, Weber T, Robin M, Stelljes M, Afanasyev B, Heim D, Deliliers GL, Onida F, Dreger P, Pini M, Guidi S, Volin L, Günther A, Bethge W, Poiré X, Kobbe G, van Os M, Brand R, de Witte T. Dose-Reduced Versus Standard Conditioning Followed by Allogeneic Stem-Cell Transplantation for Patients With Myelodysplastic Syndrome: A Prospective Randomized Phase III Study of the EBMT (RICMAC Trial). J Clin Oncol. 2017 Jul 1;35(19):2157-2164. doi: 10.1200/JCO.2016.70.7349. Epub 2017 May 2. PMID: 28463633.

189. Kubasch AS, Fenaux P, Platzbecker U. Development of luspatercept to treat ineffective erythropoiesis. Blood Adv. 2021 Mar 9;5(5):1565-1575. doi: 10.1182/bloodadvances.2020002177. PMID: 33687432; PMCID: PMC7948289.

190. Kuendgen A, Müller-Thomas C, Lauseker M, Haferlach T, Urbaniak P, Schroeder T, Brings C, Wulfert M, Meggendorfer M, Hildebrandt B, Betz B, Royer-Pokora B, Gattermann N, Haas R, Germing U, Götze KS. Efficacy of azacitidine is independent of molecular and clinical characteristics - an analysis of 128 patients with myelodysplastic syndromes or acute myeloid leukemia and a review of the literature. Oncotarget. 2018 Jun 12;9(45):27882-27894. doi: 10.18632/oncotarget.25328. PMID: 29963245; PMCID: PMC6021252.

191. Kulasekararaj AG, Smith AE, Mian SA, Mohamedali AM, Krishnamurthy P, Lea NC, Gäken J, Pennaneach C, Ireland R, Czepulkowski B, Pomplun S, Marsh JC, Mufti GJ. TP53 mutations in myelodysplastic syndrome are strongly correlated with aberrations of chromosome 5, and correlate with adverse prognosis. Br J Haematol. 2013 Mar;160(5):660-72. doi: 10.1111/bjh.12203. Epub 2013 Jan 9. PMID: 23297687.

192. Kumar MS, Narla A, Nonami A, Mullally A, Dimitrova N, Ball B, McAuley JR, Poveromo L, Kutok JL, Galili N, Raza A, Attar E, Gilliland DG, Jacks T, Ebert BL. Coordinate loss of a microRNA and protein-coding gene cooperate in the pathogenesis of 5q- syndrome. Blood. 2011 Oct 27;118(17):4666-73. doi: 10.1182/blood-2010-12-324715. Epub 2011 Aug 26. PMID: 21873545; PMCID: PMC3208282.

193. Kwon YR, Kim HJ, Sohn MJ, Lim JY, Park KS, Lee S, Chung NG, Jeong DC, Min CK, Kim YJ. Effects of decitabine on allogeneic immune reactions of donor lymphocyte infusion via activation of dendritic cells. Exp Hematol Oncol. 2020 Sep 3;9:22. doi: 10.1186/s40164-020-00178-y. PMID: 32908796; PMCID: PMC7470611.

194. Lambert JM, Gorzov P, Veprintsev DB, Söderqvist M, Segerbäck D, Bergman J, Fersht AR, Hainaut P, Wiman KG, Bykov VJ. PRIMA-1 reactivates mutant p53 by covalent binding to the core domain. Cancer Cell. 2009 May 5;15(5):376-88. doi: 10.1016/j.ccr.2009.03.003. PMID: 19411067.

195. Lamprianidou E, Kordella C, Kazachenka A, Zoulia E, Bernard E, Filia A, Laidou S, Garantziotis P, Vassilakopoulos TP, Papageorgiou SG, Pappa V, Galanopoulos AG, Viniou N, Nakou E, Kalafati L, Chatzidimitriou A, Kassiotis G, Papaemmanuil E, Mitroulis I, Kotsianidis I. Modulation of IL-6/STAT3

signaling axis in CD4+FOXP3- T cells represents a potential antitumor mechanism of azacitidine. Blood Adv. 2021 Jan 12;5(1):129-142. doi: 10.1182/bloodadvances.2020002351. PMID: 33570632; PMCID: PMC7805308.

196. Lane AA, Sweet KL, Wang ESW, Donnellan WB, Walter RB, Stein AS, et al.. Results from Ongoing Phase 2 Trial of SL-401 As Consolidation Therapy in Patients with Acute Myeloid Leukemia (AML) in Remission with High Relapse Risk Including Minimal Residual Disease (MRD). Blood (2016) 128:215. 10.1182/blood.V128.22.215.215

197. Lechner MG, Liebertz DJ, Epstein AL. Characterization of cytokine-induced myeloid-derived suppressor cells from normal human peripheral blood mononuclear cells. J Immunol. 2010 Aug 15;185(4):2273-84. doi: 10.4049/jimmunol.1000901. Epub 2010 Jul 19. Erratum in: J Immunol. 2010 Nov 1;185(9):5668. PMID: 20644162; PMCID: PMC2923483.

198. Lee S, Kim HS, Roh KH, Lee BC, Shin TH, Yoo JM, Kim YL, Yu KR, Kang KS, Seo KW. DNA methyltransferase inhibition accelerates the immunomodulation and migration of human mesenchymal stem cells. Sci Rep. 2015 Jan 26;5:8020. doi: 10.1038/srep08020. PMID: 25620445; PMCID: PMC4306122.

199. Lee YG, Kim I, Yoon SS, Park S, Cheong JW, Min YH, Lee JO, Bang SM, Yi HG, Kim CS, Park Y, Kim BS, Mun YC, Seong CM, Park J, Lee JH, Kim SY, Lee HG, Kim YK, Kim HJ; Korean Society of Haematology AML/MDS working party. Comparative analysis between azacitidine and decitabine for the treatment of myelodysplastic syndromes. Br J Haematol. 2013 May;161(3):339-47. doi: 10.1111/bjh.12256. Epub 2013 Feb 21. PMID: 23432512.

200. Legros L, Slama B, Karsenti JM, Vey N, Natarajan-Amé S, Watel E, Richard B, Bouabdallah K, Mannone L, Benchetrit M, Touitou I, Huault S, Durivault J, Ambroseti D, Hueber AO, Fenaux P, Dreyfus F; Groupe Francophone des Myélodysplasies. Treatment of myelodysplastic syndromes with excess of blasts by bevacizumab is well tolerated and is associated with a decrease of VEGF plasma level. Ann Hematol. 2012 Jan;91(1):39-46. doi: 10.1007/s00277-011-1242-z. Epub 2011 May 7. PMID: 21553011.

201. Li H, Hu F, Gale RP, Sekeres MA, Liang Y. Myelodysplastic syndromes. Nat Rev Dis Primers. 2022 Nov 17;8(1):74. doi: 10.1038/s41572-022-00402-5. PMID: 36396662.

202. Li J, Yue L, Wang H, Liu C, Liu H, Tao J, Qi W, Wang Y, Zhang W, Fu R, Shao Z. Th17 Cells Exhibit Antitumor Effects in MDS Possibly through Augmenting Functions of CD8+ T Cells. J Immunol Res. 2016;2016:9404705. doi: 10.1155/2016/9404705. Epub 2016 Sep 19. PMID: 27722177; PMCID: PMC5046048.

203. Li K, Shi H, Zhang B, Ou X, Ma Q, Chen Y, Shu P, Li D, Wang Y. Myeloid-derived suppressor cells as immunosuppressive regulators and therapeutic targets in cancer. Signal Transduct Target Ther. 2021 Oct 7;6(1):362. doi: 10.1038/s41392-021-00670-9. PMID: 34620838; PMCID: PMC8497485.

204. Lindblad KE, Goswami M, Hourigan CS, Oetjen KA. Immunological effects of hypomethylating agents. Expert Rev Hematol. 2017 Aug;10(8):745-752. doi: 10.1080/17474086.2017.1346470. Epub 2017 Jul 3. PMID: 28644756; PMCID: PMC6071309.

205. Lindsley C, Ebert B.L. The biology and clinical impact of genetic lesions in myeloid malignancies. Blood. 2013 Nov; 122(23): 3741-3748. doi: 10.1182/blood-2013-06-460295

206. Lindsley RC, Saber W, Mar BG, Redd R, Wang T, Haagenson MD, Grauman PV, Hu ZH, Spellman SR, Lee SJ, Verneris MR, Hsu K, Fleischhauer K, Cutler C, Antin JH, Neuberg D, Ebert BL. Prognostic Mutations in Myelodysplastic Syndrome after Stem-Cell Transplantation. N Engl J Med. 2017 Feb 9;376(6):536-547. doi: 10.1056/NEJMoa1611604. PMID: 28177873; PMCID: PMC5438571.

207. Liu W, Zhou Z, Chen L, Wang X. Comparison of Azacitidine and Decitabine in Myelodysplastic Syndromes and Acute Myeloid Leukemia: A Network Meta-analysis. Clin Lymphoma Myeloma Leuk. 2021 Jun;21(6):e530-e544. doi: 10.1016/j.clml.2021.01.024. Epub 2021 Feb 24. PMID: 33716056.

208. Liu YC, Kwon J, Fabiani E, Xiao Z, Liu YV, Follo MY, Liu J, Huang H, Gao C, Liu J, Falconi G, Valentini L, Gurnari C, Finelli C, Cocco L, Liu JH, Jones AI, Yang J, Yang H, Thoms JAI, Unnikrishnan A, Pimanda JE, Pan R, Bassal MA, Voso MT, Tenen DG, Chai L. Demethylation and Up-Regulation of an Oncogene after Hypomethylating Therapy. N Engl J Med. 2022 May 26;386(21):1998-2010. doi: 10.1056/NEJMoa2119771. PMID: 35613022; PMCID: PMC9514878.
209. Lopes MR, Traina F, Campos Pde M, Pereira JK, Machado-Neto JA, Machado Hda C, Gilli SC, Saad ST, Favaro P. IL10 inversely correlates with the percentage of $CD8^+$ cells in MDS patients. Leuk Res. 2013 May;37(5):541-6. doi: 10.1016/j.leukres.2013.01.019. Epub 2013 Feb 28. PMID: 23453286.
210. López-Otín C, Blasco MA, Partridge L, Serrano M, Kroemer G. The hallmarks of aging. Cell. 2013 Jun 6;153(6):1194-217. doi: 10.1016/j.cell.2013.05.039. PMID: 23746838; PMCID: PMC3836174.
211. Lübbert M, Suciu S, Baila L, Rüter BH, Platzbecker U, Giagounidis A, Selleslag D, Labar B, Germing U, Salih HR, Beeldens F, Muus P, Pflüger KH, Coens C, Hagemeijer A, Eckart Schaefer H, Ganser A, Aul C, de Witte T, Wijermans PW. Low-dose decitabine versus best supportive care in elderly patients with intermediate- or high-risk myelodysplastic syndrome (MDS) ineligible for intensive chemotherapy: final results of the randomized phase III study of the European Organisation for Research and Treatment of Cancer Leukemia Group and the German MDS Study Group. J Clin Oncol. 2011 May 20;29(15):1987-96. doi: 10.1200/JCO.2010.30.9245. Epub 2011 Apr 11. PMID: 21483003.
212. Lübbert M, Wijermans P, Kunzmann R, Verhoef G, Bosly A, Ravoet C, Andre M, Ferrant A. Cytogenetic responses in high-risk myelodysplastic syndrome following low-dose treatment with the DNA methylation inhibitor 5-aza-2'-deoxycytidine. Br J Haematol. 2001 Aug;114(2):349-57. doi: 10.1046/j.1365-2141.2001.02933.x. PMID: 11529854.
213. Lübbert M, Bertz H, Wäsch R, Marks R, Rüter B, Claus R, Finke J. Efficacy of a 3-day, low-dose treatment with 5-azacytidine followed by donor lymphocyte infusions in older patients with acute myeloid leukemia or chronic myelomonocytic leukemia relapsed after allografting. Bone Marrow Transplant. 2010 Apr;45(4):627-32. doi: 10.1038/bmt.2009.222. Epub 2009 Aug 31. PMID: 19718057.
214. Lucas F, Michaels PD, Wang D, Kim AS. Mutational analysis of hematologic neoplasms in 164 paired peripheral blood and bone marrow samples by next-generation sequencing. Blood Adv. 2020 Sep 22;4(18):4362-4365. doi: 10.1182/bloodadvances.2020002306. PMID: 32926123; PMCID: PMC7509881.
215. Luo N, Nixon MJ, Gonzalez-Ericsson PI, Sanchez V, Opalenik SR, Li H, Zahnow CA, Nickels ML, Liu F, Tantawy MN, Sanders ME, Manning HC, Balko JM. DNA methyltransferase inhibition upregulates MHC-I to potentiate cytotoxic T lymphocyte responses in breast cancer. Nat Commun. 2018 Jan 16;9(1):248. doi: 10.1038/s41467-017-02630-w. PMID: 29339738; PMCID: PMC5770411.
216. Luquette LJ, Bohrson CL, Sherman MA, Park PJ. Identification of somatic mutations in single cell DNA-seq using a spatial model of allelic imbalance. Nat Commun. 2019 Aug 29;10(1):3908. doi: 10.1038/s41467-019-11857-8. PMID: 31467286; PMCID: PMC6715686.
217. Lv J, Zhao Y, Zong H, Ma G, Wei X, Zhao Y. Increased Levels of Circulating Monocytic- and Early-Stage Myeloid-Derived Suppressor Cells (MDSC) in Acute Myeloid Leukemia. Clin Lab. 2021 Mar 1;67(3). doi: 10.7754/Clin.Lab.2020.200719. PMID: 33739029.
218. Ma L, Delforge M, van Duppen V, Verhoef G, Emanuel B, Boogaerts M, Hagemeijer A, Vandenberghe P. Circulating myeloid and lymphoid precursor dendritic cells are clonally involved in myelodysplastic syndromes. Leukemia. 2004 Sep;18(9):1451-6. doi: 10.1038/sj.leu.2403430. PMID: 15284864.
219. Ma L, Ceuppens J, Kasran A, Delforge M, Boogaerts M, Vandenberghe P. Immature and mature monocyte-derived dendritic cells in myelodysplastic syndromes of subtypes refractory

anemia or refractory anemia with ringed sideroblasts display an altered cytokine profile. Leuk Res. 2007 Oct;31(10):1373-82. doi: 10.1016/j.leukres.2006.11.007. Epub 2006 Dec 22. PMID: 17188353.

220. Ma X, Does M, Raza A, Mayne ST. Myelodysplastic syndromes: incidence and survival in the United States. Cancer. 2007 Apr 15;109(8):1536-42. doi: 10.1002/cncr.22570. PMID: 17345612.

221. Maffei R, Bulgarelli J, Fiorcari S, Bertoncelli L, Martinelli S, Guarnotta C, Castelli I, Deaglio S, Debbia G, De Biasi S, Bonacorsi G, Zucchini P, Narni F, Tripodo C, Luppi M, Cossarizza A, Marasca R. The monocytic population in chronic lymphocytic leukemia shows altered composition and deregulation of genes involved in phagocytosis and inflammation. Haematologica. 2013 Jul;98(7):1115-23. doi: 10.3324/haematol.2012.073080. Epub 2013 Jan 24. PMID: 23349302; PMCID: PMC3696616.

222. Makishima H, Visconte V, Sakaguchi H, Jankowska AM, Abu Kar S, Jerez A, Przychodzen B, Bupathi M, Guinta K, Afable MG, Sekeres MA, Padgett RA, Tiu RV, Maciejewski JP. Mutations in the spliceosome machinery, a novel and ubiquitous pathway in leukemogenesis. Blood. 2012 Apr 5;119(14):3203-10. doi: 10.1182/blood-2011-12-399774. Epub 2012 Feb 9. PMID: 22323480; PMCID: PMC3321850.

223. Makishima H, Yoshizato T, Yoshida K, Sekeres MA, Radivoyevitch T, Suzuki H, Przychodzen B, Nagata Y, Meggendorfer M, Sanada M, Okuno Y, Hirsch C, Kuzmanovic T, Sato Y, Sato-Otsubo A, LaFramboise T, Hosono N, Shiraishi Y, Chiba K, Haferlach C, Kern W, Tanaka H, Shiozawa Y, Gómez-Seguí I, Husseinzadeh HD, Thota S, Guinta KM, Dienes B, Nakamaki T, Miyawaki S, Saunthararajah Y, Chiba S, Miyano S, Shih LY, Haferlach T, Ogawa S, Maciejewski JP. Dynamics of clonal evolution in myelodysplastic syndromes. Nat Genet. 2017 Feb;49(2):204-212. doi: 10.1038/ng.3742. Epub 2016 Dec 19. PMID: 27992414; PMCID: PMC8210656.

224. Malcovati L, Germing U, Kuendgen A, Della Porta MG, Pascutto C, Invernizzi R, Giagounidis A, Hildebrandt B, Bernasconi P, Knipp S, Strupp C, Lazzarino M, Aul C, Cazzola M. Time-dependent prognostic scoring system for predicting survival and leukemic evolution in myelodysplastic syndromes. J Clin Oncol. 2007 Aug 10;25(23):3503-10. doi: 10.1200/JCO.2006.08.5696. PMID: 17687155.

225. Malcovati, L., Papaemmanuil, E., Bowen, D.T., Boultwood, J., Della Porta, M.G., Pascutto, C., Travaglino, E., Groves, M.J., Godfrey, A.L., Ambaglio, I., Gallì, A., DaVi`a, M.C., Conte, S., Tauro, S., Keenan, N., Hyslop, A., Hinton, J., Mudie, L.J., Wainscoat, J.S., Futreal, P.A., Stratton, M.R., Campbell, P.J., Hellstr¨om-Lindberg, E., Cazzola, M., Chronic Myeloid Disorders Working Group of the International Cancer Genome Consortium and of the Associazione Italiana per la Ricerca sul CancroGruppo Italiano Malattie Mieloproliferative, 2011. Clinical significance of SF3B1 mutations in myelodysplastic syndromes and myelodysplastic/myeloproliferative neoplasms. Blood 118, 6239–6246.

226. Malcovati L, Gallì A, Travaglino E, Ambaglio I, Rizzo E, Molteni E, Elena C, Ferretti VV, Catricalà S, Bono E, Todisco G, Bianchessi A, Rumi E, Zibellini S, Pietra D, Boveri E, Camaschella C, Toniolo D, Papaemmanuil E, Ogawa S, Cazzola M. Clinical significance of somatic mutation in unexplained blood cytopenia. Blood. 2017 Jun 22;129(25):3371-3378. doi: 10.1182/blood-2017-01-763425. Epub 2017 Apr 19. PMID: 28424163; PMCID: PMC5542849.

227. Malcovati L, Karimi M, Papaemmanuil E, Ambaglio I, Jädersten M, Jansson M, Elena C, Gallì A, Walldin G, Della Porta MG, Raaschou-Jensen K, Travaglino E, Kallenbach K, Pietra D, Ljungström V, Conte S, Boveri E, Invernizzi R, Rosenquist R, Campbell PJ, Cazzola M, Hellström Lindberg E. SF3B1 mutation identifies a distinct subset of myelodysplastic syndrome with ring sideroblasts. Blood. 2015 Jul 9;126(2):233-41. doi: 10.1182/blood-2015-03-633537. Epub 2015 May 8. PMID: 25957392; PMCID: PMC4528082.

228. Malcovati L, Stevenson K, Papaemmanuil E, Neuberg D, Bejar R, Boultwood J, Bowen DT, Campbell PJ, Ebert BL, Fenaux P, Haferlach T, Heuser M, Jansen JH, Komrokji RS, Maciejewski JP,

Walter MJ, Fontenay M, Garcia-Manero G, Graubert TA, Karsan A, Meggendorfer M, Pellagatti A, Sallman DA, Savona MR, Sekeres MA, Steensma DP, Tauro S, Thol F, Vyas P, Van de Loosdrecht AA, Haase D, Tüchler H, Greenberg PL, Ogawa S, Hellstrom-Lindberg E, Cazzola M. SF3B1-mutant MDS as a distinct disease subtype: a proposal from the International Working Group for the Prognosis of MDS. Blood. 2020 Jul 9;136(2):157-170. doi: 10.1182/blood.2020004850. Erratum in: Blood. 2021 May 27;137(21):3003. PMID: 32347921; PMCID: PMC7362582.

229. Maratheftis CI, Andreakos E, Moutsopoulos HM, Voulgarelis M. Toll-like receptor-4 is up-regulated in hematopoietic progenitor cells and contributes to increased apoptosis in myelodysplastic syndromes. Clin Cancer Res. 2007 Feb 15;13(4):1154-60. doi: 10.1158/1078-0432.CCR-06-2108. PMID: 17317824.

230. Martinez-Høyer S, Deng Y, Parker J, Jiang J, Mo A, Docking TR, Gharaee N, Li J, Umlandt P, Fuller M, Jädersten M, Kulasekararaj A, Malcovati L, List AF, Hellström-Lindberg E, Platzbecker U, Karsan A. Loss of lenalidomide-induced megakaryocytic differentiation leads to therapy resistance in del(5q) myelodysplastic syndrome. Nat Cell Biol. 2020 May;22(5):526-533. doi: 10.1038/s41556-020-0497-9. Epub 2020 Apr 6. PMID: 32251398.

231. McGinley AM, Sutton CE, Edwards SC, Leane CM, DeCourcey J, Teijeiro A, Hamilton JA, Boon L, Djouder N, Mills KHG. Interleukin-17A Serves a Priming Role in Autoimmunity by Recruiting IL-1β-Producing Myeloid Cells that Promote Pathogenic T Cells. Immunity. 2020 Feb 18;52(2):342-356.e6. doi: 10.1016/j.immuni.2020.01.002. Epub 2020 Feb 4. PMID: 32023490.

232. McGraw KL, Nguyen J, Komrokji RS, Sallman D, Al Ali NH, Padron E, Lancet JE, Moscinski LC, List AF, Zhang L. Immunohistochemical pattern of p53 is a measure of TP53 mutation burden and adverse clinical outcome in myelodysplastic syndromes and secondary acute myeloid leukemia. Haematologica. 2016 Aug;101(8):e320-3. doi: 10.3324/haematol.2016.143214. Epub 2016 Apr 14. PMID: 27081179; PMCID: PMC4967580.

233. Medyouf H, Mossner M, Jann JC, Nolte F, Raffel S, Herrmann C, Lier A, Eisen C, Nowak V, Zens B, Müdder K, Klein C, Obländer J, Fey S, Vogler J, Fabarius A, Riedl E, Roehl H, Kohlmann A, Staller M, Haferlach C, Müller N, John T, Platzbecker U, Metzgeroth G, Hofmann WK, Trumpp A, Nowak D. Myelodysplastic cells in patients reprogram mesenchymal stromal cells to establish a transplantable stem cell niche disease unit. Cell Stem Cell. 2014 Jun 5;14(6):824-37. doi: 10.1016/j.stem.2014.02.014. Epub 2014 Apr 3. PMID: 24704494.

234. Mekinian A, Grignano E, Braun T, Decaux O, Liozon E, Costedoat-Chalumeau N, Kahn JE, Hamidou M, Park S, Puéchal X, Toussirot E, Falgarone G, Launay D, Morel N, Trouiller S, Mathian A, Gombert B, Schoindre Y, Lioger B, De Wazieres B, Amoura Z, Buchdaul AL, Georgin-Lavialle S, Dion J, Madaule S, Raffray L, Cathebras P, Piette JC, Rose C, Ziza JM, Lortholary O, Montestruc F, Omouri M, Denis G, Rossignol J, Nimubona S, Adès L, Gardin C, Fenaux P, Fain O. Systemic inflammatory and autoimmune manifestations associated with myelodysplastic syndromes and chronic myelomonocytic leukaemia: a French multicentre retrospective study. Rheumatology (Oxford). 2016 Feb;55(2):291-300. doi: 10.1093/rheumatology/kev294. Epub 2015 Sep 8. PMID: 26350487.

235. Meldi K, Qin T, Buchi F, Droin N, Sotzen J, Micol JB, Selimoglu-Buet D, Masala E, Allione B, Gioia D, Poloni A, Lunghi M, Solary E, Abdel-Wahab O, Santini V, Figueroa ME. Specific molecular signatures predict decitabine response in chronic myelomonocytic leukemia. J Clin Invest. 2015 May;125(5):1857-72. doi: 10.1172/JCI78752. Epub 2015 Mar 30. PMID: 25822018; PMCID: PMC4611703.

236. Méndez-Ferrer S, Bonnet D, Steensma DP, Hasserjian RP, Ghobrial IM, Gribben JG, Andreeff M, Krause DS. Bone marrow niches in haematological malignancies. Nat Rev Cancer. 2020 May;20(5):285-298. doi: 10.1038/s41568-020-0245-2. Epub 2020 Feb 28. PMID: 32112045; PMCID: PMC9912977.

237. Meng F, Li L, Lu F, Yue J, Liu Z, Zhang W, Fu R. Overexpression of TIGIT in NK and T Cells Contributes to Tumor Immune Escape in Myelodysplastic Syndromes. Front Oncol. 2020 Aug 7;10:1595. doi: 10.3389/fonc.2020.01595. PMID: 32903786; PMCID: PMC7438899.
238. Mengos AE, Gastineau DA, Gustafson MP. The CD14+HLA-DRlo/neg Monocyte: An Immunosuppressive Phenotype That Restrains Responses to Cancer Immunotherapy. Front Immunol. 2019 May 22;10:1147. doi: 10.3389/fimmu.2019.01147. PMID: 31191529; PMCID: PMC6540944.
239. Menssen AJ, Khanna A, Miller CA, Nonavinkere Srivatsan S, Chang GS, Shao J, Robinson J, O'Laughlin M, Fronick CC, Fulton RS, Brendel K, Heath SE, Saba R, Welch JS, Spencer DH, Payton JE, Westervelt P, DiPersio JF, Link DC, Schuelke MJ, Jacoby MA, Duncavage EJ, Ley TJ, Walter MJ. Convergent Clonal Evolution of Signaling Gene Mutations Is a Hallmark of Myelodysplastic Syndrome Progression. Blood Cancer Discov. 2022 Jul 6;3(4):330-345. doi: 10.1158/2643-3230.BCD-21-0155. PMID: 35709710; PMCID: PMC9338759.
240. Menssen AJ, Walter MJ. Genetics of progression from MDS to secondary leukemia. Blood. 2020 Jul 2;136(1):50-60. doi: 10.1182/blood.2019000942. PMID: 32430504; PMCID: PMC7332895.
241. Mercier FE, Ragu C, Scadden DT. The bone marrow at the crossroads of blood and immunity. Nat Rev Immunol. 2011 Dec 23;12(1):49-60. doi: 10.1038/nri3132. PMID: 22193770; PMCID: PMC4013788.
242. Metzeler KH, Walker A, Geyer S, Garzon R, Klisovic RB, Bloomfield CD, Blum W, Marcucci G. DNMT3A mutations and response to the hypomethylating agent decitabine in acute myeloid leukemia. Leukemia. 2012 May;26(5):1106-7. doi: 10.1038/leu.2011.342. Epub 2011 Nov 29. PMID: 22124213; PMCID: PMC3696987.
243. Mian SA, Smith AE, Kulasekararaj AG, Kizilors A, Mohamedali AM, Lea NC, Mitsopoulos K, Ford K, Nasser E, Seidl T, Mufti GJ. Spliceosome mutations exhibit specific associations with epigenetic modifiers and proto-oncogenes mutated in myelodysplastic syndrome. Haematologica. 2013 Jul;98(7):1058-66. doi: 10.3324/haematol.2012.075325. Epub 2013 Jan 8. PMID: 23300180; PMCID: PMC3696609.
244. Miari KE, Guzman ML, Wheadon H, Williams MTS. Macrophages in Acute Myeloid Leukaemia: Significant Players in Therapy Resistance and Patient Outcomes. Front Cell Dev Biol. 2021 Jun 24;9:692800. doi: 10.3389/fcell.2021.692800. PMID: 34249942; PMCID: PMC8264427.
245. Miltiades P, Lamprianidou E, Vassilakopoulos TP, Papageorgiou SG, Galanopoulos AG, Kontos CK, Adamopoulos PG, Nakou E, Vakalopoulou S, Garypidou V, Papaioannou M, Hatjiharissi E, Papadaki HA, Spanoudakis E, Pappa V, Scorilas A, Tsatalas C, Kotsianidis I; Hellenic MDS Study Group. The Stat3/5 Signaling Biosignature in Hematopoietic Stem/Progenitor Cells Predicts Response and Outcome in Myelodysplastic Syndrome Patients Treated with Azacitidine. Clin Cancer Res. 2016 Apr 15;22(8):1958-68. doi: 10.1158/1078-0432.CCR-15-1288. Epub 2015 Dec 23. PMID: 26700206.
246. Misawa S, Horiike S. TP53 mutations in myelodysplastic syndrome. Leuk Lymphoma. 1996 Nov;23(5-6):417-22. doi: 10.3109/10428199609054848. PMID: 9031070.
247. Mittelbrunn M, Kroemer G. Hallmarks of T cell aging. Nat Immunol. 2021 Jun;22(6):687-698. doi: 10.1038/s41590-021-00927-z. Epub 2021 May 13. PMID: 33986548.
248. Mohamedali MA, Gaken J, Ahmed M, Kulasekararaj A, Smith AE, Malik F, Mufti G. Comparison of Peripheral Blood and Bone Marrow Molecular Profiling in Primary Myelodysplastic Syndromes (MDS). Blood 2014; 124 (21): 4655. doi: https://doi.org/10.1182/blood.V124.21.4655.4655
249. Molteni A, Ravano E, Riva M, Nichelatti M, Bandiera L, Crucitti L, Truini M, Cairoli R. Prognostic Impact of Immunohistochemical p53 Expression in Bone Marrow Biopsy in Higher Risk MDS: a Pilot Study. Mediterr J Hematol Infect Dis. 2019 Mar 1;11(1):e2019015. doi: 10.4084/MJHID.2019.015. PMID: 30858953; PMCID: PMC6402551.

250. Montalban-Bravo G, Garcia-Manero G. Myelodysplastic syndromes: 2018 update on diagnosis, risk-stratification and management. Am J Hematol. 2018 Jan;93(1):129-147. doi: 10.1002/ajh.24930. PMID: 29214694.

251. Montalban-Bravo G, Kanagal-Shamanna R, Benton CB, Class CA, Chien KS, Sasaki K, Naqvi K, Alvarado Y, Kadia TM, Ravandi F, Daver N, Takahashi K, Jabbour E, Borthakur G, Pemmaraju N, Konopleva M, Soltysiak KA, Pierce SR, Bueso-Ramos CE, Patel KP, Kantarjian H, Garcia-Manero G. Genomic context and TP53 allele frequency define clinical outcomes in TP53-mutated myelodysplastic syndromes. Blood Adv. 2020 Feb 11;4(3):482-495. doi: 10.1182/bloodadvances.2019001101. PMID: 32027746; PMCID: PMC7013259.

252. Moreno Berggren D, Folkvaljon Y, Engvall M, Sundberg J, Lambe M, Antunovic P, Garelius H, Lorenz F, Nilsson L, Rasmussen B, Lehmann S, Hellström-Lindberg E, Jädersten M, Ejerblad E. Prognostic scoring systems for myelodysplastic syndromes (MDS) in a population-based setting: a report from the Swedish MDS register. Br J Haematol. 2018 Jun;181(5):614-627. doi: 10.1111/bjh.15243. Epub 2018 Apr 29. PMID: 29707769.

253. Mossner M, Jann JC, Wittig J, Nolte F, Fey S, Nowak V, Obländer J, Pressler J, Palme I, Xanthopoulos C, Boch T, Metzgeroth G, Röhl H, Witt SH, Dukal H, Klein C, Schmitt S, Gelß P, Platzbecker U, Balaian E, Fabarius A, Blum H, Schulze TJ, Meggendorfer M, Haferlach C, Trumpp A, Hofmann WK, Medyouf H, Nowak D. Mutational hierarchies in myelodysplastic syndromes dynamically adapt and evolve upon therapy response and failure. Blood. 2016 Sep 1;128(9):1246-59. doi: 10.1182/blood-2015-11-679167. Epub 2016 Jun 6. PMID: 27268087.

254. Mozessohn L, Cheung MC, Fallahpour S, Gill T, Maloul A, Zhang L, Lau O, Buckstein R. Azacitidine in the 'real-world': an evaluation of 1101 higher-risk myelodysplastic syndrome/low blast count acute myeloid leukaemia patients in Ontario, Canada. Br J Haematol. 2018 Jun;181(6):803-815. doi: 10.1111/bjh.15273. Epub 2018 May 16. PMID: 29767427.

255. Mussai F, De Santo C, Abu-Dayyeh I, Booth S, Quek L, McEwen-Smith RM, Qureshi A, Dazzi F, Vyas P, Cerundolo V. Acute myeloid leukemia creates an arginase-dependent immunosuppressive microenvironment. Blood. 2013 Aug 1;122(5):749-58. doi: 10.1182/blood-2013-01-480129. Epub 2013 Jun 3. PMID: 23733335; PMCID: PMC3731930.

256. Nahas MR, Stroopinsky D, Rosenblatt J, Cole L, Pyzer AR, Anastasiadou E, Sergeeva A, Ephraim A, Washington A, Orr S, McMasters M, Weinstock M, Jain S, Leaf RK, Ghiasuddin H, Rahimian M, Liegel J, Molldrem JJ, Slack F, Kufe D, Avigan D. Hypomethylating agent alters the immune microenvironment in acute myeloid leukaemia (AML) and enhances the immunogenicity of a dendritic cell/AML vaccine. Br J Haematol. 2019 May;185(4):679-690. doi: 10.1111/bjh.15818. Epub 2019 Mar 3. PMID: 30828801; PMCID: PMC6590084.

257. Nakao S, Gale RP. Are mild/moderate acquired idiopathic aplastic anaemia and low-risk myelodysplastic syndrome one or two diseases or both and how should it/they be treated? Leukemia. 2016 Nov;30(11):2127-2130. doi: 10.1038/leu.2016.206. Epub 2016 Sep 2. PMID: 27585953.

258. Nannya Y, Tobiasson M, Sato S, Bernard E, Ohtake S, Takeda J, Creignou M, Zhao L, Kusakabe M, Shibata Y, Nakamura N, Watanabe M, Hiramoto N, Shiozawa Y, Shiraishi Y, Tanaka H, Yoshida K, Kakiuchi N, Makishima H, Nakagawa MM, Usuki K, Watanabe M, Imada K, Handa H, Taguchi M, Kiguchi T, Ohyashiki K, Ishikawa T, Takaori-Kondo A, Tsurumi H, Kasahara S, Chiba S, Naoe T, Miyano S, Papaemmanuil E, Miyazaki Y, Hellström Lindberg E, Ogawa S. Post-azacitidine clone size predicts outcome of patients with myelodysplastic syndromes and related myeloid neoplasms. Blood Adv. 2023 Mar 29:bloodadvances.2022009564. doi: 10.1182/bloodadvances.2022009564. Epub ahead of print. PMID: 36989067.

259. Narasimhan PB, Marcovecchio P, Hamers AAJ, Hedrick CC. Nonclassical Monocytes in Health and Disease. Annu Rev Immunol. 2019 Apr 26;37:439-456. doi: 10.1146/annurev-immunol-042617-053119. PMID: 31026415.
260. Ndhlovu LC, Lopez-Vergès S, Barbour JD, Jones RB, Jha AR, Long BR, Schoeffler EC, Fujita T, Nixon DF, Lanier LL. Tim-3 marks human natural killer cell maturation and suppresses cell-mediated cytotoxicity. Blood. 2012 Apr 19;119(16):3734-43. doi: 10.1182/blood-2011-11-392951. Epub 2012 Mar 1. PMID: 22383801; PMCID: PMC3335380.
261. Nie J, Zhang Y, Li X, Chen M, Liu C, Han W. DNA demethylating agent decitabine broadens the peripheral T cell receptor repertoire. Oncotarget. 2016 Jun 21;7(25):37882-37892. doi: 10.18632/oncotarget.9352. PMID: 27191266; PMCID: PMC5122357.
262. Nishiwaki S, Ito M, Watarai R, Okuno S, Harada Y, Yamamoto S, Suzuki K, Kurahashi S, Iwasaki T, Sugiura I. A new prognostic index to make short-term prognoses in MDS patients treated with azacitidine: A combination of p53 expression and cytogenetics. Leuk Res. 2016 Feb;41:21-6. doi: 10.1016/j.leukres.2015.11.014. Epub 2015 Nov 25. PMID: 26651421.
263. Obeng EA, Chappell RJ, Seiler M, Chen MC, Campagna DR, Schmidt PJ, Schneider RK, Lord AM, Wang L, Gambe RG, McConkey ME, Ali AM, Raza A, Yu L, Buonamici S, Smith PG, Mullally A, Wu CJ, Fleming MD, Ebert BL. Physiologic Expression of Sf3b1(K700E) Causes Impaired Erythropoiesis, Aberrant Splicing, and Sensitivity to Therapeutic Spliceosome Modulation. Cancer Cell. 2016 Sep 12;30(3):404-417. doi: 10.1016/j.ccell.2016.08.006. PMID: 27622333; PMCID: PMC5023069.
264. Oduro KA Jr, Liu F, Tan Q, Kim CK, Lubman O, Fremont D, Mills JC, Choi K. Myeloid skewing in murine autoimmune arthritis occurs in hematopoietic stem and primitive progenitor cells. Blood. 2012 Sep 13;120(11):2203-13. doi: 10.1182/blood-2011-11-391342. Epub 2012 Jul 31. PMID: 22855602; PMCID: PMC3447779.
265. Ogawa S. Genetics of MDS. Blood. 2019 Mar 7;133(10):1049-1059. doi: 10.1182/blood-2018-10-844621. Epub 2019 Jan 22. PMID: 30670442; PMCID: PMC6587668.
266. Olnes MJ, Sloand EM. Targeting immune dysregulation in myelodysplastic syndromes. JAMA. 2011 Feb 23;305(8):814-9. doi: 10.1001/jama.2011.194. PMID: 21343581.
267. Ørskov AD, Treppendahl MB, Skovbo A, Holm MS, Friis LS, Hokland M, Grønbæk K. Hypomethylation and up-regulation of PD-1 in T cells by azacytidine in MDS/AML patients: A rationale for combined targeting of PD-1 and DNA methylation. Oncotarget. 2015 Apr 20;6(11):9612-26. doi: 10.18632/oncotarget.3324. PMID: 25823822; PMCID: PMC4496243.
268. Pang WW, Pluvinage JV, Price EA, Sridhar K, Arber DA, Greenberg PL, Schrier SL, Park CY, Weissman IL. Hematopoietic stem cell and progenitor cell mechanisms in myelodysplastic syndromes. Proc Natl Acad Sci U S A. 2013 Feb 19;110(8):3011-6. doi: 10.1073/pnas.1222861110. Epub 2013 Feb 6. PMID: 23388639; PMCID: PMC3581956.
269. Papaemmanuil E, Cazzola M, Boultwood J, Malcovati L, Vyas P, Bowen D, Pellagatti A, Wainscoat JS, Hellstrom-Lindberg E, Gambacorti-Passerini C, Godfrey AL, Rapado I, Cvejic A, Rance R, McGee C, Ellis P, Mudie LJ, Stephens PJ, McLaren S, Massie CE, Tarpey PS, Varela I, Nik-Zainal S, Davies HR, Shlien A, Jones D, Raine K, Hinton J, Butler AP, Teague JW, Baxter EJ, Score J, Galli A, Della Porta MG, Travaglino E, Groves M, Tauro S, Munshi NC, Anderson KC, El-Naggar A, Fischer A, Mustonen V, Warren AJ, Cross NC, Green AR, Futreal PA, Stratton MR, Campbell PJ; Chronic Myeloid Disorders Working Group of the International Cancer Genome Consortium. Somatic SF3B1 mutation in myelodysplasia with ring sideroblasts. N Engl J Med. 2011 Oct 13;365(15):1384-95. doi: 10.1056/NEJMoa1103283. Epub 2011 Sep 26. PMID: 21995386; PMCID: PMC3322589.
270. Papaemmanuil E, Gerstung M, Malcovati L, Tauro S, Gundem G, Van Loo P, Yoon CJ, Ellis P, Wedge DC, Pellagatti A, Shlien A, Groves MJ, Forbes SA, Raine K, Hinton J, Mudie LJ, McLaren S, Hardy C, Latimer C, Della Porta MG, O'Meara S, Ambaglio I, Galli A, Butler AP, Walldin G, Teague JW, Quek L, Sternberg A, Gambacorti-Passerini C, Cross NC, Green AR, Boultwood J, Vyas P, Hellstrom-Lindberg

E, Bowen D, Cazzola M, Stratton MR, Campbell PJ; Chronic Myeloid Disorders Working Group of the International Cancer Genome Consortium. Clinical and biological implications of driver mutations in myelodysplastic syndromes. Blood. 2013 Nov 21;122(22):3616-27; quiz 3699. doi: 10.1182/blood-2013-08-518886. Epub 2013 Sep 12. PMID: 24030381; PMCID: PMC3837510.

271. Papayannopoulou T, Nakamoto B. Peripheralization of hemopoietic progenitors in primates treated with anti-VLA4 integrin. Proc Natl Acad Sci U S A. 1993 Oct 15;90(20):9374-8. doi: 10.1073/pnas.90.20.9374. PMID: 7692447; PMCID: PMC47570.

272. Papayannopoulou T, Scadden DT. Stem-cell ecology and stem cells in motion. Blood. 2008 Apr 15;111(8):3923-30. doi: 10.1182/blood-2007-08-078147. PMID: 18398055; PMCID: PMC2288715.

273. Paracatu LC, Monlish DA, Greenberg ZJ, Fisher DAC, Walter MJ, Oh ST, Schuettpelz LG. Toll-like receptor and cytokine expression throughout the bone marrow differs between patients with low- and high-risk myelodysplastic syndromes. Exp Hematol. 2022 Jun;110:47-59. doi: 10.1016/j.exphem.2022.03.011. Epub 2022 Apr 1. PMID: 35367529; PMCID: PMC9590644.

274. Parker JE, Fishlock KL, Mijovic A, Czepulkowski B, Pagliuca A, Mufti GJ. 'Low-risk' myelodysplastic syndrome is associated with excessive apoptosis and an increased ratio of pro- versus anti-apoptotic bcl-2-related proteins. Br J Haematol. 1998 Dec;103(4):1075-82. doi: 10.1046/j.1365-2141.1998.01114.x. PMID: 9886323.

275. Parker JE, Mufti GJ, Rasool F, Mijovic A, Devereux S, Pagliuca A. The role of apoptosis, proliferation, and the Bcl-2-related proteins in the myelodysplastic syndromes and acute myeloid leukemia secondary to MDS. Blood. 2000 Dec 1;96(12):3932-8. PMID: 11090080.

276. Parker JE, Mufti GJ, Rasool F, Mijovic A, Devereux S, Pagliuca A. The role of apoptosis, proliferation, and the Bcl-2-related proteins in the myelodysplastic syndromes and acute myeloid leukemia secondary to MDS. Blood. 2000;96(12):3932-3938.

277. Passweg JR, Giagounidis AA, Simcock M, Aul C, Dobbelstein C, Stadler M, Ossenkoppele G, Hofmann WK, Schilling K, Tichelli A, Ganser A. Immunosuppressive therapy for patients with myelodysplastic syndrome: a prospective randomized multicenter phase III trial comparing antithymocyte globulin plus cyclosporine with best supportive care--SAKK 33/99. J Clin Oncol. 2011 Jan 20;29(3):303-9. doi: 10.1200/JCO.2010.31.2686. Epub 2010 Dec 13. PMID: 21149672.

278. Patel K, Dickson J, Din S, Macleod K, Jodrell D, Ramsahoye B. Targeting of 5-aza-2'-deoxycytidine residues by chromatin-associated DNMT1 induces proteasomal degradation of the free enzyme. Nucleic Acids Res. 2010 Jul;38(13):4313-24. doi: 10.1093/nar/gkq187. Epub 2010 Mar 25. PMID: 20348135; PMCID: PMC2910061.

279. Pellagatti A, Cazzola M, Giagounidis A, Perry J, Malcovati L, Della Porta MG, Jädersten M, Killick S, Verma A, Norbury CJ, Hellström-Lindberg E, Wainscoat JS, Boultwood J. Deregulated gene expression pathways in myelodysplastic syndrome hematopoietic stem cells. Leukemia. 2010 Apr;24(4):756-64. doi: 10.1038/leu.2010.31. Epub 2010 Mar 11. PMID: 20220779.

280. Pellagatti A, Roy S, Di Genua C, Burns A, McGraw K, Valletta S, Larrayoz MJ, Fernandez-Mercado M, Mason J, Killick S, Mecucci C, Calasanz MJ, List A, Schuh A, Boultwood J. Targeted resequencing analysis of 31 genes commonly mutated in myeloid disorders in serial samples from myelodysplastic syndrome patients showing disease progression. Leukemia. 2016 Jan;30(1):247-50. doi: 10.1038/leu.2015.129. Epub 2015 May 20. PMID: 25991409; PMCID: PMC4705423.

281. Pellagatti A, Armstrong RN, Steeples V, Sharma E, Repapi E, Singh S, Sanchi A, Radujkovic A, Horn P, Dolatshad H, Roy S, Broxholme J, Lockstone H, Taylor S, Giagounidis A, Vyas P, Schuh A, Hamblin A, Papaemmanuil E, Killick S, Malcovati L, Hennrich ML, Gavin AC, Ho AD, Luft T, Hellström-Lindberg E, Cazzola M, Smith CWJ, Smith S, Boultwood J. Impact of spliceosome mutations on RNA splicing in myelodysplasia: dysregulated genes/pathways and clinical associations. Blood. 2018 Sep

20;132(12):1225-1240. doi: 10.1182/blood-2018-04-843771. Epub 2018 Jun 21. PMID: 29930011; PMCID: PMC6172604.

282. Pich A, Godio L, Davico Bonino L. p53 protein expression in patients with myelodysplasia treated with allogeneic bone marrow transplantation. Mol Clin Oncol. 2017 Jun;6(6):876-880. doi: 10.3892/mco.2017.1225. Epub 2017 Apr 21. PMID: 28588781; PMCID: PMC5451870.

283. Pitel BA, Sharma N, Zepeda-Mendoza C, Smadbeck JB, Pearce KE, Cook JM, Vasmatzis G, Sachs Z, Kanagal-Shamanna R, Viswanatha D, Xiao S, Jenkins RB, Xu X, Hoppman NL, Ketterling RP, Peterson JF, Greipp PT, Baughn LB. Myeloid malignancies with 5q and 7q deletions are associated with extreme genomic complexity, biallelic TP53 variants, and very poor prognosis. Blood Cancer J. 2021 Feb 8;11(2):18. doi: 10.1038/s41408-021-00416-4. PMID: 33563889; PMCID: PMC7873204.

284. Peng X, Zhang MQ, Conserva F, Hosny G, Selivanova G, Bykov VJ, Arnér ES, Wiman KG. APR-246/PRIMA-1MET inhibits thioredoxin reductase 1 and converts the enzyme to a dedicated NADPH oxidase. Cell Death Dis. 2017 Apr 13;8(4):e2751. doi: 10.1038/cddis.2016.137. Erratum for: Cell Death Dis. 2013 Oct 24;4:e881. PMID: 28406483; PMCID: PMC5477569.

285. Pollyea DA, Hedin BR, O'Connor BP, Alper S. Monocyte function in patients with myelodysplastic syndrome. J Leukoc Biol. 2018 Sep;104(3):641-647. doi: 10.1002/JLB.5AB1017-419RR. Epub 2018 Apr 14. PMID: 29656609; PMCID: PMC6113098.

286. Pollyea DA, Harris C, Rabe JL, Hedin BR, De Arras L, Katz S, Wheeler E, Bejar R, Walter MJ, Jordan CT, Pietras EM, Alper S. Myelodysplastic syndrome-associated spliceosome gene mutations enhance innate immune signaling. Haematologica. 2019 Sep;104(9):e388-e392. doi: 10.3324/haematol.2018.214155. Epub 2019 Mar 7. PMID: 30846499; PMCID: PMC6717580.

287. Poon Z, Dighe N, Venkatesan SS, Cheung AMS, Fan X, Bari S, Hota M, Ghosh S, Hwang WYK. Bone marrow MSCs in MDS: contribution towards dysfunctional hematopoiesis and potential targets for disease response to hypomethylating therapy. Leukemia. 2019 Jun;33(6):1487-1500. doi: 10.1038/s41375-018-0310-y. Epub 2018 Dec 21. Erratum in: Leukemia. 2019 Feb 20;: PMID: 30575819; PMCID: PMC6756222.

288. Prébet T, Gore SD, Esterni B, Gardin C, Itzykson R, Thepot S, Dreyfus F, Rauzy OB, Recher C, Adès L, Quesnel B, Beach CL, Fenaux P, Vey N. Outcome of high-risk myelodysplastic syndrome after azacitidine treatment failure. J Clin Oncol. 2011 Aug 20;29(24):3322-7. doi: 10.1200/JCO.2011.35.8135. Epub 2011 Jul 25. PMID: 21788559; PMCID: PMC4859209.

289. Priestley GV, Ulyanova T, Papayannopoulou T. Sustained alterations in biodistribution of stem/progenitor cells in Tie2Cre+ alpha4(f/f) mice are hematopoietic cell autonomous. Blood. 2007 Jan 1;109(1):109-11. doi: 10.1182/blood-2006-06-026427. Epub 2006 Aug 24. PMID: 16931623; PMCID: PMC1785077.

290. Pronk E, Raaijmakers MHGP. The mesenchymal niche in MDS. Blood. 2019 Mar 7;133(10):1031-1038. doi: 10.1182/blood-2018-10-844639. Epub 2019 Jan 22. PMID: 30670448.

291. Pyzer AR, Stroopinsky D, Rajabi H, Washington A, Tagde A, Coll M, Fung J, Bryant MP, Cole L, Palmer K, Somaiya P, Karp Leaf R, Nahas M, Apel A, Jain S, McMasters M, Mendez L, Levine J, Joyce R, Arnason J, Pandolfi PP, Kufe D, Rosenblatt J, Avigan D. MUC1-mediated induction of myeloid-derived suppressor cells in patients with acute myeloid leukemia. Blood. 2017 Mar 30;129(13):1791-1801. doi: 10.1182/blood-2016-07-730614. Epub 2017 Jan 26. PMID: 28126925; PMCID: PMC5813734.

292. Qi X, Jiang H, Liu P, Xie N, Fu R, Wang H, Liu C, Zhang T, Wang H, Shao Z. Increased myeloid-derived suppressor cells in patients with myelodysplastic syndromes suppress CD8+ T lymphocyte function through the STAT3-ARG1 pathway. Leuk Lymphoma. 2021 Jan;62(1):218-223. doi: 10.1080/10428194.2020.1817431. Epub 2020 Sep 26. PMID: 32985300.

293. Qin T, Castoro R, El Ahdab S, Jelinek J, Wang X, Si J, Shu J, He R, Zhang N, Chung W, Kantarjian HM, Issa JP. Mechanisms of resistance to decitabine in the myelodysplastic syndrome. PLoS One.

2011;6(8):e23372. doi: 10.1371/journal.pone.0023372. Epub 2011 Aug 17. PMID: 21858090; PMCID: PMC3157379.

294. Radwan SM, Elleboudy NS, Nabih NA, Kamal AM. The immune checkpoints Cytotoxic T lymphocyte antigen-4 and Lymphocyte activation gene-3 expression is up-regulated in acute myeloid leukemia. HLA. 2020 Jul;96(1):3-12. doi: 10.1111/tan.13872. Epub 2020 Mar 29. PMID: 32189430.
295. Raj K, John A, Ho A, Chronis C, Khan S, Samuel J, Pomplun S, Thomas NS, Mufti GJ. CDKN2B methylation status and isolated chromosome 7 abnormalities predict responses to treatment with 5-azacytidine. Leukemia. 2007 Sep;21(9):1937-44. doi: 10.1038/sj.leu.2404796. Epub 2007 Jul 5. PMID: 17611569.
296. Reagan MR, Rosen CJ. Navigating the bone marrow niche: translational insights and cancer-driven dysfunction. Nat Rev Rheumatol. 2016 Mar;12(3):154-68. doi: 10.1038/nrrheum.2015.160. Epub 2015 Nov 26. PMID: 26607387; PMCID: PMC4947935.
297. Ren Y, Wang J, Zhang H, Mei C, Ye L, Luo Y, Zhou X, Zhu S, Jiang L, Wang L, Jin J, Tong H. TP53 mutations are associated with very complex karyotype and suggest poor prognosis in newly diagnosed myelodysplastic syndrome patients with monosomal karyotype. Asia Pac J Clin Oncol. 2020 Jun;16(3):172-179. doi: 10.1111/ajco.13316. Epub 2020 Feb 7. PMID: 32030889.
298. Rettig MP, Godwin J, Vey N, Fox B, Ballesteros-Merino C, Bifulco CB, Li D, Primo D, Ballesteros J, Sun J, Lelièvre H, Baughman J, La Motte-Mohs R, Muth J, Moore P, Bonvini E, Wigginton J, DiPersio JF, Davidson-Moncada J. Preliminary Translational Results from an Ongoing Phase 1 Study of Flotetuzumab, a CD123 x CD3 Dart®, in AML/MDS: Rationale for Combining Flotetuzumab and Anti-PD-1/PD-L1 Immunotherapies. Blood 2017; 130 (Supplement 1): 1365. doi: https://doi.org/10.1182/blood.V130.Suppl_1.1365.1365
299. Rhyasen GW, Bolanos L, Fang J, Jerez A, Wunderlich M, Rigolino C, Mathews L, Ferrer M, Southall N, Guha R, Keller J, Thomas C, Beverly LJ, Cortelezzi A, Oliva EN, Cuzzola M, Maciejewski JP, Mulloy JC, Starczynowski DT. Targeting IRAK1 as a therapeutic approach for myelodysplastic syndrome. Cancer Cell. 2013 Jul 8;24(1):90-104. doi: 10.1016/j.ccr.2013.05.006. PMID: 23845443; PMCID: PMC3711103.
300. Ries C, Loher F, Zang C, Ismair MG, Petrides PE. Matrix metalloproteinase production by bone marrow mononuclear cells from normal individuals and patients with acute and chronic myeloid leukemia or myelodysplastic syndromes. Clin Cancer Res. 1999 May;5(5):1115-24. PMID: 10353746.
301. Rodrigues CP, Shvedunova M, Akhtar A. Epigenetic Regulators as the Gatekeepers of Hematopoiesis. Trends Genet. 2020 Oct 21:S0168-9525(20)30251-1. doi: 10.1016/j.tig.2020.09.015. Epub ahead of print. PMID: 34756331.
302. Saber W, Horowitz MM. Transplantation for myelodysplastic syndromes: who, when, and which conditioning regimens. Hematology Am Soc Hematol Educ Program. 2016 Dec 2;2016(1):478-484. doi: 10.1182/asheducation-2016.1.478. PMID: 27913519; PMCID: PMC6142436.
303. Saft L, Björklund E, Berg E, Hellström-Lindberg E, Porwit A. Bone marrow dendritic cells are reduced in patients with high-risk myelodysplastic syndromes. Leuk Res. 2013 Mar;37(3):266-73. doi: 10.1016/j.leukres.2012.10.010. Epub 2012 Nov 13. PMID: 23153526.
304. Sakaguchi S. Naturally arising CD4+ regulatory t cells for immunologic self-tolerance and negative control of immune responses. Annu Rev Immunol. 2004;22:531-62. doi: 10.1146/annurev.immunol.21.120601.141122. PMID: 15032588.
305. Sallman DA, Komrokji R, Vaupel C, Cluzeau T, Geyer SM, McGraw KL, Al Ali NH, Lancet J, McGinniss MJ, Nahas S, Smith AE, Kulasekararaj A, Mufti G, List A, Hall J, Padron E. Impact of TP53 mutation variant allele frequency on phenotype and outcomes in myelodysplastic syndromes. Leukemia. 2016 Mar;30(3):666-73. doi: 10.1038/leu.2015.304. Epub 2015 Oct 30. PMID: 26514544; PMCID: PMC7864381.

306. Sallman DA, Padron E. Integrating mutation variant allele frequency into clinical practice in myeloid malignancies. Hematol Oncol Stem Cell Ther. 2016 Sep;9(3):89-95. doi: 10.1016/j.hemonc.2016.04.003. Epub 2016 May 11. PMID: 27187622.
307. Sallman DA, List A. The central role of inflammatory signaling in the pathogenesis of myelodysplastic syndromes. Blood. 2019 Mar 7;133(10):1039-1048. doi: 10.1182/blood-2018-10-844654. Epub 2019 Jan 22. PMID: 30670444; PMCID: PMC7022316.
308. Sallman DA, McLemore AF, Aldrich AL, Komrokji RS, McGraw KL, Dhawan A, Geyer S, Hou HA, Eksioglu EA, Sullivan A, Warren S, MacBeth KJ, Meggendorfer M, Haferlach T, Boettcher S, Ebert BL, Al Ali NH, Lancet JE, Cleveland JL, Padron E, List AF. TP53 mutations in myelodysplastic syndromes and secondary AML confer an immunosuppressive phenotype. Blood. 2020 Dec 10;136(24):2812-2823. doi: 10.1182/blood.2020006158. PMID: 32730593; PMCID: PMC7731792.
309. Sallman DA, DeZern AE, Garcia-Manero G, Steensma DP, Roboz GJ, Sekeres MA, Cluzeau T, Sweet KL, McLemore A, McGraw KL, Puskas J, Zhang L, Yao J, Mo Q, Nardelli L, Al Ali NH, Padron E, Korbel G, Attar EC, Kantarjian HM, Lancet JE, Fenaux P, List AF, Komrokji RS. Eprenetapopt (APR-246) and Azacitidine in TP53-Mutant Myelodysplastic Syndromes. J Clin Oncol. 2021 May 10;39(14):1584-1594. doi: 10.1200/JCO.20.02341. Epub 2021 Jan 15. PMID: 33449813; PMCID: PMC8099410.
310. Sallman DA, Al Malki MM, Asch AS, Wang ES, Jurcic JG, Bradley TJ, Flinn IW, Pollyea DA, Kambhampati S, Tanaka TN, Zeidner JF, Garcia-Manero G, Jeyakumar D, Komrokji R, Lancet J, Kantarjian HM, Gu L, Zhang Y, Tan A, Chao M, O'Hear C, Ramsingh G, Lal I, Vyas P, Daver NG. Magrolimab in Combination With Azacitidine in Patients With Higher-Risk Myelodysplastic Syndromes: Final Results of a Phase Ib Study. J Clin Oncol. 2023 May 20;41(15):2815-2826. doi: 10.1200/JCO.22.01794. Epub 2023 Mar 8. PMID: 36888930.
311. Sand K, Theorell J, Bruserud Ø, Bryceson YT, Kittang AO. Reduced potency of cytotoxic T lymphocytes from patients with high-risk myelodysplastic syndromes. Cancer Immunol Immunother. 2016 Sep;65(9):1135-47. doi: 10.1007/s00262-016-1865-y. Epub 2016 Aug 1. PMID: 27481108.
312. Santini V. How I treat MDS after hypomethylating agent failure. Blood. 2019 Feb 7;133(6):521-529. doi: 10.1182/blood-2018-03-785915. Epub 2018 Dec 13. PMID: 30545832.
313. Sarhan D, Wang J, Sunil Arvindam U, Hallstrom C, Verneris MR, Grzywacz B, Warlick E, Blazar BR, Miller JS. Mesenchymal stromal cells shape the MDS microenvironment by inducing suppressive monocytes that dampen NK cell function. JCI Insight. 2020 Mar 12;5(5):e130155. doi: 10.1172/jci.insight.130155. PMID: 32045384; PMCID: PMC7141401.
314. Sauta E, Robin M, Bersanelli M, Travaglino E, Meggendorfer M, Zhao LP, Caballero Berrocal JC, Sala C, Maggioni G, Bernardi M, Di Grazia C, Vago L, Rivoli G, Borin L, D'Amico S, Tentori CA, Ubezio M, Campagna A, Russo A, Mannina D, Lanino L, Chiusolo P, Giaccone L, Voso MT, Riva M, Oliva EN, Zampini M, Riva E, Nibourel O, Bicchieri M, Bolli N, Rambaldi A, Passamonti F, Savevski V, Santoro A, Germing U, Kordasti S, Santini V, Diez-Campelo M, Sanz G, Sole F, Kern W, Platzbecker U, Ades L, Fenaux P, Haferlach T, Castellani G, Della Porta MG. Real-World Validation of Molecular International Prognostic Scoring System for Myelodysplastic Syndromes. J Clin Oncol. 2023 Mar 17:JCO2201784. doi: 10.1200/JCO.22.01784. Epub ahead of print. PMID: 36930857.
315. Schanz J, Tüchler H, Solé F, Mallo M, Luño E, Cervera J, Granada I, Hildebrandt B, Slovak ML, Ohyashiki K, Steidl C, Fonatsch C, Pfeilstöcker M, Nösslinger T, Valent P, Giagounidis A, Aul C, Lübbert M, Stauder R, Krieger O, Garcia-Manero G, Faderl S, Pierce S, Le Beau MM, Bennett JM, Greenberg P, Germing U, Haase D. New comprehensive cytogenetic scoring system for primary myelodysplastic syndromes (MDS) and oligoblastic acute myeloid leukemia after MDS derived from an international database merge. J Clin Oncol. 2012 Mar 10;30(8):820-9. doi: 10.1200/JCO.2011.35.6394. Epub 2012 Feb 13. PMID: 22331955; PMCID: PMC4874200.

316. Schipani E, Wu C, Rankin EB, Giaccia AJ. Regulation of Bone Marrow Angiogenesis by Osteoblasts during Bone Development and Homeostasis. Front Endocrinol (Lausanne). 2013 Jul 10;4:85. doi: 10.3389/fendo.2013.00085. PMID: 23847596; PMCID: PMC3706978.
317. Schnegg-Kaufmann AS, Thoms JAI, Bhuyan GS, Hampton HR, Vaughan L, Rutherford K, Kakadia PM, Lee HM, Johansson EMV, Failes TW, Arndt GM, Koval J, Lindeman R, Warburton P, Rodriguez-Meira A, Mead AJ, Unnikrishnan A, Davidson S, Polizzotto MN, Hertzberg M, Papaemmanuil E, Bohlander SK, Faridani OR, Jolly CJ, Zanini F, Pimanda JE. Contribution of mutant HSC clones to immature and mature cells in MDS and CMML, and variations with AZA therapy. Blood. 2023 Mar 16;141(11):1316-1321. doi: 10.1182/blood.2022018602. PMID: 36493342.
318. Schmiedel BJ, Arélin V, Gruenebach F, Krusch M, Schmidt SM, Salih HR. Azacytidine impairs NK cell reactivity while decitabine augments NK cell responsiveness toward stimulation. Int J Cancer. 2011 Jun 15;128(12):2911-22. doi: 10.1002/ijc.25635. Epub 2010 Oct 19. PMID: 20960460.
319. Schneider M, Rolfs C, Trumpp M, Winter S, Fischer L, Richter M, Menger V, Nenoff K, Grieb N, Metzeler KH, Kubasch AS, Sockel K, Thiede C, Wu J, Woo J, Brüderle A, Hofbauer LC, Lützner J, Roth A, Cross M, Platzbecker U. Activation of distinct inflammatory pathways in subgroups of LR-MDS. Leukemia. 2023 Jul 7. doi: 10.1038/s41375-023-01949-2. Epub ahead of print. PMID: 37420006.
320. Schroeder T, Czibere A, Platzbecker U, Bug G, Uharek L, Luft T, Giagounidis A, Zohren F, Bruns I, Wolschke C, Rieger K, Fenk R, Germing U, Haas R, Kröger N, Kobbe G. Azacitidine and donor lymphocyte infusions as first salvage therapy for relapse of AML or MDS after allogeneic stem cell transplantation. Leukemia. 2013 Jun;27(6):1229-35. doi: 10.1038/leu.2013.7. Epub 2013 Jan 14. PMID: 23314834.
321. Schroeder T, Geyh S, Germing U, Haas R. Mesenchymal stromal cells in myeloid malignancies. Blood Res. 2016 Dec;51(4):225-232. doi: 10.5045/br.2016.51.4.225. Epub 2016 Dec 23. PMID: 28090484; PMCID: PMC5234241.
322. Schroeder T, Ruf L, Bernhardt A, Hildebrandt B, Aivado M, Aul C, Gattermann N, Haas R, Germing U. Distinguishing myelodysplastic syndromes (MDS) from idiopathic cytopenia of undetermined significance (ICUS): HUMARA unravels clonality in a subgroup of patients. Ann Oncol. 2010 Nov;21(11):2267-2271. doi: 10.1093/annonc/mdq233. Epub 2010 May 3. PMID: 20439346.
323. Schulz F, Nachtkamp K, Kasprzak A, Gattermann N, Haas R, Germing U. Luspatercept as a therapy for myelodysplastic syndromes with ring sideroblasts. Expert Rev Hematol. 2021 Jun;14(6):509-516. doi: 10.1080/17474086.2021.1947791. Epub 2021 Jun 30. PMID: 34161752.
324. Scott LM, Priestley GV, Papayannopoulou T. Deletion of alpha4 integrins from adult hematopoietic cells reveals roles in homeostasis, regeneration, and homing. Mol Cell Biol. 2003 Dec;23(24):9349-60. doi: 10.1128/MCB.23.24.9349-9360.2003. PMID: 14645544; PMCID: PMC309677.
325. Shi X, Zheng Y, Xu L, Cao C, Dong B, Chen X. The inflammatory cytokine profile of myelodysplastic syndromes: A meta-analysis. Medicine (Baltimore). 2019 May;98(22):e15844. doi: 10.1097/MD.0000000000015844. PMID: 31145332; PMCID: PMC6708708.
326. Shestak AG, Bukaeva AA, Saber S, Zaklyazminskaya EV. Allelic Dropout Is a Common Phenomenon That Reduces the Diagnostic Yield of PCR-Based Sequencing of Targeted Gene Panels. Front Genet. 2021 Feb 1;12:620337. doi: 10.3389/fgene.2021.620337. PMID: 33633783; PMCID: PMC7901947.
327. Sica A, Mantovani A. Macrophage plasticity and polarization: in vivo veritas. J Clin Invest. 2012 Mar;122(3):787-95. doi: 10.1172/JCI59643. Epub 2012 Mar 1. PMID: 22378047; PMCID: PMC3287223.
328. Silverman LR, Fenaux P, Mufti GJ, Santini V, Hellström-Lindberg E, Gattermann N, Sanz G, List AF, Gore SD, Seymour JF. Continued azacitidine therapy beyond time of first response improves quality of response in patients with higher-risk myelodysplastic syndromes. Cancer. 2011 Jun

15;117(12):2697-702. doi: 10.1002/cncr.25774. Epub 2011 Jan 10. PMID: 21656747; PMCID: PMC4000012.

329. Sébert M, Komrokji RS, Sekeres MA, Prebet T, Cluzeau T, Santini V, Gyan E, Sanna A, Ali NH, Hobson S, Eclache V, List A, Fenaux P, Adès L. Impact of baseline cytogenetic findings and cytogenetic response on outcome of high-risk myelodysplastic syndromes and low blast count AML treated with azacitidine. Leuk Res. 2017 Dec;63:72-77. doi: 10.1016/j.leukres.2017.10.013. Epub 2017 Oct 27. PMID: 29112938.

330. Seif F, Khoshmirsafa M, Aazami H, Mohsenzadegan M, Sedighi G, Bahar M. The role of JAK-STAT signaling pathway and its regulators in the fate of T helper cells. Cell Commun Signal. 2017 Jun 21;15(1):23. doi: 10.1186/s12964-017-0177-y. PMID: 28637459; PMCID: PMC5480189.

331. Sekeres MA. Epidemiology, natural history, and practice patterns of patients with myelodysplastic syndromes in 2010. J Natl Compr Canc Netw. 2011 Jan;9(1):57-63. doi: 10.6004/jnccn.2011.0006. PMID: 21233244.

332. Selimoglu-Buet D, Badaoui B, Benayoun E, Toma A, Fenaux P, Quesnel B, Etienne G, Braun T, Abermil N, Morabito M, Droin N, Solary E, Wagner-Ballon O; Groupe Francophone des Myélodysplasies. Accumulation of classical monocytes defines a subgroup of MDS that frequently evolves into CMML. Blood. 2017 Aug 10;130(6):832-835. doi: 10.1182/blood-2017-04-779579. Epub 2017 Jun 13. PMID: 28611023.

333. Serrano-López J, Martín-Antonio B. Inflammaging, an Imbalanced Immune Response That Needs to Be Restored for Cancer Prevention and Treatment in the Elderly. Cells. 2021 Sep 28;10(10):2562. doi: 10.3390/cells10102562. PMID: 34685542; PMCID: PMC8533838.

334. Sezaki M, Hayashi Y, Wang Y, Johansson A, Umemoto T, Takizawa H. Immuno-Modulation of Hematopoietic Stem and Progenitor Cells in Inflammation. Front Immunol. 2020 Nov 24;11:585367. doi: 10.3389/fimmu.2020.585367. PMID: 33329562; PMCID: PMC7732516.

335. Shiozawa Y, Malcovati L, Gallì A, Sato-Otsubo A, Kataoka K, Sato Y, Watatani Y, Suzuki H, Yoshizato T, Yoshida K, Sanada M, Makishima H, Shiraishi Y, Chiba K, Hellström-Lindberg E, Miyano S, Ogawa S, Cazzola M. Aberrant splicing and defective mRNA production induced by somatic spliceosome mutations in myelodysplasia. Nat Commun. 2018 Sep 7;9(1):3649. doi: 10.1038/s41467-018-06063-x. PMID: 30194306; PMCID: PMC6128865.

336. Smith MA, Choudhary GS, Pellagatti A, Choi K, Bolanos LC, Bhagat TD, Gordon-Mitchell S, Von Ahrens D, Pradhan K, Steeples V, Kim S, Steidl U, Walter M, Fraser IDC, Kulkarni A, Salomonis N, Komurov K, Boultwood J, Verma A, Starczynowski DT. U2AF1 mutations induce oncogenic IRAK4 isoforms and activate innate immune pathways in myeloid malignancies. Nat Cell Biol. 2019 May;21(5):640-650. doi: 10.1038/s41556-019-0314-5. Epub 2019 Apr 22. PMID: 31011167; PMCID: PMC6679973.

337. Sohlberg E, Pfefferle A, Andersson S, Baumann BC, Hellström-Lindberg E, Malmberg KJ. Imprint of 5-azacytidine on the natural killer cell repertoire during systemic treatment for high-risk myelodysplastic syndrome. Oncotarget. 2015 Oct 27;6(33):34178-90. doi: 10.18632/oncotarget.6213. PMID: 26497557; PMCID: PMC4741444.

338. Sommer S, Cruijsen M, Claus R, Bertz H, Wäsch R, Marks R, Zeiser R, Bogatyreva L, Blijlevens NMA, May A, Duyster J, Huls G, van der Velden WJFM, Finke J, Lübbert M. Decitabine in combination with donor lymphocyte infusions can induce remissions in relapsed myeloid malignancies with higher leukemic burden after allogeneic hematopoietic cell transplantation. Leuk Res. 2018 Sep;72:20-26. doi: 10.1016/j.leukres.2018.07.005. Epub 2018 Jul 7. PMID: 30064039.

339. Sperling AS, Gibson CJ, Ebert BL. The genetics of myelodysplastic syndrome: from clonal haematopoiesis to secondary leukaemia. Nat Rev Cancer. 2017 Jan;17(1):5-19. doi: 10.1038/nrc.2016.112. Epub 2016 Nov 11. PMID: 27834397; PMCID: PMC5470392.

340. Starczynowski DT, Kuchenbauer F, Argiropoulos B, Sung S, Morin R, Muranyi A, Hirst M, Hogge D, Marra M, Wells RA, Buckstein R, Lam W, Humphries RK, Karsan A. Identification of miR-145 and miR-146a as mediators of the 5q- syndrome phenotype. Nat Med. 2010 Jan;16(1):49-58. doi: 10.1038/nm.2054. Epub 2009 Nov 8. PMID: 19898489.
341. Steensma David P., Stone Richard M., in Abeloff's Clinical Oncology (Sixth Edition), 2020
342. Steensma DP. The Clinical Challenge of Idiopathic Cytopenias of Undetermined Significance (ICUS) and Clonal Cytopenias of Undetermined Significance (CCUS). Curr Hematol Malig Rep. 2019 Dec;14(6):536-542. doi: 10.1007/s11899-019-00547-3. PMID: 31696381.
343. Steensma DP, Bejar R, Jaiswal S, Lindsley RC, Sekeres MA, Hasserjian RP, Ebert BL. Clonal hematopoiesis of indeterminate potential and its distinction from myelodysplastic syndromes. Blood. 2015 Jul 2;126(1):9-16. doi: 10.1182/blood-2015-03-631747. Epub 2015 Apr 30. PMID: 25931582; PMCID: PMC4624443.
344. Stomper J, Rotondo JC, Greve G, Lübbert M. Hypomethylating agents (HMA) for the treatment of acute myeloid leukemia and myelodysplastic syndromes: mechanisms of resistance and novel HMA-based therapies. Leukemia. 2021 Jul;35(7):1873-1889. doi: 10.1038/s41375-021-01218-0. Epub 2021 May 6. PMID: 33958699; PMCID: PMC8257497.
345. Stubbins RJ, Karsan A. Differentiation therapy for myeloid malignancies: beyond cytotoxicity. Blood Cancer J. 2021 Dec 4;11(12):193. doi: 10.1038/s41408-021-00584-3. PMID: 34864823; PMCID: PMC8643352.
346. Stubbins RJ, Platzbecker U, Karsan A. Inflammation and myeloid malignancy: quenching the flame. Blood. 2022 Sep 8;140(10):1067-1074. doi: 10.1182/blood.2021015162. PMID: 35468199.
347. Stübig T, Badbaran A, Luetkens T, Hildebrandt Y, Atanackovic D, Binder TM, Fehse B, Kröger N. 5-azacytidine promotes an inhibitory T-cell phenotype and impairs immune mediated antileukemic activity. Mediators Inflamm. 2014;2014:418292. doi: 10.1155/2014/418292. Epub 2014 Mar 13. PMID: 24757283; PMCID: PMC3976863.
348. Sugiyama T, Kohara H, Noda M, Nagasawa T. Maintenance of the hematopoietic stem cell pool by CXCL12-CXCR4 chemokine signaling in bone marrow stromal cell niches. Immunity. 2006 Dec;25(6):977-88. doi: 10.1016/j.immuni.2006.10.016. PMID: 17174120.
349. Takahashi K, Jabbour E, Wang X, Luthra R, Bueso-Ramos C, Patel K, Pierce S, Yang H, Wei Y, Daver N, Faderl S, Ravandi F, Estrov Z, Cortes J, Kantarjian H, Garcia-Manero G. Dynamic acquisition of FLT3 or RAS alterations drive a subset of patients with lower risk MDS to secondary AML. Leukemia. 2013 Oct;27(10):2081-3. doi: 10.1038/leu.2013.165. Epub 2013 Jun 7. PMID: 23774633.
350. Takahashi K, Patel K, Bueso-Ramos C, Zhang J, Gumbs C, Jabbour E, Kadia T, Andreff M, Konopleva M, DiNardo C, Daver N, Cortes J, Estrov Z, Futreal A, Kantarjian H, Garcia-Manero G. Clinical implications of TP53 mutations in myelodysplastic syndromes treated with hypomethylating agents. Oncotarget. 2016 Mar 22;7(12):14172-87. doi: 10.18632/oncotarget.7290. PMID: 26871476; PMCID: PMC4924706.
351. Takahashi K, Patel KP, Kantarjian H, Luthra R, Pierce S, Cortes J, Verstovsek S. JAK2 p.V617F detection and allele burden measurement in peripheral blood and bone marrow aspirates in patients with myeloproliferative neoplasms. Blood. 2013 Nov 28;122(23):3784-6. doi: 10.1182/blood-2013-07-515676. Epub 2013 Sep 25. PMID: 24068492; PMCID: PMC3952679.
352. Tao J, Li L, Wang Y, Fu R, Wang H, Shao Z. Increased TIM3+CD8+T cells in Myelodysplastic Syndrome patients displayed less perforin and granzyme B secretion and higher CD95 expression. Leuk Res. 2016 Dec;51:49-55. doi: 10.1016/j.leukres.2016.11.003. Epub 2016 Nov 2. PMID: 27846431.
353. Tao J, Han D, Gao S, Zhang W, Yu H, Liu P, Fu R, Li L, Shao Z. CD8+ T cells exhaustion induced by myeloid-derived suppressor cells in myelodysplastic syndromes patients might be through

TIM3/Gal-9 pathway. J Cell Mol Med. 2020 Jan;24(1):1046-1058. doi: 10.1111/jcmm.14825. Epub 2019 Nov 22. PMID: 31756785; PMCID: PMC6933355.

354. Tcvetkov NY, Morozova EV, Epifanovskaya OS, Babenko EV, Barabanshikova MV, Lepik KV, et al. Profile of checkpoint molecules expression on bone marrow cell populations in patients with high-risk myelodysplastic syndrome. Blood. 2020;136(Supplement 1):43–4.

355. Tehranchi R, Woll PS, Anderson K, Buza-Vidas N, Mizukami T, Mead AJ, Astrand-Grundström I, Strömbeck B, Horvat A, Ferry H, Dhanda RS, Hast R, Rydén T, Vyas P, Göhring G, Schlegelberger B, Johansson B, Hellström-Lindberg E, List A, Nilsson L, Jacobsen SE. Persistent malignant stem cells in del(5q) myelodysplasia in remission. N Engl J Med. 2010 Sep 9;363(11):1025-37. doi: 10.1056/NEJMoa0912228. PMID: 20825315.

356. Teofili L, Martini M, Nuzzolo ER, Capodimonti S, Iachininoto MG, Cocomazzi A, Fabiani E, Voso MT, Larocca LM. Endothelial progenitor cell dysfunction in myelodysplastic syndromes: possible contribution of a defective vascular niche to myelodysplasia. Neoplasia. 2015 May;17(5):401-9. doi: 10.1016/j.neo.2015.04.001. PMID: 26025663; PMCID: PMC4468365.

357. Teoh PJ, Bi C, Sintosebastian C, Tay LS, Fonseca R, Chng WJ. PRIMA-1 targets the vulnerability of multiple myeloma of deregulated protein homeostasis through the perturbation of ER stress via p73 demethylation. Oncotarget. 2016 Sep 20;7(38):61806-61819. doi: 10.18632/oncotarget.11241. PMID: 27533450; PMCID: PMC5308692.

358. Tessoulin B, Descamps G, Moreau P, Maïga S, Lodé L, Godon C, Marionneau-Lambot S, Oullier T, Le Gouill S, Amiot M, Pellat-Deceunynck C. PRIMA-1Met induces myeloma cell death independent of p53 by impairing the GSH/ROS balance. Blood 2014; 124 (10): 1626–1636. doi: https://doi.org/10.1182/blood-2014-01-548800

359. Thol F, Kade S, Schlarmann C, Löffeld P, Morgan M, Krauter J, Wlodarski MW, Kölking B, Wichmann M, Görlich K, Göhring G, Bug G, Ottmann O, Niemeyer CM, Hofmann WK, Schlegelberger B, Ganser A, Heuser M. Frequency and prognostic impact of mutations in SRSF2, U2AF1, and ZRSR2 in patients with myelodysplastic syndromes. Blood. 2012 Apr 12;119(15):3578-84. doi: 10.1182/blood-2011-12-399337. Epub 2012 Mar 2. PMID: 22389253.

360. Togashi Y, Shitara K, Nishikawa H. Regulatory T cells in cancer immunosuppression - implications for anticancer therapy. Nat Rev Clin Oncol. 2019 Jun;16(6):356-371. doi: 10.1038/s41571-019-0175-7. PMID: 30705439.

361. Tohumeken S, Baur R, Böttcher M, Stoll A, Loschinski R, Panagiotidis K, Braun M, Saul D, Völkl S, Baur AS, Bruns H, Mackensen A, Jitschin R, Mougiakakos D. Palmitoylated Proteins on AML-Derived Extracellular Vesicles Promote Myeloid-Derived Suppressor Cell Differentiation via TLR2/Akt/mTOR Signaling. Cancer Res. 2020 Sep 1;80(17):3663-3676. doi: 10.1158/0008-5472.CAN-20-0024. Epub 2020 Jun 30. PMID: 32605996.

362. Tong WG, Sandhu VK, Wood BL, Hendrie PC, Becker PS, Pagel JM, Walter RB, Estey EH. Correlation between peripheral blood and bone marrow regarding FLT3-ITD and NPM1 mutational status in patients with acute myeloid leukemia. Haematologica. 2015 Mar;100(3):e97-8. doi: 10.3324/haematol.2014.118422. Epub 2014 Dec 19. PMID: 25527567; PMCID: PMC4349287.

363. Traina F, Visconte V, Elson P, Tabarroki A, Jankowska AM, Hasrouni E, Sugimoto Y, Szpurka H, Makishima H, O'Keefe CL, Sekeres MA, Advani AS, Kalaycio M, Copelan EA, Sauntharajah Y, Olalla Saad ST, Maciejewski JP, Tiu RV. Impact of molecular mutations on treatment response to DNMT inhibitors in myelodysplasia and related neoplasms. Leukemia. 2014 Jan;28(1):78-87. doi: 10.1038/leu.2013.269. Epub 2013 Sep 18. PMID: 24045501.

364. Travaglino E, Benatti C, Malcovati L, Della Porta MG, Gallì A, Bonetti E, Rosti V, Cazzola M, Invernizzi R. Biological and clinical relevance of matrix metalloproteinases 2 and 9 in acute myeloid leukaemias and myelodysplastic syndromes. Eur J Haematol. 2008 Mar;80(3):216-26. doi: 10.1111/j.1600-0609.2007.01012.x. Epub 2007 Dec 10. PMID: 18081721.

365. Triozzi PL, Aldrich W, Achberger S, Ponnazhagan S, Alcazar O, Saunthararajah Y. Differential effects of low-dose decitabine on immune effector and suppressor responses in melanoma-bearing mice. Cancer Immunol Immunother. 2012 Sep;61(9):1441-50. doi: 10.1007/s00262-012-1204-x. Epub 2012 Feb 5. PMID: 22310929.
366. Troy JD, de Castro CM, Pupa MR, Samsa GP, Abernethy AP, LeBlanc TW. Patient-Reported Distress in Myelodysplastic Syndromes and Its Association With Clinical Outcomes: A Retrospective Cohort Study. J Natl Compr Canc Netw. 2018 Mar;16(3):267-273. doi: 10.6004/jnccn.2017.7048. PMID: 29523665; PMCID: PMC5921897.
367. Tsukamoto H, Fujieda K, Senju S, Ikeda T, Oshiumi H, Nishimura Y. Immune-suppressive effects of interleukin-6 on T-cell-mediated anti-tumor immunity. Cancer Sci. 2018;109(3):523-530.
368. Unnikrishnan A, Papaemmanuil E, Beck D, Deshpande NP, Verma A, Kumari A, Woll PS, Richards LA, Knezevic K, Chandrakanthan V, Thoms JAI, Tursky ML, Huang Y, Ali Z, Olivier J, Galbraith S, Kulasekararaj AG, Tobiasson M, Karimi M, Pellagatti A, Wilson SR, Lindeman R, Young B, Ramakrishna R, Arthur C, Stark R, Crispin P, Curnow J, Warburton P, Roncolato F, Boultwood J, Lynch K, Jacobsen SEW, Mufti GJ, Hellstrom-Lindberg E, Wilkins MR, MacKenzie KL, Wong JWH, Campbell PJ, Pimanda JE. Integrative Genomics Identifies the Molecular Basis of Resistance to Azacitidine Therapy in Myelodysplastic Syndromes. Cell Rep. 2017 Jul 18;20(3):572-585. doi: 10.1016/j.celrep.2017.06.067. PMID: 28723562.
369. Unnikrishnan A, Vo ANQ, Pickford R, Raftery MJ, Nunez AC, Verma A, Hesson LB, Pimanda JE. AZA-MS: a novel multiparameter mass spectrometry method to determine the intracellular dynamics of azacitidine therapy in vivo. Leukemia. 2018 Apr;32(4):900-910. doi: 10.1038/leu.2017.340. Epub 2017 Nov 29. PMID: 29249821; PMCID: PMC5886051.
370. Uy GL, Duncavage EJ, Chang GS, Jacoby MA, Miller CA, Shao J, Heath S, Elliott K, Reineck T, Fulton RS, Fronick CC, O'Laughlin M, Ganel L, Abboud CN, Cashen AF, DiPersio JF, Wilson RK, Link DC, Welch JS, Ley TJ, Graubert TA, Westervelt P, Walter MJ. Dynamic changes in the clonal structure of MDS and AML in response to epigenetic therapy. Leukemia. 2017 Apr;31(4):872-881. doi: 10.1038/leu.2016.282. Epub 2016 Oct 14. PMID: 27740633; PMCID: PMC5382101.
371. Uy GL, Godwin J, Rettig MP, Vey N, Foster M, Arellano ML, Rizzieri DA, Topp MS, Huls G, Lowenberg B, Martinelli G, Paolini S, Ciceri F, Carrabba MG, Ballesteros-Merino C, Bifulco CB, Lelièvre H, La Motte-Mohs R, Li D, Sun J, DiPersio JF. Preliminary Results of a Phase 1 Study of Flotetuzumab, a CD123 x CD3 Bispecific Dart® Protein, in Patients with Relapsed/Refractory Acute Myeloid Leukemia and Myelodysplastic Syndrome. Blood. 2017 Dec;130(8):637. https://doi.org/10.1182/blood.V130.Suppl_1.637.637
372. Vadakekolathu J, Lai C, Reeder S, Church SE, Hood T, Lourdusamy A, Rettig MP, Aldoss I, Advani AS, Godwin J, Wieduwilt MJ, Arellano M, Muth J, Yau TO, Ravandi F, Sweet K, Altmann H, Foulds GA, Stölzel F, Middeke JM, Ciciarello M, Curti A, Valk PJM, Löwenberg B, Gojo I, Bornhäuser M, DiPersio JF, Davidson-Moncada JK, Rutella S. TP53 abnormalities correlate with immune infiltration and associate with response to flotetuzumab immunotherapy in AML. Blood Adv. 2020 Oct 27;4(20):5011-5024. doi: 10.1182/bloodadvances.2020002512. PMID: 33057635; PMCID: PMC7594389.
373. Valencia A, Masala E, Rossi A, Martino A, Sanna A, Buchi F, Canzian F, Cilloni D, Gaidano V, Voso MT, Kosmider O, Fontenay M, Gozzini A, Bosi A, Santini V. Expression of nucleoside-metabolizing enzymes in myelodysplastic syndromes and modulation of response to azacitidine. Leukemia. 2014 Mar;28(3):621-8. doi: 10.1038/leu.2013.330. Epub 2013 Nov 6. PMID: 24192812; PMCID: PMC3948159.
374. Valent P, Bain BJ, Bennett JM, Wimazal F, Sperr WR, Mufti G, Horny HP. Idiopathic cytopenia of undetermined significance (ICUS) and idiopathic dysplasia of uncertain significance (IDUS), and

their distinction from low risk MDS. Leuk Res. 2012 Jan;36(1):1-5. doi: 10.1016/j.leukres.2011.08.016. Epub 2011 Sep 13. PMID: 21920601.

375. Van Leeuwen-Kerkhoff N, Westers TM, Poddighe PJ, Povoleri GAM, Timms JA, Kordasti S, De Gruijl TD, Van de Loosdrecht AA. Reduced frequencies and functional impairment of dendritic cell subsets and non-classical monocytes in myelodysplastic syndromes. Haematologica. 2022 Mar 1;107(3):655-667. doi: 10.3324/haematol.2020.268136. PMID: 33567812; PMCID: PMC8883570.

376. Varney ME, Niederkorn M, Konno H, Matsumura T, Gohda J, Yoshida N, Akiyama T, Christie S, Fang J, Miller D, Jerez A, Karsan A, Maciejewski JP, Meetei RA, Inoue J, Starczynowski DT. Loss of Tifab, a del(5q) MDS gene, alters hematopoiesis through derepression of Toll-like receptor-TRAF6 signaling. J Exp Med. 2015 Oct 19;212(11):1967-85. doi: 10.1084/jem.20141898. Epub 2015 Oct 12. PMID: 26458771; PMCID: PMC4612089.

377. Vasu S, He S, Cheney C, Gopalakrishnan B, Mani R, Lozanski G, Mo X, Groh V, Whitman SP, Konopitzky R, Kössl C, Bucci D, Lucas DM, Yu J, Caligiuri MA, Blum W, Adam PJ, Borges E, Rueter B, Heider KH, Marcucci G, Muthusamy N. Decitabine enhances anti-CD33 monoclonal antibody BI 836858-mediated natural killer ADCC against AML blasts. Blood. 2016 Jun 9;127(23):2879-89. doi: 10.1182/blood-2015-11-680546. Epub 2016 Mar 24. PMID: 27013443; PMCID: PMC4900955.

378. Veillette A, Tang Z. Signaling Regulatory Protein (SIRP)α-CD47 Blockade Joins the Ranks of Immune Checkpoint Inhibition. J Clin Oncol. 2019 Apr 20;37(12):1012-1014. doi: 10.1200/JCO.19.00121. Epub 2019 Feb 27. PMID: 30811295.

379. Velegraki M, Papakonstanti E, Mavroudi I, Psyllaki M, Tsatsanis C, Oulas A, Iliopoulos I, Katonis P, Papadaki HA. Impaired clearance of apoptotic cells leads to HMGB1 release in the bone marrow of patients with myelodysplastic syndromes and induces TLR4-mediated cytokine production. Haematologica. 2013 Aug;98(8):1206-15. doi: 10.3324/haematol.2012.064642. Epub 2013 Feb 12. PMID: 23403315; PMCID: PMC3729900.

380. Velegraki M, Papakonstantinou N, Kalaitzaki L, Ntoufa S, Laidou S, Tsagiopoulou M, Bizymi N, Damianaki A, Mavroudi I, Pontikoglou C, Papadaki HA. Increased proportion and altered properties of intermediate monocytes in the peripheral blood of patients with lower risk Myelodysplastic Syndrome. Blood Cells Mol Dis. 2021 Feb;86:102507. doi: 10.1016/j.bcmd.2020.102507. Epub 2020 Sep 28. PMID: 33032166.

381. Velegraki M, Stiff A, Papadaki HA, Li Z. Myeloid-Derived Suppressor Cells: New Insights into the Pathogenesis and Therapy of MDS. J Clin Med. 2022 Aug 21;11(16):4908. doi: 10.3390/jcm11164908. PMID: 36013147; PMCID: PMC9410159.

382. Verma A, Suragani RN, Aluri S, Shah N, Bhagat TD, Alexander MJ, Komrokji R, Kumar R. Biological basis for efficacy of activin receptor ligand traps in myelodysplastic syndromes. J Clin Invest. 2020 Feb 3;130(2):582-589. doi: 10.1172/JCI133678. PMID: 31961337; PMCID: PMC6994157.

383. Vidal V, Robert G, Goursaud L, Durand L, Ginet C, Karsenti JM, Luciano F, Gastaud L, Garnier G, Braun T, Hirsch P, Raffoux E, Nloga AM, Padua RA, Dombret H, Rohrlich P, Ades L, Chomienne C, Auberger P, Fenaux P, Cluzeau T. BCL2L10 positive cells in bone marrow are an independent prognostic factor of azacitidine outcome in myelodysplastic syndrome and acute myeloid leukemia. Oncotarget. 2017 Jul 18;8(29):47103-47109. doi: 10.18632/oncotarget.17482. PMID: 28514758; PMCID: PMC5564547.

384. Walter MJ, Shen D, Ding L, Shao J, Koboldt DC, Chen K, Larson DE, McLellan MD, Dooling D, Abbott R, Fulton R, Magrini V, Schmidt H, Kalicki-Veizer J, O'Laughlin M, Fan X, Grillot M, Witowski S, Heath S, Frater JL, Eades W, Tomasson M, Westervelt P, DiPersio JF, Link DC, Mardis ER, Ley TJ, Wilson RK, Graubert TA. Clonal architecture of secondary acute myeloid leukemia. N Engl J Med. 2012 Mar 22;366(12):1090-8. doi: 10.1056/NEJMoa1106968. Epub 2012 Mar 14. PMID: 22417201; PMCID: PMC3320218.

385. Walter MJ, Shen D, Shao J, Ding L, White BS, Kandoth C, Miller CA, Niu B, McLellan MD, Dees ND, Fulton R, Elliot K, Heath S, Grillot M, Westervelt P, Link DC, DiPersio JF, Mardis E, Ley TJ, Wilson RK, Graubert TA. Clonal diversity of recurrently mutated genes in myelodysplastic syndromes. Leukemia. 2013 Jun;27(6):1275-82. doi: 10.1038/leu.2013.58. Epub 2013 Feb 27. PMID: 23443460; PMCID: PMC3736571.

386. Wan Y, Zhang C, Xu Y, Wang M, Rao Q, Xing H, Tian Z, Tang K, Mi Y, Wang Y, Wang J. Hyperfunction of CD4 CD25 regulatory T cells in de novo acute myeloid leukemia. BMC Cancer. 2020 May 26;20(1):472. doi: 10.1186/s12885-020-06961-8. PMID: 32456622; PMCID: PMC7249438.

387. Wang Z, Tang X, Xu W, Cao Z, Sun L, Li W, Li Q, Zou P, Zhao Z. The different immunoregulatory functions on dendritic cells between mesenchymal stem cells derived from bone marrow of patients with low-risk or high-risk myelodysplastic syndromes. PLoS One. 2013;8(3):e57470. doi: 10.1371/journal.pone.0057470. Epub 2013 Mar 4. PMID: 23469196; PMCID: PMC3587596.

388. Weber J, Salgaller M, Samid D, Johnson B, Herlyn M, Lassam N, Treisman J, Rosenberg SA. Expression of the MAGE-1 tumor antigen is up-regulated by the demethylating agent 5-aza-2'-deoxycytidine. Cancer Res. 1994 Apr 1;54(7):1766-71. PMID: 7511051.

389. Wei AH, Jacqueline S Garcia, Uma Borate, Chun Yew Fong, Maria R. Baer, Florian Nolte, Pierre Peterlin, Joseph G. Jurcic, Guillermo Garcia-Manero, Wan-Jen Hong, Uwe Platzbecker, Olatoyosi Odenike, Martin Dunbar, Ying Zhou, Jason Harb, Poonam Tanwani, Johannes E. Wolff, Meagan Jacoby; A Phase 1b Study Evaluating the Safety and Efficacy of Venetoclax in Combination with Azacitidine in Treatment-Naïve Patients with Higher-Risk Myelodysplastic Syndrome. Blood 2019; 134 (Supplement_1): 568. doi: https://doi.org/10.1182/blood-2019-124437

390. Wei Y, Dimicoli S, Bueso-Ramos C, Chen R, Yang H, Neuberg D, Pierce S, Jia Y, Zheng H, Wang H, Wang X, Nguyen M, Wang SA, Ebert B, Bejar R, Levine R, Abdel-Wahab O, Kleppe M, Ganan-Gomez I, Kantarjian H, Garcia-Manero G. Toll-like receptor alterations in myelodysplastic syndrome. Leukemia. 2013 Sep;27(9):1832-40. doi: 10.1038/leu.2013.180. Epub 2013 Jun 14. PMID: 23765228; PMCID: PMC4011663.

391. Weinberg OK, Siddon A, Madanat YF, Gagan J, Arber DA, Dal Cin P, Narayanan D, Ouseph MM, Kurzer JH, Hasserjian RP. TP53 mutation defines a unique subgroup within complex karyotype de novo and therapy-related MDS/AML. Blood Adv. 2022 May 10;6(9):2847-2853. doi: 10.1182/bloodadvances.2021006239. PMID: 35073573; PMCID: PMC9092405.

392. Welch JS, Ley TJ, Link DC, Miller CA, Larson DE, Koboldt DC, Wartman LD, Lamprecht TL, Liu F, Xia J, Kandoth C, Fulton RS, McLellan MD, Dooling DJ, Wallis JW, Chen K, Harris CC, Schmidt HK, Kalicki-Veizer JM, Lu C, Zhang Q, Lin L, O'Laughlin MD, McMichael JF, Delehaunty KD, Fulton LA, Magrini VJ, McGrath SD, Demeter RT, Vickery TL, Hundal J, Cook LL, Swift GW, Reed JP, Alldredge PA, Wylie TN, Walker JR, Watson MA, Heath SE, Shannon WD, Varghese N, Nagarajan R, Payton JE, Baty JD, Kulkarni S, Klco JM, Tomasson MH, Westervelt P, Walter MJ, Graubert TA, DiPersio JF, Ding L, Mardis ER, Wilson RK. The origin and evolution of mutations in acute myeloid leukemia. Cell. 2012 Jul 20;150(2):264-78. doi: 10.1016/j.cell.2012.06.023. PMID: 22817890; PMCID: PMC3407563.

393. Welch JS, Petti AA, Miller CA, Fronick CC, O'Laughlin M, Fulton RS, Wilson RK, Baty JD, Duncavage EJ, Tandon B, Lee YS, Wartman LD, Uy GL, Ghobadi A, Tomasson MH, Pusic I, Romee R, Fehniger TA, Stockerl-Goldstein KE, Vij R, Oh ST, Abboud CN, Cashen AF, Schroeder MA, Jacoby MA, Heath SE, Luber K, Janke MR, Hantel A, Khan N, Sukhanova MJ, Knoebel RW, Stock W, Graubert TA, Walter MJ, Westervelt P, Link DC, DiPersio JF, Ley TJ. TP53 and Decitabine in Acute Myeloid Leukemia and Myelodysplastic Syndromes. N Engl J Med. 2016 Nov 24;375(21):2023-2036. doi: 10.1056/NEJMoa1605949. PMID: 27959731; PMCID: PMC5217532.

394. Wenk C, Garz AK, Grath S, Huberle C, Witham D, Weickert M, Malinverni R, Niggemeyer J, Kyncl M, Hecker J, Pagel C, Mulholland CB, Müller-Thomas C, Leonhardt H, Bassermann F, Oostendorp RAJ, Metzeler KH, Buschbeck M, Götze KS. Direct modulation of the bone marrow

mesenchymal stromal cell compartment by azacitidine enhances healthy hematopoiesis. Blood Adv. 2018 Dec 11;2(23):3447-3461. doi: 10.1182/bloodadvances.2018022053. PMID: 30518537; PMCID: PMC6290099.

395. Westwood NB, Mufti GJ. Apoptosis in the myelodysplastic syndromes. Curr Hematol Rep. 2003 May;2(3):186-92. PMID: 12901339.

396. Williams P, Basu S, Garcia-Manero G, Hourigan CS, Oetjen KA, Cortes JE, Ravandi F, Jabbour EJ, Al-Hamal Z, Konopleva M, Ning J, Xiao L, Hidalgo Lopez J, Kornblau SM, Andreeff M, Flores W, Bueso-Ramos C, Blando J, Galera P, Calvo KR, Al-Atrash G, Allison JP, Kantarjian HM, Sharma P, Daver NG. The distribution of T-cell subsets and the expression of immune checkpoint receptors and ligands in patients with newly diagnosed and relapsed acute myeloid leukemia. Cancer. 2019 May 1;125(9):1470-1481. doi: 10.1002/cncr.31896. Epub 2018 Nov 30. PMID: 30500073; PMCID: PMC6467779.

397. Wilson A, Trumpp A. Bone-marrow haematopoietic-stem-cell niches. Nat Rev Immunol. 2006 Feb;6(2):93-106. doi: 10.1038/nri1779. PMID: 16491134.

398. Wiman KG. Pharmacological reactivation of mutant p53: from protein structure to the cancer patient. Oncogene. 2010 Jul 29;29(30):4245-52. doi: 10.1038/onc.2010.188. Epub 2010 May 24. PMID: 20498645.

399. Wimazal F, Fonatsch C, Thalhammer R, Schwarzinger I, Müllauer L, Sperr WR, Bennett JM, Valent P. Idiopathic cytopenia of undetermined significance (ICUS) versus low risk MDS: the diagnostic interface. Leuk Res. 2007 Nov;31(11):1461-8. doi: 10.1016/j.leukres.2007.03.015. Epub 2007 May 16. PMID: 17507091.

400. Wimazal F, Krauth MT, Vales A, Böhm A, Agis H, Sonneck K, Aichberger KJ, Mayerhofer M, Simonitsch-Klupp I, Müllauer L, Sperr WR, Valent P. Immunohistochemical detection of vascular endothelial growth factor (VEGF) in the bone marrow in patients with myelodysplastic syndromes: correlation between VEGF expression and the FAB category. Leuk Lymphoma. 2006 Mar;47(3):451-60. doi: 10.1080/10428190500353083. PMID: 16396768.

401. Wolf Y, Anderson AC, Kuchroo VK. TIM3 comes of age as an inhibitory receptor. Nat Rev Immunol. 2020 Mar;20(3):173-185. doi: 10.1038/s41577-019-0224-6. Epub 2019 Nov 1. PMID: 31676858; PMCID: PMC7327798.

402. Wolff F, Leisch M, Greil R, Risch A, Pleyer L. The double-edged sword of (re)expression of genes by hypomethylating agents: from viral mimicry to exploitation as priming agents for targeted immune checkpoint modulation. Cell Commun Signal. 2017 Mar 31;15(1):13. doi: 10.1186/s12964-017-0168-z. PMID: 28359286; PMCID: PMC5374693.

403. Wong KK, Hassan R, Yaacob NS. Hypomethylating Agents and Immunotherapy: Therapeutic Synergism in Acute Myeloid Leukemia and Myelodysplastic Syndromes. Front Oncol. 2021 Feb 25;11:624742. doi: 10.3389/fonc.2021.624742. PMID: 33718188; PMCID: PMC7947882.

404. Wu A, Gao P, Wu N, Shi C, Huang Z, Rong C, Sun Y, Sheng L, Ouyang G, Mu Q. Elevated mature monocytes in bone marrow accompanied with a higher IPSS-R score predicts a poor prognosis in myelodysplastic syndromes. BMC Cancer. 2021 May 13;21(1):546. doi: 10.1186/s12885-021-08303-8. PMID: 33985456; PMCID: PMC8117396.

405. Wynn TA, Chawla A, Pollard JW. Macrophage biology in development, homeostasis and disease. Nature. 2013 Apr 25;496(7446):445-55. doi: 10.1038/nature12034. PMID: 23619691; PMCID: PMC3725458.

406. Xie M, Lu C, Wang J, McLellan MD, Johnson KJ, Wendl MC, McMichael JF, Schmidt HK, Yellapantula V, Miller CA, Ozenberger BA, Welch JS, Link DC, Walter MJ, Mardis ER, Dipersio JF, Chen F, Wilson RK, Ley TJ, Ding L. Age-related mutations associated with clonal hematopoietic expansion and malignancies. Nat Med. 2014 Dec;20(12):1472-8. doi: 10.1038/nm.3733. Epub 2014 Oct 19. PMID: 25326804; PMCID: PMC4313872.

407. Xie M, Jiang Q, Xie Y. Comparison between decitabine and azacitidine for the treatment of myelodysplastic syndrome: a meta-analysis with 1,392 participants. Clin Lymphoma Myeloma Leuk. 2015 Jan;15(1):22-8. doi: 10.1016/j.clml.2014.04.010. Epub 2014 Jun 12. PMID: 25042977.
408. Xie N, Shen G, Gao W, Huang Z, Huang C, Fu L. Neoantigens: promising targets for cancer therapy. Signal Transduct Target Ther. 2023 Jan 6;8(1):9. doi: 10.1038/s41392-022-01270-x. PMID: 36604431; PMCID: PMC9816309.
409. Xiong B, Nie Y, Yu Y, Wang S, Zuo X. Reduced miR-16 levels are associated with VEGF upregulation in high-risk myelodysplastic syndromes. J Cancer. 2021 Jan 30;12(7):1967-1977. doi: 10.7150/jca.52455. PMID: 33753995; PMCID: PMC7974534.
410. Xu XQ, Wang JM, Gao L, et al. Characteristics of acute myeloid leukemia with myelodysplasia-related changes: A retrospective analysis in a cohort of Chinese patients. American Journal of Hematology. 2014 Sep;89(9):874-881. DOI: 10.1002/ajh.23772. PMID: 24861848.
411. Xu Y, Mou J, Wang Y, Zhou W, Rao Q, Xing H, Tian Z, Tang K, Wang M, Wang J. Regulatory T cells promote the stemness of leukemia stem cells through IL10 cytokine-related signaling pathway. Leukemia. 2022 Feb;36(2):403-415. doi: 10.1038/s41375-021-01375-2. Epub 2021 Aug 11. PMID: 34381181.
412. Yachoui R, Kristianto J, Sitwala K, Blank RD. Role of Endothelin-1 in a Syndrome of Myelofibrosis and Osteosclerosis. J Clin Endocrinol Metab. 2015 Nov;100(11):3971-4. doi: 10.1210/jc.2015-2729. Epub 2015 Sep 10. PMID: 26358171; PMCID: PMC5399504.
413. Yang H, Bueso-Ramos C, DiNardo C, Estecio MR, Davanlou M, Geng QR, Fang Z, Nguyen M, Pierce S, Wei Y, Parmar S, Cortes J, Kantarjian H, Garcia-Manero G. Expression of PD-L1, PD-L2, PD-1 and CTLA4 in myelodysplastic syndromes is enhanced by treatment with hypomethylating agents. Leukemia. 2014 Jun;28(6):1280-8. doi: 10.1038/leu.2013.355. Epub 2013 Nov 25. PMID: 24270737; PMCID: PMC4032802.
414. Yang X, Ma L, Zhang X, Huang L, Wei J. Targeting PD-1/PD-L1 pathway in myelodysplastic syndromes and acute myeloid leukemia. Exp Hematol Oncol. 2022 Mar 2;11(1):11. doi: 10.1186/s40164-022-00263-4. PMID: 35236415; PMCID: PMC8889667.
415. Yang, Y.;Wu, Y. The Clinical Significance of Tumor Associated Macrophages in Myelodysplastic Syndromes. Blood 2018, 132, 5505.
416. Ye J, Livergood RS, Peng G. The role and regulation of human Th17 cells in tumor immunity. Am J Pathol. 2013 Jan;182(1):10-20. doi: 10.1016/j.ajpath.2012.08.041. Epub 2012 Nov 14. PMID: 23159950; PMCID: PMC3532708.
417. Yi M, Niu M, Xu L, Luo S, Wu K. Regulation of PD-L1 expression in the tumor microenvironment. J Hematol Oncol. 2021 Jan 7;14(1):10. doi: 10.1186/s13045-020-01027-5. PMID: 33413496; PMCID: PMC7792099.
418. Yoshida K, Sanada M, Shiraishi Y, Nowak D, Nagata Y, Yamamoto R, Sato Y, Sato-Otsubo A, Kon A, Nagasaki M, Chalkidis G, Suzuki Y, Shiosaka M, Kawahata R, Yamaguchi T, Otsu M, Obara N, Sakata-Yanagimoto M, Ishiyama K, Mori H, Nolte F, Hofmann WK, Miyawaki S, Sugano S, Haferlach C, Koeffler HP, Shih LY, Haferlach T, Chiba S, Nakauchi H, Miyano S, Ogawa S. Frequent pathway mutations of splicing machinery in myelodysplasia. Nature. 2011 Sep 11;478(7367):64-9. doi: 10.1038/nature10496. PMID: 21909114.
419. Yoshizato T, Nannya Y, Atsuta Y, Shiozawa Y, Iijima-Yamashita Y, Yoshida K, Shiraishi Y, Suzuki H, Nagata Y, Sato Y, Kakiuchi N, Matsuo K, Onizuka M, Kataoka K, Chiba K, Tanaka H, Ueno H, Nakagawa MM, Przychodzen B, Haferlach C, Kern W, Aoki K, Itonaga H, Kanda Y, Sekeres MA, Maciejewski JP, Haferlach T, Miyazaki Y, Horibe K, Sanada M, Miyano S, Makishima H, Ogawa S. Genetic abnormalities in myelodysplasia and secondary acute myeloid leukemia: impact on outcome of stem cell transplantation. Blood. 2017 Apr 27;129(17):2347-2358. doi: 10.1182/blood-2016-12-754796. Epub 2017 Feb 21. PMID: 28223278; PMCID: PMC5409449.

420. You L, Han Q, Zhu L, Zhu Y, Bao C, Yang C, Lei W, Qian W. Decitabine-Mediated Epigenetic Reprograming Enhances Anti-leukemia Efficacy of CD123-Targeted Chimeric Antigen Receptor T-Cells. Front Immunol. 2020 Aug 18;11:1787. doi: 10.3389/fimmu.2020.01787. PMID: 32973749; PMCID: PMC7461863.
421. Yue J, Li J, Ma J, Zhai Y, Shen L, Zhang W, Li L, Fu R. Myeloid-derived suppressor cells inhibit natural killer cells in myelodysplastic syndromes through the TIGIT/CD155 pathway. Hematology. 2023 Dec;28(1):2166333. doi: 10.1080/16078454.2023.2166333. PMID: 36651499.
422. Yue LZ, Fu R, Wang HQ, Li LJ, Hu HR, Fu L, Shao ZH. Expression of CD123 and CD114 on the bone marrow cells of patients with myelodysplastic syndrome. Chin Med J (Engl). 2010 Aug 5;123(15):2034-7. PMID: 20819538.
423. Zeidan AM, Kharfan-Dabaja MA, Komrokji RS. Beyond hypomethylating agents failure in patients with myelodysplastic syndromes. Curr Opin Hematol. 2014 Mar;21(2):123-30. doi: 10.1097/MOH.0000000000000016. PMID: 24335709; PMCID: PMC4124617.
424. Zeidan AM, Sekeres MA, Garcia-Manero G, Steensma DP, Zell K, Barnard J, Ali NA, Zimmerman C, Roboz G, DeZern A, Nazha A, Jabbour E, Kantarjian H, Gore SD, Maciejewski JP, List A, Komrokji R; MDS Clinical Research Consortium. Comparison of risk stratification tools in predicting outcomes of patients with higher-risk myelodysplastic syndromes treated with azanucleosides. Leukemia. 2016 Mar;30(3):649-57. doi: 10.1038/leu.2015.283. Epub 2015 Oct 14. PMID: 26464171; PMCID: PMC4775363.
425. Zeidan AM, Borate U, Pollyea DA, Brunner AM, Roncolato F, Garcia JS, Filshie R, Odenike O, Watson AM, Krishnadasan R, Bajel A, Naqvi K, Zha J, Cheng WH, Zhou Y, Hoffman D, Harb JG, Potluri J, Garcia-Manero G. A phase 1b study of venetoclax and azacitidine combination in patients with relapsed or refractory myelodysplastic syndromes. Am J Hematol. 2023 Feb;98(2):272-281. doi: 10.1002/ajh.26771. Epub 2022 Nov 10. PMID: 36309981; PMCID: PMC10100228.
426. Zhang G, Yang L, Han Y, Niu H, Yan L, Shao Z, Xing L, Wang H. Abnormal Macrophage Polarization in Patients with Myelodysplastic Syndrome. Mediators Inflamm. 2021 Jul 9;2021:9913382. doi: 10.1155/2021/9913382. PMID: 34335093; PMCID: PMC8286189.
427. Zhang Q, Bi J, Zheng X, Chen Y, Wang H, Wu W, Wang Z, Wu Q, Peng H, Wei H, Sun R, Tian Z. Blockade of the checkpoint receptor TIGIT prevents NK cell exhaustion and elicits potent anti-tumor immunity. Nat Immunol. 2018 Jul;19(7):723-732. doi: 10.1038/s41590-018-0132-0. Epub 2018 Jun 18. PMID: 29915296.
428. Zhang W, Shao Z, Fu R, Wang H, Li L, Liu H. Expressions of CD96 and CD123 in Bone Marrow Cells of Patients with Myelodysplastic Syndromes. Clin Lab. 2015;61(10):1429-34. doi: 10.7754/clin.lab.2015.141240. PMID: 26642704.
429. Zhang W, Xie X, Mi H, Sun J, Ding S, Li L, Liu H, Wang H, Fu R, Shao Z. Abnormal populations and functions of natural killer cells in patients with myelodysplastic syndromes. Oncol Lett. 2018 Apr;15(4):5497-5504. doi: 10.3892/ol.2018.8062. Epub 2018 Feb 15. PMID: 29556297; PMCID: PMC5844044.
430. Zhang X, Ulm A, Somineni HK, Oh S, Weirauch MT, Zhang HX, Chen X, Lehn MA, Janssen EM, Ji H. DNA methylation dynamics during ex vivo differentiation and maturation of human dendritic cells. Epigenetics Chromatin. 2014 Aug 20;7:21. doi: 10.1186/1756-8935-7-21. PMID: 25161698; PMCID: PMC4144987.
431. Zhang Z, Li X, Guo J, Xu F, He Q, Zhao Y, Yang Y, Gu S, Zhang Y, Wu L, Chang C. Interleukin-17 enhances the production of interferon-γ and tumour necrosis factor-α by bone marrow T lymphocytes from patients with lower risk myelodysplastic syndromes. Eur J Haematol. 2013 May;90(5):375-84. doi: 10.1111/ejh.12074. Epub 2013 Mar 1. PMID: 23331180.
432. Zhao C, Jia B, Wang M, Schell TD, Claxton DF, Ehmann WC, Rybka WB, Mineishi S, Naik S, Songdej N, Sivik JM, Hohl RJ, Zeng H, Zheng H. Multi-dimensional analysis identifies an immune

signature predicting response to decitabine treatment in elderly patients with AML. Br J Haematol. 2020 Mar;188(5):674-684. doi: 10.1111/bjh.16228. Epub 2019 Oct 1. PMID: 31573077; PMCID: PMC7065206.

433. Zhao Z, Wang Z, Li Q, Li W, You Y, Zou P. The different immunoregulatory functions of mesenchymal stem cells in patients with low-risk or high-risk myelodysplastic syndromes. PLoS One. 2012;7(9):e45675. doi: 10.1371/journal.pone.0045675. Epub 2012 Sep 21. PMID: 23029178; PMCID: PMC3448671.

434. Zhao G, Wang Q, Li S, Wang X. Resistance to Hypomethylating Agents in Myelodysplastic Syndrome and Acute Myeloid Leukemia From Clinical Data and Molecular Mechanism. Front Oncol. 2021 Sep 28;11:706030. doi: 10.3389/fonc.2021.706030. PMID: 34650913; PMCID: PMC8505973.

435. Zhao LP, Boy M, Azoulay C, Clappier E, Sébert M, Amable L, Klibi J, Benlagha K, Espéli M, Balabanian K, Preudhomme C, Marceau-Renaut A, Benajiba L, Itzykson R, Mekinian A, Fain O, Toubert A, Fenaux P, Dulphy N, Adès L. Genomic landscape of MDS/CMML associated with systemic inflammatory and autoimmune disease. Leukemia. 2021 Sep;35(9):2720-2724. doi: 10.1038/s41375-021-01152-1. Epub 2021 Feb 23. PMID: 33623140.

436. Zhao LP, Schell B, Sébert M, Kim R, Lemaire P, Boy M, Mathis S, Larcher L, Chauvel C, Dhouaieb MB, Bisio V, Preudhomme C, Marceau-Renaut A, Itzykson R, Mekinian A, Fain O, Toubert A, Fenaux P, Dulphy N, Clappier E, Adès L. Prevalence of UBA1 mutations in MDS/CMML patients with systemic inflammatory and auto-immune disease. Leukemia. 2021 Sep;35(9):2731-2733. doi: 10.1038/s41375-021-01353-8. Epub 2021 Aug 3. PMID: 34344988.

437. Zheng L, Zhang L, Guo Y, Xu X, Liu Z, Yan Z, Fu R. The immunological role of mesenchymal stromal cells in patients with myelodysplastic syndrome. Front Immunol. 2022 Dec 7;13:1078421. doi: 10.3389/fimmu.2022.1078421. PMID: 36569863; PMCID: PMC9767949.

438. Zhou J, Yao Y, Shen Q, Li G, Hu L, Zhang X. Demethylating agent decitabine disrupts tumor-induced immune tolerance by depleting myeloid-derived suppressor cells. J Cancer Res Clin Oncol. 2017 Aug;143(8):1371-1380. doi: 10.1007/s00432-017-2394-6. Epub 2017 Mar 20. PMID: 28321548.

439. Zhou J, Shen Q, Lin H, Hu L, Li G, Zhang X. Decitabine shows potent anti-myeloma activity by depleting monocytic myeloid-derived suppressor cells in the myeloma microenvironment. J Cancer Res Clin Oncol. 2019 Feb;145(2):329-336. doi: 10.1007/s00432-018-2790-6. Epub 2018 Nov 13. PMID: 30426212.

440. Zhou JD, Zhang TJ, Xu ZJ, Deng ZQ, Gu Y, Ma JC, Wen XM, Leng JY, Lin J, Chen SN, Qian J. Genome-wide methylation sequencing identifies progression-related epigenetic drivers in myelodysplastic syndromes. Cell Death Dis. 2020 Nov 20;11(11):997. doi: 10.1038/s41419-020-03213-2. PMID: 33219204; PMCID: PMC7679421.

Deciphering the role of immune system dysfunction in classification and prognosis of Myelodysplastic Syndromes patients

Elena Riva, Michela Calvi, Matteo Zampini, Clara Di Vito, Lorenzo Dall'Olio, Alessandra Merlotti, Giulia Maggioni, Antonio Russo, Elena Saba, Marta Ubezio, Francesca Ficara, Laura Crisafulli, Elisabetta Sauta, Enrico Lugli, Daniel Remondini, Gastone Castellani, Domenico Mavilio and Matteo G Della Porta.

Introduction

Myelodysplastic syndromes (MDS) are a heterogeneous group of myeloid neoplasms with an increased risk of progression to acute myeloid leukemia (AML), characterized by ineffective hematopoiesis, peripheral cytopenia, genetic instability and chromosomal abnormalities [1-2]. Given the high heterogeneity of MDS, several classifications and prognostic score systems have been introduced to identify the biological subset of the disease or the prognosis of the patients. In particular, the World Health Organization (WHO)2016, WHO2022 and International Consensus Classification (ICC)2022 represent the main MDS classifications to distinguish different disease subtypes, while International Prognostic Scoring System (IPSS) Revised (-R) and the more recent IPSS Molecular (-M) are used to define the prognosis of the patients, in terms of disease progression and survival [3].

MDS pathogenesis is a complex multi-step process which can develop over many years and consists in the outgrowth and spread of a malignant hematopoietic stem cell (HSC) clone who becomes dominant in the bone marrow niche. It is actually known that this clonal expansion is the result of a complex interplay between genetic mutations, epigenetic alterations, a corrupted bone marrow microenvironment and immune system dysfunctions [4-7].

Of note, the immune profile of MDS patients dynamically changes along disease progression. Indeed, an aberrant and chronic innate immune signaling hyperactivation at a stem cell level initially set the background for MDS development, favoring myeloid skewing and genetic instability. Then, in the advanced stages of the disease, the immune contexture shifts towards an immunosuppressive environment that favor immune evasion and expansion of malignant blasts [8-12].

With the advent of high dimensional flow cytometry, that to date allows to simultaneously detect up to 50 different parameters at a single cell level, many studies have been done with the aim of characterizing both innate and adaptive immune compartments in MDS patients; however, the use of different clinical classifications for the stratification of data, the involvement of distinct patients cohorts and technical discrepancies (such as the differences in included markers, panel design and gating strategies) often leads to controversial results.

Nowadays, the use of hypomethylating agents (HMAs), azacytidine or decitabine, represents the only treatment in MDS patients with a higher risk of AML evolution who are ineligible for transplantation [13-14], and no alternative therapies are currently available in case of HMA failure [15-16]. Moreover, HMAs are not curative since they do not completely eliminate the founder clone [17-18], and only half of the patients have a hematologic response [19]. Despite the revised international prognostic scoring system (IPSS-R) and the more recent IPSS-Molecular (IPSS-M) are reliable tools to estimate the overall survival (OS) and the risk of leukemic transformation, they ineffectively predict response to therapies [20-22].

Here, we perform a comprehensive analysis of the immunologic landscape in 154 MDS and AML post MDS patients, investigating T lymphocytes, NK and myeloid cells firstly with a classical approach of manual gating, and then implementing an unsupervised pipeline for immune cells subsets analysis and the identification of groups of patients characterized by a different immune profile. We show that these groups possess prognostic power and present peculiar transcriptomic profiles of the MDS blasts and we propose a decision tree for the automatic classification of MDS patients according to their immune signature. Finally, through both manual gating and decision tree approach, we demonstrate that the response to HMA treatment correlates with the patient's immune context, before and after the therapy.

Altogether, these data further support the need of adding, to the existing scoring systems, the immune status of the patient, not only to better assess his prognosis but also to predict those individuals that will response to the HMA therapy, while evaluating different therapeutic options for the other, paving the way for a personalized management of the MDS patient.

Material and methods

Patient recruitment and sample collection

This study has been approved by the Institutional Review Boards of the Clinical and Research Institute Humanitas (Approval number 2175, AIRC IG 2018 Rif. 22053). All subjects enrolled in the study signed a written informed consent form in accordance with the Declaration of Helsinki. A total of 191 patients affected by hematological diseases, including MDS, sAML and ICUS were recruited at the Leukemia and Myelodysplasia Unit, IRCCS Humanitas Research Hospital, Rozzano, Milan, Italy. Table 1 summarizes patient's characteristics. Bone marrow (BM) and peripheral blood (PB) samples were withdrawn, by using EDTA as anticoagulant, from patients at the time of diagnosis and during the follow-up (every 4 months for patients receiving HMA treatment and every year for the others). In collaboration with the Orthopedics Hip and Prosthesis Unit, IRCCS Humanitas Research Hospital, Rozzano, Milan, Italy, we also collected BM and PB samples from 21 healthy sex and age matched individuals undergoing total hip replacement interventions. BM mononuclear cells (BMNCs) and PB mononuclear cells (PBMCs) were isolated by density gradient separation with Lympholyte®-H Cell Separation Media (Cedarlane corporation, Burlington, USA) according to manufacturer's instructions, frozen in fetal bovine serum (FBS) (Lonza, Basel, Switzerland) containing 10% Dimethyl Sulfoxide (DMSO) (Sigma Aldrich, St. Louis, Missouri, USA) and cryopreserved in liquid nitrogen. A total of 483 different timepoints were analyzed, 283 BM samples and 200 PB samples.

Flow cytometry

To minimize technical variability, flow cytometry experiments were performed in batches on frozen cells. BMMNCs and PBMCs were thawed in Roswell Park Memorial Institute-1640 (RPMI, Lonza) supplemented with 10% FBS, 1% penicillin-streptomycin (Invitrogen, Paisley, UK) and 1% L-glutamine (Lonza) containing benzonase nuclease (Sigma-Aldrich) and UltraPure EDTA (Invitrogen). After Live/Dead staining for 15 minutes at room temperature (RT) in the dark with Zombie Aqua™ Fixable viability Kit (Biolegend, San Diego, California, USA), cells were split in three different tubes and stained 30 minutes at 4°C in the dark with different mixes of fluorescent-conjugated monoclonal antibodies (mAbs), respectively specific for NK cells, Myeloid cells or T cells surface markers. All mAbs are listed in the Supplementary table 1. Every antibody lot was previously titrated on human PBMCs and used at the concentration giving the highest signal-to-noise ratio over background [23]. After extracellular mAbs staining, cells were washed with 2 mL of FACS buffer (PBS + 2%FBS) and, only for T cells panel, intracellular staining was performed using Foxp3/Transcription Factor set (eBioscience™, Thermo Fisher Scientific Inc, Massachusetts, USA), according to manufacturer's instructions. Cells stained with NK and Myeloid panels were fixed in PFA 1% for 10 minutes at RT and washed with FACS buffer. Samples were acquired at BD FACSymphonyTM A5 flow cytometer (San Jose, California, USA) and Flow Cytometry Standard (FCS) 3.0 files were analyzed using FlowJo software (version 10.9, TreeStar). The gating strategy to identify T, NK and myeloid cells is shown in Supplementary Figures 1, 2 and 3.

High-dimensional flow cytometry data analysis with Phenograph

Following the removal of debris, doublets, and dead cells, NK, CD4+ and CD8+ T cells were selected and exported from each BM sample using Flowjo, in comma separated value (CSV) files to be further analyzed in an unsupervised manner. Firstly, to have an equal contribution of cells from each sample, a downsample has been applied. In particular, the maximum number of cells per sample has been set at 5000 for CD4+ and CD8+

T cells, and 1000 for CD56+ NK cells. Then, downsampled CSV files were corrected for the batch effect exploiting the cyCombine tool using the control samples acquired in each experimental session as reference for correction [24]. In the supplementary figures is possible to see the cell clusters before and after batch correction. After the correction, CSV files were analyzed in Python (version 3.7.3) using the pipeline of PhenoGraph with the seed fixed as unsupervised method for clustering [25]. Physical and time parameters, viability dye and lineage markers were excluded from clustering and the K-value, indicating the number of nearest neighbors identified in the first iteration of the algorithm, was set at 300. PhenoGraph clusters were visualized using Uniform Manifold Approximation and Projection for Dimension Reduction (UMAP) algorithm. Different types of files were exported when the analysis finished: these include a .txt file containing the frequency of each PhenoGraph cluster in every sample, 1 CSV file per cluster containing all cells belonging to it, and 1 CSV files per each sample with the UMAP coordinates of all its cells and the PhenoGraph cluster information. Clusters representing less than 5% were excluded from the analysis and, to avoid sample-specific clusters thus not representative of the cohort, the sample composition of all clusters was checked. The CSV corresponding to the selected clusters were re-imported in FlowJo and for each of them, the frequency and the median fluorescence intensity (MFI) of positive cells for each marker were extracted and visualized in a heatmap. Moreover, these two values were used to visualize the phenotypic characteristics of the clusters through the creation of bubble plots, where the bubble diameters represent the frequency of positive cells and the bubble color intensity represents the MFI.

CD34+ Isolation from bone marrow, RNA extraction and library preparation

CD34+ cells were selected using the MACS CD34 microbead kit on autoMACS (Miltenyi Biotech Inc, San Diego, CA). A purity of >96% CD34+ cells after isolation was confirmed by flow cytometry. RNA was isolated through RNeasy Micro kit (Qiagen) according to manifacturer's protocol. RNA quality control was performed with the Agilent 2200 Tape Station system, and only RNAs having a RIN >7 were used for library preparation. Libraries for mRNA sequencing were prepared starting from 50 ng of total RNA for each sample by using the SMART-Seq v4 Ultra Low Input RNA Kit (Clontech-Takara). All samples were sequenced at an average of 20 million 75-bp single-end reads with Novaseq 2000.

Features selection and decision tree development

To identify the most relevant immunological features for the assignment to HDBSCAN groups we performed a Recursive Feature Elimination (RFE), a feature selection method – based on random forest approach - that allows to identify the most relevant features in predicting the target variable in a specific dataset (in our case, the target is to be assigned to one group over another). The method recursively removes, one by one, the weakest features until only the essential ones for the group's assignment are left, and in this way, it eliminates dependencies and redundancies that may exist in the model. After identifying the most important features for the assignment to each HDBSCAN groups, the model also creates a decision tree with the selected features. SHapley Additive exPlanations (SHAP) was then questioned to evaluate the importance of each selected feature for every cluster.

	N	Age (mean; min-max)	Sex (M;F)
All patients	191	68; 21-91	116; 75
WHO 2016			
ICUS/CCUS/ITP	37	63; 30-89	16; 21
MDS5q-	3	57; 50-68	0; 3
MDS-RS-SLD	21	73; 47-89	14; 7
MDS-RS-MLD	14	66; 46-81	12; 2
MDS-SLD	12	63; 31-91	8; 4
MDS-MLD	21	70; 37-88	19; 2
MDS-EB1	17	70; 53-91	13; 4
MDS-EB2	17	70; 58-86	12; 5
AML with MDS-related changes	49	71; 51-85	22; 27
WHO 2022			
ICUS/CCUS/ITP	37	63; 30-89	16; 21
MDS5q-	3	57; 50-68	0; 3
MDS-SF3B1	26	71; 46-87	20; 6
MDS-LB-RS	8	69; 56-89	5; 3
MDS-LB	33	68; 31-91	27; 6
MDS-IB1	16	70; 53-91	12; 4
MDS-IB2	15	70; 58-86	10; 5
MDS-biTP53	4	67; 50-73	4; 0
AML with MDS-related changes	49	71; 51-85	22; 27
ICC 2022			
ICUS/CCUS/ITP	37	63; 30-89	16; 21
MDS5q-	3	57; 50-68	0; 3
MDS-SF3B1	26	71; 46-87	20; 6
MDS NOS SLD	14	66; 31-91	9; 5
MDS NOS MLD	27	69; 37-88	23; 4
MDS-EB	16	70; 53-91	12; 4
MDS/AML	15	70; 58-86	10; 5
MDS-biTP53	2	61; 50-72	2; 0
MDS/AML-biTP53	2	72; 71-73	2; 0
AML with mutated TP53	11	75; 61-85	5; 6
AML with MDS changes	38	68; 47-83	17; 21

	N	Age (mean; min-max)	Sex (M;F)
MDS	105	69; 31-91	78; 27
IPSS-R			
Very low	20	71; 53-88	16; 4
Low	37	68; 31-91	28; 9
Intermediate	25	68; 47-89	17; 8
High	12	71; 53-91	7; 5
Very high	11	69; 50-81	10; 1
IPSS-M			
Very low	16	72; 47-91	12; 4
Low	42	67; 31-89	33; 9
Moderate low	14	71; 53-85	10; 4
Moderate high	7	71; 53-91	6; 1
High	15	69; 50-84	8; 7
Very high	11	69; 50-86	9; 2

Table 1. *List of patients included in the study classified according to (from top to bottom) WHO 2016, WHO 2022, ICC 2022, IPSS-R and IPSS-M criteria.*

Results

IPSS-R and IPSS-M risk categories do not correspond to a specific immune status of MDS patients

To conduct a first explorative evaluation of the immune cell composition in different MDS stages, we performed a manual gating on the main T, NK and Myeloid cells subpopulations and we visualized their frequencies across MDS categories by stratifying patients according to WHO 2016, WHO 2022, ICC 2022, IPSS-R and IPSS-M criteria.

T cells were identified as $CD3^+$ viable lymphocytes and, according to the expression of CD4 or CD8, helper and cytotoxic T cell populations were respectively identified (Supplementary figure 1A). According to the expression of CD45RO, CCR7, CD127, CD95 and CD25, Naïve, Central memory (Tcm), Effector memory (Tem) and Regulatory T cells (Tregs) were identified among CD4+ T cells, whereas within CD8+ T cells, Naïve, Terminal effectors (Temra) and Cytotoxic T cells were identified according to the expression of CD45RO, CCR7, CD127, CD95, CD28, GrzB and GrzK. Immune checkpoint expression was also evaluated on CD8+ Tcells (Supplementary figure 1B-C).

Among NK cells, less differentiated and cytokine producer $CD56^{bright}$ and the more differentiated and cytotoxic $CD56^{dim}$ subsets were identified according to the expression of CD56 and CD16 (Supplementary figure 2). The expression of several NK cell receptors (NKp30, NKp46, NKG2A/CD94, NKG2C/CD94, CD158b1b2j), markers of differentiation (CD57), residency/activation (CD69) and inhibition (PD1) was also evaluated.

Within myeloid compartment, we investigated different subsets of monocytes ($CD14^+$ $CD16^-$ classical monocytes, $CD14^+$ $CD16^+$ intermediate monocytes, $CD14^-$ $CD16^+$ nonclassical monocytes and the recently described $CD14^+HLA\text{-}DR^{low}$), classical dendritic cells (DCs) and the two classes of myeloid-derived suppressor cells, the monocytic (M-MDSCs) and the granulocytic/polymorphonuclear (PMN-MDSCs) (Supplementary figure 3).

To focus on the immunological changes along the natural course of MDS, we started by analyzing only BM samples collected at diagnosis or evolution, before any treatment with HMAs. Immune cell population frequencies and phenotype for T, NK and myeloid cells are respectively reported in the main figures 1, 2 and 3 using the ICC 2022 classification, whereas the comparison between all the classification systems for each immune population is reported in supplementary figures 4, 5 and 6 as indicated.

Total $CD3^+$ T cell frequency was decreased in AML post MDS compared to HC and MDS patients in all classifications and also in $SF3B1^{mut}$ MDS (WHO 2022, ICC 2022) or MDS with Ring Sideroblast (MDS-RS) in WHO 2016 compared to other MDS categories (Figure 1A, Supplementary figure 4A). However, with IPSS-R and IPSS-M these differences among MDS patients were no more observable, probably because $SF3B1^{mut}$/MDS-RS patients are split across very low/low/mid-low risk categories (Supplementary figure 4A). MDS-RS/$SF3B1^{mut}$ MDS patients were also marked by the decreased frequency of CD4 Naïve and CD8 terminal effectors and an increased frequency of $CD4^+$ central memory, $CD8^+$ effector memory, $CD8^+$ cytotoxic and $CD8^+$ expressing the checkpoint inhibitors $PD1^+$ $TIGIT^+$ (Figure 1 B-F, Supplementary figure 4 B, D, E-H). As before, IPSS-R and IPSS-M were not able to reproduce all these features. In WHO 2016, WHO 2022 and ICC 2022, Tregs showed a wave trend, increasing in ICUS/CCUS compared to HC, decreasing in $SF3B1^{mut}$/MDS-RS and significantly increasing again in MDS EB/IB, MDS/AML, MDS $TP53^{mut}$ and AML post MDS (Figure 1G, Supplementary figure 4C). This increase was also observable in intermediate, high-risk and very-high risk IPSS-R categories and in very-high risk IPSS-M category. $CD8^+$ terminal effectors cells were increased in all disease categories, except in MDS-RS/$SF3B1^{mut}$ MDS, compared to HC, while $CD8^+$ Naïve T cells were instead decreased (Figure 1D and Supplementary figure 4I). $TIM3^+$ $CD8^+$ T cells were significantly increased in

ICUS/CCUS, AML post MDS and TP53^{mut} MDS compared to HC and in high-risk and very-high risk MDS compared to low and very-low MDS in IPSS-R and IPSS-M (Figure 1I and Supplementary figure 4L).

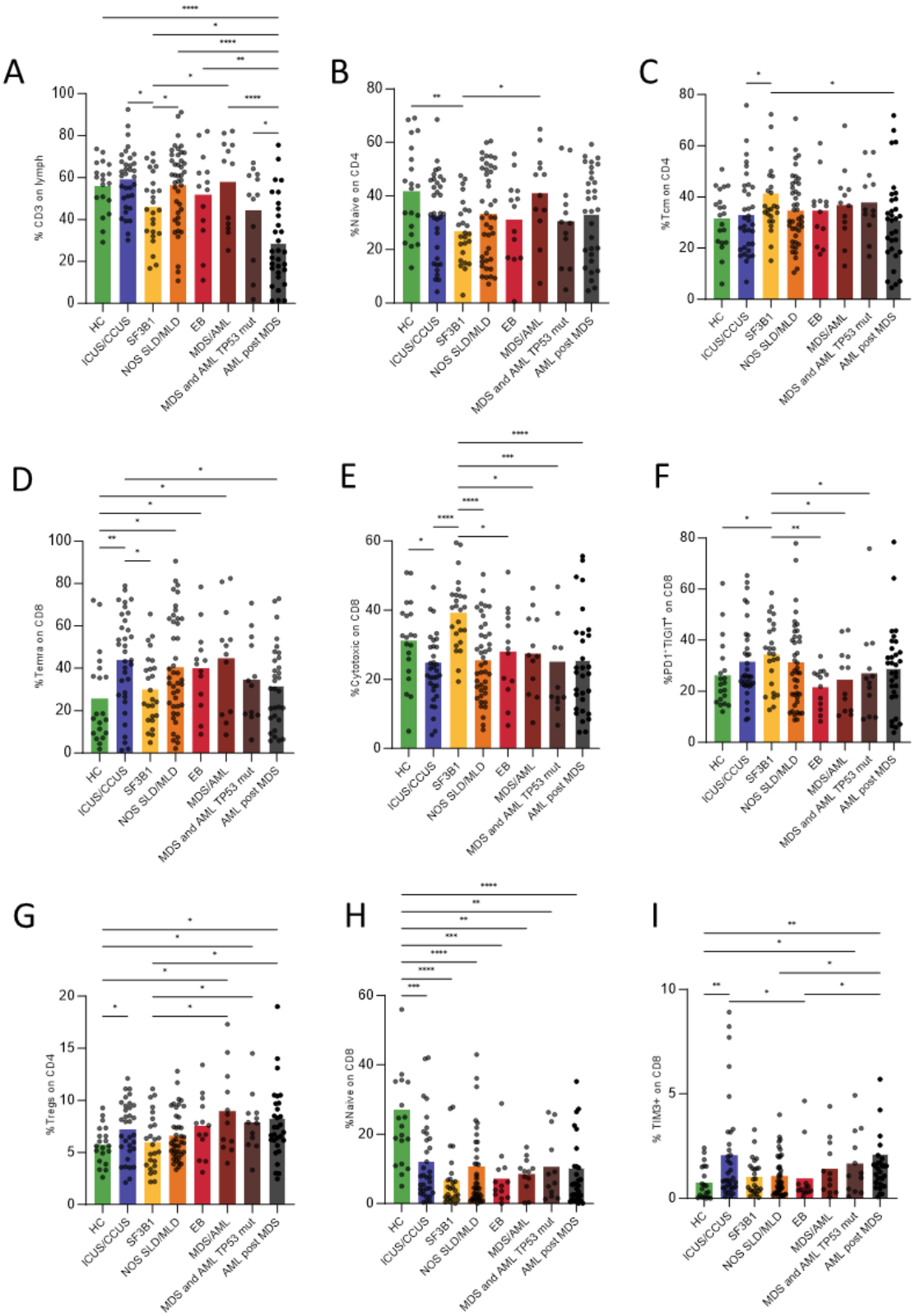

Figure 1. T cells subpopulations frequencies on bone marrow samples collected at diagnosis or at disease evolution, before HMA treatment*. The bar graphs show the frequency of a specific T cell subpopulation (indicated on the Y axis) across the ICC2022 disease categories. Mann Whitney U test was used to compare groups and significance was set at a P value less than .05.*

Focusing on NK cells, the total frequency of NK was decreased in MDS/AML and in AML post MDS categories in WHO 2016, WHO 2022 and ICC 2022 (Figure 2A). Within these classifications, less differentiated $CD56^{bright}$ NK cells were increased in $SF3B1^{mut}$/MDS-RS, MDS EB/IB and MDS/AML at the expense of more differentiated $CD56^{dim}$ NK cells, that were instead decreased (Figure 2B-C). As for T cells, IPSS-M and IPSS-R poorly captured such features, only showing a decrease of NK in high IPSS-M risk category, and an increase of $CD56^{bright}$ counterbalanced by a decrease of $CD56^{dim}$ NK cells in very high IPSS-M group (Supplementary Figure 5A-C). Moreover, looking at the phenotype of NK cells, patients classified as EB, MDS/AML, $TP53^{mut}$ MDS and AML post MDS, showed a decreased expression of CD69, a marker involved in activation/homing, NCRs (NKp30 and NKp46) involved in target recognition, NKG2A essential for NK cell licensing and a higher expression of the checkpoint inhibitor PD1 (Figure 1D-H).

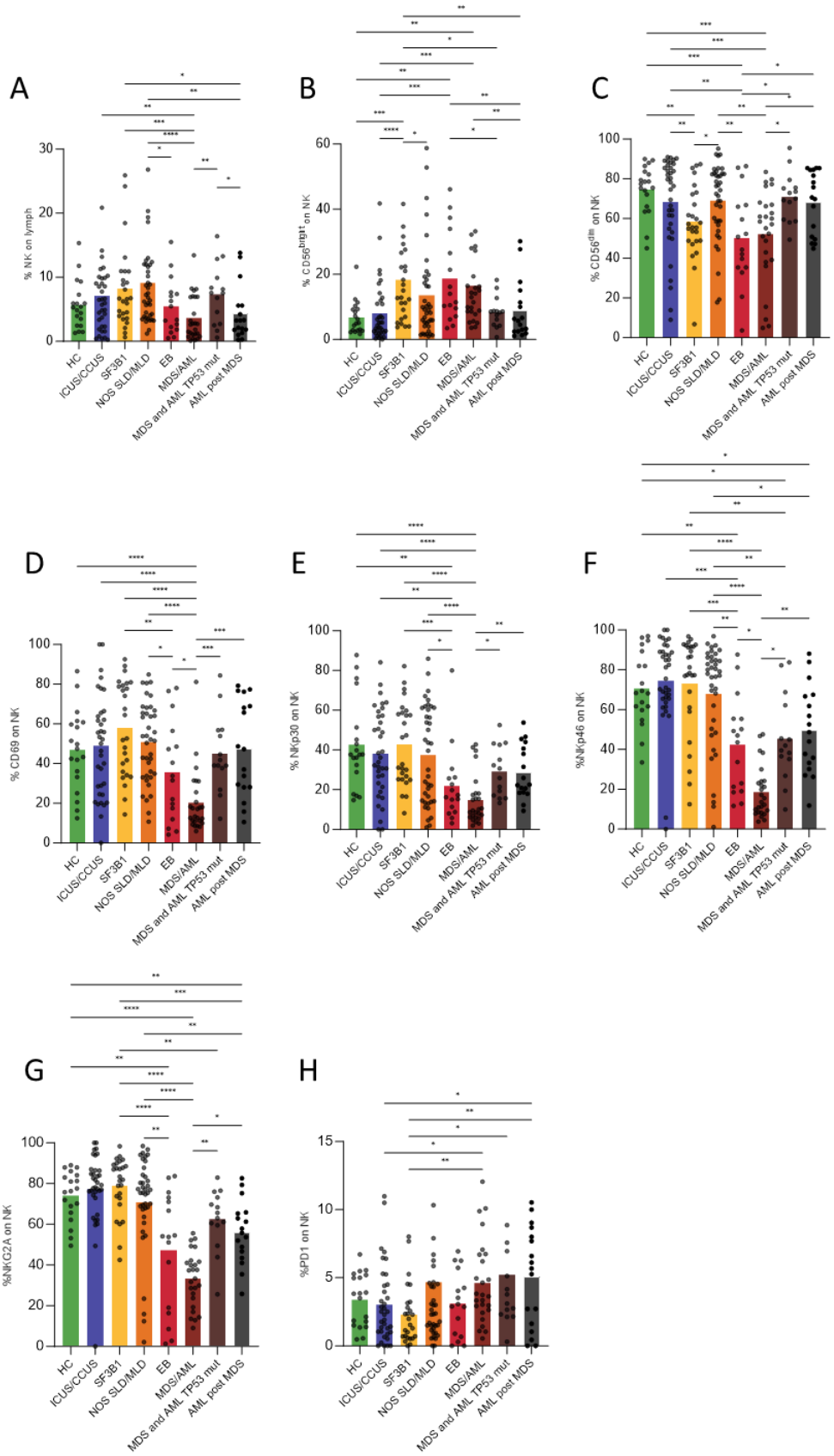

Figure 2. NK cells subpopulations frequencies on bone marrow samples collected at diagnosis or at disease evolution, before HMA treatment*. The bar graphs show the frequency of a specific NK cell subpopulation (indicated on the Y axis) across the ICC2022 disease categories. Mann Whitney U test was used to compare groups and significance was set at a P value less than .05.*

Moving to myeloid compartment, classical monocytes frequency decreased in MDS EB/IB, MDS/AML, MDS TP53^{mut} and AML post MDS (Figure 3A, Supplementary Figure 6A). This decrease was also observable in very high IPSS-R and IPSS-M risk categories (Supplementary Figure 6A). By contrast, dendritic cells displayed an opposite trend, increasing in MDS EB/IB, MDS/AML, MDS TP53^{mut} and AML post MDS (Figure 3E, Supplementary Figure 6E). DCs significantly increased only in high-risk IPSS-R category, while showed a not significant increasing trend in very-high IPSS-M categories (Supplementary Figure 6E). Intermediate monocytes (iMono) were risen in MDS/AML, MDS TP53^{mut} and AML post MDS in WHO 2016, WHO2022 and ICC 2022 classification and in very-high risk IPSS-R category (Figure 3B, Supplementary Figure 6B). Nonclassical Monocytes (ncMono) were instead decreased in all disease groups compared to HC except for MDS EB/IB, MDS/AML, MDS TP53^{mut} and AML post MDS, and showed higher frequency in IPSS-R very high and IPSS-M high and very high categories (Figure 3C, Supplementary Figure 6C). Monocytes with low expression of HLA-II molecules (HLA-DR^{low} mono) were uniquely increased in SF3B1^{mut}/MDS-RS, in MDS+AML mutated for TP53 gene (Figure 3D, Supplementary Figure 6D). In the end, immunosuppressive PMN-MDSCs showed higher frequency in MDS EB, MDS TP53^{mut}, AML post MDS and high-risk IPSS-R, while M-MDSCs were increased in SF3B1^{mut}/MDS-RS, MDS+AML TP53^{mut} classes and low-risk category in both IPSS-R and IPSS-M (Figure 3F-G, Supplementary Figure 6F-G).

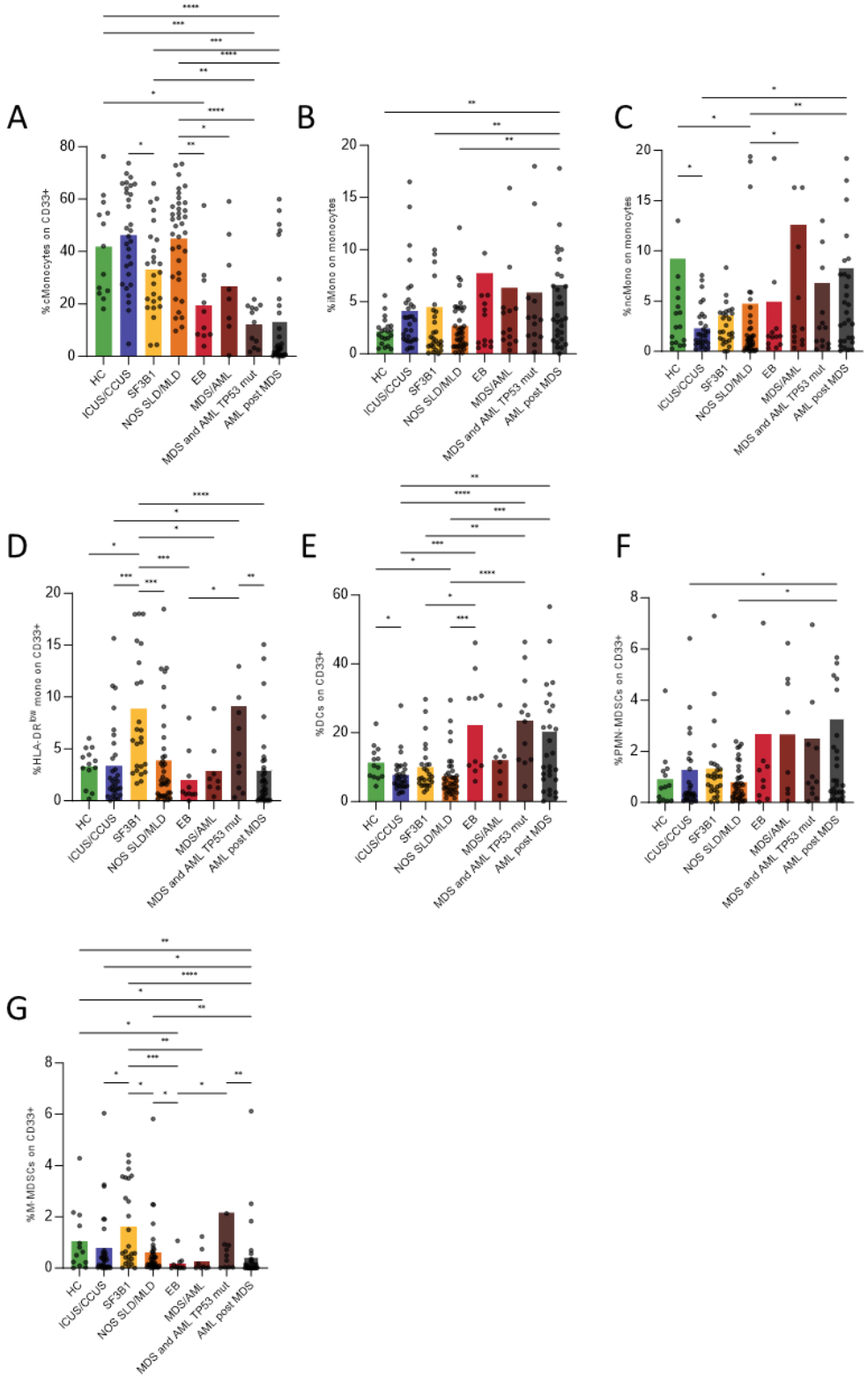

Figure 3. Myeloid cells subpopulations frequencies on bone marrow samples collected at diagnosis or at disease evolution, before HMA treatment*. The bar graphs show the frequency of a specific Myeloid subpopulation (indicated on the Y axis) across the ICC2022 disease categories. Mann Whitney U test was used to compare groups and significance was set at a P value less than .05.*

Peripheral blood recapitulates most of the bone marrow immunological features

We then evaluated whether PB can reflect the alterations of the immune microenvironment observed in the BM. To do so we performed the same analysis on PB samples collected at the time of diagnosis together with BM.

PB samples were able to recapitulate great part of T cells features such as the decrease of CD3+ T cells in AML and naïve CD8 T cells in all disease stages compared to HC, the increase of TIM3+ T cells in ICUS/CCUS, AML post MDS and TP53^{mut} MDS, and all the SF3B1^{mut}/MDS-RS peculiarities previously mentioned (Supplementary figure 7A-L). Tregs were significantly increased only in AML and ICUS/CCUS samples but not in MDS EB/IB and high-risk categories (Supplementary figure 7C).

In peripheral blood it was possible to observe the decrease of total NK cell frequency in MDS with EB/IB, MDS/AML and AML post MDS (Supplementary Figure 8A). PB samples were also able to recapitulate the altered balance between CD56^{bright} and CD56^{dim} in SF3B1^{mut}/MDS-RS, EB/IB and in AML post MDS (Supplementary Figure 8B,C). The altered NK cell phenotype, in terms of NCR, NKG2A, CD69 and PD1 expression remained detectable too in PB of MDS EB/IB, MDS/AML, TP53^{mut} MDS and AML.

Also in myeloid compartment, PB reflected most of the BM features such as the decrease of monocytes in MDS EB/IB, MDS/AML and AML post MDS accompanied with dendritic cells increase, and the increased frequency of HLA-DR^{low} monocytes in SF3B1^{mut}/MDS-RS and MDS and AML TP53^{mut} (Supplementary Figure 9A, D-E). PB recapitulated also iMono and ncMono observed in bone marrow (Supplementary Figure 9B-C). However, both PMN-MDSCs and M-MDSCs were not detectable.

Some immune cell subpopulations follow HMA treatment response and are correlated with patient's survival

Subsequently, we evaluated the variations of all immune subpopulations before and after the treatment with HMA, stratifying patients according to the clinical response in order to understand the effect of the therapy on immune cell subpopulations and to find putative predictive signatures. In particular, MDS patients were divided in complete remissions (CR), stable diseases (SD) and AML evolutions, whereas for AML patients we separated complete remissions from non-responses (NR) or AML relapses.

Focusing on T cell compartment, the frequency of total CD3$^+$, Tregs and Central memory followed the clinical response to HMA treatment in both BM and PB compartments. In particular, CD3$^+$ T lymphocytes and CD4+ central memory T cells increased in MDS and AML with CR and decreased in AML evolutions, non-responses and relapses compared to pre-treatment samples (Figure 4A-B and Supplementary figure 10A-B). By contrast, Tregs decreased in MDS and AML CR and in MDS SD, while increased in AML evolution, NR and relapse cases (Figure 4C and Supplementary figure 10C).

Also the longitudinal analysis, comparing BM pre-treatment and post-treatment samples of each patient, showed that Tregs faithfully followed treatment response, with an increasing trend in relapse, progression or non-response cases, a stable rate in stable disease timepoints and a decreased frequency in CR and long CR timepoints (Figure 4D). Similar results were observed following Tregs frequencies in longitudinal PB samples (Supplementary Figure 10F). CD3$^+$ frequencies in sequential samples from single patients showed too a coherent trend with the treatment response in both BM and PB compartments (data not shown).

We thus wondered if the rate of Tregs and CD3$^+$ at diagnosis were related to prognosis of the patients. Thus, the median value of CD3 and Tregs frequencies were calculated on all MDS pre-HMA bone marrow samples and patients were divided in lower or higher frequencies than each cell median value. We found that the median value of Tregs (= 6.5% on CD4$^+$ T cells), but not the one of CD3, significantly divided patients according

to overall survival (OS), where patients with a higher frequency displayed a worse prognosis ($p<0.05$, Figure 4E). However, this result was not reproducible in PB compartment (Supplementary figure 10G).

NK cells did not show any significant change upon treatment with hypomethylating agents in high-risk MDS bone marrow and peripheral blood samples, while AML post-HMA with CR showed an increased NK frequency compared to the pre-HMA timepoints in both BM and PB compartments (Figure 4F and Supplementary figure 10F). NK cell frequency also significantly decreased in bone marrow samples of patients who experienced a post-HMA AML evolution and relapse. We thus calculated the NK frequency median value on both PB and BM MDS samples and, only in peripheral blood, the NK median frequency (=6.5% on lymphocytes) significantly stratified patients for their OS (*$p>0.05$, Supplementary Figure 10I).

Inside Myeloid compartment, classical monocytes and dendritic cells exhibited peculiar behaviors in BM following HMA treatment; in particular, monocytes increased in AML patients with CR compared to the pre-treatment samples and decreased in the other cases (Figure 4F), whereas DCs displayed instead the opposite trend (Figure 4G). These results were reproducible in PB (Supplementary Figure 10D-E) Also in this case, we determined the median frequency of both populations in the BM and we found that only the median frequency value of monocytes at diagnosis (=21.9% on CD33+ myeloid cells) was significantly correlated with prognosis and patients with higher frequency of monocytes showed a better survival compared to those with lower frequency (Figure 4H). As for Tregs, also the frequency of monocytes in PB did not significantly divided patients according to OS, even if a trend is visible (Supplementary Figure 10H).

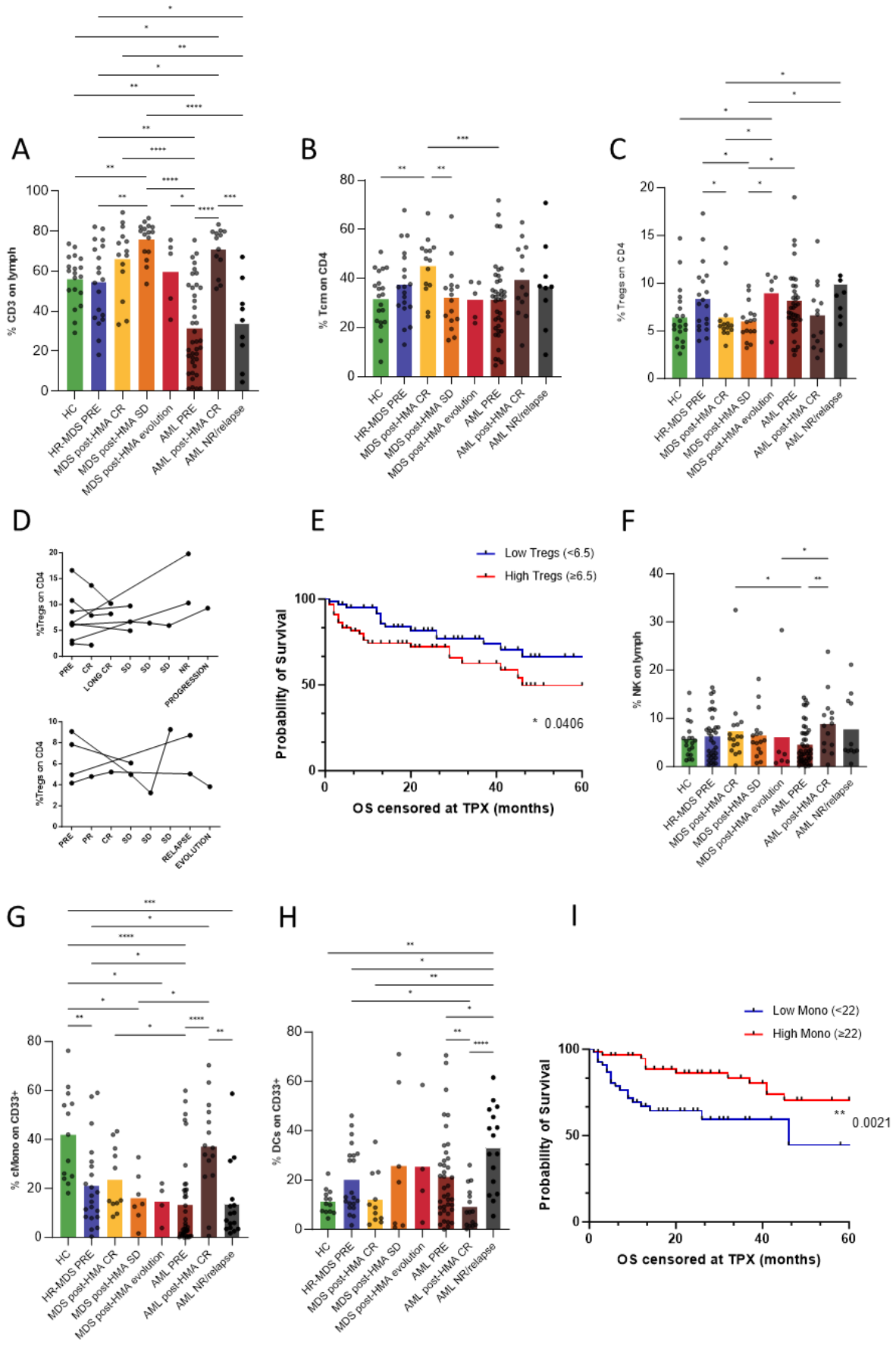
A
% CD3 on lymph
B
% Tem on CD4
C
% Tregs on CD4
HC
HR-MDS PRE
MDS post-HMA CR
MDS post-HMA SD
MDS post-HMA evolution
AML PRE
AML post-HMA CR
AML NR/relapse
D
%Tregs on CD4
PRE
CR
LONG CR
SD
SD
SD
NR
PROGRESSION
%Tregs on CD4
PRE
PR
CR
SD
SD
SD
RELAPSE
EVOLUTION
E
Low Tregs (<6.5)
High Tregs (≥6.5)
Probability of Survival
* 0.0406
OS censored at TPX (months)
F
% NK on lymph
G
% cMono on CD33+
H
% DCs on CD33+
I
Low Mono (<22)
High Mono (≥22)
Probability of Survival
** 0.0021
OS censored at TPX (months)

***Figure 4. Pre- and Post-HMAs cell frequencies comparison in bone marrow**. A-C) Bar graphs showing the frequency of CD3 on lymphocytes, CD4 central memory on total CD4 and Tregs on total CD4, respectively, in the bone marrow of High-risk and AML post MDS patients before and after the treatment with HMAs. The post-treatment samples are stratified according to clinical response. D) Tregs frequencies measured along longitudinal samples (pre- and post-HMA). Each line represents a patient and each dot a specific timepoint. E) Kaplan-Meier showing the OS of patients divided for higher or lower %Tregs than the median Treg frequency value calculated on MDS bone marrow samples at diagnosis (median = 6.5). *p<0.05. F-G) Bar graphs depicting the frequency of classical Monocytes and dendritic cells on total myeloid cells ($CD33^+$), in the bone marrow of High-risk and AML post MDS patients before and after the treatment with HMAs. H) Kaplan-Meier showing the OS of patients divided for higher or lower %Monocytes than the median monocytes frequency value calculated on MDS bone marrow samples at diagnosis (median = 22). **p<0.01. For all bar graphs, Mann Whitney U test was used to compare groups and significance was set at a P value less than .05. For Kaplan-Meier curves, log-rank test was performed to assess statistical significance.*

Unsupervised clustering of MDS patients based on T and NK cells features identified different immunologically characterized groups with prognostic power

To gain more insight in the high complexity of T and NK cell panels, we decided to proceed with a multidimensional analysis of all BM samples (both at diagnosis and post-HMAs) using the unsupervised Phenograph clustering algorithm. We tested different values of k-nearest neighbors (K) for their capacity to identify different numbers of non-redundant cell subpopulations possessing a phenotype in accordance with biological knowledge. We selected a K = 300 as the best value for identifying CD4, CD8 and NK cells subpopulations. With this K value, Phenograph identified 13 CD4+ T, 12 CD8+ T and 11 NK cell clusters (Supplemenrary Figures 11-13). CD4+ clusters number 11 and 12 and NK cluster 10 were excluded because with a frequency <5%, whereas for all the others we proceeded with cluster annotation according to marker expression, as described in the material and methods section. Phenograph algorithm was able to recognize the main T and NK subpopulations identified with manual gating, plus additional ones.

Within NK cell compartment, Phenograph algorithm was able to recapitulate NK cell differentiation. In particular, it identified three clusters of less differentiated resident $CD56^{bright}$, three clusters of maturing $CD56^{dim}$ expressing NKG2A, two clusters of mature NKG2A-CD57- $CD56^{dim}$ and two clusters of terminally differentiated CD57+ $CD56^{dim}$ NK cells, with or without the expression of NCRs, NKG2C and KIR receptors (Figure 5A).

Among CD4+ T cells, Phenograph identified one cluster of T stem cell memory (Tscm), one cluster of Tissue Resident Memory (Trm), two clusters of Naïve T cells with different CD127 expression, one Tregs and one Terminal effector cluster, two clusters of Central memory and three clusters of effector memory with different expression of PD1 (Figure 5B). Inside CD8+ T cells were identified three different Terminal effector and Effector memory subpopulations, and one cluster each of Mucosal-associated invariant T cells (MAIT), Naïve, NKG2A+, Effector/Antigen-activated, Exhausted and Granzyme B-K double positive T cells (Figure 5C).

Importantly, both the frequencies and trends of the main cell populations identified with manual gating were reproducible by the correspondent Phenograph clusters, thus validating the results and the assigned biological interpretation (Supplementary Figure 14).

A) NK Phenograph clusters

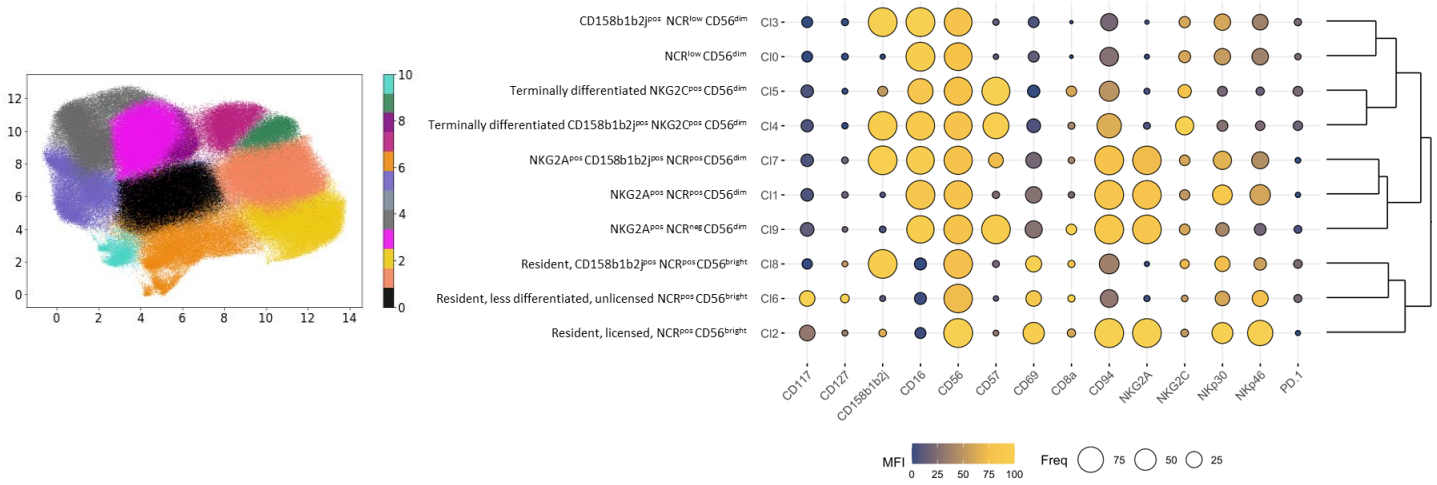

B) CD4+ T cells Phenograph clusters

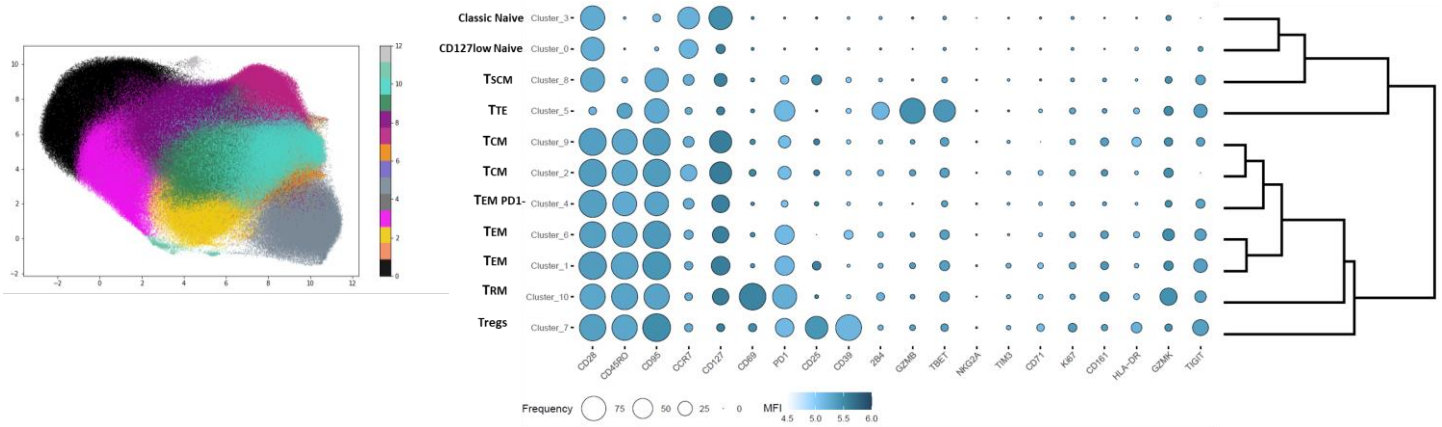

C) CD8+ T cells Phenograph clusters

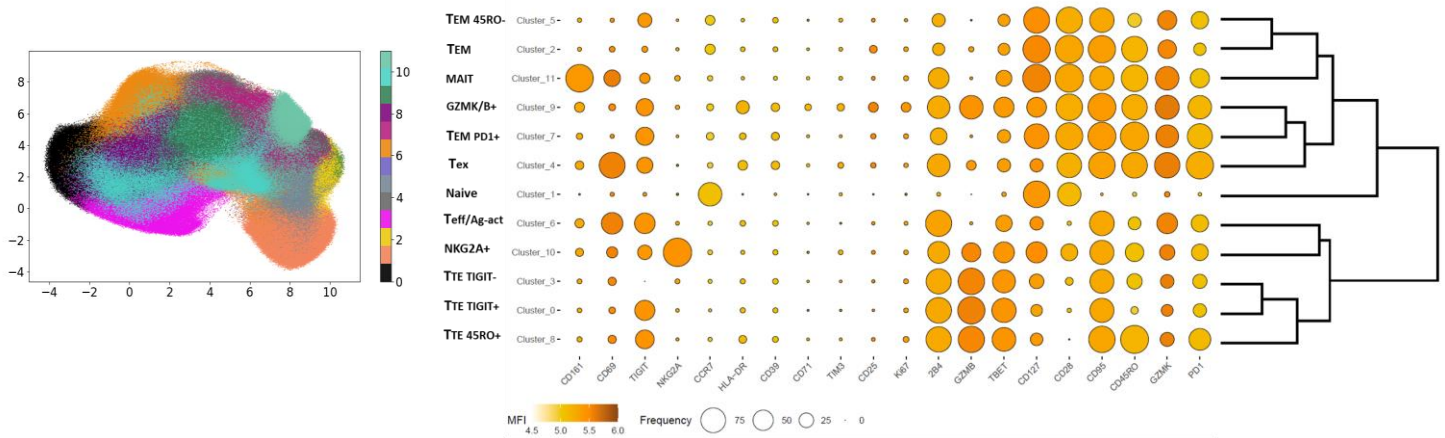

Figure 5. NK, CD4 and CD8 Phenograph clusters annotation*. The Phenograph analysis on A) NK cells B) CD4+ T cells and C) CD8+ T cells is shown. For each cell compartment, all clusters are reported in UMAP data reduction (on the left), and their biological interpretation is shown in bubble plots (on the right) with hierarchical metaclustering to show clusters with similar immunophenotypes.*

Given these premises, we wonder if starting with the immunologic signature of patients from our cohort, we were able to identify different groups characterized by similar immunological dysfunction and clinical features. To do so, after creating a matrix with all NK, CD4 and CD8 Phenograph cluster frequencies, we analyzed it performing an unsupervised clustering of all pre-HMAs BM samples (excluding ICUS/CCUS and HC) through Hierarchical Density-Based Spatial Clustering of Applications with Noise (HDBSCAN). The algorithm identified seven groups of patients marked by similar CD4, CD8 and NK cell Phenograph cluster frequencies (Supplementary Figure 15A): group -1 (composed by 10 patients), group 0 (n=25), group 1 (n=20), group 2 (n=26), group 3(n=19), group 4 (n=10), group 5 (n=24). Group -1 included all the samples not assigned to any of the other groups and thus was excluded from the analysis. For any other group we proceeded with deeper investigation of the immunological features by extracting the average frequencies of each CD4, CD8 and NK cells cluster (Supplementary Figure 15B-G) and their expression of functional and inhibitory markers (Supplementary Figure 16A-C).

To dissect the immune features of each HDBSCAN group, the frequencies of similar CD4, CD8 or NK Phenograph clusters in every patient were merged by arithmetic sum and the average frequency of immune subpopulations of all patients in the same group was calculated. In particular, for T cells, we merged CD4 Naïve clusters 0 and 3, CD4 Central memory clusters 2 and 9, CD4 effector memory clusters 1, 4 and 6, CD8 terminal effectors clusters 0, 3 and 8, CD8 effector memory clusters 2, 5 and 8. For NK cells, we merged NKG2A+ $CD56^{dim}$ clusters 1, 7 and 9, $NKG2A^{-}$ $CD57^{-}$ $CD56^{dim}$ clusters 0 and 3, and terminally differentiated $CD57^{+}$ $CD56^{dim}$ clusters 4 and 5.

The overall immune panorama of each patient group is summarized in Figure 6A, while the statistics of each immune cell subpopulation for every HDBSCAN group is reported in Supplementary Figure 17. HDBSCAN group 0 was characterized by high frequency of CD4 and CD8 terminal effectors at the expense of Naïve T cells, high Tregs but low T exhausted. Terminally differentiated NK cells with high expression of PD-1, NKG2C and CD8a were enriched, while mature $CD56^{dim}$ NK were decreased and showed low NCR expression. We thus decided to rename the group as “Activated T and NK cells, but immunosuppressed”. Group 1 showed even worse impaired immune environment, with high CD4 and CD8 terminal effector T cell, low Naïve, high Tregs and CD8 GRZB/K double positive T cells and very high T exhausted. Also NK cell compartment was severely compromised, characterized by elevated frequency of less differentiated $CD56^{bright}$ NK at the expense of mature $CD56^{dim}$ and terminally differentiated NK, which also expressed low NCRs and NKG2C. This group was then renamed “Exhausted and immunosuppressed”. Group number 2 was instead characterized by high frequency of CD4 and CD8 Naïve T cells at the expense of terminally differentiated ones, low Tregs, high MAIT, high less differentiated $CD56^{bright}$ NK at the expense of terminally differentiated NK, indicating an immune environment similar to healthy condition, and thus we named it “Naïve”. HDBSCAN group 3 was mostly enriched in CD4 and CD8 central and effector memory T cells, with low Naïve and terminal effector T cells but high antigen-activated, indicative of an activated and functional immune system with an expanded memory compartment. NK cells were characterized by high frequency of $CD56^{bright}$ NK and maturing $CD56^{dim}$ expressing NKG2A. This group was renamed as “Memory and activated”. In the end, groups 4 and 5 were observed to be very similar, both characterized by mid-high levels of CD4 and CD8 Naïve, high CD8 effector memory and terminal effector T cells, very low antigen-activated and MAIT. NK cells showed a terminally differentiated phenotype with high PD1, CD8a and NKG2C at the expense of mature $CD56^{dim}$ NK, which expressed low levels of NCRs. We thus decided to consider these two groups as unique one, characterized by less differentiated and inactivated T cells and dysfunctional terminally differentiated NK cells and we called it “Not activated”.

Interestingly, OS reflected the immune status of the groups (Figure 6A, Kaplan-Meier curve on the right of each group): this was even more evident in all OS curves together (Figure 6B), where is possible to see that the “exhausted and immunosuppressed” group shows the worse outcome, followed by the “activated immunosuppressed” and the “not activated” ones, while the other two groups, characterized by a functional

or healthy-similar immune system, display a good prognosis. Moreover, the three dysfunctional groups also comprise most of the disease evolution events, in particular group 1 (Supplementary Figure 18A).

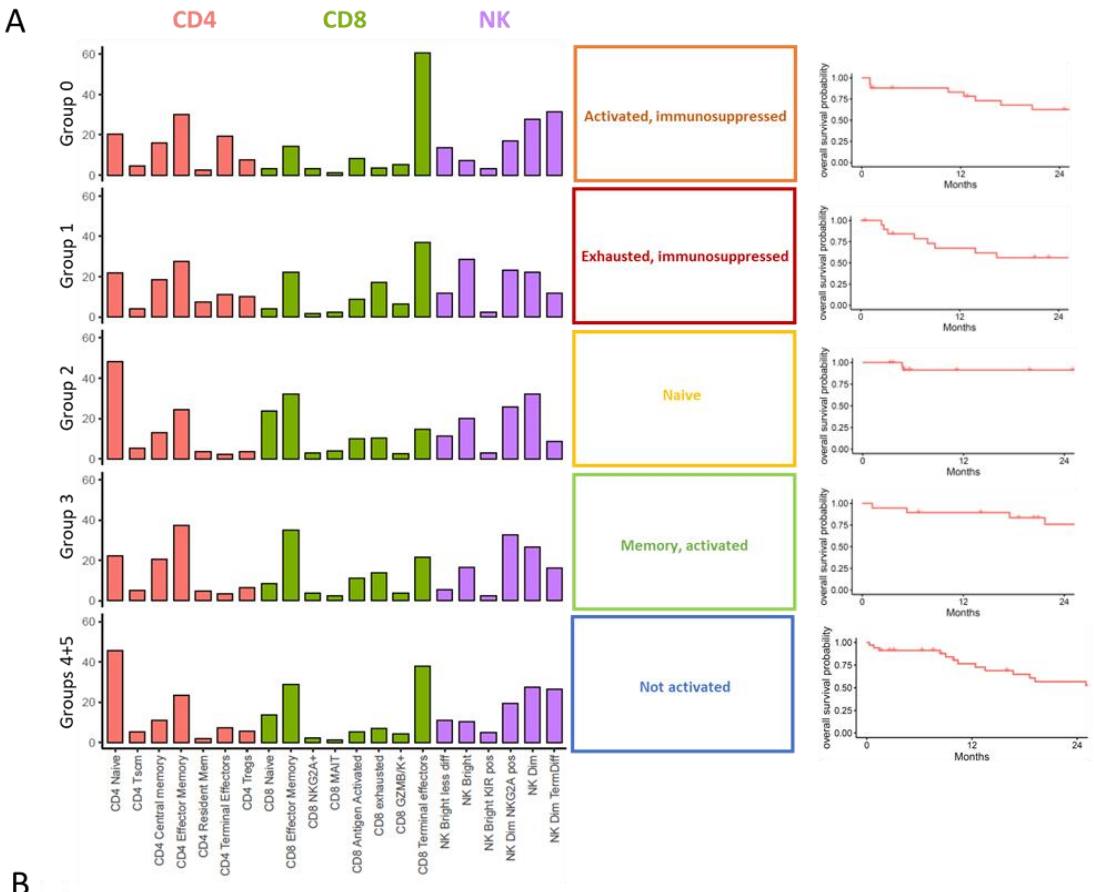

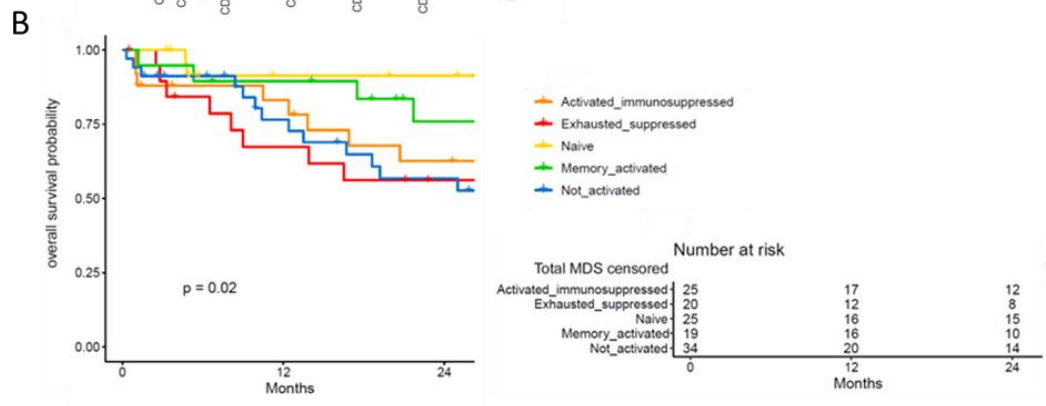

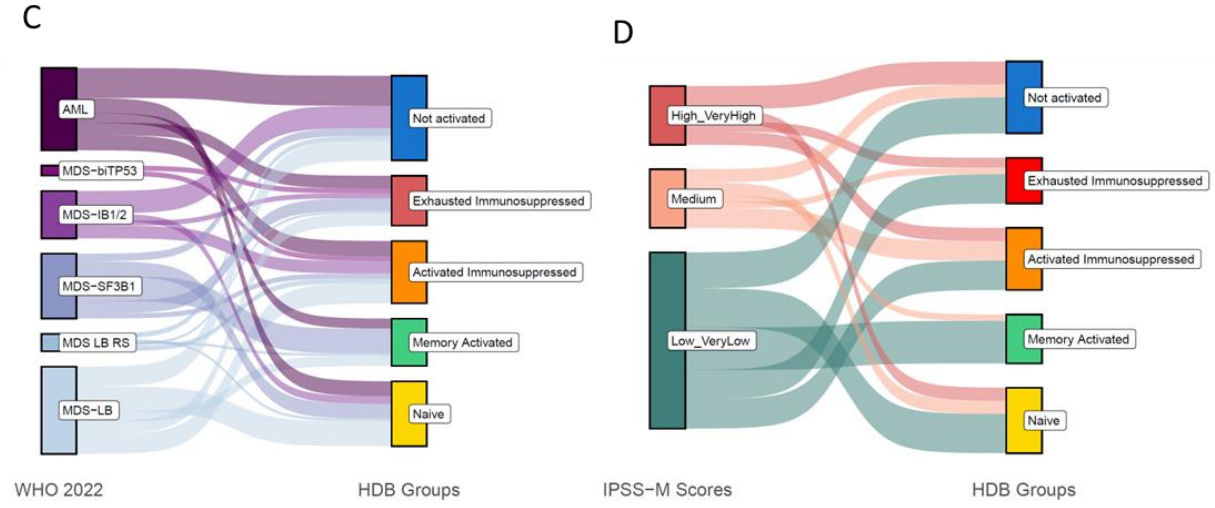

Figure 6. Immune features of HDBSCAN groups and correlations with clinical parameters and current classifications*. A) Bar graph depicting the average frequency of each CD4, CD8 and NK cell Phenograph cluster in patient's group identified through HDBSCAN algorithm. Groups 4 and 5 were merged for their similarities in immune composition. In the box is reported the summary "immune tag" of the group. On the right is shown the Kaplan-Meier curve of patients belonging to the specific group. B) Kaplan-Meier curve of all HDBSCAN groups C-D) Sankey diagrams showing the re-distribution of patients from their original WHO2022 class or IPSS-M risk category to the immune group.*

Using a univariate cox proportional hazards model, we found that the "Activated immunosuppressed", "Exhausted Immunosuppressed" and "Not activated" groups possess a significantly higher risk of death than Naïve group (*p<0.05, **p<0.01, *p<0.05), confirming what observed with Kaplan-Meier curves Supplementary Figure 18B). We did the same type of analysis also considering the single CD4, CD8 and NK cell subpopulations and we observed that the cells clusters enriched in HDB groups 0, 1 and 4+5 were mostly assigned to a higher hazard ratio compared to cell clusters enriched in HDB groups 2 and 3 (Supplementary Figure 18 C-E).

We subsequently checked how patients were re-stratified in those immune groups from their original WHO2022 class, ICC2022 class, IPSS-M or IPSS-R risk category (Figure 6 C-D, Supplementary Figure 18 F-G). Great part of the AML post MDS fell in the "not activated" group while the rest was mostly distributed in the "exhausted immunosuppressed" and in the "activated immunosuppressed", and only a small part in the "Naïve" and "Memory and Activated" ones. Half of MDS biTP53 was relocated in the "exhausted and immunosuppressed" class and the other half in the "activated but immunosuppressed", confirming the high grade of immune dysfunction and suppression associated to TP53 mutations described in literature [26-28]. MDS IB1/2 for WHO22 and MDS EB for ICC22 showed two major branches: one converging to the "not activated" group and one to the "activated but immunosuppressed". MDS/AML in ICC22 were mostly relocated to "Not Activated" group, underlining their similarity with AML. MDS SF3B1^{mut} mostly fell in the "Memory and activated" group, while MDS-LB for WHO22 and MDS NOS SLD/MLD for ICC22 were in great part connected to the "Naïve" group.

For IPSS-M and IPSS-R, high/very high categories were relocated in the three dysfunctional immune groups "exhausted and immunosuppressed", "not activated" and "activated but immunosuppressed". The majority of the Intermediate IPSS-R and mid-low/mid-high IPSS-M categories were partitioned into the "activated immunosuppressed" and then equally disseminated between "not activated", "memory activated" and "Naïve", while only few of them in the "exhausted immunosuppressed". In the end, half of very-low/low risk categories fell in the two immune categories with good prognosis (naïve and memory activated), while the other half is distributed between the other three categories with immunological dysfunction and worse survival. Taken together, these results demonstrate that immune features characterization represents an additional layer providing further prognostic information that can refine MDS classification.

Transcriptome analysis of MDS tumor cells revealed distinct inflammatory signatures associated with immunologic groups

Bulk RNAseq was performed on magnetically sorted CD34^{+} cells on 86 out of the 124 BM samples included in the immune profile analysis done for the identification of the HDBSCAN groups, to further investigate the immunological groups looking at their tumor transcriptional profile.

We started by performing an Upstream Regulator Analysis (URA) with IPA (Figure 7A), a tool able to estimate the presence or absence, within the microenvironment, of several molecules and factors (the so-called "upstream regulators") that could be responsible for the observed gene expression changes, based on what has been experimentally observed in literature [29]. This analysis revealed an increased inflammatory niche in

the three immunologically dysfunctional groups, compared to the naïve and memory activated ones, characterized by the presence of pro-inflammatory cytokines such as interferon (IFN)γ, tumor necrosis factor (TNF), interleukin (IL)-4, IL-5, IFNα and IFNβ. The two groups characterized by immunosuppression were specifically enriched also in IL27 (and its subunit EBI3), a cytokine with immunomodulatory properties [30-31], and IL15, an anti-apoptotic cytokine important for T and NK activation that have been also shown to promote Tregs function [32-33]. By contrast, naïve and memory activated groups were enriched in interleukin-1 receptor antagonist protein (IL-1RN), an inhibitor of the pro-inflammatory cytokine IL-1 activity, and Naïve group also showed higher presence of Osteopontin (SPP1) and Colony-stimulating factor 1 and 2 (CSF1/2), all factors important for bone marrow homeostasis that are secreted in normal conditions.

Similar results were observed through differential gene expression analysis on inflammatory pathways (Figure 7B), where the two groups characterized by immunosuppression were enriched in genes involved in inflammatory and IFNγ response, while the naïve and memory activated groups did not show any enrichment of inflammation-related signatures. The activated and immunosuppressed group showed the highest tumoral expression of TNFα/ Nuclear Factor kappa B (NFkB), IL-2/ Signal transducer and activator of transcription (STAT)5, IL-6/ Janus kinase (JAK)/STAT3 pathways and was the only enriched in TGFβ signaling. Not activated group showed an enrichment of TNFα/NFkB, IL-2/STAT5, IL-6/JAK/STAT3 and IFNα response pathways, but not in the inflammatory and IFNγ response ones.

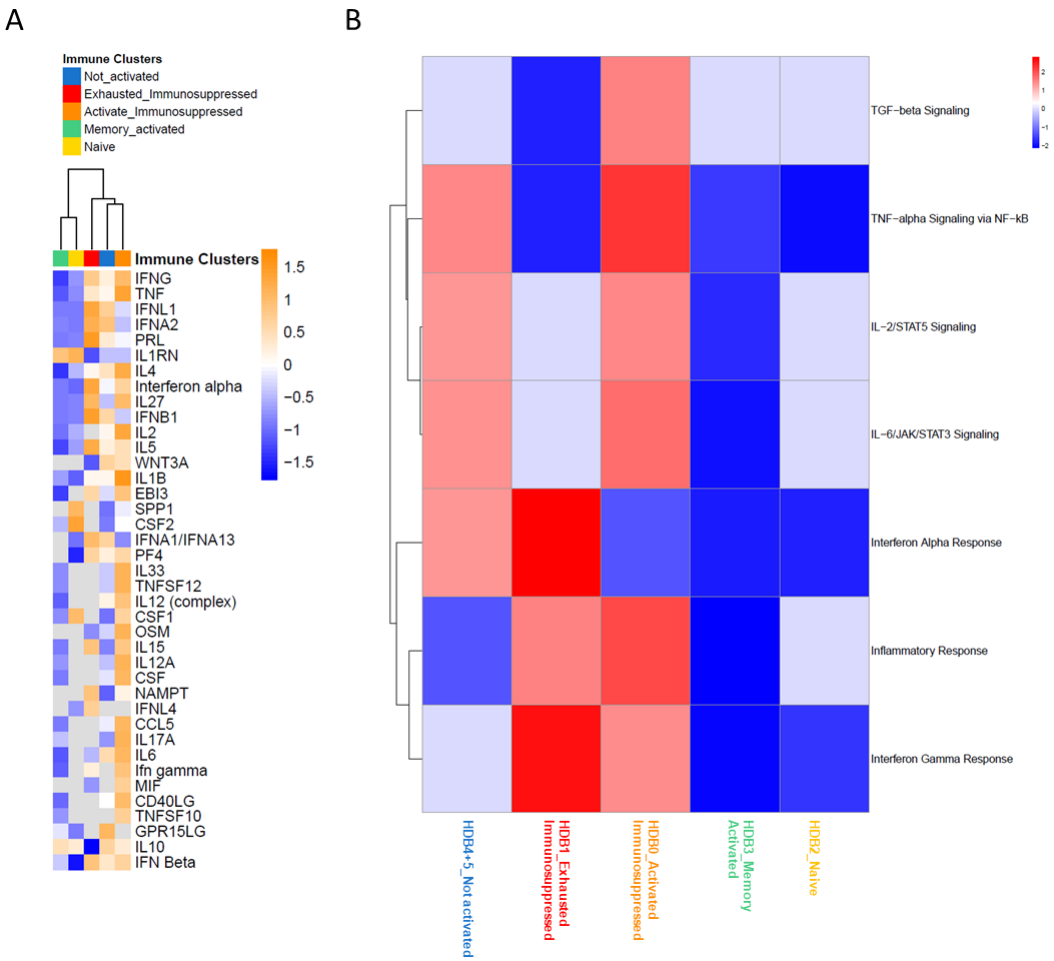

Figure 7. RNAseq data integration*. A) IPA analysis showing the predicted molecules and factors enriched in the bone marrow microenvironment of the different HDBSCAN groups. B) Heatmap of the differential expressed genes (DEGs) involved in inflammatory pathways.*

Development of a Decision Tree model for the automatic assignment of patients to immune groups and assessment of the prognostic value of immune characterization for HMA treatment outcome prediction

In the end, we aimed to design a decision tree to classify patients across the identified immunological groups. We thus performed a Recursive Feature Elimination (RFE) on our T and NK dataset to identify the most relevant immunological features for the assignment to each HDBSCAN group. The method selected the frequencies of $CD4^+$ naïve, $CD8^+$ terminal effectors, $CD4^+$ effector memory and $CD57^+$ terminally differentiated NK cells as the 4 most important features that allow patient allocation, with an accuracy of 75%, to a specific group (Figure 8A). We then evaluated the importance of each selected feature for every cluster association with SHapley Additive exPlanations (SHAP) (Figure 8B). Both the tree and SHAP value show that the first feature to be considered for the assignment to all groups is the frequency of $CD4^+$ Naïve, followed by the frequency of $CD8^+$ terminal effectors. Then, the frequency of $CD4^+$ effector memory is important for the assignment to HDBSCAN groups 0, 1, 2 and 3, while the frequency of terminally differentiated NK cells is relevant just for the assignment between groups 0 and 1.

We applied the decision tree on all pre-HMAs samples from our cohort, and we confirmed that 72% of patients were correctly assigned to group 0, 85% to group 1, 88% to group 2, 90% to group 3 and 76% to group 4/5. Interestingly, 80% of healthy controls were assigned to the “Naïve” group, and the residual 20% to “Memory activated” one, further confirming the similarity of these groups to a healthy immune system (Figure 8C). We applied the decision tree thresholds also on post-HMAs samples, stratifying for response to therapy (LONG CR vs LOST CR vs SD vs NR). Complete remissions that were maintained for more than 6 months from the start of the treatment and until last available follow-up (Long CR, n=11) were composed for 2/3 of cases from samples classified within the “Naïve” or “Memory activated” group and 1/3 from “Not activated” one (Figure 8D). Conversely, complete remissions that were lost before or after 6 months from the beginning of HMAs administration (n= 9) presented a dysfunctional immune profile, composed from the three immune dysfunctional groups (Figure 8E). More than half of sable diseases samples (n=17) were instead “not activated”, followed by “Activated immunosuppressed”, “Naïve” and “Exhausted immunosuppressed” (Figure 8F). In the end, non-responses samples (n=9) were mostly classified as “Activated immunosuppressed” (44%), followed by 33% of “Naïve” or “Memory activated” and 22% of “Exhausted Immunosuppressed” or “Not activated” (Figure 8G). In the end, we looked to how immune landscape changed in each patient with sequential timepoints (n = 15), comparing immune classification at diagnosis with the one at first evaluation post-HMA (after 2-6 cycles of HMAs), according to the decision tree tresholds (Figure 8H). For each patient we also checked the therapy outcome at last available follow-up. Interestingly, it was possible to observe that the immune group did not change in most of the cases from pre-HMA compared to post-HMA timepoints, indicating that HMAs do not profoundly affect the global immune panorama. Patients that displayed an “Exhausted immunosuppressed” phenotype in pre-HMA samples became “Activated immunosuppressed” after the therapy, showing anyway a failed response. Patients with “not activated” immune classification at diagnosis maintained in most of the cases the same immune group also after HMA, with just one of them converting to “Activated immunosuppressed” and evolving to AML. Compressively, the “not activated” group showed a bad treatment outcome at long follow-up. Naïve and “Memory Activated” displayed a certain grade of interchangeability and long response to HMA treatment, with one exception consisting in a SD.

Taken together, these data indicate that the immune landscape post-HMA does not radically change from the pre-HMA status, and this affects the long-term treatment outcome. Thus, immune evaluation at MDS diagnosis is important to perform a prediction of therapy response.

A

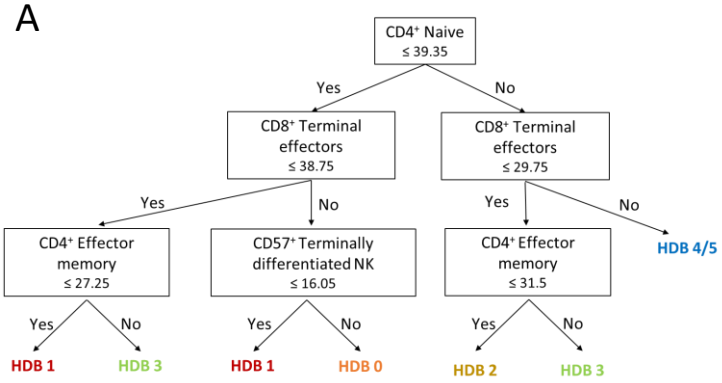
CD4⁺ Naive
≤ 39.35
Yes
No
CD8⁺ Terminal effectors
≤ 38.75
CD8⁺ Terminal effectors
≤ 29.75
Yes
No
Yes
No
CD4⁺ Effector memory
≤ 27.25
CD57⁺ Terminally differentiated NK
≤ 16.05
CD4⁺ Effector memory
≤ 31.5
HDB 4/5
Yes
No
Yes
No
Yes
No
HDB 1
HDB 3
HDB 1
HDB 0
HDB 2
HDB 3

B

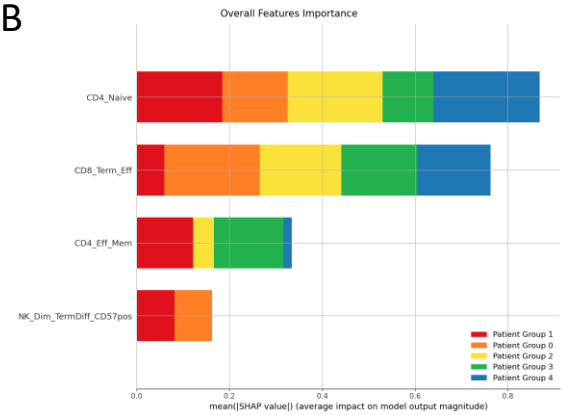
Overall Features Importance
CD4_Naive
CD8_Term_Eff
CD4_Eff_Mem
NK_Dim_TermDiff_CD57pos
Patient Group 1
Patient Group 0
Patient Group 2
Patient Group 3
Patient Group 4
0.0
0.2
0.4
0.6
0.8
mean(|SHAP value|) (average impact on model output magnitude)

C

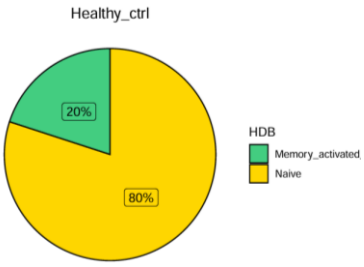
Healthy_ctrl
20%
80%
HDB
Memory_activated
Naive

D

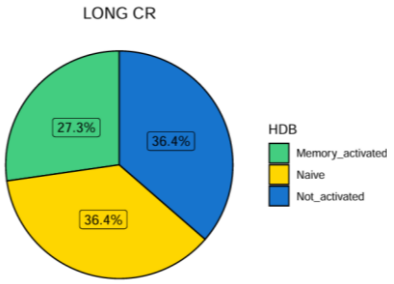
LONG CR
27.3%
36.4%
36.4%
HDB
Memory_activated
Naive
Not_activated

E

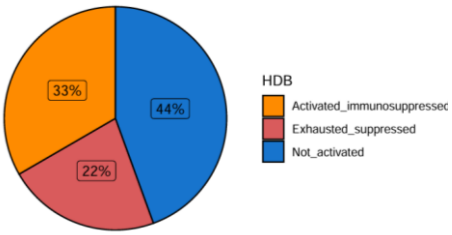
LOST CR
33%
44%
22%
HDB
Activated_immunosuppressed
Exhausted_suppressed
Not_activated

F

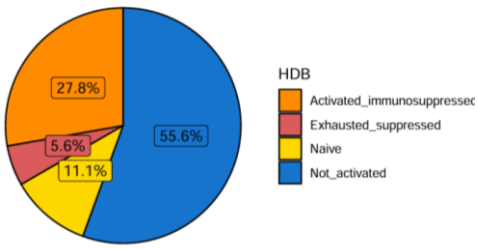
SD
27.8%
55.6%
5.6%
11.1%
HDB
Activated_immunosuppressed
Exhausted_suppressed
Naive
Not_activated

G

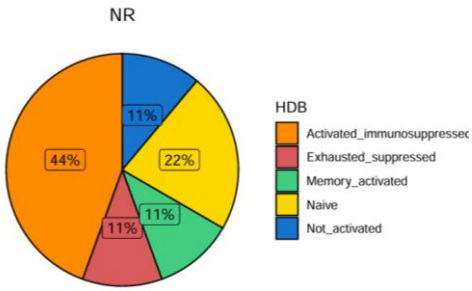
NR
11%
44%
22%
11%
11%
HDB
Activated_immunosuppressed
Exhausted_suppressed
Memory_activated
Naive
Not_activated

H

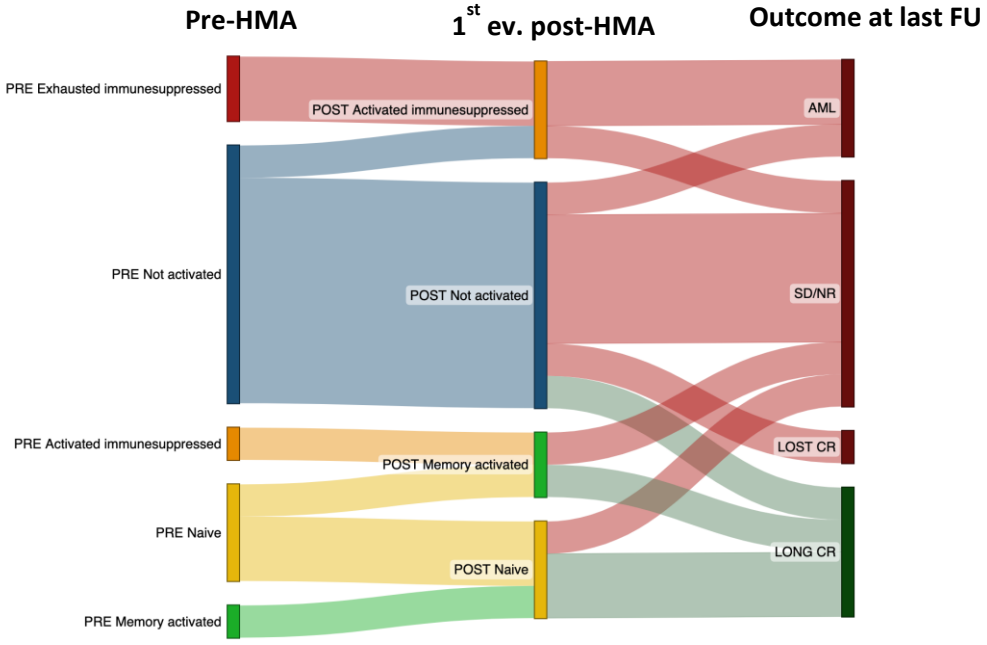
Pre-HMA
1st ev. post-HMA
Outcome at last FU
PRE Exhausted immunesuppressed
PRE Not activated
PRE Activated immunesuppressed
PRE Naive
PRE Memory activated
POST Activated immunesuppressed
POST Not activated
POST Memory activated
POST Naive
AML
SD/NR
LOST CR
LONG CR

***Figure 8. Decision tree model development and immune classification of post-HMA samples**. A) Schematic representation of the decision tree model based on the four most important features selected by recursive feature elimination. B) SHAP analysis result showing the impact of the selected four features for the assignment to each HDBSCAN group. C) Pie chart displaying the immune classification of healthy controls samples based on the decision tree features. D-G) Pie charts depicting the classification of post-HMA samples divided for type of response (LONG CR, LOST CR, SD, NR) based on the decision tree features. H) Sankey plot showing, on the left, the immune group assignment of patients with coupled pre- and post-HMA samples at first evaluation (2-6 cycles of therapy). On the right is reported the treatment outcome (AML evolution, SD or NR, LOST CR, LONG CR) at last available follow-up.*

Discussion

Myelodysplastic Syndromes are a group of diseases that comprises a wide spectrum of hematological disorders with different clinical manifestations and associated mortality risk. Given this heterogeneity, the use of classifications and scoring systems is of fundamental importance in order to identify the disease subtype and evaluate the patient's prognosis.

It is now certain that the immune system plays a major role in the initiation and progression of MDS [34-35]. For this reason, including the evaluation of the immune context in the actual risk stratification scores could indeed ameliorate their prognostic and predictive ability. Nevertheless, a deep characterization of the immune profile and its alterations in MDS patients is still lacking since the disease is highly heterogeneous and there are not standard ways for evaluating patient's immune status [36].

HMAs represent the first line treatment for MDS patients, however only half of patients respond to HMA and responses tend to be transient. Moreover, the identification of patients who will respond to HMAs is challenging since mechanisms underlying resistance to HMA are not clear yet. Indeed, the two current risk stratification scores, IPSS-R and IPSS-M, reliable predict the chance of leukemic evolution and the overall survival on the basis of clinical and cytogenetic parameters and, only in IPSS-M, the presence of specific gene mutations, but none of them can predict treatment outcome and neither the WHO and ICC classification can identify patients that will respond to the therapy [22;37].

In the present study, we assessed the immune profile of a large cohort of MDS patients with focus on T lymphocytes, NK and myeloid cells, taking advantage of high-dimensional flow cytometry combined with unsupervised methods of analysis and clustering. Immune features were firstly investigated in both BM and PB compartments by manual gating, stratifying patients according to WHO 2016, WHO 2022, ICC 2022, IPSS-R and IPSS-M criteria, to assess the ability of each classification or risk score method to capture differences in immune profiles and also the capacity of PB to reflect the BM immune niche.

Manual gating analysis revealed that WHO and ICC classifications can capture many immune differences between disease subtypes, while IPSS-R and IPSS-M risk scores only showed the major ones. This is reasonable since the risk stratification scores scope is only to evaluate parameters important for disease progression, while WHO and ICC classify MDS also under cytomorphological and genetic aspects, and thus are more comprehensive of the biology of the disease.

In summary, all the stages of the disease were characterized by an expansion of terminal effector T cells at the expense of the naïve compartment compared to age-matched healthy controls, indicating a general T cell activation and differentiation. MDS with ring sideroblast/SF3B1^{mut} showed an activated and functional T cell compartment, with less CD8$^+$ terminal effectors and CD4$^+$ naïve, more CD4$^+$ central memory, CD8$^+$ effector memory and cytotoxic CD8$^+$ T cells and the expansion of the cytokine producer CD56^{bright} NK cells. Advanced stages of the disease and TP53^{mut} MDS displayed instead a compromised immune environment that favors tumor immune evasion and expansion, characterized by the increased presence of immunosuppressive Tregs

and TIM3 expression on $CD8^+$ T cells, and impaired NK cell tumor immune surveillance due to a defective NK cell maturation coupled with a decreased expression of markers related to activation and licensing and the increased expression of PD1, confirming what described in literature [38-43]. Classical monocytes and dendritic cells were respectively decreased and increased in MDS EB/IB, MDS/AML, $TP53^{mut}$ MDS and AML post MDS, indicating enhanced monocytic maturation towards DCs. Those DCs should be further investigated for their activity since it has been shown, in cancer settings, that tolerogenic DCs can exert immunomodulatory functions and induce the differentiation of Tregs [44-46]. MDSCs have been shown in MDS to contribute increasing BM niche immunosuppression thanks to their capacity to recruit Tregs [47] and induce CD8+ T cell exhaustion through the expression of TIM3 ligand Galectin-9 [48]. In our cohort we just observed an increasing trend of PMN-MDSCs in advanced stages of the disease that was significant only in AML post MDS. The other MDSCs class, M-MDSCs, were instead significantly higher in $SF3B1^{mut}$ and $TP53^{mut}$, the two categories which also showed increased frequencies of HLA-DR^{low} monocytes. Monocytes with low HLA-DR expression are often considered as M-MDSCs since they share the same phenotypic markers and are known to possess immunoregulatory properties thanks to their low antigen presentation [49-51]. We think that in the case of $SF3B1^{mut}$ MDS, the decreased antigen presentation is counterbalanced by a functional T and NK state, while in $TP53^{mut}$ MDS it probably contributes to tumor immune evasion.

To evaluate the effects of HMA therapy on immune profile of MDS patients, we included in the experiments also BM and PB samples collected during the follow-up. Here, we showed that $CD3^+$ T lymphocytes, $CD4^+$ central memory, Tregs, NK cells, dendritic cells and classical monocytes frequencies in the BM follow the treatment response and, in particular, in patients that respond to the therapy the frequencies of these populations are partially restored. Moreover, as for pre-HMA samples, PB reflected many of the observed trends: we can thus conclude that, in a context of patient's immune characterization at diagnosis and immune monitoring along HMA treatment, bone marrow evaluation is preferable for a deeper and precise cellular characterization, but since BM aspiration is an invasive practice that cannot be frequently performed, PB represents a valid alternative. We also investigated the prognostic value of the immune populations here identified and interestingly, the BM frequency of Tregs and monocytes, and the PB frequency of NK cells at diagnosis are correlated with patient's OS, supporting the idea of a complete evaluation of immunological profile of MDS patients at the time of disease diagnosis, in addition to clinical ones, to better assess their prognosis.

However, the data obtained, even if showed the alteration of the immune compartment in MDS niche, especially in high grade patients, were still marked by high heterogeneity. Thus, to wriggle out from the limits of patients classifications and scoring systems and to identify prognostic and predictive markers in an unbiased manner, we deeply analyzed T and NK cells with Phenograph algorithm and patients were classified in an unsupervised manner according to their immune features. We found 5 immunological groups with different grades of immune dysfunction: two groups were characterized by immunosuppression with different marks of exhaustion, one by general T cell inactivation and NK cell impaired activity and two groups with a more functional immune system, of which one characterized by the expansion of naïve compartment and the other one by memory T cells and activated T and NK cells. Interestingly, each group was characterized by a different prognosis and in particular, the grade of T and NK dysfunction was correlated with better or worse overall survival, as assessed by Kaplan-Meier curves and cox models. Moreover, we demonstrated for the first time that patients initially classified within the same MDS class or IPSS-R/M risk category display, at diagnosis, immunological differences that will influence the clinical course of the disease, once again supporting the need of integrating information about the patient's immune status for a better stratification and outcome prediction.

Bulk RNA-seq analysis on $CD34^+$ bone marrow cells were integrated to further investigate such immunological groups. Pathway and upstream regulator analysis showed that the bone marrow niche of the three HDB groups characterized by major immune dysfunctions and worse prognosis (groups 0, 1 and 4/5) were enriched

in pro-inflammatory cytokines, while the groups with healthy-similar features and better prognosis (groups 2 and 3) only showed an enrichment in molecules released in homeostatic conditions. Differential gene expression analysis revealed a strong upregulation of inflammatory and IFNγ response pathways in the two groups characterized by immunosuppression (HDB 0 and 1), indicative of a highly inflamed niche. In addition, the group "Activated but immunosuppressed" (HDB 0) was enriched in TNFα/NFkB, IL-6/JAK/STAT3, IL-2/STAT5 and TGFβ signaling. The TNFα/NFkB pathway is involved in both adaptive and innate immune response triggering, and its deregulated activation is associated to exacerbated inflammatory response and autoimmunity [52-53]. The IL-6/JAK/STAT3 has been associated with tumorigenesis, since its hyperactivation contributes to the creation of inflammatory microenvironment which promotes tumor cells survival and proliferation while strongly suppress the anti-tumor immune response [54-55]. IL-2 is a cytokine with fundamental roles for T cell activation and proliferation [56-57]. IL-2 signals are propagated via activation of STAT5, a transcription factor whose aberrant hyperexpression plays a critical role in suppression of antitumor immunity through the development of Tregs [58-59]. Finally, TGFβ signaling is well known to induce an immunosuppressive microenvironment, especially in tumor setting [60-61]. The "Not activated" group (HDB 4/5) was less enriched in TNFα/NFkB, IL-6/JAK/STAT3, IL-2/STAT5 compared to "Activated but immunosuppressed" one (HDB 0), and in IFNα response compared to "Exhausted and Immunosuppressed" group (HDB 1), indicating a moderate inflammatory status. Collectively, RNAseq data indicate that the increased immune dysfunction is accompanied by a rise in the inflammatory status at the niche level, which favor tumor aggressiveness and immunosuppression. These data also suggest that patients with high grade of immune dysfunction could benefit from inhibitors of IL-6/JAK/STAT3 and/or IL-2/STAT5 axes. Agents that target IL-6, IL-6R and JAKs are already approved by the FDA for the management of inflammatory conditions [62-63] and myeloproliferative neoplasm. In particular, the JAK1/2 inhibitor ruxolitinib is widely used for the treatment of myelofibrosis and polycythemia vera [64-65]. Moreover, since IL-6/JAK/STAT3 signaling induces the expression of PD1/PDL1 [66-68], the co-targeting of these pathways could improve the inhibition of the clonal hematopoiesis, as recently described in mouse models [69-70]. Finally, the inhibition of STAT5 is another active field of research, especially in leukemia [71-73], that could be exploited also for MDS management.

In the end, with a Recursive Feature Elimination model we identified the most relevant cell populations for the assignment to the immunological groups previously identified, and with these features we developed a decision tree for patient's classification. Essentially, the four features at the basis of all groups rely on the frequencies of $CD4^+$ naïve, $CD8^+$ terminal effectors, $CD4^+$ effector memory and $CD57^+$ terminally differentiated NK cells, highlighting the importance of the proportion between an early stage of T cell differentiation (Naïve and memory T cells) and late stages of T cells activation and NK cell maturation (terminal effectors T cells and $CD57^+$ NK cells). To understand the role of the identified immunological groups in therapy response, we applied the decision tree on post-HMA samples and we observed that, subdividing them according to the response to the treatment, their distribution among immunological groups was different. In particular, post-HMA samples of patients with prolonged complete remissions were mostly composed by the two groups with low immune dysfunction and better prognosis, while patients who lost the initial CR were from the beginning characterized by a prevalence of dysfunctional and immunosuppressed immunological groups. Similarly, stable diseases and non-responses samples were composed by a prevalence of the three dysfunctional groups, underlying that the immune context is different depending on the type of response. Moreover, comparison between pre-HMA and post-HMA samples at first evaluation (2-4 HMA cycles) from the same patients revealed that the treatment does not change the assigned immune group and the final treatment response, and thus it does not have a profound impact on the global immune panorama. These results strongly support the importance of evaluating the immune status at MDS diagnosis and along HMA administration to improve the prediction of HMA treatment.

To sum up, we identified, for the first time and in a totally unsupervised way, different immunological groups of MDS and AML post MDS patients whose immune features are correlated with prognosis and response to

HMA therapy. We then validated a pipeline able to classify patients within these immunological groups with high precision considering few immune populations that are easy to detect with a restricted number of markers, demonstrating the feasibility of developing a model for immune characterization and integration of immunological features to clinical data. Taken together, our data provide evidence that the addition of immune signatures can refine MDS risk stratification and classification, determine prognostic and predictive markers for disease course and HMA response as well as identify innovative and specific therapeutic targets to overcome tumor growth and immunosuppression.

References

1. Tefferi A, Vardiman JW. Myelodysplastic syndromes. N Engl J Med. 2009 Nov 5;361(19):1872-85. doi: 10.1056/NEJMra0902908. PMID: 19890130.
2. Adès L, Itzykson R, Fenaux P. Myelodysplastic syndromes. Lancet. 2014 Jun 28;383(9936):2239-52. doi: 10.1016/S0140-6736(13)61901-7. Epub 2014 Mar 21. PMID: 24656536.
3. Lee WH, Tsai MT, Tsai CH, Tien FM, Lo MY, Tseng MH, Kuo YY, Liu MC, Yang YT, Chen JC, Tang JL, Sun HI, Chuang YK, Lin LI, Chou WC, Lin CC, Hou HA, Tien HF. Validation of the molecular international prognostic scoring system in patients with myelodysplastic syndromes defined by international consensus classification. Blood Cancer J. 2023 Aug 9;13(1):120. doi: 10.1038/s41408-023-00894-8. PMID: 37558665; PMCID: PMC10412560.
4. Itzykson R, Fenaux P. Epigenetics of myelodysplastic syndromes. Leukemia. 2014 Mar;28(3):497-506. doi: 10.1038/leu.2013.343. Epub 2013 Nov 19. PMID: 24247656.
5. Lynch OF, Calvi LM. Immune Dysfunction, Cytokine Disruption, and Stromal Changes in Myelodysplastic Syndrome: A Review. Cells. 2022 Feb 8;11(3):580. doi: 10.3390/cells11030580. PMID: 35159389; PMCID: PMC8834462.
6. Bravo GM, Lee E, Merchan B, Kantarjian HM, García-Manero G. Integrating genetics and epigenetics in myelodysplastic syndromes: advances in pathogenesis and disease evolution. Br J Haematol. 2014 Sep;166(5):646-59. doi: 10.1111/bjh.12957. Epub 2014 Jun 5. PMID: 24903747; PMCID: PMC5553700.
7. Ghobrial, I., Detappe, A., Anderson, K. et al. The bone-marrow niche in MDS and MGUS:implications for AML and MM. Nat Rev Clin Oncol 15, 219–233 (2018). https://doi.org/10.1038/nrclinonc.2017.197
8. Stubbins RJ, Platzbecker U, Karsan A. Inflammation and myeloid malignancy: quenching the flame. Blood. 2022 Sep 8;140(10):1067-1074. doi: 10.1182/blood.2021015162. PMID: 35468199.
9. Kordasti SY, Afzali B, Lim Z, Ingram W, Hayden J, Barber L, Matthews K, Chelliah R, Guinn B, Lombardi G, Farzaneh F, Mufti GJ. IL-17-producing CD4(+) T cells, pro-inflammatory cytokines and apoptosis are increased in low risk myelodysplastic syndrome. Br J Haematol. 2009 Apr;145(1):64-72. doi: 10.1111/j.1365-2141.2009.07593.x. Epub 2009 Feb 3. PMID: 19210506.
10. Aggarwal S, van de Loosdrecht AA, Alhan C, Ossenkoppele GJ, Westers TM, Bontkes HJ. Role of immune responses in the pathogenesis of low-risk MDS and high-risk MDS: implications for immunotherapy. Br J Haematol. 2011 Jun;153(5):568-81. doi: 10.1111/j.1365-2141.2011.08683.x. Epub 2011 Apr 13. PMID: 21488861.
11. Barakos GP, Hatzimichael E. Microenvironmental Features Driving Immune Evasion in Myelodysplastic Syndromes and Acute Myeloid Leukemia. Diseases. 2022 Jun 10;10(2):33. doi: 10.3390/diseases10020033. PMID: 35735633; PMCID: PMC9221594.
12. Velegraki M, Stiff A, Papadaki HA, Li Z. Myeloid-Derived Suppressor Cells: New Insights into the Pathogenesis and Therapy of MDS. J Clin Med. 2022 Aug 21;11(16):4908. doi: 10.3390/jcm11164908. PMID: 36013147; PMCID: PMC9410159.

13. Garcia-Manero G, Chien KS, Montalban-Bravo G. Myelodysplastic syndromes: 2021 update on diagnosis, risk stratification and management. Am J Hematol. 2020 Nov;95(11):1399-1420. doi: 10.1002/ajh.25950. PMID: 32744763.
14. Li, H., Hu, F., Gale, R.P. et al. Myelodysplastic syndromes. Nat Rev Dis Primers 8, 74 (2022). https://doi.org/10.1038/s41572-022-00402-5
15. Carraway HE. Treatment options for patients with myelodysplastic syndromes after hypomethylating agent failure. Hematology Am Soc Hematol Educ Program. 2016 Dec 2;2016(1):470-477. doi: 10.1182/asheducation-2016.1.470. PMID: 27913518; PMCID: PMC6142467.
16. Valeria Santini; How I treat MDS after hypomethylating agent failure. Blood 2019; 133 (6): 521–529. doi: https://doi.org/10.1182/blood-2018-03-785915
17. Unnikrishnan A, Papaemmanuil E, Beck D, Deshpande NP, Verma A, Kumari A, Woll PS, Richards LA, Knezevic K, Chandrakanthan V, Thoms JAI, Tursky ML, Huang Y, Ali Z, Olivier J, Galbraith S, Kulasekararaj AG, Tobiasson M, Karimi M, Pellagatti A, Wilson SR, Lindeman R, Young B, Ramakrishna R, Arthur C, Stark R, Crispin P, Curnow J, Warburton P, Roncolato F, Boultwood J, Lynch K, Jacobsen SEW, Mufti GJ, Hellstrom-Lindberg E, Wilkins MR, MacKenzie KL, Wong JWH, Campbell PJ, Pimanda JE. Integrative Genomics Identifies the Molecular Basis of Resistance to Azacitidine Therapy in Myelodysplastic Syndromes. Cell Rep. 2017 Jul 18;20(3):572-585. doi: 10.1016/j.celrep.2017.06.067. PMID: 28723562.
18. Schnegg-Kaufmann AS, Thoms JAI, Bhuyan GS, Hampton HR, Vaughan L, Rutherford K, Kakadia PM, Lee HM, Johansson EMV, Failes TW, Arndt GM, Koval J, Lindeman R, Warburton P, Rodriguez-Meira A, Mead AJ, Unnikrishnan A, Davidson S, Polizzotto MN, Hertzberg M, Papaemmanuil E, Bohlander SK, Faridani OR, Jolly CJ, Zanini F, Pimanda JE. Contribution of mutant HSC clones to immature and mature cells in MDS and CMML, and variations with AZA therapy. Blood. 2023 Mar 16;141(11):1316-1321. doi: 10.1182/blood.2022018602. PMID: 36493342.
19. Fenaux P, Mufti GJ, Hellstrom-Lindberg E, Santini V, Finelli C, Giagounidis A, Schoch R, Gattermann N, Sanz G, List A, Gore SD, Seymour JF, Bennett JM, Byrd J, Backstrom J, Zimmerman L, McKenzie D, Beach C, Silverman LR; International Vidaza High-Risk MDS Survival Study Group. Efficacy of azacitidine compared with that of conventional care regimens in the treatment of higher-risk myelodysplastic syndromes: a randomised, open-label, phase III study. Lancet Oncol. 2009 Mar;10(3):223-32. doi: 10.1016/S1470-2045(09)70003-8. Epub 2009 Feb 21. PMID: 19230772; PMCID: PMC4086808.
20. Cazzola M. Myelodysplastic Syndromes. N Engl J Med. 2020 Oct 1;383(14):1358-1374. doi: 10.1056/NEJMra1904794. PMID: 32997910.
21. Bernard E, Nannya Y, Hasserjian RP, Devlin SM, Tuechler H, Medina-Martinez JS, Yoshizato T, Shiozawa Y, Saiki R, Malcovati L, Levine MF, Arango JE, Zhou Y, Solé F et al. Implications of TP53 allelic state for genome stability, clinical presentation and outcomes in myelodysplastic syndromes. Nat Med. 2020 Oct;26(10):1549-1556. doi: 10.1038/s41591-020-1008-z. Epub 2020 Aug 3. Erratum in: Nat Med. 2021 Mar;27(3):562. Erratum in: Nat Med. 2021 May;27(5):927. PMID: 32747829; PMCID: PMC8381722.
22. Sauta E, Robin M, Bersanelli M, Travaglino E, Meggendorfer M, Zhao LP, Caballero Berrocal JC, Sala C, Maggioni G, Bernardi M, Di Grazia C, Vago L, Rivoli G, Borin L, D'Amico S, Tentori CA, Ubezio M, Campagna A, Russo A et al. Real-World Validation of Molecular International Prognostic Scoring System for Myelodysplastic Syndromes. J Clin Oncol. 2023 May 20;41(15):2827-2842. doi: 10.1200/JCO.22.01784. Epub 2023 Mar 17. PMID: 36930857; PMCID: PMC10414702.
23. Cossarizza A, Chang HD, Radbruch A, Abrignani S, Addo R, Akdis M, Andrä I, Andreata F, Annunziato F, Arranz E, Bacher P, Bari S, Barnaba V, Barros-Martins J, Baumjohann D, Beccaria CG, Bernardo D, Boardman DA, Borger J, Böttcher C, Brockmann L et al. Guidelines for the use of flow cytometry and

cell sorting in immunological studies (third edition). Eur J Immunol. 2021 Dec;51(12):2708-3145. doi: 10.1002/eji.202170126. Epub 2021 Dec 7. PMID: 34910301.
24. Pedersen CB, Dam SH, Barnkob MB, Leipold MD, Purroy N, Rassenti LZ, Kipps TJ, Nguyen J, Lederer JA, Gohil SH, Wu CJ, Olsen LR. cyCombine allows for robust integration of single-cell cytometry datasets within and across technologies. Nat Commun. 2022 Mar 31;13(1):1698. doi: 10.1038/s41467-022-29383-5. PMID: 35361793; PMCID: PMC8971492.
25. Levine JH, Simonds EF, Bendall SC, Davis KL, Amir el-AD, Tadmor MD, Litvin O, Fienberg HG, Jager A, Zunder ER, Finck R, Gedman AL, Radtke I, Downing JR, Pe'er D, Nolan GP. Data-Driven Phenotypic Dissection of AML Reveals Progenitor-like Cells that Correlate with Prognosis. Cell. 2015 Jul 2;162(1):184-97. doi: 10.1016/j.cell.2015.05.047. Epub 2015 Jun 18. PMID: 26095251; PMCID: PMC4508757.
26. Sallman DA, McLemore AF, Aldrich AL, Komrokji RS, McGraw KL, Dhawan A, Geyer S, Hou HA, Eksioglu EA, Sullivan A, Warren S, MacBeth KJ, Meggendorfer M, Haferlach T, Boettcher S, Ebert BL, Al Ali NH, Lancet JE, Cleveland JL, Padron E, List AF. TP53 mutations in myelodysplastic syndromes and secondary AML confer an immunosuppressive phenotype. Blood. 2020 Dec 10;136(24):2812-2823. doi: 10.1182/blood.2020006158. PMID: 32730593; PMCID: PMC7731792.
27. Shi, Y., Xie, T., Wang, B. et al. Mutant p53 drives an immune cold tumor immune microenvironment in oral squamous cell carcinoma. Commun Biol 5, 757 (2022). https://doi.org/10.1038/s42003-022-03675-4
28. Jiang Z, Liu Z, Li M, Chen C, Wang X. Immunogenomics Analysis Reveals that TP53 Mutations Inhibit Tumor Immunity in Gastric Cancer. Transl Oncol. 2018 Oct;11(5):1171-1187. doi: 10.1016/j.tranon.2018.07.012. Epub 2018 Jul 27. PMID: 30059832; PMCID: PMC6078052.
29. Krämer A, Green J, Pollard J Jr, Tugendreich S. Causal analysis approaches in Ingenuity Pathway Analysis. Bioinformatics. 2014 Feb 15;30(4):523-30. doi: 10.1093/bioinformatics/btt703. Epub 2013 Dec 13. PMID: 24336805; PMCID: PMC3928520.
30. Wang Q, Liu J. Regulation and Immune Function of IL-27. Adv Exp Med Biol. 2016;941:191-211. doi: 10.1007/978-94-024-0921-5_9. PMID: 27734414.
31. Mascanfroni ID, Yeste A, Vieira SM, Burns EJ, Patel B, Sloma I, Wu Y, Mayo L, Ben-Hamo R, Efroni S, Kuchroo VK, Robson SC, Quintana FJ. IL-27 acts on DCs to suppress the T cell response and autoimmunity by inducing expression of the immunoregulatory molecule CD39. Nat Immunol. 2013 Oct;14(10):1054-63. doi: 10.1038/ni.2695. Epub 2013 Sep 1. PMID: 23995234; PMCID: PMC3964005.
32. Waldmann, T. The biology of interleukin-2 and interleukin-15: implications for cancer therapy and vaccine design. Nat Rev Immunol 6, 595–601 (2006). https://doi.org/10.1038/nri1901
33. Xia J, Liu W, Hu B, Tian Z, Yang Y. IL-15 promotes regulatory T cell function and protects against diabetes development in NK-depleted NOD mice. Clin Immunol. 2010 Feb;134(2):130-9. doi: 10.1016/j.clim.2009.09.011. Epub 2009 Oct 28. PMID: 19875339.
34. Barreyro L, Chlon TM, Starczynowski DT. Chronic immune response dysregulation in MDS pathogenesis. Blood. 2018 Oct 11;132(15):1553-1560. doi: 10.1182/blood-2018-03-784116. Epub 2018 Aug 13. PMID: 30104218; PMCID: PMC6182269.
35. Wang C, Yang Y, Gao S, Chen J, Yu J, Zhang H, Li M, Zhan X, Li W. Immune dysregulation in myelodysplastic syndrome: Clinical features, pathogenesis and therapeutic strategies. Crit Rev Oncol Hematol. 2018 Feb;122:123-132. doi: 10.1016/j.critrevonc.2017.12.013. Epub 2018 Jan 3. PMID: 29458780.
36. Winter S, Shoaie S, Kordasti S, Platzbecker U. Integrating the "Immunome" in the Stratification of Myelodysplastic Syndromes and Future Clinical Trial Design. J Clin Oncol. 2020 May 20;38(15):1723-1735. doi: 10.1200/JCO.19.01823. Epub 2020 Feb 14. PMID: 32058844.
37. Greenberg PL, Tuechler H, Schanz J, Sanz G, Garcia-Manero G, Solé F, Bennett JM, Bowen D, Fenaux P, Dreyfus F, Kantarjian H, Kuendgen A, Levis A, Malcovati L, Cazzola M, Cermak J, Fonatsch C, Le Beau

MM, Slovak ML, Krieger O, Luebbert M, Maciejewski J, Magalhaes SM, Miyazaki Y, Pfeilstöcker M, Sekeres M, Sperr WR, Stauder R, Tauro S, Valent P, Vallespi T, van de Loosdrecht AA, Germing U, Haase D. Revised international prognostic scoring system for myelodysplastic syndromes. Blood. 2012 Sep 20;120(12):2454-65. doi: 10.1182/blood-2012-03-420489. Epub 2012 Jun 27. PMID: 22740453; PMCID: PMC4425443.

38. Kordasti SY, Ingram W, Hayden J, Darling D, Barber L, Afzali B, Lombardi G, Wlodarski MW, Maciejewski JP, Farzaneh F, Mufti GJ. CD4+CD25high Foxp3+ regulatory T cells in myelodysplastic syndrome (MDS). Blood. 2007 Aug 1;110(3):847-50. doi: 10.1182/blood-2007-01-067546. Epub 2007 Apr 5. PMID: 17412885.
39. Tao J, Li L, Wang Y, Fu R, Wang H, Shao Z. Increased TIM3+CD8+T cells in Myelodysplastic Syndrome patients displayed less perforin and granzyme B secretion and higher CD95 expression. Leuk Res. 2016 Dec;51:49-55. doi: 10.1016/j.leukres.2016.11.003. Epub 2016 Nov 2. PMID: 27846431.
40. Rezaei M, Tan J, Zeng C, Li Y, Ganjalikhani-Hakemi M. TIM-3 in Leukemia; Immune Response and Beyond. Front Oncol. 2021 Sep 30;11:753677. doi: 10.3389/fonc.2021.753677. PMID: 34660319; PMCID: PMC8514831.
41. Hejazi M, Manser AR, Fröbel J, Kündgen A, Zhao X, Schönberg K, Germing U, Haas R, Gattermann N, Uhrberg M. Impaired cytotoxicity associated with defective natural killer cell differentiation in myelodysplastic syndromes. Haematologica. 2015 May;100(5):643-52. doi: 10.3324/haematol.2014.118679. Epub 2015 Feb 14. PMID: 25682594; PMCID: PMC4420213.
42. Epling-Burnette PK, Bai F, Painter JS, Rollison DE, Salih HR, Krusch M, Zou J, Ku E, Zhong B, Boulware D, Moscinski L, Wei S, Djeu JY, List AF. Reduced natural killer (NK) function associated with high-risk myelodysplastic syndrome (MDS) and reduced expression of activating NK receptors. Blood. 2007 Jun 1;109(11):4816-24. doi: 10.1182/blood-2006-07-035519. Epub 2007 Mar 6. PMID: 17341666; PMCID: PMC1885518.
43. Cianga VA, Campos Catafal L, Cianga P, Pavel Tanasa M, Cherry M, Collet P, Tavernier E, Guyotat D, Rusu C, Aanei CM. Natural Killer Cell Subpopulations and Inhibitory Receptor Dynamics in Myelodysplastic Syndromes and Acute Myeloid Leukemia. Front Immunol. 2021 Apr 27;12:665541. doi: 10.3389/fimmu.2021.665541. PMID: 33986753; PMCID: PMC8112610.
44. Sharma MD, Baban B, Chandler P, Hou DY, Singh N, Yagita H, Azuma M, Blazar BR, Mellor AL, Munn DH. Plasmacytoid dendritic cells from mouse tumor-draining lymph nodes directly activate mature Tregs via indoleamine 2,3-dioxygenase. J Clin Invest. 2007 Sep;117(9):2570-82. doi: 10.1172/JCI31911. PMID: 17710230; PMCID: PMC1940240.
45. Janikashvili N, Bonnotte B, Katsanis E, Larmonier N. The dendritic cell-regulatory T lymphocyte crosstalk contributes to tumor-induced tolerance. Clin Dev Immunol. 2011;2011:430394. doi: 10.1155/2011/430394. Epub 2011 Nov 3. PMID: 22110524; PMCID: PMC3216392.
46. Ge W, Ma X, Li X, Wang Y, Li C, Meng H, Liu X, Yu Z, You S, Qiu L. B7-H1 up-regulation on dendritic-like leukemia cells suppresses T cell immune function through modulation of IL-10/IL-12 production and generation of Treg cells. Leuk Res. 2009 Jul;33(7):948-57. doi: 10.1016/j.leukres.2009.01.007. Epub 2009 Feb 23. PMID: 19233469.
47. Kittang AO, Kordasti S, Sand KE, Costantini B, Kramer AM, Perezabellan P, Seidl T, Rye KP, Hagen KM, Kulasekararaj A, Bruserud Ø, Mufti GJ. Expansion of myeloid derived suppressor cells correlates with number of T regulatory cells and disease progression in myelodysplastic syndrome. Oncoimmunology. 2015 Jun 24;5(2):e1062208. doi: 10.1080/2162402X.2015.1062208. PMID: 27057428; PMCID: PMC4801428.
48. Tao J, Han D, Gao S, Zhang W, Yu H, Liu P, Fu R, Li L, Shao Z. CD8+ T cells exhaustion induced by myeloid-derived suppressor cells in myelodysplastic syndromes patients might be through TIM3/Gal-9 pathway. J Cell Mol Med. 2020 Jan;24(1):1046-1058. doi: 10.1111/jcmm.14825. Epub 2019 Nov 22. PMID: 31756785; PMCID: PMC6933355.

49. Yi Lin, Michael P. Gustafson, Peggy A. Bulur, Dennis A. Gastineau, Thomas E. Witzig, Allan B. Dietz; Immunosuppressive CD14+HLA-DRlow/− monocytes in B-cell non-Hodgkin lymphoma. Blood 2011; 117 (3): 872–881. doi: https://doi.org/10.1182/blood-2010-05-283820
50. Gustafson MP, Lin Y, New KC, Bulur PA, O'Neill BP, Gastineau DA, Dietz AB. Systemic immune suppression in glioblastoma: the interplay between CD14+HLA-DRlo/neg monocytes, tumor factors, and dexamethasone. Neuro Oncol. 2010 Jul;12(7):631-44. doi: 10.1093/neuonc/noq001. Epub 2010 Feb 23. PMID: 20179016; PMCID: PMC2940665.
51. Mengos AE, Gastineau DA, Gustafson MP. The CD14+HLA-DRlo/neg Monocyte: An Immunosuppressive Phenotype That Restrains Responses to Cancer Immunotherapy. Front Immunol. 2019 May 22;10:1147. doi: 10.3389/fimmu.2019.01147. PMID: 31191529; PMCID: PMC6540944.
52. Liu, T., Zhang, L., Joo, D. et al. NF-κB signaling in inflammation. Sig Transduct Target Ther 2, 17023 (2017). https://doi.org/10.1038/sigtrans.2017.23
53. Barnabei L, Laplantine E, Mbongo W, Rieux-Laucat F, Weil R. NF-κB: At the Borders of Autoimmunity and Inflammation. Front Immunol. 2021 Aug 9;12:716469. doi: 10.3389/fimmu.2021.716469. PMID: 34434197; PMCID: PMC8381650.
54. Huang B, Lang X, Li X. The role of IL-6/JAK2/STAT3 signaling pathway in cancers. Front Oncol. 2022 Dec 16;12:1023177. doi: 10.3389/fonc.2022.1023177. PMID: 36591515; PMCID: PMC9800921.
55. Johnson DE, O'Keefe RA, Grandis JR. Targeting the IL-6/JAK/STAT3 signalling axis in cancer. Nat Rev Clin Oncol. 2018 Apr;15(4):234-248. doi: 10.1038/nrclinonc.2018.8. Epub 2018 Feb 6. PMID: 29405201; PMCID: PMC5858971.
56. Spolski, R., Li, P. & Leonard, W.J. Biology and regulation of IL-2: from molecular mechanisms to human therapy. Nat Rev Immunol 18, 648–659 (2018). https://doi.org/10.1038/s41577-018-0046-y
57. Boyman, O., Sprent, J. The role of interleukin-2 during homeostasis and activation of the immune system. Nat Rev Immunol 12, 180–190 (2012). https://doi.org/10.1038/nri3156
58. Rani A, Murphy JJ. STAT5 in Cancer and Immunity. J Interferon Cytokine Res. 2016 Apr;36(4):226-37. doi: 10.1089/jir.2015.0054. Epub 2015 Dec 30. PMID: 26716518.
59. Jones DM, Read KA, Oestreich KJ. Dynamic Roles for IL-2-STAT5 Signaling in Effector and Regulatory CD4+ T Cell Populations. J Immunol. 2020 Oct 1;205(7):1721-1730. doi: 10.4049/jimmunol.2000612. PMID: 32958706; PMCID: PMC7513451.
60. Massagué J, Sheppard D. TGF-β signaling in health and disease. Cell. 2023 Sep 14;186(19):4007-4037. doi: 10.1016/j.cell.2023.07.036. PMID: 37714133.
61. Tauriello DVF, Sancho E, Batlle E. Overcoming TGFβ-mediated immune evasion in cancer. Nat Rev Cancer. 2022 Jan;22(1):25-44. doi: 10.1038/s41568-021-00413-6. Epub 2021 Oct 20. PMID: 34671117.
62. Scott LJ. Tocilizumab: A Review in Rheumatoid Arthritis. Drugs. 2017 Nov;77(17):1865-1879. doi: 10.1007/s40265-017-0829-7. Erratum in: Drugs. 2017 Dec 19;: PMID: 29094311; PMCID: PMC5736769.
63. van Rhee F, Wong RS, Munshi N, Rossi JF, Ke XY, Fosså A, Simpson D, Capra M, Liu T, Hsieh RK, Goh YT, Zhu J, Cho SG, Ren H, Cavet J, Bandekar R, Rothman M, Puchalski TA, Reddy M, van de Velde H, Vermeulen J, Casper C. Siltuximab for multicentric Castleman's disease: a randomised, double-blind, placebo-controlled trial. Lancet Oncol. 2014 Aug;15(9):966-74. doi: 10.1016/S1470-2045(14)70319-5. Epub 2014 Jul 17. Erratum in: Lancet Oncol. 2014 Sep;15(10):417. PMID: 25042199.
64. Bose P, Verstovsek S. JAK2 inhibitors for myeloproliferative neoplasms: what is next? Blood. 2017 Jul 13;130(2):115-125. doi: 10.1182/blood-2017-04-742288. Epub 2017 May 12. PMID: 28500170; PMCID: PMC5510786.
65. Senkevitch E, Durum S. The promise of Janus kinase inhibitors in the treatment of hematological malignancies. Cytokine. 2017 Oct;98:33-41. doi: 10.1016/j.cyto.2016.10.012. Epub 2016 Oct 27. PMID: 28277287; PMCID: PMC5854188.

66. Zhang N, Zeng Y, Du W, Zhu J, Shen D, Liu Z, Huang JA. The EGFR pathway is involved in the regulation of PD-L1 expression via the IL-6/JAK/STAT3 signaling pathway in EGFR-mutated non-small cell lung cancer. Int J Oncol. 2016 Oct;49(4):1360-8. doi: 10.3892/ijo.2016.3632. Epub 2016 Jul 26. PMID: 27499357.
67. Bu LL, Yu GT, Wu L, Mao L, Deng WW, Liu JF, Kulkarni AB, Zhang WF, Zhang L, Sun ZJ. STAT3 Induces Immunosuppression by Upregulating PD-1/PD-L1 in HNSCC. J Dent Res. 2017 Aug;96(9):1027-1034. doi: 10.1177/0022034517712435. Epub 2017 Jun 12. PMID: 28605599; PMCID: PMC6728673.
68. Atsaves V, Tsesmetzis N, Chioureas D, Kis L, Leventaki V, Drakos E, Panaretakis T, Grander D, Medeiros LJ, Young KH, Rassidakis GZ. PD-L1 is commonly expressed and transcriptionally regulated by STAT3 and MYC in ALK-negative anaplastic large-cell lymphoma. Leukemia. 2017 Jul;31(7):1633-1637. doi: 10.1038/leu.2017.103. Epub 2017 Mar 27. PMID: 28344319.
69. Liu H, Shen J, Lu K. IL-6 and PD-L1 blockade combination inhibits hepatocellular carcinoma cancer development in mouse model. Biochem Biophys Res Commun. 2017 Apr 29;486(2):239-244. doi: 10.1016/j.bbrc.2017.02.128. Epub 2017 Mar 1. PMID: 28254435.
70. Mace TA, Shakya R, Pitarresi JR, Swanson B, McQuinn CW, Loftus S, Nordquist E, Cruz-Monserrate Z, Yu L, Young G, Zhong X, Zimmers TA, Ostrowski MC, Ludwig T, Bloomston M, Bekaii-Saab T, Lesinski GB. IL-6 and PD-L1 antibody blockade combination therapy reduces tumour progression in murine models of pancreatic cancer. Gut. 2018 Feb;67(2):320-332. doi: 10.1136/gutjnl-2016-311585. Epub 2016 Oct 21. PMID: 27797936; PMCID: PMC5406266.
71. Wingelhofer, B., Maurer, B., Heyes, E.C. et al. Pharmacologic inhibition of STAT5 in acute myeloid leukemia. Leukemia 32, 1135–1146 (2018). https://doi.org/10.1038/s41375-017-0005-9
72. Kaneshige, A., Bai, L., Wang, M. et al. A selective small-molecule STAT5 PROTAC degrader capable of achieving tumor regression in vivo. Nat Chem Biol 19, 703–711 (2023). https://doi.org/10.1038/s41589-022-01248-4
73. Tolomeo M, Meli M, Grimaudo S. STAT5 and STAT5 Inhibitors in Hematological Malignancies. Anticancer Agents Med Chem. 2019;19(17):2036-2046. doi: 10.2174/1871520619666190906160848. PMID: 31490767.

Supplementary Figures

Supplementary Figure 1

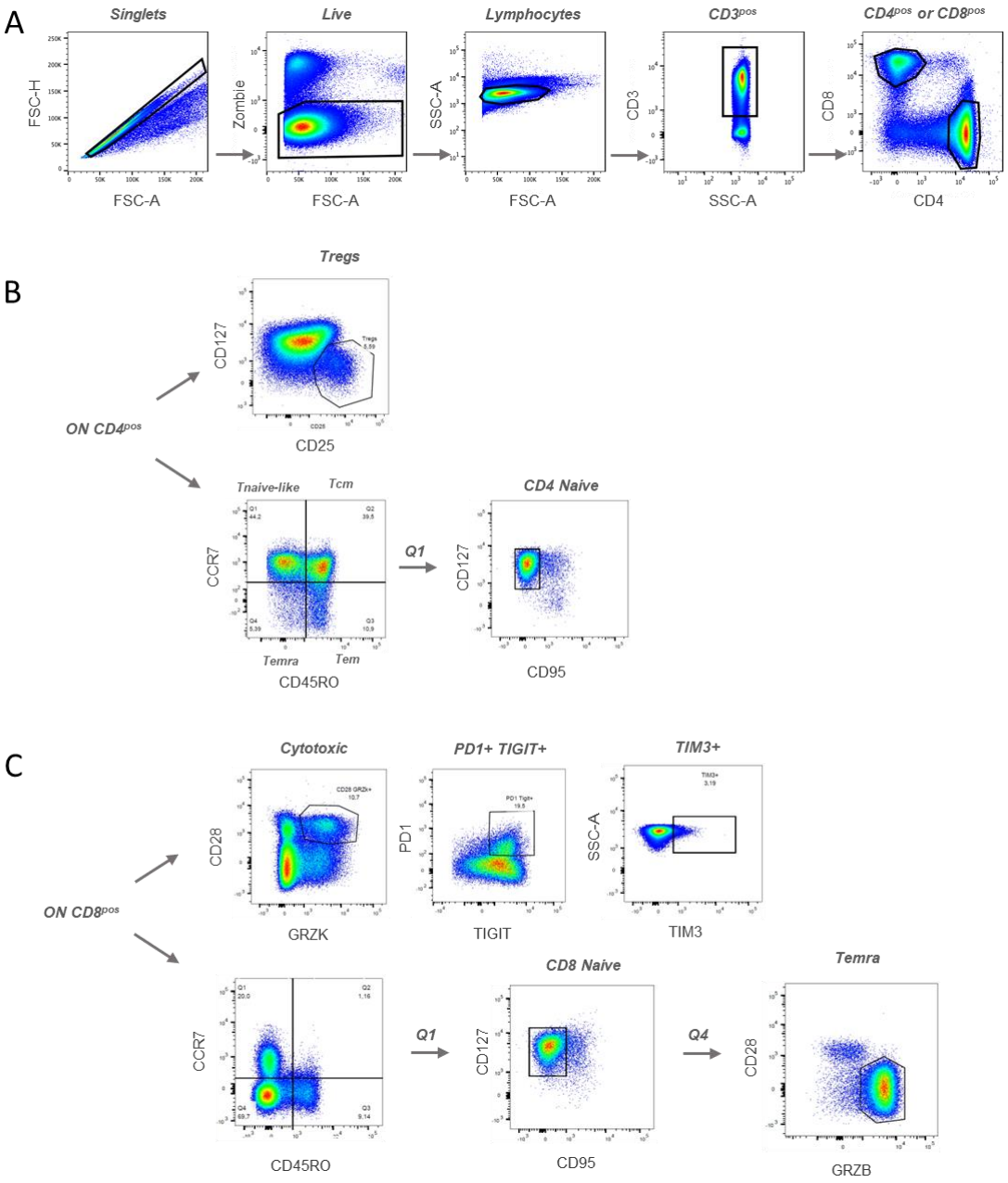

S1. Manual gating strategy for the identification of T cells subpopulations.

Supplementary Figure 2

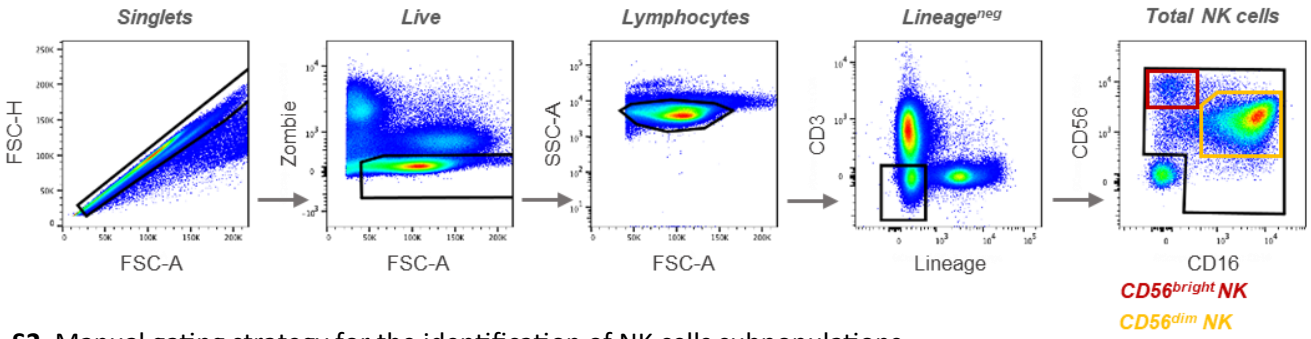

S2. Manual gating strategy for the identification of NK cells subpopulations.

Supplementary Figure 3

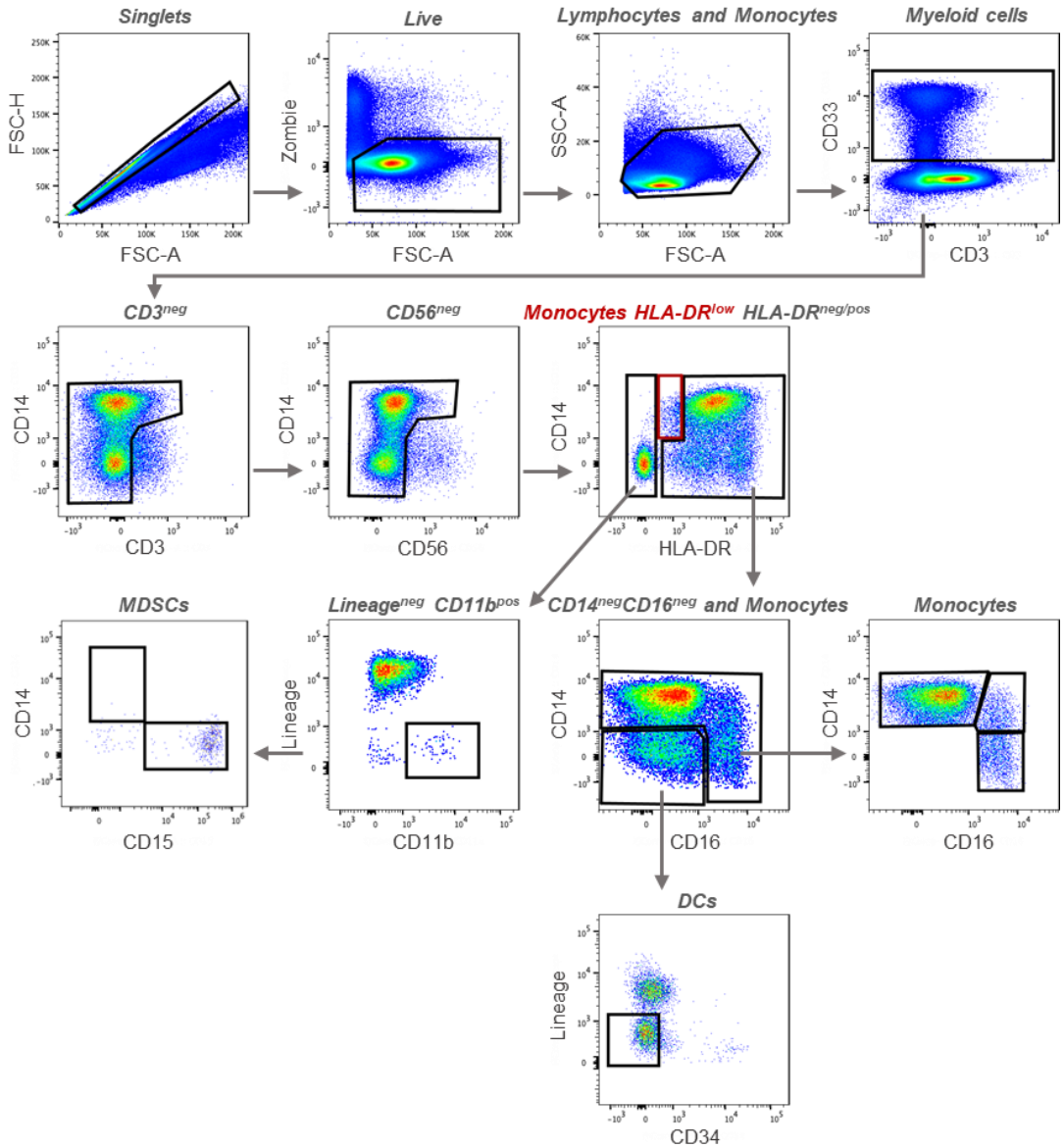

S3. Manual gating strategy for the identification of Myeloid cells subpopulations.

Supplementary Figure 4

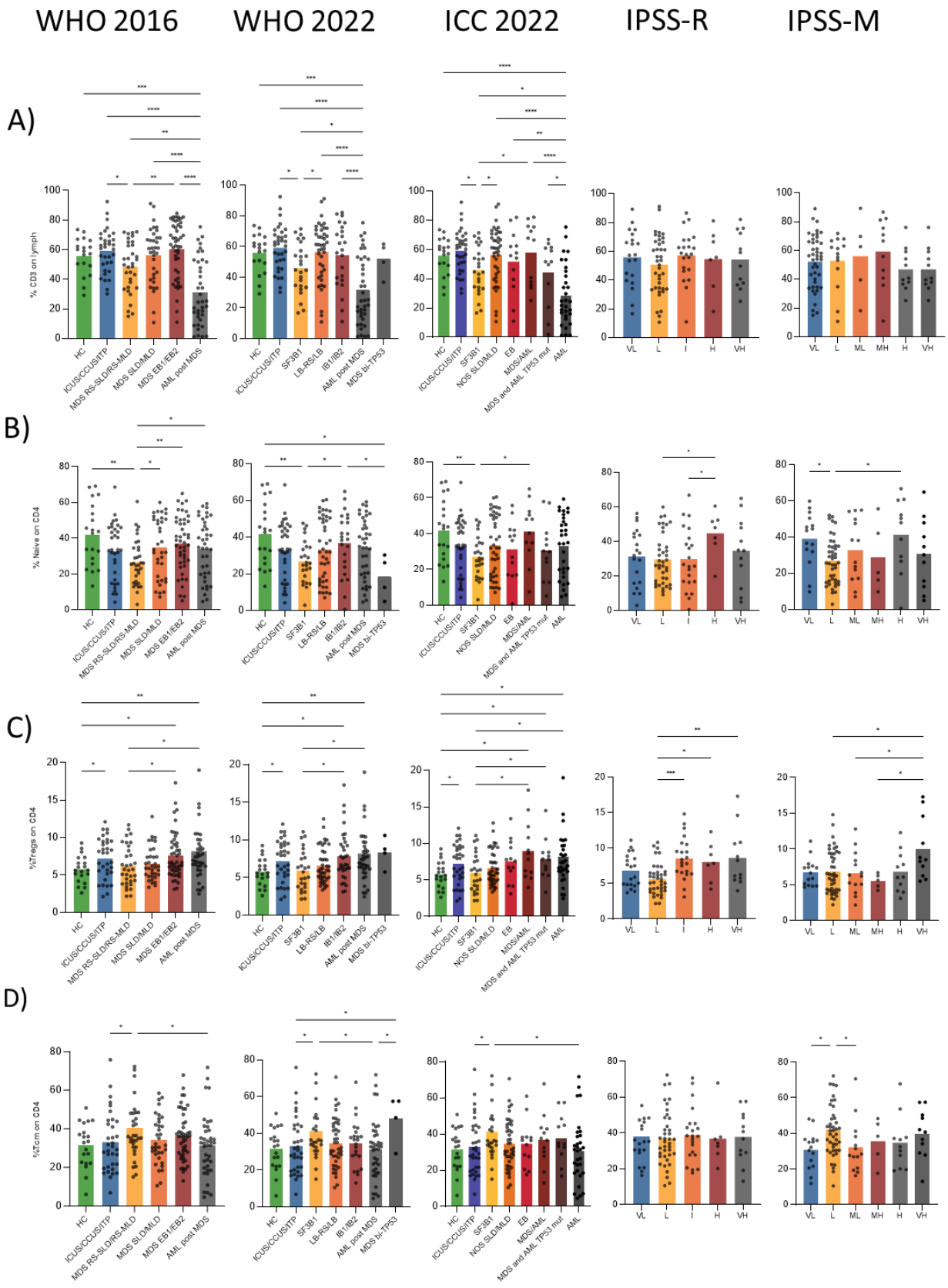

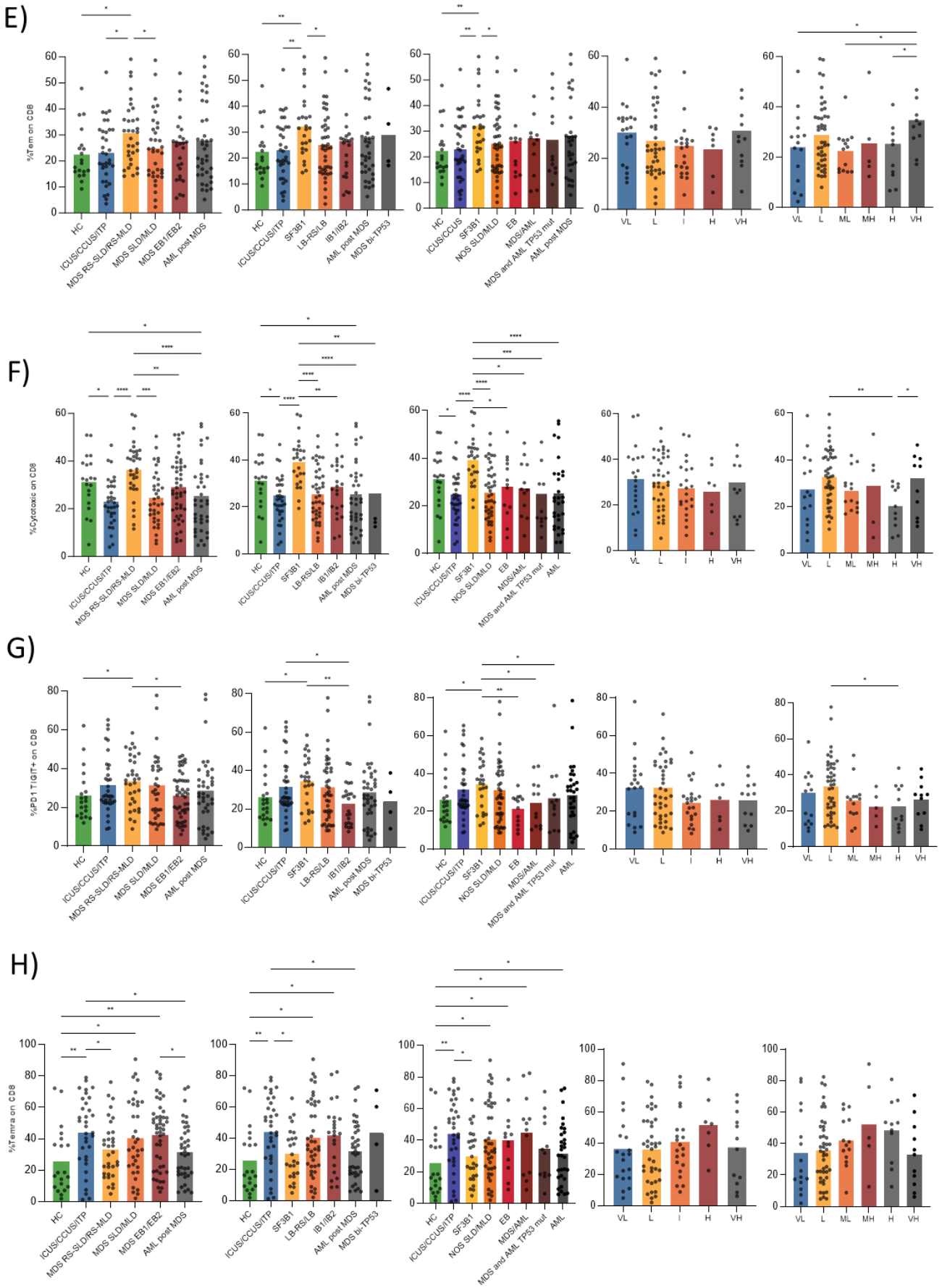
E)
%Tem on CD8
HC
ICUS/CCUS/ITP
MDS RS-SLD/RS-MLD
MDS SLD/MLD
MDS EB1/EB2
AML post MDS
HC
ICUS/CCUS/ITP
SF3B1
LB-RS/LB
IB1/IB2
AML post MDS
MDS bi-TP53
HC
ICUS/CCUS
SF3B1
NOS SLD/MLD
EB
MDS/AML
MDS and AML TP53 mut
AML post MDS
VL
L
I
H
VH
VL
L
ML
MH
H
VH
F)
%Cytotoxic on CD8
HC
ICUS/CCUS/ITP
MDS RS-SLD/RS-MLD
MDS SLD/MLD
MDS EB1/EB2
AML post MDS
HC
ICUS/CCUS/ITP
SF3B1
LB-RS/LB
IB1/IB2
AML post MDS
MDS bi-TP53
HC
ICUS/CCUS/ITP
SF3B1
NOS SLD/MLD
EB
MDS/AML
MDS and AML TP53 mut
AML
VL
L
I
H
VH
VL
L
ML
MH
H
VH
G)
%PD1 TIGIT+ on CD8
HC
ICUS/CCUS/ITP
MDS RS-SLD/RS-MLD
MDS SLD/MLD
MDS EB1/EB2
AML post MDS
HC
ICUS/CCUS/ITP
SF3B1
LB-RS/LB
IB1/IB2
AML post MDS
MDS bi-TP53
HC
ICUS/CCUS/ITP
SF3B1
NOS SLD/MLD
EB
MDS/AML
MDS and AML TP53 mut
AML
VL
L
I
H
VH
VL
L
ML
MH
H
VH
H)
%Temra on CD8
HC
ICUS/CCUS/ITP
MDS RS-SLD/RS-MLD
MDS SLD/MLD
MDS EB1/EB2
AML post MDS
HC
ICUS/CCUS/ITP
SF3B1
LB-RS/LB
IB1/IB2
AML post MDS
MDS bi-TP53
HC
ICUS/CCUS/ITP
SF3B1
NOS SLD/MLD
EB
MDS/AML
MDS and AML TP53 mut
AML
VL
L
I
H
VH
VL
L
ML
MH
H
VH

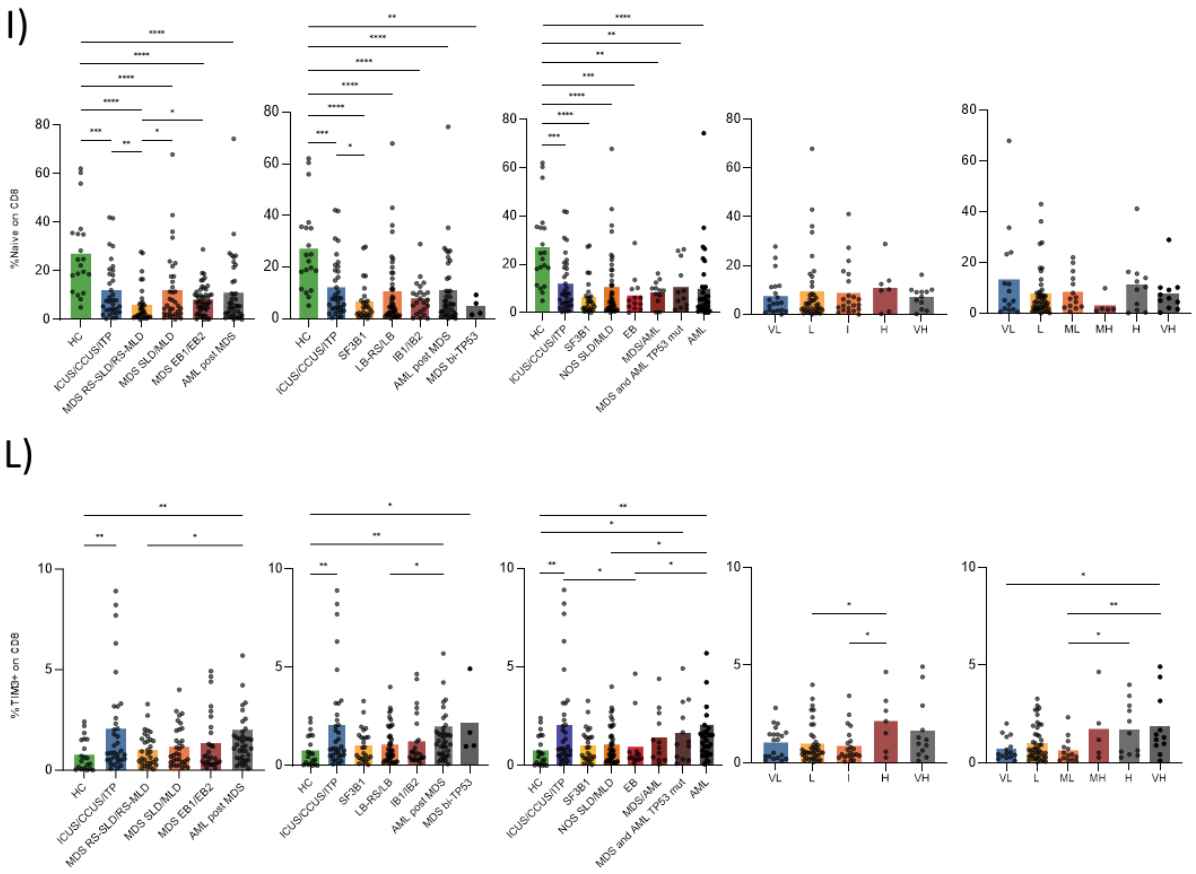

S4. T cell subpopulations frequencies on bone marrow samples collected at diagnosis or at disease evolution, before HMA treatment.

The bar graphs show the frequency of a specific T cell subpopulation (indicated on the Y axis of the first graph in each row) in the different MDS and risk categories. Mann whitney U test was used to compare groups and significance was set at a P value less than .05.

Supplementary Figure 5

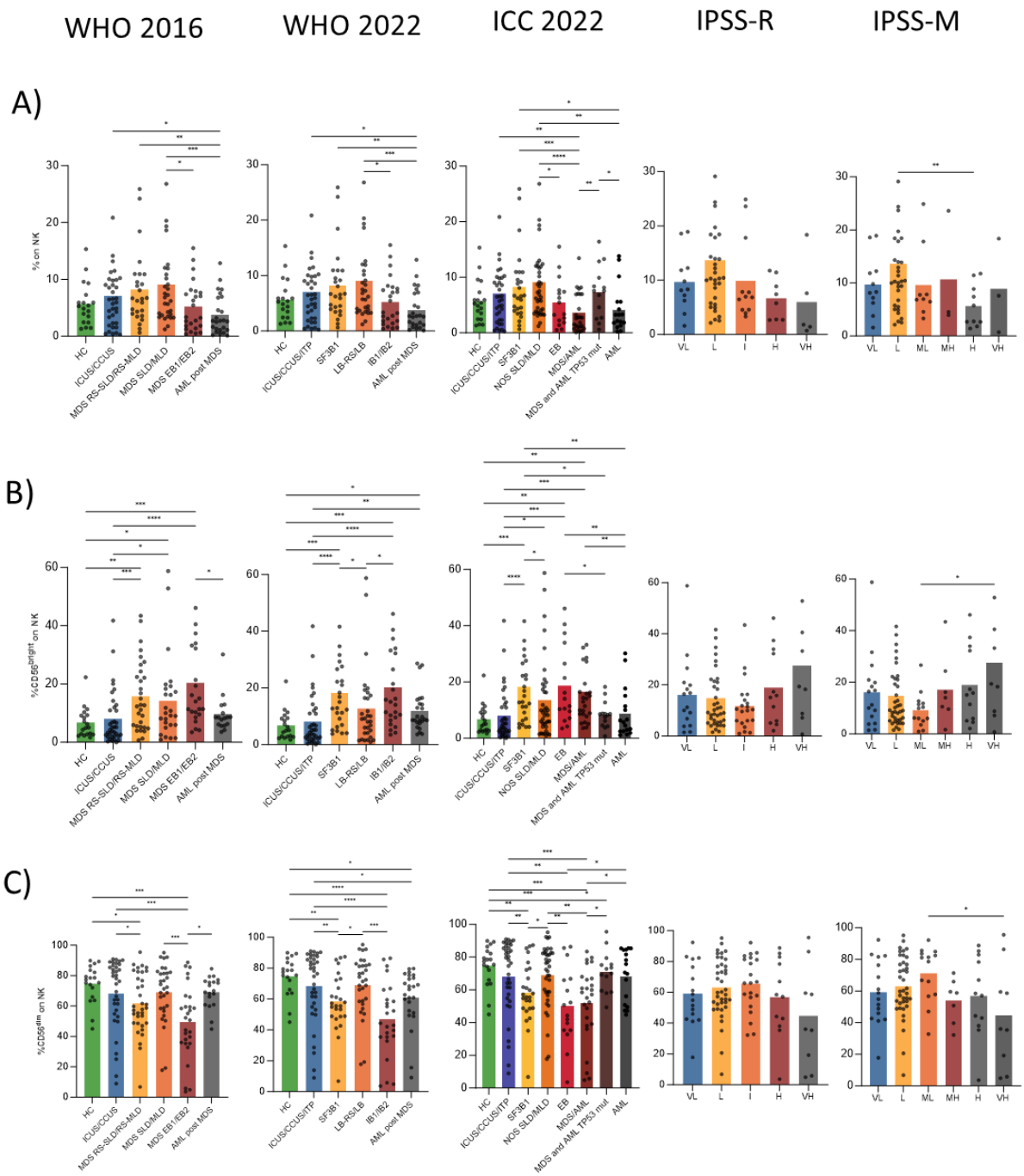

S5. Main NK cell subpopulations frequencies on bone marrow samples collected at diagnosis or at disease evolution, before HMA treatment.

The bar graphs show the frequency of a specific NK subpopulation (indicated on the Y axis of the first graph in each row) in the different MDS and risk categories. Mann whitney U test was used to compare

Supplementary Figure 6

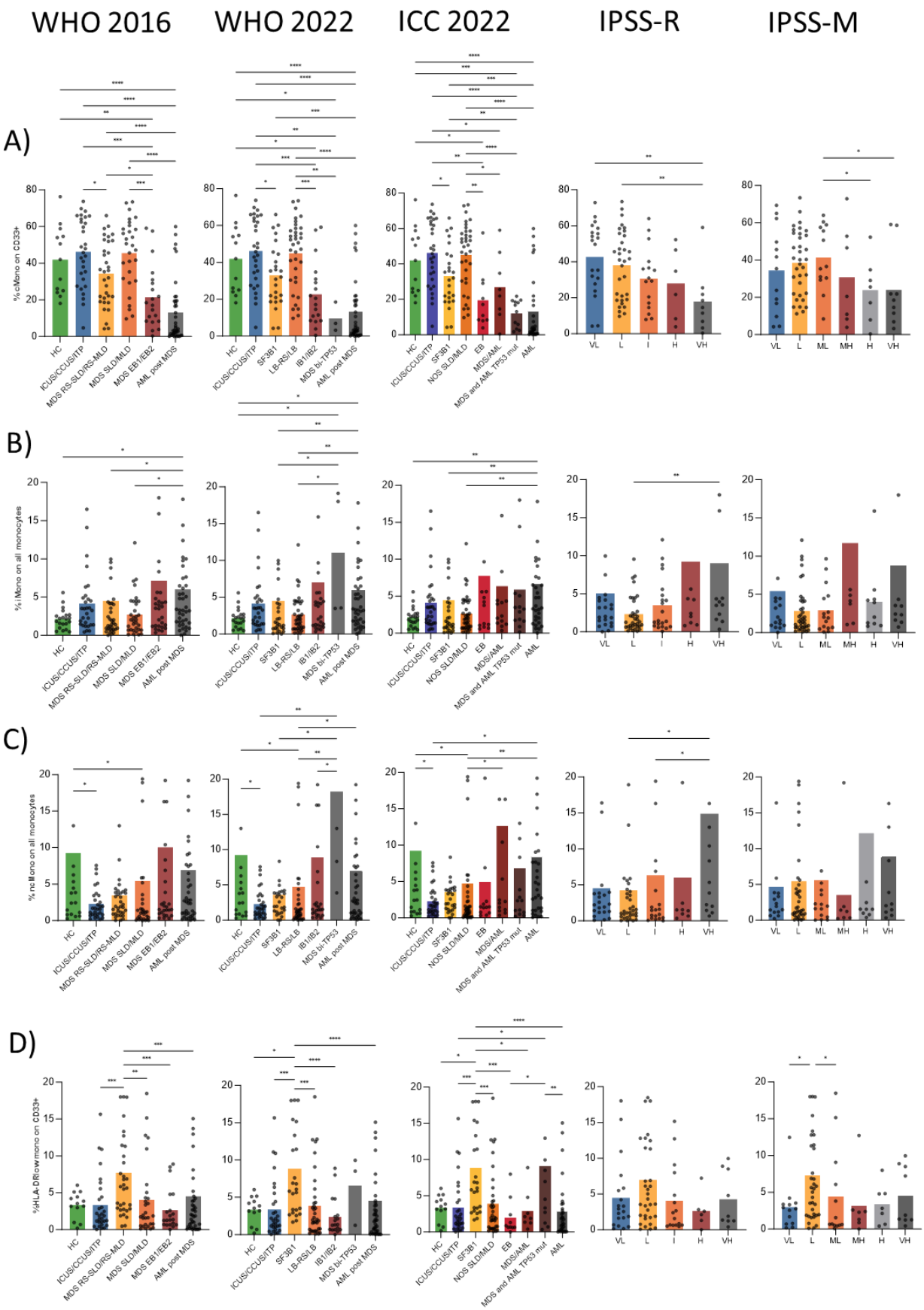

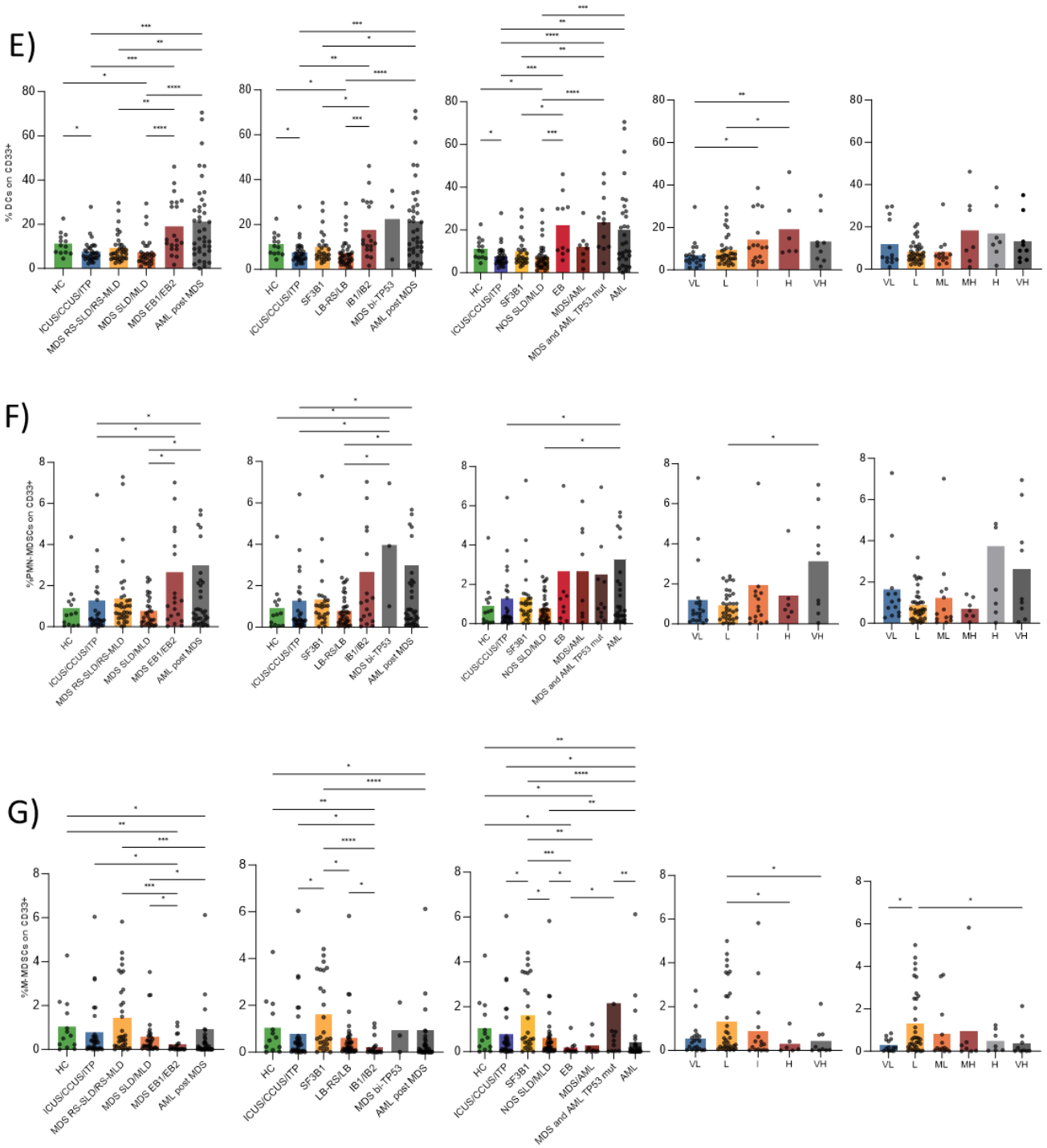

S6. Myeloid cells subpopulations frequencies on bone marrow samples collected at diagnosis or at disease evolution, before HMA treatment.

The bar graphs show the frequency of a specific myeloid cell subpopulation (indicated on the Y axis of the first graph in each row) in the different MDS and risk categories. Mann whitney U test was used to compare groups and significance was set at a P value less than .05.

Supplementary Figure 7

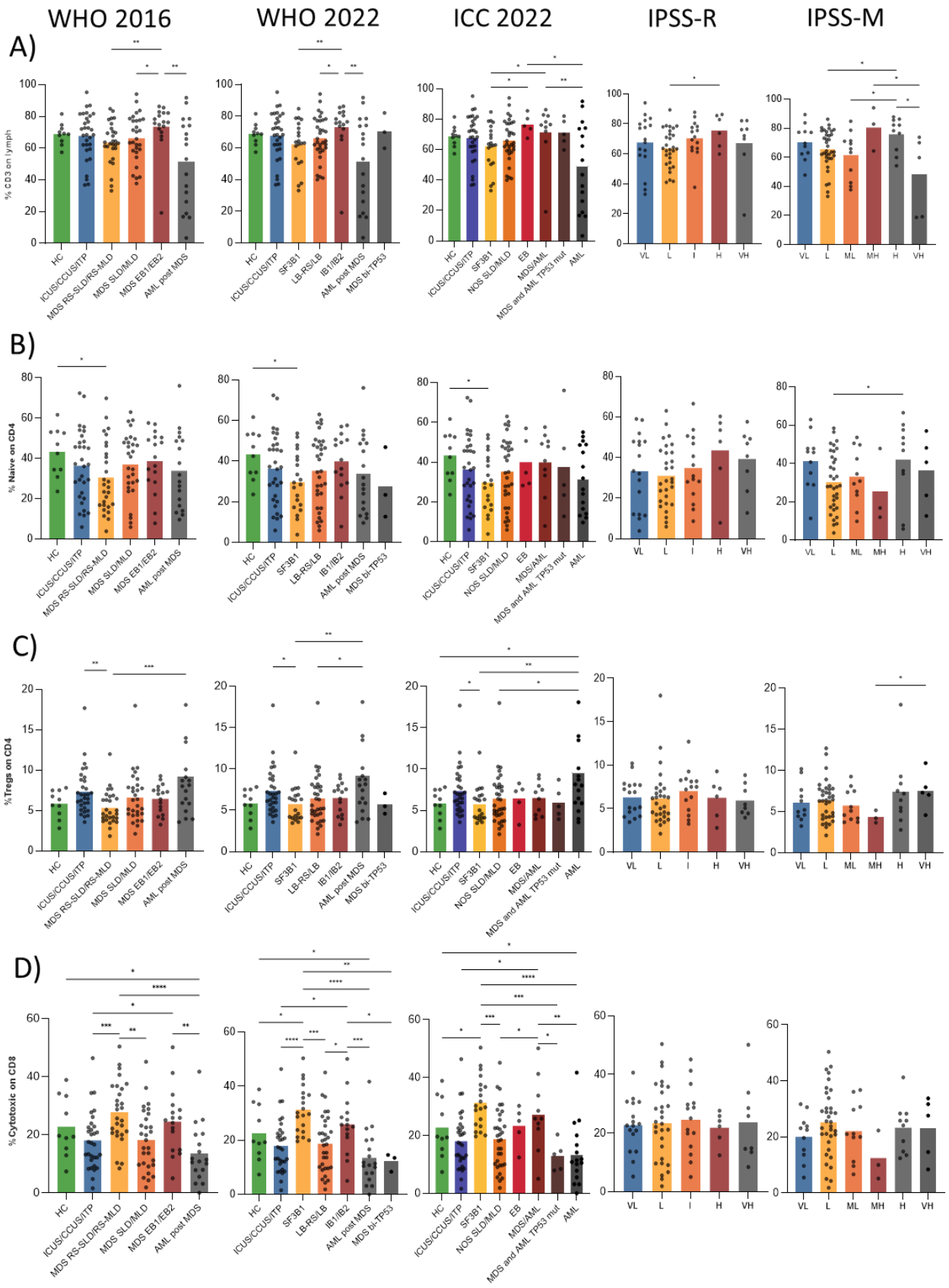

E)

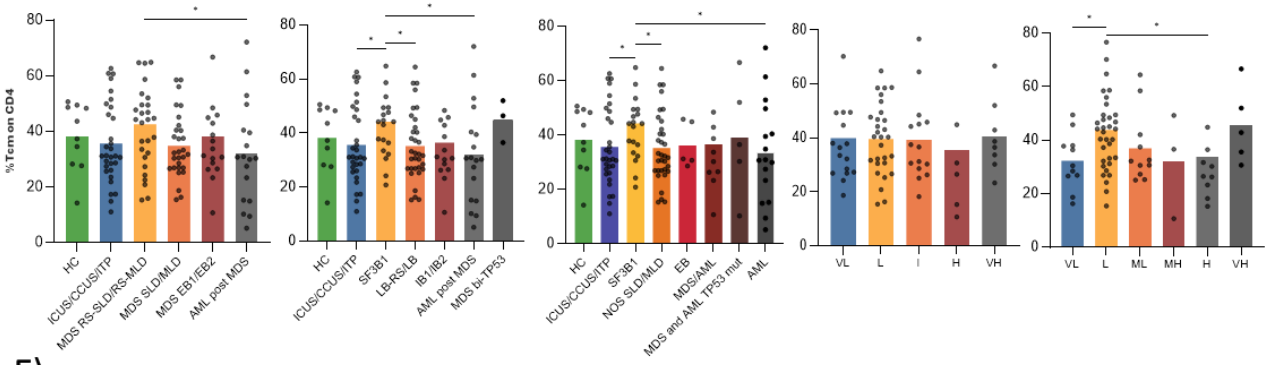
% Tem on CD4
HC
ICUS/CCUS/ITP
MDS RS-SLD/RS-MLD
MDS SLD/MLD
MDS EB1/EB2
AML post MDS
SF3B1
LB-RS/LB
IB1/IB2
MDS bi-TP53
NOS SLD/MLD
EB
MDS/AML
MDS and AML TP53 mut
AML
VL
L
I
H
VH
ML
MH

F)

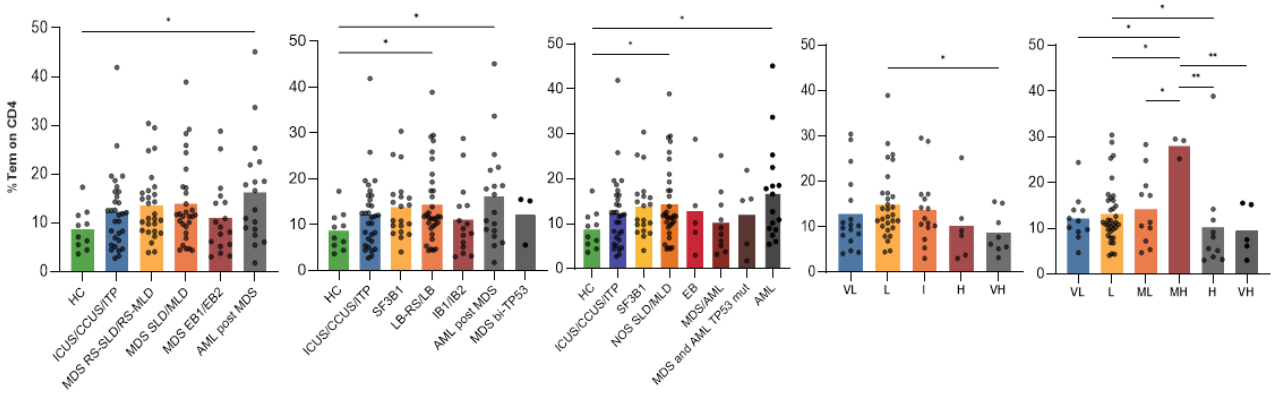
% Tem on CD4
HC
ICUS/CCUS/ITP
MDS RS-SLD/RS-MLD
MDS SLD/MLD
MDS EB1/EB2
AML post MDS
SF3B1
LB-RS/LB
IB1/IB2
MDS bi-TP53
NOS SLD/MLD
EB
MDS/AML
MDS and AML TP53 mut
AML
VL
L
I
H
VH
ML
MH

G)

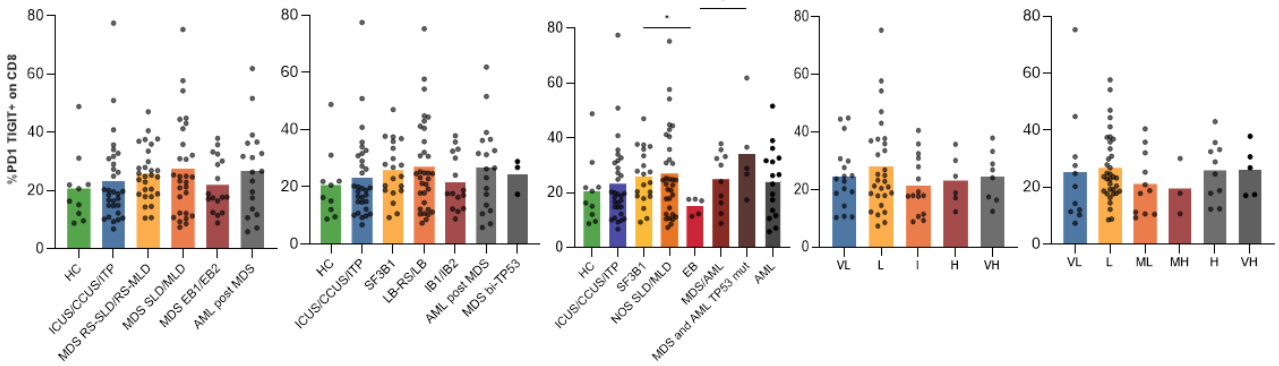
% PD1 TIGIT+ on CD8
HC
ICUS/CCUS/ITP
MDS RS-SLD/RS-MLD
MDS SLD/MLD
MDS EB1/EB2
AML post MDS
SF3B1
LB-RS/LB
IB1/IB2
MDS bi-TP53
NOS SLD/MLD
EB
MDS/AML
MDS and AML TP53 mut
AML
VL
L
I
H
VH
ML
MH

H)

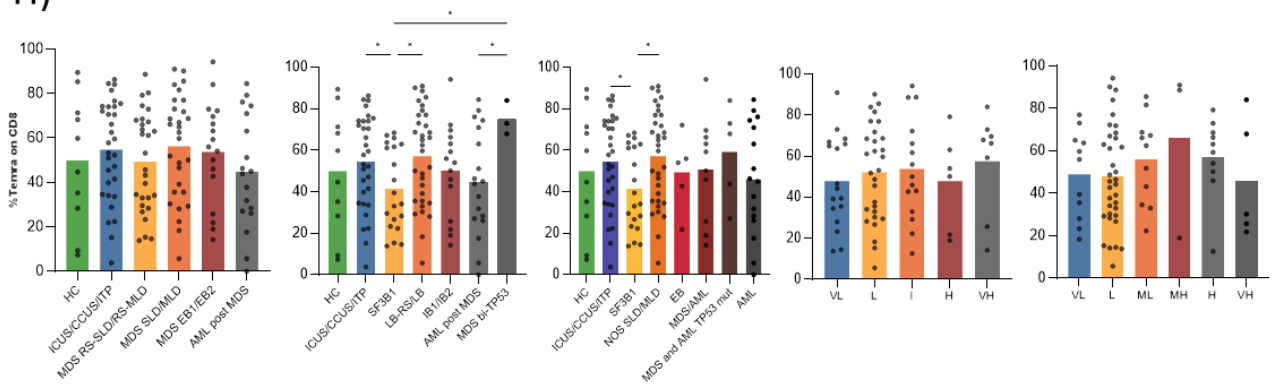
% Temra on CD8
HC
ICUS/CCUS/ITP
MDS RS-SLD/RS-MLD
MDS SLD/MLD
MDS EB1/EB2
AML post MDS
SF3B1
LB-RS/LB
IB1/IB2
MDS bi-TP53
NOS SLD/MLD
EB
MDS/AML
MDS and AML TP53 mut
AML
VL
L
I
H
VH
ML
MH

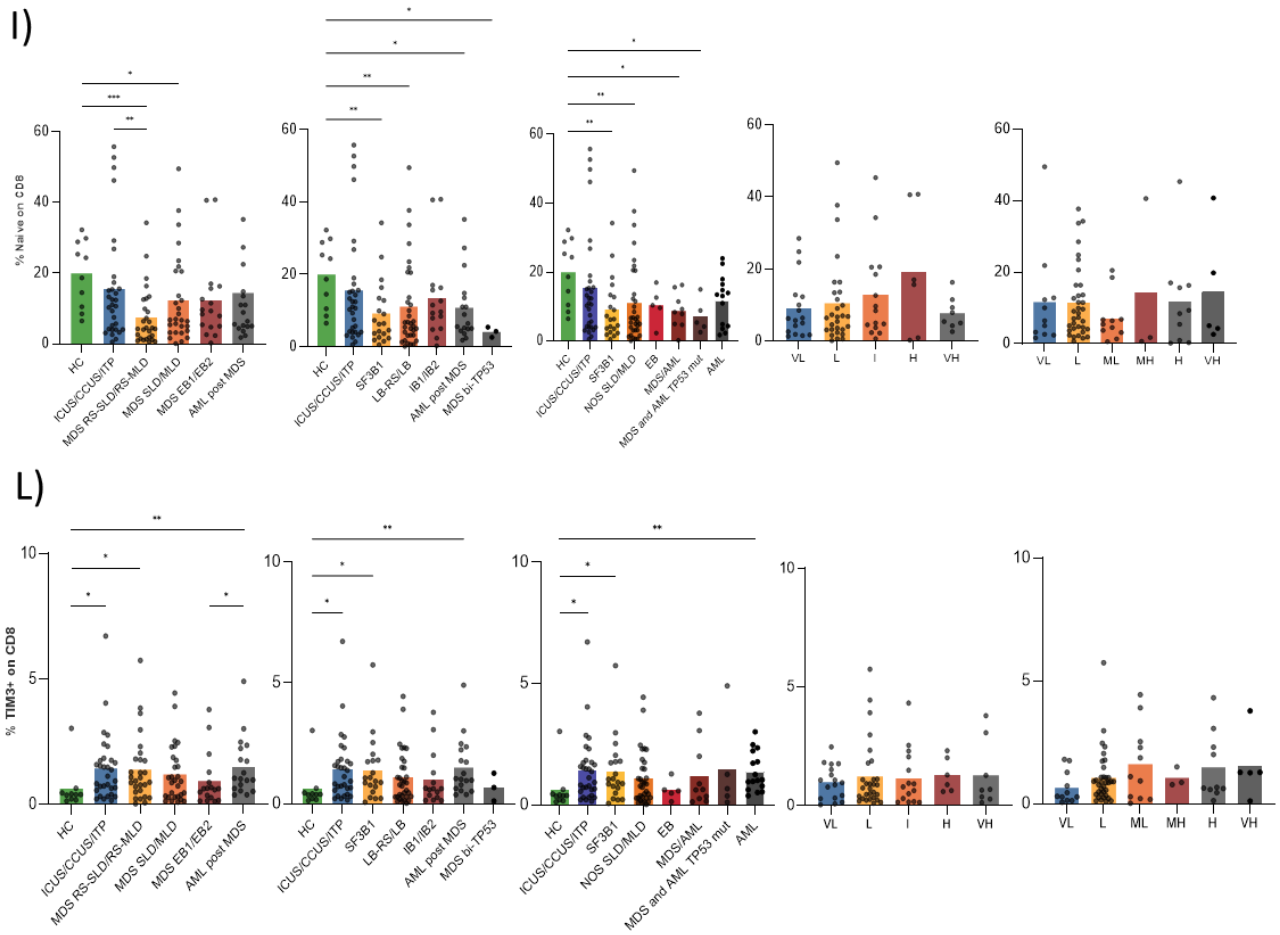

S7. T cell subpopulations frequencies on peripheral blood samples collected at diagnosis or at disease evolution, before HMA treatment.

The bar graphs show the frequency of a specific T cell subpopulation (indicated on the Y axis of the first graph in each row) in the different MDS and risk categories. Mann whitney U test was used to compare groups and significance was set at a P value less than .05.

Supplementary Figure 8

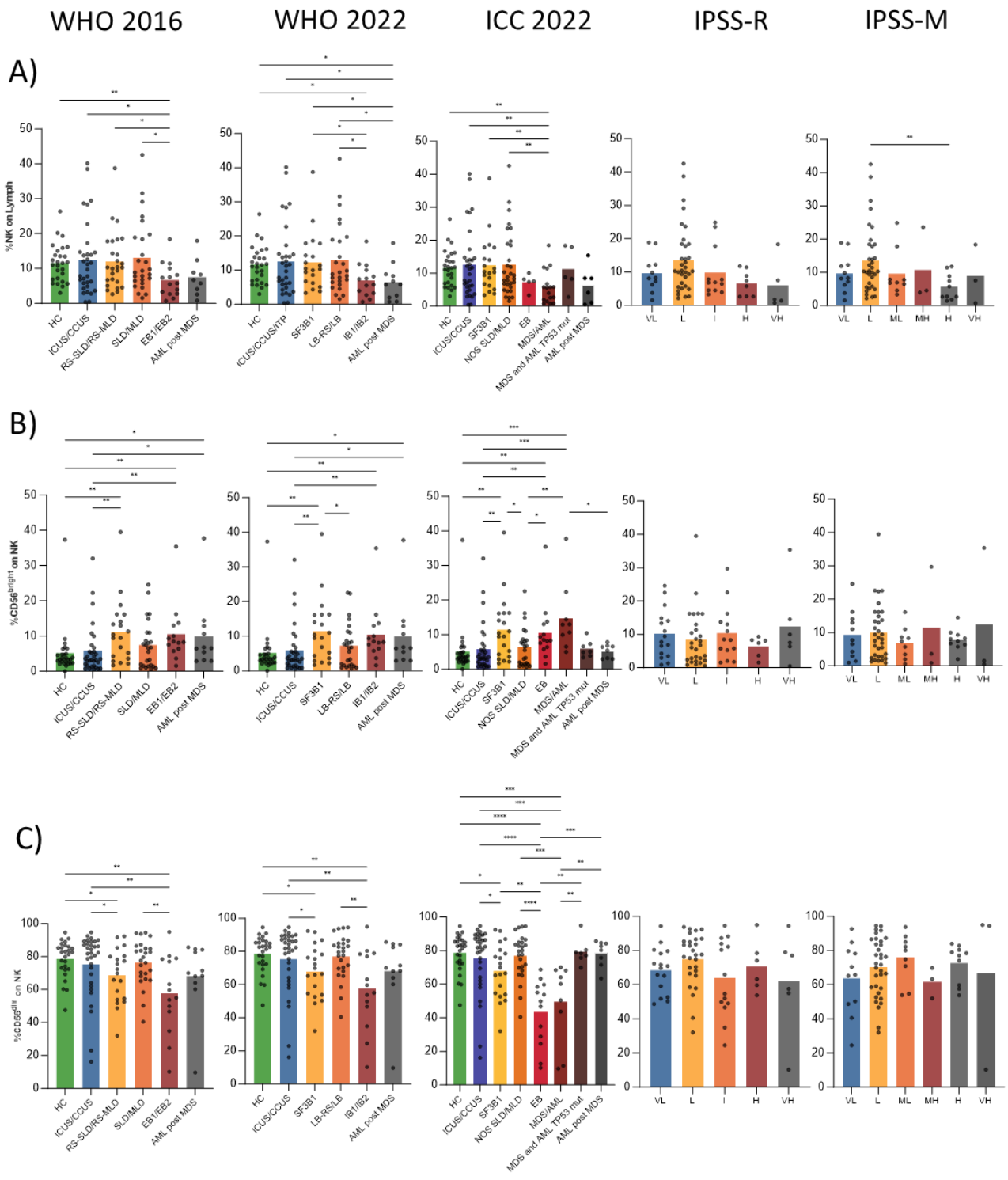

S8. NK cell subpopulations frequencies on peripheral blood samples collected at diagnosis or at disease evolution, before HMA treatment.

The bar graphs show the frequency of a specific NK subpopulation (indicated on the Y axis of the first graph in each row) in the different MDS and risk categories. Mann whitney U test was used to compare groups and significance was set at a P value less than .05.

Supplementary Figure 9

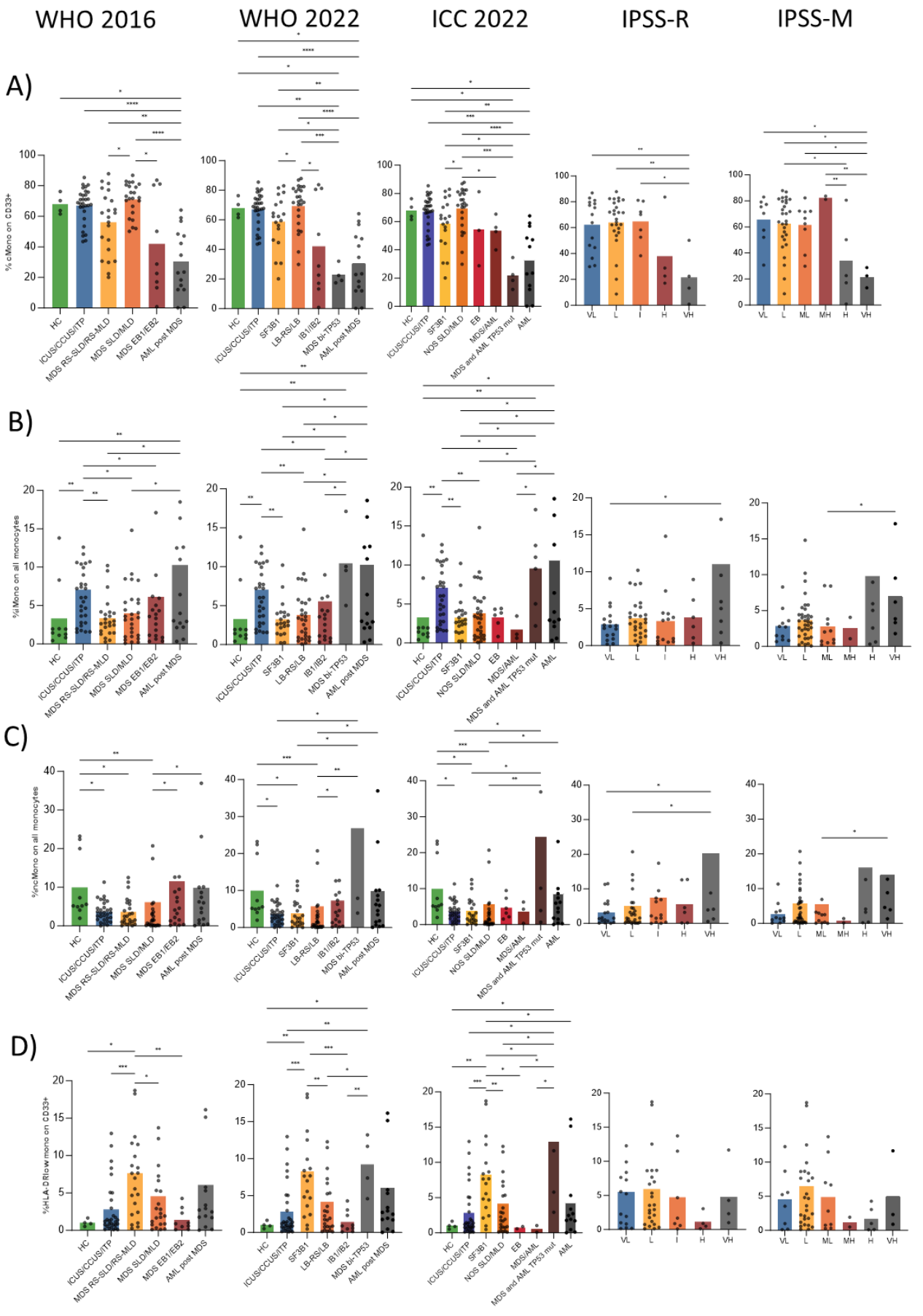

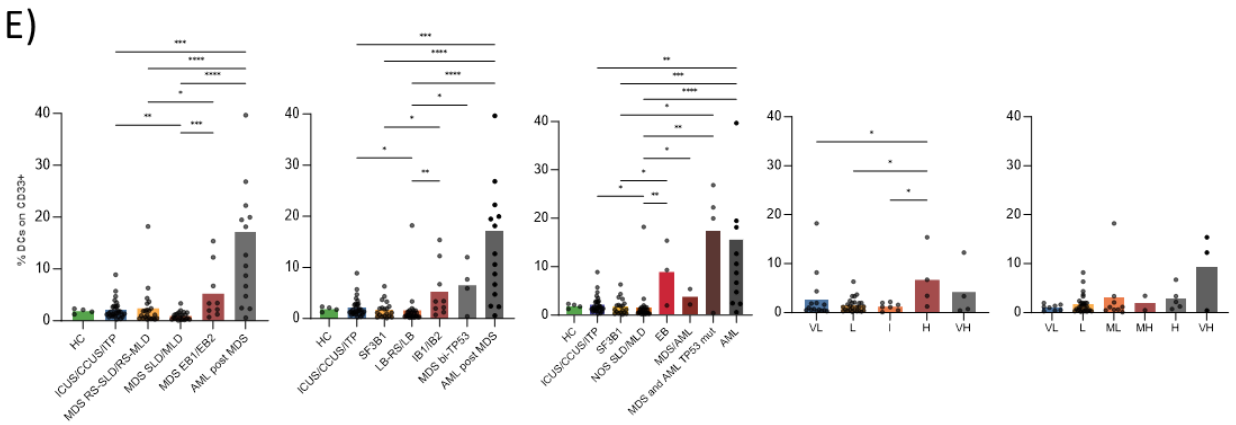

S9. Myeloid cell subpopulations frequencies on peripheral blood samples collected at diagnosis or at disease evolution, before HMA treatment.

The bar graphs show the frequency of a specific myeloid subpopulation (indicated on the Y axis of the first graph in each row) in the different MDS and risk categories. Mann whitney U test was used to compare groups and significance was set at a P value less than .05.

Supplementary Figure 10

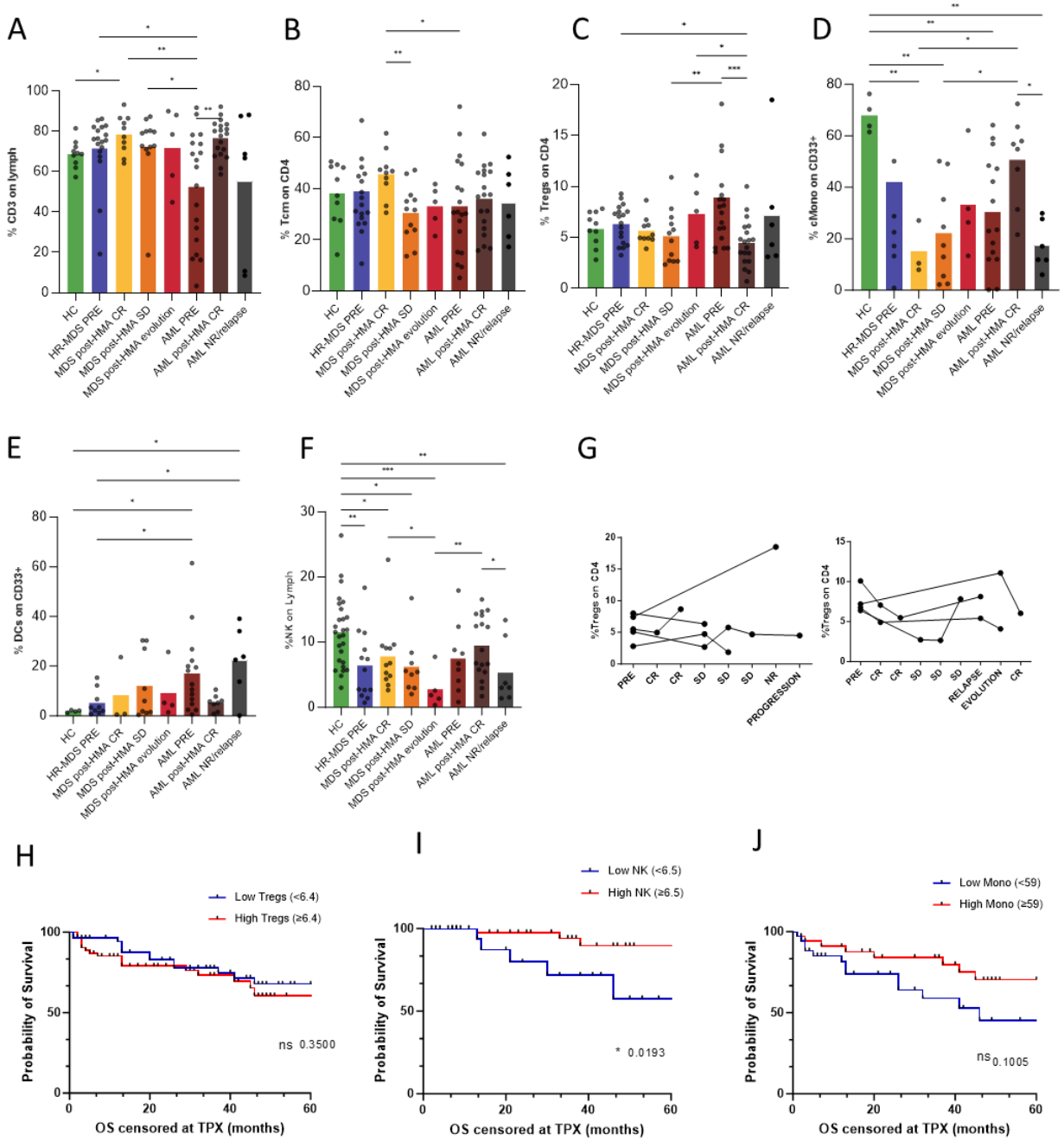

S10. Pre- and Post-HMAs cell frequencies comparison in peripheral blood. A-F) The bar graphs show the frequency of a specific immune subpopulation (indicated on the Y axis) in High-risk MDS and AML-post MDS, before and after treatment with HMAs. Post-HMAs samples are divided for treatment response (CR – Complete remission; SD – Stable Disease; NR – Non response). Mann whitney U test was used to compare groups and significance was set at a P value less than .05. G) Tregs frequencies measured along longitudinal samples (pre- and post-HMA). Each line represents a patient and each dot a specific timepoint. H-J) Kaplan-Meier showing the OS of patients divided for higher or lower %Tregs, %cMonocytes or %NK cells than the respective median frequency value calculated on MDS peripheral blood samples at diagnosis. Log-rank test was performed to assess statistical significance.

Supplementary Figure 11

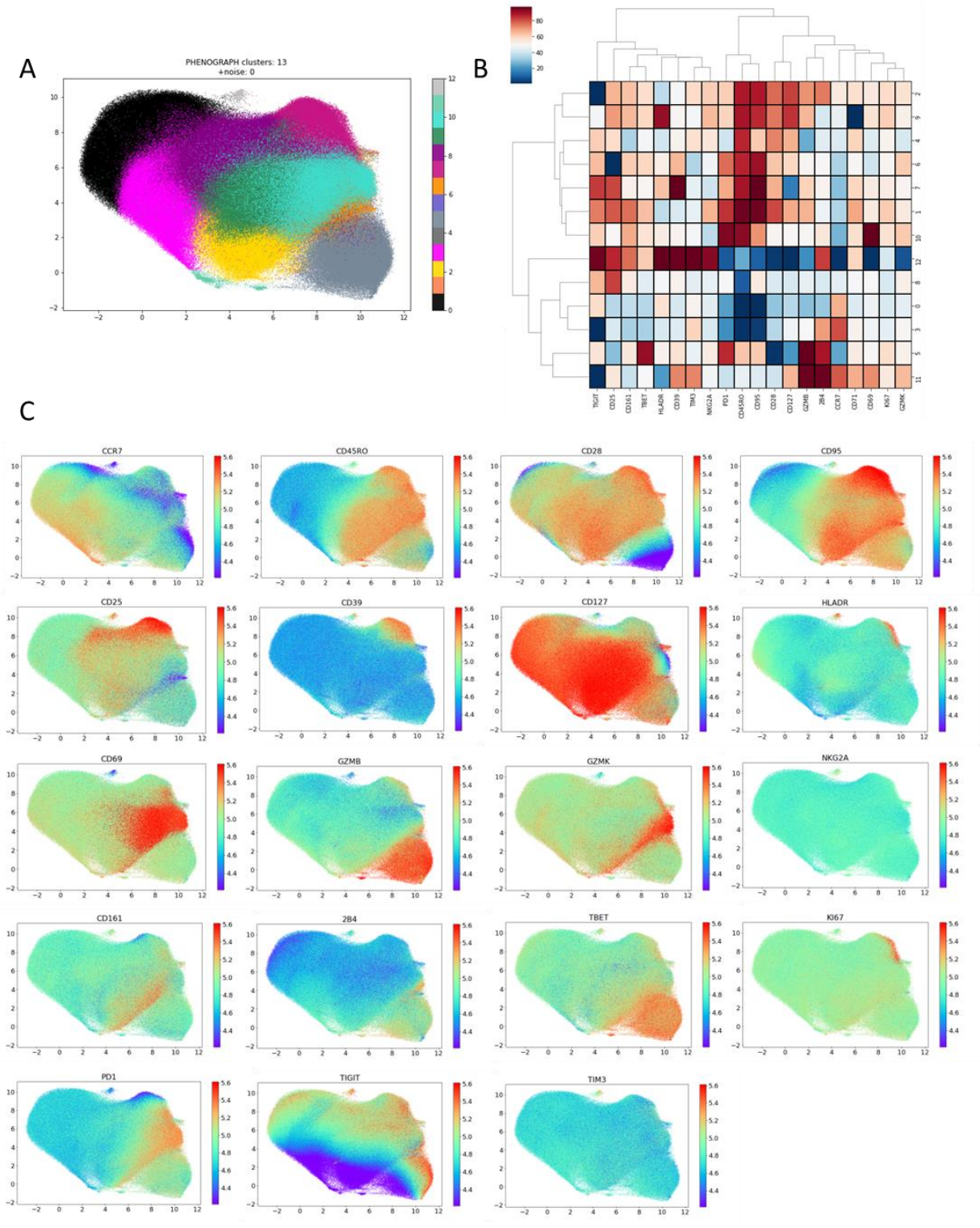

S11. CD4 Phenograph clusters. A) UMAP representation of the 13 CD4 Phenograph clusters. B) Heatmap representing the markers expression in each cluster. C) Visualization of single marker expression across Phenograph clusters.

Supplementary Figure 12

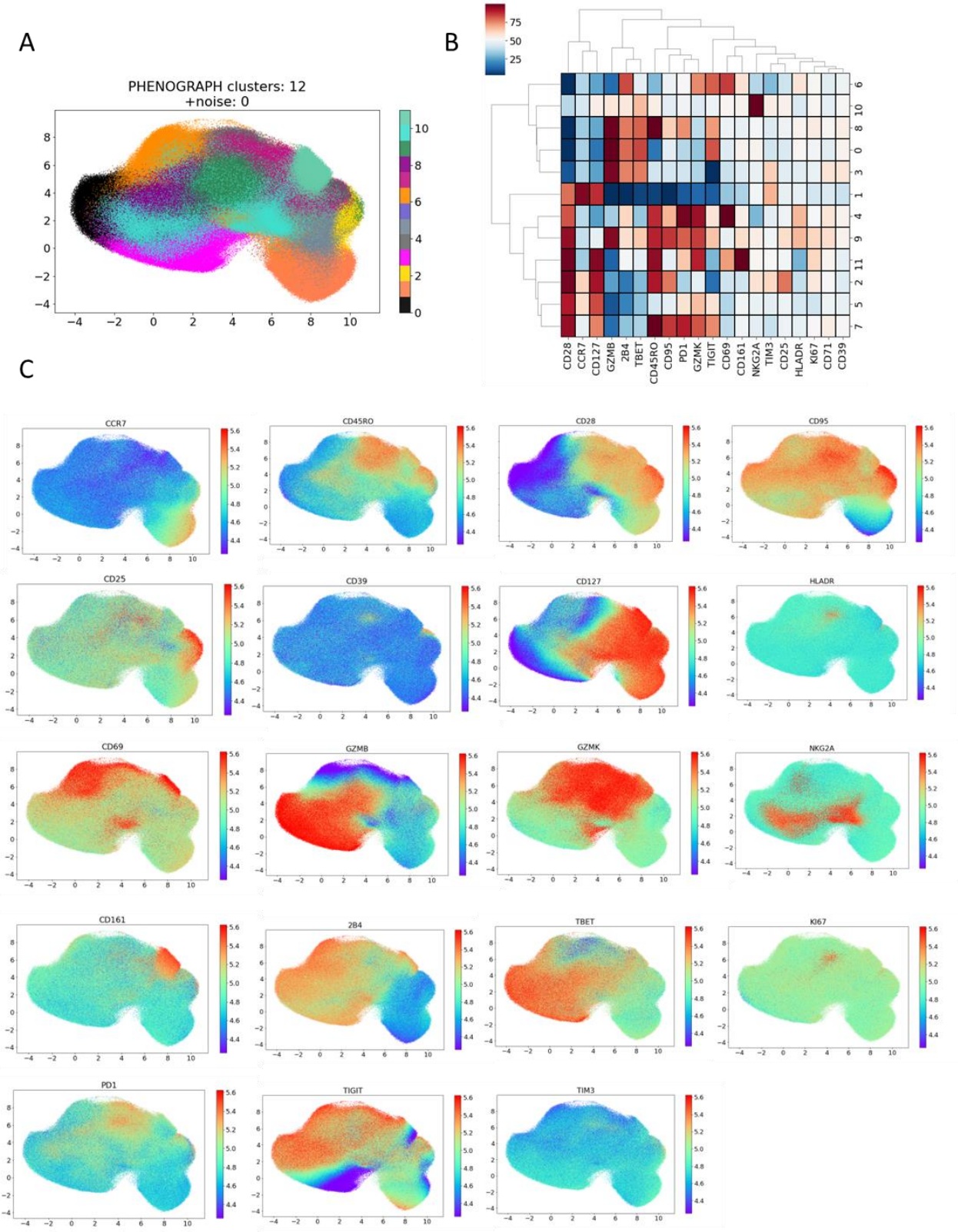

S12. CD8 Phenograph clusters. A) UMAP representation of the 12 CD8 Phenograph clusters. B) heatmap representing the markers expression in each cluster. C) Visualization of single marker expression across Phenograph clusters.

Supplementary Figure 13

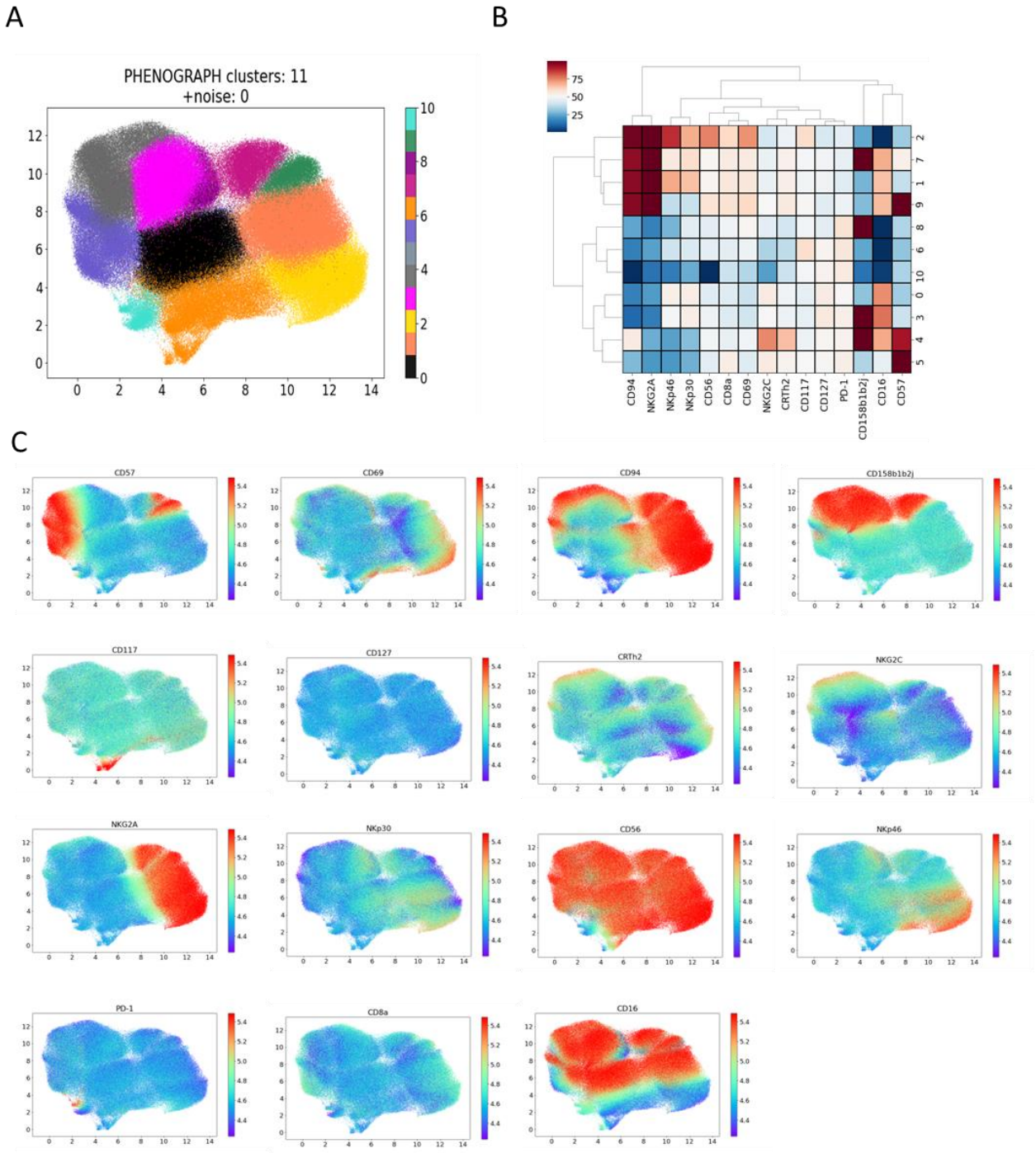

S13. NK Phenograph clusters. A) UMAP representation of the 11 NK Phenograph clusters. B) heatmap representing the markers expression in each cluster. C) Visualization of single marker expression across Phenograph clusters.

Supplementary Figure 14

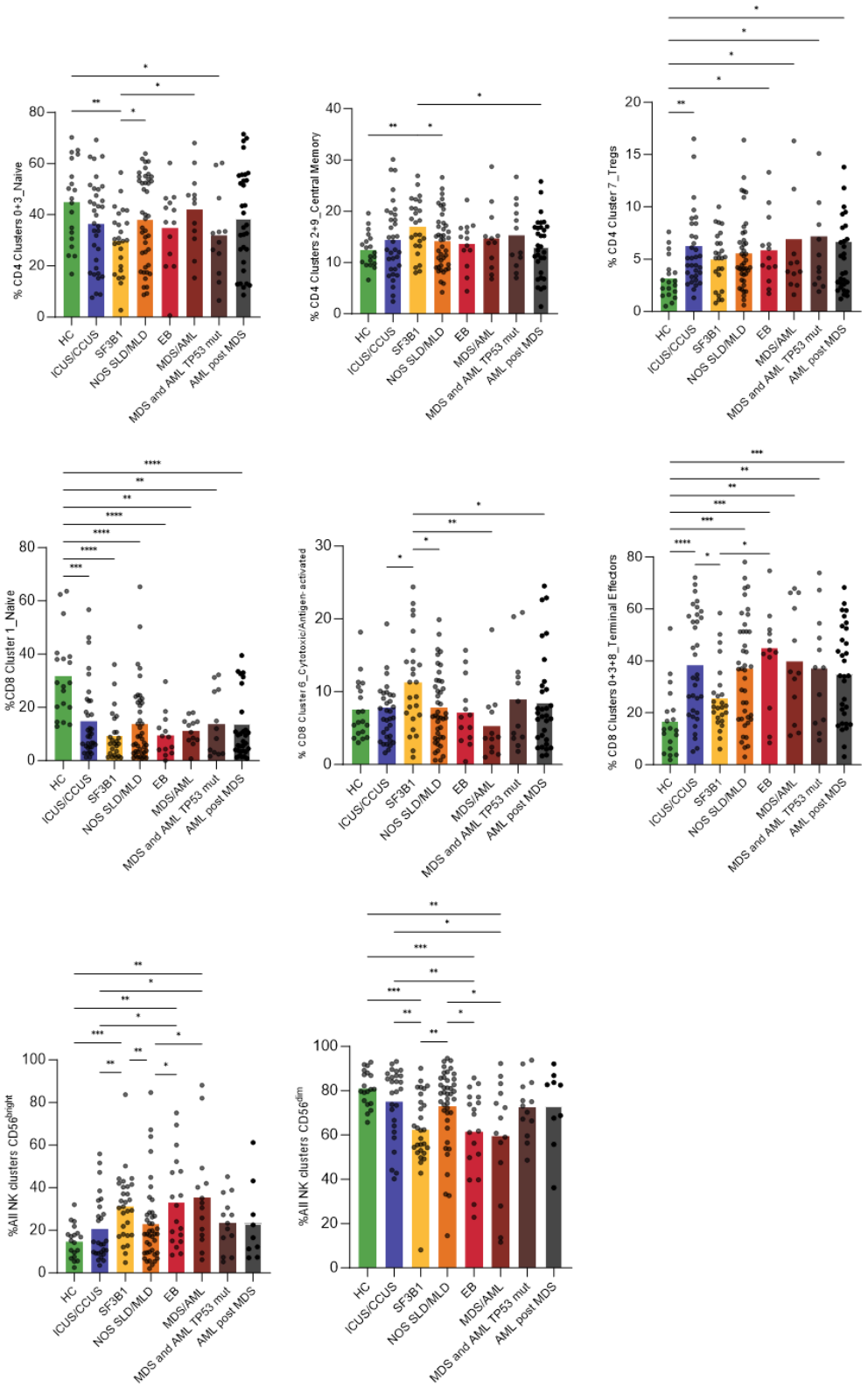

S14. Phenograph clusters frequencies of the major T and NK cell populations identified by manual gating. Both the frequency and the trend of each represented cell type reflects what observed with manual gating analysis.

Supplementary Figure 15

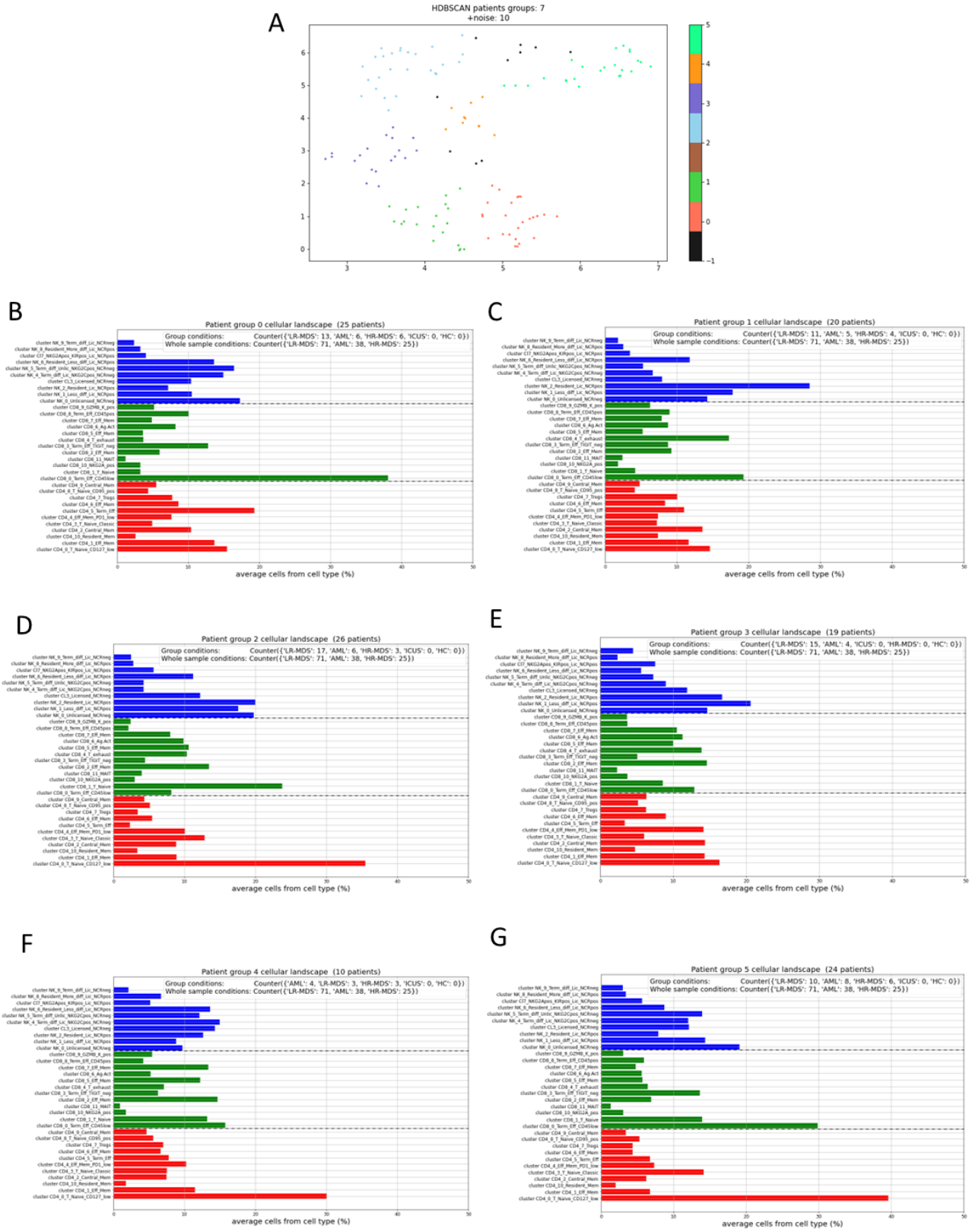

S15. HDBSCAN clustering of MDS patients. A) UMAP visualization of the 7 groups of patients identified through HDBSCAN algorithm. B-G) Frequency of each CD4, CD8 and NK Phenograph cluster in a specific HDBSCAN group.

Supplementary Figure 16

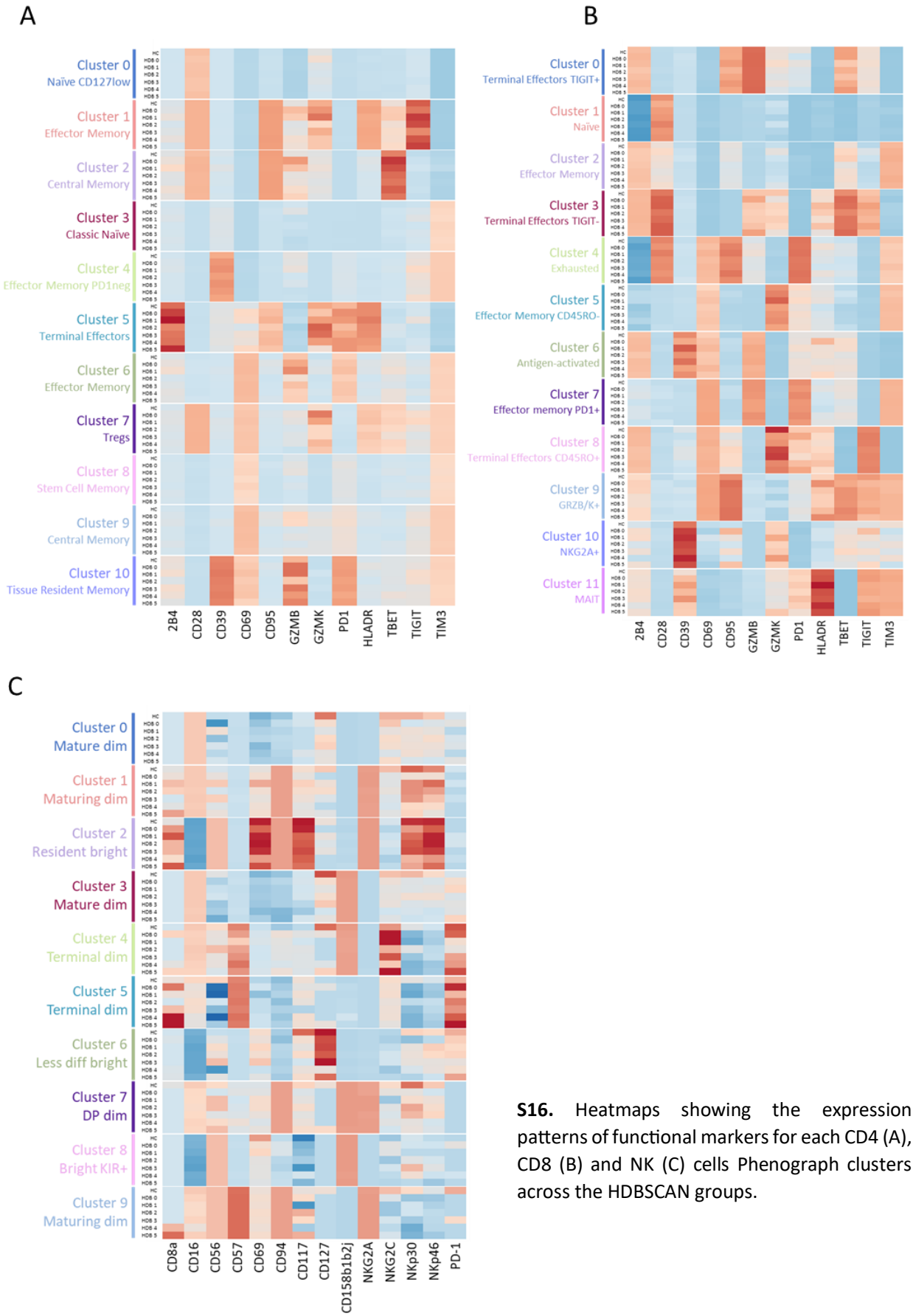

S16. Heatmaps showing the expression patterns of functional markers for each CD4 (A), CD8 (B) and NK (C) cells Phenograph clusters across the HDBSCAN groups.

Supplementary Figure 17

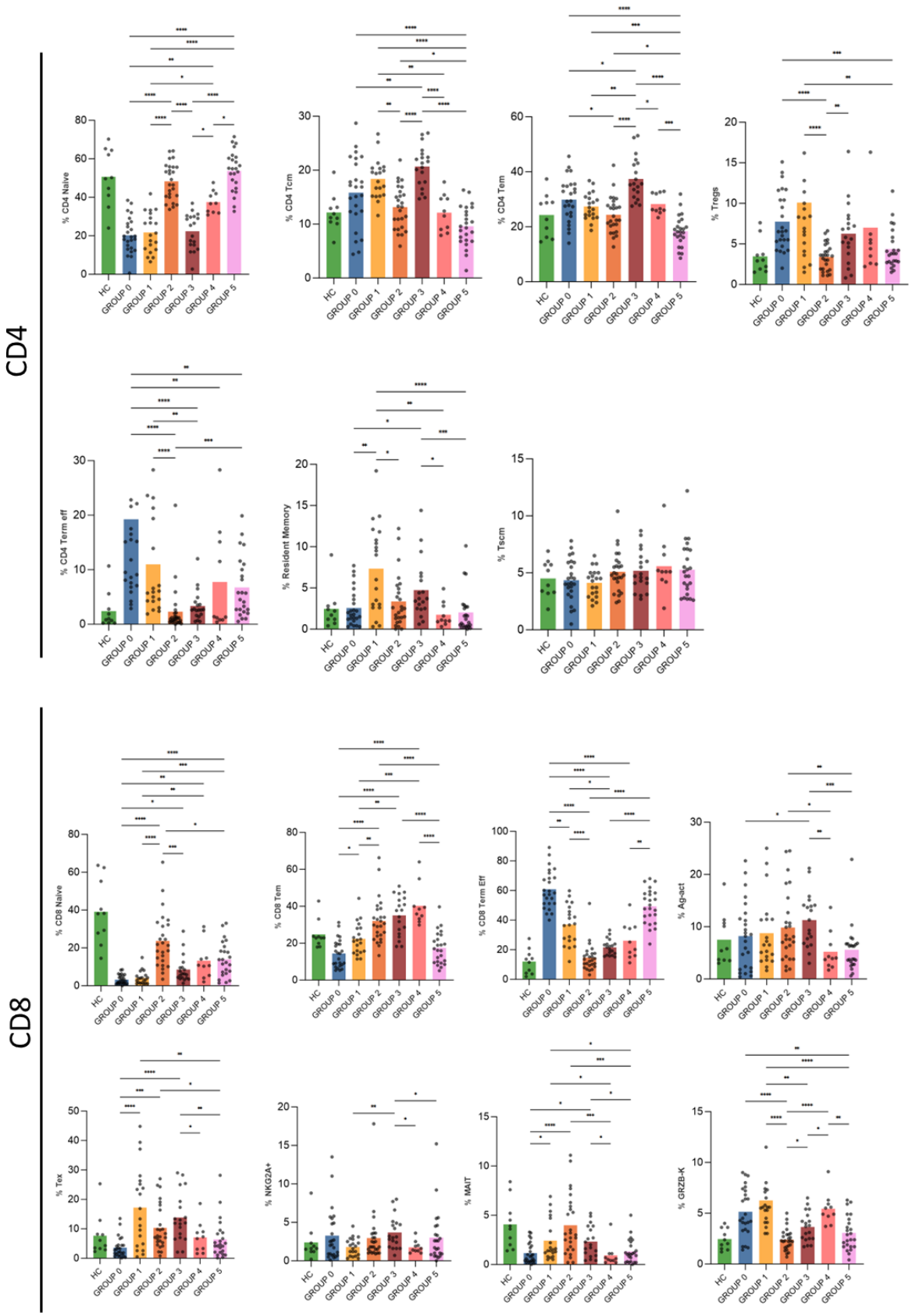

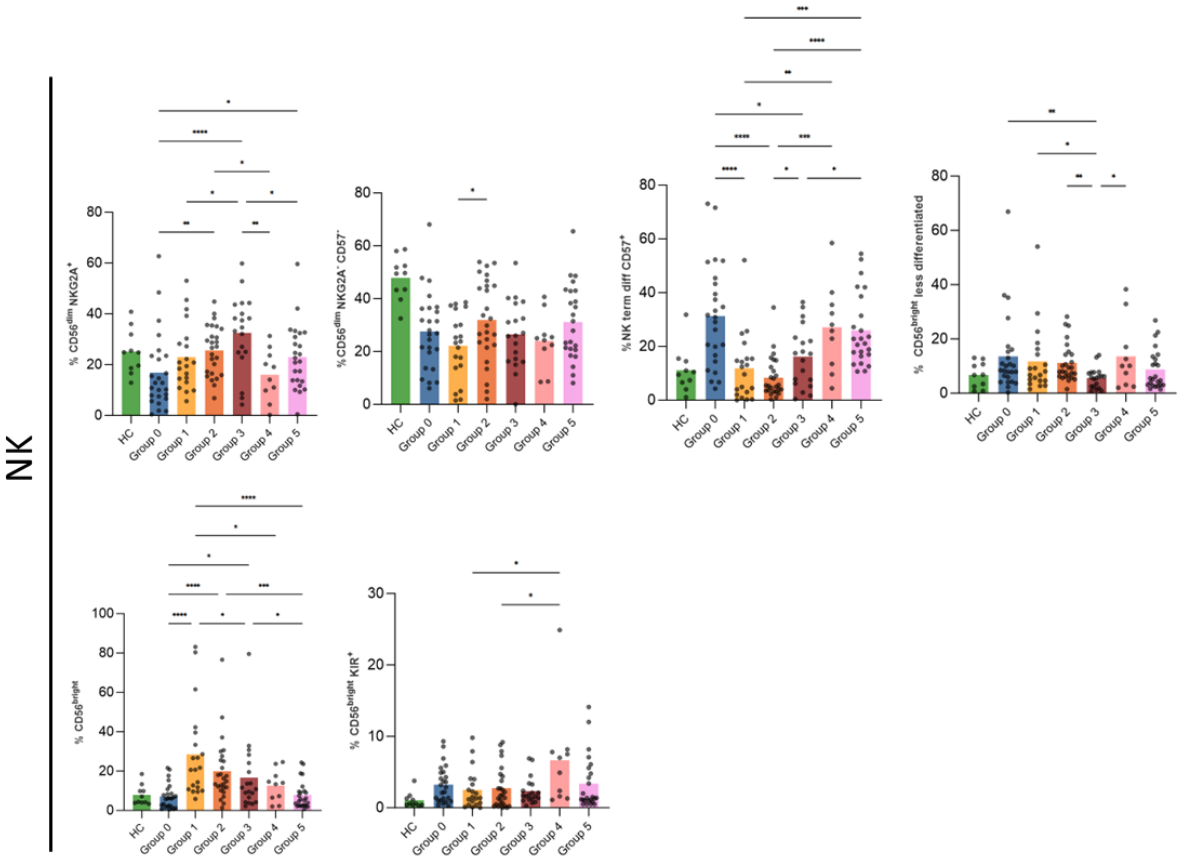

S17. Characterization of immune cell composition of HDBSCAN groups. The bar graphs show the frequency of a specific immune subpopulation (indicated on the Y axis) in the different HDBSCAN groups. Healthy controls (HC) frequencies are reported just as a reference, but are not included in the statistics. Mann whitney U test was used to compare groups and significance was set at a P value less than .05.

Supplementary Figure 18

A

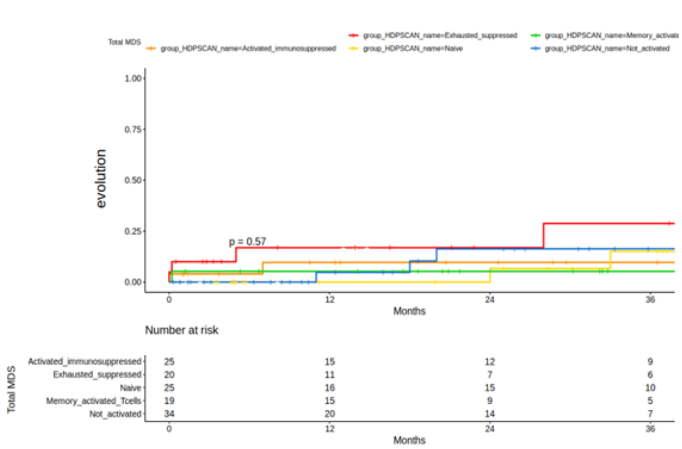

B

Variable		N	Hazard ratio	p
group_HDPSCAN_name	Naive	25	Reference	
	Memory_activatec	19	3.30 (0.66, 16.42)	0.15
	Activated_immunosuppressed	25	5.28 (1.16, 24.16)	0.03
	Exhausted_suppressed	20	6.78 (1.48, 31.01)	0.01
	Not_activated	34	6.18 (1.41, 27.11)	0.02

C

Variable		N	Hazard ratio	p
NK_2_Resident_Lic_NCRpos	↑ HDB 1 HDB 2	133	0.99 (0.97, 1.01)	0.456
NK_6_Resident_Less_diff_Lic_NCRpos	↑ HDB 1	133	1.02 (1.00, 1.05)	0.088
NK_8_Resident_More_diff_Lic_NCRpos	↑ HDB 1	133	1.05 (1.01, 1.11)	0.028
NK_Dim_NKG2A_pos	↑ HDB 2 HDB 3	133	0.96 (0.94, 0.99)	0.002
NK_Dim_NKG2Aneg_CD57neg	↓ in all HDB	133	1.00 (0.98, 1.02)	0.855
NK_Dim_TermDiff_CD57pos	↑ HDB 0 HDB 4/5	133	1.02 (1.00, 1.03)	0.052

D

Variable		N	Hazard ratio	p
CD8_Term_Eff	↑HDB 0/1/4-5	133	1.01 (1.00, 1.02)	0.17
CD8_1_T_Naive	↑HDB 2 HDB 4-5	133	0.99 (0.96, 1.01)	0.28
CD8_10_NKG2A_pos	↓ HDB 1 ↑HDB 3	133	0.92 (0.81, 1.05)	0.23
CD8_11_MAIT	↓ HDB 0/1/4-5 ↑HDB 2	133	0.83 (0.68, 1.00)	0.05
CD8_Eff_Mem	↑HDB 2 HDB 3	133	0.98 (0.95, 1.00)	0.06
CD8_4_T_exhaust	↑ HDB 1 ↑HDB 3	133	1.02 (0.99, 1.06)	0.12
CD8_6_Ag.Act	↑HDB 3 ↓ HDB 4-5	133	1.01 (0.97, 1.06)	0.55
CD8_9_GZMB_K_pos	↑ HDB 0/1/4-5	133	1.05 (0.93, 1.18)	0.41

E

Variable		N	Hazard ratio	p
CD4_Naive	↑HDB 2 HDB 4-5	133	0.99 (0.98, 1.01)	0.42
CD4_Eff_Mem	↑HDB 3 ↓ HDB 4-5	133	0.97 (0.94, 1.00)	0.10
CD4_10_Resident_Mem	↑ HDB 1	133	1.09 (1.01, 1.17)	0.02
CD4_Central_Mem	↑HDB 3 ↓ HDB 4-5	133	0.97 (0.92, 1.02)	0.19
CD4_5_Term_Eff	↑HDB 0/1/4-5	133	1.02 (1.00, 1.05)	0.08
CD4_7_Tregs	↑HDB 0 HDB 1	133	1.09 (1.04, 1.15)	<0.001

F

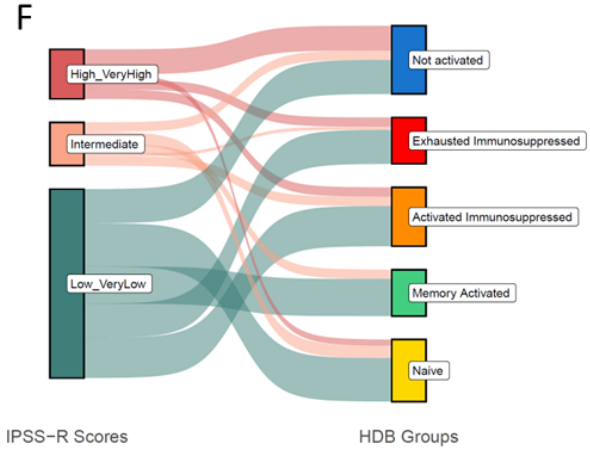

G

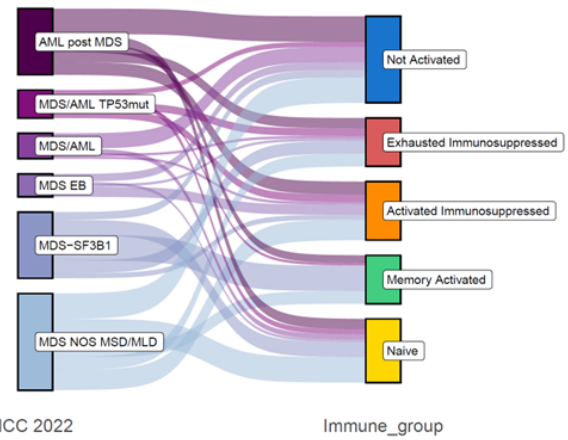

S18. Immune features of HDBSCAN groups and correlations with clinical parameters. A) Kaplan-Meier curves showing the events of MDS evolution in the different groups. B) Hazard ratio of HDBSCAN groups. Naïve group (HDBSCAN group n°2) was chosen as reference due to the best survival, as assessed by Kaplan-Meier curves. C-E) Hazard ratio of each T CD4, T CD8 and NK cell subtype and respective group(s) enrichment. F-G) Sankey Plots representing the re-distribution of patients from IPSS-R risk classes and ICC2022 categories to immunological groups.

Supplementary Tables

Supplementary Table 1. List of Antibodies included in the three flow cytometry panels for the characterization of T lymphocytes, NK and Myeloid cells.

Antibody	Fluorochrome	Company	Identifier	Panel
2B4	PECy5.5	Beckman Coulter	B21171	T
CCR7	PE-CF594	BD	562381	T
CD117	BV786	BioLegend	313238	NK, Myeloid
CD11b	BV480	BD	746572	Myeloid
CD127	APC-e780	eBioscience	47-1278-42	NK, Myeloid
CD127	PE-Cy5	eBioscience	15-1278-42	T
CD14	BV510	BioLegend	301842	NK, T
CD14	BUV805	BD	565779	Myeloid
CD15	FITC	BC	B36298	NK
CD15	BUV395	BD	740318	Myeloid
CD158b1b2j	BUV395	BD	743456	NK
CD16	BUV737	BD	564434	NK, Myeloid
CD161	BV421	Biolegend	339913	Myeloid
CD161	BV605	Biolegend	339916	T
CD19	FITC	BD	345776	NK, Myeloid
CD20	FITC	Biolegend	302304	NK, Myeloid
CD203c	FITC	Biolegend	324614	NK, Myeloid
CD25	BV786	BD	741035	T
CD28	BUV737	BD	564438	T
CD3	BUV661	BD	565065	NK, Myeloid
CD3	BUV496	BD	564809	T
CD33	FITC	Biolegend	303304	NK
CD33	BV711	BioLegend	303424	Myeloid
CD34	FITC	Biolegend	343604	NK
CD34	APC	Biolegend	343510	Myeloid
CD38	BUV496	BD	564657	Myeloid
CD39	APC-Cy7	BioLegend	328226	T
CD4	BUV615	BD	624297	T
CD45RA	BV605	BioLegend	304134	Myeloid
CD45RO	BV570	BioLegend	304226	T
CD56	BUV563	BD	565704	NK, Myeloid
CD57	BV605	BD	393304	NK
CD69	PE-CF594	BD	562617	NK
CD69	BUV395	BD	564364	T
CD71	APC	BD	551375	T
CD8	BUV805	BD	564912	T
CD8a	BV570	Biolegend	301038	NK, Myeloid
CD94	PE	BD	555889	NK, Myeloid
CD95	BV711	BioLegend	305644	T
CRTh2	PerCP-Cy5,5	Biolegend	350116	NK, Myeloid
FcERI	FITC	Biolegend	334608	NK, Myeloid
Granzyme B	AF700	BD	560213	T
Granzyme K	PE	Santa Cruz	sc-56125	T
HLA-DR	BUV615	BD	624297	Myeloid
HLA-DR	BUV661	BD	565073	T
IL1R1	AF700	R&D	FAB269N-025	Myeloid
Ki67	BV480	BD	566109	T
NKG2A	PE-Vio770	Miltenyi	130-113-567	NK
NKG2A	VioBright FITC	Miltenyi	130-113-568	T
NKG2C	AF700	R&D	FAB138N	NK
NKp30	PE-Cy5	BC	A66904	NK
NKp44	PE-Cy5	BC	A66903	Myeloid
NKp46	APC	BD	558051	NK
PD-1	BV711	BD	564017	NK
PD1	BV421	BioLegend	329920	T
T-bet	PE-Cy7	eBioscience	BMS25-5825-82	T
TIGIT	PerCP-eF710	eBioscience	46-9500-42	T
TIM3	BV650	BD	565564	T
Vδ1	BV421	Miltenyi	130-100-553	NK
Vδ2	BV650	BD	743752	NK

Clinical Implications of p53 Dysfunction in Patients with Myelodysplastic Syndromes

Matteo Zampini, Elena Riva, Alberto Termanini, Lorenzo Dall'Olio, Alessandra Merlotti, Austin Kulasekararaj, Michela Calvi, Clara Di Vito, Daoud Rahal, Arturo Bonometti, Giorgio Croci, Emanuela Boveri, Umberto Gianelli, Maurilio Ponzoni, Antonio Russo, Benedetta Tinterri, Francesca Re, Elisabetta Sauta, Elena Saba, Erica Travaglino, Marta Ubezio, Alessia Campagna, , Luca Lanino, Giulia Maggioni, Cristina A Tentori, Chiara Milanesi, Nicla Manes, Saverio D'Amico, Francesca Ficara, Laura Crisafulli, Domenico Mavilio, Enrico Lugli, Armando Santoro, Maria Diez-Campelo, Guillermo Sanz, Francesc Solé, Uwe Platzbecker, Valeria Santini, Shahram Kordasti, Pierre Fenaux, Torsten Haferlach, Daniel Remondini, Gastone Castellani, and Matteo G Della Porta.

Introduction

TP53 gene encodes for the transcription factor p53, whose functions and activities as tumor suppressor are so broad and crucial such that it was nicknamed as "the guardian of the genome". In fact, p53 main role is to avoid the propagation of cells that carry damaged DNA with potentially oncogenic mutations through the induction of cell cycle arrest, DNA repair mechanisms activation and, when the damage is too severe to be solved, apoptosis [1-3]. More recently, also roles in regulation of both innate and adaptive immune responses such as T and myeloid cells recruitment, immune checkpoint regulation, cytokine production and MHC expression have emerged, implying a potential additional p53 role as "guardian of immune integrity" [4-6]. Mutations in TP53 occur in more than 50% of human primary tumors, thus making it the most common mutated gene in cancer [3,7-8]. Myelodysplastic syndromes (MDS) comprise a heterogeneous group of hematopoietic stem cell disorders characterized by bone marrow failure, peripheral blood cytopenia, increased risk of Acute Myeloid Leukemia (AML) transformation and recurrent genetic and cytogenetic abnormalities [9]. Our understanding of MDS genetic landscape has massively increased in the last decade thanks to the advent of next generation sequencing (NGS), that allowed to understand the central role of genetic alterations in MDS pathogenesis and evolution [10-11]. It is now well known that mutations in some genes, in particular SF3B1 and TP53, possess independent prognostic power and were thus recently introduced in the new MDS classification systems as distinct disease categories [12-13].

Among patients with MDS, 8-10% harbor mutations in TP53 gene [14-15], which can hit just one TP53 allele (monoallelic mutations) or both alleles (biallelic mutations) and are generally correlated with high-risk disease. In particular, patients carrying biallelic mutations represent a peculiar clinical entity associated with reduced survival due to the increased risk of leukemic evolution, high rate of relapse after transplantation and short duration of response to hypomethylating agents (HMAs) [16].

Surprisingly, in a general genetic screening on a large cohort of MDS patients, we observed that a small fraction of MDS patients possess the same dismal outcome of biallelic TP53 mutated ones despite carrying a wild type (WT) TP53 gene. In this paper, we show that those patients are characterized by a nuclear hyperexpression of p53 protein in bone marrow progenitors, assessed by immunohistochemistry (IHC). Moreover, we performed RNAseq analysis of isolated CD34+ progenitors and high-dimensional flow cytometry of immune cell populations on a large cohort of MDS patients respectively $TP53^{WT}$, $TP53^{mut}$ and $TP53^{WT}$ with p53 protein hyperexpression.

Our data suggest that this non-mutational p53 dysfunction may occur through different inactivating mechanisms which result in peculiar transcriptomic profile and immunosuppressive phenotype, as recently described in TP53 mutation cases [17]. Furthermore, our results highlight a group of $TP53^{wt}$ MDS patients that could potentially benefit from MDM2 inhibitory therapy.

Results

MDS patients with TP53^{wt} gene and p53 hyperexpression show poor outcome

In a previous explorative screening, we assessed on bone marrow progenitor cells from 1.244 MDS patients the presence of gene mutations and/or chromosomal aberrations mainly involved in MDS pathogenesis, in particular we included mutations in SF3B1, TET2, DNMT3A, ZRSR2, SRSF2, ASXL1, RUNX1, TP53, IDH1/2, U2AF1, STAG1, N/KRAS, JAK2 genes and main chromosomal aberrations such as del(5q), –7/del(7q), del(17p), +8 and -Y. Patients were clustered and classified according to their genetic and cytogenetic features using Hierarchical Density-Based Spatial Clustering of Applications with Noise (HDBSCAN) algorithm and visualized with dimension reduction by Uniform Manifold Approximation and Projection (UMAP). In this way, we were able to identify twenty different genomic clusters (Fig 1A). Among them, two were TP53-related and respectively characterized by monoallelic TP53 lesions and biallelic and/or complex karyotype. Interestingly, within the latter group we noticed the presence of MDS patients, approximately representing the 5% of the group, who carried a wild type TP53 gene. We selected those patients for a deeper molecular characterization and, through immunohistochemistry staining on bone marrow sections, we could observe that they were characterized by a nuclear hyperexpression of p53 protein within the bone marrow progenitors (Fig 1B). Despite the presence of a WT TP53 gene, those patients showed the same dismal outcome of the patients carrying biallelic TP53 mutations in terms of overall survival probability (Fig 1C). We hence decided to further characterize the molecular and biological similarities and/or differences of these patients with TP53^{WT} without p53 hyperexpression and TP53^{mut} ones.

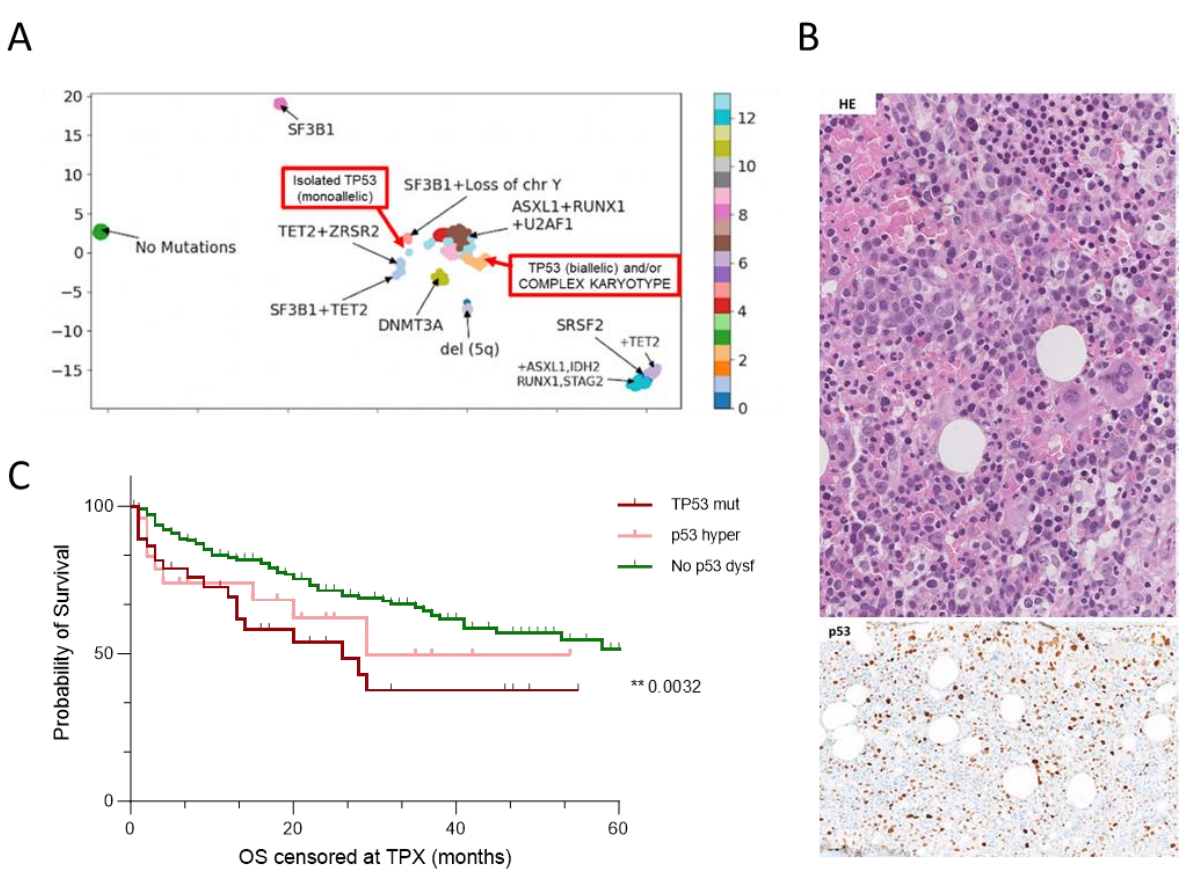

Figure 1. Identification of MDS group with p53 nuclear hyperexpression and TP53^{wt} with same dismal outcome as TP53^{mut} patients*. A) Genomic-based classification of MDS by HDBSCAN and UMAP data reduction. Each dot represents a patient and patient location is defined on the basis of its cytogenetic and genomic features; B) Bone marrow trephine biopsy showing dysplasia assessed by hematoxylin/eosin staining (upper) and p53 protein hyperexpression within >2% of progenitors nuclei assessed by IHC (lower); C) Kaplan-Meier curves showing OS in MDS patients without p53 dysfunctions, with TP53 mutations and with p53 hyperexpression. Patients with p53 hyperexpression show the same trend as TP53^{mut} ones, with significative worse survival compared to patients with no p53 dysfunction (** p<.01).*

Transcriptional profiles of MDS with p53 dysfunction share an impairment of p53-related pathways

We initially investigated the transcriptional differences between MDS with p53 dysfunction (i.e. TP53^{mut} or TP53^{WT} with p53 hyperexpression) and those without p53 dysfunctions (i.e. TP53^{WT} with no p53 protein hyperexpression) by performing bulk RNA-Seq experiment on selected CD34+ bone marrow (BM) cells in two different myeloid neoplasms cohorts: in the principal cohort we analyzed CD34+ BM cells of 75 samples (44 WT vs 31 p53 dysfunction) while in the validation cohort we analyzed CD34+ BM cells of 34 samples (16 WT vs 18 p53 dysfunction).

MDS and AML that arises from MDS are heterogeneous and the array of mutations in these diseases has generally differential effects on gene expression, nevertheless, unsupervised correlation plot of normalized gene expression in both RNA-Seq datasets shows good dichotomization between p53 dysfunction and wild-type samples (WT) independently of *TP53* mutation or p53 hyperexpression (Fig 2A; Supplementary Fig1A). Multidimensional Scaling (MDS) plot also demonstrates high within-group reproducibility and substantial between-group differences in both cohorts (Fig 2B; Supplemental Fig1B). To understand if the groups were different, we performed pairwise comparison by permutational multivariate analysis of variance (PERMANOVA) revealing that the differences between the two groups (p53 dysfunction vs WT) were statistically significant (p<.001). PERMANOVA analysis within p53 dysfunction samples did not show significant separation between p53 hyper-expressed and TP53 mutated samples in both cohorts (p= .342 and p=.227 respectively; Supplemental Fig2).

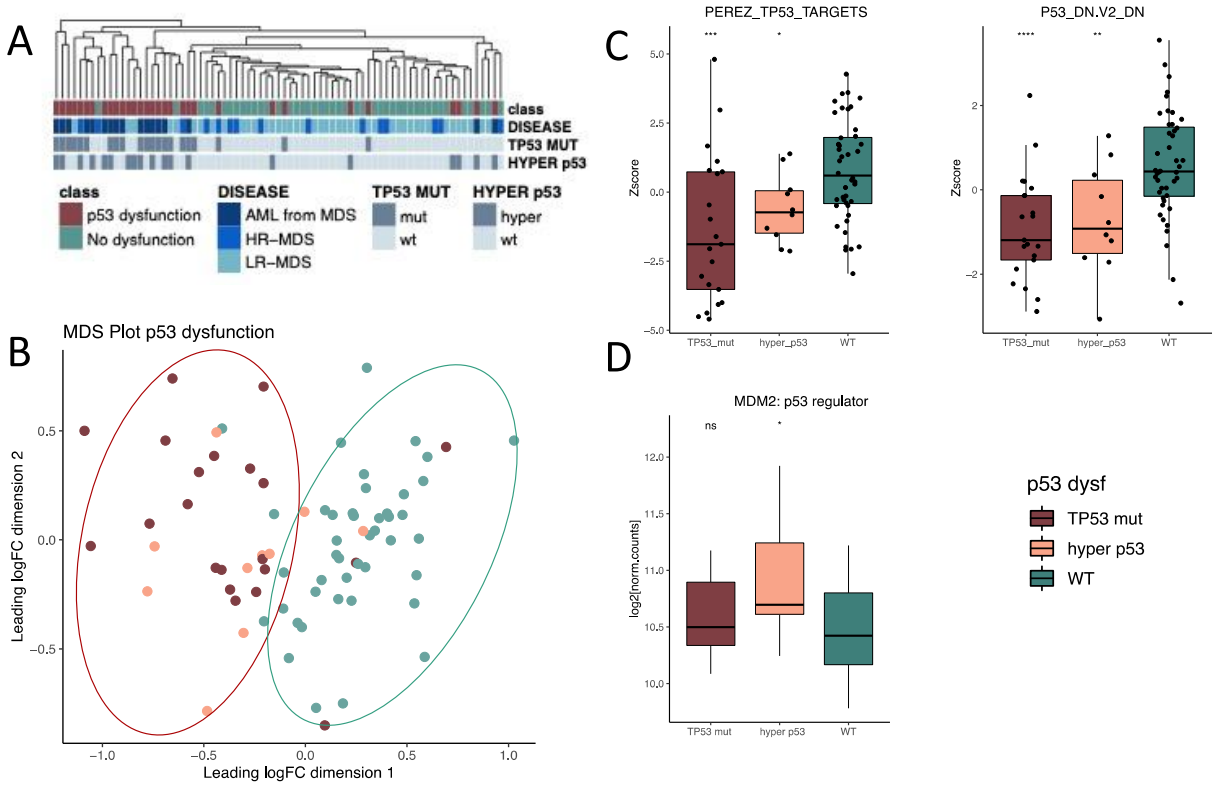

Figure 2. P53 dysfunction MDS patients show a peculiar transcriptomic profile with an impairment of p53 pathway. *A) Dendrogram of unsupervised correlation plot obtained by RNA-Seq data; B) Multidimensional Scaling plot of RNA-Seq data. Each dot represents a patient. Red dots highlight TP53 mutated patients, pink dots hyper mutated patients, and green dots wild type patients; C) Box plots of RNA-seq z-scores of p53 target signatures retrieved by MsigDB; D) Boxplot of gene expression of MDM2 gene. In all box plots, the median is indicated by the horizontal line and the first and third quartiles are represented by the box edges. The lower and upper whiskers extend from the hinges to the smallest and largest values, respectively, with individual values included. * p<.05; ** p<.01; *** p<.001; ns: not significant*

To determine whether there was a common impairment in the p53 pathway among samples with p53 dysfunction, we analyzed the normalized expression (z-score) of p53 target signatures in our cohorts. We found that p53 targets were significantly decreased in both TP53 mutated and p53 hyper-expressed samples compared to WT samples (Mann-Whitney test, $p < .05$, Fig 2C; Supplemental Fig 1C, 3, and 4), indicating a non-genetic downregulation of p53 downstream targets in hyper expressed patients potentially due to the retention of the protein in the nucleus.

Additionally, we observed a significant overexpression of the p53 negative regulator MDM2 in p53 hyper-expressed samples compared to WT samples (t-test, $p < .05$, Fig 2D), but not in mutated vs. WT samples. We confirmed MDM2 upregulation in p53 hyperexpressed patients using MDM2 IHC staining (Supplemental Fig 5A). In 5 out of 10 hyper-expressed patients we identified genomic MDM2 gene amplification by fluorescence in situ hybridization (FISH) (Supplemental Fig 5B).

Moreover, we also investigated other possible mechanisms able to suppress wt p53 function through MDM2 axis in absence of TP53 mutations. In particular, NPM1/FLT3-mutated AML are often accompanied by wt p53

dysfunction due to several inactivating processes [18]. In our cohorts we did not identify these mutations in TP53 mutated patients while we found 2 FLT3 and 1 NPM1 mutated samples in p53 hyper-expressed patients. In addition, several aberrant signaling pathways are well-known to suppress wt p53 function by various inter-related mechanisms involving MDM2 upregulation. Specifically, we identified aberrant activation of the PI3K/AKT, RAS/RAF/MEK/ERK, and non-canonical NF-κB pathways in p53 hyper-expressed samples compared to WT samples, but not in TP53 mutated vs. WT samples (Mann-Whitney test, $p < .05$, Supplemental Fig 6).

MDS patients with p53 dysfunction show an immunosuppressive transcriptional program

To investigate the impact of p53 dysfunction on the biological mechanisms in myeloid neoplasm patients, we analyzed differential gene expression between p53 dysfunction and WT samples. In the principal cohort, we identified 701 genes that were differentially expressed (FDR < .01), with 323 genes upregulated in p53 dysfunction and 378 genes downregulated (Figure 3A). These differentially expressed genes were able to accurately distinguish between p53 dysfunction samples and WT samples (Figure 3B). Among the most upregulated genes, we found some that have been previously associated with worse prognosis in myeloid malignancies, such as HBG1, or related to p53 dysfunction in cancer, such as CKB [19-20]. In the downregulated genes, there are those often downregulated in hematopoietic stem cells (HSCs), such as VCAN and FCN1, or genes associated with immune infiltration in cancer, such as CLEC10A [21-22]. We conducted over-representation analysis (ORA) to determine which pathways were significantly enriched in our gene list. Figure 3C shows the Reactome database pathways that were overrepresented in downregulated or upregulated genes (q-value < .01). We found several immunological pathways, such as the Innate Immune System and Adaptive Immune System presentation, were downregulated, while oxidative stress-related pathways were upregulated.

We obtained similar results in the validation cohort, where we observed the downregulation of immunological pathways (such as Adaptive immune system and MHC class II antigen presentation) and upregulation of transcription and MYC targets (Supplemental Fig 7). Therefore, our results suggest that p53 dysfunction in MDS patients is associated with an immunosuppressive transcriptional program.

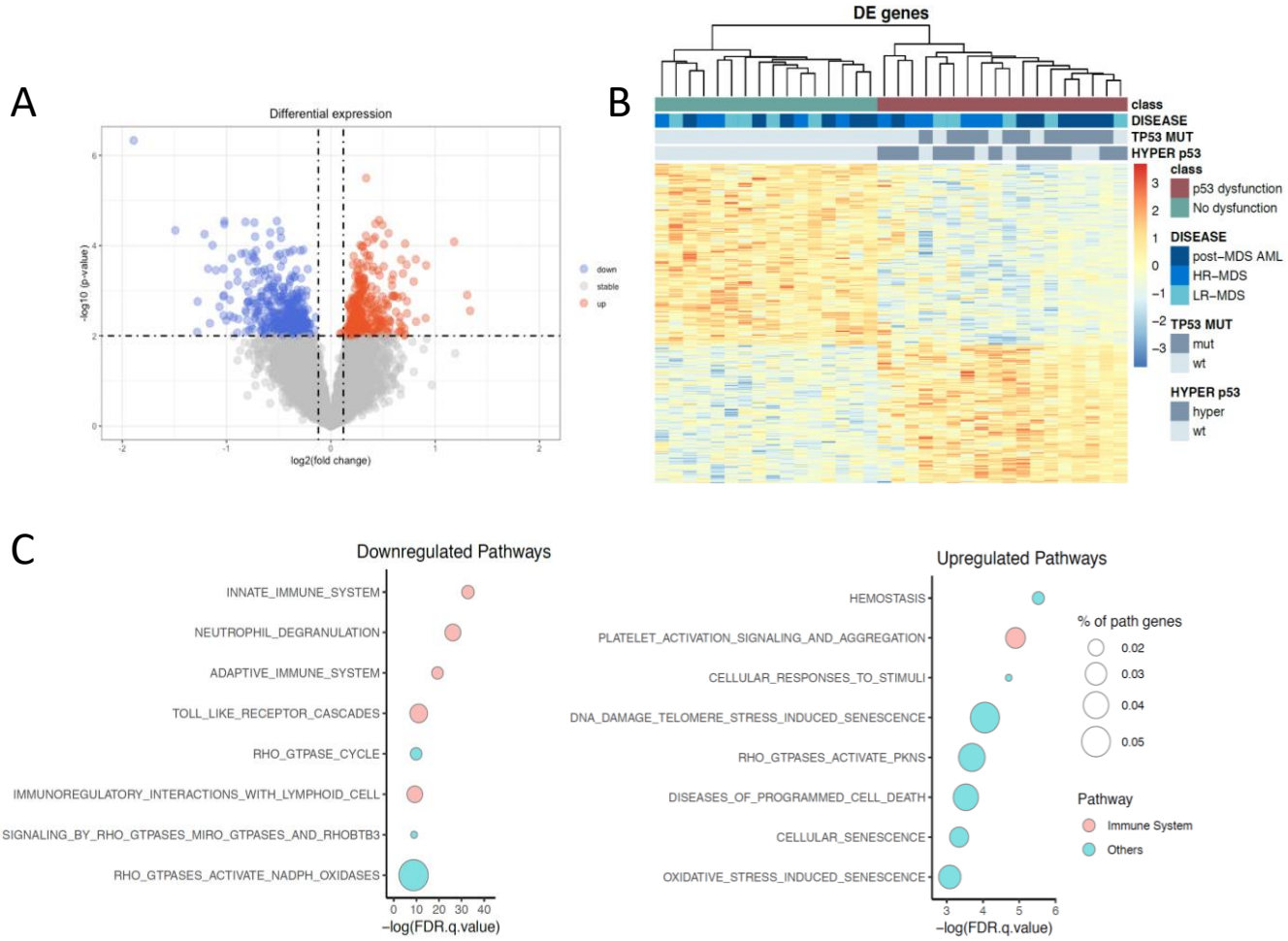

Figure 3. Analysis of gene expression in principal cohort. *A) Volcano plot of differentially expressed genes between p53 dysfunction and WT samples; red dots are significant upregulated genes in p53 dysfunction patients while blue dots are downregulated genes; B) Heatmap of differentially expressed gene; C) Functional enrichment analysis visualization: the dotplot depicts the activity of Reactome pathways starting from significant downregulated genes (on the left) or significant upregulated genes (on the right). Dot size indicates k/n ratio ("% of path genes"), where k is the number of genes participating in the pathway and n is the number of genes annotated as participants of any Reactome pathway. Dot color indicates if the pathway is related to the immune system or not. The x axis represents the log of the enrichment test FDR ((Hypergeometric test).*

In an MDS cohort harboring TP53 mutations, Sallman and colleagues identified the upregulation of MYC that could confer an immunosuppressive phenotype [17]. Although MYC gene is not significantly upregulated in p53 dysfunction in our cohort, we performed Gene Set Enrichment Analysis (GSEA) and we identified significant upregulation of MYC targets in both our cohorts (p<.01, FDR<.01; Fig4A). Furthermore, we found upregulation of MYC targets also in TP53 mutated or p53 hyperexpressed samples separately versus WT patients (Supplemental Figure 8).

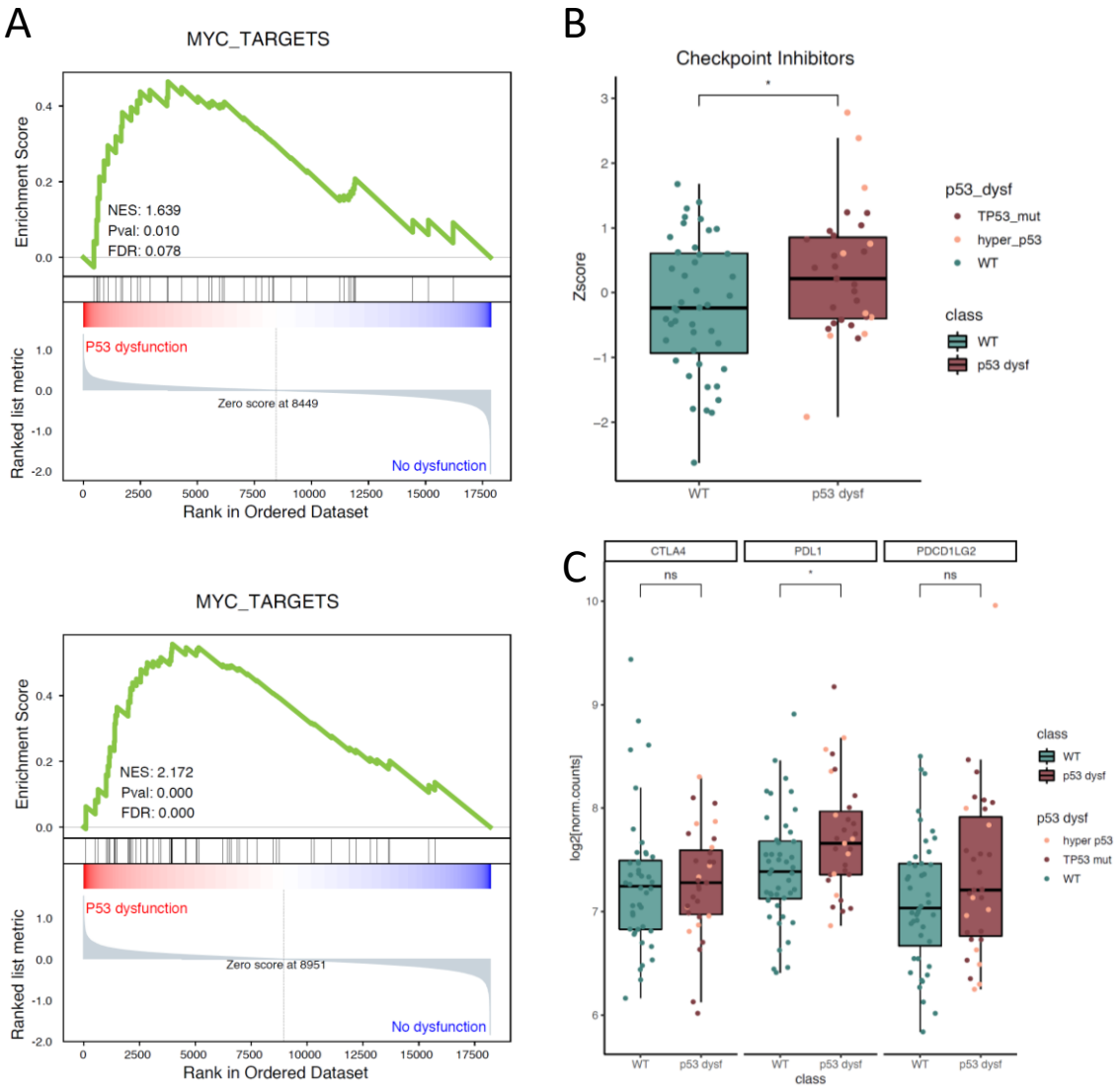

Figure 4*. A) GSEA results of MYC targets gene signature in principal cohort (upper plot) and validation cohort (lower plot). In both plots, we observe a positive gene set enrichment in MDS samples harboring p53 dysfunction. NES, Normalized Enrichment Score. B) Box plots of RNA-seq z-scores of Checkpoint inhibitors (Mann-Whitney Test); B) Boxplot of gene expression of CTLA4, PDL1, and PDL2 gene. Red dots highlight TP53 mutated patients, pink dots hyper mutated patients, and green dots wild type patients. In all box plots, the median is indicated by the horizontal line and the first and third quartiles are represented by the box edges. The lower and upper whiskers extend from the hinges to the smallest and largest values, respectively. * p<.05; ** p<.01; ns: not significant*

Given that RNA-seq suggests an immunosuppressive phenotype in our population, we investigated the possible immune evasion mechanisms driven by p53 dysfunction.

We initially examined the mRNA expression of immune checkpoint in CD34+ MDS cells. Gene expression profiling revealed upregulation of immune checkpoints PDL1, PDL2, and CTLA4 in p53 dysfunction patients (Z-score, Mann-Whitney test, p<.05; Fig 4B), with a particularly strong upregulation of PDL1 transcript (T-test, p<.05), while PDL2 and CTLA4 only showed a positive trend (Fig 4C).

As suggested by pathway analysis, we also examined the downregulation of HLA class II molecules in hematological malignancies as a mechanism of immune evasion that impairs blast cell recognition [23-24]. GSEA analysis in p53 dysfunction samples showed significant downregulation of HLA class II members and their master regulator CIITA in both the cohorts (Fig 5A, p<.01, FDR<.1).

Other known mechanisms of immune evasion in myeloid malignancies context include the increase of anti-inflammatory cytokines production and the decrease of pro-inflammatory ones [25-27]. To understand if p53 dysfunction can directly or indirectly affect cytokine regulation in the microenvironment, we performed upstream regulator analysis (Ingenuity Pathway Analysis suite) to our RNA-Seq data. Figure 5B depict the top activated and inhibited cytokines in p53 dysfunction samples (p<.01, fold change >1.5) inferred by variations in their downstream target molecules. We identified a possible general increase of anti-inflammatory cytokines activation and the reduce of pro-inflammatory cytokines, in particular interferon-gamma (IFN-γ) and IL-33 which are common in both the cohorts.

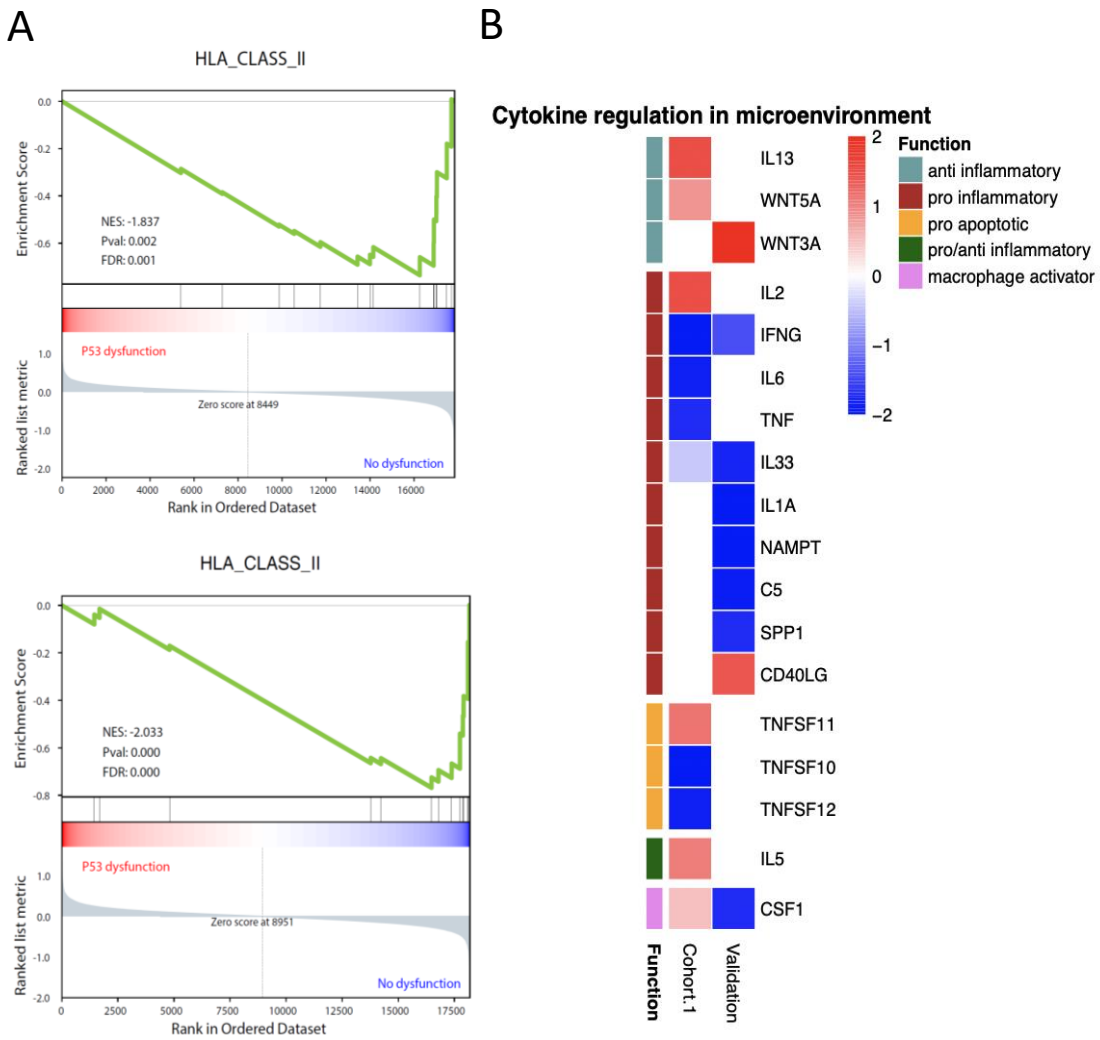

Figure 5. Immune evasion mechanism in p53 dysfunction patients. *A) GSEA results of HLA Class II genes signature in principal cohort (upper plot) and validation cohort (lower plot). In both plots, we observe a negative gene set enrichment in MDS samples harboring p53 dysfunction. NES, Normalized Enrichment Score. B) Upstream regulator analysis utilizing Ingenuity Pathway Analysis (IPA). The results are shown only for the top activated and inhibited cytokines in p53*

dysfunction samples (p<.01, fold change >1.5) as a heatmap of the activated z-scores. Regulators are ranked according to the z-score that predicts activation (red)/suppression (blue).

In p53 dysfunction samples we identified also the up-regulation of enzymes that mediate immunosuppression. In particular, we found a significant increase of NT5E gene (CD73) in validation cohort (t-test, p<.01) but not in principal cohort.

P53 dysfunction MDS microenvironment is characterized by an immunosuppressive phenotype

RNA-seq analysis revealed an immunosuppressive phenotype in MDS patients with p53 dysfunction, affecting both the adaptive and innate immune systems. Therefore, we conducted further investigations on the bone marrow microenvironment using high-dimensional flow cytometry with three panels targeting T lymphocytes, Natural Killer (NK), and myeloid cells (Supplemental Table 1-3) and integrating them with RNA-seq data. Specifically, we analyzed T cells in 76 MDS patients (21 p53 dysfunction vs. 55 WT), NK cells in 66 MDS patients (19 p53 dysfunction vs. 47 WT), and myeloid cells in 77 MDS patients (22 p53 dysfunction vs. 55 WT). We also added to the analysis 20 age-matched healthy controls.

Initially, we examined by manual gating the lymphocyte populations frequencies in MDS patients and found that the $CD3^+$, $CD4^+$ $CD8^+$ T cells and NK cells counts did not significantly differ between p53 dysfunction and WT patients, suggesting possible changes in T and NK cell subtypes ratios rather than in absolute count (Supplemental Fig. 9; Mann-Whitney test).
To analyze T and NK cell subsets we used PhenoGraph, a computational algorithm capable of clustering single cells based on their relative expression of antigens in the multidimensional space [28]. PhenoGraph identified eight clusters of CD4+ cells (Fig. 6A): Cluster 7 - Regulatory T cells (Treg), Cluster 5 - Terminal Effector T cells (Temra), Cluster 4/6 - Effector Memory T cells (Tem), Cluster 0/8 - Central Memory T cells (Tcm), and Cluster 1/2/3 - Naïve T-cells (Tnaïve).

Among $CD4^+$ T cells, we observed that clusters 7, 0, and 1 were associated with WT samples, while clusters 5, 6, 4, 8, and 2 were associated with p53 dysfunction samples (Fig. 6B; Fisher test p<.01). The clusters with the largest variation from the expected frequency (> 2%, Fig. 6B) were a Naïve T-cells cluster associated with WT samples and two clusters of Tregs and Central Memory T-cells associated with the p53 dysfunction category. Through manual gating, we confirmed the increase of Tregs and the decrease of Naïve T cells frequencies in p53dysf samples (Mann-Whitney test, p<.05, Fig. 6C-D), supporting the possible immune suppressive environment in the BM of these patients.

Regarding $CD8^+$ T cells, PhenoGraph identified eight clusters (see Supplemental Fig. 10): three clusters of Temra (Clusters 1/4/7), one of Tcm (Cluster 3), one of Tnaïve (Cluster 2), one of Tem (Cluster 0), one of Exhausted T cells (Tex, Cluster 6), one of GRZB+ GRZK+ T cells (Cluster 8), and one of antigen-activated T cells (Ag-act, Cluster 5).
In $CD8^+$ cells, clusters 5, 6, 3, and 0 were associated with WT samples, while clusters 8, 7, 4, and 2 were associated with p53 dysfunction samples (Supplemental Fig. 10B; Fisher test p < .01). The clusters with the largest variation from the expected frequency were antigen-activated and effector memory T cell clusters, which are associated with WT samples, and terminal effector and $GRZB^+$ $GRZK^+$ T cell clusters associated with p53 dysfunction. The increase of Temra and the decrease of antigen-activated T cells are hallmarks of adaptive immune system aging and progressive loss of function. Through manual gating, we were able to

confirm the increase of $CD28^+$ $CD69^+$ $GRZK^+$ antigen-activated $CD8^+$ T cells in WT samples (Mann-Whitney test, $p < .05$, Fig 6E).

A study in a mouse model of AML showed the increase in of Treg cells and functionally exhausted $CD8^+$ T cells coexpressing the PD-1 and TIM3 immune checkpoint inhibitors during disease progression [29]. Thus, through manual gating, we found an increase in exhausted $PD1^+$ $TIM3^+$ $CD8^+$ cells in p53 dysfunction samples (Mann-Whitney test, $p<.05$; Fig 6F).

As gene expression profiling in CD34+ cells showed the upregulation of the PD1 ligand (PDL1), we also investigated whether this change was associated with the increased of T-cell exhaustion through the crosstalk PD1/PDL1. We identified a significative positive correlation between PDL1 mRNA expression on blasts cells and the percentage of PD1 surface expression on $CD8^+$ T cells (R=.67; p=.0031; Fig 6G) in our cohort.

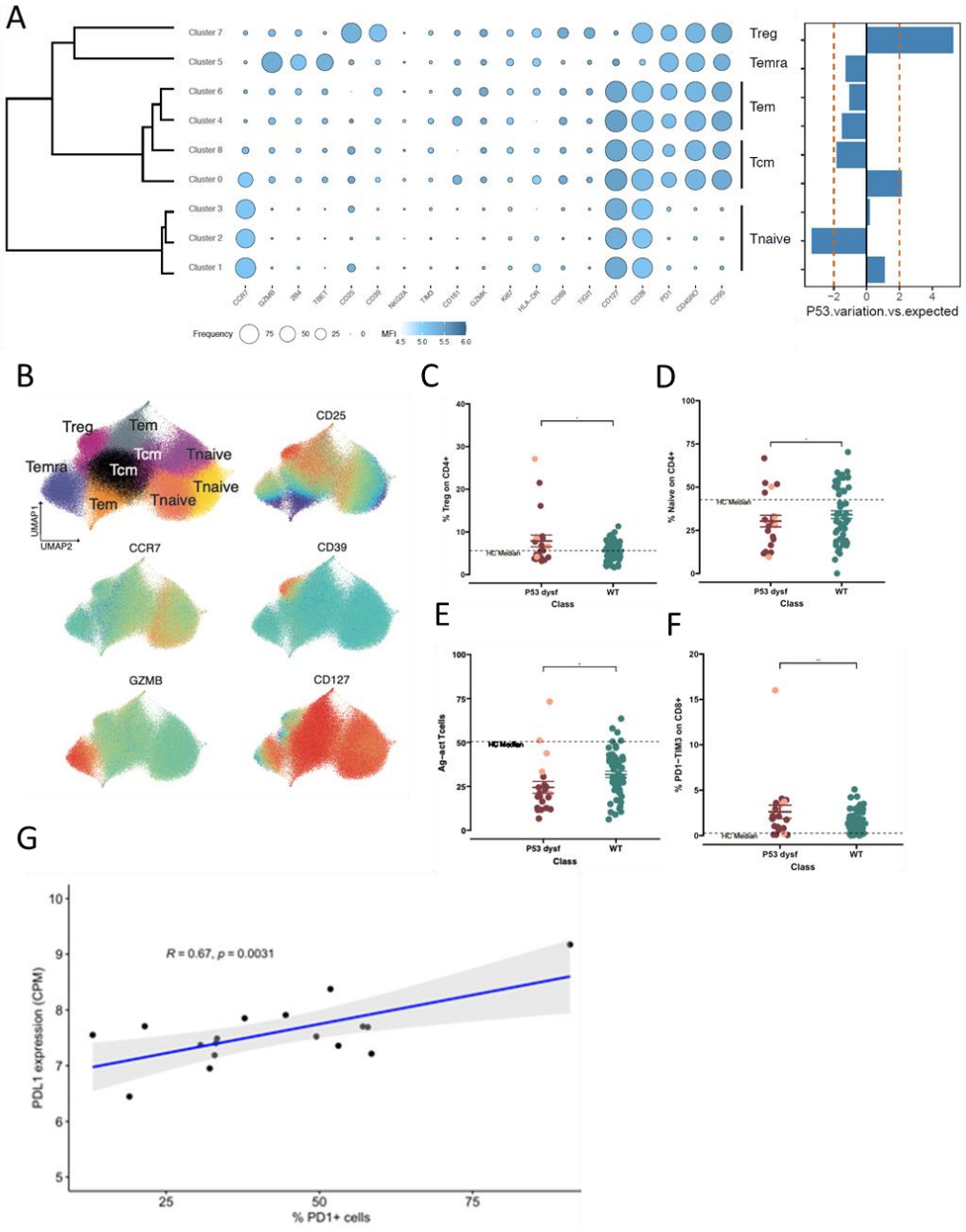

Figure 6. T cells profiling in p53 dysfunction patients microenvironment. *A) UMAP plot depicting CD4+ T cell heterogeneity. PhenoGraph clustering was performed using concatenated CD3+ CD4+ CD8- T cells (3,000 cells/sample) from 76 BM profiling (21 p53 dysfunction vs 55 WT). Cells are colored according to the eight clusters identified by Phenograph in an unsupervised manner. Other UMAP plots show the expression of selected markers among CD4+ T cells. B) Balloon plot showing the percent expression and the median fluorescence intensity (MFI) of specific markers (columns) in each Phenograph clusters (rows). The Barplot on the right shows the variation of p53 dysfunction cells frequency from expected frequency for each cluster. C-G) Dot plots showing the frequencies depicted with mean ± SEM of different CD4+ and CD8+ T cells populations (respectively indicated on Y axes) between p53 dysfunction and WT patients. The dashed line indicates the median value of the cell population in HC donors. Red dots highlight TP53 mutated patients, pink dots hyper mutated patients, and green dots wild type patients; T-Test. From the left: CD25+ CD127- Tregs, CD45RO- CD95- CCR7+ CD127+ CD28+ CD4+ Naïve, CD28+ CD69+ GRZK+ CD8+ antigen-activated and PD1+ TIM1+ exhausted CD8+ T cells. G) Correlation of PDL1 expression in CD34+ cells with the percent of CD8+ cells expressing PD1 in the BM microenvironment. T-Test. * p<.05; ** p<.01.*

Phenograph analysis identified 8 clusters of NK cells differentially distributed in WT and p53 dysfunctional patients. In particular, we observed an enrichment of NK cells belonging to cluster 3, mainly composed by less differentiated and cytokine producer $CD56^{bright}$ cells, in WT patients, while p53 dysfunctional were characterized by an enrichment of clusters of more differentiated $CD56^{dim}$ KIR^{pos} NK cells, namely cluster 2 and cluster 5, composed by $CD94^{low}$ NK cells and terminally differentiated $NKG2^{pos}CD57^{pos}$ NK cells, respectively. In addition, cluster 3 is characterized by the highest expression of natural cytotoxicity receptors (NCRs) NKp30 and NKp46 compared to all the other clusters (Fig 7A). This result was further confirmed by manual gating of flow cytometry data, which showed a reduced percentage of NK cells expressing NCRs (NKp30 and/or NKp46) in p53 dysfunctional patients (Fig 7B, Mann-Whitney test, p<.05).
Moreover, since an upregulation of PDL1 was observed in CD34pos cells from p53 dysfunctional patients, we investigated the expression of PD1 on NK cells by manual gating on and we found out an upregulation of PD1 on CD56bright NK cells from p53 dysfunctional patients (Fig 7C, Mann-Whitney test, p<.05).

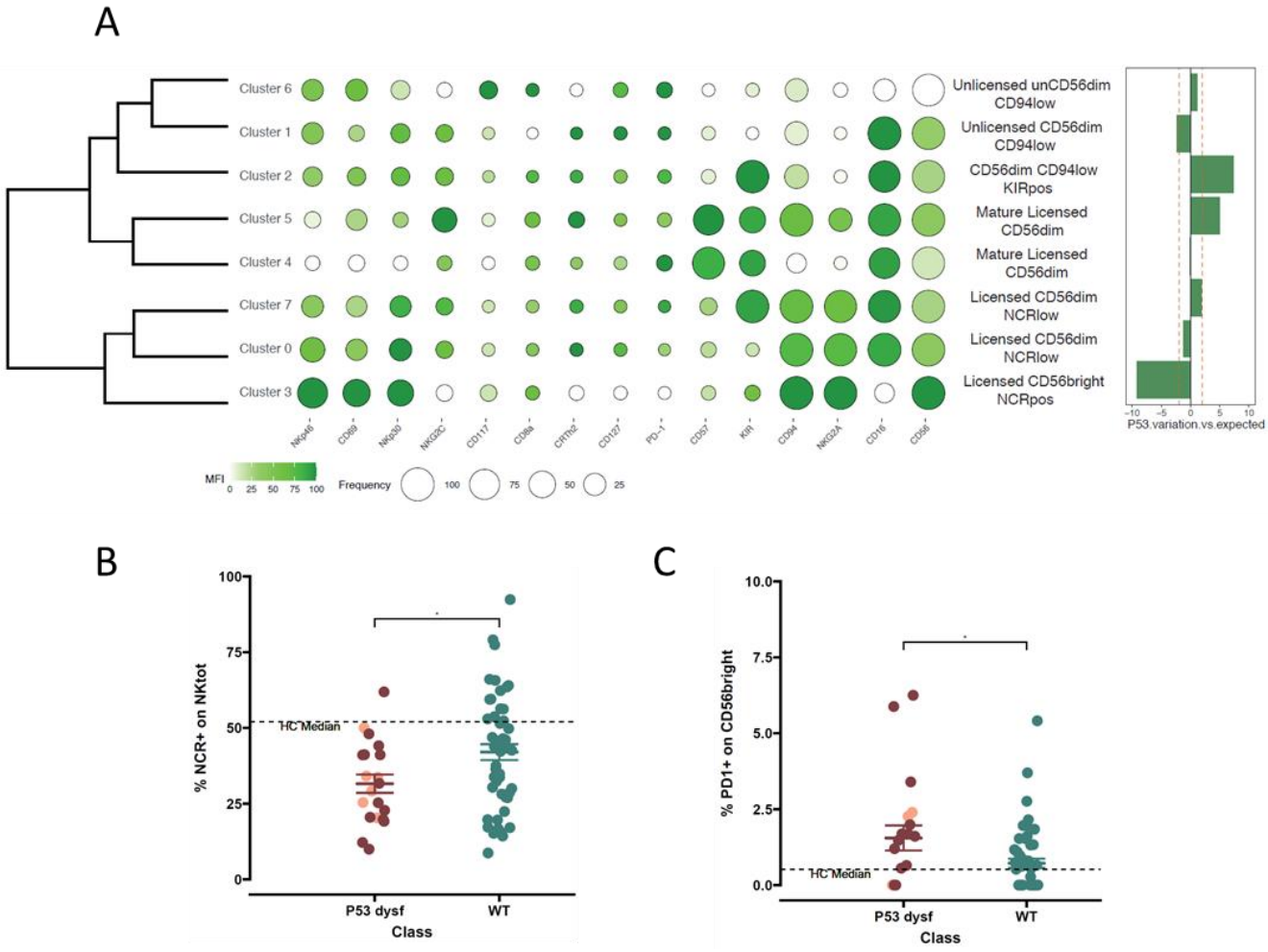

Figure 7. NK cells profiling in p53 dysfunction patient's microenvironment*. A) Balloon plot showing the percent expression and the median fluorescence intensity (MFI) of specific markers (columns) in each PhenoGraph clusters (rows). The Barplot on the right shows the variation of p53 dysfunction NK cells frequency from expected frequency for each cluster. B-C) Dot plots showing the frequency depicted with mean ± SEM of NK cells expressing NKp30 receptor and/or NKp46 receptor (NCRs) (B), and CD56^{bright} expressing PD1 (C). The dashed line indicates the median value of the cell population in HC donors. Red dots highlight TP53 mutated patients, pink dots hyper mutated patients, and green dots wild type patients; T-Test. * p<.05; ** p<.01.*

In the end, we analyzed myeloid cells through manual gating and we looked to the frequencies of classical, intermediate and nonclassical monocytes, dendritic cells and polymorphonuclear myeloid-derived suppressor cells (PMN-MDSCs). We found no significant changes between the two categories except for classical monocytes and dendritic cells that were respectively decreased and increased in p53 dysfunction category compared to p53 non-dysfunction one (p<.05 and p<.01; Supplementary Fig. 11).

Taken together, flow cytometry data indicate an impaired function of adaptive immune system in p53 dysfunction category compared to non-dysfunction, while innate immune system display a shift in monocytes maturation towards dendritic cells.

Discussion

In this paper, we identified a subset of MDS patients with very poor outcome that are characterized by hyperexpression of p53 protein within the bone marrow progenitors cell nucleus, in the absence of TP53 mutations. Through RNAseq analysis, we demonstrated that p53 hyper expressed patients are transcriptionally similar to TP53 mutated ones, both showing a downregulation of p53-related pathways. In the case of hyper-expressed patients, p53 inactivity is not due to a mutated isoform of the protein, since the TP53 gene is wild type, thus suggesting a post-translational inhibition of the oncosuppressor. Given the broad and important functions of p53, its activity and abundance are tightly regulated by a complex protein network, and in particular MDM2 and its homolog MDMX (also known as MDM4) are the main negative regulators, as they bind to the transcriptional activation domains of p53, thereby impeding p53 tetramerization and transactivation functions [30-33]. MDM2 can also promote p53 degradation through ubiquitination and proteasomal degradation by acting as an E3 ubiquitin ligase [34-37]. Furthermore, MDM2 is part of the p53 auto-regulatory feedback loop, since MDM2 is transcriptionally activated by p53 to inhibit its own activity [37-39].

We thus decided to investigate MDM2 expression, observing that p53 hyper-expressed patients are characterized by an upregulation of p53 inhibitor MDM2 at both transcriptional and nuclear protein level, that in half of the cases is due to MDM2 gene amplification, as assessed by FISH.

MDM2 has been shown to be abnormally upregulated due to gene amplification, increased transcription, and enhanced translation in many malignancies such as lung, liver, colorectal, breast and esophagogastric cancers [40-41]. The MDM2 gene amplification could explain the high expression of MDM2 protein despite the absence of its transcriptional induction from a fully functional p53 form.

Moreover, covalent post-translational modifications are very common on p53 and some are necessary for its correct function, in particular phosphorylation and acetylation generally result in its stabilization and activation [42]. However, it has been observed that both mutant and non-mutant p53 protein in cancer is generally more intensely phosphorylated and acetylated than p53 from non-transformed tissues and, since the p53 acetylation sites are the same as for ubiquitylation, a high level of acetylation could hamper the ubiquitination and degradation of p53, thus facilitating the accumulation of dysfunctional p53 protein in the nucleus [42-43].

We hence hypothesize that, in these patients, p53 could undergo some post-translational modifications that strongly limit its functions and still allow the inhibitory interaction with MDM2 within the nucleus but impede ubiquitination and nuclear export for cytoplasmic proteasomal degradation. Deeper p53 biochemical investigation in p53 hyper-expressed MDS patients should be performed to confirm this hypothesis.

Additionally, MDM2 upregulation can hamper p53 functions and improve cancer cell survival through other ways that include the activation of non-canonical NF-κB pathway [44-45], PI3K/AKT signaling [46-47] and MEK/ERK cascade [48-49]. We indeed found an aberrant activation of such pathways in p53 hyper-expressed samples compared to wt.

We further demonstrated that the p53 loss of function in both $TP53^{mut}$ and p53 hyper-expressed MDS lead to the downstream activation of Myc pathway, indicating that p53 is no more able to activate target genes that induce cell cycle arrest through Myc repression [50-51].

The p53 impairment in p53 dysfunction category showed also other peculiarities related to immunosuppression, that have been widely described to occur in hematological malignancies and could further favor tumor outgrowth and poor prognosis by conferring to tumor cells the ability to escape immune system control. In particular we observed, on a transcriptional level, an increased expression of immune checkpoint molecules and ligands [52-54] and CD73 immunosuppressive enzyme [55-56] and a decreased

expression of HLA-II molecules [23-24, 52, 57-58] on tumor blasts, accompanied by a possible increase of anti-inflammatory cytokines and the reduction of pro-inflammatory cytokines, in particular IFNγ, within bone marrow milieu [25; 58].

These immunosuppressive features of the blast cells seem to exert a detrimental influence on immune cells since, by high dimensional flow cytometry analysis, we observed an increased frequency of Tregs and effector $CD8^+$ T cells expressing high levels of immune checkpoint inhibitors TIM3 and PD1, with a reduction of the functional Naïve compartment, indicative of a general T cell exhaustion. Increased Tregs frequency have been previously associated to disease progression, increased aggressiveness, and poor prognosis in MDS and AML [59-61]. We observed similar exhausted features also on NK cells, that displayed an up-regulation of PD1 and a downregulation of natural cytotoxicity receptors (NCRs) NKp30 and NKp46 in MDS patients with p53 dysfunction compared to non-dysfunction. Downregulation of NCRs have been associated to NK poor cytolytic functions, and both NKp30 and NKp46 expression levels have shown to be prognostic markers in AML [62-64]. Dendritic cells are responsible for the priming of T cell responses through phagocytosis of infected or transformed cells and antigen presentation [65]. It is also known that dendritic cells can promote immune tolerance through the release of cytokines that favor Naïve differentiation towards Tregs within the thymus, a process that is normally necessary to avoid the release of auto-reactive T cells that could lead to autoimmune diseases [66-68]. We could speculate that tumor-derived factors may arrest dendritic cells maturation to an immature stage in which they poorly express costimulatory molecules that are necessary to initiate an immune response, a phenomenon already observed to occur in cancer [69-71]. Moreover, such tolerogenic DCs can release cytokines within the bone marrow niche and express immunosuppressive enzymes (such as IDO) to induce Tregs differentiation in a tumor setting [72-73].

Taken together, our data indicate that patients with p53 disfunction, defined by either TP53 mutation or p53 protein hyper-expression, share common transcriptional and microenvironmental features that could be the primary driver of their dismal prognosis. From a clinical perspective, we propose to consider p53 hyper expression as a marker of p53 dysfunction leading to adverse clinical outcome similar to that observed in TP53 mutated patients. Identification of such patients can be easily performed in routine diagnostic with immunohistochemistry. In the end, p53 hyper-expressed MDS patients may benefit from MDM2 inhibitory therapy that can be further combined with PI3K/AKT and MEK/ERK pathways co-inhibition, as is being currently tested in AML [35; 74-75]. Interestingly, the combined MEK/MDM2 inhibition have demonstrated great antitumor efficacy in both *in vitro* and *in vivo* models of TP53 wild-type thyroid and colorectal cancers with MAPK alterations [76], further supporting the possible positive impact of clinical translation of these therapies on MDS patients with p53 hyperexpression.

Material and methods

Patients material collection and gene sequencing

Study procedures are in accordance with the Declaration of Helsinki. Ethics Committees of Humanitas Research Hospital, Milan, Italy approved the study. Written informed consent was obtained prior to Bone Marrow (BM) sampling. In total 135 patients with a diagnosis of MDS according to WHO 2022 and International International Consensus Classification of Myeloid Neoplasms and Acute Leukemia (ICC) criteria have been enrolled in this study between 2010 and 2022. Data on hospitalization and mortality were available for all subjects. TP53 mutational status has been performed through targeted deep sequencing using a 30-gene panel of genes recurrently mutated in myeloid neoplasms as utilized in routine diagnostic workup at our institution (SOPHiA Genetics, Saint Sulpice, Switzerland). Bioinformatics analysis was performed with Sophia DDM (Sophia Genetics).

Immunohistochemistry and FISH

Immunohistochemical stain experiments were performed on formalin-fixed and paraffin-embedded biopsies. Trephine biopsies were formalin-fixed, decalcified and paraffin-embedded. Consecutive 3-µm-thick sections were cut from the BM tissue block, and then stained with hematoxylin and eosin, Giemsa stain and silver impregnation. Immunohistochemical stain was performed using an automated staining system (Discovery XT; Ventana Medical Systems, Oro Valley, AZ) according to the manufacturer's instructions and using antibodies against p53 (clone DO-7, prediluited, Ventana, Tucson, AZ, USA) and MDM2 (clone IF2, dilition 1:40, calbiochem, Merck KGaA, Darmstadt, Germany). All stained slides were reviewed by two experenced hematopathologists (AB, RD).

In situ hybridization protocol was performed to assess MDM2 genomic amplification using Poseidon FISH digestion kit (Leica biosystem – Kreatech biotecnology B.V. – Amsterdam – Netherlands) as manufacturer's instructions starting from FFPE tissue sections. The evaluation of copy number gain of MDM2 gene has been assessed using Probes mixed is Zytolight® SPEC MDM2/CEN12 Dual Color Probe (locus 12q15), (ZytoVision GmbH – Bremerhaven – Germany). Using a Leica DM 5500 B Fluorescence microscope (Leica Microsystem SRL, Milan, Italy), histological samples for each single case were evaluated and interpreted as follow: normal interphase cells are indicated by two green (CEP12) and two orange (MDM2) signals per nucleus; nuclei with amplified MDM2 showed clusters of green signals versus normal CEP12 signals status. The average number of MDM2 and CEP12 ratio was calculated and a ratio>2.0 was considered amplified.

CD34+ Isolation from bone marrow, RNA extraction and library preparation

CD34+ cells were selected using the MACS CD34 microbead kit on autoMACS (Miltenyi Biotech Inc, San Diego, CA). A purity of >96% CD34+ cells after isolation was confirmed by flow cytometry. RNA was isolated through RNeasy Micro kit (Qiagen) according to manifacturer's protocol. RNA quality control was performed with the Agilent 2200 Tape Station system, and only RNAs having a RIN >7 were used for library preparation. Libraries for mRNA sequencing were prepared starting from 50 ng of total RNA for each sample by using the SMART-Seq v4 Ultra Low Input RNA Kit (Clontech-Takara). All samples were sequenced at an average of 20 million 75-bp single-end reads. The 2 cohorts of patients sequenced with different sequencers have been analyzed separately in order to minimize batch effects. Principal cohort has been sequenced with Novaseq 2000 and it contain 75 samples while validation cohort has been sequenced with Nextseq550 and it contain 34 samples.

Flow Cytometry

Mononucleated cells were isolated from bone marrow samples by Ficoll density gradient centrifugation (Cedarlane, Burlington, Canada) and frozen in liquid nitrogen according to standard procedures. All the experiments were performed in batch on frozen cells to minimize variability. Cells were thawed and stained as we previously described. The anti-human monoclonal antibodies (mAbs) used are listed in supplementary tables 1 and 2.
Samples were acquired at BD FACSymphonyA5 flow cytometer (BD Bioscience, San Jose, California, USA). Flow Cytometry data were analysed using the FlowJo software (TreeStar Inc, Ashland, Oregon, USA), version 10.7.1.

Batch correction and Phenograph analysis on flow cytometry data

Flow Cytometry Standard (FCS) 3.0 files were analysed by standard gating in FlowJo to remove dead cells and spurious events. Data were downsampled to 3,000 events per sample through FlowJo and they were biexponentially transformed and exported for further analysis with PhenoGraph python package. Samples were labelled with a unique computational barcode for further identification and converted in comma separated (CSV) files and concatenated in a single matrix by using the merge function of pandas package. Data were first batch-corrected via cyCombine [77] and subsequently clustered via Phenograph [78]. The former

tool was recently developed to correct for batch effect in single cell data and operates as follows: the expression from every marker is converted to rank, for every batch; subsequently, each batch is reorganized into M different sub-clusters, and for every sub-cluster the batch normalization is performed separately using ComBat [79]. The result is a dataset where every marker has a comparable distribution across different batches (Supplemental Fig 9).
Batch-corrected data were then partitioned into subpopulations by means of Phenograph algorithm, which mainly operates through the following steps: for each cell, a set of k nearest neighbors is identified using Euclidean distance; a weighted graph is then build, where nodes represent single cells and the weight between two nodes represents their distance (Gaussian kernel); finally, nodes are grouped into clusters using Louvain method [80], which maximizes modularity, namely a measure representing the density of links inside communities compared to density of links between communities. Different K values (number of nearest neighbours identified in the first iteration of the algorithm) were tested in preliminary analysis, and were arbitrarily set at 300 for CD4+ and CD8+ T cells clustering and K=600 in NK cell clustering. The data were then reorganized and saved as new CSV files, one for each cluster, that were further analysed in FlowJo to determine the frequency of positive cells for each marker and the corresponding median fluorescent intensity (MFI). Subsequent metaclustering of these values was performed using the gplots R package. Uniform Manifold Approximation and Projection (UMAP) was obtained by UMAP Python package.

Statistical Analysis

All the statistical analyses were performed using R software (4.4.1 version) or Python 3 software. We performed prerank GSEA using the gseapy package in python for Reactome pathways enrichment analyses. To identify significant overlaps between gene signatures and differential expressed we performed hypergeometric test using MsigDB 7.0 investigation tool. Values are presented as mean ± SEM. In all box plots, the median is indicated by the horizontal line and the first and third quartiles are represented by the box edges. The lower and upper whiskers extend from the hinges to the smallest and largest values, respectively, with individual values included. Significance between expression or zscore values was determined by Student's unpaired t-test and Wilcoxon rank sum test. $P < .05$ was considered significant. The association between clusters and conditions (p53 dysfunction or wild type) was assessed by a Fisher test followed by Benjamini-Hochberg correction for multiple tests with $P < .01$ considered as significant.

References

1. Levine AJ, Oren M. The first 30 years of p53: growing ever more complex. Nat Rev Cancer. 2009 Oct;9(10):749-58. doi: 10.1038/nrc2723. PMID: 19776744; PMCID: PMC2771725.
2. Boutelle AM, Attardi LD. p53 and Tumor Suppression: It Takes a Network. Trends Cell Biol. 2021 Apr;31(4):298-310. doi: 10.1016/j.tcb.2020.12.011. Epub 2021 Jan 28. PMID: 33518400; PMCID: PMC7954925.
3. Vaddavalli PL, Schumacher B. The p53 network: cellular and systemic DNA damage responses in cancer and aging. Trends Genet. 2022 Jun;38(6):598-612. doi: 10.1016/j.tig.2022.02.010. Epub 2022 Mar 25. PMID: 35346511.
4. Muñoz-Fontela C, Mandinova A, Aaronson SA, Lee SW. Emerging roles of p53 and other tumour-suppressor genes in immune regulation. Nat Rev Immunol. 2016 Dec;16(12):741-750. doi: 10.1038/nri.2016.99. Epub 2016 Sep 26. PMID: 27667712; PMCID: PMC5325695.
5. Shi D, Jiang P. A Different Facet of p53 Function: Regulation of Immunity and Inflammation During Tumor Development. Front Cell Dev Biol. 2021 Oct 18;9:762651. doi: 10.3389/fcell.2021.762651. PMID: 34733856; PMCID: PMC8558413.

6. Blagih J, Buck MD, Vousden KH. p53, cancer and the immune response. J Cell Sci. 2020 Mar 6;133(5):jcs237453. doi: 10.1242/jcs.237453. PMID: 32144194.
7. Chen X, Zhang T, Su W, Dou Z, Zhao D, Jin X, Lei H, Wang J, Xie X, Cheng B, Li Q, Zhang H, Di C. Mutant p53 in cancer: from molecular mechanism to therapeutic modulation. Cell Death Dis. 2022 Nov 18;13(11):974. doi: 10.1038/s41419-022-05408-1. PMID: 36400749; PMCID: PMC9674619.
8. Kandoth C, McLellan MD, Vandin F, Ye K, Niu B, Lu C, Xie M, Zhang Q, McMichael JF, Wyczalkowski MA, Leiserson MDM, Miller CA, Welch JS, Walter MJ, Wendl MC, Ley TJ, Wilson RK, Raphael BJ, Ding L. Mutational landscape and significance across 12 major cancer types. Nature. 2013 Oct 17;502(7471):333-339. doi: 10.1038/nature12634. PMID: 24132290; PMCID: PMC3927368.
9. Li H, Hu F, Gale RP, Sekeres MA, Liang Y. Myelodysplastic syndromes. Nat Rev Dis Primers. 2022 Nov 17;8(1):74. doi: 10.1038/s41572-022-00402-5. PMID: 36396662.
10. Ogawa S. Genetics of MDS. Blood 2019; 133 (10): 1049–1059. doi: https://doi.org/10.1182/blood-2018-10-844621
11. Sperling AS, Gibson CJ, Ebert BL. The genetics of myelodysplastic syndrome: from clonal haematopoiesis to secondary leukaemia. Nat Rev Cancer. 2017 Jan;17(1):5-19. doi: 10.1038/nrc.2016.112. Epub 2016 Nov 11. PMID: 27834397; PMCID: PMC5470392.
12. Khoury JD, Solary E, Abla O, Akkari Y, Alaggio R, Apperley JF, Bejar R, Berti E, Busque L, Chan JKC, Chen W, Chen X, Chng WJ, Choi JK, Colmenero I, Coupland SE, Cross NCP, De Jong D, Elghetany MT, Takahashi E, Emile JF, Ferry J, Fogelstrand L, Fontenay M, Germing U, Gujral S, Haferlach T, Harrison C, Hodge JC, Hu S, Jansen JH, Kanagal-Shamanna R, Kantarjian HM, Kratz CP, Li XQ, Lim MS, Loeb K, Loghavi S, Marcogliese A, Meshinchi S, Michaels P, Naresh KN, Natkunam Y, Nejati R, Ott G, Padron E, Patel KP, Patkar N, Picarsic J, Platzbecker U, Roberts I, Schuh A, Sewell W, Siebert R, Tembhare P, Tyner J, Verstovsek S, Wang W, Wood B, Xiao W, Yeung C, Hochhaus A. The 5th edition of the World Health Organization Classification of Haematolymphoid Tumours: Myeloid and Histiocytic/Dendritic Neoplasms. Leukemia. 2022 Jul;36(7):1703-1719. doi: 10.1038/s41375-022-01613-1. Epub 2022 Jun 22. PMID: 35732831; PMCID: PMC9252913.
13. Arber DA, Orazi A, Hasserjian RP, Borowitz MJ, Calvo KR, Kvasnicka HM, Wang SA, Bagg A, Barbui T, Branford S, Bueso-Ramos CE, Cortes JE, Dal Cin P, DiNardo CD, Dombret H, Duncavage EJ, Ebert BL, Estey EH, Facchetti F, Foucar K, Gangat N, Gianelli U, Godley LA, Gökbuget N, Gotlib J, Hellström-Lindberg E, Hobbs GS, Hoffman R, Jabbour EJ, Kiladjian JJ, Larson RA, Le Beau MM, Loh ML, Löwenberg B, Macintyre E, Malcovati L, Mullighan CG, Niemeyer C, Odenike OM, Ogawa S, Orfao A, Papaemmanuil E, Passamonti F, Porkka K, Pui CH, Radich JP, Reiter A, Rozman M, Rudelius M, Savona MR, Schiffer CA, Schmitt-Graeff A, Shimamura A, Sierra J, Stock WA, Stone RM, Tallman MS, Thiele J, Tien HF, Tzankov A, Vannucchi AM, Vyas P, Wei AH, Weinberg OK, Wierzbowska A, Cazzola M, Döhner H, Tefferi A. International Consensus Classification of Myeloid Neoplasms and Acute Leukemias: integrating morphologic, clinical, and genomic data. Blood. 2022 Sep 15;140(11):1200-1228. doi: 10.1182/blood.2022015850. PMID: 35767897; PMCID: PMC9479031.
14. Haferlach T, Nagata Y, Grossmann V, Okuno Y, Bacher U, Nagae G, Schnittger S, Sanada M, Kon A, Alpermann T, Yoshida K, Roller A, Nadarajah N, Shiraishi Y, Shiozawa Y, Chiba K, Tanaka H, Koeffler HP, Klein HU, Dugas M, Aburatani H, Kohlmann A, Miyano S, Haferlach C, Kern W, Ogawa S. Landscape of genetic lesions in 944 patients with myelodysplastic syndromes. Leukemia. 2014 Feb;28(2):241-7. doi: 10.1038/leu.2013.336. Epub 2013 Nov 13. PMID: 24220272; PMCID: PMC3918868.
15. Stengel A, Kern W, Haferlach T, Meggendorfer M, Fasan A, Haferlach C. The impact of TP53 mutations and TP53 deletions on survival varies between AML, ALL, MDS and CLL: an analysis of 3307 cases. Leukemia. 2017 Mar;31(3):705-711. doi: 10.1038/leu.2016.263. Epub 2016 Sep 29. PMID: 27680515.
16. Bernard E, Nannya Y, Hasserjian RP, Devlin SM, Tuechler H, Medina-Martinez JS, Yoshizato T, Shiozawa Y, Saiki R, Malcovati L, Levine MF, Arango JE, Zhou Y, Solé F, Cargo CA, Haase D, Creignou M, Germing U, Zhang Y, Gundem G, Sarian A, van de Loosdrecht AA, Jädersten M, Tobiasson M, Kosmider O, Follo MY, Thol F, Pinheiro RF, Santini V, Kotsianidis I, Boultwood J, Santos FPS, Schanz J, Kasahara S, Ishikawa T, Tsurumi H, Takaori-Kondo A, Kiguchi T, Polprasert C, Bennett JM, Klimek VM, Savona MR, Belickova M, Ganster C, Palomo L, Sanz G, Ades L, Della Porta MG, Elias HK, Smith AG,

Werner Y, Patel M, Viale A, Vanness K, Neuberg DS, Stevenson KE, Menghrajani K, Bolton KL, Fenaux P, Pellagatti A, Platzbecker U, Heuser M, Valent P, Chiba S, Miyazaki Y, Finelli C, Voso MT, Shih LY, Fontenay M, Jansen JH, Cervera J, Atsuta Y, Gattermann N, Ebert BL, Bejar R, Greenberg PL, Cazzola M, Hellström-Lindberg E, Ogawa S, Papaemmanuil E. Implications of TP53 allelic state for genome stability, clinical presentation and outcomes in myelodysplastic syndromes. Nat Med. 2020 Oct;26(10):1549-1556. doi: 10.1038/s41591-020-1008-z. Epub 2020 Aug 3. Erratum in: Nat Med. 2021 Mar;27(3):562. Erratum in: Nat Med. 2021 May;27(5):927. PMID: 32747829; PMCID: PMC8381722.

17. Sallman DA, McLemore AF, Aldrich AL, Komrokji RS, McGraw KL, Dhawan A, Geyer S, Hou HA, Eksioglu EA, Sullivan A, Warren S, MacBeth KJ, Meggendorfer M, Haferlach T, Boettcher S, Ebert BL, Al Ali NH, Lancet JE, Cleveland JL, Padron E, List AF. TP53 mutations in myelodysplastic syndromes and secondary AML confer an immunosuppressive phenotype. Blood. 2020 Dec 10;136(24):2812-2823. doi: 10.1182/blood.2020006158. PMID: 32730593; PMCID: PMC7731792.
18. Prokocimer M, Molchadsky A, Rotter V. Dysfunctional diversity of p53 proteins in adult acute myeloid leukemia: projections on diagnostic workup and therapy. Blood. 2017 Aug 10;130(6):699-712. doi: 10.1182/blood-2017-02-763086. Epub 2017 Jun 12. PMID: 28607134; PMCID: PMC5659817.
19. Bullinger L, Ehrich M, Döhner K, Schlenk RF, Döhner H, Nelson MR, van den Boom D. Quantitative DNA methylation predicts survival in adult acute myeloid leukemia. Blood. 2010 Jan 21;115(3):636-42. doi: 10.1182/blood-2009-03-211003. Epub 2009 Nov 10. PMID: 19903898.
20. Zhou F, Dou X, Li C. CKB affects human osteosarcoma progression by regulating the p53 pathway. Am J Cancer Res. 2022 Oct 15;12(10):4652-4665. PMID: 36381321; PMCID: PMC9641398.
21. Jaatinen T, Hemmoranta H, Hautaniemi S, Niemi J, Nicorici D, Laine J, Yli-Harja O, Partanen J. Global gene expression profile of human cord blood-derived CD133+ cells. Stem Cells. 2006 Mar;24(3):631-41. doi: 10.1634/stemcells.2005-0185. Epub 2005 Oct 6. PMID: 16210406.
22. Tang S, Zhang Y, Lin X, Wang H, Yong L, Zhang H, Cai F. CLEC10A can serve as a potential therapeutic target and its level correlates with immune infiltration in breast cancer. Oncol Lett. 2022 Jun 28;24(2):285. doi: 10.3892/ol.2022.13405. PMID: 35814828; PMCID: PMC9260715.
23. Christopher MJ, Petti AA, Rettig MP, Miller CA, Chendamarai E, Duncavage EJ, Klco JM, Helton NM, O'Laughlin M, Fronick CC, Fulton RS, Wilson RK, Wartman LD, Welch JS, Heath SE, Baty JD, Payton JE, Graubert TA, Link DC, Walter MJ, Westervelt P, Ley TJ, DiPersio JF. Immune Escape of Relapsed AML Cells after Allogeneic Transplantation. N Engl J Med. 2018 Dec 13;379(24):2330-2341. doi: 10.1056/NEJMoa1808777. Epub 2018 Oct 31. PMID: 30380364; PMCID: PMC6322675.
24. Toffalori C, Zito L, Gambacorta V, Riba M, Oliveira G, Bucci G, Barcella M, Spinelli O, Greco R, Crucitti L, Cieri N, Noviello M, Manfredi F, Montaldo E, Ostuni R, Naldini MM, Gentner B, Waterhouse M, Zeiser R, Finke J, Hanoun M, Beelen DW, Gojo I, Luznik L, Onozawa M, Teshima T, Devillier R, Blaise D, Halkes CJM, Griffioen M, Carrabba MG, Bernardi M, Peccatori J, Barlassina C, Stupka E, Lazarevic D, Tonon G, Rambaldi A, Cittaro D, Bonini C, Fleischhauer K, Ciceri F, Vago L. Immune signature drives leukemia escape and relapse after hematopoietic cell transplantation. Nat Med. 2019 Apr;25(4):603-611. doi: 10.1038/s41591-019-0400-z. Epub 2019 Mar 25. PMID: 30911134.
25. Zeiser R, Vago L. Mechanisms of immune escape after allogeneic hematopoietic cell transplantation. Blood. 2019 Mar 21;133(12):1290-1297. doi: 10.1182/blood-2018-10-846824. Epub 2018 Dec 21. PMID: 30578254.
26. Barakos GP, Hatzimichael E. Microenvironmental Features Driving Immune Evasion in Myelodysplastic Syndromes and Acute Myeloid Leukemia. Diseases. 2022 Jun 10;10(2):33. doi: 10.3390/diseases10020033. PMID: 35735633; PMCID: PMC9221594.
27. Luciano M, Krenn PW, Horejs-Hoeck J. The cytokine network in acute myeloid leukemia. Front Immunol. 2022 Sep 28;13:1000996. doi: 10.3389/fimmu.2022.1000996. PMID: 36248849; PMCID: PMC9554002.
28. Levine JH, Simonds EF, Bendall SC, Davis KL, Amir el-AD, Tadmor MD, Litvin O, Fienberg HG, Jager A, Zunder ER, Finck R, Gedman AL, Radtke I, Downing JR, Pe'er D, Nolan GP. Data-Driven Phenotypic Dissection of AML Reveals Progenitor-like Cells that Correlate with Prognosis. Cell. 2015 Jul

2;162(1):184-97. doi: 10.1016/j.cell.2015.05.047. Epub 2015 Jun 18. PMID: 26095251; PMCID: PMC4508757.
29. Zhou Q, Munger ME, Highfill SL, Tolar J, Weigel BJ, Riddle M, Sharpe AH, Vallera DA, Azuma M, Levine BL, June CH, Murphy WJ, Munn DH, Blazar BR. Program death-1 signaling and regulatory T cells collaborate to resist the function of adoptively transferred cytotoxic T lymphocytes in advanced acute myeloid leukemia. Blood. 2010 Oct 7;116(14):2484-93. doi: 10.1182/blood-2010-03-275446. Epub 2010 Jun 22. PMID: 20570856; PMCID: PMC2953885.
30. Momand J, Zambetti GP, Olson DC, George D, Levine AJ. The mdm-2 oncogene product forms a complex with the p53 protein and inhibits p53-mediated transactivation. Cell. 1992 Jun 26;69(7):1237-45. doi: 10.1016/0092-8674(92)90644-r. PMID: 1535557.
31. Chen J, Marechal V, Levine AJ. Mapping of the p53 and mdm-2 interaction domains. Mol Cell Biol. 1993 Jul;13(7):4107-14. doi: 10.1128/mcb.13.7.4107-4114.1993. PMID: 7686617; PMCID: PMC359960.
32. Danovi D, Meulmeester E, Pasini D, Migliorini D, Capra M, Frenk R, de Graaf P, Francoz S, Gasparini P, Gobbi A, Helin K, Pelicci PG, Jochemsen AG, Marine JC. Amplification of Mdmx (or Mdm4) directly contributes to tumor formation by inhibiting p53 tumor suppressor activity. Mol Cell Biol. 2004 Jul;24(13):5835-43. doi: 10.1128/MCB.24.13.5835-5843.2004. Erratum in: Mol Cell Biol. 2019 Jul 16;39(15): PMID: 15199139; PMCID: PMC480894.
33. Chène P. Inhibiting the p53-MDM2 interaction: an important target for cancer therapy. Nat Rev Cancer. 2003 Feb;3(2):102-9. doi: 10.1038/nrc991. PMID: 12563309.
34. Haupt Y, Maya R, Kazaz A, Oren M. Mdm2 promotes the rapid degradation of p53. Nature. 1997 May 15;387(6630):296-9. doi: 10.1038/387296a0. PMID: 9153395.
35. Konopleva M, Martinelli G, Daver N, Papayannidis C, Wei A, Higgins B, Ott M, Mascarenhas J, Andreeff M. MDM2 inhibition: an important step forward in cancer therapy. Leukemia. 2020 Nov;34(11):2858-2874. doi: 10.1038/s41375-020-0949-z. Epub 2020 Jul 10. PMID: 32651541.
36. Yu ZK, Geyer RK, Maki CG. MDM2-dependent ubiquitination of nuclear and cytoplasmic P53. Oncogene. 2000 Nov 30;19(51):5892-7. doi: 10.1038/sj.onc.1203980. PMID: 11127820.
37. Wu X, Bayle JH, Olson D, Levine AJ. The p53-mdm-2 autoregulatory feedback loop. Genes Dev. 1993 Jul;7(7A):1126-32. doi: 10.1101/gad.7.7a.1126. PMID: 8319905.
38. Barak Y, Juven T, Haffner R, Oren M. mdm2 expression is induced by wild type p53 activity. EMBO J. 1993 Feb;12(2):461-8. doi: 10.1002/j.1460-2075.1993.tb05678.x. PMID: 8440237; PMCID: PMC413229.
39. Picksley SM, Lane DP. The p53-mdm2 autoregulatory feedback loop: a paradigm for the regulation of growth control by p53? Bioessays. 1993 Oct;15(10):689-90. doi: 10.1002/bies.950151008. PMID: 7506024.
40. Momand J, Jung D, Wilczynski S, Niland J. The MDM2 gene amplification database. Nucleic Acids Res. 1998 Aug 1;26(15):3453-9. doi: 10.1093/nar/26.15.3453. PMID: 9671804; PMCID: PMC147746.
41. Hou H, Sun D, Zhang X. The role of MDM2 amplification and overexpression in therapeutic resistance of malignant tumors. Cancer Cell Int. 2019 Aug 22;19:216. doi: 10.1186/s12935-019-0937-4. PMID: 31440117; PMCID: PMC6704499.
42. Bode AM, Dong Z. Post-translational modification of p53 in tumorigenesis. Nat Rev Cancer. 2004 Oct;4(10):793-805. doi: 10.1038/nrc1455. PMID: 15510160.
43. Minamoto T, Buschmann T, Habelhah H, Matusevich E, Tahara H, Boerresen-Dale AL, Harris C, Sidransky D, Ronai Z. Distinct pattern of p53 phosphorylation in human tumors. Oncogene. 2001 Jun 7;20(26):3341-7. doi: 10.1038/sj.onc.1204458. PMID: 11423984.
44. Thomasova D, Mulay SR, Bruns H, Anders HJ. p53-independent roles of MDM2 in NF-κB signaling: implications for cancer therapy, wound Healing, and autoimmune diseases. Neoplasia. 2012;14:1097–101.
45. Vaughan C, Mohanraj L, Singh S, Dumur CI, Ramamoorthy M, Garrett CT, et al. Human oncoprotein MDM2 up-regulates expression of NF-κB2 precursor p100 conferring a survival advantage to lung cells. Genes Cancer. 2011;2:943–55.

46. Singh S, Ramamoorthy M, Vaughan C, Yeudall WA, Deb S, Palit Deb S. Human oncoprotein MDM2 activates the Akt signaling pathway through an interaction with the repressor element-1 silencing transcription factor conferring a survival advantage to cancer cells. Cell Death Differ. 2013 Apr;20(4):558-66. doi: 10.1038/cdd.2012.153. Epub 2012 Dec 14. PMID: 23238568; PMCID: PMC3595481.
47. Chibaya L, Karim B, Zhang H, Jones SN. Mdm2 phosphorylation by Akt regulates the p53 response to oxidative stress to promote cell proliferation and tumorigenesis. Proc Natl Acad Sci U S A. 2021 Jan 26;118(4):e2003193118. doi: 10.1073/pnas.2003193118. Erratum in: Proc Natl Acad Sci U S A. 2021 Mar 2;118(9): PMID: 33468664; PMCID: PMC7848548.
48. Roy S, Laroche-Clary A, Verbeke S, Derieppe MA, Italiano A. MDM2 Antagonists Induce a Paradoxical Activation of Erk1/2 through a P53-Dependent Mechanism in Dedifferentiated Liposarcomas: Implications for Combinatorial Strategies. Cancers (Basel). 2020 Aug 12;12(8):2253. doi: 10.3390/cancers12082253. PMID: 32806555; PMCID: PMC7465494.
49. Pairawan S, Akcakanat A, Kopetz S, Tapia C, Zheng X, Chen H, Ha MJ, Rizvi Y, Holla V, Wang J, Evans KW, Zhao M, Busaidy N, Fang B, Roth JA, Dumbrava EI, Meric-Bernstam F. Combined MEK/MDM2 inhibition demonstrates antitumor efficacy in TP53 wild-type thyroid and colorectal cancers with MAPK alterations. Sci Rep. 2022 Jan 24;12(1):1248. doi: 10.1038/s41598-022-05193-z. PMID: 35075200; PMCID: PMC8786858.
50. Ho JS, Ma W, Mao DY, Benchimol S. p53-Dependent transcriptional repression of c-myc is required for G1 cell cycle arrest. Mol Cell Biol. 2005 Sep;25(17):7423-31. doi: 10.1128/MCB.25.17.7423-7431.2005. PMID: 16107691; PMCID: PMC1190302.
51. Olivero CE, Martínez-Terroba E, Zimmer J, Liao C, Tesfaye E, Hooshdaran N, Schofield JA, Bendor J, Fang D, Simon MD, Zamudio JR, Dimitrova N. p53 Activates the Long Noncoding RNA Pvt1b to Inhibit Myc and Suppress Tumorigenesis. Mol Cell. 2020 Feb 20;77(4):761-774.e8. doi: 10.1016/j.molcel.2019.12.014. Epub 2020 Jan 20. PMID: 31973890; PMCID: PMC7184554.
52. Roemer MGM, Redd RA, Cader FZ, Pak CJ, Abdelrahman S, Ouyang J, Sasse S, Younes A, Fanale M, Santoro A, Zinzani PL, Timmerman J, Collins GP, Ramchandren R, Cohen JB, De Boer JP, Kuruvilla J, Savage KJ, Trneny M, Ansell S, Kato K, Farsaci B, Sumbul A, Armand P, Neuberg DS, Pinkus GS, Ligon AH, Rodig SJ, Shipp MA. Major Histocompatibility Complex Class II and Programmed Death Ligand 1 Expression Predict Outcome After Programmed Death 1 Blockade in Classic Hodgkin Lymphoma. J Clin Oncol. 2018 Apr 1;36(10):942-950. doi: 10.1200/JCO.2017.77.3994. Epub 2018 Feb 2. PMID: 29394125; PMCID: PMC5877802.
53. Williams P, Basu S, Garcia-Manero G, Hourigan CS, Oetjen KA, Cortes JE, Ravandi F, Jabbour EJ, Al-Hamal Z, Konopleva M, Ning J, Xiao L, Hidalgo Lopez J, Kornblau SM, Andreeff M, Flores W, Bueso-Ramos C, Blando J, Galera P, Calvo KR, Al-Atrash G, Allison JP, Kantarjian HM, Sharma P, Daver NG. The distribution of T-cell subsets and the expression of immune checkpoint receptors and ligands in patients with newly diagnosed and relapsed acute myeloid leukemia. Cancer. 2019 May 1;125(9):1470-1481. doi: 10.1002/cncr.31896. Epub 2018 Nov 30. PMID: 30500073; PMCID: PMC6467779.
54. Annibali O, Crescenzi A, Tomarchio V, Pagano A, Bianchi A, Grifoni A, Avvisati G. PD-1 /PD-L1 checkpoint in hematological malignancies. Leuk Res. 2018 Apr;67:45-55. doi: 10.1016/j.leukres.2018.01.014. Epub 2018 Jan 31. PMID: 29428449.
55. Serra S, Horenstein AL, Vaisitti T, Brusa D, Rossi D, Laurenti L, D'Arena G, Coscia M, Tripodo C, Inghirami G, Robson SC, Gaidano G, Malavasi F, Deaglio S. CD73-generated extracellular adenosine in chronic lymphocytic leukemia creates local conditions counteracting drug-induced cell death. Blood. 2011 Dec 1;118(23):6141-52. doi: 10.1182/blood-2011-08-374728. Epub 2011 Oct 13. PMID: 21998208; PMCID: PMC3342854.
56. Chen S, Wainwright DA, Wu JD, Wan Y, Matei DE, Zhang Y, Zhang B. CD73: an emerging checkpoint for cancer immunotherapy. Immunotherapy. 2019 Aug;11(11):983-997. doi: 10.2217/imt-2018-0200. Epub 2019 Jun 21. PMID: 31223045; PMCID: PMC6609898.
57. Rimsza LM, Roberts RA, Miller TP, Unger JM, LeBlanc M, Braziel RM, Weisenberger DD, Chan WC, Muller-Hermelink HK, Jaffe ES, Gascoyne RD, Campo E, Fuchs DA, Spier CM, Fisher RI, Delabie J,

Rosenwald A, Staudt LM, Grogan TM. Loss of MHC class II gene and protein expression in diffuse large B-cell lymphoma is related to decreased tumor immunosurveillance and poor patient survival regardless of other prognostic factors: a follow-up study from the Leukemia and Lymphoma Molecular Profiling Project. Blood. 2004 Jun 1;103(11):4251-8. doi: 10.1182/blood-2003-07-2365. Epub 2004 Feb 19. PMID: 14976040.

58. Tarafdar A, Hopcroft LE, Gallipoli P, Pellicano F, Cassels J, Hair A, Korfi K, Jørgensen HG, Vetrie D, Holyoake TL, Michie AM. CML cells actively evade host immune surveillance through cytokine-mediated downregulation of MHC-II expression. Blood. 2017 Jan 12;129(2):199-208. doi: 10.1182/blood-2016-09-742049. Epub 2016 Oct 28. PMID: 27793879; PMCID: PMC5305055.
59. Kordasti SY, Ingram W, Hayden J, Darling D, Barber L, Afzali B, Lombardi G, Wlodarski MW, Maciejewski JP, Farzaneh F, Mufti GJ. CD4+CD25high Foxp3+ regulatory T cells in myelodysplastic syndrome (MDS). Blood. 2007 Aug 1;110(3):847-50. doi: 10.1182/blood-2007-01-067546. Epub 2007 Apr 5. PMID: 17412885.
60. Shenghui Z, Yixiang H, Jianbo W, Kang Y, Laixi B, Yan Z, Xi X. Elevated frequencies of $CD4^+$ $CD25^+$ CD127lo regulatory T cells is associated to poor prognosis in patients with acute myeloid leukemia. Int J Cancer. 2011 Sep 15;129(6):1373-81. doi: 10.1002/ijc.25791. Epub 2011 Feb 26. PMID: 21105040.
61. Xu Y, Mou J, Wang Y, Zhou W, Rao Q, Xing H, Tian Z, Tang K, Wang M, Wang J. Regulatory T cells promote the stemness of leukemia stem cells through IL10 cytokine-related signaling pathway. Leukemia. 2022 Feb;36(2):403-415. doi: 10.1038/s41375-021-01375-2. Epub 2021 Aug 11. PMID: 34381181.
62. Fauriat C, Just-Landi S, Mallet F, Arnoulet C, Sainty D, Olive D, Costello RT. Deficient expression of NCR in NK cells from acute myeloid leukemia: Evolution during leukemia treatment and impact of leukemia cells in NCRdull phenotype induction. Blood. 2007 Jan 1;109(1):323-30. doi: 10.1182/blood-2005-08-027979. Epub 2006 Aug 29. PMID: 16940427.
63. Chretien AS, Fauriat C, Orlanducci F, Rey J, Borg GB, Gautherot E, Granjeaud S, Demerle C, Hamel JF, Cerwenka A, von Strandmann EP, Ifrah N, Lacombe C, Cornillet-Lefebvre P, Delaunay J, Toubert A, Arnoulet C, Vey N, Olive D. NKp30 expression is a prognostic immune biomarker for stratification of patients with intermediate-risk acute myeloid leukemia. Oncotarget. 2017 Jul 25;8(30):49548-49563. doi: 10.18632/oncotarget.17747. Erratum in: Oncotarget. 2019 Sep 10;10(52):5493. PMID: 28548938; PMCID: PMC5564787.
64. Chretien AS, Devillier R, Fauriat C, Orlanducci F, Harbi S, Le Roy A, Rey J, Bouvier Borg G, Gautherot E, Hamel JF, Ifrah N, Lacombe C, Cornillet-Lefebvre P, Delaunay J, Toubert A, Arnoulet C, Vey N, Blaise D, Olive D. NKp46 expression on NK cells as a prognostic and predictive biomarker for response to allo-SCT in patients with AML. Oncoimmunology. 2017 Mar 24;6(12):e1307491. doi: 10.1080/2162402X.2017.1307491. PMID: 29209559; PMCID: PMC5706596.
65. Hilligan KL, Ronchese F. Antigen presentation by dendritic cells and their instruction of CD4+ T helper cell responses. Cell Mol Immunol. 2020 Jun;17(6):587-599. doi: 10.1038/s41423-020-0465-0. Epub 2020 May 20. PMID: 32433540; PMCID: PMC7264306.
66. Watanabe N, Wang YH, Lee HK, Ito T, Wang YH, Cao W, Liu YJ. Hassall's corpuscles instruct dendritic cells to induce CD4+CD25+ regulatory T cells in human thymus. Nature. 2005 Aug 25;436(7054):1181-5. doi: 10.1038/nature03886. PMID: 16121185.
67. Hanabuchi S, Ito T, Park WR, Watanabe N, Shaw JL, Roman E, Arima K, Wang YH, Voo KS, Cao W, Liu YJ. Thymic stromal lymphopoietin-activated plasmacytoid dendritic cells induce the generation of FOXP3+ regulatory T cells in human thymus. J Immunol. 2010 Mar 15;184(6):2999-3007. doi: 10.4049/jimmunol.0804106. Epub 2010 Feb 19. PMID: 20173030; PMCID: PMC3325785.
68. Besin G, Gaudreau S, Ménard M, Guindi C, Dupuis G, Amrani A. Thymic stromal lymphopoietin and thymic stromal lymphopoietin-conditioned dendritic cells induce regulatory T-cell differentiation and protection of NOD mice against diabetes. Diabetes. 2008 Aug;57(8):2107-17. doi: 10.2337/db08-0171. Epub 2008 May 13. PMID: 18477807; PMCID: PMC2494678.

69. Janikashvili N, Bonnotte B, Katsanis E, Larmonier N. The dendritic cell-regulatory T lymphocyte crosstalk contributes to tumor-induced tolerance. Clin Dev Immunol. 2011;2011:430394. doi: 10.1155/2011/430394. Epub 2011 Nov 3. PMID: 22110524; PMCID: PMC3216392.
70. Almand B, Clark JI, Nikitina E, van Beynen J, English NR, Knight SC, Carbone DP, Gabrilovich DI. Increased production of immature myeloid cells in cancer patients: a mechanism of immunosuppression in cancer. J Immunol. 2001 Jan 1;166(1):678-89. doi: 10.4049/jimmunol.166.1.678. PMID: 11123353.
71. Steinman RM, Hawiger D, Nussenzweig MC. Tolerogenic dendritic cells. Annu Rev Immunol. 2003;21:685-711. doi: 10.1146/annurev.immunol.21.120601.141040. Epub 2001 Dec 19. PMID: 12615891.
72. Sharma MD, Baban B, Chandler P, Hou DY, Singh N, Yagita H, Azuma M, Blazar BR, Mellor AL, Munn DH. Plasmacytoid dendritic cells from mouse tumor-draining lymph nodes directly activate mature Tregs via indoleamine 2,3-dioxygenase. J Clin Invest. 2007 Sep;117(9):2570-82. doi: 10.1172/JCI31911. PMID: 17710230; PMCID: PMC1940240.
73. Ge W, Ma X, Li X, Wang Y, Li C, Meng H, Liu X, Yu Z, You S, Qiu L. B7-H1 up-regulation on dendritic-like leukemia cells suppresses T cell immune function through modulation of IL-10/IL-12 production and generation of Treg cells. Leuk Res. 2009 Jul;33(7):948-57. doi: 10.1016/j.leukres.2009.01.007. Epub 2009 Feb 23. PMID: 19233469.
74. Erba HP, Becker PS, Shami PJ, Grunwald MR, Flesher DL, Zhu M, Rasmussen E, Henary HA, Anderson AA, Wang ES. Phase 1b study of the MDM2 inhibitor AMG 232 with or without trametinib in relapsed/refractory acute myeloid leukemia. Blood Adv. 2019 Jul 9;3(13):1939-1949. doi: 10.1182/bloodadvances.2019030916. PMID: 31253596; PMCID: PMC6616264.
75. Zeng Z, Liu W, Tsao T, Qiu Y, Zhao Y, Samudio I, Sarbassov DD, Kornblau SM, Baggerly KA, Kantarjian HM, Konopleva M, Andreeff M. High-throughput profiling of signaling networks identifies mechanism-based combination therapy to eliminate microenvironmental resistance in acute myeloid leukemia. Haematologica. 2017 Sep;102(9):1537-1548. doi: 10.3324/haematol.2016.162230. Epub 2017 Jun 28. PMID: 28659338; PMCID: PMC5685227.
76. Pairawan S, Akcakanat A, Kopetz S, Tapia C, Zheng X, Chen H, Ha MJ, Rizvi Y, Holla V, Wang J, Evans KW, Zhao M, Busaidy N, Fang B, Roth JA, Dumbrava EI, Meric-Bernstam F. Combined MEK/MDM2 inhibition demonstrates antitumor efficacy in TP53 wild-type thyroid and colorectal cancers with MAPK alterations. Sci Rep. 2022 Jan 24;12(1):1248. doi: 10.1038/s41598-022-05193-z. PMID: 35075200; PMCID: PMC8786858.
77. Pedersen CB, Dam SH, Barnkob MB, Leipold MD, Purroy N, Rassenti LZ, Kipps TJ, Nguyen J, Lederer JA, Gohil SH, Wu CJ, Olsen LR. cyCombine allows for robust integration of single-cell cytometry datasets within and across technologies. Nat Commun. 2022 Mar 31;13(1):1698. doi: 10.1038/s41467-022-29383-5. PMID: 35361793; PMCID: PMC8971492.
78. Levine JH, Simonds EF, Bendall SC, Davis KL, Amir el-AD, Tadmor MD, Litvin O, Fienberg HG, Jager A, Zunder ER, Finck R, Gedman AL, Radtke I, Downing JR, Pe'er D, Nolan GP. Data-Driven Phenotypic Dissection of AML Reveals Progenitor-like Cells that Correlate with Prognosis. Cell. 2015 Jul 2;162(1):184-97. doi: 10.1016/j.cell.2015.05.047. Epub 2015 Jun 18. PMID: 26095251; PMCID: PMC4508757.
79. Johnson WE, Li C, Rabinovic A. Adjusting batch effects in microarray expression data using empirical Bayes methods. Biostatistics. 2007 Jan;8(1):118-27. doi: 10.1093/biostatistics/kxj037. Epub 2006 Apr 21. PMID: 16632515.
80. Blondel VD et al J. Fast unfolding of communities in large networks. Stat. Mech. (2008) P10008 DOI 10.1088/1742-5468/2008/10/P10008

Supplementary figures

Supplementary Figure 1

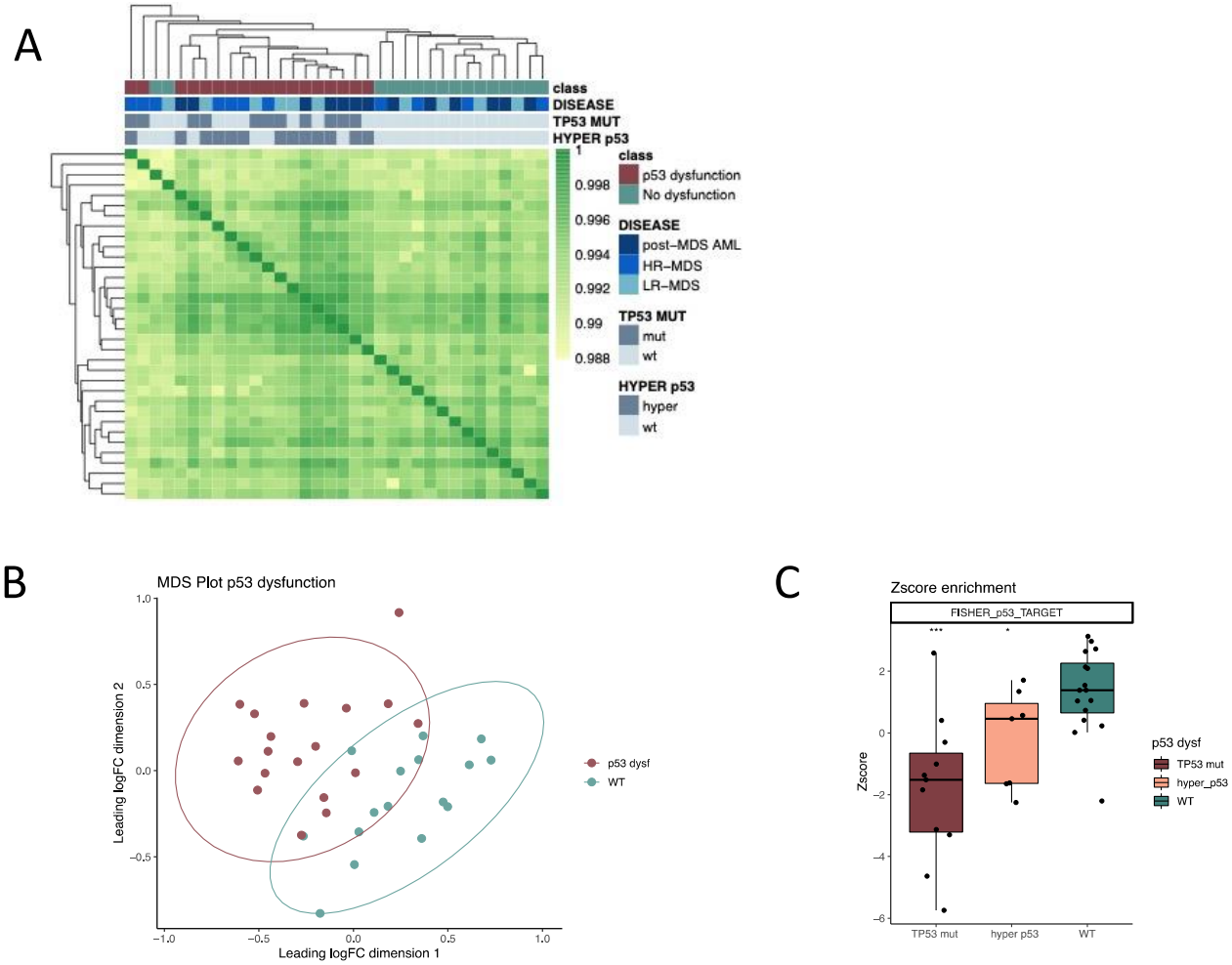

S1. *A) Unsupervised correlation plot obtained by RNA-Seq data. B) Multidimensional Scaling plot of RNA-Seq data. Each dot represents a patient. Brown dots highlight TP53 dysf patients, green dots wild type patients. C) Box plots of RNA-seq z-scores of p53 target signatures retrieved by MsigDB; In all box plots, the median is indicated by the horizontal line and the first and third quartiles are represented by the box edges. The lower and upper whiskers extend from the hinges to the smallest and largest values, respectively, with individual values included. * p<0.05; ** p<0.01; *** p<0.001; ns: not significant*

Supplementary Figure 2

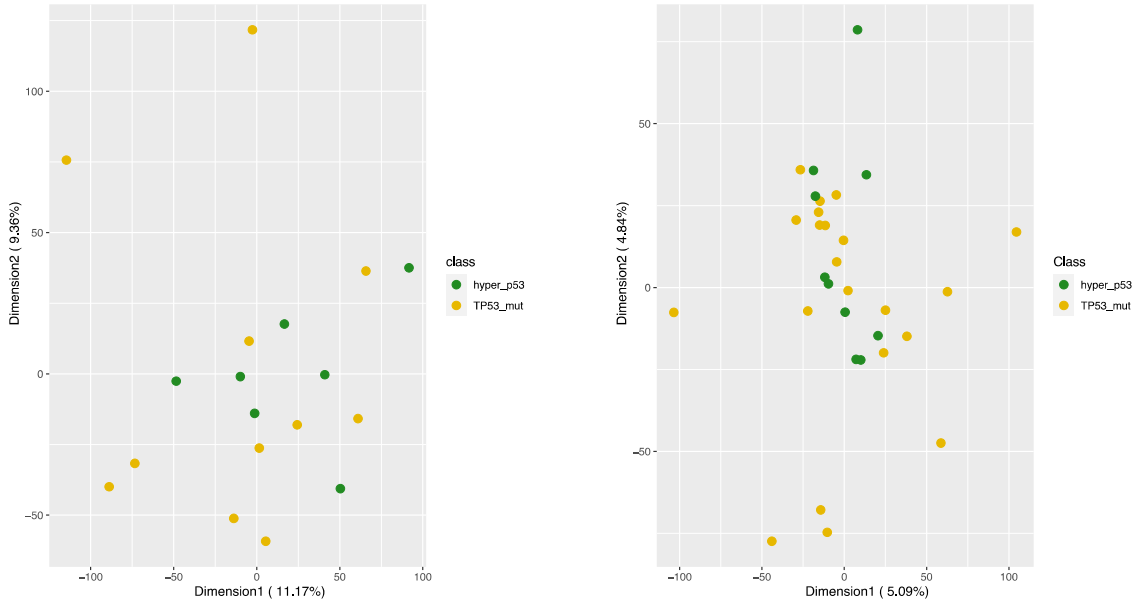

S2. *Multidimensional Scaling plot of RNA-Seq data of p53 dysfunction patients in principal cohort (on the right) and validation cohort (on the left). Each dot represents a patient. Yellow dots highlight TP53 mutated patients and green dots hyper mutated patients; PERMANOVA tests are not significant p=.227 and p= .342 respectively.*

Supplementary Figure 3

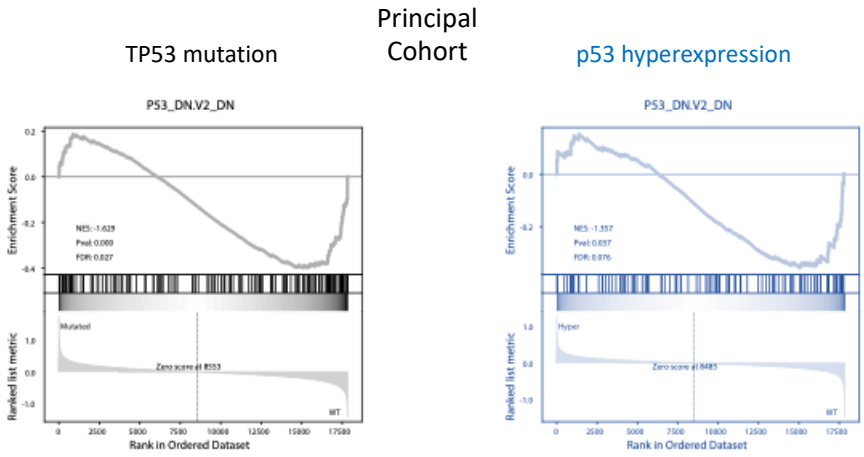

P<0.05, FDR <0.25

S3*. A) GSEA results of a P53 pathway related gene signature in principal cohort in the analysis TP53 mut vs WT and p53 hyperexpressed vs WT. In both plots, we observe a significant negative gene set enrichment in MDS samples harboring p53 dysfunction. NES, Normalized Enrichment Score.*

Supplementary Figure 4

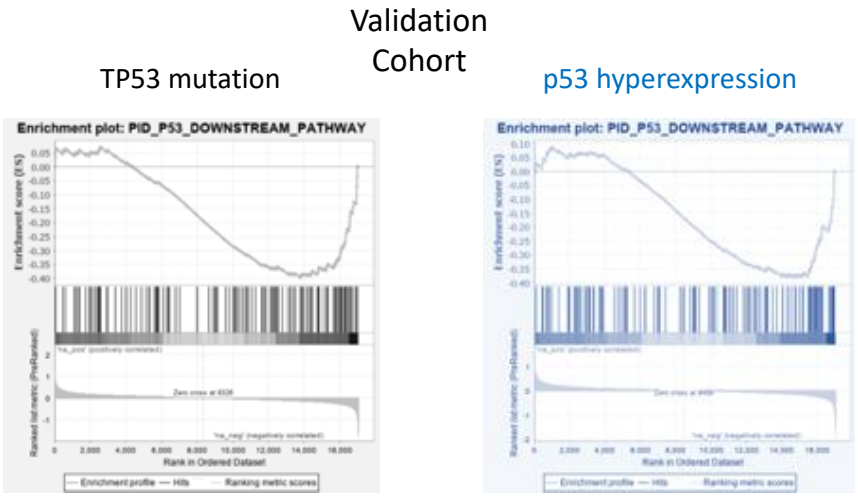

P<0.05, FDR <0.25

S4. *A) GSEA results of a P53 pathway related gene signature in validation cohort in the analysis TP53 mut vs WT and p53 hyperexpressed vs WT. In both plots, we observe a significant negative gene set enrichment in MDS samples harboring p53 dysfunction. NES, Normalized Enrichment Score.*

Supplementary Figure 5

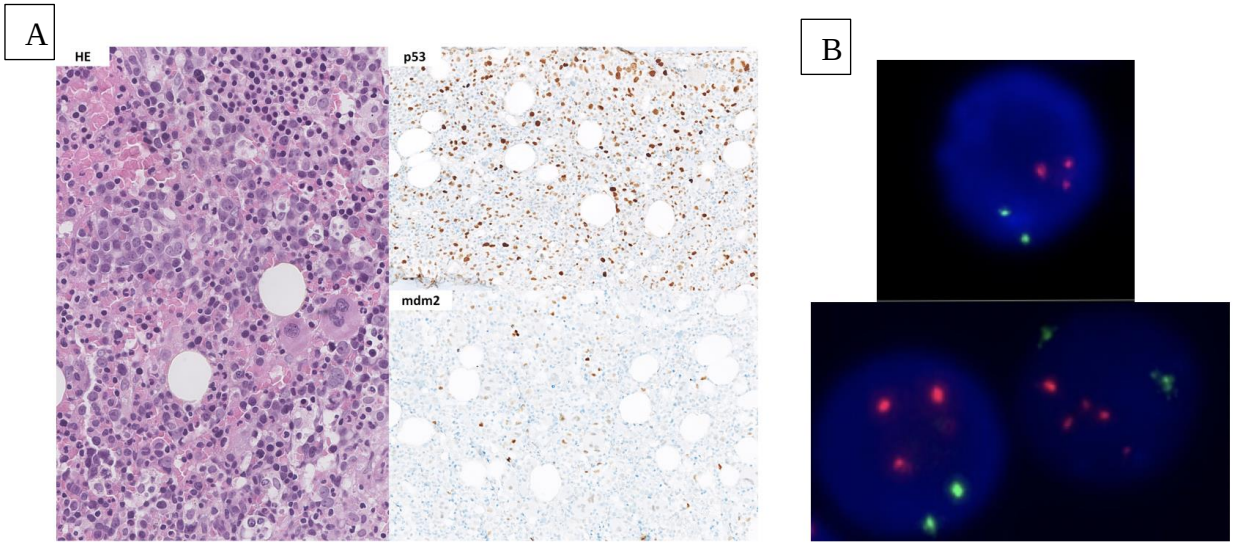

S5. *Trephine biopsy examination showed a left-shifted hematopoiesis with dysplasia (A), strong expression of p53 immunostain in more than 2% of bone marrow cells, and also nuclear positivity for mdm2, that could be linked to a gene amplification of MDM2, as assessed by FISH (B).*

Supplementary Figure 6

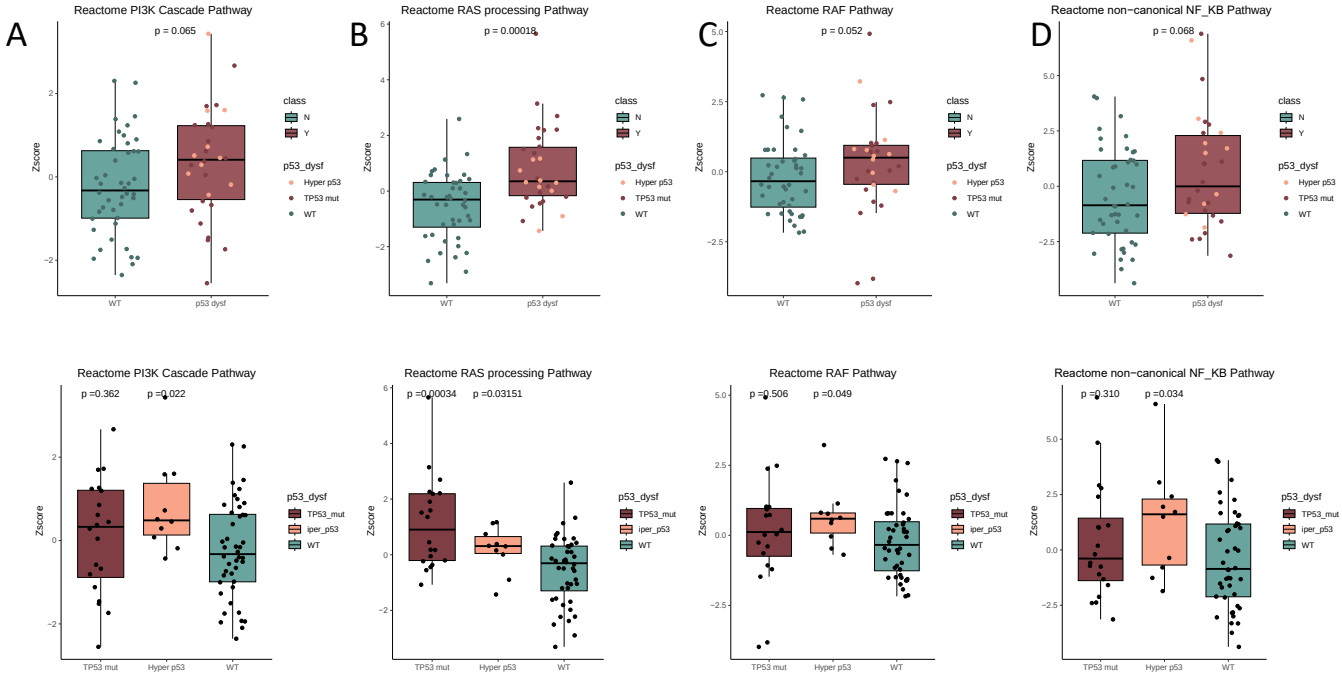

S6. *Box plots of RNA-seq z-scores of Reactome signatures retrieved by MsigDB;Samples are divided by the presence of p53 dysfunction (upper plots) or by the type of p53 dysfunction (lower plots);In all box plots, the median is indicated by the horizontal line and the first and third quartiles are represented by the box edges. The lower and upper whiskers extend from the hinges to the smallest and largest values, respectively, with individual values included. P-value of Mann-Whitney test is indicated in the figure.*

Supplementary Figure 7

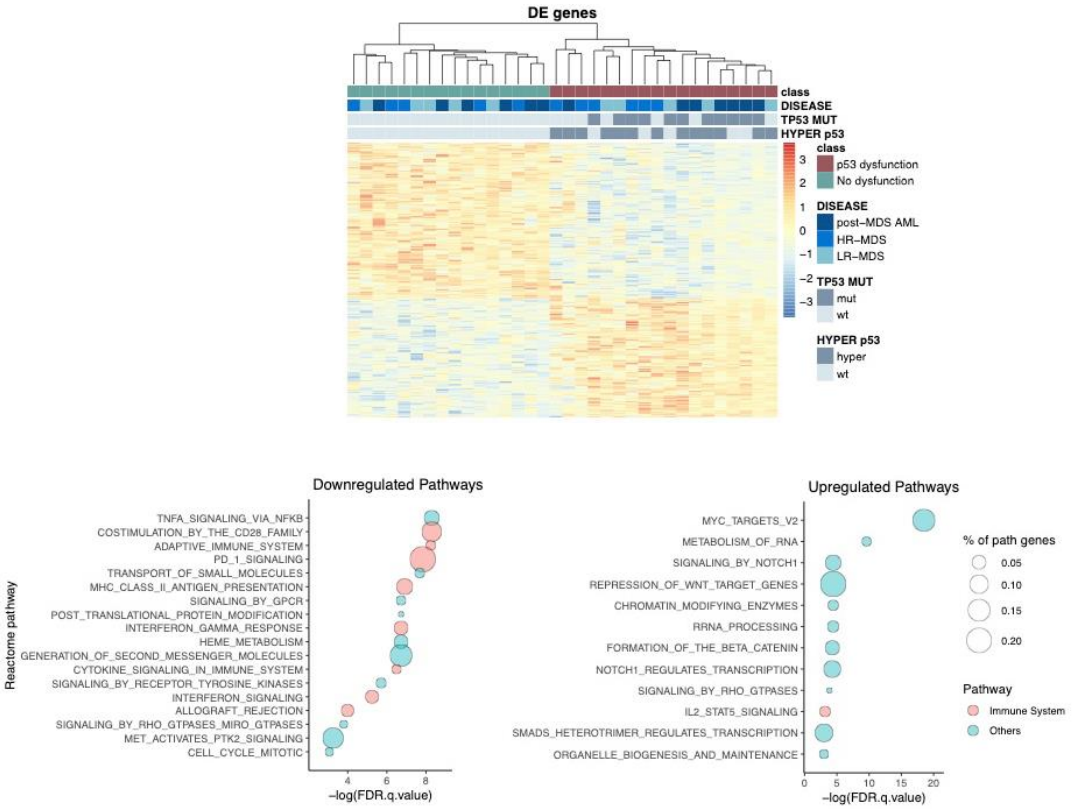

***S7**. A) Heatmap of differentially expressed genes. B) Functional enrichment analysis visualization: the dotplot depicts the activity of Reactome pathways starting from significant downregulated genes (on the left) or significant upregulated genes (on the right). Dot size indicates k/n ratio ("% of path genes"), where k is the number of genes participating in the pathway and n is the number of genes annotated as participants of any Reactome pathway. Dot color indicates if the pathway is related to the immune system or not. The x axis represents the log of the enrichment test FDR (Hypergeometric test).*

Supplementary Figure 8

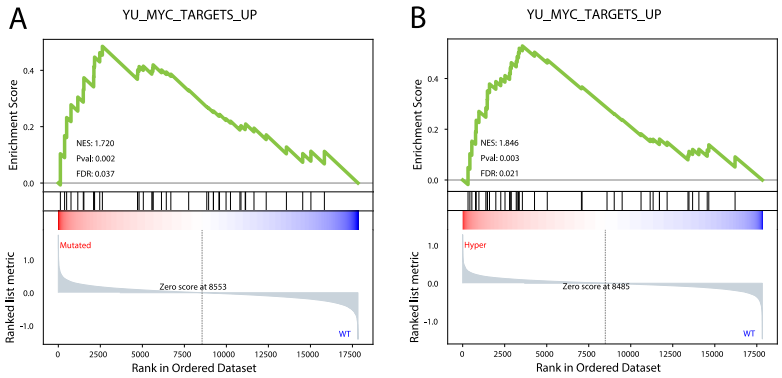

***S8.** A) GSEA results of a Myc targets signature in the analysis TP53 mut vs WT (A) and p53 hyperexpressed vs WT (B). In both plots, we observe a significant positive gene set enrichment in MDS samples harboring p53 dysfunction. NES, Normalized Enrichment Score.*

Supplementary Figure 9

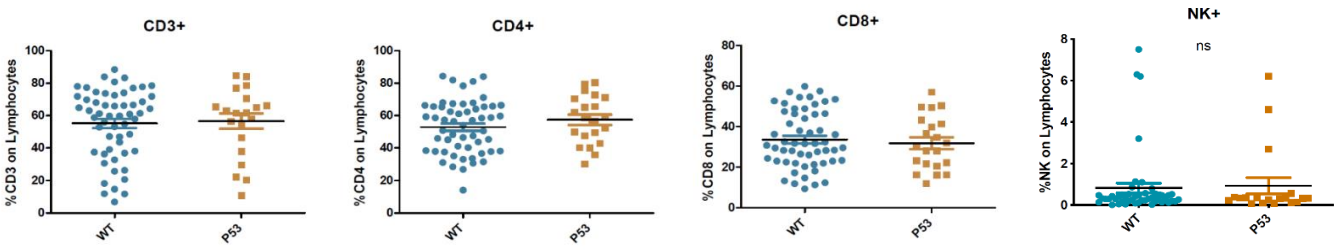

***S9**. CD3+, CD4+, CD8+ and NK cells percentage on total lymphocyte in p53 dysfuntion vs WT samples.*

Supplementary Figure 10

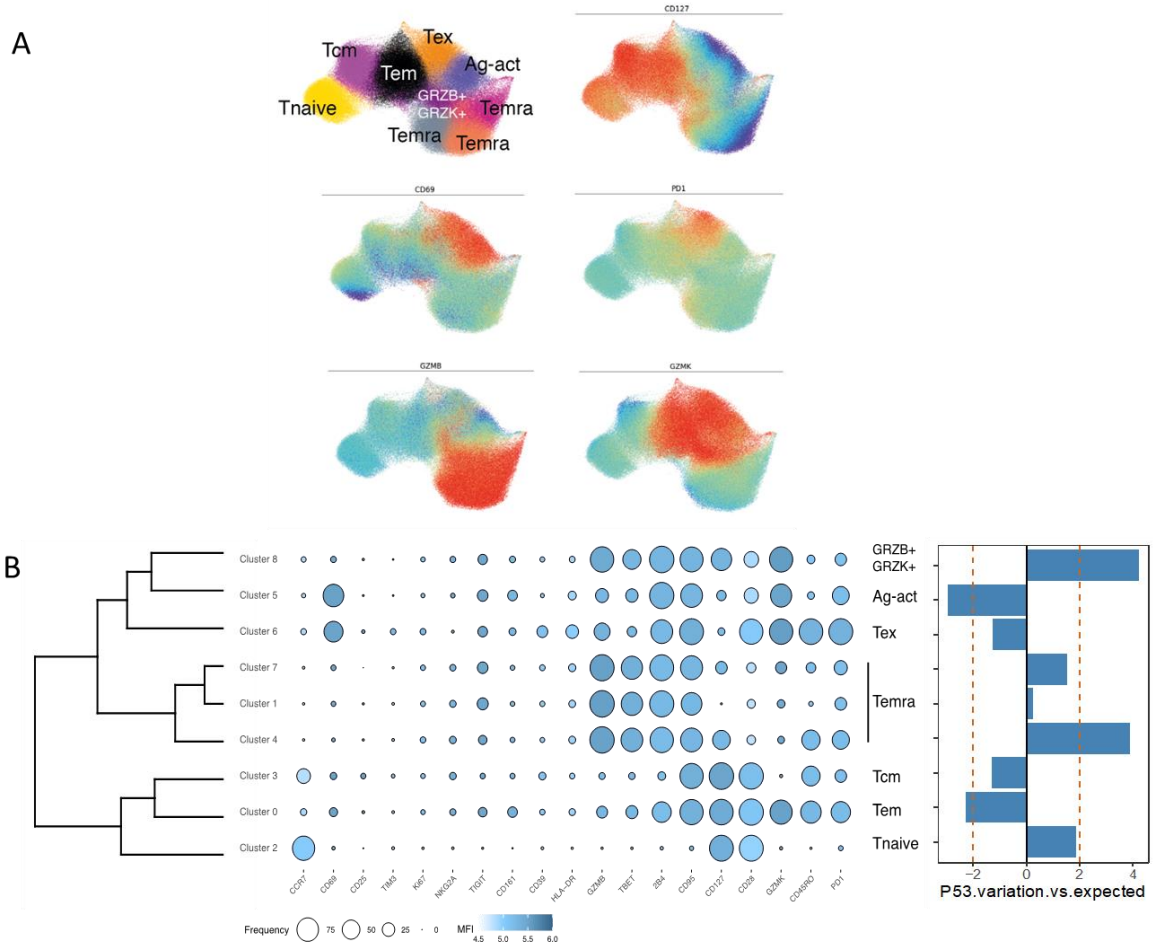

***S10**. A) UMAP plot depicting CD8+ T cell heterogeneity. PhenoGraph clustering was performed using concatenated CD3+ CD4- CD8+ T cells (3.000 cells/sample) from 76 BMMNCs (21 p53 dysfunction vs 55 WT). Cells are colored according to the 13 clusters identified by Phenograph in an unsupervised manner. Other UMAP plots show the expression of selected markers among CD8+ T cells. B) Balloon plot showing the percent expression and the median fluorescence intensity (MFI) of specific markers (columns) in each PhenoGraph clusters (rows). Barplot on the right shows the variation of p53 dysfunction cells frequency from expected frequency for each cluster.*

Supplementary Figure 11

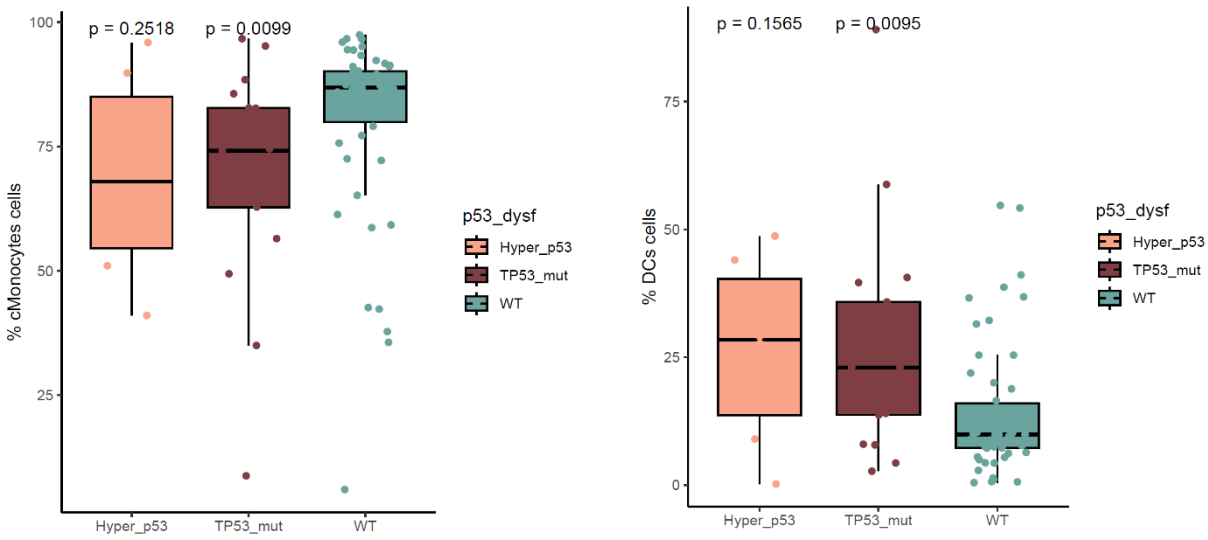

S11. *Classical monocytes (left) and Dendritic cells (right) percentage on total CD33^{+} Myeloid cells in p53 hyper-expressed, TP53^{mut} and WT samples.*

Supplementary Figure 12

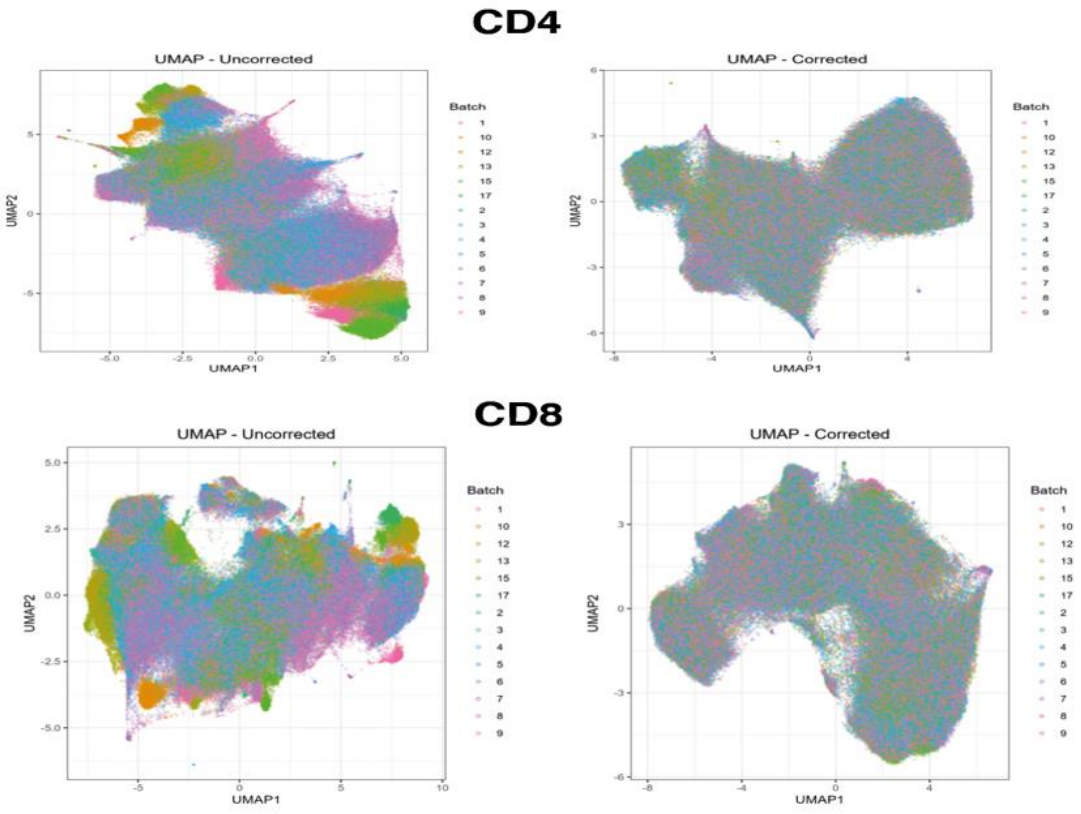

S12. *UMAP plot before and after cyCombine batch correction in CD4+ and CD8+ T cells*

Supplementary tables

Supplementary table 1 **-** List of antibodies used for the analysis of T cells.

fluorochrome	antibody	Company	Catalogue	Lot. N
BV510	**hCD14**	BioLegend	301842	B265263
APC	**hCD71**	BD	551375	8297711
BUV737	**hCD28**	BD	564438	8236693
PerCP-eF710	**hTIGIT**	eBioscience	46-9500-42	1993643
BV605	**hCD161**	Biolegend	339916	B265242
BV421	**hPD1 (CD279)**	BioLegend	329920	B263659
BUV496	**hCD3**	BD	564809	9037570
PECy5.5	**hCD244 (2B4)**	Beckman Coulter	B21171	200030
PE-Cy5	**hCD127**	eBioscience	15-1278-42	2025251
BV711	**hCD95**	Biolegend	305644	B270181
BUV395	**hCD69**	BD	564364	8242749
PE-CF594	**hCD197 (CCR7)**	BD	562381	8270954
APC-Cy7	**hCD39**	Biolegend	328226	B277400
BV570	**hCD45RO**	BioLegend	304226	B280396
BUV805	**hCD8**	BD	564912	9030908
VioBright FITC	**CD159a (NKG2A)**	Miltenyi	130-113-568	8190603637
BV786	**hCD25**	BD	741035	9150522
BUV661	**hHLA-DR**	BD	565073	9060584
BV650	**hCD366 (TIM3)**	BD	565564	9046621
BUV615	**hCD4**	BD	624297	9101901
BV480	**hKi67**	BD	566109	8274704
PE	**hGranzyme K**	Santa Cruz	sc-56125	E2214
AF700	**hGranzyme B**	BD	560213	9002854
PE-Cy7	**hT-bet**	eBioscience	BMS25-5825-82	1995491

Supplementary table 2 **-** List of antibodies used for the analysis of NK cells.

fluorochrome	antibody	Company	Catalogue	Lot. N
FITC	**CD20**	Biolegend	302304	B218411
BV650	**Vdelta2**	BD	743752	9129618
PE-Vio770	**NKG2A**	Miltenyi	130-113-567	5190314532
BV570	**CD8a**	Biolegend	301038	B262531
BV510	**CD14**	BioLegend	301842	B265263
BV421	**vd1**	Miltenyi	130-100-553	5190603572
BUV737	**CD16**	BD	564434	8260751
BUV661	**CD3**	BD	565065	9070786
BUV563	**CD56**	BD	565704	9022780
FITC	**FcERI**	Biolegend	334608	B226717
FITC	**CD19**	BD	345776	9016952
BV605	**CD57**	BD	393304	B277530
BUV395	**CD158b1b2j**	BD	743456	9129609
PE-CF594	**CD69**	BD	562617	8208742
FITC	**CD34**	Biolegend	343604	B241061
APC-e780	**CD127**	eBioscience	47-1278-42	1978210
AF700	**NKG2C**	R&D	FAB138N	ACUA0217121
APC	**NKp46**	BD	558051	8151558
BV786	**CD117**	BioLegend	313238	B271292
BV711	**PD-1**	BD	564017	8164557
FITC	**CD33**	Biolegend	303304	B217222
FITC	**CD203c**	Biolegend	324614	B267681
PE-Cy5	**NKp30**	BC	A66904	23
FITC	**CD15**	BC	B36298	13
PerCP-Cy5,5	**CRTh2**	Biolegend	350116	B266750
PE	**CD94**	BD	555889	7174991

SF3B1 splicing mutations distinctly shape monocyte signatures in lower-risk myelodysplastic Neoplasms

Susann Winter, Marie Schneider, Uta Oelschlaegel, Giulia Maggioni, Elena Riva, Marco Gabriele Raddi5, Sara Bencini, Benedetta Peruzzi, Desmond Choy, Rita Antunes Dos Reis, Jessica Timms, Nicolas Sompairac, Antje Tunger, Matteo Giovanni Della Porta, Valeria Santini, Marc Schmitz, Uwe Platzbecker, Shahram Kordasti

Introduction

Somatic mutations in the splicing factor SF3B1 occur in 25% of all MDS cases and arise early in MDS development. In fact, SF3B1-driven clonal hematopoiesis is almost invariably associated with anemia and usually progresses to overt MDS characterized by ring sideroblasts (RS), ineffective erythropoiesis, and an indolent disease course in lower-risk (LR) MDS [1–5]. The impact of SF3B1 mutations on erythroid progenitors has become apparent but much less is known about cellular immune phenotypes downstream of SF3B1 mutations [6–8]. SF3B1 change-of-function mutations in MDS and other cancers promote alternative 3' splice site selection, generating a complex repertoire of aberrant transcripts [9]. These mutations are typically heterozygous missense substitutions, which most frequently (> 50%) involve p.K700E [10] (SF3B1 NM_012433.4: c.2098A>G (p.Lys700Glu), henceforth referred to as $SF3B1^{K700E}$) and appear to affect splicing in MDS in a hematopoietic cell type-specific manner [11]. Differential splicing has been shown to contribute to disease phenotypes and may support the oncogenic phenotype of SF3B1-mutant MDS [6,11–16]. In particular, mutant SF3B1 induces missplicing of important genes throughout erythroid differentiation, including RS driver genes, resulting in erythroid dysplasia with RS and anemia [7,8,16]. SF3B1 mutations target multipotent lymphomyeloid hematopoietic stem cells and are clonally propagated to myeloid progenitors [17], yet their impact on myeloid phenotype and function remains largely unexplored [17,18]. In general, morphologic dysplasia of myeloid cells in SF3B1-mutant MDS with multilineage dysplasia is very mild without significant effects on peripheral cytopenia [5]. Mutations in SF3B1 may, however, alter the magnitude or nature of innate and adaptive antitumor immune responses via altered splicing of key regulatory genes [19,20]. The clinical consequences of SF3B1 mutations and mutation subtype are emerging [21–23]. Recent data suggest that different hotspots may produce divergent disease consequences. Specifically, only the $SF3B1^{K700E}$ mutation subtype independently predicted better overall survival in MDS [22]. In contrast, the p.K666N hotspot mutation associated with increased progression of MDS and these patients may need more aggressive management than patients with other SF3B1 mutations [23]. Regarding treatment, patients with SF3B1 mutations show high response rates to the erythroid maturation agent luspatercept [24,25]. Conversely, mutations in SF3B1 negatively predicted response to immunosuppressive treatment with anti-thymocyte globulin-based combination regiments in MDS [26,27]. Thus, identification of patient characteristics downstream of the pathogenic mutations in SF3B1 may reveal immunological determinants of disease phenotype and response to therapeutic interventions. In the present study, we applied multiplex immunophenotyping technologies in combination with machine learning-based analytical approaches to identify genotype-immunophenotype correlations that may affect disease course and clinical outcomes in SF3B1-mutant MDS. We further investigated the prevailing immunophenotype of classical monocytes on the transcriptional level to evaluate functional impairment.

Material and Methods

Patient cohort

Overall, bone marrow (BM) and peripheral blood (PB) samples from 168 MDS patients were analyzed for this study. We first analyzed BM/PB samples from 37 mostly treatment-naïve MDS patients (experimental cohort: 19 $SF3B1^{mut}$, 18 $SF3B1^{wt}$; Supplemental Figure 1 and Supplemental Table 1 summarize somatic mutational data, performed analyses, clinical characteristics) and hematologically healthy donors (HD). Additionally, we validated findings in two independent cohorts comprising 131 treatment-naïve MDS patients (validation cohort 1: 28 $SF3B1^{mut}$, 39 $SF3B1^{wt}$; validation cohort 2: 32 $SF3B1^{mut}$, 32 $SF3B1^{wt}$; Supplemental Figure 6), including HD as reference. Biosamples from the experimental cohort were collected with approval from local ethics committees at the University Hospitals Dresden and Leipzig under broad research informed consent with unspecified future use as part of the MDS registry (EK289112008) or BoHemE study (EK393092016, 137/19-lk). The study of biosamples from the validation cohorts was approved by the Independent Ethics Committee of Humanitas Clinical Institute [validation cohort 1; n. 2175/AIRC-IG-2018-Rif. 22053] and the Comitato Etico Area Vasta Centro [validation cohort 2; Em. 2020-298 Rif. CEAVC Studio 6277_oss (già 14.104)]).

NanoString gene expression analysis

Total RNA was isolated with the AllPrep DNA/RNA Kit (QIAGEN, Germantown, MD, USA) from fresh BM mononuclear cells (BM-MNCs) separated by density centrifugation in Ficoll-Paque PLUS (GE Healthcare, Chicago, IL, USA). The expression levels of 770 genes were analyzed using the nCounter®PanCancer Immune Profiling Panel (NanoString Technologies, Inc., Seattle, WA, USA). Quality-checked raw data were background-subtracted and normalized using the NanoString nSolver 4.0 software and default settings. Differential expression of genes was inferred by fitting generalized linear models using the R package edgeR (http://bioconductor.org). Genes with false discovery rate (FDR) < 0.05 were considered significant. Pathway and process enrichment analysis of differentially expressed genes (DEG) was performed using the web-based Metascape resource (http://metascape.org) [28] as described in Supplemental Methods. The list of DEG was further analyzed by Ingenuity Pathway Analysis (IPA) core analysis (QIAGEN).

CyTOF and clinical flow data analysis

Viably frozen BM-MNCs were thawed and stained with a customized Maxpar Direct Immune Profiling Assay (Standard BioTools Inc., CA, USA), employing a CD45-based barcoding approach for multiplex Cytometry by Time-of-Flight (CyTOF). Debarcoded CyTOF data (live $CD45^+$ cells or further gated subpopulations as indicated) were concatenated at the group level (LR-MDS [IPSS-R ≤ 3.5] vs. HD, $SF3B1^{K700E}$ vs. $SF3B1^{wt}$) using a customized R-based script, then arcsinh-transformed using a cofactor of 5, and analyzed with the Tracking Responders Expanding (T-REX) algorithm [29]. T-REX provides a rapid, unsupervised machine learning approach that combines Uniform Manifold Approximation and Projection (UMAP), k-Nearest Neighbour Classification (KNN), and Marker Enrichment Modeling (MEM) to reveal regions of great difference between patients. For our setting, we adapted the publicly available script (https://github.com/cytolab/T-REX) to calculate the percentage of cells within the identified regions for individual patients. For validation, we retrieved flow cytometric data on fresh BM/PB samples acquired independently as part of the diagnostic work142 (experimental cohort/validation cohort 2) or cryopreserved BM-MNCs (validation cohort 1), and analyzed monocyte subsets by expert manual gating.

Transcriptional analysis of monocytes using RNA-seq

Classical monocytes ($CD14^+$ $CD16^-$) were isolated from viably frozen PB mononuclear cells (PBMCs). Initially, we also tried to isolate this monocyte subset from viably frozen BM-MNCs but monocyte cell counts were variable and often too low for downstream experiments. We used a two-step isolation procedure. After

depletion of $CD16^+$ cells using CD16 MicroBeads, $CD14^+$ monocytes were magnetically separated using CD14 MicroBeads over two sequential LS columns (Miltenyi Biotec, Bergisch Gladbach, Germany), yielding routinely >95% $CD14^+$ $CD16^-$ monocytes based on flow cytometric assessment. Monocytes (195000 – 500000 cells per 96-well in 250 µl RPMI 1640/PenStrep [Life Technologies Corp., NY, USA]/5% heat-inactivated human serum [Sigma-Aldrich, MO, USA]) were then stimulated with 100 ng/mL LPS (#L3024, Sigma-Aldrich) for 4 hours or left untreated. Following RNA isolation with TRIzol and Direct-zol™ RNA Microprep (Zymo Research, Irvine, CA, USA), mRNA library preparations and sequencing reactions were conducted at GENEWIZ, LLC. A detailed description of the RNA-seq protocol and downstream data analysis (EBSeq [30], rMATS [31]) is provided in Supplemental Methods.

Results

Patients with SF3B1 mutations exhibit a distinct immune gene signature in the bone marrow

The initial transcriptional profiling of more than 700 immune-related genes identified 110 DEG between $SF3B1^{mut}$ and $SF3B1^{wt}$ BM samples (66 down-/44 upregulated, Supplemental Table 4). Pathway and process enrichment analysis of DEG showed that the majority of the downregulated genes in $SF3B1^{mut}$ patients were related to lymphocyte (T, B, and NK cell) function, whereas upregulated genes were mainly related to myeloid cell function and innate host defense (Figure 1A). Gene expression of key cell markers for T (CD3D) and B cells (CD79A) correlated positively with the percentage of BM $CD3^+$ T (Spearman, R = 0.6; p = 0.0073) and $CD19^+$ B cells (Spearman, R = 0.78; p =7.5e-05) assessed by diagnostic flow cytometry of corresponding fresh BM samples, respectively, indicating that lower relative lymphocyte frequencies in $SF3B1^{mut}$ BM may account for differential expression of lymphocyte-related genes. $SF3B1^{mut}$ BM samples exhibited predicted reduced activity of several canonical pathways pertaining to T cell immune responses and adaptive immunity (Figure 1B). On the other hand, upregulation of myeloid cell-related genes in SF3B1mut BM (e.g. CYBB, NCF4, CEACAM8, CSF1R, S100A8, S100A12, Supplemental Table 4) implied a myeloid bias, as also evidenced by significantly higher absolute monocyte counts in PB compared to $SF3B1^{wt}$ MDS (Supplemental Table 1). Upregulated genes in $SF3B1^{mut}$ MDS further included genes related to immune regulation/immunosuppression (ARG1/2, ADORA2A, AXL), cell cycle (CDK1, CCND3, BIRC5), stress induced responses (MICB, ATG7), and apoptosis regulation (BIRC5, CASP10, IGFR1) (Supplemental Table 4). Despite the prevailing myeloid gene signature, $SF3B1^{mut}$ BM exhibited significantly reduced expression of IL1β, a gene transcriptionally induced in myeloid cells upon activation. Overall, the mRNA expression levels of IL1β showed no correlation with the frequency of BM monocytes assessed by flow cytometry of corresponding fresh samples (Spearman, R = 0.062; p = 0.8) or the monocyte marker gene CD14 (R = 0.24; p = 0.33). However, lower levels of IL1β in $SF3B1^{mut}$ BM correlated with lower expression of inflammatory genes, including NLRP3 (R = 0.74; p = 0.00043), CXCL5 (R = 0.59; p = 0.0073), and NFKB1/2 (R = 0.61, p = 0.0071; R = 0.68, p = 0.0017, respectively). IPA-based pathway analysis further suggested that pathways pertaining to inflammatory cytokine signaling (e.g. Pathogen Induced Cytokine Storm Signaling Pathway, NFkB Signaling) and myeloid activation (e.g. Dendritic Cell Maturation, Macrophage Classical Activation Signaling Pathway) were less activated in $SF3B1^{mut}$ BM (Figure 1B). Overall, these results point toward a myeloid-biased gene signature, yet less pronounced myeloid-driven inflammation in this patient subgroup.

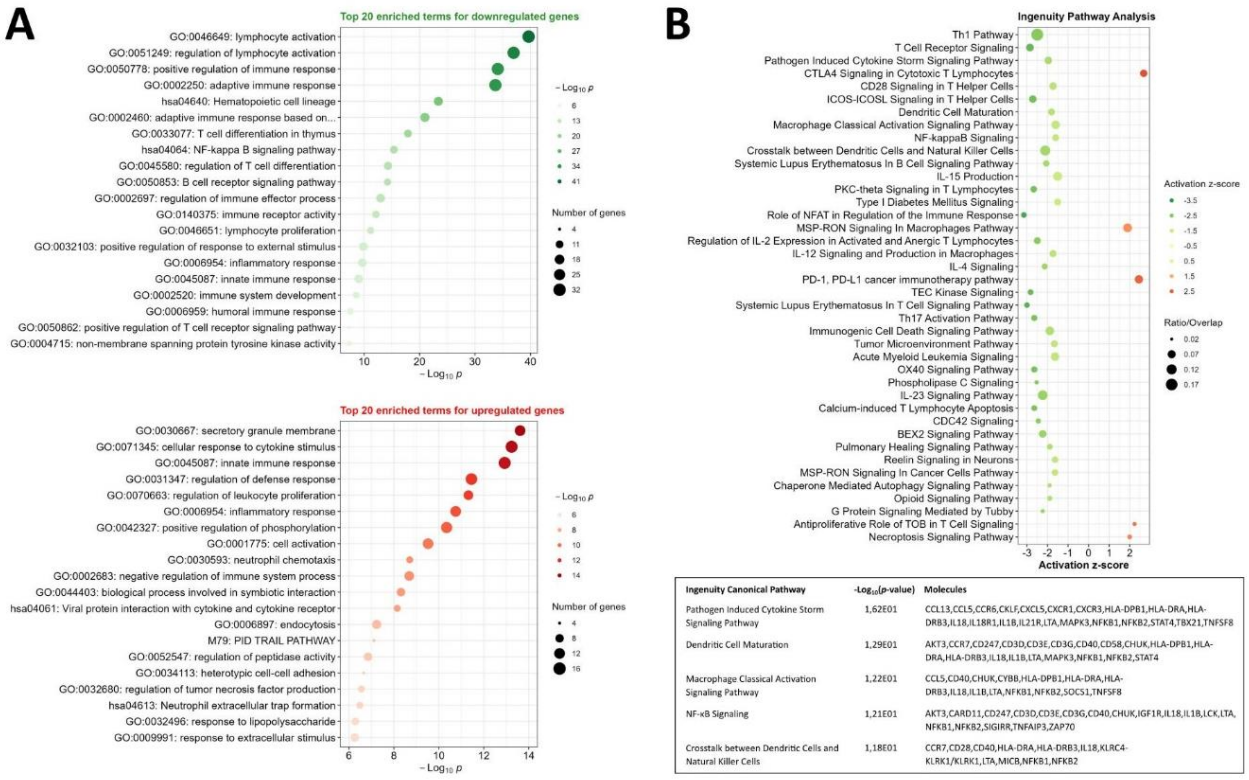

Figure 1. Transcriptional immune profiling using bulk bone marrow samples fromSF3B1^{mut} compared to SF3B1^{wt} MDS. (A) Pathway and process enrichment analysis (top 20 representative terms) of down and upregulated genes in SF3B1^{mut} (n = 9 SF3B1^{K700E} and n = 3 SF3B1^{nonK700E}, mean age = 71 years) compared to SF3B1^{wt} (n = 7, mean age = 62 years) bulk BM samples profiled using the NanoStringnCounter® PanCancer Immune Profiling Panel. (B) IPA core pathway analysis showing the predicted activity (cutoff z-score of > |1.5|) of overrepresented annotations (p-value < 0.05 [right-tailed Fisher's exact test]) based on the list of DEG in SF3B1^{mut} compared to SF3B1^{wt} BM samples. For selected pathways, DEG overlapping the pathway are listed.

High-dimensional immunophenotyping of SF3B1^{K700E} LR-MDS reveals distinct cluster of monocytes in the bone marrow

Next, we performed high-dimensional CyTOF coupled with unsupervised T-REX-based data analysis to identify the immunophenotypic differences in the BM associated with LR-MDS in general and with SF3B1^{K700E} LR-MDS in particular. First, we explored immunophenotypic changes evident in 14 LR-MDS patients compared to HD (n = 4). As expected, LR-MDS displayed several immunophenotypic changes consistent with an activated immune response in the presence of MDS precursor clones (Figure 2A-B, Supplemental Figure 2). This included a heterogeneous cluster of CD4$^+$ T cells (cluster 195) in LR-MDS (Figure 2B). We further gated CD4$^+$ T cell subsets, which revealed a significantly reduced proportion of naïve CD4$^+$ T cells (TNV) in LR-MDS compared to HD (Supplemental Figure 3). LR-MDS samples further comprised specific clusters resembling terminally differentiated effector memory CD8$^+$ T cells (TTE/TEMRA, cluster 1295), mature CD57$^+$ NK cells (cluster 2495), CD27$^+$ IgD- memory B cells (cluster 795), and γδ T cells exhibiting an exhausted immunophenotype (coexpressing TIGIT and PD-1, cluster 1395), respectively. Consistent with this, we found a higher proportion of TTE/TEMRA CD8$^+$ T cells and an increase in the frequency of overall NK as well as CD57$^+$ NK cells in LR-MDS (Supplemental Figure 3). Within the monocytic lineage, we observed aberrant expression of CD56 (clusters 1495, 295) (Supplemental Figure 2), which has been well documented in MDS [32]. Subsequently, we explored the immunophenotypic changes specific to SF3B1^{K700E} (n = 5) compared to SF3B1^{wt} (n = 9) LR-MDS. T-REX analysis of CD45$^+$ BM-MNCs identified a SF3B1^{K700E}-specific cluster comprising CD33$^+$

CD14^{+} cells (cluster 495, $p < 0.01$) (Figure 2C-D, Supplemental Figure 4). Further analysis of pre-gated CD33^{+} CD14^{+} cells showed that a remarkable proportion of the monocytes in SF3B1^{K700E} LR-MDS adopt a HLA-DR$^{low/neg}$ phenotype (median = 10.7%, IQR = 16.9 vs. median = 0.9%, IQR = 1.0 in SF3B1wt, $p < 0.05$) (Figure 2E-F). Some SF3B1^{K700E} samples contained a cluster of naïve CD4^{+} T cells (cluster 3895) featuring lower expression of the co-stimulatory molecule CD27 (MEM score CD27^{+1}), which is involved in cellular activation (Supplemental Figure 4). Additional gating of naïve CD4^{+} T cells (TN) confirmed that CD27 expression tends to be higher in SF3B1^{wt} LR-MDS, possibly a result of transient upregulation upon recent T cell activation [33], but was comparable between SF3B1^{K700E} LR-MDS and HD (Supplemental Figure 3C and 4). T-REX also revealed specific immunophenotypes evident in some SF3B1^{wt} LR-MDS that were not expanded in other SF3B1^{wt} patients, including clusters resembling mature CD57^{+} NK cells (cluster 1305) and more differentiated memory CD8^{+} T cells (cluster 1005) (Figure 2C-D, Supplemental Figure 4). Overall, our results point out a distinct cluster of monocytes in the BM of SF3B1^{K700E} LR-MDS, which is characterized by lower surface expression of the MHC class II molecule HLA-DR. LR-MDS-related shifts in CD4^{+} and CD8^{+} T cell differentiation are noticable, yet naïve CD4^{+} T cells in SF3B1^{K700E} patients showed subtle immunophenotypic differences indicative of less recent activation.

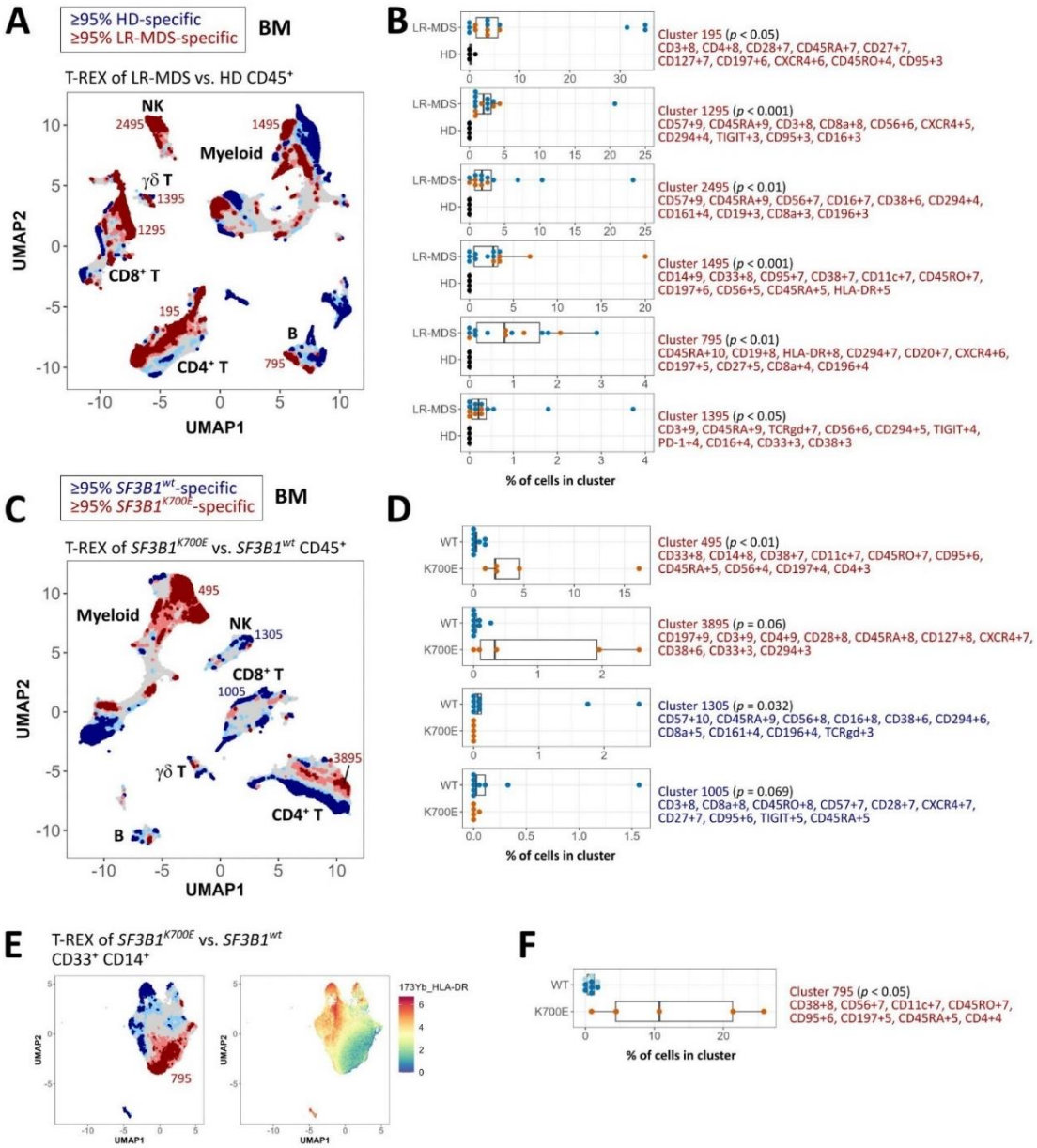

Figure 2. High dimensional single-cell profiling of the bone marrow immune landscape in SF3B1^{K700E} LR-MDS. (A) T-REX plot of regions of significant change on Uniform Manifold Approximation (UMAP) axes for CD45+ BM-MNCs stained for CyTOF showing distinct LR-MDS-specific (dark red, ≥ 95% of cells are contributed by LR-MDS samples) and HD-specific (dark blue, ≥ 95% of cells are contributed by HD) cell clusters. 14 LR-MDS (mean age = 74 years, 4 women, 10 men) and 4 HD (mean age = 58 years, all men) were included in the analysis. (B) Top 10 Marker Enrichment Modeling (MEM) labels with enrichment scores are shown for statistically significant (i.e. commonly found) LR-MDS-specific clusters (cutoff > 2000 cells) indicated on T-REX plot in (A). LR-MDS group comprises SF3B1^{K700E} (n = 5, orange dots; mean age = 75 years, 2 women, 3 men) and SF3B1^{wt} (n = 9, blue dots; mean age = 74 years, 2 women, 7 men) patients. (C) T-REX analysis of CD45^{+} BM-MNCs stained for CyTOF showing distinct SF3B1^{K700E}-specific (dark red) and SF3B1^{wt}-specific (dark blue) cell clusters. (D) Top 10 MEM labels are shown for statistically significant and trend clusters (cutoff > 1000 cells) indicated on T-REX plot in (C). (E, F) T-REX analysis of CD33^{+} CD14^{+} pre-gated monocytes showing SF3B1^{K700E}-specific (dark red) and SF3B1^{wt}-specific (dark blue) clusters. Cluster 795 depicts a distinct monocyte subset in SF3B1^{K700E} LR565 MDS (NOTE: this cluster is not related to cluster 795 shown in (B)). (A, C) Labels on T-REX plot indicate major immune cell subsets (Myeloid, myeloid cells; NK, NK cells; γδ, γδT cells; CD4^{+} and CD8^{+} T cells). (B, D, F) Mann-Whitney-U-test/Wilcoxon-test was performed for indicated clusters ($p < 0.05$ was considered significant; p-values are shown in brackets). Box plots depict median, IQR (lower and upper hinges), and 1.5 * IQR (lower and upper whiskers).

Monocytes from SF3B1-mutant MDS frequently display diminished HLA-DR expression

To confirm the presence of HLA-DR$^{low/neg}$ monocytes in SF3B1^{mut} MDS, we retrospectively analyzed diagnostic flow data collected on fresh BM samples from a larger cohort of LR and higher-risk (HR) patients (18 SF3B1^{mut}, 16 SF3B1^{wt}), comprising mainly SF3B1^{K700E} MDS (n = 14). In line with the CyTOF data, we found an increased frequency of HLA-DR$^{low/neg}$ monocytes, accounting for more than one third of the CD33^{+} CD14^{+} monocytes in the majority of SF3B1^{mut} BM samples (median = 35.6%, IQR = 34.85 vs. median = 6.25%, IQR = 11.15 in SF3B1^{wt}, $p < 0.001$) (Figure 3A-B). Higher frequencies of HLA-DR$^{low/neg}$ monocytes correlated positively with the mutational burden of SF3B1, while co-occuring mutations in TET2 or DNMT3A and the IPSS-R showed no correlation (Figure 3C). A significant increase in the proportion of HLA-DR$^{low/neg}$ monocytes was also detectable in BM and PB of SF3B1^{mut} MDS compared to HD ($p < 0.05$ and $p < 0.001$, respectively) (Figure 3A-B, Supplemental Figure 5A). Among studied patients, we found a strong correlation between BM and PB regarding HLA-DR$^{low/neg}$ monocyte frequencies (Supplemental Figure 5B). The CD14^{+} HLA-DR$^{low/neg}$ BM monocytes in SF3B1^{mut} MDS were mainly classical monocytes based on the absent surface expression of CD16 (≤ 0.4% CD16+) (Supplemental Figure 5C). Conversely, the proportion of CD16^{+} intermediate/non-classical monocytes was increased in the majority of SF3B1^{wt} compared to SF3B1^{mut} LR-MDS (median = 27.95%, IQR = 15.025 vs. median = 9.9%, IQR = 6.6, $p < 0.05$) and HD (median = 5.3%, IQR = 9.5, $p < 0.01$) (Figure 3D), whereas no difference was observed for HR (IPSS-R > 3.5) patients (data not shown). Analysis of available longitudinal data for 4 SF3B1^{K700E} patients showed a consistently high frequency of HLA-DR$^{low/neg}$ monocytes (Figure 3E). Importantly, external validation in two independent patient cohorts, which combined included 131 MDS patients, confirmed an increased frequency of HLA-DR$^{low/neg}$ monocytes in SF3B1mut (SF3B1^{K700E} and SF3B1^{nonK700E}) compared to SF3B1^{wt} LR-MDS (Supplemental Figure 6).

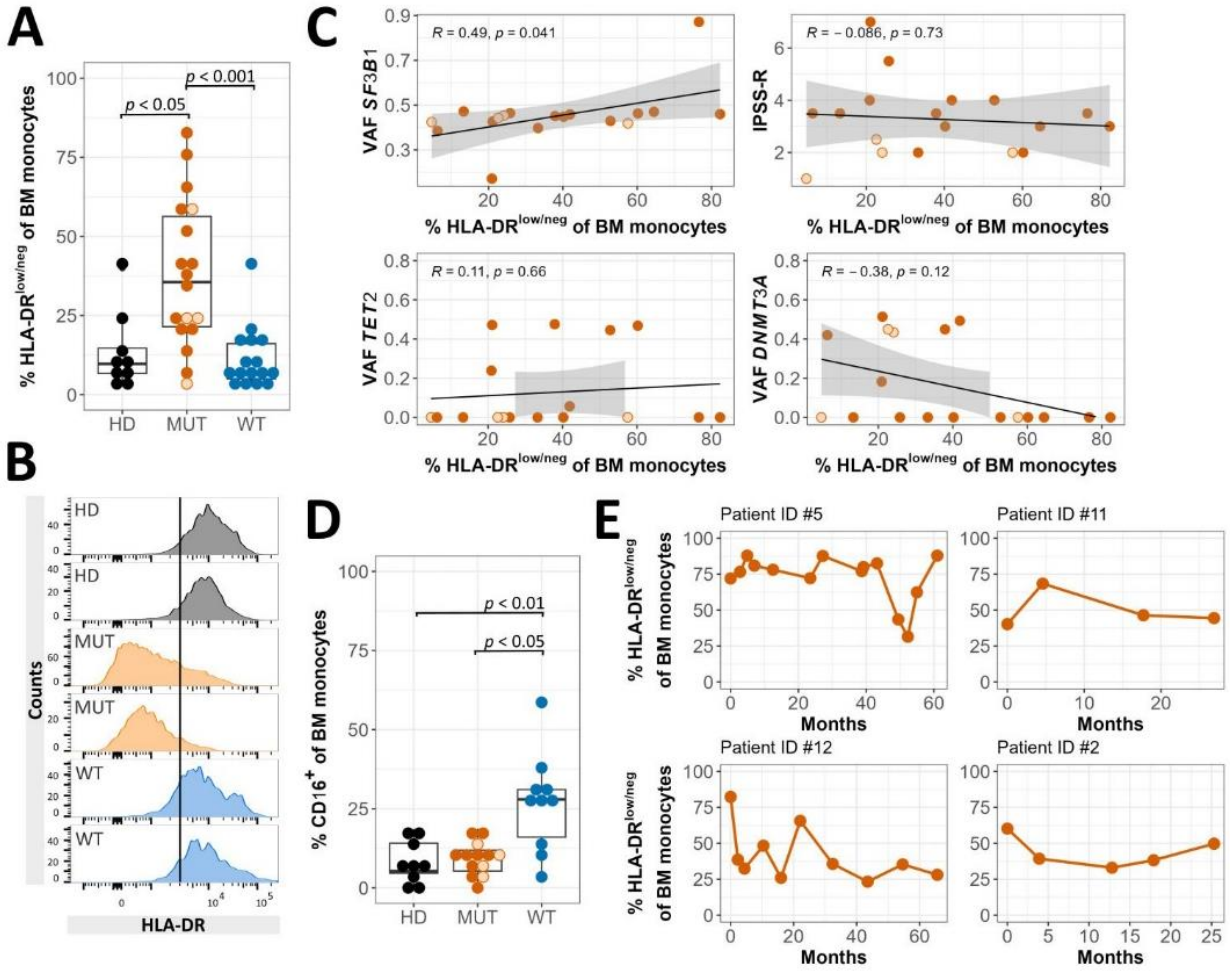

Figure 3. Monocytes with HLA-DRlow/neg immunophenotype emerge frequently in the bone marrow of SF3B1mut MDS. (A) Percentage of CD33^{+} CD14^{+} BM monocytes with HLA-DR$^{low/neg}$ immunophenotype in HD (n = 9, mean age = 69 years, 6 women, 3 men), SF3B1^{mut} (n = 18; orange dots, K700E; light orange filled circles, nonK700E; mean age = 71 years, 7 women, 11 men), and SF3B1^{wt} (n = 16, mean age = 66 years, 8 women, 8 men) MDS assessed by diagnostic flow cytometry of freshly stained BM samples. (B) Representative HLA-DR staining on gated CD33^{+} CD14^{+} BM monocytes. The black line indicates set threshold distinguishing low or negative from high HLA-DR expression. (C) Correlation of the percentage of BM HLA-DR$^{low/neg}$ monocytes with variant allele frequency (VAF) of SF3B1 mutation, IPSS579R, and VAF of confounding TET2 and DNMT3A co-mutations. Scatter plots show Spearman's rank correlation coefficient R and p-value with linear regression line and confidence interval. (D) Percentage of BM monocytes with surface CD16 expression (intermediate and non-classical monocytes) assessed by diagnostic flow cytometry of freshly stained BM samples obtained from HD (n = 9), SF3B1^{mut} (n = 13, orange dots, K700E; light orange-filled circles, nonK700E; mean age = 73 years, 3 women, 10 men), and SF3B1^{wt} (n = 10, mean age = 66 years, 4 women, 6 men) LR-MDS (IPSS-R ≤ 3.5). (E) Percentage of CD33^{+} CD14^{+} BM monocytes with HLA-DRlow/neg immunophenotype in 4 SF3B1^{K700E} MDS patients over time. (A and D) Kruskal-Wallis test with Dunn's post-hoc test (Bonferroni adjusted p-values).

Classical monocytes with isolated SF3B1^{K700E} mutation lack activated immune gene signature seen in other LR-MDS

As CD14^{+} monocytes lose HLA-DR expression, they convert from an inflammatory to an anti-inflammatory/immunosuppressive phenotype [34]. To confirm this is the case in SF3B1^{K700E} MDS, we studied the inflammatory profile of the CD14^{+} classical monocyte subset using RNA-seq. Variant calling from RNA-seq data confirmed clonal involvement of mutant SF3B1 in sorted monocytes, with similar variant allele frequency (VAF) compared to mutational screening of whole BM-MNCs (Figure 4A-B). Principal component analysis applied to examine the global distribution of gene expression profiles showed clustering of HD (n = 3) and scattering of LR-MDS monocytes (n = 3 SF3B1^{K700E}, n = 3 SF3B1^{wt}), reflecting the transcriptional heterogeneity of the latter (Figure 4C). Differential gene expression analysis identified 545 up- and 812 downregulated genes in SF3B1^{K700E} LR-MDS monocytes with isolated K700E hotspot mutation compared to HD (PostFC ≥ 1.5 or ≤ 0.67, respectively), including 172 genes not mapped to Entrez ID. IPA-based pathway analysis of DEG (PostFC ≥ 2 or ≤ 0.5) predicted reduced activity of enriched pathways ($p < 0.05$) pertaining to inflammatory cytokine signaling (i.e. TREM1 Signaling [z-score = -1.9], NF-kB Signaling [z-score = -2.8], LPS/IL1 Mediated Inhibition of RXR Function [z-score = -2.6], IL-6 Signaling [z-score = -3.2], Acute Phase Response Signaling [z-score = -2.5], PI3K/AKT Signaling [z-score = -2.3]) and inflammatory conditions (i.e. Hepatic Fibrosis Signaling Pathway [z-score = -3.5]) (Figure 4D). Accordingly, SF3B1^{K700E} monocytes expressed lower levels of many genes involved in inflammatory responses, such as TREM1, IL6R, and MAP3K7 (Figure 4E, Supplemental Table 5). In contrast, monocytes from SF3B1^{wt} LR-MDS patients, of whom 2 out of 3 carried somatic mutations in TET2, were predicted to have increased activity of enriched pathways ($p< 0.05$) pertaining to inflammatory processes and conditions (i.e. S100 Family Signaling Pathway [zscore = 2.3], Pathogen Induced Cytokine Storm Signaling Pathway [z-score = 0.6], Cardiac Hypertrophy Signaling (Enhanced) [z-score = 2.8]) (Figure 4F). Despite their transcriptionally immunosuppressed signature, SF3B1^{K700E} monocytes readily secreted inflammatory cytokines such as TNFα, IL-1β, and IL-6 following in vitro stimulation with the Toll-like receptor 4 (TLR4) agonist LPS, unless the mutational burden was extremely high (VAF = 0.86), in which case LPS-induced cytokine production was diminished for these and other cytokines compared to HD (Supplemental Figure 7). Taken together, these data showed that circulating classical monocytes in SF3B1^{K700E} LR-MDS patients display a less inflammatory/activated gene signature, which was clearly different from other LR-MDS, but these monocytes are still proficient to initiate inflammatory cytokine production for host defense.

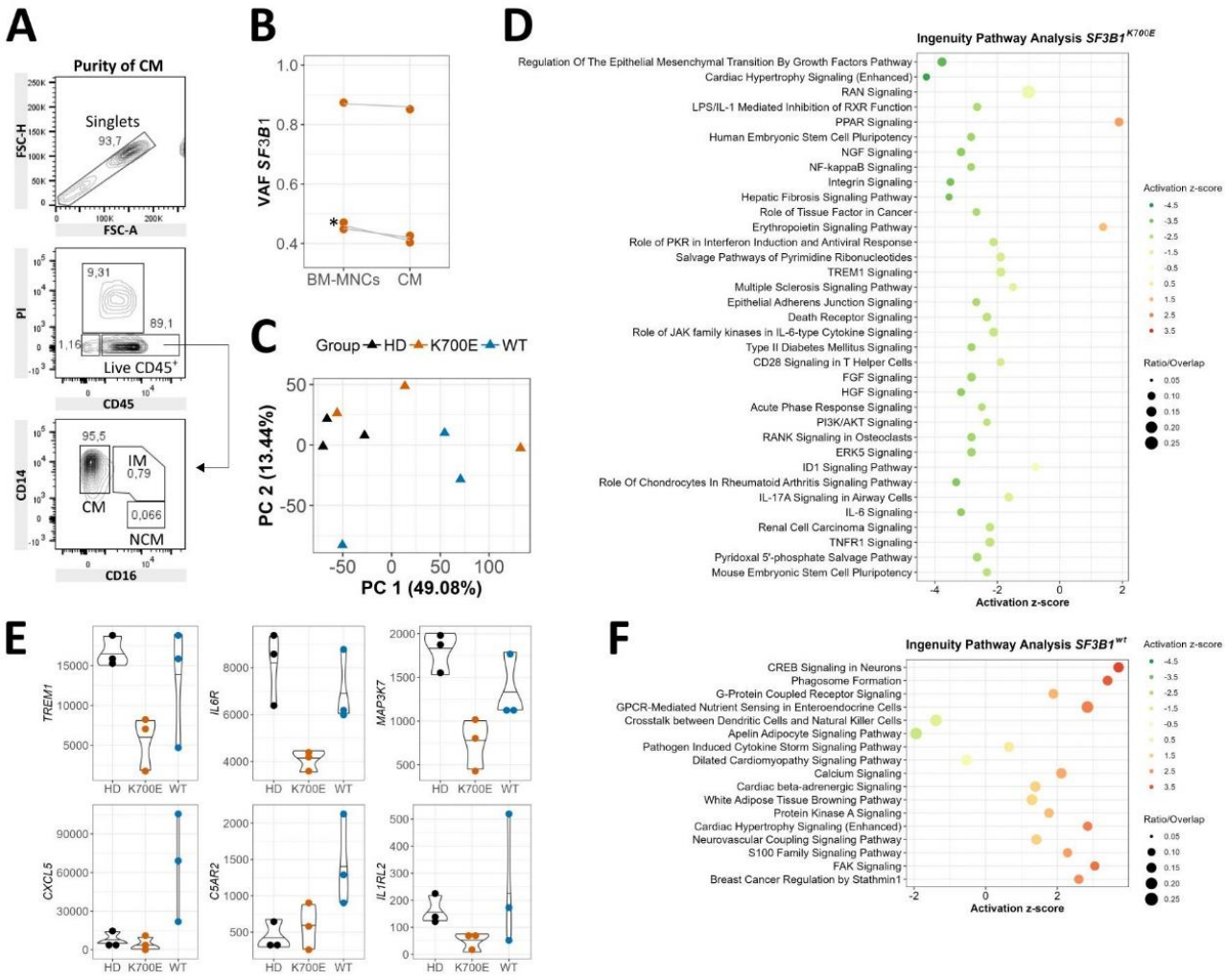

Figure 4. Classical monocytes from SF3B1K700E LR-MDS exhibited reduced predicted activity of inflammatory pathways based on gene expression profile. (A) Representative flow cytometric evaluation of purity of MACS-sorted CD14^{+} CD16^{-} classical monocytes (CM) and percentages of intermediate (IM) and non-classical (NCM) monocytes. (B) VAF of SF3B1^{K700E} mutation in sorted peripheral CD14^{+} CD16^{-} CM (RNA-seq data) and paired BM-MNCs (Archer® VariantPlex® Myeloid panel). Asterisk (*) denotes one patient with time lag of 1 year between CM and BM-MNC sampling. Patient with VAF = 0.86 has proven somatic SF3B1^{K700E} mutation. (C) Principal component analysis of TPM (transcripts per kilobase million) values from RNA-seq of LR-MDS (n = 3 SF3B1^{K700E} [mean age = 70 years, all men], n = 3 SF3B1^{wt} [mean age = 71 years, all men]) compared to HD (n = 3, mean age = 66 years, 1 woman, 2 men) classical monocytes. Scatterplot illustrates variation along the first (PC1) and second (PC2) principal component. (D, F) IPA core pathway analysis showing the predicted activity (cutoff z-score of > |0.5|) of overrepresented annotations (p-value < 0.05 [right-tailed Fisher's exact test]) based on the list of DEG (PostFC ≥ 2 or ≤ 0.5, PPDE > 0.95) in (D) SF3B1^{K700E} or (F) SF3B1^{wt} compared to HD classical monocytes. (E) Violin plot of normalized read counts for selected genes based on RNA-seq data. Abbreviations: PI, propidium iodide.

Mis-spliced gene signature in monocytes with isolated SF3B1^{K700E} mutation

To further characterize the functional effects of SF3B1^{K700E} mutation in classical monocytes, we investigated their alternative splicing (AS) signature in comparison to HD monocytes using rMATS [31]. Altogether, we observed 834 differentially spliced genes (DSG) (1226 events), with exon skipping (SE) constituting the most frequent AS event (651), followed by inclusion of mutually exclusive exons (318), alternative 3' splice site (156), alternative 5' splice site (59), and retained intron events (42) (Figure 5A). The identified SF3B1^{K700E} splicing signature included genes previously reported as mis-spliced in SF3B1^{mut} cells, such as BRD9 [35], COASY [36], and TMEM214 [15] (Figure 5B). For example, mis-splicing of COASY affected the same junctions as described before [36]. Many of the identified genes (416) were also observed using EBSeq, which identifies differentially expressed isoforms (DEI) (Figure 5C). Subsequent Isoprofiler filtering of all DEI identified several protein-coding isoforms of genes implicated in inflammatory processes, including TREM1, IL6R, and WNT5A (Supplemental Table 7). However, EBSeq does not provide accurate splice site event information and hence we focused our analysis on the event-based approach rMATS. Pathway and process enrichment analysis of all DSG pointed to regulation of the immune response and cytokine signaling, next to mRNA metabolism, apoptotic signaling, and mitotic cell cycle (Figure 5D, Supplemental Table 8). We concentrated on splicing eve 297 nts related to activation and inflammatory signaling. DSG associated with activation of the immune response and/or cytokine signaling included genes involved in the NF-kB signaling pathway (TLR2, MYD88, IRAK4, CYLD, IKBKB, MAP3K7) and innate immune response (TLR2, C2, NOD2, Ly96) (Figure 5E-F). For instance, the observed SE event for TLR2 aligned with EBSeq data, which showed reduced expression of two isoforms with incomplete 3' coding sequence (ENST00000643501, ENST00000646219) and a principal isoform (ENST00000260010) in SF3B1^{K700E} monocytes (Supplemental Table 6). SF3B1^{K700E} monocytes also exhibited AS of IRAK4 in line with increased expression of an IRAK4 transcript undergoing nonsense-mediated decay (ENST00000431837) (Supplemental Table 6). Furthermore, we observed a high proportion of exon skipping (ILD = 0.651, FDR = 2.5925e-09) for the stimulatory immunoreceptor LILRA2, corresponding to exon 2 of the principal transcript (ENST00000391738). ANXA2, which fulfills a spectrum of pro- and anti-inflammatory functions, showed a complex dysregulation of AS (Figure 5F). Importantly, 369 (out of the 834) DSG were also differentially spliced in SF3B1^{K700E} compared to SF3B1^{wt} LR-MDS monocytes (Supplemental Table 9). Altogether, our findings reveal differential mRNA splicing of a multitude of genes implicated in inflammatory responses and cellular activation, which adds to the complex transcriptional dysregulation of immune pathways in SF3B1^{K700E} MDS.

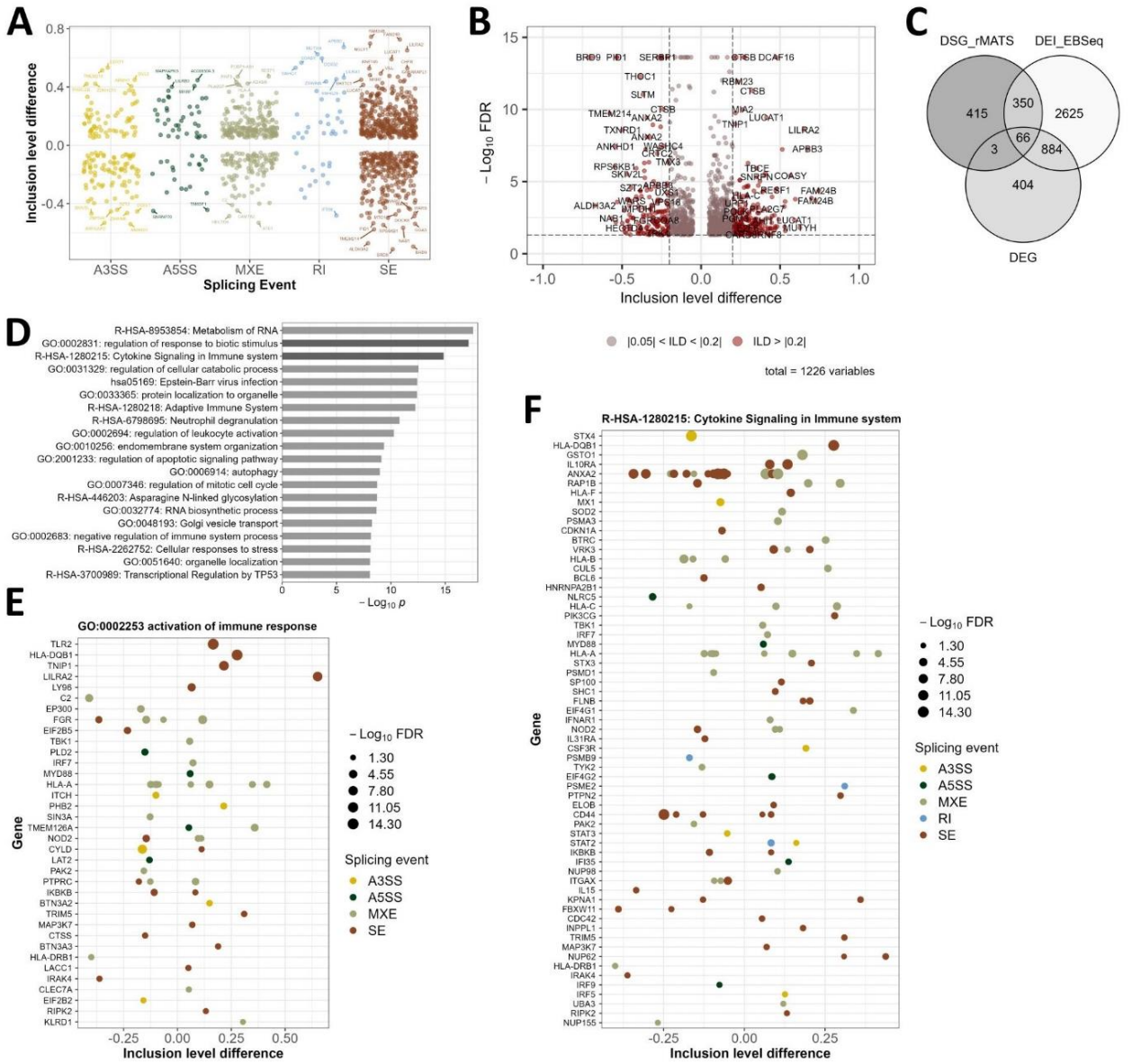

Figure 5. Alternative splicing signature in SF3B1^{K700E} classical monocytes. (A) Overview of differential splicing events detectable in SF3B1^{K700E} LR-MDS (n = 3, mean age = 70 years, all men) compared to HD (n = 3, mean age = 66 years, 1 woman, 2 men) classical monocytes using rMATS. (B) Volcano plot highlighting DSG with inclusion level difference (ILD) > |0.2|. (C) Venn diagram showing overlap of DSG, DEI, and DEG based on Ensembl gene ID. (D) Enrichment analysis of DSG using Metascape. Top 20 enriched terms across input DSG are shown. (E, F) DSG associated with terms related to activation and inflammatory signaling are shown with their type of differential splicing event(s). Abbreviations: A3SS, alternative 3' 611 splice site; A5SS, alternative 5' splice site; MXE, mutually exclusive exon; RI, retained intron; SE, skipped exon.

Discussion

The inherent mechanisms subverting effective antitumor immunity in myeloid malignancies such as MDS are diverse and shaped by the somatic mutational background. In this study, we investigated the immunophenotype of a subgroup of MDS patients genetically defined by somatic mutations in SF3B1, with a majority of the patients fulfilling the recent WHO 2022 criteria for MDS-SF3B1 classification [37], in comparison to healthy controls and other MDS. First, we broadly assessed immune cell signatures and phenotypes using multiplex immunophenotyping technologies in combination with machine learning-based analytical approaches. Second, we used RNA-seq to study the global gene expression changes and splicing abnormalities associated with the presence of $SF3B1^{K700E}$ mutations in $CD14^+$ classical monocytes from LR-MDS.

Prevailing in the BM of $SF3B1^{mut}$ patients was a myeloid cell-related immune gene signature exhibiting immunoregulatory facets (e.g. increased ARG1/2, ADORA2A, and AXL [38,39]) and lacking signs of overt myeloid-driven inflammation. Lymphoid-related genes were underrepresented, accordant with the previously reported lower proportion of lymphocytes in the BM of $SF3B1^{mut}$ patients [40]. Since total BM cell counts were not available for extrapolating absolute lymphocyte subset counts, it remains to be investigated whether this translates into reduced lymphoid infiltration in $SF3B1^{mut}$ BM. Further analysis of the T cell compartment showed a similarly disturbed T cell homeostasis in $SF3B1^{K700E}$ and $SF3B1^{wt}$ LR-MDS compared to HD, with less naïve $CD4^+$ and $CD8^+$ T cells, and memory phenotype skewing toward effector memory (TEM) and TTE $CD8^+$ T cells, consistent with progressive memory differentiation entailing loss of survival [41]. Such skewing of T cells is typically seen in MDS, potentially contributing to impaired long-term antitumor immunosurveillance [42]. In addition, our data support a dysregulated NK cell phenotype with an increased percentage of phenotypically more mature $CD57^+$ NK cells in the BM of $SF3B1^{K700E}$ and $SF3B1^{wt}$ LR-MDS compared to HD. While a more in-depth investigation of the defects in NK cell phenotype and function was beyond the scope of this study, recent data strongly encourage consideration of the patients' somatic mutational profiles for evaluation of NK cell deficits, especially with regard to (co-)mutations in TET2 [43].

The most remarkable immunophenotypic difference distinguishing $SF3B1^{mut}$ ($SF3B1^{K700E}$ and $SF3B1^{nonK700E}$) patients was, however, the frequent and persistent emergence of $HLA\text{-}DR^{low/neg}$ $CD14^+$ $CD16^-$ classical monocytes in the BM and PB in comparison to HD and other MDS. To the best of our knowledge, the only other study to date investigating immunophenotypic features in the BM of $SF3B1^{mut}$ MDS patients reported lower expression of CD11b, CD36, and CD64 on SF3B1mut monocytes [40]. While we can confirm these findings (data not included), our study revealed an even more profound impact of SF3B1 mutations on monocyte immunophenotype and potentially function. $HLA\text{-}DR^{low/neg}$ monocytes have known immunoregulatory properties via multiple mechanisms, including effector T cell inhibition, decreased antigen presentation, and defective dendritic cell maturation [34,44–48]. A possible scenario is that the early acquisition of SF3B1 mutations and the presence of inflammation during this early-stage disease fosters the emergence of $HLA\text{-}DR^{low/neg}$ monocytes, which then contribute to counteract and balance inflammatory responses in established $SF3B1^{mut}$ MDS. Further comprehensive transcriptional profiling of the peripheral classical monocyte subset affirmed a less activated state and reduced activity of inflammatory pathways in $SF3B1^{K700E}$ MDS. Importantly, this signature was directly attributable to $SF3B1^{K700E}$ and not confounded by co-mutations or cytogenetic aberrations. Nevertheless, $SF3B1^{K700E}$ (VAF ~ 0.4) monocytes were capable of responding to *in vitro* TLR4 stimulation with adequate secretion of different cytokines required for innate host defense comparable to HD monocytes, suggesting that TLR4-mediated NF-kB signaling can be activated. On that account, the less activated constitutive state appears likely to be a result of a less inflammatory microenvironment in $SF3B1^{K700E}$ MDS.

To date, only few studies have investigated the contribution of clonally involved, yet mutationally undefined monocyte subsets to the immune dysregulation in MDS. Our previous collaborative study found a higher

frequency of classical monocytes expressing immunoregulatory thrombomodulin, especially in MDS subtypes with lower percentage of blasts (< 5%) and RS, a hallmark of SF3B1^{mut} MDS [49]. Sorted thrombomodulin-expressing monocytes from MDS patients with RS supported *in vitro* polarization of CD4^{+} T cells to an immunosuppressive phenotype. Moreover, according to another recent study, non-classical slan^{+} monocytes from MDS patients with RS showed disrupted expression of receptors and signaling pathways involved in innate and inflammatory responses [50]. Thus, monocyte signatures that could contribute to the complex picture of immune dysregulation and immune escape in MDS are currently emerging. Our study now shows that splicing factor mutations, in particular SF3B1^{K700E}, distinctly shape monocyte signatures on various levels. Specifically, our data inform on monocyte-specific splicing differences, which may affect certain innate and chronic inflammatory responses in patients with an isolated SF3B1^{K700E} mutation.

In conclusion, the monocyte signatures identified in SF3B1^{K700E} MDS suggest a lower level of harmful sterile inflammation known to contribute to genomic instability in MDS and further suggest that therapies targeting myeloid-driven hyperinflammation, such as canakinumab [51], need to be properly chosen and maybe ultimately personalized.

References

1. Gallì A, Todisco G, Catamo E, et al. Relationship between clone metrics and clinical outcome in clonal cytopenia. Blood. 2021;138(11):965–976.
2. Todisco G, Moura PL, Hellström-Lindberg E. Clinical manifestations of clonal hematopoiesis: What has SF3B1-mutant MDS taught us? Semin. Hematol. 2022;59(3):150–155.
3. Papaemmanuil E, Cazzola M, Boultwood J, et al. Somatic SF3B1 Mutation in Myelodysplasiawith Ring Sideroblasts. N. Engl. J. Med. 2011;365(15):1384–1395.
4. Sarchi M, Gallì A, Clough CA, et al. Modeling Clonal Progression in SF3B1-Mutant Myelodysplastic Syndrome. Blood. 2021;138(Supplement 1):149.
5. Malcovati L, Stevenson K, Papaemmanuil E, et al. SF3B1-mutant MDS as a distinct disease subtype: A proposal from the International Working Group for the Prognosis of MDS. Blood. 2020;136(2):157–170.
6. Bondu S, Alary AS, Lefèvre C, et al. A variant erythroferrone disrupts iron homeostasis in SF3B1-mutated myelodysplastic syndrome. Sci. Transl. Med. 2019;11(500):eaav5467.
7. Lieu YK, Liu Z, Ali AM, et al. SF3B1 mutant-induced missplicing of MAP3K7 causes anemia in myelodysplastic syndromes. bioRxiv. 2020.
8. Clough CA, Pangallo J, Sarchi M, et al. Coordinated mis-splicing of TMEM14C and ABCB7 causes ring sideroblast formation in SF3B1-mutant myelodysplastic syndrome. Blood. 2021.
9. Hershberger CE, Moyer DC, Adema V, et al. Complex landscape of alternative splicing in myeloid neoplasms. Leukemia. 2021;35(4):1108–1120.
10. Huber S, Haferlach T, Meggendorfer M, et al. SF3B1 mutated MDS: Blast count, genetic co432 abnormalities and their impact on classification and prognosis. Leukemia. 2022;36(12):2894–2902.
11. Pellagatti A, Armstrong RN, Steeples V, et al. Impact of spliceosome mutations on RNA splicing in myelodysplasia: Dysregulated genes/pathways and clinical associations. Blood. 2018;132(12):1225–1240.
12. Dolatshad H, Pellagatti A, Fernandez-Mercado M, et al. Disruption of SF3B1 results in deregulated expression and splicing of key genes and pathways in myelodysplastic syndrome hematopoietic stem and progenitor cells. Leukemia. 2015;29(5):1092–1103.
13. Clough C, Pangallo J, Sarchi M, et al. Coordinated Mis-Splicing of Multiple Mitochondrial Iron Metabolism Genes Causes Ring Sideroblast Formation in SF3B1-Mutant MDS. Blood. 2020;136(Supplement 1):4–4.

14. Choudhary GS, Pellagatti A, Agianian B, et al. Activation of targetable inflammatory immune signaling is seen in myelodysplastic syndromes with SF3B1 mutations. Elife. 2022;11.
15. Asimomitis G, Deslauriers AG, Kotini AG, et al. Patient-specific MDS-RS iPSCs define the mis446 spliced transcript repertoire and chromatin landscape of SF3B1-mutant HSPCs. Blood Adv. 2022;6(10):2992–3005.
16. Moura PL, Mortera-Blanco T, Hofman IJF, et al. Erythroid differentiation intensifies RNA mis449 splicing in SF3B1-mutant myelodysplastic syndromes with ring sideroblasts. bioRxiv. 2023;2023.04.11.536355.
17. Mortera-Blanco T, Dimitriou M, Woll PS, et al. SF3B1-initiating mutations in MDS-RSs target lymphomyeloid hematopoietic stem cells. Blood. 2017;130(7):881–890.
18. Mian SA, Rouault-Pierre K, Smith AE, et al. SF3B1 mutant MDS-initiating cells may arise from the haematopoietic stem cell compartment. Nat. Commun. 2015;6.
19. De Arras L, Alper S. Limiting of the Innate Immune Response by SF3A-Dependent Control of MyD88 Alternative mRNA Splicing. PLoS Genet. 2013;9(10):e1003855.
20. Pollyea DA, Harris C, Rabe JL, et al. Myelodysplastic syndrome-associated spliceosome gene mutations enhance innate immune signaling. Haematologica. 2019;104(9):e388–e392.
21. Nazha A, Komrokji R, Meggendorfer M, et al. Personalized Prediction Model to Risk Stratify Patients With Myelodysplastic Syndromes. J. Clin. Oncol. 2021;39(33):3737–3746.
22. Kanagal-Shamanna R, Montalban-Bravo G, Sasaki K, et al. Only SF3B1 mutation involving K700E independently predicts overall survival in myelodysplastic syndromes. Cancer. 2021;127(19):3552–3565.
23. Brian Dalton W, Helmenstine E, Pieterse L, et al. The K666N mutation in SF3B1 is associated with increased progression of MDS and distinct RNA splicing. Blood Adv. 2020;4(7):1192–1196.
24. Platzbecker U, Germing U, Götze KS, et al. Luspatercept for the treatment of anaemia in patients with lower-risk myelodysplastic syndromes (PACE-MDS): a multicentre, open-label phase 2 dose-finding study with long-term extension study. Lancet Oncol. 2017;18(10):1338–1347.
25. Fenaux P, Platzbecker U, Mufti GJ, et al. The Medalist Trial: Results of a Phase 3, Randomized, Double-Blind, Placebo-Controlled Study of Luspatercept to Treat Anemia in Patients with Very Low-, Low-, or Intermediate-Risk Myelodysplastic Syndromes (MDS) with Ring Sideroblasts (RS) Who Require Red. Blood. 2018;132(Supplement 1):1–1.
26. Stahl M, DeVeaux M, De Witte T, et al. The use of immunosuppressive therapy in MDS: Clinical outcomes and their predictors in a large international patient cohort. Blood Adv. 2018;2(14):1765–1772.
27. Zhang Q, Haider M, Al Ali NH, et al. SF3B1 Mutations Negatively Predict for Response to Immunosuppressive Therapy in Myelodysplastic Syndromes. Clin. Lymphoma Myeloma Leuk. 2020;20(6):400-406.e2.
28. Zhou Y, Zhou B, Pache L, et al. Metascape provides a biologist-oriented resource for the analysis of systems-level datasets. Nat. Commun. 2019;10(1):.
29. Barone SM, Paul AGA, Muehling LM, et al. Unsupervised machine learning reveals key immune cell subsets in covid-19, rhinovirus infection, and cancer therapy. Elife. 2021;10:1–23.
30. Leng N, Dawson JA, Thomson JA, et al. EBSeq: an empirical Bayes hierarchical model for inference in RNA-seq experiments. Bioinformatics. 2013;29(8):1035–1043.
31. Shen S, Park JW, Lu ZX, et al. rMATS: Robust and flexible detection of differential alternative splicing from replicate 487 RNA-Seq data. Proc. Natl. Acad. Sci. U. S. A. 2014;111(51):E5593–E5601.
32. Bento LC, Correia RP, Mangueira CLP, et al. The Use of Flow Cytometry in Myelodysplastic Syndromes: A Review. Front. Oncol. 2017;7(NOV):270.
33. Van De Ven K, Borst J. Targeting the T-cell co-stimulatory CD27/CD70 pathway in cancer immunotherapy: Rationale and potential. Immunotherapy. 2015;7(6):655–667.

34. Mengos AE, Gastineau DA, Gustafson MP. The CD14+HLA-DrlO/NEG monocyte: An immunosuppressive phenotype that restrains responses to cancer immunotherapy. Front. Immunol. 2019;10(MAY):1147.
35. Inoue D, Chew GL, Liu B, et al. Spliceosomal disruption of the non-canonical BAF complex in cancer. Nat. 2019 5747778. 2019;574(7778):432–436.
36. Mian SA, Philippe C, Maniati E, et al. Vitamin B5 and succinyl-CoA improve ineffective erythropoiesis in SF3B1-mutated myelodysplasia. Sci. Transl. Med. 2023;15(685):eabn5135.
37. Khoury JD, Solary E, Abla O, et al. The 5th edition of the World Health Organization Classification of Haematolymphoid Tumours: Myeloid and Histiocytic/Dendritic Neoplasms. Leukemia. 2022;36(7):1703–1719.
38. Medyouf H, Tirado-Gonzalez I, Mies A, et al. The identification of the AXL/Gas6 signalling axis as a key player of myelodysplastic syndrome (MDS) and the potential of the oral selective AXL inhibitor bemcentinib in the treatment of MDS. Ann. Oncol. 2018;29:viii361.
39. Tirado-Gonzalez I, Descot A, Soetopo D, et al. Axl inhibition in macrophages stimulates host506 versus-leukemia immunity and eradicates naïve and treatment-resistant leukemia. Cancer Discov. 2021;11(11):2924–2943.
40. Duetz C, Westers TM, in 't Hout FEM, et al. Distinct bone marrow immunophenotypic features define the splicing factor 3B subunit 1 (SF3B1)-mutant myelodysplastic syndromes subtype. Br. J. Haematol. 2021;193(4):798–803.
41. Mahnke YD, Brodie TM, Sallusto F, Roederer M, Lugli E. The who's who of T-cell differentiation: Human memory T-cell subsets. Eur. J. Immunol. 2013;43(11):2797–2809.
42. Zou JX, Rollison DE, Boulware D, et al. Altered naive and memory CD4+ T-cell homeostasis and immunosenescence characterize younger patients with myelodysplastic syndrome. Leukemia. 2009;23(7):1288–1296.
43. Boy M, Bisio V, Zhao LP, et al. Myelodysplastic Syndrome associated TET2 mutations affect NK cell function and genome methylation. Nat. Commun. 2023 141. 2023;14(1):1–14.
44. Hoechst B, Ormandy LA, Ballmaier M, et al. A new population of myeloid-derived suppressor cells in hepatocellular carcinoma patients induces CD4(+)CD25(+)Foxp3(+) T cells. Gastroenterology. 2008;135(1):234–243.
45. Gustafson MP, Lin Y, New KC, et al. Systemic immune suppression in glioblastoma: the interplay between CD14+HLA-DRlo/neg monocytes, tumor factors, and dexamethasone. Neuro. Oncol. 2010;12(7):631–644.
46. Lin Y, Gustafson MP, Bulur PA, et al. Immunosuppressive CD14+HLA-DR(low)/- monocytes in B525 cell non-Hodgkin lymphoma. Blood. 2011;117(3):872–881.
47. 47. Laborde RR, Lin Y, Gustafson MP, Bulur PA, Dietz AB. Cancer Vaccines in the World of Immune Suppressive Monocytes (CD14(+)HLA-DR(lo/neg) Cells): The Gateway to Improved Responses. Front. Immunol. 2014;5(APR):
48. Jitschin R, Braun M, Büttner M, et al. CLL-cells induce IDOhi CD14+HLA-DRlo myeloid-derived suppressor cells that inhibit T-cell responses and promote TRegs. Blood. 2014;124(5):750–760.
49. van Leeuwen-Kerkhoff N, Westers TM, Poddighe PJ, et al. Thrombomodulin-expressing monocytes are associated with low-risk features in myelodysplastic syndromes and dampen excessive immune activation. Haematologica. 2020;105(4):961–970.
50. van Leeuwen-Kerkhoff N, Westers TM, Poddighe PJ, et al. Reduced frequencies and functional impairment of dendritic cell subsets and non-classical monocytes in myelodysplastic syndromes. Haematologica. 2022;107(3):655.
51. Garcia-Manero G, Adema V, Urrutia S, et al. Clinical and Biological Effects of Canakinumab in Lower-Risk Myelodysplastic Syndromes (MDS): Results from a Phase 2 Clinical Trial. Blood. 539 2022;140(Supplement 1):2078–2080.

SUPPLEMENTAL METHODS

Patient cohort

Supplemental Table 1: Clinical characteristics of MDS experimental cohort

Variable	*SF3B1*^{wt}	*SF3B1*^{mut}	*p*-value
Number of patients	18	19	
Sex			
Female	8	8	
Male	10	11	
Age, years (median)	72.1	72	NS
Age, years (range)	27.5 - 83.5	55.8 - 83.7	
Age, years (IQR)	61.8 - 75.5	67.7 - 76	
RS, % (median)	0	62	< 0.001*
RS, % (range)	0 - 75	29 - 89	
RS, % (IQR)	0 - 7	42 - 71	
BM blasts, % (median)	3	4	NS
BM blasts, % (range)	0.5 - 16	2 - 13	
BM blasts, % (IQR)	2.1 - 5.3	2.3 - 4.8	
Hb, g/dL (median)	8.9	8.7	NS
Hb, g/dL (range; ref. range 11.92 - 17.24)	7.7 - 13.7	5.8 - 10.3	
Hb, g/dL (IQR)	8.7 - 10.8	7.9 - 9.6	
WBC, GPt/L (median)	3	4.2	NS
WBC, GPt/L (range; ref. range 3.8 - 9.8)	0.8 - 6	1.1 - 8.7	
WBC, GPt/L (IQR)	2 - 4.4	3.1 - 6.5	
ANC, GPt/L (median)	1.7	2.5	NS
ANC, GPt/L (range; ref. range 1.8 - 7.55)	0.1 - 4.2	0.4 - 6.4	
ANC, GPt/L (IQR)	0.7 - 2.8	1.6 - 3.7	
Platelets, GPt/L (median)	184.5	239	NS
Platelets, GPt/L (range; ref. range 150 - 400)	57 - 392	42 - 1471	
Platelets, GPt/L (IQR)	110 - 266.5	113.5 - 354.5	
ALC, GPt/L (median)	1	1.2	NS
ALC, GPt/L (range; ref. range 1.5 - 4)	0.4 - 1.9	0.2 - 2.8	
ALC, GPt/L (IQR)	0.7 - 1.3	0.7 - 1.5	
AMC, GPt/L (median)	0.2	0.5	0.02*
AMC, GPt/L (range; ref. range 0.2 - 1)	0.02 - 0.71	0.01 - 1	
AMC, GPt/L (IQR)	0.1 - 0.42	0.3 - 0.6	
IPSS-R			
IPSS-R ≤ 3.5 (number of patients)	13	13	
IPSS-R > 3.5 - 4.5 (number of patients)	2	3	
IPSS-R > 4.5 (number of patients)	3	3	
CRP, mg/L (median)	4.4	1.6	NS
CRP, mg/L (range; ref. range < 5)	0.3 - 37.5	0.5 - 18.3	
CRP, mg/L (IQR)	1.6 - 8.7	0.9 - 2.9	

Mann-Whitney-U-test/Wilcoxon-test was performed for laboratory variables ($p < 0.05$ was considered significant).

Abbreviations: ALC, absolute lymphocyte count; AMC, absolute monocyte count; ANC, absolute neutrophil count; CRP, C-reactive protein; IQR, interquartile range; NS, not significant; RS, ring sideroblasts; WBC, white blood cell count.

*Similar to the IWG cohort,[1] *SF3B1*^{mut} MDS patients had RS phenotype and higher absolute PB monocyte counts.

CyTOF staining and panel design

Viably frozen BM-MNCs were thawed in 10 mL RPMI medium containing 10% FBS and 1x CTL anti-aggregate wash supplement (CTL-AA-005 CTL, Cellular Technology Limited, USA). Following centrifugation (300 x g for 5 min), cells were resuspended in 10 mL CTL wash medium and counted using trypan blue and a hemocytometer. Samples were incubated with 103Rh-Intercalator, washed, and FcR were blocked with 50 µg/sample human IgG blend (KIOVIG, Baxalta Belgium Manufacturing SA/Baxter SA, Belgium). Two differently mass-tagged CD45 antibodies were used to barcode samples prior to their joint surface and intracellular staining. Barcoded samples were stained with APC-conjugated anti-human CD95 for 30 min at 4°C, washed, and transferred into a new tube containing the dried antibody pellet from the Maxpar Direct Immune Profiling Assay. A custom mastermix containing antibodies from the Maxpar Direct T cell Expansion Panel 2 and others as indicated in Supplemental Table 2 was added and cells were incubated for 30 min at RT. After washing, cells were fixed with freshly prepared 1.6% PFA solution for 10 min at RT. Cells were stained intracellularly using the Foxp3/Transcription Factor Staining Buffer Set according to manufacturer's instructions (Thermo Fisher Scientific, USA). Cells were then resuspended in Maxpar Fix & Perm buffer containing Cell-ID™ Intercalator-Ir for nucleated cell discrimination (Standard BioTools Inc., CA, USA) and incubated at 4°C overnight. On the next day, cells were centrifuged and resuspended in 1 mL freezing medium (10% DMSO, 90% FBS) for storage at -80°C until data acquisition. Upon thawing and washing, cells were counted using a Countess® II FL Automated Cell Counter (Thermo Fisher Scientific, USA) before loading for acquisition. All cell washes were performed with Maxpar Cell Staining Buffer. Samples were acquired on a Helios™ mass cytometer (Standard BioTools Inc., CA, USA). Raw FCS files were normalized using the free CyTOF 6.7 system control software. Data were cleaned, gated on $CD45^+$ cells, and debarcoded using FlowJo v10.8 (FlowJo, Ashland, OR, USA). Due to unspecific staining, the data on Foxp3 were not included. Further gating of key immune cell populations was done using FlowJo. T cell subpopulations were gated based on differential expression of CD45RO, CCR7, CD28, and CD95 according to published gating strategies.[2]

Supplemental Table 2: CyTOF panel

Target	Clone	Metal	Information
Anti-human CD45	HI30	89Y	Maxpar Direct Immune Profiling Assay
Live/dead 103Rh-Intercalator	N/A	103Rh	Maxpar Direct Immune Profiling Assay
Anti-human CD196/CCR6	G034E3	141Pr	Maxpar Direct Immune Profiling Assay
Anti-human CD123	6H6	143Nd	Maxpar Direct Immune Profiling Assay
Anti-human CD19	HIB19	144Nd	Maxpar Direct Immune Profiling Assay
Anti-human CD4	RPA-T4	145Nd	Maxpar Direct Immune Profiling Assay
Anti-human CD8a	RPA-T8	146Nd	Maxpar Direct Immune Profiling Assay
Anti-human CD11c	Bu15	147Sm	Maxpar Direct Immune Profiling Assay
Anti-human CD16	3G8	148Nd	Maxpar Direct Immune Profiling Assay
Anti-human CD45RO	UCHL1	149Sm	Maxpar Direct Immune Profiling Assay
Anti-human CD45RA	HI100	150Nd	Maxpar Direct Immune Profiling Assay
Anti-human CD161	HP-3G10	151Eu	Maxpar Direct Immune Profiling Assay
Anti-human CD194/CCR4	L291H4	152Sm	Maxpar Direct Immune Profiling Assay
Anti-human CD25	BC96	153Eu	Maxpar Direct Immune Profiling Assay
Anti-human CD27	O323	154Sm	Maxpar Direct Immune Profiling Assay
Anti-human CD57	HCD57	155Gd	Maxpar Direct Immune Profiling Assay
Anti-human CD183/CXCR3	G025H7	156Gd	Maxpar Direct Immune Profiling Assay
Anti-human CD185/CXCR5	J252D4	158Gd	Maxpar Direct Immune Profiling Assay
Anti-human CD28	CD28.2	160Gd	Maxpar Direct Immune Profiling Assay
Anti-human CD38	HB-7	161Dy	Maxpar Direct Immune Profiling Assay
Anti-human CD56/NCAM	NCAM16.2	163Dy	Maxpar Direct Immune Profiling Assay
Anti-human TCRgd	B1	164Dy	Maxpar Direct Immune Profiling Assay
Anti-human CD294	BM16	166Er	Maxpar Direct Immune Profiling Assay
Anti-human CD197/CCR7	G043H7	167Er	Maxpar Direct Immune Profiling Assay
Anti-human CD14	63D3	168Er	Maxpar Direct Immune Profiling Assay
Anti-human CD3	UCHT1	170Er	Maxpar Direct Immune Profiling Assay
Anti-human CD20	2H7	171Yb	Maxpar Direct Immune Profiling Assay
Anti-human CD66b	G10F5	172Yb	Maxpar Direct Immune Profiling Assay
Anti-human HLA-DR	LN3	173Yb	Maxpar Direct Immune Profiling Assay
Anti-human IgD	IA6-2	174Yb	Maxpar Direct Immune Profiling Assay
Anti-human CD127	A019D5	176Yb	Maxpar Direct Immune Profiling Assay
Anti-human PD-1/CD279	EH12.2H7	165Ho	Maxpar Direct T cell Expansion Panel 2
Anti-APC (Maxpar® Ready)	APC003	106Cd	Biolegend, custom metal labeling
APC anti-CD95	DX2	NA	Biolegend
Anti-human CD33 (Maxpar® Ready)	WM53	111Cd	Biolegend, custom metal labeling
Anti-human OX40/CD134	ACT35	142Nd	Standard BioTools
Anti-human TIM-3/CD366	F38-2E2	159Tb	Maxpar Direct T cell Expansion Panel 2
Anti-human ICOS/CD278	C398.4A	169Tm	Maxpar Direct T cell Expansion Panel 2
Anti-human CD184/CXCR4	12G5	175Lu	Maxpar Direct T cell Expansion Panel 2
Anti-human TIGIT	MBSA43	209Bi	Maxpar Direct T cell Expansion Panel 2
Anti-human CD45	HI30	110Cd	Standard BioTools, used for barcoding
Anti-human CD45	HI30	112Cd	Standard BioTools, used for barcoding

Clinical flow cytometry staining (experimental cohort)

The monoclonal antibody panels consisted of 8-color-tubes that are part of routine diagnostic flow cytometric analysis of MDS patients. Cell preparation was performed within 24 hours after BM aspiration or PB collection in EDTA tubes. Prior to staining, erythrocytes were removed by bulk lysis for

10 min at RT using BD Pharm Lyse buffer (1:10 dilution with distilled water; BD Biosciences, USA), followed by two washing steps with PBS (Thermo Fisher Scientific, USA). For surface labeling, cells were incubated with monoclonal antibodies (Supplemental Table 3) in the dark (15 min at RT) according to the recommendations of the manufacturer. Subsequently, cells were washed twice and resuspended in 500 µl PBS. Samples were stored at 4°C and acquired within 1 hour on a FACS Canto II cytometer (BD Biosciences) equipped with three lasers (405, 488, and 633 nm). The analysis of FCS files was performed using BD FACSDiva v9.0.1 software. $CD33^{+}$ $CD36^{+}$ monocytes were routinely backgated within CD45/SSC-A to verify that all events fall within the traditional monocyte gate. The same threshold for HLA-$DR^{low/neg}$ $CD14^{+}$ monocytes was set for all samples according to the upper limit of HLA-DR in HLA-DR^{neg} lymphocytes. FlowJo v10.8.1 was used for visualization of data.

Supplemental Table 3: Clinical flow cytometry antibodies

Target	Clone	Source
Anti-human HLA-DR	L243	BD Biosciences
Anti-human CD19	HD37	Agilent Dako
Anti-human CD3	SK7	eBioscience
Anti-human CD16	3G8	Beckman Coulter/Biolegend
Anti-human CD64	10.1	Biolegend
Anti-human CD11b	ICRF44	Biolegend
Anti-human CD14	M5E2/HCD14	BD Biosciences/Biolegend
Anti-human CD36	CB38 (also known as NL07)	BD Biosciences
Anti-human CD33	P67.6	BD Biosciences
Anti-human Lineage Cocktail (CD3, CD14, CD16, CD19, CD20, CD56)*	UCHT1; HCD14; 3G8; HIB19; 2H7; HCD56;	Biolegend
Anti-human CD45	HI30	BD Biosciences

Flow cytometric evaluation of isolated classical monocytes

The purity of the isolated $CD14^{+}$ $CD16^{-}$ monocytes was checked by flow cytometry using a cocktail of monoclonal antibodies (anti-human CD45 [clone 2D1], anti-human CD14 [clone MΦP9], anti-human CD33 [clone P67.6], anti-human CD16 [clone NKP15], anti-human CD34 [clone 8G12], anti-human HLA-DR [clone L243], BD Biosciences).

RNA-seq of classical monocytes and downstream data analysis

The mRNA library preparations and sequencing reactions were conducted at GENEWIZ, LLC. (South Plainfield, NJ, USA). The SMART-Seq HT kit (Takara, San Jose, CA, USA) was used for full-length cDNA synthesis and amplification, and Illumina Nextera XT (Illumina, San Diego, CA, USA) was used for sequencing library preparation according to manufacturer's instructions. The samples were sequenced on the Illumina HiSeq 4000 instrument using a 2x150 bp paired-end configuration. Image analysis and base calling were conducted by the HiSeq Control Software. Raw sequence data (.bcl files) generated

from Illumina HiSeq was converted into FASTQ files and de-multiplexed using Illumina's bcl2fastq Conversion Software v2.20. Sequencing quality of raw FASTQ files was checked using FastQC 0.11.8 (https://www.bioinformatics.babraham.ac.uk/projects/fastqc/). Adapter trimming and quality filtering of sequence reads were performed using Seqtk and cutadapt. The adapter clipped reads were also aligned to ribosomal RNA sequences using Bowtie 2 (v2.4.1) and the mapped reads were discarded. After that, mapping against the human genome (GRCh38 version 32/Ensembl 98) was performed using STAR aligner v2.7.9a.

SeqPilot software (JSI medical systems GmbH, Ettenheim, Germany) was used for *SF3B1* variant calling using FASTQ files as inputs. RSEM (v1.3.3) was used for quantifying gene and transcript abundances from RNA-seq data. The R package EBSeq (v1.28.0) was used to infer differential gene and isoform expressions.[3] Downstream pathway analysis of DEG was conducted using IPA core pathway and upstream regulator analysis (QIAGEN Ingenuity Systems, CA, USA) by applying the following filters: posterior probability of being differentially expressed (PPDE) > (1-α) (with significance level α set to 0.05) and posterior fold change (PostFC) of ≥ 2 or ≤ 0.5. The right-tailed Fisher's exact test was used to estimate the probability that an association between a set of molecules and a biological function or pathway might be due to random chance. The IPA activation z-score was used to infer the activation states ("increased" or "decreased") of implicated biological functions. Furthermore, the Isoprofiler tool in IPA was utilized to filter protein-coding isoforms associated with known diseases or functions (PostFC of ≥ 2 or ≤ 0.5 [values below 1 were converted to -1/PostFC within IPA application]; isoform-specific disease or function count set to 1). Replicate multivariate analysis of transcript splicing (rMATS[4] v4.0.2) was used to assess differential alternative splicing events. rMATS detects differential usage of exons by comparing exon-inclusion levels defined with junction reads. Splicing events with FDR < 0.05, inclusion level difference of > |0.05|, average read counts ≥ 10, and average inclusion levels within 0.05 and 0.95 were taken forward (events with missing read count values and events affecting genes on X or Y chromosome were omitted). The EnhancedVolcano and ggvenn R packages were used for data visualization.

Pathway and process enrichment analysis

Pathway and process enrichment analysis of DEG (NanoString gene expression analysis, Figure 1A) has been carried out using Metascape (http://metascape.org)[5] with the following ontology sources: GO Biological Processes, GO Cellular Components, GO Molecular Functions, KEGG Pathway, and Canonical Pathways. Ontology sources for Metascape pathway and process enrichment analysis of DSG (rMATS data, Figure 5D) included: KEGG Pathway, GO Biological Processes, Reactome Gene Sets, Canonical Pathways, CORUM, WikiPathways, and PANTHER Pathway. Significant enrichment was indicated by a minimum overlap of 3, *p*-value cut-off of 0.01, and minimum enrichment of 1.5. The most significant term within a cluster was chosen to represent the cluster.

Luminex analysis of secreted cytokines

Cytokine levels in supernatants were determined in duplicate using a customized Luminex™ panel for IFN-α2, IFN-γ, IL-1β, IL-1RA, IL-6, IL-10, IL-17A, IL-18, IL-27, CXCL10 (IP-10), MCP-1, and TNF-α (Merck Millipore, MA, USA) on a FLEXMAP 3D™ system (Luminex Corp., Austin, TX, USA) according to the manufacturer´s instructions. The background-subtracted averaged median fluorescence intensity (MFI) values for LPS-stimulated samples were corrected for non-stimulated cytokine secretion through subtraction. We added +1 to all values and plotted log2-transformed LPS-induced MFI values using the R package pheatmap.

Statistical analysis

Statistical analyses were performed using R (v4.2.3, R Foundation for Statistical Computing, Vienna, Austria) and R Studio (v2023.03.0, Posit Software). A *p*-value of < 0.05 was considered statistically significant.

Supplemental Figure 1

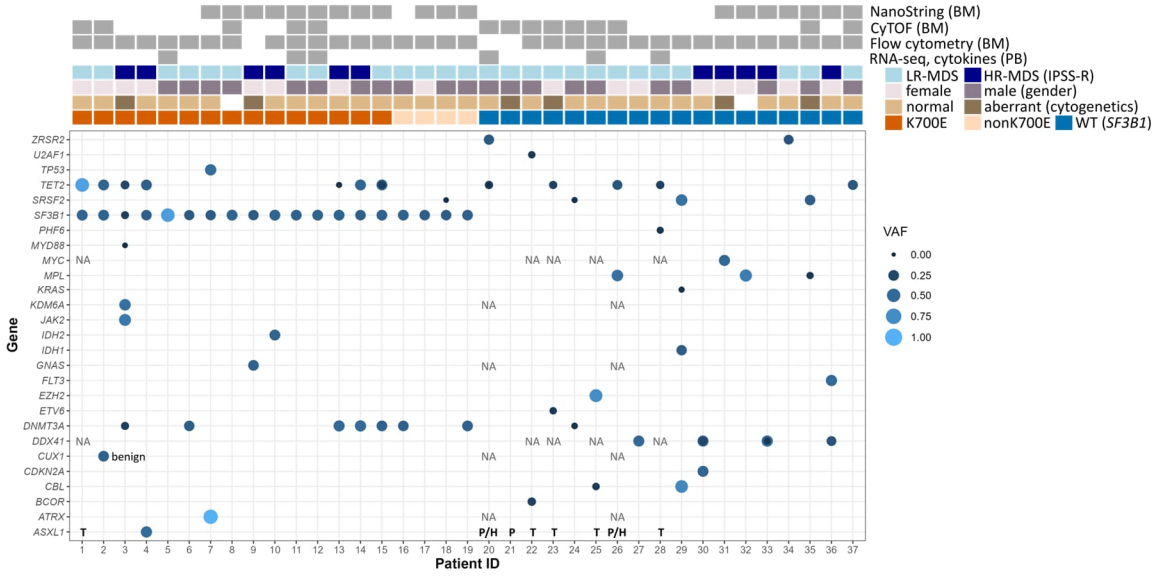

Supplemental Figure 1: Overview of somatic mutational data of MDS patients (experimental cohort) and performed analyses. Summary of somatic mutational data assessed by next generation sequencing showing VAF of gene variants for individual patients. BM samples were screened using the Archer® VariantPlex® Myeloid panel (75 genes) unless otherwise indicated (T, Illumina TrueSight Myeloid Sequencing Panel [54 genes]; P, PB samples used for mutational screening; P/H, PB samples used for mutational screening with a customized Agilent HaloPlex Panel [71 genes]). *SF3B1*^{mut} MDS patients showed a restricted spectrum of co-mutations, with *TET2* and *DNMT3A* being the most frequently mutated co-occurring genes (both 36.8%). Mutations in splicing genes other than *SF3B1* (i.e. *SRSF2*, *U2AF1*, *ZRSR2*) or splicing regulatory genes (i.e. *DDX41*) were detected in 10/18 *SF3B1*^{wt} MDS patients, while 18/19 *SF3B1*^{mut} MDS patients were devoid of mutations in these genes. Annotations above indicate the analyses performed on individual patient samples and clinical characteristics including IPSS-R (LR-MDS, IPSS-R ≤ 3.5; HR-MDS, IPSS-R > 3.5), cytogenetic profile, and *SF3B1* mutation status (K700E, nonK700E, WT). MDS patients were treatment-naïve (i.e. EPO, supportive care) with the following exceptions: patient #3 has documented lenalidomide/valproic acid treatment until 3 months before sampling; patients #18 and #32 had documented administration of LY2157299 monohydrate in medical history; patient #33 was enrolled in the randomized, placebo-controlled AZA-MDS-003 trial (NCT01566695) before sampling; and patient #37 had documented ATG/CSA 6 years before sampling.

Supplemental Figure 2

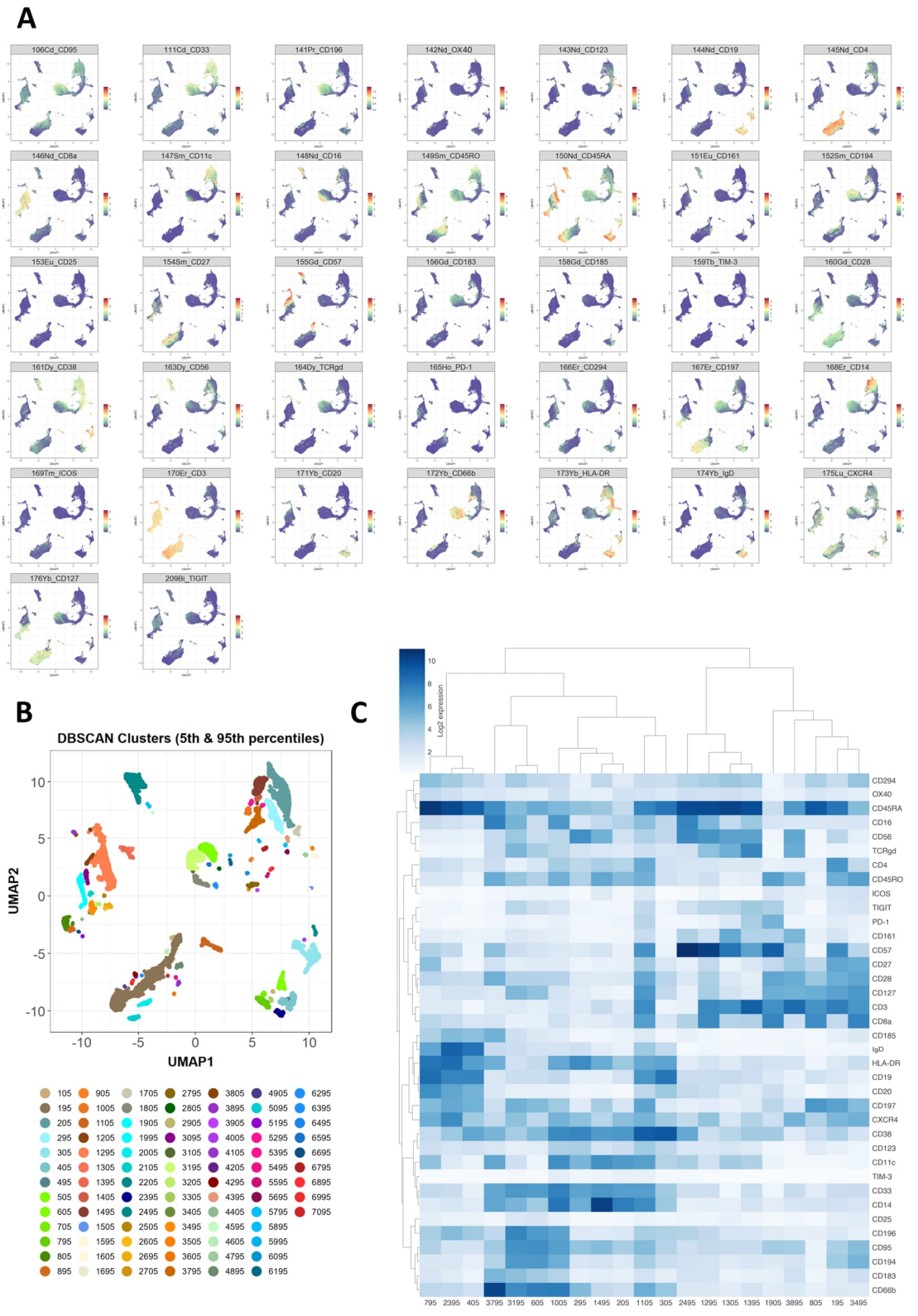

Supplemental Figure 2: T-REX analysis of CyTOF data comparing CD45^{+} BM-MNCs from LR-MDS (n = 14) and HD (n = 4). (A) Protein marker expression projected onto UMAP. (B) Cluster analysis using density-based spatial clustering of applications with noise (DBSCAN) within T-REX workflow. (C) Heatmap depicting the average marker expression (in log2) across DBSCAN clusters containing > 2000 cells. Clusters were grouped using hierarchical clustering with the complete linkage method and correlation as a distance metric.

Supplemental Figure 3

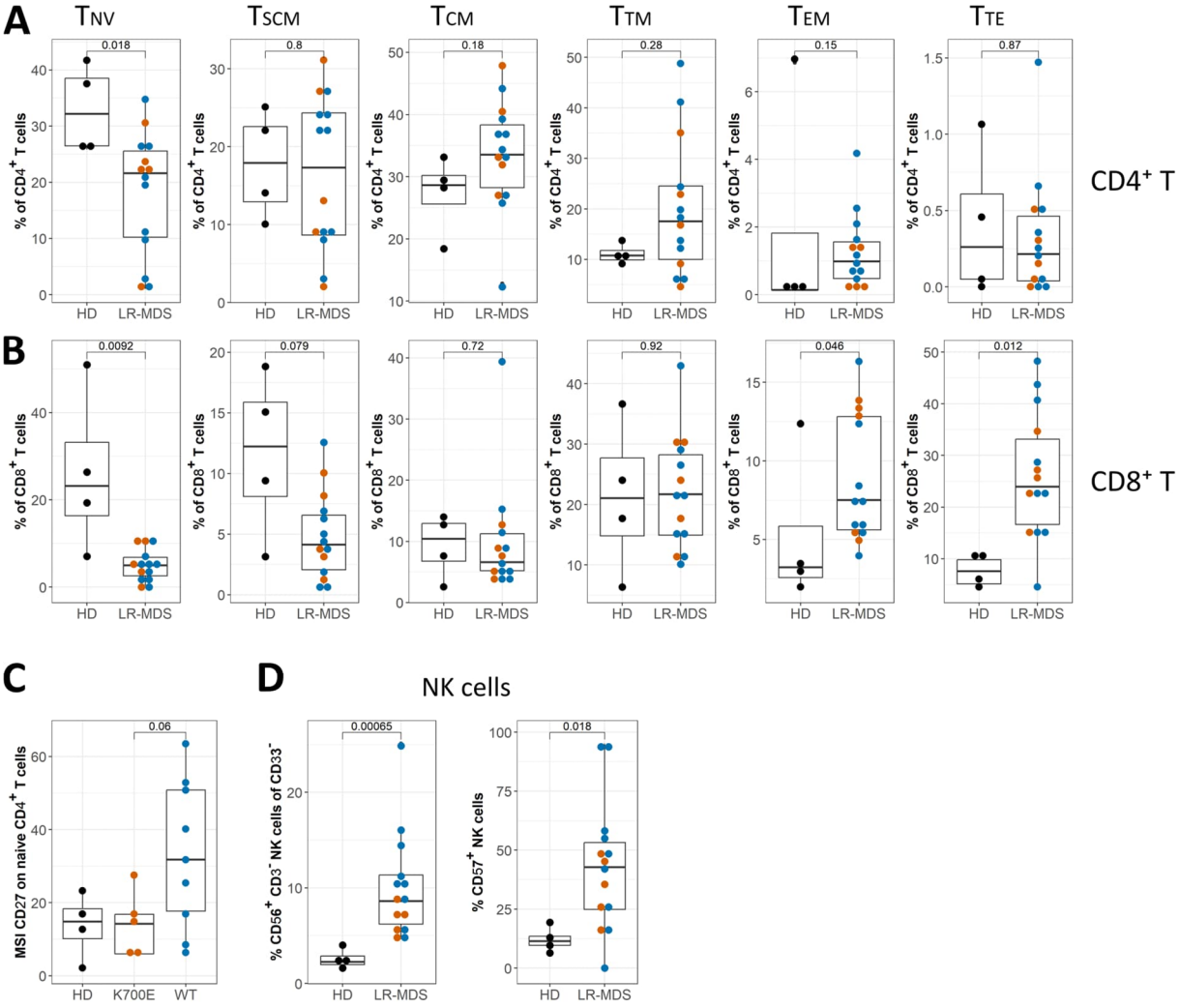

Supplemental Figure 3: Distribution of key immune cell subpopulations in the BM of LR-MDS. CyTOF data gated on live CD45$^+$ BM-MNCs from HD, *SF3B1^{K700E}* (orange dots), or *SF3B1^{wt}* (blue dots) LR-MDS were further gated for (A, C) CD4$^+$ T, (B) CD8$^+$ T, and (D) NK cell subsets. (C) Geometric mean signal intensity (MSI) of CD27 expression on naïve CD4$^+$ T cells. (D) The frequency of CD56$^+$ CD3$^-$ NK cells relative to (non-myeloid) CD33$^-$ CD45$^+$ cells and the proportion of CD57$^+$ NK cells. (A-D) Mann-Whitney-U-test/Wilcoxon-test was performed for indicated comparisons. Abbreviations: T_{CM}, central memory T cells; T_{EM}, effector memory T cells; T_{NV}, naïve T cells; T_{SCM}, T stem cell-like memory cells; T_{TE}, terminal effector T cells; T_{TM}, transitional memory T cells.

Supplemental Figure 4

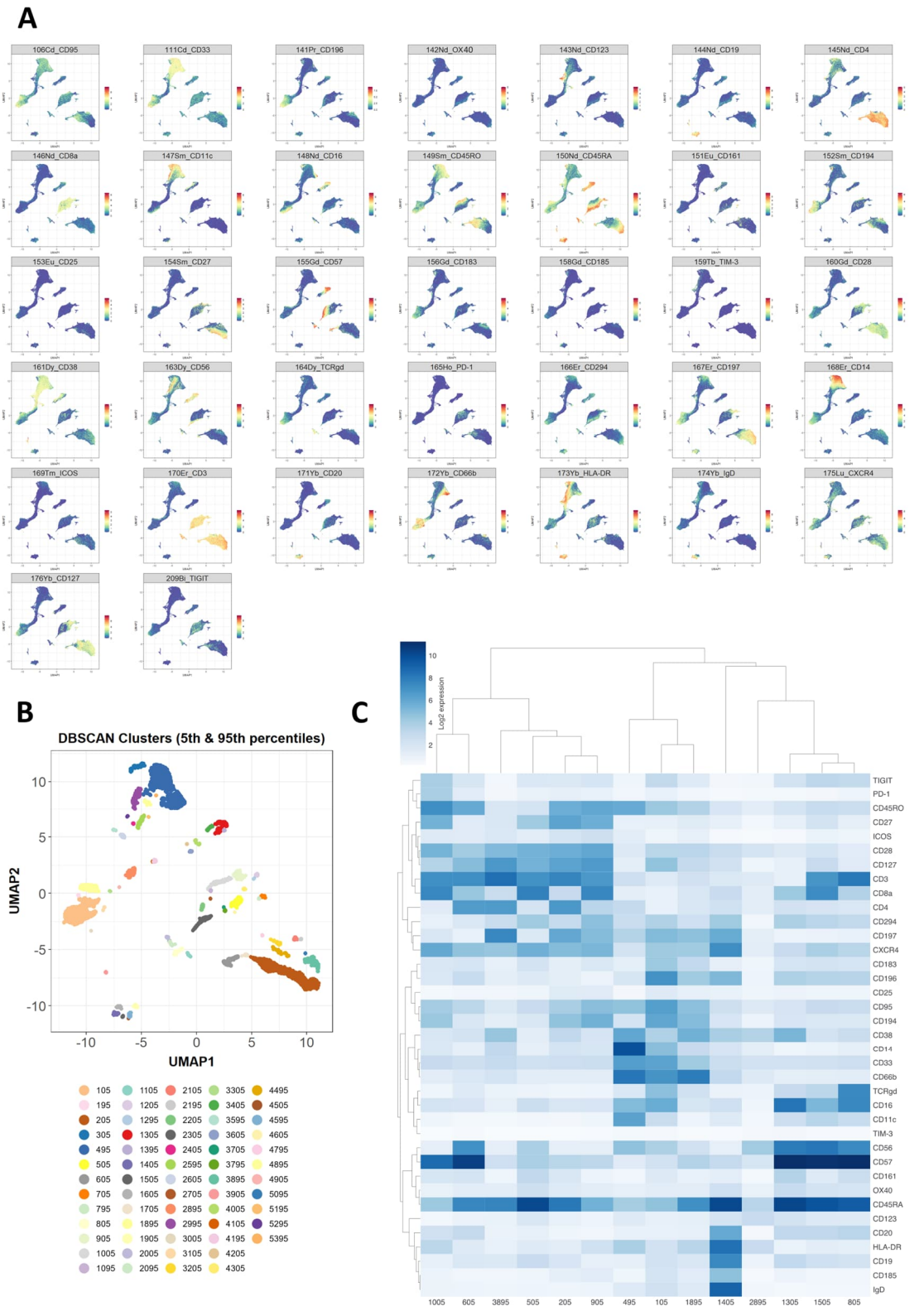

Supplemental Figure 4: T-REX analysis of CyTOF data comparing CD45^{+} BM-MNCs from *SF3B1*^{K700E} (n = 5) and *SF3B1*^{wt} (n = 9) LR-MDS. (A) Protein marker expression projected onto UMAP. (B) Cluster analysis using density-based spatial clustering of applications with noise (DBSCAN) within T-REX workflow. (C) Heatmap depicting the average marker expression (in log2) across DBSCAN clusters containing > 1000 cells. Clusters were grouped using hierarchical clustering with the complete linkage method and correlation as a distance metric.

Supplemental Figure 5

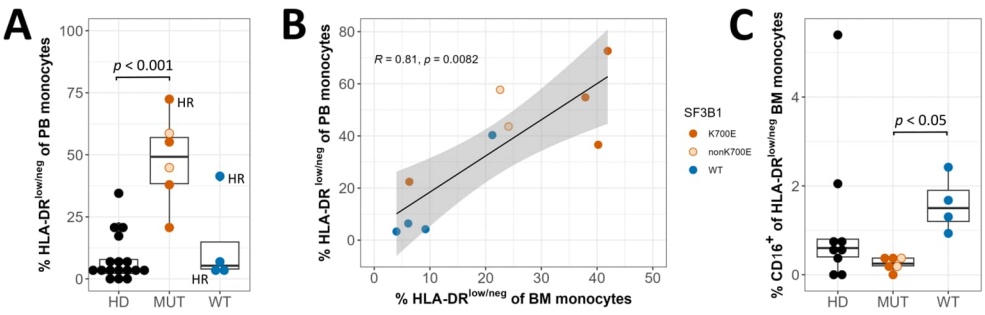

Supplemental Figure 5: Increased proportion of HLA-DR$^{low/neg}$ monocytes in peripheral blood of *SF3B1*^{mut} MDS and further characterization of HLA-DR$^{low/neg}$ BM monocytes. (A) Percentage of PB monocytes with HLA-DR$^{low/neg}$ immunophenotype in HD (n = 17, mean age = 51 years), *SF3B1*^{mut} (n = 6; orange dots, K700E; light orange-filled circles, nonK700E; mean age = 74 years), and *SF3B1*^{wt} (n = 4, mean age = 71 years) MDS assessed by diagnostic flow cytometry of freshly stained PB samples. "HR" labels indicate patients with IPSS-R > 3.5. (B) Correlation of frequency of HLA-DR$^{low/neg}$ monocytes in BM and PB. Data show Spearman's rank correlation coefficient *R* and *p*-value with linear regression line and confidence interval. (C) Proportion of HLA-DR$^{low/neg}$ BM monocytes expressing CD16. (A, C) Kruskal-Wallis test with Dunn's post-hoc test (Bonferroni adjusted *p*-values).

Supplemental Figure 6

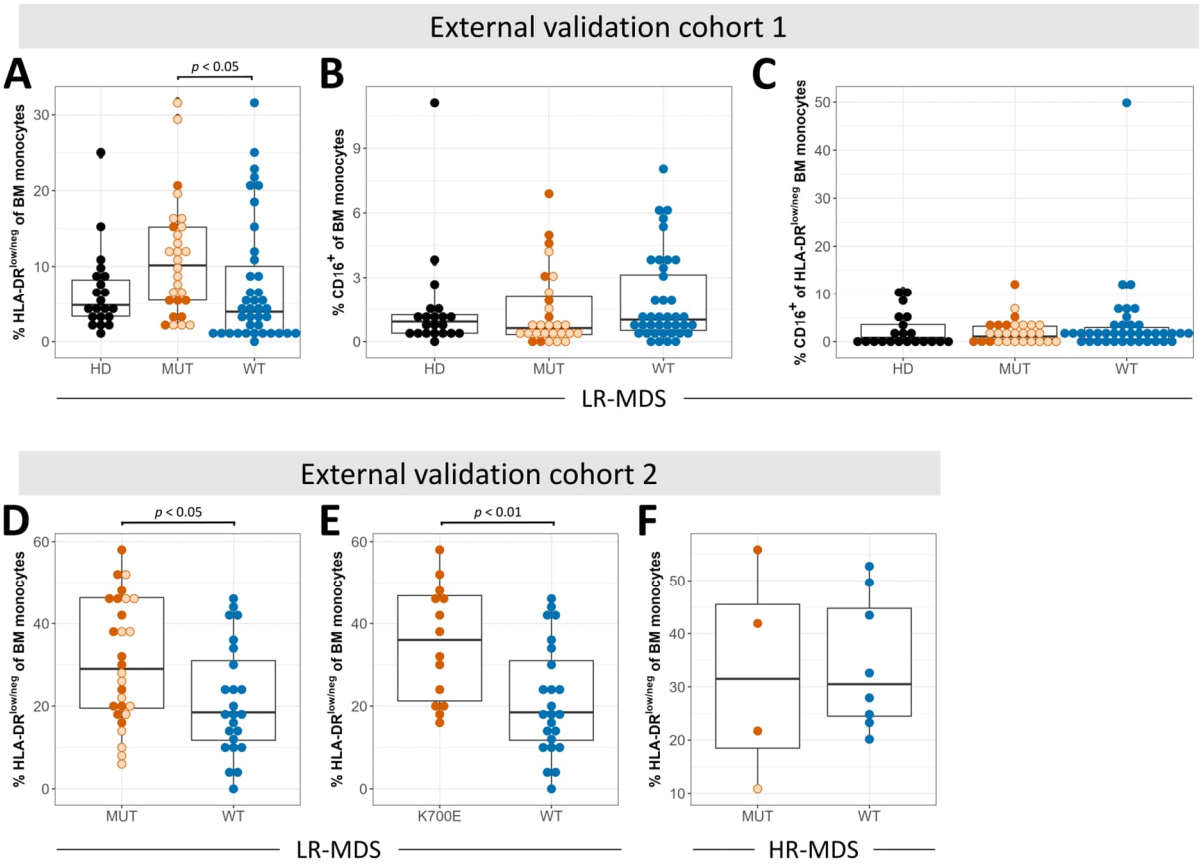

Supplemental Figure 6: External validation confirms increased frequency of HLA-DR$^{low/neg}$ monocytes in *SF3B1*^{mut} compared to *SF3B1*^{wt} LR-MDS. (A-C) Shown are data from external validation cohort 1 comprising 21 HD (mean age = 60 years), 28 *SF3B1*^{mut} (orange dots, K700E; light orange-filled circles, nonK700E; mean age = 71 years), and 39 *SF3B1*^{wt} (mean age = 68 years) treatment-naïve LR-MDS (IPSS-R ≤ 3.5) assessed by flow cytometry of viably frozen BM-MNCs isolated by density gradient centrifugation in Lympholyte®-H separation medium (Cedarlane). Kruskal-Wallis test with Dunn's post-hoc test (Bonferroni adjusted *p*-values < 0.05 were considered significant). (A) Percentage of CD33$^+$ CD14$^+$ BM monocytes with HLA-DR$^{low/neg}$ immunophenotype. (B) Percentage of BM monocytes with surface CD16 expression (intermediate and non-classical monocytes). (C) Proportion of HLA-DR$^{low/neg}$ BM monocytes expressing CD16. (D-F) Shown are data from external validation cohort 2 comprising 32 *SF3B1*^{mut} (orange dots, K700E; light orange-filled circles, nonK700E; mean age = 71 years) and 32 *SF3B1*^{wt} (mean age = 69 years) treatment-naïve (at diagnosis) or largely untreated (i.e. EPO in 4 out of 64) LR- and HR-MDS patients assessed by flow cytometry of freshly stained BM samples as part of the diagnostic work-up. The gating of HLA-DR$^{low/neg}$ monocytes was performed using Infinicyt flow cytometry software (Cytognos, S.L.) according to the gating strategy applied to the experimental cohort. Mann-Whitney-U-test/Wilcoxon-test was performed ($p < 0.05$ was considered significant). (D) Percentage of CD33$^+$ CD14$^+$ BM monocytes with HLA-DR$^{low/neg}$ immunophenotype including 28 *SF3B1*^{mut} (n = 14 *SF3B1*^{K700E}, n = 14 *SF3B1*^{nonK700E}) compared to 24 *SF3B1*^{wt} LR-MDS (IPSS-R ≤ 3.5). (E) Percentage of CD33$^+$ CD14$^+$ BM monocytes with HLA-DR$^{low/neg}$ immunophenotype in *SF3B1*^{K700E} compared to *SF3B1*^{wt} LR-MDS. (F) Percentage of CD33$^+$ CD14$^+$ BM monocytes with HLA-DR$^{low/neg}$ immunophenotype including 4 *SF3B1*^{mut} (n = 3 *SF3B1*^{K700E}, n = 1 *SF3B1*^{nonK700E}) compared to 8 *SF3B1*^{wt} HR-MDS (IPSS-R > 3.5).

Supplemental Figure 7

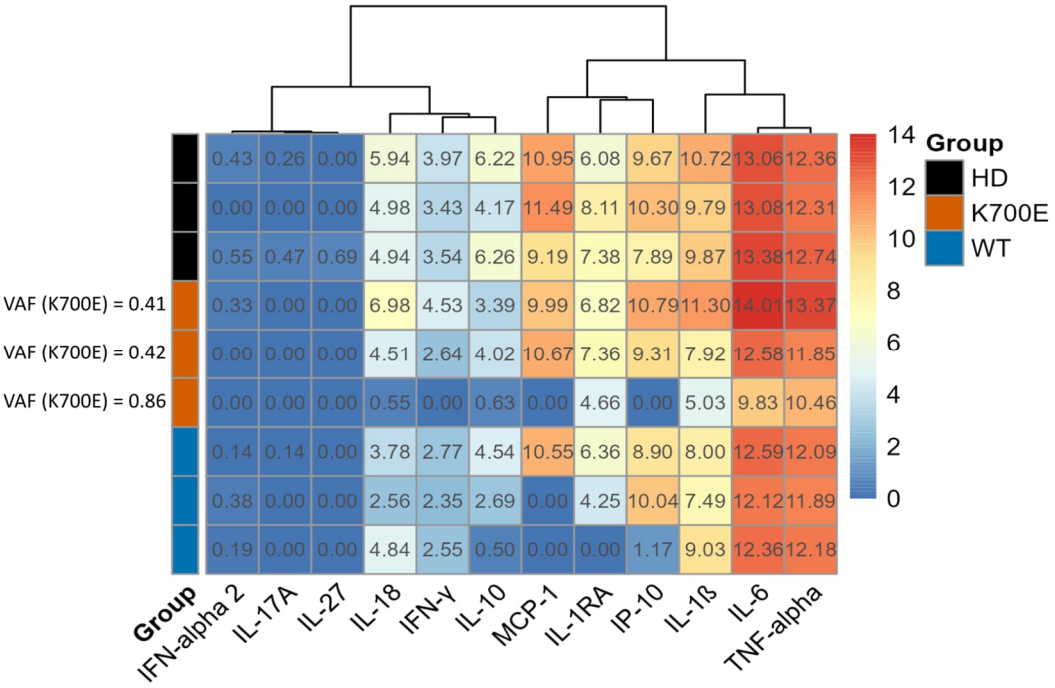

Supplemental Figure 7: Cytokine secretion by LPS-stimulated classical monocytes. Heatmap depicts log2-transformed normalized median fluorescence intensity values for the indicated cytokines produced by HD (n = 3), *SF3B1*^{K700E} (n = 3), or *SF3B1*^{wt} (n = 3) LR-MDS classical monocytes following *in vitro* LPS stimulation. The variant allele frequency (VAF) of *SF3B1*^{K700E} mutation in classical monocytes is shown on the left side.

Chapter 6

Summary, conclusions and future perspectives

In the present project, we focused our attention in dissecting the role of immune dysregulation in MDS, with the aim of finding additional signatures that could help to deepen the knowledge about the molecular features underlying MDS pathogenesis, an urgent medical need given the restricted choice and limited efficacy of available treatments. With the recent development of the IPSS-M score, which integrates genomic information to risk score calculation, a significantly improvement of MDS classification has been achieved [1-4]. However, our group demonstrated that even if IPSS-M ameliorates the prediction of survival and relapse in patients undergone HSCT, and thus it could be helpful in the selection of eligible patients, it fails in predicting the response to HMA therapy [4]. This means that there are other factors, beyond gene mutations, that are involved in disease progression and therapy response. One of these factors rely on immune system capacity to properly work and eliminate tumor cells. In fact, it is known that the immune system suppress tumor outgrowth, but on the other hand can also shape the immunological characteristic of the malignant cells, promoting the selection of edited cancers able to bypass immunosurveillance and carry out immune escape: this phenomenon is called "cancer immunoediting", and its discovery revolutionized cancer treatment of the last two decades, paving the way to "immuno-oncology" field and to the development of immunotherapies [5-7]. As for the other cancers, also in MDS it has been shown an involvement of immune dysregulation in MDS origination and progression [8-10], but the addition of immune features to clinical information is still difficult due to the high heterogeneity of the disease and the controversial results obtained from different patients' cohorts and methods of investigation.

Given the complexity of tumor microenvironment and the multitude of cell-to-cell interactions and pathways involved in tumorigenesis and treatment outcome, multi-omics data integration has recently emerged as a powerful tool to identify predictive biomarkers in cancer [11-13]. For this reason, we thought that a multi-omics analysis would have helped to identify more robust immune signatures for the prediction of survival and treatment response in MDS. Our multi-omic approach, consisting in the integration of immunophenotyping data with transcriptomic, genetic mutations and clinical information, allowed us to deeply characterize a large and heterogeneous MDS cohort in the first paper, and also genetically-characterized MDS groups ($TP53^{mut}$ and $SF3B1^{mut}$) in the second and third projects, respectively.

In the first work we demonstrated, in both supervised and unsupervised manner, the value of adding immunological information at MDS diagnosis and along HMA administration for a better stratification, outcome prediction and treatment response estimation. With unsupervised methods of clustering, we classified MDS patients in five groups characterized by different grades of immune dysfunction, from an immunosuppressed and exhausted phenotype, via an anergic state to a naïve and functional one. Moreover, we proved that such immune groups possess prognostic power both in terms of overall survival and therapy response, and we showed how patients belonging to the same IPSS-R/M risk or WHO/ICC category are heterogeneous respective to immune system functionality. Thanks to RNAseq data integration, we were able to deeply characterize the tumor features in each immune subgroup, highlighting the presence of different inflammatory signatures that could be specifically targeted. Two independent studies on AML recently showed how the characterization of immune features can improve stratification and predict treatment outcome, in particular inflammation has emerged as a key factor impacting on both immune cell functions and patient's survival [14-15]. As in the work of Lasry et al., we found that high levels of inflammation are associated with immunologic dysfunction and poor outcome [15]. We also demonstrated the feasibility of developing a decision model for the automatic assignment of patients to the different immune groups and we identified four immune cell subpopulations whose balance is important for immunologic classification. For these four cell types, we are actually working on refining the decision tree thresholds for their adaptation from Phenograph clusters frequencies to manual gating ones, in order to simplify the approach and allow a broad validation of our findings on other MDS cohorts. Furthermore, we are developing an "immune score", based on the grade of immune dysfunction, that could be integrated to the actual parameters for IPSS-R and IPSS-M calculation. In the end, given our findings confirming the power of peripheral blood in reflecting bone

marrow environment, we designed three cytometry panels with few markers relevant for T, NK and Myeloid cells characterization that will be applied in clinical routine evaluation of MDS PB samples.

In the second paper we characterized the transcriptional and immunological features of MDS patients with p53 dysfunction ($TP53^{mut}$ or $TP53^{wt}$ with p53 protein hyperexpression) versus MDS without p53 dysfunctions. Through RNAseq analysis of tumor blasts we showed that p53 dysfunctional patients present an aggressive phenotype with p53 pathway downregulation, myc targets upregulation and an immunosuppressive transcriptional program compared to other MDS patients, characterized by major expression of immune checkpoints molecules, downregulation of HLA class II members and their master regulator CIITA and an enrichment in immunosuppressive cytokines within the bone marrow niche. With flow cytometry analysis we confirmed that the transcriptional programs expressed by blast cells also have an impact on immune cell functions. In fact, we identified an increased presence of Tregs, exhausted $PD1^+$ $CD8^+$ T cells and $PD1^+$ NK cells with low expression of activation receptors, and decreased frequency of Naïve and antigen-actived $CD8^+$ T cells, indicative of a general loss of function of immune cells. Moreover, we identified a new MDS patients subgroup characterized by p53 protein hyperexpression without TP53 gene mutations that is molecularly similar to TP53 mutated patients and could benefit from specific therapies.

In the third paper we firstly investigated the transcriptional differences in $SF3B1^{mut}$ vs $SF3B1^{wt}$ low-risk MDS through RNAseq, observing that $SF3B1^{mut}$ MDS have an increased myeloid gene signature compared to lymphocytes and a minor inflamed niche characterized by less expression of IL-1β and inflammatory genes. High-dimensional immunophenotyping of bone marrow cells in MDS patients vs healthy donors revealed coherent results with the ones observed in the first paper, with less $CD4^+$ naïve and more $CD8^+$ terminal effectors, $PD1^+$ $TIGIT^+$ T cells and $CD57^+$ NK cells. The comparison between $SF3B1^{mut}$ and $F3B1^{wt}$ showed a higher proportion of $CD33^+$ $CD14^+$ monocytes expressing low levels of HLA-DR in $SF3B1^{mut}$. RNAseq of sorted monocytes from those patients highlighted that monocytes harbor the SF3B1 mutation with similar VAF to total BMNCs, indicating their clonal origin, and a reduced pro-inflammatory profile. However, *in vitro* stimulation showed that, despite they arise from the MDS clone, they are still functional and retain their capacity to secrete inflammatory cytokines upon LPS administration. We concluded that the SF3B1 mutation shapes not only MDS blast inflammatory properties, but also monocyte ones, and $SF3B1^{mut}$ MDS are characterized by a lower level of inflammation; thus, therapies that target myeloid-driven hyperinflammation are not useful.

Taken together, our works underline how the integration of data coming from different -omics technologies can give an important help in elucidating the complex molecular and cellular panorama of MDS, in particular for the study of immune system deregulations. In fact, the results from each single technique helped us to confirm and dissect in many ways what we were observing on one hand, and in the other hand allowed us to give conceivable explanations about the link between molecular features and clinical data, and to identify possible targeted therapies.

Additional future perspectives in our MDS studies involve the use of single-cell RNA sequencing with CITE-seq (Cellular Indexing of Transcriptomes and Epitopes by Sequencing), an innovative sequencing method that simultaneously allow, at a single cell level, to obtain both transcriptome information and quantity and quality protein expression [16]. Furthermore, since bone marrow is a complex tissue whose functions depend not only on a balanced cell composition and correct cellular behaviors, but also on the spatial localization and interactions of all the niche components, we are planning to perform spatial analyses on MDS bone marrow slides. In fact, even if RNA-seq and flow cytometry can provide a huge amount of data about cell composition and functionality, they can't give any information about their original localization and distribution in the tissue. Imaging mass cytometry (IMC) is a technology that uses tissue laser ablation to generate plumes of particles which are channeled to a mass cytometer by inert gas [17]. Briefly, the tissue slide is marked with heavy metal-tagged antibodies specific for intra- and extra-cellular markers of interest. Then, a laser with

1µM diameter size ablates the tissue and thus the metals are released from each cell and are detected and measured with a (Time of flight) TOF system. In this way, the tissue is scanned spot-by-spot, allowing to obtain information about quantity and spatial expression of each marker. IMC has been employed in important publications for the study of tumor immune microenvironment [18-19] and its relevance has been recently underlined [20]. Our idea is to apply the IMC analysis of BM slides from the same patients that we will sequence with the CITE-seq technique. For these experiments we specifically selected two MDS cohorts of patients: one cohort composed of people that experienced a disease evolution in absence of medical treatments, in order to study the natural course of the disease, and the second cohort composed of patients who experienced a relapse of the disease after an initial response to therapy with HMA or HSCT, in order to understand the molecular and cellular changes that caused the lost remission.

Overall, we believe that the knowledge deriving from our present and future projects will have a significant impact in improving the understanding of MDS molecular pathogenesis, as well as opening new frontiers in MDS management and personalized treatment.

References

1. Bernard E, Tuechler H, Greenberg Peter L, Hasserjian Robert P, Arango Ossa Juan E, Nannya Y, et al. Molecular international prognostic scoring system for myelodysplastic syndromes. NEJM Evid. 2022;1:EVIDoa2200008.
2. Lee, WH., Tsai, MT., Tsai, CH. et al. Validation of the molecular international prognostic scoring system in patients with myelodysplastic syndromes defined by international consensus classification. Blood Cancer J. 13, 120 (2023). https://doi.org/10.1038/s41408-023-00894-8
3. Aguirre LE, Al Ali N, Sallman DA, Ball S, Jain AG, Chan O, Tinsley-Vance SM, Kuykendall A, Sweet K, Lancet JE, Padron E, Komrokji RS. Assessment and validation of the molecular international prognostic scoring system for myelodysplastic syndromes. Leukemia. 2023 Jul;37(7):1530-1539. doi: 10.1038/s41375-023-01910-3. Epub 2023 May 5. PMID: 37147425.
4. Sauta E, Robin M, Bersanelli M, Travaglino E, Meggendorfer M, Zhao LP, Caballero Berrocal JC, Sala C, Maggioni G, Bernardi M, Di Grazia C, Vago L, Rivoli G, Borin L, D'Amico S, Tentori CA, Ubezio M, Campagna A, Russo A, Mannina D, Lanino L, Chiusolo P, Giaccone L, Voso MT, Riva M, Oliva EN, Zampini M, Riva E, Nibourel O, Bicchieri M, Bolli N, Rambaldi A, Passamonti F, Savevski V, Santoro A, Germing U, Kordasti S, Santini V, Diez-Campelo M, Sanz G, Sole F, Kern W, Platzbecker U, Ades L, Fenaux P, Haferlach T, Castellani G, Della Porta MG. Real-World Validation of Molecular International Prognostic Scoring System for Myelodysplastic Syndromes. J Clin Oncol. 2023 May 20;41(15):2827-2842. doi: 10.1200/JCO.22.01784. Epub 2023 Mar 17. PMID: 36930857; PMCID: PMC10414702.
5. Schreiber RD, Old LJ, Smyth MJ. Cancer immunoediting: integrating immunity's roles in cancer suppression and promotion. Science. 2011 Mar 25;331(6024):1565-70. doi: 10.1126/science.1203486. PMID: 21436444.
6. Gubin MM, Vesely MD. Cancer Immunoediting in the Era of Immuno-oncology. Clin Cancer Res. 2022 Sep 15;28(18):3917-3928. doi: 10.1158/1078-0432.CCR-21-1804. PMID: 35594163; PMCID: PMC9481657.
7. O'Donnell JS, Teng MWL, Smyth MJ. Cancer immunoediting and resistance to T cell-based immunotherapy. Nat Rev Clin Oncol. 2019 Mar;16(3):151-167. doi: 10.1038/s41571-018-0142-8. PMID: 30523282.

8. Barreyro L, Chlon TM, Starczynowski DT. Chronic immune response dysregulation in MDS pathogenesis. Blood. 2018 Oct 11;132(15):1553-1560. doi: 10.1182/blood-2018-03-784116. Epub 2018 Aug 13. PMID: 30104218; PMCID: PMC6182269.
9. Vegivinti CTR, Keesari PR, Veeraballi S, Martins Maia CMP, Mehta AK, Lavu RR, Thakur RK, Tella SH, Patel R, Kakumani VK, Pulakurthi YS, Aluri S, Aggarwal RK, Ramachandra N, Zhao R, Sahu S, Shastri A, Verma A. Role of innate immunological/inflammatory pathways in myelodysplastic syndromes and AML: a narrative review. Exp Hematol Oncol. 2023 Jul 8;12(1):60. doi: 10.1186/s40164-023-00422-1. PMID: 37422676; PMCID: PMC10329313.
10. Barakos GP, Hatzimichael E. Microenvironmental Features Driving Immune Evasion in Myelodysplastic Syndromes and Acute Myeloid Leukemia. Diseases. 2022 Jun 10;10(2):33. doi: 10.3390/diseases10020033. PMID: 35735633; PMCID: PMC9221594.
11. Sammut, SJ., Crispin-Ortuzar, M., Chin, SF. et al. Multi-omic machine learning predictor of breast cancer therapy response. Nature 601, 623–629 (2022). https://doi.org/10.1038/s41586-021-04278-5
12. Vantaku V, Dong J, Ambati CR, Perera D, Donepudi SR, Amara CS, Putluri V, Ravi SS, Robertson MJ, Piyarathna DWB, Villanueva M, von Rundstedt FC, Karanam B, Ballester LY, Terris MK, Bollag RJ, Lerner SP, Apolo AB, Villanueva H, Lee M, Sikora AG, Lotan Y, Sreekumar A, Coarfa C, Putluri N. Multi-omics Integration Analysis Robustly Predicts High-Grade Patient Survival and Identifies CPT1B Effect on Fatty Acid Metabolism in Bladder Cancer. Clin Cancer Res. 2019 Jun 15;25(12):3689-3701. doi: 10.1158/1078-0432.CCR-18-1515. Epub 2019 Mar 7. PMID: 30846479; PMCID: PMC6571061.
13. Lu M, Zhan X. The crucial role of multiomic approach in cancer research and clinically relevant outcomes. EPMA J. 2018 Feb 21;9(1):77-102. doi: 10.1007/s13167-018-0128-8. PMID: 29515689; PMCID: PMC5833337.
14. Vadakekolathu J, Minden MD, Hood T, Church SE, Reeder S, Altmann H, Sullivan AH, Viboch EJ, Patel T, Ibrahimova N, Warren SE, Arruda A, Liang Y, Smith TH, Foulds GA, Bailey MD, Gowen-MacDonald J, Muth J, Schmitz M, Cesano A, Pockley AG, Valk PJM, Löwenberg B, Bornhäuser M, Tasian SK, Rettig MP, Davidson-Moncada JK, DiPersio JF, Rutella S. Immune landscapes predict chemotherapy resistance and immunotherapy response in acute myeloid leukemia. Sci Transl Med. 2020 Jun 3;12(546):eaaz0463. doi: 10.1126/scitranslmed.aaz0463. PMID: 32493790; PMCID: PMC7427158.
15. Lasry A, Nadorp B, Fornerod M, Nicolet D, Wu H, Walker CJ, Sun Z, Witkowski MT, Tikhonova AN, Guillamot-Ruano M, Cayanan G, Yeaton A, Robbins G, Obeng EA, Tsirigos A, Stone RM, Byrd JC, Pounds S, Carroll WL, Gruber TA, Eisfeld AK, Aifantis I. An inflammatory state remodels the immune microenvironment and improves risk stratification in acute myeloid leukemia. Nat Cancer. 2023 Jan;4(1):27-42. doi: 10.1038/s43018-022-00480-0. Epub 2022 Dec 29. Erratum in: Nat Cancer. 2023 Jan 19;: PMID: 36581735; PMCID: PMC9986885.
16. Stoeckius, M., Hafemeister, C., Stephenson, W. et al. Simultaneous epitope and transcriptome measurement in single cells. Nat Methods 14, 865–868 (2017). https://doi.org/10.1038/nmeth.4380
17. Chang Q, Ornatsky OI, Siddiqui I, Loboda A, Baranov VI, Hedley DW. Imaging Mass Cytometry. Cytometry A. 2017 Feb;91(2):160-169. doi: 10.1002/cyto.a.23053. Epub 2017 Feb 3. PMID: 28160444.
18. Sorin, M., Rezanejad, M., Karimi, E. et al. Single-cell spatial landscapes of the lung tumour immune microenvironment. Nature 614, 548–554 (2023). https://doi.org/10.1038/s41586-022-05672-3
19. Karimi E, Yu MW, Maritan SM, Perus LJM, Rezanejad M, Sorin M, Dankner M, Fallah P, Doré S, Zuo D, Fiset B, Kloosterman DJ, Ramsay L, Wei Y, Lam S, Alsajjan R, Watson IR, Roldan Urgoiti G, Park M, Brandsma D, Senger DL, Chan JA, Akkari L, Petrecca K, Guiot MC, Siegel PM, Quail DF, Walsh LA. Single-cell spatial immune landscapes of primary and metastatic brain tumours. Nature. 2023 Feb;614(7948):555-563. doi: 10.1038/s41586-022-05680-3. Epub 2023 Feb 1. PMID: 36725935; PMCID: PMC9931580.

20. Piyadasa, H., Angelo, M. & Bendall, S.C. Spatial proteomics of tumor microenvironments reveal why location matters. Nat Immunol 24, 565–566 (2023). https://doi.org/10.1038/s41590-023-01471-8